

American Society of Echocardiography
30th Annual Scientific Sessions

ASE 2019



30

YEARS OF
INNOVATION

June 21 - 25, 2019

Oregon Convention Center • Portland, OR

• ORIGINAL SCIENCE PRESENTATIONS •

ASE gratefully acknowledges the following individuals for their contribution to the 30th Annual ASE Scientific Sessions as an Abstract Grader.

ABSTRACT CHAIR

Theodore P. Abraham, MD, FASE

ABSTRACT CO-CHAIR

Michael L. Main, MD, FASE

Karima Addetia, MD, FASE

Srinath Adusumalli, MD, MSc

Clara I. Angulo, BS, ACS, RDCS, FASE

Alicia C. Armour, BA, MA, RDCS, FASE

Rima Arnaout, MD

Federico M. Asch, MD, FASE

Jose Banchs, MD, FASE

Ana Barac, MD, PhD

Piers C.A. Barker, MD, FASE

Harald Becher, MD, PhD

Ricardo J. Benenstein, MD, FASE

Himani Bhatt, MD, MPA, FASE

Paul F. Braum, BS, RDCS, RCS, RVT,
RVS, ACS, FASE

Su Min Chang, MD

Annabel A. Chen-Tournoux, MD

Frederick C. Cobey, MD, FASE

Keith A. Collins, MS, RDCS, FASE

Mary C. Corretti, MD, FASE

Clifford Cua, MD

Jacob P. Dal-Bianco, MD, FASE

Ravin Davidoff, MBBCh, FASE

Brian P. Davidson, MD, FASE

Jeanne M. DeCara, MD, FASE

Francesca Delling, MD

John M. Dent, MD, MS, MHCM, FASE

Adam L. Dorfman, MD, FASE

Nowell M. Fine, MD, MS, FASE

Craig E. Fleishman, MD, FASE

Benjamin H. Freed, MD, FASE

Steven A. Goldstein, MD, FASE

Aasha S. Gopal, MD, FASE

John Gorcsan, III, MD, FASE

Joy D. Guthrie, PhD, ACS, RDMS,
RDCS, RVT, FASE

Yuchi Han, MD, MMSc, FASE

Brian D. Hoit, MD, FASE

Lanqi Hua, RDCS, MS, FASE

Rajesh Janardhanan, MD,
MRCP, FASE

Madeline Jankowski, RDCS, FASE

Harish Jarrett, MD

Amer M. Johri, MD, FASE

Ravi V. Joshi, MD, FASE

Bonnie J. Kane, BS, RDCS, FASE

Martin G. Keane, MD, FASE

James N. Kirkpatrick, MD, FASE

Kyle W. Klarich, MD, FASE

Allan L. Klein, MD, FASE

Megan C. Koivisto, RDCS

Karla M. Kurrelmeyer, MD, FASE

Arthur J. Labovitz, MD, FASE

Roberto M. Lang, MD, FASE

Michael Lanspa, MD, FASE

Howard Leong-Poi, MD, FASE

Hsin-Yueh Liang, MD

Jonathan R. Lindner, MD, FASE

Sheldon E. Litwin, MD, FASE

Juan C. Lopez-Mattei, MD, FASE

Ying Hui Low, MD

Dai-yin Lu, MD

Jimmy C. Lu, MD, FASE

George K. Lui, MD, FASE

G. Burkhard Mackensen, MD,
PhD, FASE

Anthony Magalski, MD, FASE

Kameswari Maganti, MD, FASE

Judy R. Mangion, MD, FASE

Sunil V. Mankad, MD, FASE

Thomas H. Marwick, MBBS, PhD,
MPH, MD

Shiraz Maskatia, MD, FASE

Susan A. Mayer, MD, FASE

Robert L. McNamara, MD, FASE

Carol K.C. Mitchell, PhD, RDMS,
RDCS, RVT, RT(R), ACS, FASE

Victor Mor-Avi, PhD, FASE

Shaine A. Morris, MD

Sharon L. Mulvagh, MD, FASE

Akhil Narang, MD

Matthew Parker, MD, FASE

David Parra, MD, FASE

Anitha Parthiban, MD, FASE

Ayan R. Patel, MD, FASE

Patricia A. Pellikka, MD, FASE

Shabnam Peyvandi, MD, FASE

Dermot Phelan, MD, PhD, FASE

Sue D. Phillip, RCS, FASE

Nelangi M. Pinto, MD, FASE

Juan Carlos Plana, MD, FASE

Thomas R. Porter, MD, FASE

Michael D. Puchalski, MD, FASE

Jyothy J. Puthumana, MD, FASE

Atif N. Qasim, MD, FASE

Miguel A. Quiñones, MD, FASE

Vera H. Rigolin, MD, FASE

Mary Jo R. Rizzo, RDCS, RDMS, FASE

Ana Clara T. Rodrigues, MD

Geoffrey A. Rose, MD, FASE

Thomas Ryan, MD, FASE

Ritu Sachdeva, MBBS, FASE

Stephen G. Sawada, MD

Jennifer L. Schaaf, BS, ACS,
RDCS, FASE

Marielle Scherrer-Crosbie, MD,
PhD, FASE

Nelson B. Schiller, MD, FASE

Elif Seda Selamet Tierney, MD, FASE

Partho P. Sengupta, MBBS, MD,
DM, FASE

Fadi Shamoun, MD, FASE

Elaine A. Shea, ACS, RCS,
RCCS, FASE

Takahiro Shiota, MD, FASE

Timothy C. Slesnick, MD, FASE

Wendy Sowa-Maldarelli, MS,
RT, RDCS, FASE

Lissa Sugeng, MD, MPH, FASE

Madhav Swaminathan, MD, FASE

James D. Thomas, MD, FASE

Kirsten Tolstrup, MD, FASE

Wendy Tsang, MD

Joel Turner, MD, MSc

Matt M. Umland, ACS, RDCS, FASE

Anne Marie Valente, MD, FASE

Thomas Van Houten, MPH, ACS,
RDCS, FASE

Hector R. Villarraga, MD, FASE

Constance G. Weismann, MD, FASE

Bryan Wells, MD, FASE

Gillian A. Whalley, PhD, DMU, FASE

David H. Wiener, MD, FASE

Sandra A. Witt, RDCS, FASE

Anna Woo, MD, SM

Danita M. Yoerger Sanborn, MD,
MMSc, FASE

Luciana T. Young, MD, FASE

Qiong Zhao, MD, PhD, FASE

William A. Zoghbi, MD, FASE

Young Investigator's Award Competition (YIA)

Monday, June 24, 2019

2019 ARTHUR E. WEYMAN
YOUNG INVESTIGATOR'S AWARD
COMPETITION FINALISTS

Presented Monday, June 24, 3:30 PM-5:30 PM

New Technology
YIA-1

Ischemic Heart Disease
YIA-2

Artificial Intelligence / Machine Learning
YIA-3

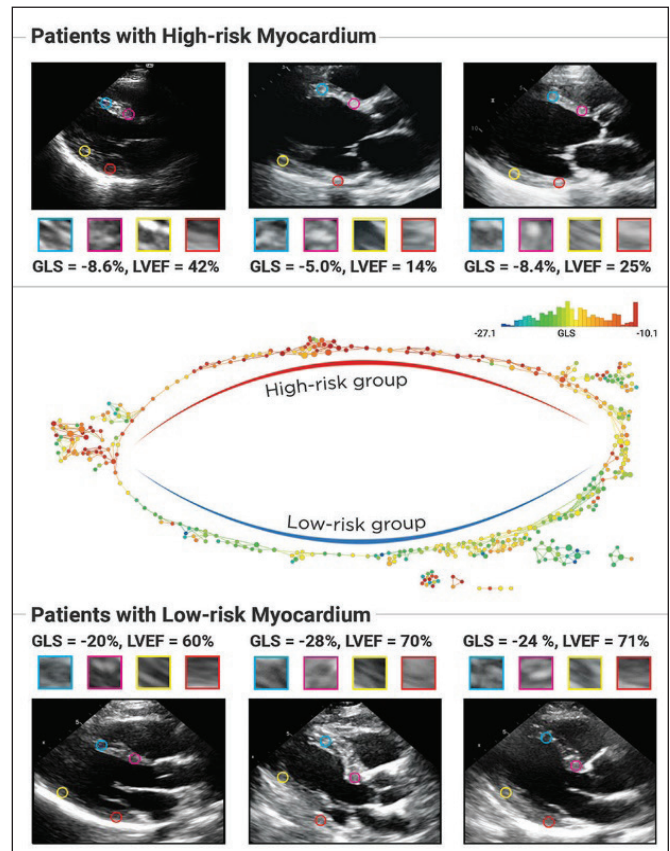
3D Echocardiography
YIA-4

YIA-01

Cardiac Ultrasonic Fingerprinting: A Radiomics Approach for High-throughput Feature Phenotyping of Dysfunctional Myocardium

Nobuyuki Kagiya, Sirish Shrestha, Jung Sun Cho, Muhammad Ashraf, Muhammad Khalil, Lan Hu, Sudarshan Balla, Grace Casalang-Verzosa, Partho P. Sengupta. West Virginia University Heart Vascular Institute Innovation Center, Morgantown, WV

Background: Cyclic variation of the integrated backscatter and video densitometric analysis have been used previously for left ventricular (LV) tissue characterization. We studied a radiomic-based approach for extracting information from noisy multidimensional medical images and identifying quantitative features of myocardial tissue remodeling from static cardiac ultrasound images. **Methods:** Total 256 radiomic texture indices were extracted from cardiac ultrasound images in 446 patients and compared with conventional echocardiography and 2D speckle tracking derived global longitudinal strain (GLS). Unsupervised feature extraction was performed using topological data analysis for predicting the presence of a high-risk myocardial fingerprint. In a subgroup of 40 patients undergoing cardiac magnetic resonance (CMR), we subsequently assessed high-risk fingerprint in total 160 LV segments for predicting the presence of myocardial fibrosis as defined by late gadolinium enhanced CMR. **Results:** Radiomic feature analysis was feasible in 433 (97%) patients (56±17 years, 55% female). Topological data analysis clustered the patients with high and low-risk myocardial fingerprint (Figure A) in an unsupervised manner. The high-risk features were associated with conventional markers of LV remodeling including LV end-diastolic (p=0.006) and systolic volumes (p<0.001), ejection fraction (p<0.001) and impaired GLS (p<0.001). Furthermore, the high-risk fingerprint predicted presence of advanced heart failure (ACC/AHA stage ≥ C: odds ratio [OR] 1.69, p=0.009) and symptoms (NYHA class ≥ III, OR 2.17, p<0.001). In patients undergoing CMR, the high-risk fingerprint was an independent predictor of fibrosis (OR 8.06, p=0.03). Adding fingerprint information to GLS improved prediction of myocardial fibrosis (net reclassification improvement 1.17, p<0.001; sensitivity 95.8% and specificity 81.2%, C-statistic 0.89). **Conclusions:** Radiomic-based cardiac ultrasound fingerprinting identifies high-risk features associated with LV remodeling in early and advanced clinical stages of heart failure. Further clinical validation of this quantitative approach may address critical barriers in adoption of ultrasound techniques for myocardial tissue characterization.



YIA-02

Molecular Imaging of Microvascular Endothelial Von Willebrand Factor and Platelet Adhesion in Myocardial Ischemia-Reperfusion Injury

Koya Ozawa¹, William Packwood¹, Oleg Varlamov¹, Aris Xie¹, Melinda D. Wu¹, Jose A. López², Jonathan R. Lindner¹. ¹Oregon Health & Science University, Portland, OR; ²Blood Works NW, Seattle, WA

Background: In myocardial infarction (MI), ischemia-reperfusion (IR) injury contributes to impaired microvascular reflow. The role of microvascular platelet adhesion in microvascular IR is poorly understood. We used myocardial contrast echocardiography (MCE) molecular imaging to test the hypothesis that endothelial-associated Von Willebrand Factor (VWF) and platelet adhesion contribute to myocardial IR injury. **Methods:** Closed-chest IR was produced by LAD ligation for 30 min in wild-type mice (WT), atherosclerotic mice deficient for the LDL receptor and Apobec-1 (DKO), and DKO mice receiving treatment to reduce endothelial VWF including N-acetylcysteine (NAC) or recombinant ADAMTS13 which cleaves VWF multimers. Sham-treated WT and DKO mice were also studied. Molecular imaging of platelet GPIIb/IIIa and activated VWF, and MCE perfusion imaging were performed 30-60 min after reflow. Regional analysis was performed for the remote region and the risk area which were determined by microsphere technique. Platelets and leukocyte immunohistochemistry were also performed on confocal microscopy; and infarct size was measured by TTC staining. **Results:** In DKO mice, post-IR molecular imaging signal was greater in the risk area than the remote region for microvascular platelet adhesion (25±3 vs 7±4) and VWF (23±1 vs. 5±3 IU). This signal was ~2-fold higher for DKO than WT mice (25±3 vs 12±3 IU; and 23±1 vs 13±4 IU, for platelets and VWF respectively, p<0.05). In DKO mice, platelet and VWF signal in the risk area was reduced by >50% by NAC (10±1 and 9±1 IU, respectively, p<0.01 vs untreated); and was completely eliminated by ADAMTS13 (1±2 and -2±1 IU, p<0.01). Immunohistochemistry confirmed that ADAMTS13 not only eliminated risk area platelets, but also neutrophil recruitment. Post-IR MCE perfusion (Aβ) in the risk area was lower for DKO than WT mice (20±3 vs 31±1, p<0.01). Post-IR perfusion in DKO mice was significantly (p<0.05) improved by both NAC (33±3) and ADAMTS13 (50±4); resulting in a smaller infarct size (32±2 vs 23±1 vs 15±1 % of LV risk area, for DKO, DKO+NAC, and DKO+ADAMTS13; p<0.05). **Conclusion:** After myocardial IR, abnormal regulation of microvascular endothelial VWF results in platelet adhesion which contributes to impaired microvascular reflow, post-IR inflammation, and larger infarct size. MCE molecular and perfusion imaging can be used to assess new therapeutic strategies, such as ADAMTS13 which appears to completely eliminate platelet adhesion, improve reflow, and reduce infarct size.

Young Investigator's Award Competition (YIA)

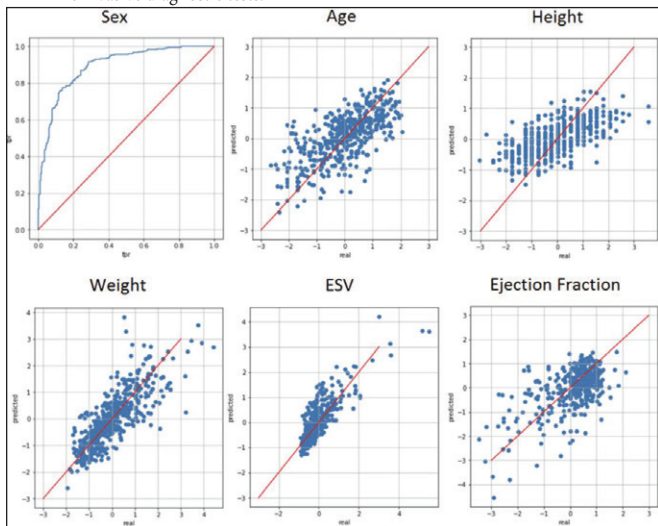
Monday, June 24, 2019

YIA-03

Deep Learning of Echocardiography to Identify Systemic Phenotypes and Unsupervised Learning of Clinical Measurements

David Ouyang, Amirata Ghorbani, David Liang, Euan Ashley, James Zou. Stanford University, Menlo Park, CA

Introduction: Medical still-images and videos are ideal data sets for machine learning algorithms given the high dimensional, granular data and established frameworks for convolutional neural networks for imaging datasets. Previous work on medical datasets have shown that deep learning can identify systemic human phenotypes not typically associated with the imaging modality. Echocardiography, given its ubiquity as both a screening modality and utility in critical disease, is a high-impact area for the application of machine learning in cardiovascular medicine. **Methods:** We developed deep learning models using echocardiography images from 2,952 patients from a large academic medical center and trained using clinical and demographic information from the electronic medical record system. From all images in each study, a dataset of over 190,000 apical 4 chamber still images was identified and extracted. A convolutional neural network with Inception-Resnet-V1 architecture was trained on phenotypes of age, gender, height, and weight, as well as echocardiography metrics of end systolic volume and ejection fraction. **Results:** We were able to accurately predict cardiovascular risk factors including age (75% binary accuracy, rank correlation 0.68, $r_2 = 0.45$), gender (81% accuracy, AUC = 0.89), height (84% binary accuracy, rank correlation 0.66, $r_2 = 0.38$) and weight (79% binary accuracy, rank correlation 0.82, $r_2 = 0.60$). Conventional echocardiography metrics were also predicted with accuracy, including end systolic volume (82% binary accuracy, rank correlation 0.75, $r_2 = 0.59$), and ejection fraction (72% binary accuracy, rank correlation 0.47, $r_2 = 0.21$). **Conclusions:** Deep learning of echocardiography images can identify cardiovascular risk factors and conventional metrics from echocardiogram images. Phenotypes difficult to identify by human echocardiographers were readily identified through deep learning. Further accuracy can be obtained by training on video images and trialing different convolutional neural network architectures. Future work will identify areas where noninvasive imaging coupled with deep learning can better aid diagnosis and minimize invasive diagnostic tests.

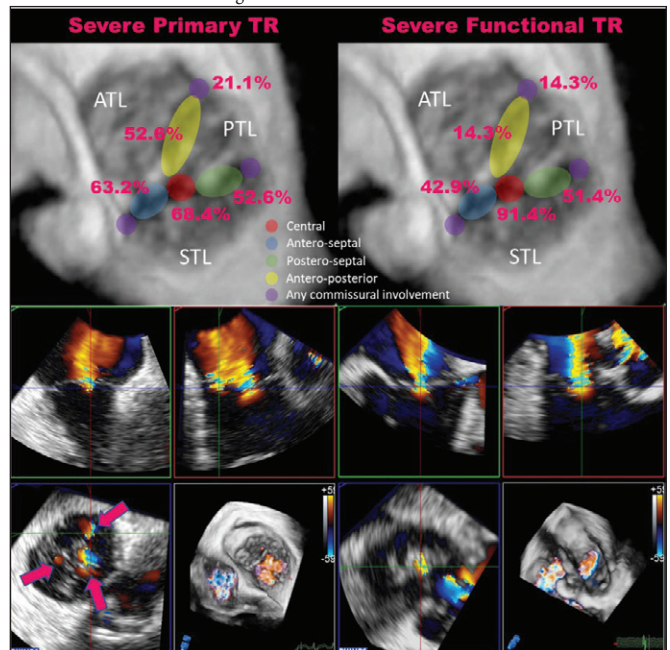


YIA-04

Comprehensive Evaluation of Tricuspid Regurgitation Location and Severity Using Vena Contracta Analysis: A Color Doppler 3-Dimensional Transesophageal Echocardiography Study

Hiroto Utsunomiya¹, Yu Harada¹, Hitoshi Susawa¹, Kosuke Takahari¹, Yusuke Ueda¹, Kanako Izumi¹, Kiho Itakura¹, Hiroki Ikenaga¹, Takayuki Hidaka¹, Yukihiko Fukuda¹, Yasuki Kihara¹, Takahiro Shiota². ¹Department of Cardiovascular Medicine, Hiroshima University Hospital, Hiroshima, Japan; ²Cedars-Sinai Medical Center, Los Angeles, CA

Background: Comprehensive evaluation of the tricuspid valve and detailed information on tricuspid regurgitation (TR) jet location and severity may assist in decision making whether a patient is anatomically suited for new transcatheter tricuspid devices. However, the number of clinical studies to evaluate the values for 3-dimensional (3D) vena contracta area (VCA) is limited. **Methods:** We retrospectively reviewed 116 patients with at least moderate TR who underwent 2D transthoracic echocardiography and color Doppler 3D transesophageal echocardiography (TEE). To assess the location and severity of TR, 3D VC analysis was performed by off-line cropping of the color Doppler 3D datasets in which 3 simultaneous orthogonal planes were provided. To obtain the 3D VCA, the short-axis plane was aligned perpendicular to the narrowest neck of the TR jet just above towards the right atrial side of the flow convergence zone. The severity of TR was graded as moderate or severe according to the 3D TEE-derived regurgitant volume (RVol) as a reference standard. **Results:** Distribution of TR jet location according to TR etiology was shown in Figure. Severe functional TR group showed the highest prevalence of central jet location (91.4%) among the TR subgroups, with a higher prevalence of postero-septal jet location than moderate TR group ($P=0.011$). In contrast, severe primary TR group had thoroughly spread jet location with the highest prevalence of antero-posterior jet location (52.6%) among the TR subgroups, resulting in a higher number of VC and greater spatial extent of TR jet location involved as compared to moderate TR (both $P<0.05$). As for grading TR severity, 3D VCA at an optimal cutoff value of 0.61 cm² yielded a sensitivity of 78% and a specificity of 97% to differentiate moderate from severe TR. 3D VCA correlated well with 2D PISA-EROA but showed a stronger correlation to the reference method compared with 2D PISA-EROA ($P=0.038$). The difference between 3D VCA and 2D PISA-EROA was correlated with the number, shape, and spatial extent of VC (all $P<0.05$), resulting in 15% were misclassified when 2D-PISA EROA alone was used for TR grading. **Conclusions:** The 3D VC technique is feasible to assess TR jet location, and 3D VCA has high diagnostic value for separating moderate from severe TR using 3D TEE-derived RVol as a reference standard.



Sonographer Research Award Competition (SIA)

Sunday, June 23, 2019

**2019 BRIAN HALUSKA SONOGRAPHER
RESEARCH AWARD
COMPETITION FINALISTS**

Presented Sunday, June 23, 3:30 PM-5:00 PM

**Value of Echocardiography (Quality and Cost) / Outcomes
/ Comparative Effectiveness**

SIA-1

New Technology

SIA-2

Ventricular Function / Myocardial Mechanics

SIA-3

Pediatric Heart Disease

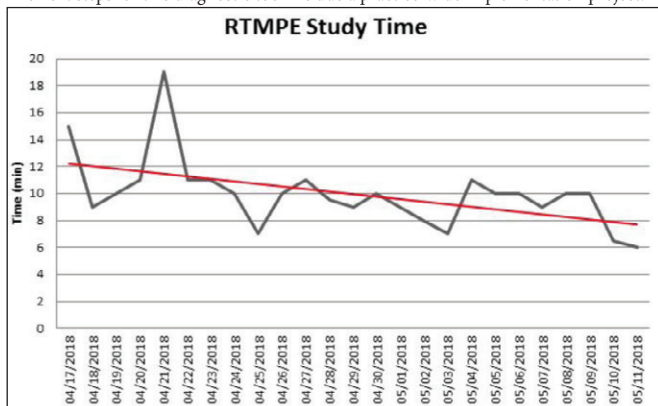
SIA-4

SIA-01

Real Time Myocardial Perfusion Stress Echocardiography: A Practice Implementation Pilot

Daniel L. McCullough, Patricia A. Pellikka, Garvan C. Kane, Robert B. McCully, Merri L. Bremer, Courtney E. Bennett. Mayo Clinic, Rochester, MN

Background: Real Time Myocardial Perfusion Echocardiography (RTMPE) has been validated to be feasible, safe, and accurate in assessing myocardial blood flow with the use of ultrasound enhancement agents (UEA). Our goal was to add this valuable diagnostic modality to dobutamine stress echocardiography (DSE) without significantly increasing study acquisition and interpretation time, decreasing study quality, and/or causing adverse events. **Methods:** This practice implementation pilot followed the Six Sigma quality improvement methodology. Key stakeholders were identified within the Mayo Clinic Rochester Echocardiography Laboratory to form a multidisciplinary team. Plan, Do, Study, Act (PDSA) cycles were completed, which included multiple focus meetings. Training was completed by 3 sonographers, 1 nurse, and 1 physician at University of Nebraska Medical Center where RTMPE is performed with every stress study. Using the skills obtained, we trained 2 additional sonographers and 2 additional nurses for the pilot. RTMPE was added to the DSE when UEA was utilized for left ventricular opacification. The metrics defined were study duration, study quality, adverse events, perfusion failures, staff satisfaction, and added value. A RedCap survey was completed by allied health staff and a written survey by the interpreting physician. **Results:** The pilot was performed over 9 months from 04/17/2018-01/10/2019. RTMPE was performed by the core group of sonographers and nurses on 25 patients referred for DSE. The studies were interpreted by a single cardiologist. The time to perform RTMPE included the UEA preparation and image acquisition, with the goal to not exceed 10 minutes total. The average RTMPE time during the pilot was 10 minutes and significantly decreased over time ($p < 0.001$) (Figure). 96% of the studies were of adequate quality. There was 1 perfusion failure and no adverse events. Staff satisfaction was 3.8 (out of 5). The added value was an average Likert of 3.4 (out of 5). **Conclusion:** We were able to add value with RTMPE to our DSE studies within a reasonable timeframe and adequate image quality. This was completed without negatively impacting the counterbalance measures of adverse events or decreased staff satisfaction. The next steps for this diagnostic tool include a practice-wide implementation project.

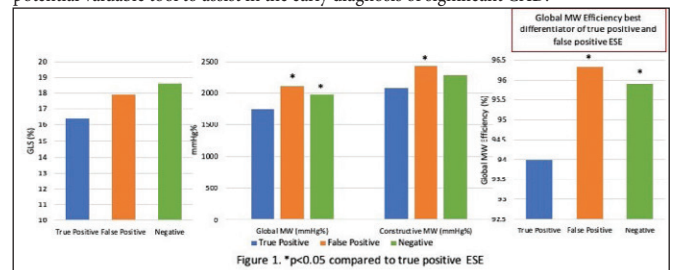


SIA-02

Resting Global Myocardial Work Derived from Non-invasive Left Ventricular Pressure-strain Loops Discriminates Between True Positive and False Positive Exercise Stress Echocardiography

Natalie F.A. Edwards¹, Gregory M. Scalia¹, Surendran Sabapathy², Bonita A. Anderson¹, Robert Chamberlain¹, Jonathan Chan². ¹The Prince Charles Hospital, Chermside, Australia; ²Griffith University, Gold Coast, Australia

Background: Exercise stress echocardiography (ESE) is an established method for non-invasive detection of obstructive coronary artery disease (CAD), however, results in varied sensitivity and specificity due to qualitative interpretation of regional wall motion abnormalities. This study sought to determine whether global myocardial work (MW), derived from non-invasive LV pressure-strain loops at rest can differentiate between true positive (TP) and false positive (FP) ESE. **Methods:** Speckle tracing echo was performed at rest on 70 patients (mean age 56 ± 12 yrs; 31 males) referred for clinically indicated ESE who had an ejection fraction $\geq 55\%$ with no evidence of resting regional wall motion abnormalities. Subsequent global MW was derived from non-invasive LV pressure-strain loops constructed from strain and brachial systolic blood pressure. Constructive work reflected positive work by myocardial shortening in systole including lengthening during isovolumic relaxation. Wasted work reflected energy loss by myocardial lengthening in systole and shortening in isovolumic relaxation. Global MW efficiency was derived from the percentage ratio of constructive and wasted work. Coronary angiography was performed on those with a positive ESE (N=18) to determine presence and/or severity of CAD. **Results:** Coronary angiography revealed significant obstructive CAD (TP ESE) in 10 patients and no evidence of CAD (FP ESE) in 8 patients. There was no significant difference ($p=0.10$) in GLS between those with TP (16.4%) and FP (17.9%) ESE. Resting global MW was significantly reduced ($p < 0.05$) in TP ESE (1733mmHg%) compared with FP ESE (2099mmHg%). Global MW efficiency was the best differentiator and also significantly reduced ($p < 0.05$) in TP (94%) compared with FP (96%) ESE due to a significant reduction ($p < 0.05$) in constructive MW (figure 1). 52 patients with a negative ESE, no symptomatic or ECG changes and a high exercise level showed a significantly higher ($p < 0.05$) resting GLS (18.6 vs 16.4%) and global MW (1971 vs 1733mmHg%) compared to TP ESE. **Conclusion:** Non-invasive estimation of global MW derived from LV pressure-strain loops at rest may be a more sensitive tool than GLS to help distinguish between TP and FP ESE. This is a potential valuable tool to assist in the early diagnosis of significant CAD.



SIA-03

Left Ventricle Longitudinal Excursion in Children Following Heart Transplantation: Utility of Tissue Motion Annular Displacement Index

Gilda Kadiu, Jennifer Blake, Swati Sehgal, Sanjeev Aggarwal. Children's Hospital of Michigan, Detroit, MI

Background: Heart transplantation (HT) is an established treatment modality for end stage heart failure in children. Early diagnosis of rejection, often associated with myocardial dysfunction, is critical for HT recipients. However, assessment of left ventricular (LV) function by M mode measurement is limited by abnormal septal motion in these patients. Recently, Tissue Motion Annular Displacement (TMAD) of the mitral valve has been shown to be a reliable measure of longitudinal LV function that is independent of endothelial definition. **Objective:** To compare TMAD in pediatric HT recipients without acute rejection and normal controls and to assess its correlation with ejection fraction (EF) calculated by the biplane Simpson's method. **Method:** This was a retrospective review of echocardiograms on HT recipients who had no evidence of clinical or biopsy-proven rejection. Patients with pericardial effusion or acute illness were excluded. Patients with chest pain, murmur or syncope who had normal echocardiograms were controls. Echocardiograms (Philips iE33) were read by a single reader blinded to clinical data. TMAD was measured in the apical four chamber view using a CMQ advanced technique (Qlab 10.8 Philips Medical System) in duplicate and an average was taken. EF was calculated in apical 4 chamber and 2 chamber views using Simpson's method. Student t-test and Chi-square test were used for comparisons between groups. **Results:** Our cohort (n=111) included 48 (43%) HT recipients and 63 controls. The median (range) age at transplant was 1.5 (2-18) years and follow up duration was 7.2 (4.4) years. Primary reasons for HT were cardiomyopathy in 32 (65%) and congenital heart disease in 16 (35%) patients. The groups were similar in age and gender distribution. TMAD and EF were significantly abnormal in HT group compared to control. TMAD correlated significantly with EF ($r 0.49, p=0.001$). **Conclusions:** Pediatric HT recipients, even without acute rejection, had significant abnormalities in longitudinal

Oral Abstracts (OA)

Friday, June 21, 2019 — Tuesday, June 25, 2019

LV excursion as assessed by TMAD and low normal EF. The two measures were strongly correlated. It is plausible that the longitudinal LV function becomes abnormal first, while EF is preserved by compensatory circumferential contraction. TMAD may be a useful additional measure of LV function in the surveillance of HT recipients.

Echo parameters (mean ± SD) (n%)	OHT (n=48)	Normal Controls (n= 63)	P value
Age (years)	12.3±5.4	12.1±4.1	0.2
Gender (male)	23(47.9%)	36 (57.1%)	0.2
Ht (cm)	141.8 ± 25.8	151.6± 22.4	0.7
Wt (kg)	42.8 ± 22.2	48.9 ± 18.9	0.2
BSA	1.3 ± 0.44	1.4 ± 0.38	0.06
SBP (mmHg)	110±12	112±12	0.2
DBP (mmHg)	69±10	61±8	0.005*
TMAD%	19.2±6	21.9±2.3	0.0001*
EF%	57.4±5.3	64.8±5.6	0.0001*

SIA-04

Fetal Brain Resistance is Abnormal in Neonates with Coarctation of the Aorta Despite Antegrade Aortic Arch Flow

Michele Clouse, Kaitlyn Freeman, Jeffrey Conwell, Luciana Young, Mark Lewin, Bhawna Arya. Seattle Children's Hospital Heart Center, Seattle, WA

Background: Middle cerebral artery (MCA) resistance (RI) and pulsatility (PI) index are often lower in fetuses with coarctation of the aorta (CoA) and generally result in lower cerebroplacental RI ratio (CPR) and cerebroplacental PI ratio (CPP). Retrograde aortic arch (AoA) flow from the ductus arteriosus and low oxygen delivery to the brain are the proposed cause. We hypothesize that a low fetal MCA RI, PI, CPR and CPP are present in a majority of CoA patients and expect fetal AoA directionality to correlate. Fetal brain flow changes may help predict CoA when prenatal suspicion is high. **Methods:** Retrospective case control study of fetuses with prenatal suspicion for CoA (recommendation for postnatal CoA evaluation) from 1/2014-9/2018. True CoA was defined as need for prostaglandin at time of surgery. Measurements were obtained from first fetal echo: MCA RI, PI, MCA RI, PI, CPR and CPP. Directionality of the AoA was noted to be antegrade, retrograde, or bidirectional on fetal echo. Student's *t* test compared differences in fetal measurements between postnatal CoA and non-CoA groups. **Results:** Thirty five fetuses met criteria for inclusion (mean GA at diagnosis 28.2±5.9 weeks). CoA was confirmed in 27/35 neonates. Abnormal AoA flow was present in 8 fetuses, 7 with CoA (5 reversed, 2 bidirectional) and 1 non-CoA (bidirectional). MCA RI (mean 0.68 vs 0.76; $p<0.01$), CPR (mean 1.00 vs 1.33; $p<0.01$ and CPP (mean 1.41 vs 2.08; $p=0.01$) were significantly lower in the CoA vs non-CoA group. MCA PI was not different between groups. There was no difference in MCA RI, PI, CPR or CPP between fetuses with normal and abnormal AoA flow. **Conclusion:** Fetal brain resistance appears to be lower in neonates with CoA, regardless of AoA flow directionality. Presence of low MCA RI, CPR, and CPP in fetuses with CoA suspicion may aid in identifying true neonatal CoA. Fetal brain flow may be affected in neonates with CoA despite AoA antegrade flow. Fetal physiologic causes for low brain resistance and neurodevelopmental outcomes in CoA should be explored.

ORAL ABSTRACTS

Presented Friday, June 21 through Tuesday, June 25

Echocardiography in Systemic Disease (DM, HTN, Obesity) / Pericardial Disease / Primary Myocardial Disease

OA-01

Pediatric Heart Disease

OA-02, OA-04 through OA-05, OA-07 through OA-09, and OA-11

Cardio-Oncology

OA-03

Echocardiography in SOE / Arrhythmias / Atrial Function

OA-06

3D Echocardiography

OA-10

Critical Care Ultrasound / Point of Care Ultrasound

OA-12

OA-01

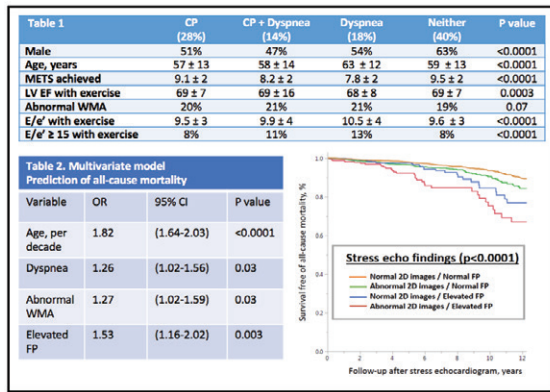
Assessment of Left Ventricular Filling Pressure with Exercise is Independently Associated with All-cause Mortality in a Cohort of 14,446 Patients

Christina L. Luong, Ratnasari Padang, Jae K. Oh, Patricia A. Pellikka, Robert B. McCully, Garvan C. Kane. Mayo Clinic, Rochester, MN

Introduction: The prevalence, associated characteristics and outcome of patients with an elevation in left ventricular (LV) filling pressures (FP) with exercise obtained on routine assessment in patients referred for exercise echocardiography is not well known. **Methods:** Subjects were adult patients referred for a treadmill exercise stress echocardiogram for the evaluation of known or suspected coronary artery disease, including the symptoms of chest pain or dyspnea. All underwent assessment of regional wall motion, mitral inflow (E) and early diastolic mitral annulus relaxation (e') velocities before and immediately following maximum symptom-limited exercise. Patients were excluded if they had significant valvular heart disease (defined by any mitral stenosis, moderate or greater other valvular stenosis, regurgitation, valve repair or replacement), atrial fibrillation, or if they refused to participate in research. Subjects were stratified as those with chest pain (CP), dyspnea, both or neither symptom. Elevated LVFP with exercise was defined as an $E/e' \geq 15$. **Results:** The cohort comprised 14,446 subjects (Table 1). Patients with elevated filling pressure with exercise ($n=1287$; 9%) were older (67 ± 10 versus 58 ± 13 years, $p<0.0001$), more likely dyspneic (69% versus 59%, $p<0.0001$), had lower exercise capacity (7.3 ± 2.1 versus 9.1 ± 2.4 METS, $p<0.0001$) and a higher rate of wall motion abnormalities (WMA) with stress (38% versus 18%, $p<0.0001$). Patients with dyspnea were 1.5-fold (1.2-1.8) more likely to die at follow-up than those without dyspnea, $p=0.0002$. An elevated filling pressure with exercise ($E/e' \geq 15$) was a strong predictor of all-cause mortality, with incremental association with death over and above evidence of myocardial ischemia on the stress echocardiogram (Figure) and other variables including age (Table 2). **Conclusion:** Elevation in LV filling pressures defined as $E/e' \geq 15$ with exercise is found in 9% of patients referred for stress echocardiography, is associated with increasing age, dyspnea, an impaired functional capacity and stress-induced ischemia and is independently associated with all-cause mortality over long term follow-up.

Oral Abstracts (OA)

Friday, June 21, 2019 — Tuesday, June 25, 2019

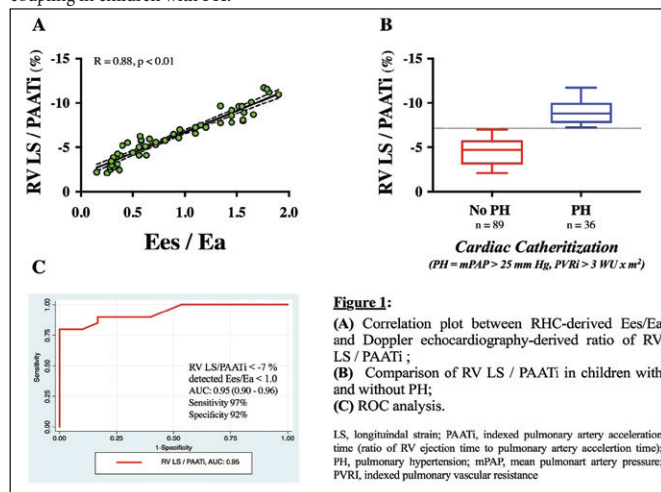


OA-02

Altered Right Ventricle Pulmonary Arterial Coupling in Children with Pulmonary Hypertension: A Novel Approach to Cardiopulmonary Phenotyping in Pediatrics

Philip T. Levy¹, Kel Vin Woo², Georganne Groh², Amanda Hauck³, Aaron Hamvas³, Gautam K. Singh². ¹Boston Children's Hospital, Boston, MA; ²Washington University School of Medicine, Saint Louis, MO; ³Northwestern University Feinberg School of Medicine, Chicago, IL

Background: The right ventricle (RV) to pulmonary arterial vasculature (PV) coupling is a key determinant of outcome in cardiopulmonary disease in children. RV-PV coupling is usually derived by right heart catheterization (RHC) that measures the ratio of ventricular elastance (Ees, contractility) to arterial elastance (Ea, afterload) and is based on the work-energy principle that states a change in energy is equal to the work expended by a force through displacement. Non-invasive echocardiography derived surrogates to the Ees/Ea ratio that account for the length-force relationships to estimate RV-PV coupling clinically remain to be established. We hypothesize that the relationship of RV deformation by strain to the pulmonary arterial systolic pressure (PASP), as non-invasive index of RV length-force relationship, is a reliable measure of invasive RV-PV coupling (Ees/Ea) in children. **Methods:** Prospectively acquired simultaneous RHC-derived Ees/Ea and echocardiography-derived ratio of RV free wall longitudinal strain (LS,%) to pulmonary artery acceleration time (PAAT,sec) was compared using regression analysis in a cohort of 125 children (median age, 5 years; IQR, 1-13 years) with a wide range of pulmonary hemodynamics. Ees/Ea was calculated using the single beat method with the following equation: (RV systolic pressure - mean PASP) / mean PASP. RV LS, as a measure of RV shortening, was substituted for length and PAAT as a reliable estimate of PASP was exchanged for force. PAAT was adjusted for RV ejection time (PAATi=RVET/PAAT) to account for heart rate variability. **Results:** RV LS/PAATi correlated with invasive Ees/Ea (r = 0.88, p < 0.01, Figure 1A). RV LS/PAATi was decreased (p<0.001) in children with pulmonary hypertension (PH) diagnosed by RHC (mPAP>25 mmHg and PVRI>3 WU.m2, Figure 1B). With ROC analysis, RV LS/PAATi < -7 % detected Ees/Ea < 1.0 with sensitivity of 97% and specificity of 92% with an AUC of 0.95 (95% CI, 0.90-0.96), Figure 1C. **Conclusions:** We established that RV LS/PAATi, a novel non-invasive index of the length-force relationship, provides a clinically reliable estimate of invasive RV-PV coupling in children with PH.



OA-03

Global Longitudinal versus Circumferential Strain to Identify Cardiotoxicity in Women with HER2+ Breast Cancer

Maryam Esmailzadeh¹, Babitha Thampinathan¹, Oscar Calvillo Arguelles¹, Eitan Amir², Yobiga Thevakumar¹, Maria Michalowska¹, Camila M. Urzua Fresno¹, Bernd J. Wintersperger³, Paaladinesh Thavendiranathan, on behalf of the EMBRACE-MRI¹. ¹University Health Network, Toronto General Hospital, Peter Munk Cardiac Centre, Dept. of Cardiology, Toronto, ON, Canada; ²Cancer Clinical Research Unit, Princess Margaret Cancer Centre, Toronto, ON, Canada; ³University Health Network, Toronto General Hospital, Dept. of Medical Imaging, Toronto, ON, Canada

Background: Global longitudinal strain (GLS) is recommended as the preferred method for sequential monitoring of cardiac function during cancer therapy. However, recent data suggests that global circumferential strain (GCS) may also be a marker of early myocardial dysfunction. We sought to compare the diagnostic characteristics of a relative change in GLS versus GCS to detect cardiotoxicity during cancer therapy. **Methods:** 53 women (mean age 52.2±9.3 years) with HER2+early stage breast cancer were prospectively recruited. Echocardiography was performed at baseline, after anthracycline, and at 3, 6, 9, and 12 months during trastuzumab therapy by experienced sonographers (GE Vivid 7). 3D LVEF was measured by 4D Auto LVQ software and 2D speckle tracking echocardiography (STE) was used for the assessment of GLS from 3 apical long axis views and GCS from the basal, mid and apical short axis views (EchoPAC, Q-analysis). All strain images were acquired at >50 frames per second and 3D data set at >20 volumes per second. Analyses were performed by an experienced reader blinded to patient information or imaging time point. A significant relative change in GLS or GCS was defined as 15%. **Results:** Amongst recruited patients 10 (18.9%) had hypertension and 10 (18.9%) had smoking history. Mean baseline LVEF was 58.1 ± 4.3% and mean GLS and GCS were -21.6% ± 2.3 and -21.3% ± 2.9 respectively. 12 (22.6%) patients experienced cardiotoxicity (>10% relative reduction in 3D LVEF to <55%). A>15% relative reduction in GLS or GCS was seen in 19 and 30 patients respectively. Amongst those who had a reduction in GCS the majority (43%) occurred immediately after anthracycline therapy but no pattern was seen with GLS (Table 1). Respective sensitivity and specificity for identification of cardiotoxicity was 58.3% [95%CI: 22.7 - 84.8] and 70.7% [95%CI: 54.5 - 83.9] for GLS, and 72.7% [95%CI: 39.0 - 94.0] and 46.3% [95%CI: 30.7 - 62.6] for GCS. **Conclusion:** In women with breast cancer undergoing anthracycline and trastuzumab combination therapy a >15% relative change in both GLS and GCS identify patients at risk for cardiotoxicity. Changes in GCS occurred earlier and was more sensitive while changes in GLS was more specific. The test characteristics of both methods were only modest for the identification of cardiotoxicity as defined per current guidelines.

OA-04

Unique Challenges Associated with a Large Biorepository of Clinical Echocardiograms from a Multicenter Retrospective Cohort of Childhood Cancer Survivors: Lessons Learned from Central Core Lab Analysis

Ritu Sachdeva¹, Kayla L. Stratton², Saro H. Armenian³, Aarti Bhar⁴, William L. Border⁵, David E. Cox¹, Kasey J. Leger⁶, Wendy M. Leisenring⁷, Lillian R. Meacham¹, Karim T. Sadak⁸, Shanthi Sivanandam⁹, Eric J. Chow¹, Paul C. Nathan⁶. ¹Emory University School of Medicine, Children's Healthcare of Atlanta, Atlanta, GA; ²Fred Hutchinson Cancer Research Center, Seattle, WA; ³City of Hope, Duarte, CA; ⁴University of Washington, Seattle Children's Hospital, Seattle, WA; ⁵University of Minnesota, Masonic Children's Hospital, Minneapolis, MN; ⁶University of Toronto, The Hospital for Sick Children, Toronto, ON, Canada

Background: Multicenter research studies using archived echocardiograms (echos) obtained for clinical care are limited by the image quality and center variability. The purpose of this study was to assess the quality of archived clinical studies from a cohort of childhood cancer survivors and determine imaging and patient characteristics associated with poorer quality. **Methods:** A single blinded-reviewer at a central core lab used 8 elements (Table) to grade the image quality of clinical echos from childhood cancer survivors at 5 centers. These echos were retrospectively analyzed to assess cardiac function using a vendor-neutral software (TomTec). 2D and M-Mode fractional shortening (FS), biplane Simpson ejection fraction (EF), myocardial performance index (MPI), tissue Doppler imaging (TDI) derived velocities and global longitudinal strain (GLS) were obtained. The relationships of image quality with age and body mass index (BMI) at echo, sex, year of echo, and center were assessed. **Results:** Of the 535 studies analyzed (102 patients), all measures of cardiac function could be assessed in 35 (7%) and in 178 (33%) if GLS was excluded. 2D FS could not be measured in 6 (1%), M-Mode FS in 69 (13%), EF in 254 (48%), MPI in 125 (24%), mitral E/E' in 167 (31%), septal E/E' in 83 (16%) and GLS in 483 (90%). The quality measures and significant risk factors are shown in the table. At least one problem was identified in 355 (66.4%) studies, with technical issues (lung artifact, poor endocardial definition) being the most common. Lack of 2- and 3-chamber views was associated with the performing center. Younger patients had a higher risk of apex cut-off in 4-chamber views. Overall, there was a modestly increased risk of quality issues associated with low BMI, earlier era of echo, and center. **Conclusion:** Cardiac function parameters, excluding strain, could be assessed in 1/3 of studies and 2/3 of studies had at least one identifiable

Oral Abstracts (OA)

Friday, June 21, 2019 — Tuesday, June 25, 2019

quality issue. Factors associated with lower quality included younger age, underweight BMI, earlier year of study, and center. These findings highlight the challenges of retrospectively using clinical studies for research. Standardizing clinical echo protocols to include 2- and 3-chamber views and TDI will improve the ability to assess cardiac function in future research studies using an echo biorepository.

Factors (age and body mass index at echo, sex, year of echo, and center) significantly associated with echocardiogram quality measures				
Quality measure	No. affected (%)	Factor	††RR (95%CI)	P-value
No 2 chamber view	116 (21.7)	Center 2 vs 1*	58.88 (8.63-401.71)	< 0.0001
		Center 3 vs 1*	45.83 (6.71 - 313.12)	< 0.0001
		Year of echo (2004-08 vs 2014-17)	3.55 (1.84-6.83)	0.0002
		Year of echo (2009-13 vs 2014-17)	3.61 (2.10-6.23)	< 0.0001
No 3 chamber view	34 (6.4%)	Center 2 vs 1*	19.20 (2.44-151.16)	0.005
		Center 3 vs 1*	7.77 (1.07-56.23)	0.0424
Apex cut-off in 4 chamber view	74 (13.8%)	Age at echo (0-5 vs. 16-35 yrs)	2.77 (1.55-4.93)	0.0006
No parasternal short-axis view	1 (0.2%)	†		
No M-mode	11 (2.1%)	†		
No spectral Doppler	19 (3.6%)	Year of echo (2009-13 vs 2014-17)	0.21 (0.08-0.55)	0.0016
Technical issues	177 (33.1%)	BMI (Underweight vs. Normal)	1.42 (1.00-2.01)	0.0493
Any quality issue	355 (66.4%)	Center 2 vs 1*	1.96 (1.46-2.64)	<0.0001
		Center 3 vs 1*	1.88 (1.41-2.51)	<0.0001
		Year of echo (2004-08 vs 2014-17)	1.34(1.10-1.63)	0.0040
		BMI (Underweight vs. Normal)	1.19 (1.00-1.41)	0.0453

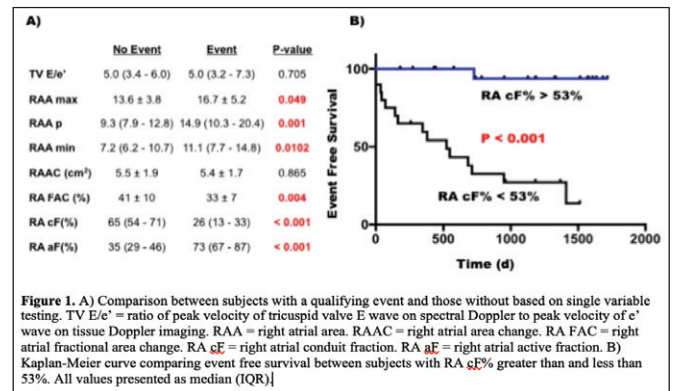
BMI = Body Mass Index; Categorized into underweight, healthy, overweight and obese based on CDC age percentiles at ages less than 20 years and standard adult reference values for those > 20 years.
*Two centers were excluded from this analysis due to low volume resulting in non-estimable models.
†No significant risk factors identified.
††Relative risk (RR) for not meeting the quality measures was estimated using generalized linear regression models with robust errors.

OA-05

Decreased Reliance on Right Atrial Contraction for Atrial Emptying Predicts Decreased Risk of Adverse Events in Pediatric Pulmonary Hypertension

Benjamin S. Frank, Michal Schafer, D. Dunbar Ivy, Pei-Ni Jone. Children's Hospital Colorado, Aurora, CO

Background: Increased right atrial (RA) pressure is a risk factor for adverse outcomes in pediatric pulmonary hypertension (PH). Retrospective studies suggest that abnormal RA mechanics may also be associated with clinical worsening. To validate these findings, we undertook a prospective study evaluating whether changes in RA geometry during the cardiac cycle have prognostic value for children with PH. We hypothesized that decreased dependence on RA contraction for atrial emptying would be associated with lower risk of adverse clinical events. **Methods:** Subjects <18 years old with idiopathic or heritable PH were prospectively enrolled from 2014-2018 at the time of their first clinical echocardiogram during the study period. RA area was measured from the apical 4-chamber view at end-systole, during the electrical p wave, and at end-diastole. RA conduit filling percent (RA cF%) was defined as the ratio of the area change between end-systole and the electrical p wave to the total RA area change (end-systolic area minus end-diastolic area). Qualifying adverse clinical events were initiation of parenteral prostacyclin, death, Potts shunt, lung transplant, and heart failure admission. **Results:** 41 subjects (median age 11.9 y, IQR 7.8-15.7 y) were enrolled. 16 subjects had a qualifying event during a median follow-up of 39 months. Subjects without an event had a median RA cF% of 65% (IQR 53-71%) at enrollment compared to 27% (IQR 13-33%) in those with an event ($p < 0.001$). RA cF% > 53% was prognostic for decreased risk of clinical event (HR 0.09, 95% CI 0.03-0.24, $p < 0.001$). ROC curve demonstrated an AUC of 0.90 to predict a clinical event (specificity 93.8%, sensitivity 92%). Maximum ($16.7 \pm 13.6 \text{ cm}^2$, $p = 0.049$) and minimum ($11.1 \pm 7.2 \text{ cm}^2$, $p = 0.01$) RA size were larger in the event group than the non-event group but neither was prognostic (HR = 1.4, 95% CI 0.52-3.74, $p = 0.44$ for maximum; HR = 1.5, 95% CI 0.52-4.23, $p = 0.45$ for minimum). **Conclusion:** Among children with PH, subjects with RA cF% > 53% have a decreased risk of adverse clinical event. Having a larger fraction of RA emptying occur prior to atrial contraction conferred a better prognosis while smaller atrial size alone did not. We speculate that decreased dependence on atrial contraction for RA emptying might identify a lower-risk group of PH patients.



OA-06

Immediate Recovery of Left Atrial Function is Associated with Maintenance of Sinus Rhythm After Electrical Cardioversion in Patients with Atrial Fibrillation and Atrial Flutter

Edward Chu, Anton Camaj, Asaf Rabinovitz, William Whang, Vivek Reddy, Martin Goldman. Icahn School of Medicine at Mount Sinai, New York, NY

Background: The extent of atrial stunning following direct current cardioversion (DCCV) in patients with atrial fibrillation (AF) and atrial flutter (AFL) can be variable and its impact on long term clinical outcomes remain unclear. The objective of this study was to determine if pre and post-DCCV transthoracic echo-Doppler (TTE) parameters of left atrial (LA) function can predict the maintenance of sinus rhythm at 1-year follow-up. **Methods:** Patients with non-valvular AF or AFL underwent TTE evaluation immediately before and after outpatient DCCV. Exclusion criteria included prior mitral valve intervention, recent cardiac surgery, and unsuccessful DCCV. By TTE, LA function was quantified by the absence, inconsistent presence or consistent presence of mitral inflow Doppler velocities (E and A wave), and medial and lateral mitral annular velocities (e', a' and s' wave), as well as the magnitude of these velocities. All patients were monitored for recurrence of atrial fibrillation or atrial flutter for 1-year after DCCV. **Results:** Of the 33 patients (age 71.4 ± 3.8 years, 76% male, 15% amiodarone) who underwent successful DCCV, 13 (39%) demonstrated complete contractile recovery of LA function, defined as the consistent presence of A wave, medial a' wave and lateral a' wave on post-DCCV TTE. At 1-year follow-up, only 4/33 patients (12%; 24% amiodarone) maintained sinus. Compared to patients who developed recurrence (n=29, 28% amiodarone), those who maintained sinus were more likely to have complete contractile recovery of LA function (31% vs 100%, $p=0.02$) and post-DCCV lateral s' ≥ 0.09 cm/s (21% vs 100%, $p = 0.005$). The presence of complete recovery of LA function with lateral s' ≥ 0.09 cm/s had a sensitivity, specificity and accuracy of 100%, 86%, and 88%, respectively, for predicting sinus rhythm ($p = 0.002$). **Conclusion:** In patients with AF or AFL, immediate return of complete contractile LA function after DCCV is a significant predictor of sinus rhythm at 1-year follow-up. Individuals who demonstrate this finding may benefit from post-DCCV antiarrhythmic therapy to preserve LA electrical-mechanical synchrony.

OA-07

Serial Fetal Echocardiograms in Hypoplastic Left Heart Syndrome Fetuses: Does it Affect Immediate Post-Natal Care

Bernadette Richards, Lesley Freely, Corey Stiver, Karen Texter, Cliff Cua. Nationwide Children's Hospital, Columbus, OH

Introduction: Guidelines recommend serial fetal echocardiograms when congenital heart disease is diagnosed. Necessity, timing, and frequency of serial echocardiograms are based on clinical judgment. Fetuses with hypoplastic left heart syndrome (fHLHS) may undergo multiple studies prior to birth. The goal of this study was to determine if the need for unexpected, emergent cardiac procedures were identified on follow up studies, if there were no concerns on the initial fetal echocardiogram. **Methods:** All fetal echocardiograms performed between 2006 - 2018 on fHLHS were reviewed. fHLHS were excluded if the initial fetal scan documented an abnormal rhythm, pericardial effusion, obstruction at the atrial or pulmonary vein levels, ≥ moderate ventricular dysfunction or atrioventricular valve regurgitation, or any other concerns. Unexpected, emergent catheterization or surgical procedures within the first 48 hours of life and death < 1 week of age were recorded. **Results:** Total of 81 fHLHS studies were reviewed. Thirty-one patients were excluded because of concerns on the initial fetal echocardiogram (19 = atrial septum restriction, 3 = atrioventricular valve regurgitation, 7 = other, 2 = comfort care), thus 50 fHLHS were analyzed. Sixteen fHLHS had one scan (27.1 ± 5.5 weeks), 16 had two scans (30.3 ± 3.5 weeks), 13 had 3 scans (33.6 ± 2.3 weeks), and 5 had four scans (36.0 ± 1.6 weeks). No patient underwent an unexpected, emergent catheterization or surgical procedure within the first 48 hours of life. Five patients died at less than 1 week of age (2 = comfort care, 1 = sudden arrest, 1 = complications from trisomy 13, 1 = surgical death). **Conclusion:** No

Oral Abstracts (OA)

Friday, June 21, 2019 — Tuesday, June 25, 2019

fHLHS underwent an unexpected, emergent catheterization or surgical procedure within the first 48 hours of life if the initial fetal echocardiogram had no significant concerns. No early deaths were associated with a missed fetal echocardiographic diagnosis. Serial fetal echocardiograms may not be necessary to predict the need for an unexpected, emergent procedure. Larger studies are needed in the fHLHS population to determine the cost effectiveness of serial fetal echocardiograms if the initial scan had no significant concerns.

OA-08

Management of Paediatric Cardiology Cases in Developing Countries Utilising Cardiac Point of Care Ultrasound via a Telemedicine Platform - a Descriptive Study

Rugambwa M. Muhame¹, Andreea R. Dragulescu¹, Cedric Manhiot¹, Kyle Runeckles¹, Raghu Venugopal², Adi Nadimpalli³, Daniel Martinez Garcia⁴, Marie-Claude Bottineau², Lynne E. Niell¹. ¹The Hospital for Sick Children, Department of Pediatrics, Division of Cardiology, Toronto, ON, Canada; ²Medecins Sans Frontieres, Toronto, ON, Canada; ³Medecins Sans Frontieres, New York, NY; ⁴Medecins Sans Frontieres, Geneva, Switzerland

Background: In developing countries, there is limited access to pediatric cardiology programs, with poor outcomes observed in children with heart disease. The Medecins Sans Frontieres (MSF) telemedicine (TM) platform provides direct cardiology specialist access to field staff in remote and resource constrained sites. Cardiac point of care ultrasound (C-POCUS) has been utilized in these sites with the objective of improving diagnosis and case management. We describe the experience of the pediatric cardiology program on this platform. **Methods:** We conducted a retrospective review of all pediatric cardiology referrals to two pediatric cardiologists on the TM platform between Jan 2016 and Dec 2018 to ascertain the spectrum of disease and determine the outcome in children with suspected heart disease. The secondary objective was to determine the utility of C-POCUS in case management. **Results:** A total of 233 children (0-18 years) with suspected heart disease were reviewed on the MSF-TM platform with males comprising 126/233 (54%) of the referrals. An increase in referrals was observed in successive years: 2016 (N=21), 2017 (N=44), 2018 (N=168). The referrals included neonates 0-28 days (12%), children aged <1 year (35%), 1-5 years (23%), 5-10 years (12%) and >10-18 years (18%). C-POCUS was performed in 191/233 (82%) cases with a definitive cardiac diagnosis possible in 163/191 (85%). Diagnoses comprised of congenital cyanotic lesions in 30/163 (18%), acyanotic lesions in 37/163 (23%), cardiomyopathy/ myocarditis in 16/163 (10%) and acquired heart disease lesions (including rheumatic heart disease, infective endocarditis and pericardial effusions) in 41/163 (25%) among others. Management changed in 137/233 (59%) cases following cardiology case and imaging review. Mortality was 40/233 (17%) and significant morbidity was expected in 106/233 (45%) of the referrals - significantly higher than expected mortality and morbidity. **Conclusions:** The MSF-TM platform improves diagnosis and case management in children with heart disease in resource limited settings. In particular, the availability of C-POCUS has had a significant clinical impact. Resources should thus be directed towards increased C-POCUS utilization with further training and rollout to additional sites.

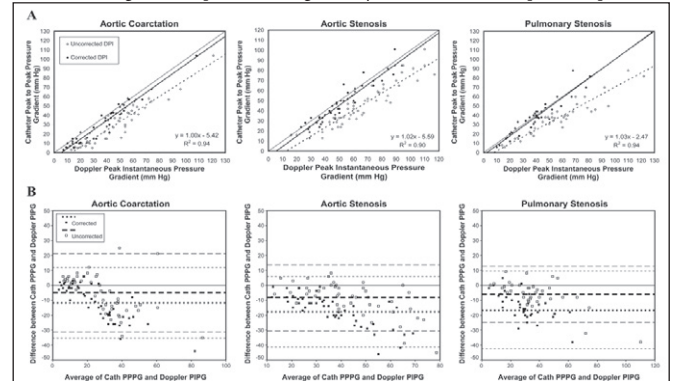
OA-09

Effect of Pressure Recovery on Pressure Gradients in Congenital Stenotic Outflow Lesions in Pediatric Patients - Clinical Implications of Lesion Severity and Geometry: A Simultaneous Doppler Echocardiography and Cardiac Catheter Correlative Study

Gautam K. Singh¹, Katie L. Mowers¹, Cynthia Marino², David Balzer¹, Syamasundar Rao³. ¹Washington University School of Medicine in St. Louis, St. Louis, MO; ²Saint Louis University School of Medicine, St. Louis, MO; ³University of Texas Houston Medical School, Houston, TX

Background: Doppler pressure gradients (PG) are routinely used as a surrogate for catheter peek-to-peek gradient (PPG) for referring pediatric patients with aortic stenosis (AS), pulmonary stenosis (PS) and coarctation of aorta (CoA) for intervention but do not predict the catheter PPG accurately. This results in misclassification of lesion severity and inappropriate referral for intervention. Pressure recovery (PR) accounts for much of the discrepancy between Doppler PG and catheter PPG in in-vitro and adult studies, but the occurrence of clinically significant PR causing misclassification of lesion severity by Doppler PG in congenital AS, PS and CoA is not well studied. **Methods:** Simultaneous Doppler and catheter PG were prospectively measured in 82 consecutive pts (median age: 12.2 mo., range 1-224 mo.; wt.: 7.5kg, range 2.8-72kg) with AS (n, 30), PS (n, 24), and CoA (n, 28) and agreement before and after correcting for PR were analyzed. PR was calculated from fluid dynamic based equation using echo-data. Effect of lesion geometry characterized by the ratio of lesion area/downstream vessel area on the magnitude of PR were analyzed. **Results:** Compared to uncorrected Doppler peak instantaneous gradient (PIG), PR-corrected Doppler PIG had significantly (p<0.001) higher correlation and closer agreement with (Figure) and prediction of catheter PPG with high specificity and accuracy in all lesions (95% CI: 36% to 97%; AUC 92%; and 95% CI 85%, 100% respectively, p <0.05 for both). The PR-corrected Doppler PIG was significantly (p <0.01) more accurate in predicting catheter PPG than mean Doppler PG which systematically underestimated it. The PR, which accounted for 4% to 42% overestimation of catheter PPG by Doppler PIG, was directly related (r = 0.33 to 0.47) to valve area and inversely related (r = -0.22 to -0.34)

to downstream vessel area. For the lesions with similar valve area > 0.5cm²/M² and vessel area < 2.75cm²/M², PR magnitude was significantly (p < 0.05) more in CoA and PS than in AS. **Conclusions:** Significant PR occurs in congenital AS, PS, and CoA accounting for misclassification of lesion severity by Doppler PIG. The PR-corrected Doppler PIG reliably predicts the catheter PPG in lesions with area > 0.5cm²/M² and vessel area < 2.75cm²/M². The PR magnitude depends on the geometry of stenotic lesion in pediatric patients.



OA-10

Right Ventricular Volumes, Ejection Fraction and Longitudinal Strain Assessed by Three-Dimensional Speckle Tracking Echocardiography: Comparisons with Cardiac Magnetic Resonance Imaging

Yuman Li^{1,2}, Xiaojing Wan^{1,2}, Yanting Zhang^{1,2}, Wei Sun^{1,2}, Yushan Wang^{1,2}, Li Zhang^{1,2}, Yali Yang^{1,2}, Jing Wang^{1,2}, Qing Lv^{1,2}, Heshui Shi³, Mingxing Xie^{1,2}. ¹Department of Ultrasound, Union Hospital, Tongji Medical College, Huazhong University of Science and Technology, Wuhan, China; ²Hubei Province Key Laboratory of Molecular Imaging, Wuhan, China; ³Department of Radiology, Union Hospital, Tongji Medical College, Huazhong University of Science and Technology, Wuhan, China

Purpose: Given the right ventricular (RV) complex structure, three-dimensional (3D) methods would be more suitable for assessing RV volumes and function than two-dimensional methods. Recently, 3D speckle tracking echocardiography (3D-STE) has been increasingly used to quantify RV function and strain. However, direct comparisons of 3D-STE and cardiac magnetic resonance (CMR) imaging for evaluation of RV function and strain are limited. The aim of this study was to test the feasibility and accuracy of 3D-STE using comparison with CMR imaging. **Methods:** We enrolled 122 patients who agreed to undergo both CMR and 3D-STE on the same day. RV end-diastolic volume (RVEDV), RV end-systolic volume (RVESV), ejection fraction (EF) and longitudinal strain of RV free wall were obtained from 3D-STE and CMR. CMR imaging was the reference standard. The Pearson correlation coefficient and Bland-Altman analysis were used to assess inter-technique agreement. **Results:** 3D-STE was feasible in 116 patients (95%). 3D-STE-determined RV volumes, EF and longitudinal strain correlated strongly with CMR values (RVEDV, r=0.94; RVESV, r=0.95; RVEF, r=0.94; RV longitudinal strain, r=0.82; P < .001 for all). Compared with CMR reference, 3D-STE-derived RVEDV and RVESV were underestimated by 7.2 ± 29.5ml and by 13.1 ± 28.1ml, respectively. 3D-STE-derived RVEF and RV longitudinal strain were overestimated by 3.5 ± 5.4% and 2.7 ± 4.5%, respectively. Compared with patients with RVEF > 30%, 3D-STE-determined RV volumes, EF and longitudinal strain had better correlations with CMR values in patients with RVEF < 30% (RVEDV, r=0.86 vs 0.92; RVESV, r=0.83 vs 0.93; RVEF, r=0.78 vs 0.86; RV longitudinal strain, r=0.50 vs 0.69; P < .001 for all). 3D-STE to measure RV volumes, EF and longitudinal strain was highly reproducible. **Conclusions:** 3D-STE is highly feasible and reproducible, and it correlates highly with the CMR method, especially in patients with severe RV dysfunction.

OA-11

Exercise Stress Echocardiography in Children with Hypertrophic Cardiomyopathy

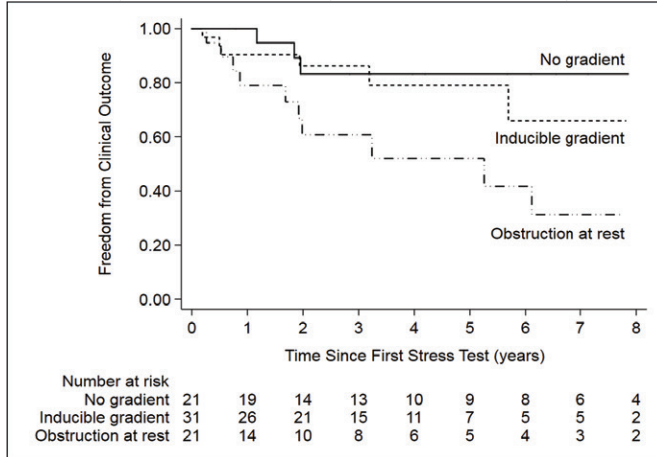
Iqbal El-Assaad, Kimberlee Gauvreau, Raheel Rizwan, Steven Colan, Ming Hui Chen. Boston Children's Hospital, Boston, MA

Background: Exercise stress echocardiography (ESE) is a valuable diagnostic and prognostic tool in adults with hypertrophic cardiomyopathy (HCM). Inducible and resting left ventricular outflow tract (LVOT) gradients are important predictors of heart failure (HF). However, the feasibility and significance of ESE in children is unknown, given its recent use. **Methods:** Retrospective review of all pediatric HCM patients who underwent ESE at our hospital between 2007-2018. Patients were assigned to 1 of 3 categories: No LVOT gradient (<30 mmHg at rest and exercise), inducible gradient (<30mmHg at rest and ≥ 30mmHg w/ exercise), and obstruction at rest (≥ 30mmHg at rest and exercise). Records were reviewed for earliest occurrence of the composite endpoint of any of following: cardiac syncope, cardiac chest pain, non-sustained/sustained ventricular tachycardia,

Poster Session 1 (P1)

Sunday, June 23, 2019

aborted cardiac arrest, NYHA class II-IV, or HCM-related death/transplant. **Results:** 91 children (34% F), median age 12yr (1d-23yr), and median LV wall thickness of 20 mm, formed the cohort. Median follow-up (f/u) was 3 yr. During ESE, 1 child experienced an event and was resuscitated. Total of 25 patients (27%) had no LVOT gradient, 40 (44%) had inducible gradient, and 26 (29%) had resting obstruction. Twenty six (29%) patients met composite endpoint including 2 heart transplant, 1 aborted cardiac arrest, and 1 sudden cardiac death. Children with rest LVOT obstruction were 5x more likely to develop symptoms and/or serious clinical outcome at any age (HR 5.18, [95% CI 1.39-19.2], $p=0.01$, Figure). During our short f/u time, patients with inducible gradients were estimated to have a higher risk of outcome, but this did not achieve statistical significance (HR 1.95 [95% CI 0.5-7.6], $p=0.33$). **Conclusion:** In this largest study assessing the value of ESE in children with HCM, ESE can be safely performed. About 40% of children have inducible LVOT gradient, which is comparable to adults, and were only unmasked by ESE testing. The clinical long-term sequelae of this finding require further studies with longer follow-up.



OA-12

Focused Cardiac Ultrasound Training for Rural Providers via Simulation

Florence H. Sheehan, Shannon McConaughy, Rosario V. Freeman, James N. Kirkpatrick. University of Washington, Seattle, WA

Background: Rural clinicians wishing to adopt focused cardiac ultrasound (FoCUS) lack access to sustained training because centralized continuing medical education (CME) courses are expensive and brief with limited opportunities for skill reinforcement. We tested the efficacy of disseminated CME using a simulator-based curriculum developed at the University of Washington. **Methods:** FoCUS was taught in a self-paced, simulator-based course with integrated didactic and hands-on training. The mannequin and computer were sent to clinicians for training at home or in their clinics. Didactic integration is a structured, stepwise approach to train on normal cases before introduction to pathology. Providers saw original patient images that morphed in real time as they manipulated a mock transducer on a mannequin. The parasternal long axis, parasternal short axis at aortic and mitral valves, apical and subcostal 4 chamber, and inferior vena cava views were taught. Providers took simulator based tests at baseline (pre), after all views were introduced (interim), and after 17 more cases (post). Psychomotor (technical) skill was measured in terms of the angle error between an acquired image and the plane of the anatomically correct image for the view, and averaged over all views in each case. Cognitive skill was judged from multiple-choice questions on image interpretation. **Results:** We present the results of 7 providers from 3 sites in Alaska of whom 5 completed the curriculum, 1 completed the curriculum up to the interim test, and 1 quit before. Psychomotor skill improved as seen from the decrease in angle error from $72 \pm 38^\circ$ (pre) to $35 \pm 19^\circ$ (interim) to $22 \pm 2^\circ$ (post, $p=0.008$, ANOVA for repeated measures, $N=5$). Skill in image interpretation also improved from $29 \pm 25\%$ (pre) to $53 \pm 33\%$ (interim) to $70 \pm 8\%$ (post, $p=0.032$, ANOVA for repeated measures) in these 5 providers. The sixth provider improved in image interpretation (from 9 to 64% correct) but not in technical skill ($83 \pm 29^\circ$ (pre), $79 \pm 50^\circ$ (interim)). **Conclusion:** A self-guided, simulator based FoCUS course improved provider skill in image acquisition and image interpretation. In place of faculty oversight the simulator's skill metrics provided immediate feedback to providers on their progress. The simulator enables repeated practice over multiple sessions in a safe learning environment, and its skill metrics enable objective competency testing. Disseminated CME achieved by shipping a mannequin simulator to rural clinicians is an inexpensive and accurate way to develop, test, and maintain FoCUS skill.

POSTER SESSION 1 (P1)

Presented Sunday, June 23, 9:00 AM-4:00 PM

Cardio-Oncology

P1-001 through P1-013

Adult Congenital Heart Disease

P1-014 through P1-020

Pediatric Heart Disease

P1-021 through P1-067

Clinical Cases: Pediatric Patients

P1-068 through P1-099

Critical Care Ultrasound / Point of Care Ultrasound

P1-100 through P1-104

Intraoperative Echocardiography (Operating Room and Interventional Lab) / TEE

P1-105 through P1-114

Valvular Heart Disease

P1-115 through P1-154

Doppler / Hemodynamics

P1-155 through P1-166

Echocardiography in SOE / Arrhythmias / Atrial Function

P1-167 through P1-181

Ischemic Heart Disease

P1-182 through P1-187

Ventricular Function / Myocardial Mechanics

P1-188 through P1-230

P1-001

Moderated Poster

Global Longitudinal Left Atrial Strain Provides an Early Index of Doxorubicin-Induced Cardiotoxicity: Validation in Chronic Canine Model

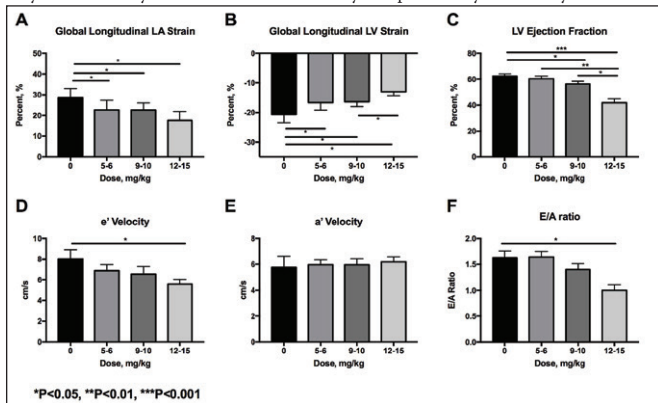
Nabil Boutagy, Nicole Guerrero, Attila Feher, Eva Romita, Christi Hawley, Carmen Booth, Chi Liu, Albert J. Sinusas. Yale University, New Haven, CT

Background: Left ventricular ejection fraction (LVEF) is used to detect doxorubicin (DOX)-induced cardiotoxicity in patients, but a decrease in LVEF often occurs after irreversible cardiotoxicity has developed. Left atrial (LA) global longitudinal strain (GLS) is a useful prognostic marker in patients with heart failure. The utility of LA GLS as early indicator of DOX-induced cardiotoxicity remains uncertain. We hypothesized that LA peak-diastolic GLS would decline prior to a fall in LVEF in chronic canine model of DOX-induced cardiotoxicity. **Methods:** Seven adult female dogs received DOX HCl (1 mg/kg) weekly for 12-15 weeks to produce progressive systolic dysfunction. Transthoracic echocardiograms (TTEs, Philips iE33) were performed in awake animals at baseline, and subsequently bi-weekly until LVEF fell below 50%, and then weekly. Endocardial LV biopsies were performed at 4-5 and 8-10 weeks, and detailed histopathology of all four-chambers was performed at terminal endpoint. LA GLS was determined from zoomed apical 2- and 4- chamber views, using 2D speckle tracking software (Epsilon, EchoInsight, Ann Arbor, MI). Similarly, peak systole LV GLS was determined from apical 2-, 3-, and 4- chamber views. LVEF and LV diastolic function were measured with system software. Baseline, early, mid and late time points were chosen for analysis that coincided with the following cumulative doses: 0, 5-6, 9-10, and 12-15 mg/kg, respectively. **Results:** A significant decrease in LA and LV GLS were observed at the early time-point (Figure 1 A, B), while LVEF was not significantly reduced until the mid-time point (Figure 1C). Diastolic dysfunction was not observed until the late-time point (Figure 1 D-F), coinciding with onset of severe systolic dysfunction. LV endocardial biopsies from the early and mid-time points did not display myocellular damage/fibrosis by light microscopy, although

Poster Session 1 (P1)

Sunday, June 23, 2019

myocyte degeneration, vacuolation and fibrosis in LA and LV were seen at the terminal timepoint. The microscopic injury in LA appeared worse than LV in some animals. **Conclusion:** LA GLS decreased prior to a fall in LVEF and myocellular toxicity in a chronic canine model of DOX-induced cardiotoxicity. These data suggest that LA strain imaging may allow for early assessment of cardiotoxicity that precedes systolic LV dysfunction.



P1-002

Effect of Iron Overload on Right Ventricular Function in Children with Sickle Cell Anemia

Yamuna Sanil, Preetha L. Balakrishnan, Neha Bansal, Sanjeev Aggarwal. Children's Hospital of Michigan, Detroit, MI

Background: Sickle cell anemia (SCA) is a common inherited hemoglobinopathy; a subset of patients need regular blood transfusions which leads to iron overload with deleterious effects on the heart. While left ventricle dysfunction is known in patients with SCA, data on right ventricular (RV) dysfunction and pulmonary hypertension are lacking. Specifically, RV function in patients with SCA with and without iron overload has not been previously explored. **Objective:** Our aim was to compare RV systolic function, in children with SCA with and without iron overload. **Methods:** This was a retrospective chart and echocardiogram review of SCA patients < 18 years of age. Patients were divided into groups with high (≥ 1000 ng/ml) and low (<1000 ng/ml) serum ferritin. Demographic and hematological data were collected. Echocardiograms were reviewed by a single reader who was blinded to clinical data. Echocardiographic parameters included a) Tricuspid annular plane systolic excursion (TAPSE) measured in the apical 4 chamber view using the 2D Doppler method, b) RV systolic pressure from the maximum velocity from the tricuspid valve regurgitation, c) right ventricular systolic (S) and diastolic (D) times and SD ratio, and d) TAPSE: RVSP ratio. Statistical analysis (SPSS 20.0) included student t-test and chi square test for comparison between groups. P value < 0.05 was considered significant. **Results:** Of the 90 children with SCD, 32 (35.5%) patients were in the high and 58 (64.5%) were in the low serum ferritin group. Demographics and hematological measures were comparable between groups except for serum iron level. TAPSE (2D) was significantly lower and SD ratio tended to be higher in the high serum ferritin group, compared to the low serum ferritin group. No significant difference was found in the RV systolic pressure or TAPSE: RV systolic pressure ratio. **Conclusion:** We found a significant difference in TAPSE using the 2D method between children with SCA who had and did not have iron overload. These intriguing findings suggest that children who undergo chronic transfusions for SCA develop RV dysfunction, even at a relatively young age. Further longitudinal evaluation of progression of RV dysfunction and associated clinical correlates is warranted in this population.

Demographic and echo parameters	High Serum Ferritin (n=32) (mean \pm SD) or n%	Low Serum Ferritin (n=58) (mean \pm SD) or n%	p value
Age (years)	10.3 \pm 4.6	11.9 \pm 4.8	0.13
Male (%)	18(56)	29 (50)	0.66
BMI	19.4 \pm 6.4	21.14 \pm 6.4	0.47
Hemoglobin (g/dl)	9.59 \pm 1.6	9.41 \pm 2	0.15
Iron	44.5\pm23.7	28.32\pm12.9	0.01*
Total Iron Binding Capacity	330 \pm 173	329.3 \pm 113.1	0.14
RVSP	21.6 \pm 4.8	24.1 \pm 8.3	0.13
TAPSE (2D)	2.06\pm0.35	2.32\pm0.48	0.005*
TAPSE:RVSP	9.8 \pm 2.9	10.7 \pm 3.6	0.28
SD ratio	1.2 \pm 1.4	0.9 \pm 0.32	0.06

P1-003

A Model for Predicting the Benefit of Cardiac Monitoring in Breast Cancer Patients Receiving Cardiotoxic Chemotherapy

Omid Amidi¹, Teodora Donisan², Dinu Balanescu², Saamir Hassan², Cezar Iliescu², Juan Lopez-Matter², Syed W. Yusuf², Jose Banchs², Nicolas Palaskas², Nicolas Palaskas². ¹Baylor College of Medicine, Houston, TX; ²MD Anderson Cancer Center, Houston, TX

Background: Anthracyclines and HER2 inhibitors are known to cause cardiotoxicity, requiring cardiac monitoring during and after therapy. Modern chemotherapy regimens against breast cancer use low-dose anthracyclines which carry a lower risk of cardiotoxicity. However, due to the lack of specific cardio-oncology guidelines, cardiac monitoring is still widely recommended, adding to overall healthcare costs. **Methods:** An IRB-approved retrospective study was performed at a large tertiary cancer center between March 2011 - March 2018. Breast cancer patients receiving anthracyclines, trastuzumab, or both, were included. Subjects were classified into 2 groups: one including patients that developed cancer therapeutics related cardiac dysfunction (CTRCD) and one including patients that did not. CTRCD was defined according to the Expert Consensus for Multimodality Imaging Evaluation of Adult Patients during and after Cancer Therapy. Baseline and follow-up clinical and echocardiographic parameters were collected. Binary multiple logistic regression analysis was performed to evaluate a prediction model for developing CTRCD. **Results:** The CTRCD group comprised 37 patients, compared to the no-CTRCD group of 126 patients. The model demonstrated a good correlation (Nagelkerke $R^2=0.804$) and accurately predicted patients that did not develop CTRCD 96.7% of the time. The model predicted no-CTRCD in 80% of patients. Assuming routine echocardiographic monitoring would be omitted for those with a negative predictive model, \$300,609 of healthcare costs would be saved in a one year period for every 100 breast cancer patients. **Conclusion:** Although echocardiography is widely available and inexpensive compared to other imaging modalities, the financial burden of monitoring large numbers of patients for a rare event is considerable. Using predictive models that incorporate clinical variables to identify patients that may not benefit from follow-up cardiac imaging is needed to safely reduce the overall cost of cardio-oncology care. With an estimated 266,126 cases of invasive breast cancer, this translates to savings of \$799,980,670 in cardiovascular monitoring costs.

P1-004

What is the Effect of Concomitant Radiation During Adjuvant Trastuzumab on Left Ventricular Function in HER2+ Breast Cancer Patients?

Lua Jafari, Sasan Raissi, Nadia El Hangouche, Kimberly Chow, Inga Vaitenas, Anjan Tiberwala, Nausheen Akhter. Northwestern University, Chicago, IL

Background: Breast cancer is the leading cause of cancer for women in the United States. Approximately 20% of breast tumors overexpress the tumor marker HER-2. In addition to chemotherapy, 12 months of adjuvant Trastuzumab (a monoclonal antibody directed against the HER2 receptor) is standard-of-care for early-stage HER-2 positive breast tumors. Depending on cancer stage and surgical approach, some women undergo adjuvant external beam breast radiation. The potential enhanced cardiac toxicity of concomitant Trastuzumab and breast radiation therapy is not well understood. The aim of this study was to evaluate early changes in LV function during treatment with concurrent Trastuzumab and breast radiation. **Methods:** Transthoracic Echocardiograms (TTEs) were obtained prior to treatment, and every 3 months on treatment for up to one year. Two-dimensional speckle tracking was performed using GE EchoPAC software. Ejection fraction was performed by Simpson's biplane. The baseline, initial TTE post-radiation, and 1 year TTE were analyzed for changes in left ventricular ejection fraction (LVEF) and global longitudinal strain (GLS). Statistical analysis was performed using a paired sample t-test, with a p-value < 0.05 considered statistically significant. **Results:** 45 female patients with HER2 positive breast cancer were included, mean age 52 years, 24% had hypertension, 8% had hyperlipidemia, and 4% had diabetes. The mean cumulative dose of radiation was 6370 cGy. Nineteen patients received right-sided radiation, 25 received left-sided radiation, and 1 patient received bilateral radiation. Compared to the baseline echocardiogram, there was a change in GLS immediately post radiation (-21.5 vs. -20.4, p = 0.001) which persisted at 1 year (-21.5 vs. -20.4, p = 0.007). Although there was a small change in LVEF immediately post radiation (63 vs. 61, p = 0.47), this was not significant at 1 year.

Table 1.

	Baseline	Early Post-Radiation	Late Post-Radiation (1 year)		
	(Mean \pm SD)	(Mean \pm SD)	P-value	(Mean \pm SD)	P-value
GLS (%)	-21.5 \pm 2.4	-20.4 \pm 2.3	0.001	-20.4 \pm 2.8	p=0.007
LVEF (%)	63 \pm 4	61 \pm 5	0.047	63 \pm 6	NS

Conclusion: These findings suggest that concomitant Trastuzumab and breast radiation is safe, and that although there is a small decline in GLS and LVEF immediately after radiation exposure, the changes in LVEF do not persist at 1 year.

Poster Session 1 (P1)

Sunday, June 23, 2019

P1-005

Temporal Changes in Diastolic Function in Women with HER2+ Breast Cancer Receiving Sequential Anthracyclines and Trastuzumab Therapy

Kate Rankin¹, Babitha Thampinathan¹, Eitan Amir¹, Paul Yip², Christine Brezden³, Kibar Yared⁴, Rossanna C. Pezo², Oscar Calvillo-Arguelles¹, Yobiga Thevakumar¹, Maria Michalowska¹, Anna Woo¹, Bernd J. Wintersperger¹, Paaladinesh Thavendiranathan¹. ¹University Health Network, Toronto, ON, Canada; ²Sunnybrook Health Sciences Centre, Toronto, ON, Canada; ³St. Michael's Hospital, Toronto, ON, Canada; ⁴Scarborough General Hospital, Toronto, ON, Canada

Background: There are limited data on the incidence and timing of diastolic dysfunction (DD) during cancer therapy. We sought to assess the incidence, timing, and impact of DD in women with HER2+ breast cancer during anthracycline and trastuzumab-based treatment. **Methods:** 99 women (50.9±9.1 years) with HER2+ early stage breast cancer treated sequentially with anthracyclines, trastuzumab ± radiotherapy (T3/4) were recruited prospectively. Using 2D echocardiography, diastolic function parameters, including indexed left atrial volume, average E/e' and TR max velocity, were measured pretreatment (T1), post anthracycline (T2) and at 3, 6, 9, and 12 months post trastuzumab initiation (T3-6). Diastolic function was graded according to 2016 ASE diastolic function guidelines. Chi-square test and unpaired t-tests were used for analysis. **Results:** There were no patients with DD at baseline (T1). During treatment 29 patients (29.3%) developed DD (p=0.005 for trend) at least at 1 time point (Figure 1). Six patients (6.1%) developed persistent DD, defined as DD occurring and remaining up to T6. Majority had grade 1 DD while 2 developed grade 2 DD with an average E/e' >14. DD was most common at T4 and T5. DD was associated with older age (53.8±9.1 vs 49.7±8.8 years, p=0.04) and diabetes (6.9% vs 0.0%, p=0.08) compared to those without DD. There was no difference in the proportion of patients with NYHA II-IV symptoms at each time point (p>0.05 for all). There were no significant differences in the trajectory of BNP values between the two groups (Figure 2). At the end of cancer therapy the mean E/e' was higher in those who developed DD at any timepoint vs those who did not (8.2±3.1 vs. 6.8±1.6 p=0.005). **Conclusion:** Amongst women with HER2+ breast cancer receiving treatment, 29% developed DD. DD was grade 1 and transient in the majority. There were no differences in BNP or NYHA class between the groups. The long-term consequences of DD during cancer therapy remain to be determined.

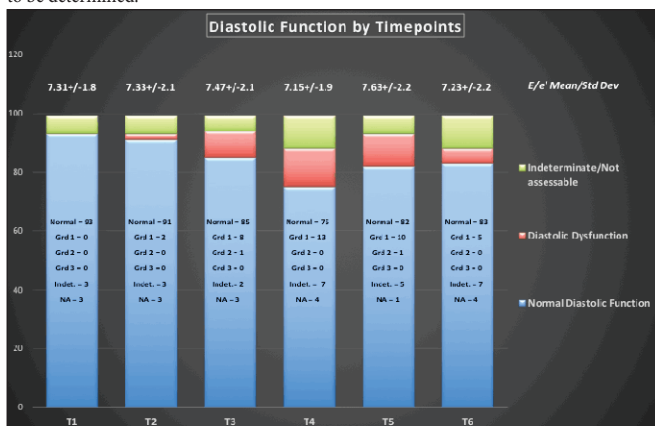


Figure 1 Proportions of normal, DD and indeterminate diastolic function by follow-up timepoint (Chi-square for trend p=0.0052). Mean E/e' by timepoint.

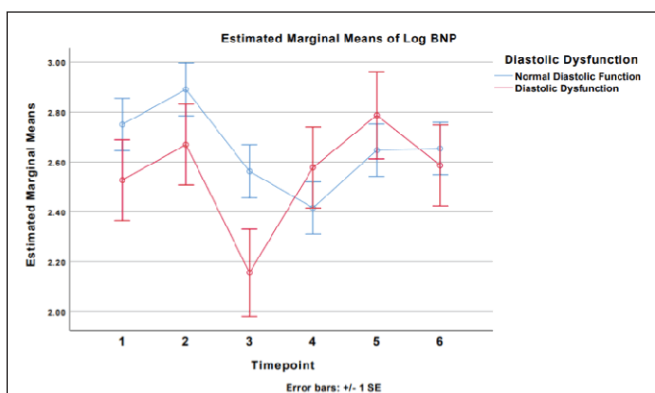


Figure 2 BNP trajectory by Log BNP estimated marginal means in patients with and without diastolic dysfunction.

P1-006

Inpatient Outcomes of Pericardial Tamponade in Patients with Cancer: Analysis from the National Inpatient Sample

Mohamed Khayata¹, Nour Tashtish², Sadeer G. Al-Kindi², Nishant P. Shah¹, Beni R. Verma¹, Chandra Ala¹, Saqer Alkharabsheh¹, Muhammad Furqan¹, Guilherme H. Oliveira³, Allan L. Klein¹. ¹Cleveland Clinic Foundation, Cleveland, OH; ²University Hospitals Cleveland Medical Center, Cleveland, OH

Background: Pericardial tamponade (PT) is a condition associated with significant morbidity and mortality and is often a complication of malignant pericardial effusions. Incidence and outcomes of PT in patients with cancer are scarce. The aim of this study was to investigate the nationwide outcomes of PT admissions in patients with versus without cancer. **Methods:** We used the 2016 national inpatient sample dataset to identify admissions among adult patients (age ≥18 years) with a primary or secondary diagnosis of PT using ICD 10 code I31.4. Primary outcome was inpatient mortality. Secondary outcomes included pericardial drainage procedures, inpatient palliative care consultation, length of stay (LOS), and hospital charges. **Results:** Out of 4104 admissions with PT, 1093 (27%) had cancer. Patients with cancer were younger (61 ± 14 vs 64 ± 16 years, P<0.001), more likely to be female (50% vs 45%, P = 0.006), less likely to be admitted electively (8.8% vs 22%, P<0.001), and less likely to have atrial fibrillation or flutter (31% vs 44%, P<0.001) compared to patients without cancer. Among patients with cancer, lung cancer was the most common (46%) followed by lymphoma (17%). Fifty nine percent of patients had metastatic cancer. Patients with cancer were more likely to undergo a pericardial drainage procedure (81% vs 75%, P<0.001), mainly due to higher utilization of pericardiocentesis (49% vs 42%, P<0.001), with no significant difference in surgical drainage (39% vs 38%, P=0.80). Pericardial drainage was associated with reduced inpatient mortality (0.39 [0.32-0.47], P<0.001). Cancer was associated with higher inpatient mortality (OR 1.52 [1.23-1.87], P<0.001), independently of demographics and pericardial drainage procedure compared to those without cancer. There was no difference in mortality by cancer type. Only 19% of patients with cancer and tamponade received inpatient palliative care. Cancer patients had lower hospital charges (82,162 [44,279-142,524] vs 118,045 [53,556-258,241] USD, P<0.001), but there was no difference in LOS (7 [4-14] vs 7 [4-14] days, P=0.16). **Conclusion:** Approximately 1 in 4 patients admitted with PT have cancer, most commonly lung neoplasms followed by lymphomas. Patients with PT and concomitant malignancy have higher inpatient mortality than those with PT without concomitant cancer. In cancer patients with PT, pericardial drainage was associated with reduced mortality, independent of whether percutaneous or surgical.

P1-007

Right Ventricular Strain Parameters Derived from Three-dimensional Speckle Tracking Imaging in Early Detection and Prediction of Cardiotoxicity Induced by Anthracycline-based Chemotherapy

R. Zhao, L.L. Cheng, X.Y. Fang, Y.C. Xu, Xianhong Shu. Zhongshan Hospital, Fudan University, Shanghai, China

Background: To investigate whether alterations of right ventricular (RV) strain indices derived from three-dimensional speckle tracking imaging (3D-STI) could predict future RV dysfunction in patients treated with anthracycline-based chemotherapy. **Methods:** Fifty patients with diffuse large B-cell lymphoma (DLBCL) who received 6 cycles of anthracycline -based treatments were enrolled. Echocardiography was performed on each patient at baseline (T1), at the end of 4 cycles (T2) and 6 cycles of the chemotherapy (T3). Right ventricular longitudinal free wall strain (RVLFS), right ventricular longitudinal septum strain (RVLSS) were calculated by 3D-STI. Right ventricular ejection fraction (RVEF) was measured by three-dimensional echocardiography (3DE). Anthracycline-induced cardiotoxicity (AIC) was defined as a decrease in the RVEF of >10 percentage points or an RVEF lower than 45%. The area under the receiver operating characteristic curve was calculated to determine the capability of RV strain parameters in predicting AIC. Correlation coefficient test was applied to evaluate the relationship between RV strains and RVEF. **Results:** Nine patients developed cardiotoxicity after the chemotherapy. Compared with baseline values (T1), RVLFS markedly reduced at T2 (-24.2±2.6% vs. -27.3±3.1%, p<0.001) as well as T3 (-21.9±2.8% vs. -27.3±3.1%, p<0.001). While, RVLSS (-22.9±2.7% vs. -25.6±2.9%, p<0.001) and RVEF (49.6±3.5% vs. 54.6±3.2%, p<0.001) did not change with significance until T3 compared with baseline. A >13.0% decrease in RVLFS [sensitivity, 89%; specificity, 71%; area under the curve (AUC)=0.748; P=0.007] from baseline to the fourth cycle of chemotherapy predicted subsequent AIC. At T3, the absolute value of RVLFS was positively related to RVEF (r=0.53, p<0.001). Furthermore, percentage change (between T0 and T3) of RVLFS was highly positively related to that of RVEF (r=0.72, p<0.001). **Conclusions:** Right ventricular strain parameters could detect subclinical changes of RV function at an early stage during anthracycline-based chemotherapy. Compared with RVLSS, RVLFS could be a more reliable method to predict future cardiac dysfunction induced by anthracycline.

Poster Session 1 (P1)

Sunday, June 23, 2019

P1-008

Noninvasive Myocardial Work and Global Longitudinal Strain in HER2+ Breast Cancer Patients Receiving Sequential Anthracycline and Trastuzumab Therapy

Oscar Calvillo-Argüelles¹, Camila Urzua-Fresno¹, Maryam Esmaeilzadeh¹, Babitha Thampinathan¹, Eitan Amir², Yobiga Thevakumaran¹, Maria Michalowska^{1,3}, Husam Abdel-Qadir^{1,3}, Bernd J. Wintersperger⁴, Paaladinesh Thavendiranathan¹. ¹University of Toronto, University Health Network, Toronto General Hospital, Peter Munk Cardiac Centre, Toronto, ON, Canada; ²University of Toronto, University Health Network, Princess Margaret Cancer Centre, Toronto, ON, Canada; ³Women's College Hospital, Toronto, ON, Canada; ⁴University of Toronto, University Health Network, Toronto General Hospital, Joint Department of Medical Imaging, Toronto, ON, Canada

Background: Global longitudinal strain (GLS) is a strong predictor of anthracycline and/or trastuzumab induced cardiotoxicity (CTX). Changes in myocardial work derived from pressure-strain analysis have not been explored in this setting. We aimed to describe longitudinal changes in Global Work Index (GWI) among patients with and without CTX. **Methods:** 17 women with HER2+ early breast cancer and cardiac MRI (CMR) defined CTX ($\geq 10\%$ decline in LVEF to value $< 55\%$) were matched (1:1) by age (± 3 years) and cardiovascular risk factors to patients without CTX. CMR and echocardiography were performed at: pretreatment (T1), anthracycline completion (T2), 3 (T3) and 6 (T4) months during trastuzumab and end of treatment (T5). Speckle tracking echocardiography based GLS and GWI from pressure-strain loops were analyzed at each time point. Univariate general linear models were constructed for GLS and GWI. **Results:** After exclusion of suboptimal studies, 32 patients with a mean age of 48.6 ± 7.2 years were included (N for CTX = 15). Mean epirubicin dose was 301.9 ± 10.1 mg/m² and 84% received radiation therapy. Baseline CMR LVEF in women with and without CTX was $60.8\% \pm 3.0$ and 60.5 ± 3.7 respectively ($p=0.76$). Amongst patients who developed CTX, 67% received ACEIs or beta-blockers. Overall temporal changes were significant for GLS ($p=0.013$) and GWI ($p=0.002$) (Fig 1A/1B) among the CTX group but not in the non-CTX group ($p=0.45$ and $p=0.24$ respectively). Post-Hoc pairwise comparisons with baseline GWI (among the CTX group), showed a significant reduction at T4 (Figure; $p=0.003$) which partially recovered by the end of cancer treatment ($p=0.73$). **Conclusion:** Amongst women with early stage breast cancer with treatment induced cardiotoxicity there was a significant reduction of GWI at T4. Since this measure is less load dependent (incorporates afterload) it may be an alternative to GLS to monitor deterioration in cardiac performance during cancer treatment. The potential clinical and prognostic additive value to GLS remains to be explored.

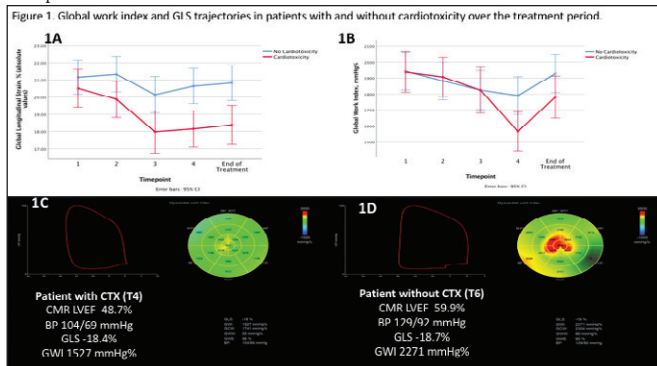


Table 1. Demographic and clinical variables in patients with and without cardiotoxicity

Variable	All patients N= 32	No Cardiotoxicity N= 17	Cardiotoxicity N= 15	P Value
Age, years \pm SD	48.6 \pm 7.2	47.6 \pm 6.4	50.1 \pm 8.1	0.29
Body mass index, kg/m ²	25.7 \pm 4.4	26.3 \pm 4.1	24.9 \pm 4.7	0.37
Baseline systolic blood pressure, mmHg \pm SD	113.9 \pm 14.3	112.2 \pm 10.6	115.9 \pm 17.7	0.49
Baseline diastolic blood pressure, mmHg \pm SD	73.0 \pm 11.1	73.1 \pm 8.9	74.7 \pm 13.4	0.7
Mean cumulative epirubicin dose, mg/m ²	301.9 \pm 10.1	303.7 \pm 6.3	299.6 \pm 15.3	0.45
Radiation treatment, n (%)	27 (84.4)	15 (88.2)	12 (80)	0.52
Baseline CMR LVEF, % \pm SD	60.7 \pm 3.3	60.5 \pm 3.7	60.8 \pm 3.0	0.76
End of treatment CMR LVEF, % \pm SD	56.3 \pm 5.2	58.7 \pm 3.9	53.23 \pm 5.3	0.005
Baseline 3D LVEF, % \pm SD	59.0 \pm 4.2	58 \pm 3.8	60.2 \pm 4.4	0.14
End of treatment 3D LVEF, % \pm SD	55.5 \pm 3.9	57.4 \pm 2.7	53.2 \pm 3.9	0.002
Secondary Cardio-protection, n (%)			10 (66.7%)	
Baseline Global Work Index, mmHg% \pm SD	1939.6 \pm 245.3	1941.7 \pm 244.4	1937 \pm 255.5	0.96
Global work index (GWI) Time-point 4, mmHg% \pm SD	1682.1 \pm 273.7	1790.1 \pm 231.7	1566.9 \pm 274.7	0.02
End of treatment GWI, mmHg% \pm SD	1862.1 \pm 215.4	1927.7 \pm 184.7	1781.3 \pm 229.7	0.068
Baseline GLS, % \pm SD	-20.9 \pm 1.5	-21.2 \pm 1.5	-20.5 \pm 1.6	0.25
GLS Time-point 4, % \pm SD	-19.4 \pm 2.5	-20.6 \pm 1.7	18.2 \pm 2.6	0.004
End of treatment GLS, % \pm SD	-19.7 \pm 2.3	-20.8 \pm 1.9	-18.4 \pm 1.9	0.003

P1-009

Quality Improvement in Completeness and Efficiency of Echocardiograms in Post-Chemotherapy Pediatric Patients

Angela Kristof¹, Poonam P. Thankavel², Mirela Dugulescu¹. ¹Children's Health, Dallas, TX; ²UT Southwestern Medical Center, Dallas, TX

Background: Transthoracic echocardiography is the main imaging tool to assess for systolic dysfunction in pediatric cancer patients who have been exposed to cardiotoxic agents. Its role in recognizing early cardiomyopathy is critical, as cardiovascular complications remain the leading cause of noncancer-related mortality in this population. Echocardiography in pediatrics has the additional challenge of uncooperative patients, sometimes limiting the time available to obtain optimal images. In order to standardize our imaging approach and improve completeness, a machine based protocol was implemented. **Methods:** A new protocol was designed and implemented into Vivid E95 and Acuson SC2000 machines in our laboratory, and education was completed in early 2018. A retrospective assessment was performed comparing follow-up studies in chemotherapy patients before (9/1/17-10/31/17) and after (9/1/18-10/31/18) protocol availability. Studies were analyzed for duration (minutes) and completeness (%) based on 14 pre-determined elements (Fig 1). **Results:** Ninety-two (92) patients were identified during the pre-protocol era. The mean duration of the study was 21 minutes and completeness was 80.8%. The elements missing were: SVC (73.9%), CA (77.2%), SF (1.1%), EF (60.9%), PSAX (5.43%), PLAX (3.3%), PA (2.2%), TVCW (14.1%), TVPW (13.0%), TAPSE (4.4%), TDI (2.2%), MVPW (2.2%), AP4CH (1.1%) and AO (2.2%). Number of complete studies was 3 (3.3%). In the post-protocol era, 80 patients were identified. The protocol was used in 78.5%. In these 62 patients, study duration average was 22 minutes and completeness was 98.9%. Number of complete studies was 52 (82.3%). The elements missing were: CA (8.1%), SF (1.6%), EF (3.2%), and TAPSE (6.5%). When comparing non-protocol to protocol studies, there was no difference in study duration (21 vs 22 minutes; $p=0.46$), but improvement in study completeness (80.8% vs 98.9%; $p<0.00001$). **Conclusions:** Implementation of a machine based protocol for echocardiographic assessment in post-chemotherapy pediatric patients improves study completeness without prolonging study duration. Even with a protocol, completeness was sometimes limited by patient cooperation.

Figure 1

Poster Session 1 (P1)

Sunday, June 23, 2019

Element	Abbreviation	Non-Protocol Studies Completeness	Protocol Studies Completeness
Apical four chamber	AP4CH	98.90%	100%
Parasternal short	PSAX	94.60%	100%
Parasternal long	PLAX	96.70%	100%
Superior Vena Cava	SVC	26.10%	100%
Coronaries	CA	22.80%	91.90%
Mitral inflow	MVPW	97.80%	100%
Tricuspid inflow	TVPW	87.00%	100%
Tricuspid CW	TVCW	85.90%	100%
Aorta	AO	97.80%	100%
Pulmonary Artery	PA	97.80%	100%
Tissue Doppler	TDI	97.80%	100%
Ejection Fraction	EF	39.10%	96.80%
Shortening Fraction	SF	98.90%	98.40%
Tricuspid Annular Plane Systolic Excursion	TAPSE	95.70%	93.60%
Total	14	80.80%	98.90%

P1-010

Tissue Motion Annular Displacement of the Mitral Valve: A Simple Index for Assessment of Left Ventricular Systolic Function in Children Following Chemotherapy

Sanjeev Aggarwal, Gilda Kadiu, Pooja Gupta, James Galas. Children's Hospital of Michigan, Detroit, MI

Background: Although anthracyclines are highly effective in the treatment of pediatric cancers, their utility is limited by progressive cardiotoxicity. Shortening fraction (SF) and ejection fraction (EF) are commonly used echocardiographic parameters to assess systolic function. Recently, Tissue Motion Annular Displacement (TMAD) of the mitral valve has been shown to be a reliable measure of longitudinal left ventricular (LV) function and to be independent of endothelial definition. **Objective:** To compare TMAD in asymptomatic children following completion of anthracycline chemotherapy vs. normal controls and to assess its correlation with EF calculated by 3D echo. **Method:** This was a retrospective review of echocardiograms on patients who had received anthracycline chemotherapy for pediatric cancers >1 year earlier and had normal SF (>28%) by M mode. Bone marrow transplant and pericardial effusion were exclusion criteria. Patients with chest pain, murmur or syncope who had normal echocardiograms were controls. Echocardiograms (Philips iE33) were read by a single reader blinded to clinical data. TMAD was measured in the apical four chamber view using the 2D speckle tracking technique (Q lab 10.8 Philips Medical System) in duplicate and an average was taken. Also, full volume data consisting of 4 adjacent sub-volumes over 4 consecutive beats were acquired during breath-hold to minimize artifacts and were analyzed offline to obtain 3D global longitudinal strain (GLS) and EF by 3D volume method (Tomtec Inc software). Student t-test and Chi-square test were used for comparisons between groups. **Results:** Our cohort (n=113) included 52 (46%) subjects who had received anthracyclines and 61 controls. The groups were similar in age and gender distribution. TMAD, EF and GLS were significantly abnormal in the anthracycline-treated group compared to controls (Table). TMAD correlated significantly with EF (r 0.3, p=0.001) and GLS (r-0.3 p=0.001). **Conclusions:** Even years after anthracycline chemotherapy, asymptomatic pediatric subjects have significant abnormalities in LV longitudinal systolic function as assessed by TMAD, EF, and 3D GLS. TMAD significantly correlated with EF as measured by 3D echo and may be a useful additional measure of LV function in the surveillance of anthracycline chemotherapy recipients.

Clinical/ Echo parameters (mean ± SD) (n%)	Chemotherapy (n=52)	Normal Controls (n= 61)	P value
Age	13.4±4.1	12.1±3.9	0.2
Gender (male)	30(57.6%)	35 (67.4%)	0.6
Ht (cm)	153.8 ± 22.5	152.4 ± 21.6	0.7
Wt (kg)	55.9 ± 25.3	49.4 ± 18.8	0.2
SBP	116±12	112±12	0.2
DBP	66±10	61±8	0.005*
Heart rate	73±10	70±12	0.3
TMAD%	19.4±3.2	21.9±2.3	0.000*
ESVindex	21.9±7.3	19.4±5.8	0.04*
EDVindex	54.4±13.5	55±12.3	0.8
Ejection Fraction (EF)	59.9 ± 7.0	64.9 ± 5.6	0.000*
3D GLS (%)	-18.3 ± 3.2	-22.6 ± 3.2	0.000*
3D GCS (%)	-28.3 ± 5.0	-31.2 ± 4.8	0.000*

P1-011

Early Changes of Right Ventricular Function and Morphology in Patients with Lymphoma Treated with Anthracycline Therapy

R. Zhao¹, L.L. Cheng¹, Y.C. Xu¹, D. Hsi², Xianhong Shu¹. ¹Zhongshan Hospital, Fudan University, Shanghai, China; ²Stamford Hospital, Stamford, NY

Background: Although left ventricular dysfunction and abnormalities have been widely illuminated in patients treated with anthracycline. Little is known about the early morphologic and functional changes of right heart. In this study, we sought to assess the subclinical alterations of right heart in patients treated with anthracycline-based chemotherapy by means of two-dimensional echocardiography (2DE) and three-dimensional echocardiography (3DE). **Methods:** Seventy-four patients aged 48.9±11.8 years old with diffuse large B-cell lymphoma who received 6 cycles of anthracycline -based treatments were enrolled. Echocardiography was performed on each patient at baseline (T0), after 2 cycles (T1), after 4 cycles (T2) and the end of the 6 cycles of the chemotherapy (T3). The end-diastolic area (EDA) of both RA (RAEDA) and RV (RVEDA) together with the end-systolic area (ESA) of RA (RAESA) and RV (RVESA) were derived from 2DE. RV end-diastolic volume (RVEDV), RV end-systolic volume (RVESV) and RV ejection fraction (RVEF) were measured by 3DE. The area under the receiver operating characteristic curve was calculated to determine the capability of various echocardiographic parameters to detect changes before and after chemotherapy. Correlation coefficient test was applied to evaluate the relationship between morphologic and functional changes. **Results:** Both RAESA and RAEDA enlarged significantly at T3 compared with baseline value (T0). Similarly, RVEDA and RVESA both expanded significantly at T3 compared with T0. Furthermore, for 3DE, RVEDV and RVESV dilated considerably at T2 when compared with T0. RVEF demonstrated worsening changes from baseline values at T3. The area under the curve for RVESV, RVEDV and RVEF were 0.886, 0.800 and 0.887, respectively. RVESV had a sensitivity of 0.79 and specificity of 0.90 to distinguish patients between baseline and T3 with the cutoff value of 31.1ml. At T3, RVESV instead of RVEDV was inversely related to RVEF (r=-0.30, p=0.01). Meanwhile, percentage change (between T0 and T3) of RVESV was highly inversely related to that of RVEF (r=-0.70, p<0.001). **Conclusions:** Among all the methods in detecting those changes of RV, 3DE is more sensitive than conventional 2DE. Right ventricular morphologic parameters especially RVEDV and RVESV change earlier than functional parameter. RVESV, which is not only an index regarding RV remodeling but also intrinsic systolic function, possesses additional value in synthetic assessment of RV.

P1-012

Aortic Stenosis Progression in Cancer Patients

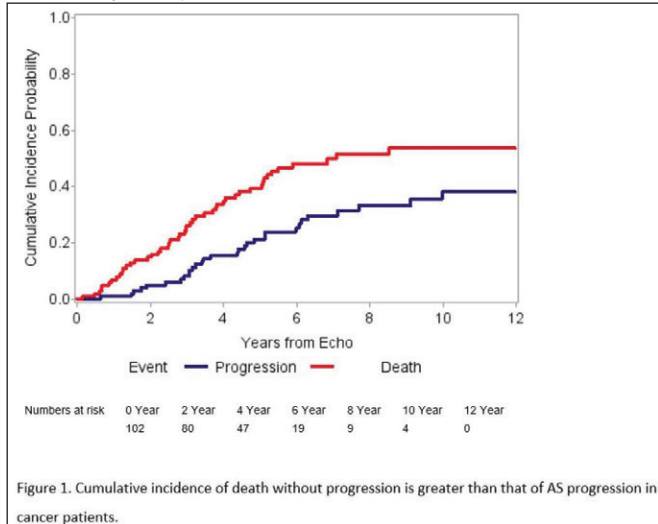
Kattia Bravo-Jaimes¹, Nadia Abellhad¹, Alveena Altaf¹, Sushanth Gouni¹, Juhee Song², Nicolas Palaskas², Syed W. Yusuf¹. ¹University of Texas Health Science Center at Houston, Houston, TX; ²MD Anderson Cancer Center, Houston, TX

BACKGROUND: Patients with cancer and aortic stenosis (AS) are exposed to several factors that could accelerate the progression of the latter, including chest radiation and chemotherapeutic agents. They are also at risk for death before AS progression occurs. This study aimed to determine the rate of aortic stenosis progression in cancer patients and which factors were associated with progression. **METHODS:** This retrospective cohort study included patients who had mild or moderate AS and at least two echocardiograms 6 months apart between January 1, 2000 and March 30, 2016 at MD Anderson Cancer Center. Patients with prior aortic valve replacement, severe aortic stenosis or left ventricular ejection fraction <50% at baseline were excluded. AS progression was defined by an increase in mean gradient of 20mmHg or peak velocity of 2 m/s by spectral Doppler echocardiography confirmed by two cardiologists or as requiring aortic valve replacement. Univariate and multivariate Fine-Gray models to account for the competing risk of death were used. **RESULTS:** 102 patients were included in the study and median follow-up

Poster Session 1 (P1)

Sunday, June 23, 2019

time was 5.2 years. Overall, 30 patients (29%) developed AS progression, while 48 (47%) died without AS progression (Figure 1). Among those with AS progression, 21 (70%) had AVR, and 10 of them (48%) died. Seven out of 9 patients (78%) with AS progression and no AVR died. Yearly rate of mean gradient change was 4.9 ± 3.9 mmHg and yearly rate of peak velocity change was 0.23 ± 0.29 m/s for patients who developed AS progression. Coronary artery disease (CAD), exposure to cyclophosphamide, VEGF inhibitor or Her2 antagonists; dyspnea; and beta-blocker use were associated with AS progression. In multivariate analysis including CAD, age, and cyclophosphamide, only CAD remained significantly associated with AS progression [sHR (subdistribution hazard ratio): 2.9 (95% CI, 1.3-6.1)]. **CONCLUSION:** Patients with aortic stenosis and cancer are more likely to die before having AS progression. Rate of AS progression is similar to the general population and CAD is significantly associated with it.

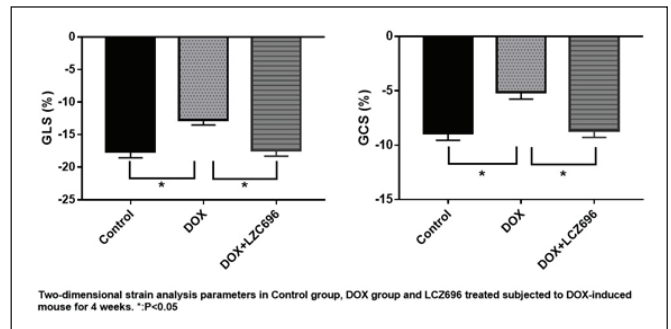


P1-013

Early Protective Effect of LCZ696 in Mice with Anthracycline-induced Cardiotoxicity Detected by Two-dimensional Echocardiographic Strain Analysis

R. Zhao, L. L. Cheng, Y. C. Xu, Y. Y. He, Xianhong Shu. Zhongshan Hospital, Fudan University, Shanghai, China

Background: This study aimed to evaluate the recovery of left ventricular systolic function detected by two-dimensional echocardiography-based strain analysis after anthracycline-based chemotherapy combined with LCZ696. **Methods:** Adult male Balb/c mice were randomly assigned to 3 groups as follows: control group received the injection of saline (one injection per 2 days for 14 days, 7 times totally; n=10); DOX group received the injection of doxorubicin at a dose of 15 mg/kg (one injection per 2 days for 14 days, 7 times totally, n=7); DOX + LCZ696 group (n=7) were given the injection of doxorubicin at a dose of 15 mg/kg (one injection per 2 days for 14 days, 7 times totally). Meanwhile, these mice were given LCZ696(60mg/kg)per gavage daily throughout the whole procedure. Echocardiography was performed using an animal specific instrument (VisualSonics Vevo770) on all animals. Conventional echocardiographic parameter included left ventricular ejection fraction (LVEF), fractional shortening (LVFS), end-diastolic dimension (LVEDD), end-systolic dimension (LVESD), end-diastolic volume (LVEDV) and end-systolic volume (LVESV). Two-dimensional strain parameter included left ventricular global longitudinal strain (GLS) and global circumferential strain (GCS). The serum N terminal pro brain natriuretic peptide (NT-proBNP), cardiac troponin I (cTnI) were measured simultaneously. **Results:** Cardiac function parameters were significantly reduced in DOX group compared with control group while improved in LCZ696 group. GLS and GCS were decreased in DOX group compared with control group. Both indices improved in LCZ696 group. NT-proBNP was significantly worse in DOX group compared with control group, which tended to be lower in LCZ696 group. Other serum biochemical markers manifested no significant difference between three groups. In addition, GLS correlated better than GCS with level of NT-proBNP. **Conclusion:** LCZ696 possessed protective effect against anthracycline-induced cardiac systolic dysfunction reflected by the recovery of left ventricular systolic parameters. GLS can be used in the early diagnosis of anthracycline-induced cardiac injury as well as the recovery of the resultant systolic dysfunction.



P1-014

Pickelhaube Under Stress: Another Risk Factor for Arrhythmic Mitral Valve Prolapse Syndrome

Andy Kieu, Lakshmi Muthukumar, Renuka Jain, M. Fuad Jan, Arshad Jahangir, Bijoy K. Khandheria, A. Jamil Tajik. Aurora Cardiovascular Services, Aurora Sinai/Aurora St. Luke's Medical Centers, Milwaukee, WI

Background: Individuals with mitral valve prolapse (MVP) present variably, from an asymptomatic state to malignant ventricular arrhythmias (VA) and sudden cardiac death (SCD). Several markers of VA/SCD in MVP patients have been defined. These include resting electrocardiographic T-wave changes in the inferolateral leads, myocardial fibrosis, mitral annular disjunction and bileaflet MVP. Our group has recently proposed a novel predictive marker, the Pickelhaube sign (Figure 1), defined as a mid-systolic spike of >16 cm/sec at the lateral/posterolateral mitral annulus on resting transthoracic echocardiogram (TTE). Herein we aimed to extrapolate this finding as a predictor of VA/SCD during exercise TTE. **Methods:** We analyzed patients with myxomatous bileaflet MVP who underwent exercise TTEs. All patients had interrogations of the lateral/posterolateral mitral annulus by tissue Doppler immediately after exercise from the apical window. **Results:** A total of 29 patients (mean age 51.5 ± 15.4 years, 62% female, n=18) were studied. The mean left ventricular ejection fraction was 58.5%. Of these 29 patients, 21 did not demonstrate any significant VA (non-VA group) on Holter monitoring. The remaining 8 (VA group) either had a prior SCD event (n=4) or episodes of non-sustained ventricular tachycardia (n=4) on Holter monitoring. The average resting annular velocity was 19.6 cm/sec in the VA group and 14.3 cm/sec in the non-VA group (95% confidence interval [CI] 0.4-10.2, p=0.04). The average exercise annular velocity was 27.0 cm/sec in the VA group and 17.1 cm/sec in the non-VA group (95% CI 2.7-17.1, p=0.01). The VA group had a 42.3% increase in velocity from rest to exercise and the non-VA group had a 25.1% increase (p=0.39, not significant likely due to insufficient patient numbers). **Conclusion:** Our data suggest that the annular Pickelhaube spike, a result of pull on the posteromedial papillary muscle in mid-systole by the large, bulky prolapsing leaflets, is a possible predictor of VA. During rest and exercise, there is a statistical significance in the Pickelhaube velocity between the VA and non-VA groups. Larger cohorts will aid in providing more significance to this finding. Arrhythmic MVP syndrome requires better risk stratification tools, especially for prediction of SCD.

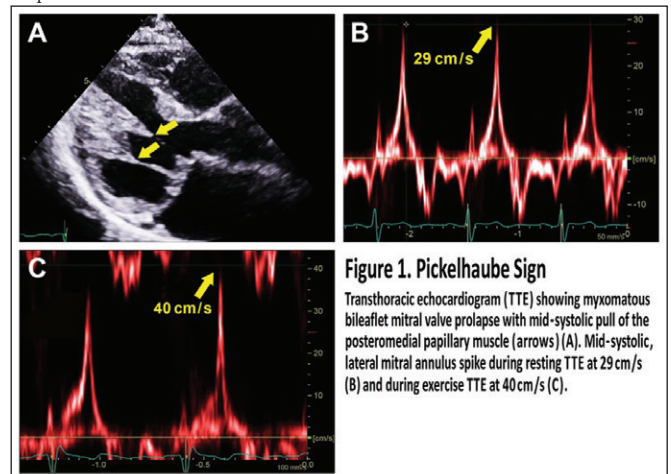


Figure 1. Pickelhaube Sign
Transthoracic echocardiogram (TTE) showing myxomatous bileaflet mitral valve prolapse with mid-systolic pull of the posteromedial papillary muscle (arrows)(A). Mid-systolic, lateral mitral annulus spike during resting TTE at 29 cm/s (B) and during exercise TTE at 40 cm/s (C).

Poster Session 1 (P1)

Sunday, June 23, 2019

P1-015

Effects of Transcatheter Pulmonary Valve Implantation on Biventricular Function and Cardiopulmonary Capacity: A Systematic Review and Meta Analysis

Mohammed Alomar, Rowan Walsh, Rajiv Verma, Marc Cohen. Newark Beth Israel Medical Center, Newark, NJ

Background: The mechanical effects of transcatheter pulmonary valve implantation (TPVI) on right and left ventricular function and exercise cardiopulmonary reserve have been limited to small cohort studies. **Methods:** Medline and Cochrane databases search for studies from inception through December 2017 was conducted using predefined criteria. Studies on TPVI effects on biventricular function in patients with right ventricular outflow tract conduit dysfunction and at least 6 months of follow up were included. Echocardiographic and exercise hemodynamics before and after TPVI were recorded. **Results:** Three studies including 54 patients with right ventricular outflow tract conduit dysfunction were identified. Mean age was 25 years, and 29% were male. Mean follow up was 6 months. TPVI indication was tetralogy of Fallot in 65% of patients, and 60% had pulmonic stenosis. Compared to pre TPVI, post TPVI mean pulmonic valve gradient and right ventricular systolic pressures were significantly lower (33.5 vs 21.4 mm Hg; $p < 0.0001$) and (69.5 vs 46 mm Hg; $p < 0.0001$), respectively. Global right and left ventricular longitudinal strain significantly improved post TPVI (-16.3 vs -17.8%; $p < 0.0001$) and (-16.2 vs -17.9%; $p < 0.0001$), respectively. In addition, right ventricular strain rate and fractional area change significantly improved post TPVI (-0.88 vs -1 s^{-1} ; $p < 0.005$) and (31.4 vs 39.5 mm^2 ; $p < 0.0001$), respectively. There was a significant improvement in peak exercise oxygen uptake (VO2) (24.6 vs 26.5 mL/Kg/min), O2 pulse (9.7 vs 10.7 mL/beat), and Ve/VCO_2 (29.7 vs 28); $p < 0.0001$. VO2 at anaerobic threshold did not significantly improve post TPVI (27.8 vs 31.7 mL/Kg/min; $p = 0.3$). **Conclusions:** In patients with right ventricular outflow tract conduit dysfunction, transcatheter pulmonary valve implantation is associated with improved biventricular function as measured by global longitudinal strain, and exercise cardiopulmonary function, when assessed by peak exercise Oxygen uptake.

P1-016

Ultrasound Enhancing Agents in Assessment of Adult Congenital Heart Disease Patients

Preeti Ramachandran¹, Bryana M. Levitan², Majd Makhoul¹, Vincent Sorrell¹. ¹Kentucky Children's Hospital, Lexington, KY; ²University of Kentucky, Lexington, KY

Background: Adult congenital heart disease (ACHD) patients are a unique population necessitating serial assessment of their congenital anatomy as well as regional and global ventricular wall motion. Due to need for multiple cardiac surgeries and cardiac geometry, image quality is often technically limited in this cohort. There is limited data on use of ultrasound enhancing agent (UEA) in ACHD patients. In this study, we review our center's experience with using UEA in ACHD patients and its impact on image quality and clinical care. **Methods:** ACHD patients with poor acoustic windows (>2 ventricular segments not visualized) undergoing echocardiograms from Jan 2017- Dec 2018 were identified. Very low mechanical index contrast imaging (VLCMI) with intravenous UEA (Definity, Lantheus Medical Imaging) was performed with mechanical index <0.2 on Phillips Epiq machine. Apical 2, 3 and 4-chamber images were obtained and compared for quality with and without UEA. Corresponding imaging views were compared in a non-serial random fashion. Ventricular regional wall segments were assessed. **Results:** A total of 10 ACHD patients were included. None of the patients had residual shunts. 7 patients had repaired tetralogy of Fallot, 2 patients had transposition of great arteries s/p Mustard procedure and 1 patient had undergone Ross procedure with right ventricle to pulmonary artery conduit. There was significant improvement in visualization of ventricular wall segments and ventricular apex with UEA compared to without UEA (Table 1). One patient with Tetralogy of Fallot and LV systolic dysfunction was noted to have thrombus at LV apex which was not appreciated on the non UEA image. No adverse effects were noted with UEA administration. **Conclusions:** Similar to experiences in other adults, UEA use was safe in ACHD patients with poor acoustic windows. It provided superior visualization of endocardial borders, ventricular wall segments and thrombus evaluation. Larger studies are required to further define application of UEA in ACHD patients.

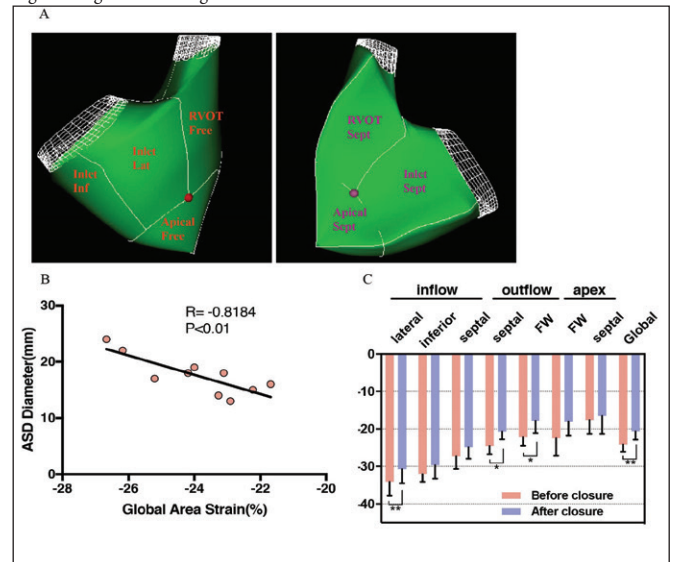
Table 1: Differences in regional wall motion assessment in images with and without UEA use			
	No UEA	With UEA	p-value
Systemic left ventricle (N=8)			
Mean total left ventricular segments seen	9	14	0.03
Mean segments seen on apical four chamber view	4	5	0.04
Mean segments seen on two chamber view	3	6	0.002
Mean segments seen on three chamber view	3	4	0.18
LV apex visualized (% of total cases)	16%	100%	N/A
Systemic Right ventricle (N=2)			
Free wall of RV (% of total cases)	0%	100%	N/A
RV apex (% of total cases)	0%	100%	N/A

P1-017

Global and Regional Right Ventricular Function in Patients with Atrial Septal Defect Assessed by Novel Three-Dimensional Speckle-Tracking Echocardiography

Z.Y. Ge, D.H. Kong, C.Z. Pan, Xianhong Shu. Zhongshan Hospital, Fudan University, Shanghai, China

Background: Two-dimensional speckle-tracking echocardiography (STE) does not allow a comprehensive evaluation owing to the right ventricle's complex, crescent-shaped structure. The aims of this study were to assess the global and regional RV strain in patients with atrial septal defect (ASD) before and after percutaneous ASD closure using a dedicated 3D STE system for RV analysis. **Methods:** Three-dimensional echocardiography was performed in 10 patients with ASD within 24 hours before and after percutaneous closure. Area strain (AS), longitudinal strain (LS), and circumferential strain (CS) of global RV and 7 RV segments (the lateral, inferior and septal segments of inlet, the free wall and septal segments of apex and outflow) were assessed. Six matched normal adults were enrolled as controls. **Results:** RV inlet compartment, especially the lateral and inferior segment showed the highest deformation in all subjects. In ASD patients, both the global RV longitudinal, and area strain were increased compared with the controls ($P < 0.01$). The regional AS and LS in the apical free wall and outflow were significantly greater compared with the controls ($P < 0.05$ for all). Global AS and apical free wall LS were negatively correlated with ASD diameters before closure ($r = -0.8184$, and $r = -0.701$ respectively, $P < 0.01$). After closure, except the apical septum, the global and regional LS of the other segments were significantly reduced. The AS of all the 7 segments showed a decreased trend after closure. **Conclusions:** Three-dimensional STE illustrates the specific physiology of RV contraction in ASD patients. Patients with ASD have enhanced RV longitudinal, and area strain. After closure, the global and regional LS of all the segments except the apical septum were significantly reduced. Fig A: 3D RV speckle-tracking echocardiographic image of seven segments(A1) The RV free wall side of the right ventricle. (A2) The septal wall side of the right ventricle Fig B: Correlations between RV global AS and ASD diameter before closure Fig C: The global and longitudinal strain before and after ASD closure



P1-018

Assessment of Right Ventricular Systolic Function and the Displacement of Tricuspid Annulus in Atrial Septal Defect Patients Using Real-time Three-dimensional Echocardiography

Lingyun Fang^{1,2}, Mingxing Xie^{1,2}, Jing Wang^{1,2}. ¹Department of Ultrasound, Union Hospital, Tongji Medical College, Huazhong University of Science and Technology, Wuhan, China; ²Hubei Key Laboratory of Molecular Imaging, Wuhan, China

Objective: Assessment of the right ventricular volume and function in atrial septal defect (ASD) patients using real-time three dimensional echocardiography (RT3DE). Assess the correlation between the right ventricular systolic function and the displacement of tricuspid annulus. **Methods:** RT3DE were performed in 36 ASD patients. The end diastolic/systolic volume (RVEDV/RVESV), and right ventricular ejection fraction (RVEF) were measured by four dimensional right ventricular quantification (4D RVQ) method. Display the spatial position of tricuspid annulus of the three dimensional imaging at the end of systole and diastole. Measure the distance of the displacement of tricuspid annulus. **Results:** RVEDV/RVESV and RVEF were $133.72 \pm 31.07 \text{ml}$, $73.04 \pm 22.62 \text{ml}$ and $42.35 \pm 5.41\%$ respectively. The displacement of tricuspid annulus was $12.01 \pm 5.06 \text{mm}$. The RVEF obtained from 4D RVQ method have an excellent correlation with the displacement of tricuspid annulus, ($r = 0.91, P < 0.01$). **Conclusions:** RT3DE can evaluate right ventricular

Poster Session 1 (P1)

Sunday, June 23, 2019

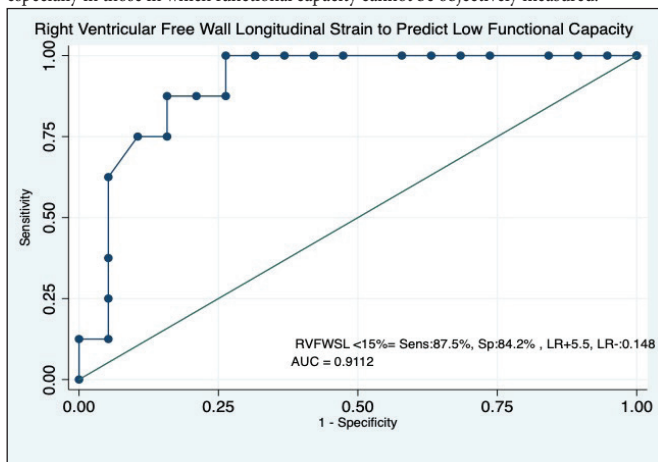
volume and function, and the correlation between the right ventricular systolic function and the displacement of tricuspid annulus. The displacement of tricuspid annulus was a reliable index for assessment right ventricular function.

P1-019

Right Ventricular Free Wall Strain Predicts Functional Capacity in Repaired Tetralogy of Fallot

Hugo Rodriguez Zanella¹, Cuatlahuac Arroyo-Rodriguez¹, Juan Francisco Fritche-Salazar¹, Paula Estrella-Cruz¹, Maria Eugenia Ruiz-Esparza¹, Edith Liliana Posada Martinez¹, Xochitl Ortiz-León¹, Laura Torres-Araujo¹, Eugenio Picano², Daniel Sierra¹, Roberto Ojeda Moreno¹, Jose Antonio Arias Godínez¹. ¹National Institute of Cardiology, Tlalpan, Mexico; ²CNR Institute of Clinical Physiology, Pisa, Italy

Background: Low functional capacity is the most important factor to perform valve replacement in repaired tetralogy of Fallot (rTOF) with severe pulmonary valve regurgitation. When measured objectively, more than 50% of asymptomatic patients have a reduced functional capacity. Because it is not always feasible to perform a stress test, finding a resting echocardiographic parameter that predicts functional capacity could be useful for decision making. **Methods:** We prospectively enrolled patients with rTOF who underwent rest and peak exercise echocardiography on a semisupine bicycle ergometer. Systolic and diastolic parameters of both ventricles were measured. Patients with a maximum oxygen consumption of <7 METS were defined to have low functional capacity. Logistic regression was used to identify parameters associated with low functional capacity. **Results:** A total of 27 patients were enrolled, mean age 26±6 years old, 11 female (40.7%). Eight patients (29.6%) had low functional capacity. These patients had a higher body mass index (24.8±4.9 vs 20.9±2.8 Kg/m², p=0.014), lower height (155±7.7 vs 162±8cm, p=0.036), tricuspid annular plane systolic excursion (15±2.4 vs 18±3mm vs, p=0.043) and right ventricular free wall longitudinal strain (RVFWSL) (12.3±3% vs 19.4±4.3, p=0.0006). Right ventricular end diastolic and end systolic dimensions (p=0.67) and right ventricular systolic pressures (p=0.1) did not differ among groups. The prevalence of severe pulmonary regurgitation was comparable among groups (63 vs 62.5%, p=0.974). On multivariate analysis RVFWSL was the only predictor of low functional capacity OR 1.53 (CI 95%, 1.096 -2.146, p=0.013) per % change. A RVFWSL <15% (absolute value) had a sensitivity of 87.5% and specificity of 84.2% to predict low functional capacity. **Conclusion:** Right ventricular free wall strain is an independent predictor of low functional capacity in repaired tetralogy of Fallot. A value <15% could be useful in deciding when to perform pulmonary valve replacement, especially in those in which functional capacity cannot be objectively measured.



P1-020

Impact of Age on Poor Reverse Right Ventricular Remodeling After Pulmonary Valve Replacement in Tetralogy of Fallot

Yuli Y. Kim¹, Jennifer Faerber², Katherine Awh², Stephanie Fuller², Lacey Gleason², Emily Ruckdeschel², Courtney Scott², Morgan Venuti², Xumei Zhang², Rosaline Zhang³, Laura Mercer-Rosa². ¹Hospital of the University of Philadelphia/Children's Hospital of Philadelphia, Philadelphia, PA; ²Children's Hospital of Philadelphia, Philadelphia, PA; ³Perelman School of Medicine at the University of Pennsylvania, Philadelphia, PA

Background: Pulmonary valve replacement (PVR) for chronic pulmonary regurgitation in tetralogy of Fallot (TOF) is associated with a decrease in right ventricular (RV) size (reverse RV remodeling) with pre-operative RV size being an important determinant of post-operative RV size. We hypothesize that older age is an independent predictor of poor reverse RV remodeling. **Methods:** Single center retrospective study of TOF patients who underwent PVR for pulmonary regurgitation from 2000-2014. Pre-operative and 1 year post-operative echocardiograms were analyzed for measurements of 1) RV end-diastolic (RVED) area, 2) RV end-systolic (RVES) area in the apical 4-chamber and 3) RV outflow

tract (RVOT) distance in the parasternal short axis. Degree of reverse RV remodeling for each dimension was calculated as the % difference in RV dimension compared to baseline with "poor reverse RV remodeling" defined as the lowest quartile. Univariable and multivariable logistic regression analyses were performed. **Results:** Forty-five patients underwent PVR (median age 16.8 years; range 3.9-43). Pre-operative and post-operative echocardiographic parameters are summarized in Table 1. There was a 16% decrease in RVED area, an 11% decrease in RVES area, and a 14% decrease in RVOT distance after PVR. On univariable analysis, pre-operative RVED area was not associated with poor reverse RV remodeling in RVED area. Age, however, was significantly associated with poor reverse RV remodeling in RVED area (Odds Ratio [OR] 1.10, 95% confidence interval [CI]: 1.02, 1.19; p=0.01) and remained significant on multivariable analysis when adjusted for pre-operative RVED area (OR 1.10, 95% CI: 1.00, 1.21; p=0.05). Age, pre-operative RVES area, and pre-operative RVOT distance were not associated with poor reverse RV remodeling in RVES area or RVOT distance. **Conclusions:** Older age at PVR is associated with poor RV reverse remodeling in end-diastolic size in TOF. Pre-operative RV dimensions were not predictive of poor reverse RV remodeling.

Table 1. Pre-operative and post-operative echocardiographic characteristics (n=45)

	Pre-operative	Post-operative	P-value
RVED area (cm ²)	36.2 ± 8.7	29.5 ± 9.0	p<0.01
RVES area (cm ²)	25.0 ± 7.0	21.6 ± 7.8	P<0.01
Fractional area change (%)	30.6 ± 9.8	27.3 ± 8.7	1.22
RVOT distance (cm)	3.4 ± 0.9	2.5 ± 0.7	<0.01
RVOT obstruction/PS (≥ moderate)	8/44 (8.2%)	1/28 (3.6%)	0.38
Tricuspid regurgitation (≥ moderate)	10/45 (22.2%)	4/41 (9.8%)	0.03
Antegrade diastolic flow	15/42 (35.7%)	15/37 (40.5%)	0.80
RV dysfunction (≥ mild)	26/43 (60.5%)	18/39 (46.2%)	0.14
LV dysfunction (≥ mild)	6/44 (13.6%)	2/34 (5.9%)	0.63

LV, left ventricular; PS, pulmonic stenosis; RV, right ventricular; RVED, right ventricular end-diastolic; RVES, right ventricular end-systolic; RVOT, right ventricular outflow tract

P1-021

Rapid Leaflet Expansion is the Main Adaptive Change to Maintain Tricuspid Valve (TV) Competency from Detrimental Remodeling: A Three-dimensional Echocardiography (3DE) Study in a Novel Chronic Right Ventricular (RV) Pressure and Volume Loaded Piglet Model

Lily Lin¹, Sanaz Hatami¹, Darren Freed¹, James Yashu Coe¹, Timothy Colen¹, Consolato Sergi², Richard Thompson¹, Elena Di Martino³, Walter Herzog⁴, Ziad Abu Sara⁴, Nee Sze Khoo¹. ¹University of Alberta, Edmonton, AB, Canada; ²University of Alberta, Faculty of Medicine and Dentistry, Department of Laboratory Medicine and Pathology, Edmonton, AB, Canada; ³University of Calgary, Department of Civil Engineering, Edmonton, AB, Canada; ⁴University of Calgary, Faculty of Kinesiology, Calgary, AB, Canada

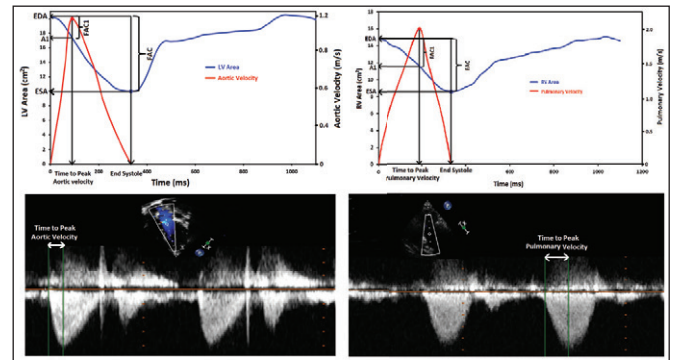
Background: Tricuspid valve regurgitation (TR) develops in 25-35% of children with hypoplastic left heart syndrome (HLHS), a risk factor for morbidity and mortality. Surgical strategies for TR in HLHS are modest in success and durability, therefore warrants improved understanding and innovation. We developed a novel piglet model simulating infant HLHS RV physiology to study TV adaptation to chronic increased preload and afterload. We hypothesize that TV competency is maintained by adaptive rapid leaflet expansion despite annular dilation. **Methods:** Sixteen piglets at 4-5 weeks of age (maturity equivalent to infants) underwent left thoracotomy. Intervention piglets (IP, n=8) had their pulmonary valve torn to produce moderate to severe pulmonary regurgitation (volume loading) and pulmonary artery band placed to increase RV pressure. Control piglets (CP, n=8), age and gender matched, had sham surgery. Following a 4-week recovery, all piglets underwent hemodynamic assessment and 3DE of TV. We assessed TV annulus and leaflet geometry in mid-systole using a custom 3DE software (MATLAB). Ex-vivo TV total leaflet area was measured. Comparisons between IP and CP were made using Student t-test with significance at p<0.05. Values were expressed as mean (standard deviation). **Results:** IP had significant pulmonary regurgitation (mean PR reverse/forward velocity time integral ratio 0.68 (0.09)) and mean RV systolic pressure 77.9% of systemic pressure, reflected in thicker RV free wall and anterior papillary muscle, consistent with an effective model. IP and CP are similar in weight and TR grade. IP TV annulus are larger (p=0.02), more circular (p=0.03) and leaflets more tethered (p=0.02) with 43% larger total leaflet area (p=0.01) [see Table]. Greatest expansion is seen in the posterior leaflet (p=0.01). 3DE TV total leaflet area correlated with ex-vivo TV pathologic specimen area (r=0.63, p=0.02). **Conclusion:** Following chronic exposure to increased RV preload and afterload, there is TV annular dilation and likely unchanged sub-valve apparatus, resulting in leaflet tethering. In-vivo 3DE identified rapid leaflet expansion as the main adaptive change to maintain competency from detrimental remodeling. Further research into modulation of TV leaflet growth may be important for understanding TV failure in HLHS.

Poster Session 1 (P1)

Sunday, June 23, 2019

Table: Comparisons of hemodynamic and echocardiographic parameters between intervention and control piglet groups. Values expressed as mean (standard deviation). Student t-test p-values reported. NS denotes non-significance.

Parameter	Control Piglets (n=8)	Intervention Piglets (n=8)	P-value
Weight (kg)	31.2 (5.8)	31.4 (6.1)	NS
RV systolic pressure/arterial systolic pressure (%)	30.3 (3.8)	77.9 (36.4)	0.003
Pulmonary regurgitation grade (0-4)	1.0 (0.5)	3.6 (0.4)	<0.0001
Tricuspid regurgitation grade (0-4)	1.9 (0.4)	2.4 (0.9)	NS
RV wall thickness (mm)	4.5 (0.9)	9.4 (1.2)	<0.0001
Anterior Papillary Muscle Cross-sectional Area (cm ²)	0.4 (0.08)	1.0 (0.3)	0.0003
TV Annulus Width/Anteroposterior dimension ratio	0.8 (0.09)	1.0 (0.2)	0.03
TV Annulus Total Area (cm ²)	6.2 (1.3)	8.3 (1.7)	0.02
TV leaflet area (cm ²) measured on pathology in relaxed state	11.0 (2.2)	12.1 (2.9)	NS
TV Leaflet Total Area (cm ²) at mid systole	7.0 (1.5)	10.1 (2.4)	0.01
TV Leaflet Area Posterior Leaflet (cm ²)	1.8 (0.6)	3.3 (1.2)	0.009
TV Total Tethering volume (ml)	1.1 (0.5)	2.6 (1.4)	0.02
TV Posterior Leaflet Tethering volume (ml)	0.2 (0.1)	0.8 (0.5)	0.01



P1-023

Fetal Left Ventricular Strain Analysis: Are High Frame Rate Images Necessary?

Alessandra M. Ferraro^{1,2}, Jamie K. Harrington^{1,2}, Wayne Tworetzky^{1,2}, Elvira D'Andrea^{3,2}, David M. Harrild^{1,2}. ¹Boston Children's Hospital, Boston, MA; ²Harvard Medical School, Boston, MA; ³Brigham and Women Hospital, Boston, MA

Background: Abnormal strain values from two-dimensional speckle-tracking echocardiography (2D-STE) are associated with clinical outcomes in children. An increasing number of studies are evaluating the association between fetal strain and postnatal outcomes. Full delineation of the clinical utility of fetal strain has been hindered, however, by typical data storage of the DICOM standard images at 30 frames per second (30FPS). High frame rate images have been recommended for STE analysis, especially at higher heart rates; and thus the analysis of images at 30FPS has been discouraged. Our aim was to determine if there is a statistically significant difference in fetal left ventricular (LV) longitudinal strain (LS) between images acquired at 30FPS versus full acquisition frame rate (FF); and to compare the magnitude of the bias between techniques to that seen with repeated measurements of the FF datasets. **Methods:** Fetuses between 18 to 36 weeks gestation with structurally and functionally normal hearts were included. Apical 4-chamber views were acquired with Philips Epiq 7 ultrasound machines at 30FPS and FF. LV LS analysis was performed using QLAB 10.8 and TomTec 2DCPA. FF images were analyzed twice to permit calculation of intra-observer variability using Bland-Altman statistics. Values resulting from 30FPS and FF images were compared using linear regression, Bland-Altman plots, and paired t-tests. P-values <0.05 were considered statistically significant. Values are listed as mean±SD unless noted otherwise. **Results:** Forty-five fetuses were studied. Mean frame rates (FPS) were: 30 (30FPS) and 93 (FF). LV LS values were not different between low and high frame rate analyses, for either QLAB (-28.5±3.1 (30FPS) vs -27.8±2.9 (FF), p=0.053) or TomTec (-27.6±3.1 (30FPS) vs -28.0±3.0 (FF), p=0.33). The figure shows that the 30FPS and FF values were highly correlated, for both software; Bland-Altman bias and 95% confidence intervals were similar for FF vs 30FPS images compared with repeated measurements of FF images, for both software. **Conclusion:** Fetal LV LS values from analyses at 30FPS are highly correlated to FF images and are not statistically different; as well their error compared to FF images is similar to the magnitude of error of repeated measures from FF images. Larger studies are needed to confirm this finding.

P1-022

First-Phase Fractional Area Change is Affected by Ventriculo-Ventricular Interaction in Repaired Tetralogy of Fallot Patients

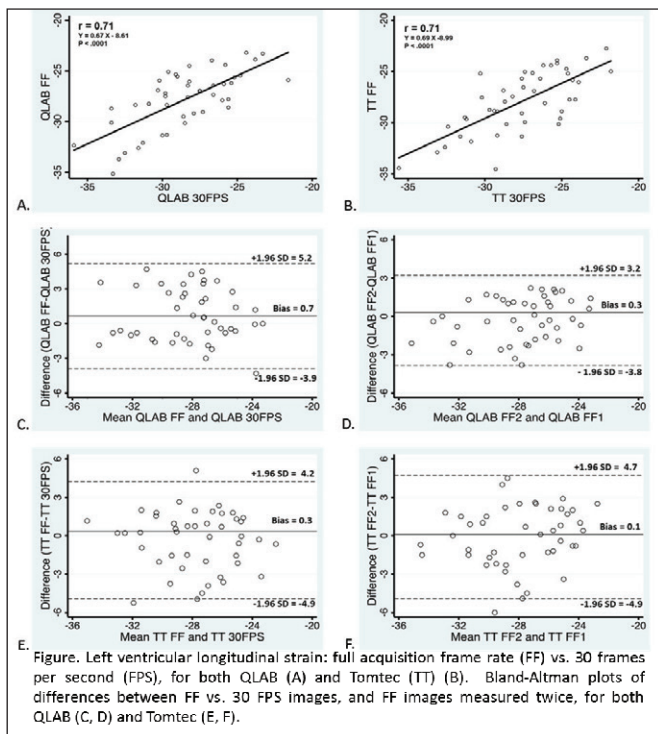
Ling Li¹, Mary Craft¹, Berthold Klas², Jason Christensen¹. ¹University Of Nebraska Medical Center; Children's Hospital and Medical Center, Omaha, NE; ²Tomtec Corp., Unterschleißheim, Germany

Background: First-phase ejection fraction is potentially a sensitive marker in detecting early left ventricular systolic dysfunction. Fractional area change correlates with ejection fraction. We hypothesized first-phase fractional area change (FAC1) can describe early systolic dysfunction and ventricular interactions in repaired tetralogy of Fallot (TOF) patients compared to normal subjects. **Methods:** 40 repaired TOF patients, age 15.2±9.2 years, 20 were male and 40 age and gender-matched controls were compared by analyzing apical 4-chamber views containing both atria and ventricles. A single observer performed deformation analysis on all 4 chambers within in the same cardiac cycle (2D CPA, TomTec). Time-to-peak pulmonary and aortic velocities were measured from spectral Doppler images. FAC1 was calculated by comparing diastolic area to early systolic area at the time to peak velocity of the respective great artery, **Figure**. Deformation indices and areas of LV and RV were computed from the spatiotemporal data. Student t-test was applied to compare measurements between patient groups. **Results:** The LV and RV time-to-peak systolic area and time-to-peak pulmonary velocity were prolonged in TOF compared to controls. Within the TOF cohort, there was no difference in time-to-peak area of the LV to the RV (p= 0.6946). LV and RV FAC were within normal range, but lower in TOF. LV FAC1 was lower in TOF than in controls. RV FAC1 was no different between groups, but RV longitudinal strain was reduced in TOF, suggesting ventricular interactions may affect early LV systolic function more than the right systolic function, **Table**. **Conclusions:** FAC1 is a novel measure of systolic function which may be valuable in TOF patients at risk for decline in ventricular contractility over time. Early systolic function needs to be further studied to determine its correlation with known risks factors in TOF and its usefulness in predicting clinical outcomes.

		Tetralogy of Fallot (N=40)	Controls (N=40)	p value
Time-to-peak (ms)	LV systolic area	374±49	341±87	0.0151*
	RV systolic area	378±83	340±38	0.0080*
	Aortic velocity	83.2±12.7	87.5±15.6	0.1780
FAC (%)	Pulmonary velocity	137.3±22.7	106.1±23.2	<0.001**
	LV	44.7±4.5	47.1±5.1	0.0238*
FAC1 (%)	RV	40.8±8.0	46.1±5.7	0.0011*
	LV	6.3±4.5	11.5±3.6	<0.001**
Global longitudinal strain (%)	RV	12.9±5.7	13.4±2.9	0.6103
	LV	-23.0±2.7	-25.6±2.9	<0.001**
	RV	-24.4±5.0	-30.0±4.2	<0.001**
	RV free wall	-27.8±6.5	-33.3±4.9	<0.001**

Poster Session 1 (P1)

Sunday, June 23, 2019



P1-024

Fetal Cerebrovascular Response to Maternal Hyperoxia: Effects of Cardiac Physiology

Shabnam Peyvand, Yili Zhao, Whitnee Hogan, Nicole Cresalia, Emilio Quezada, Hythem Nawaytou, Michael Brook, Anita Moon-Grady. UCSF, San Francisco, CA

Background: Maternal hyperoxia (MH) testing allows for acute alterations in fetal physiology. In the normal fetus, MH leads to redistribution of blood from the brain to the lungs likely secondary to intact fetal cerebral autoregulation. We sought to utilize MH testing to better understand the regulatory capacity of the fetal brain in three CHD groups: left sided obstructive lesion (LSOL), right sided obstructive lesion (RSOL) and transposition physiology (TGA). **Methods:** This is a cross-sectional study conducted from 2017- 2018. Pregnant mothers with a fetal diagnosis of CHD and no other anomalies were consented and underwent MH testing during their fetal echocardiogram in the 3rd trimester. MH testing consisted of 10 minutes of oxygen administration via a non-rebreather mask at 8L/100%FIO2. Echo images were obtained before, during and after MH testing. The pulsatility index (PI), a measure of resistance within a vascular bed, was calculated for the middle cerebral artery and umbilical artery (UA). MCA PI was converted to a z-score (MCA PIz) based on gestational age. Descriptive statistics were performed. **Results:** 40 subjects enrolled and underwent MH testing of which 36 were analyzed (LSOL-21; RSOL-8; TGA-7). The mean gestational age at echo was 32 weeks (95% CI: 31.2-32.9). At baseline, the MCA PIz was abnormal and low in LSOL (-2.2, 95% CI: -2.9, -1.5) while it was within the normal range for RSOL and TGA (table). With MH, the MCA PIz did not change significantly for LSOL (mean change +0.13, 95% CI: -0.39, 0.64). However, there was an increase in MCA PIz with MH in TGA (mean change +0.6, 95% CI: -0.4, 1.6) and a decrease in in RSOL (mean change -1.2, 95%CI: -2.6, 0.25). Within the LSOL group, there was no difference in response to MH based on the direction of flow in the aortic arch (p= 0.89). The UA PI was normal and unchanged with MH for all groups. **Conclusions:** The fetal cerebrovascular response to MH varies based on diagnostic group and suggests differences in regulatory properties of the fetal brain. Autoregulation appears to be intact in RSOL and TGA. The least response seen in LSOL suggests lack of regulation in response to variations in cerebral perfusion pressure, which may have implications for neurodevelopmental outcomes. Further studies will assess the relationship between fetal cerebral regulatory mechanisms and outcomes.

	LSOL (n= 21)	RSOL (n= 8)	TGA (n= 7)
GA at fetal echo	31.9 (30.8-33.1)	31.8 (30.3-33.4)	32.6 (30.3-34.8)
Mean MCA PI z-score			
Baseline	-2.2 (-2.9, -1.5)	-1.1 (-2.0, -0.10)	-1.0 (-1.5, -0.49)
Mat Hyperoxia	-2.0 (-2.7, -1.2)	-2.34 (-3.8, -0.83)	-0.42 (-1.8, 0.98)
Change	0.13 (-0.39,0.64)	-1.2 (-2.6, 0.25)	0.6 (-0.4, 1.6)
Mean UA PI			
Baseline	1.0 (0.89-1.1)	1.3 (1.0-1.6)	0.9 (0.7-1.1)
Mat Hyperoxia	1.1 (1.0-1.2)	1.2 (0.97-1.4)	1.0 (0.9-1.4)
Change	0.14 (0.04-0.2)	-0.19 (-0.4, 0.03)	0.09 (-0.05, 0.23)

P1-025

Prenatal Features of Ductus Related Branch Pulmonary Stenosis in Fetal Pulmonary Atresia

Deliwe P. Ngwezi^{1,2}, Marisha McClean^{1,2}, Angela McBrien^{1,2}, Luke Eckersley^{1,2}, Tim Colen^{1,2}, Jayani Abeysekera^{1,2}, Kim Haberer^{1,2}, Aisling Young^{1,2}, Lisa K. Hornberger^{1,2}. ¹Stollery Children's Hospital, Edmonton, AB, Canada; ²University of Alberta, Edmonton, AB, Canada

Background: Ductus arteriosus(DA)-related ipsilateral branch pulmonary artery(PA) stenosis (DA-PS) is common in congenital heart disease associated with pulmonary atresia (PAtr) and contributes importantly to the morbidity of affected neonates. We have recently described preoperative echocardiographic features associated with DA-PS in affected neonates, including the inability to examine the branch PAs on the same plane due to the location of ductal insertion and the presence of an obtuse posterior angle of bifurcation (>100°). In the present study, we sought to examine whether these same features can be used to identify the at risk fetus prenatally. **Methods:** We identified neonates who had been prenatally diagnosed with PAtr and a DA-dependent pulmonary circulation between 2009 and 2018 and who had undergone initial surgical/catheter intervention in our institution. Fetal echocardiograms were reviewed to examine the PA and DA anatomy for features of DA-PS best assessed from axial images with and without color Doppler. Preoperative and postoperative neonatal echocardiograms and clinical records were reviewed to confirm the presence/absence of DA-PS based on need for angioplasty at initial intervention or evolution of discrete PA stenosis postintervention. **Results:** In the study period 50 fetuses with PAtr were encountered of whom, 35 had images sufficient for analysis. Of these 35, PAtr was associated with an intact ventricular septum in 13(37%), tetralogy of Fallot (TOF) or TOF-double-outlet right ventricle in 16(46%), and with more complex heart defects in 6(17%). Twenty-one (60%) had evidence of DA-PS postnatally, including 15 who underwent arterioplasty at the time of initial intervention and 6 others who developed DA-PS postintervention. Gestational age at initial fetal echo was 26±6weeks and did not differ between groups. DA-PS was associated with an inability to image the branch PAs on the same plane in 67%, with an obtuse posterior bifurcation angle in 85% or with both features in 52% at a mean gestational age of 30±4weeks. In contrast, in those without DA-PS, the PAs could be imaged on the same plane in all and an obtuse posterior angle was present in only 3 (21%). The sensitivity, specificity and positive predictive value for an inability to image PAs on the same plane was 70%, 100%, 100% and for the finding of an obtuse posterior angle 85%, 79%, 85%. **Conclusions:** Features of DA-PS can be identified in fetal PAtr and include an inability to image the PAs on the same plane and an obtuse posterior bifurcation angle. This information is useful for prenatal counseling and planning neonatal intervention.

P1-026

Decreased Pulmonary Artery Acceleration Time is Associated with Cord Blood Biomarkers of Angiogenesis

Deidra Ansah. Ann & Robert H. Lurie Children's Hospital of Chicago; Feinberg School of Medicine at Northwestern University, Chicago, IL

Background: Bronchopulmonary dysplasia associated pulmonary hypertension (BPD-PH) is a cause of neonatal morbidity and mortality. Echocardiographic investigation of right heart function is the primary non-invasive diagnostic tool for PH in neonates. Commonly used echocardiographic parameters, such as tricuspid regurgitation velocity and qualitative right ventricular (RV) function assessment, have inherent limitations. Quantitative measurements, such as pulmonary artery acceleration times (PAAT), PAAT indexed to RV ejection time (PAAT/RVET) and eccentricity index (EI), have emerged as useful objective tools for the diagnosis of PH. Our group recently described a biochemical interplay between vascular growth factors at birth and pulmonary vascular dysfunction and identified an association between cord blood markers of angiogenesis and BPD-PH. We hypothesize that PAAT, PAAT/RVET and EI are associated with cord blood biomarkers related to angiogenesis. **Methods:** We performed a nested case-control study of infants less than 29 weeks at risk for developing BPD-PH who had available cord-blood and echocardiograms (n=31). These infants were drawn from a larger prospective cohort study at our partner institution. Multiplex immunoassay was used to measure 12 angiogenic biomarkers in cord blood. PAAT, PAAT/RVET and EI were measured on echocardiograms

Poster Session 1 (P1)

Sunday, June 23, 2019

closest to 36 weeks postmenstrual age (PMA). Multivariate linear regression was used to compare biomarker levels to PAAT, PAAT/RVET and EI. The primary outcome variable was PAAT. **Results:** Of the 31 infants with echocardiograms, 26 (mean gestational age at birth was 27 ± 1.4 weeks, and mean age at the time of echocardiogram was 35 ± 2.7 weeks PMA) had pulse wave Doppler of the pulmonary valve for assessment of PAAT. All patients had normal RV function and only 7 had reliable tricuspid regurgitation velocities to estimate RV pressure. There was no correlation between EI and any of the biomarkers. Decreased PAAT was associated with increased endothelin-1 (β: -0.72, SE: 10.6, p=0.009) and endoglin (β: -0.92, SE: 20.6, p=-.027) and decreased FGF2 (β: +0.93, SE: 10.3, p=0.01). Decreased PAAT/RVET was associated with increased endothelin-1 (β: -0.604, SE: 0.06, P=0.03) and decreased FGF2 (β: 0.71; SE: 0.055. P = 0.05). **Conclusion:** Reduced PAAT and PAAT/RVET at 36 weeks PMA are associated with increased endothelin-1 and endoglin and decreased FGF2 circulating at birth. These cord blood biomarkers may be useful to determine risk for development of objective echocardiographic findings of BPD-PH.

P1-027

Use of Tissue Doppler and Strain Imaging as Early Predictors of Fibrosis Development in Pediatric Patients with Hypertrophic Cardiomyopathy

Mansi Gaitonde¹, Janet Figueroa¹, Courtney McCracken¹, William Border², Riitu Sachdeva², Matthew E. Ferguson². ¹Emory University, Atlanta, GA; ²Children's Healthcare of Atlanta/Sibley Heart Center, Atlanta, GA

Background: The presence of myocardial fibrosis is associated with worse clinical outcomes in patients with hypertrophic cardiomyopathy (HCM). We sought to examine the prevalence of myocardial fibrosis in pediatric patients with HCM using cardiac magnetic resonance imaging (CMR). We also sought to determine whether echocardiographic measures of systolic and diastolic function using tissue Doppler imaging (TDI) and myocardial strain correlate with the development of fibrosis. We hypothesize that early abnormalities in TDI and strain will correlate with fibrosis development on CMR later in childhood. **Methods:** We reviewed records of patients < 22 years with HCM who underwent both an echocardiogram and CMR between Jan 2009 - Oct 2018 at our center. Development of fibrosis was determined by presence of late gadolinium enhancement on the patient's most recent CMR, and segments of fibrosis were described using the 17-segment left ventricle segmentation model. Left ventricular outflow tract (LVOT) gradients, left ventricular dimensions, and TDI values were recorded from the patient's earliest echocardiogram with adequate image quality. Post processing of images was performed to determine segmental and global longitudinal strain (GLS) values. Wilcoxon Rank-Sum tests were used for statistical analysis (p-value <0.05 for significance). **Results:** The study population included 96 HCM patients (40 with fibrosis; 56 without). In patients with fibrosis, the most recent CMR was performed at mean time of 15.7 months after the initial echocardiogram. The patients with fibrosis had a higher LVOT gradient at rest (42 mmHg vs 17, p=0.0024). E' and S' values of the septal annulus and A' values of the lateral annulus were significantly lower in the fibrosis group compared to the non-fibrosis group (Table 1a). Additionally, peak GLS was reduced in patients who developed fibrosis compared to those who did not (-9.1 vs -18.4, p=0.001). These findings were similar in the segmental strain analysis (Table 1b). **Conclusion:** These findings support the link between myocardial fibrosis and impaired systolic and diastolic function in HCM in children, providing further evidence of their pathophysiological relationship. This supports the use of echocardiographic indices such as TDI and strain as noninvasive early markers of myocardial fibrosis.

TDI Parameter	All		Fibrosis		p-value
	Mean [SEM]	Median [IQR]	Mean [SEM]	Median [IQR]	
Mitral E' (cm/s)	87.1 (4.4)	87.1 (4.4)	79.4 (6.5)	79.4 (6.5)	0.040
Mitral A' (cm/s)	164.1 (12.4)	164.1 (12.4)	150.1 (12.4)	150.1 (12.4)	0.096
Mitral E/A Ratio	1.9 (0.1)	1.9 (0.1)	1.7 (0.1)	1.7 (0.1)	0.335
Septum E' (cm/s)	7.5 (0.4)	7.5 (0.4)	6.3 (0.3)	6.3 (0.3)	0.008
Septum A' (cm/s)	41.1 (3.1)	41.1 (3.1)	37.9 (3.1)	37.9 (3.1)	0.023
Septum E'/A' Ratio	0.18 (0.01)	0.18 (0.01)	0.17 (0.01)	0.17 (0.01)	0.085
Lateral E' (cm/s)	11.8 (0.8)	11.8 (0.8)	10.2 (0.7)	10.2 (0.7)	0.073
Lateral A' (cm/s)	61.2 (4.1)	61.2 (4.1)	57.5 (4.0)	57.5 (4.0)	0.020
Lateral E'/A' Ratio	0.19 (0.01)	0.19 (0.01)	0.18 (0.01)	0.18 (0.01)	0.372
Lateral E'/S' Ratio	0.6 (0.1)	0.6 (0.1)	0.5 (0.1)	0.5 (0.1)	0.886

P1-028

Aortic Arch Dimensions in Determination of Surgical Approach for Aortic Arch Hypoplasia with Coarctation

Kinjal Parikh, Michael P. Fundora, Nao Sasaki, Jun Sasaki. Nicklaus Children's Hospital, Miami, FL

Background: Surgical repair of neonatal arch hypoplasia with coarctation is performed by sternotomy or thoracotomy, with thoracotomy preferred due to favorable benefits of no cardiopulmonary bypass. We performed a retrospective study of the use of pre-surgical absolute aortic arch dimensions and ratios to determine the optimal approach for arch reconstruction in neonates, and if arch dimensions predict the need for re-intervention. **Methods:** Patients < 30 days old who underwent arch reconstruction via median sternotomy

or lateral thoracotomy at Nicklaus Children's Hospital, between January 2000 and July 2018, were retrospectively reviewed. Neonates requiring additional intracardiac surgery were excluded. Aortic arch dimensions were obtained from preoperative echocardiographic images, which included the distal transverse arch, the left carotid artery, the isthmus and the distance between the left carotid artery and subclavian artery. From this, 3 distinct ratios were calculated: the distal transverse arch diameter/carotid artery diameter (DT/CA), distal transverse arch diameter/distance from the carotid to subclavian artery (CSA) and isthmus diameter/descending aorta diameter (I/D). **Results:** Of the 118 study patients, 53 underwent a lateral thoracotomy and 65 median sternotomy. Distal transverse arch (p < 0.0001), carotid artery (p = 0.035) and isthmus (p = 0.003) diameters strongly correlated with surgical approach. The DT/CA ratio had an ROC curve (p < 0.0001; AUC 0.761) identifying a ratio of 0.9 (sensitivity 89%, specificity 34%) or greater as feasible for arch reconstruction by lateral thoracotomy. The ratios did not predict the need for surgical re-intervention on the aortic arch. The re-intervention rates were similar for both approaches overall and within the first 6 months of operation. **Conclusion:** Pre-surgical aortic arch measurements and the DT/CA ratio can be utilized to determine the feasibility of a lateral thoracotomy approach. In our institution, neonates with a DT/CA ratio of 0.9 or higher have routinely undergone arch reconstruction by a lateral thoracotomy. However, the arch measurement ratios do not correlate with re-intervention on the aortic arch.

Table 1: Patient Comparison for characteristics and outcomes

	Lateral Thoracotomy (n=53)	Median Sternotomy (n=65)	P value		
Distal Transverse Arch (mm)	4.2 (2-6)	3.5 (2.2-4.5)	< 0.0001		
Isthmus (mm)*	2.1 (1.4-2.9)	2.5 (1.4-5.0)	0.003		
Smallest Diameter of Arch (mm)*	2.1 (1.4-5.4)	2.4 (1.4-5.2)	0.11		
Distal Transverse Arch Diameter Z score	-3.4 (-4.46 - -1.66)	-3.2 (-4.78 - -1.83)	0.444		
Descending Aorta (mm)	7.1 (4.3-11.4)	6.8 (4.6-10.1)	0.86		
Carotid Artery (mm)	3.4 (1.8-5.2)	3.7 (2.7-5.6)	0.035		
Distance from Carotid to Subclavian Artery (mm)	6.9 (1.5-11.9)	6.1 (1.1-15.5)	0.054		
DT/CA	1.3 (0.41-1.94)	0.98 (0.48-1.48)	< 0.0001		
CSA*	0.61 (0.3-3.53)	0.62 (0.23-3.27)	0.81		
I/D*	0.29 (0.2-0.52)	0.37 (0.18-0.85)	0.04		
Gestational Age (weeks)*	38 (78.41)	38.5 (31-41)	0.97		
Age at Surgery (days)*	8.3 (1-30)	6.2 (2-19)	0.03		
Weight at Surgery (kg)*	3.4 (1.1-5.14)	3.2 (1.9-7.1)	0.06		
Post Op Stay (days)*	4.8 (3-40)	10.9 (6-134)	< 0.0001		
Required Re-intervention within 6 months	13 (25%)	17 (26%)	0.53		
Required Re-intervention overall	15 (28%)	17 (26%)	0.27		
Comparison of Arch Measurement Ratios and Re-intervention on Aortic Arch					
Re-intervention	No	Yes	No	Yes	P
DT/CA	1.31 (0.81-2.39)	0.85 (0.41-1.94)	1.05 (0.5-1.68)	0.94 (0.7-1.20)	0.11
CSA*	0.61 (0.3-3.75)	0.64 (0.3-1.18)	0.62 (0.34-3.3)	0.6 (0.23-3.3)	0.56
I/D*	0.32 (0.2-1.0)	0.32 (0.24-0.52)	0.4 (0.2-0.68)	0.39 (0.2-0.85)	0.59

* Values expressed as n (%), mean or median (range, minimum-maximum)
* Indicates nonparametric distribution and use of median

P1-029

Hemodynamic and Echocardiographic Predictors During Venarterial Extracorporeal Membrane Oxygenation Wean in Pediatric Patients - A Multicenter Investigation

Rajesh Punn¹, Christine B. Falkensammer², Joshua J. Blinder², Carlen G. Fifer³, Thor Thorsson³, Gregory Perens⁴, Myke Sherman⁴, Punkaj Gupta⁵, Thomas Best⁶, Bhawna Arya⁶, Titus Chan⁶, Sara Sherman-Levine⁶, Shea N. Smith¹, David M. Axelrod¹, Stephen J. Roth¹, Theresa A. Tacy¹. ¹Stanford University, Lucile Packard Children's Hospital, Palo Alto, CA; ²Children's Hospital of Philadelphia, Philadelphia, PA; ³Mott Congenital Heart Center, University of Michigan, Ann Arbor, MI; ⁴David Geffen School of Medicine at UCLA, Los Angeles, CA; ⁵University of Arkansas for Medical Sciences, Arkansas Children's Hospital, Little Rock, AR; ⁶Seattle Children's Hospital and the University of Washington School of Medicine, Seattle, WA

Background: Venous-arterial extracorporeal oxygenation (VA-ECMO) supports patients with advanced cardiac dysfunction; however, mortality occurs in a significant subset of patients. We performed a multicenter, prospective study to determine hemodynamic and echocardiographic (echo) predictors of mortality in children placed on VA-ECMO for cardiac support. **Methods:** Over eight years, six heart centers prospectively assessed echo and hemodynamic variables on full and minimal ECMO flow. Hemodynamic measurements included: heart rate, vasoactive inotropic score, arterio-venous oxygen difference, pulse pressure, oxygenation index, and lactate. Echo variables included: shortening/ejection fraction, outflow tract Doppler-derived stroke distance (VTI), and degree of atrioventricular valve regurgitation (AVVR). Patients were stratified into those who died or required a ventricular assist device (VAD) or orthotopic heart transplant (OHT) (organ failure group), and those who did not (organ survival group). For each patient, we compared the variable changes from "full" versus "minimum" ECMO flow for each group. **Results:** We enrolled 65 patients ranging in age 1 day - 16 years. Thirty-one

Poster Session 1 (P1)

Sunday, June 23, 2019

formed the organ failure group (2 VAD, 4 OHT, 25 death, 48%) and 34 comprised the organ survival group. In the organ survival group, VTI (6.4 vs 8.4 cm, $p < 0.01$) and heart rate (HR, 120 vs 128 bpm, $p = 0.0032$) increased upon weaning ECMO flow, while in the organ failure group, lactate increased (1.7 vs 2.3 mmol/L, $p = 0.0062$) but the VTI (6.2 vs 6.8 cm, $p = 0.06$) and HR failed to change (127 vs 131 bpm, $p = 0.1049$). A myocarditis diagnosis predicted a benign outcome ($p = 0.01$, 26% vs 3%), while use of hemofiltration ($p = 0.04$, 39% vs 15%) and duration of ECMO ($p < 0.01$, 8 vs 6 days) associated with the organ failure group. A post-wean central venous pressure (CVP) > 12 mmHg, VTI < 7 cm, or VA-ECMO length > 7 days predicted adverse outcomes. Multivariate logistical regression showed duration of ECMO to be independently associated with adverse outcomes. **Conclusion:** Failure to augment VTI or HR during VA-ECMO weaning predicts the need for OHT or VAD support or death in children on ECMO for cardiac dysfunction. Increased post-wean CVP or prolonged ECMO course also predicted these adverse outcomes. We propose that these measurements should be utilized to discriminate who will require alternative methods of circulatory support for survival.

P1-030

Correlating Pulmonary Hypertension by Echocardiogram with Mortality in Premature Infants with Bronchopulmonary Dysplasia

Rachel Torok¹, Piers C.A. Barker¹, Andrew W. McCrary¹, Tracy G. Spears², Christoph P. Hornik², Matthew M. Laughon³. ¹Duke University Medical Center, Durham, NC; ²Duke Clinical Research Institute, Durham, NC; ³University of North Carolina at Chapel Hill, Chapel Hill, NC

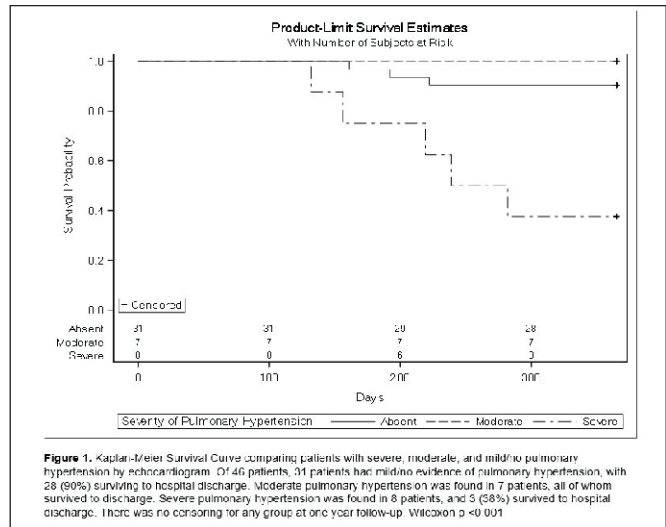
Background: Premature infants with bronchopulmonary dysplasia (BPD) are at increased risk for pulmonary hypertension (PH). Cardiac catheterization is the gold standard for diagnosing PH but often is not feasible in small, critically ill, premature infants. Data are lacking on the utility of echocardiography for diagnosing PH and predicting associated outcomes. We use *a priori* defined criteria to diagnose PH by echocardiogram and relate PH severity to mortality in extremely premature infants with BPD. **Methods:** 483 echocardiograms from 49 infants born ≤ 28 weeks gestation at two sites were independently read by 3 masked pediatric cardiologists in an echocardiography core lab to assess for PH. Diagnostic criteria for PH severity were defined *a priori* (Table 1). Survival by PH severity group was illustrated with Kaplan-Meier curves and compared by Wilcoxon test. **Results:** Of the 46 infants that met inclusion criteria, 15 (33%) had PH. Demographic characteristics, including gestational age, birth weight, sex, race, outborn status, Caesarean section rate, APGAR score, antenatal steroid administration, surfactant therapy, and treatment site were similar between infants with and without PH. Patients with severe PH had decreased survival to hospital discharge (38%) compared to moderate (100%) and mild/no PH (90%) groups. Kaplan-Meier survival curves between severity categories of PH were significantly different (Wilcoxon $p < 0.001$, Figure 1). **Conclusion:** Using predefined diagnostic criteria for PH, premature infants with severe pulmonary hypertension by echocardiogram have significantly reduced survival.

Subjective quantification of RV pressures	Absolute criteria	Supportive criteria	RV function ⁹	RV / RA size ⁹
Normal (< 1/3 systemic)	Septum round Eccentricity index ⁴ ≤ 1.0	L to R	Normal	Normal
Mildly elevated (1/3-2/3 systemic)	Septal geometry mildly distorted, Eccentricity index 1.01-1.20	L to R	Normal	Mildly dilated
Moderately elevated (2/3 systemic)	Septum moderately distorted but not flat. Eccentricity index 1.21-1.4	L to R	Mildly depressed	Moderately dilated
Severely elevated (≥ 2 systemic)	Septum flat or bowing into left ventricle, Eccentricity index > 1.4	R to L	≥Moderately depressed	Severely dilated

The presence of pulmonary hypertension was defined by tricuspid regurgitation jet velocity > 3.0 m/s or an estimated right ventricular systolic pressure / systolic blood pressure ratio ≥ 0.87 . If no tricuspid regurgitation jet velocity was present, a composite score of quantitative and qualitative echocardiographic features was used. Echocardiograms possessing 2 of the 4 criteria were considered to be at least mild right ventricular pressure category, and moderate or severe indices were considered consistent with pulmonary hypertension. RV = right ventricle; RA = right atrium; L = left; R = right. ⁴ Across a PFO/ASD or PDA; ⁹ Measures of RV function include: subjective estimates, RV fractional area change, tricuspid annular plane systolic excursion; ⁸ RV/RA size based on subjective appearance; ⁴ LV eccentricity index (LVEI) = LV antero-posterior diameter / LV septo-lateral diameter.

Characteristic	None (N=31)	Moderate (N=7)	Severe (N=8)
Gestational Age	24.0 (22.0, 28.0)	25.0 (23.0, 26.0)	25.0 (23.0, 27.0)
Birth weight--grams	670.0 (420.0, 910.0)	720.0 (477.0, 915.0)	570.0 (440.0, 882.0)
Female	16/31 (51.6%)	4/7 (57.1%)	6/8 (75.0%)
Race			
Asian	1/31 (3.2%)	0/7 (0.0%)	0/8 (0.0%)
Black/African American	16/31 (51.6%)	4/7 (57.1%)	5/8 (62.5%)
Other	2/31 (6.5%)	2/7 (28.6%)	0/8 (0.0%)
White/Caucasian	12/31 (38.7%)	1/7 (14.3%)	3/8 (37.5%)
Hispanic/Latino	1/31 (3.2%)	1/7 (14.3%)	0/8 (0.0%)
Outborn	8/31 (25.8%)	1/7 (14.3%)	2/8 (25.0%)
Caesarian Section	17/31 (54.8%)	4/7 (57.1%)	7/8 (87.5%)
5 Minute APGAR	6.0 (1.0, 9.0)	5.0 (3.0, 7.0)	5.5 (3.0, 9.0)
Antenatal Steroids	24/31 (77.4%)	5/7 (71.4%)	7/8 (87.5%)
Surfactant Therapy	30/31 (96.8%)	6/7 (85.7%)	8/8 (100.0%)
Length of stay--days	173.0 (90.0, 374.0)	138.0 (15.0, 247.0)	188.5 (120.0, 470.0)
Site			
UNC	19/31 (61.3%)	5/7 (71.4%)	3/8 (37.5%)
Duke	12/31 (38.7%)	2/7 (28.6%)	5/8 (62.5%)

Values presented are counts (%) for categorical variables



P1-031

Abnormalities of Atrial Mechanics in Fontan Patients

Robert Loar, Ricardo Pignatelli, Christopher Broda, Asela Nieuwsma, John Colquitt. Texas Children's Hospital/Baylor College of Medicine, Houston, TX

Background: Diastolic function is impaired in the Fontan circulation, but is not well assessed by conventional echocardiography. Speckle-tracking derived atrial strain (ϵ) offer insights into atrial function, which may be a surrogate for diastolic ventricular performance. We hypothesize that 1) ϵ in Fontan patients is impaired compared to healthy controls, and 2) ϵ is worse in RV vs. LV phenotypes. **Methods:** This was a cross-sectional case-control study of 42 Fontan patients and 40 healthy controls. Offline analysis of ϵ was done using GE EchoPAC with P-wave onset as the reference. A traced segment over an intra-atrial connection was excluded from analysis. ϵ was measured at the peaks of atrial active strain (ϵ_{ac} , atrial contraction) and conduit function (ϵ_{con} , early diastolic emptying); reservoir ϵ (ϵ_{res} , atrial filling) was calculated as the summation of ϵ_{ac} and ϵ_{con} . Atrial strain rates (Sr) were obtained for the same forces. Time to peaks were corrected for heart rate. Continuous variables were reported as the median (quartiles) and compared by Wilcoxon rank sum test. A sub-analysis of RV and LV phenotypes was performed in the same manner. **Results:** Compared to controls, Fontan patients had significantly worse ϵ_{con} and ϵ_{res} , less reliance on conduit function ($\% \epsilon_{con}$) for atrial emptying, and a delay in peak atrial filling. There was no difference in ϵ_{ac} or atrial electromechanical coupling (time to ϵ_{ac}). All Sr values except Sr_{ac} were worse (Table 1). Sub-analysis of RV ($n = 24$) vs. LV ($n = 18$) demonstrated no differences in age, gender, heart rate, time from Fontan, surgical type, or GLS. RV phenotype had worse ϵ_{con} and total Sr , and a delay in peak atrial filling. ϵ_{res} and $\% \epsilon_{con}$ trended towards significance (Table 2). **Conclusions:** Atrial mechanics are impaired in Fontan patients compared to normal controls. Among Fontan patients, indices of atrial filling and early atrial emptying are worse in RV phenotypes. Further study of clinical correlations and the prognostic value of atrial strain in this population is warranted.

Poster Session 1 (P1)

Sunday, June 23, 2019

Variable	Normal N = 40	Fontan N = 42	p-value
Age (years)	13.2 (8.9, 15.5)	14.0 (10.0, 16.5)	0.4
Male sex (%)	63	68	0.6
Heart rate	67 (67, 76)	74 (67, 87)	0.06
εac (%)	-9.9 (-12.7, -8.0)	-9.5 (-13.2, -6.7)	0.7
Time to εac (msec)	178 (159, 196)	184 (155, 167)	0.2
εcon (%)	28.1 (24.7, 32.6)	13.7 (7.8, 16.9)	<0.001
Atrial fill time (msec)	399 (378, 432)	450 (401, 493)	0.002
εres (%)	37.5 (34.2, 45.4)	23.0 (18.3, 27.7)	<0.001
Fraction passive (%)	74 (69, 79)	60 (41, 69)	<0.001
Sr-ac	-1.5 (-2.0, -1.2)	-1.4 (-2.0, -1.0)	0.5
Sr-ac time (msec)	120 (105, 141)	123 (99, 148)	0.9
Sr-res	1.6 (1.4, 1.9)	1.2 (0.9, 1.5)	<0.001
Sr-res time (msec)	296 (263, 352)	286 (244, 326)	0.2
Sr-con	-3.1 (-3.8, -2.5)	-1.4 (-1.9, -1.1)	<0.001
Sr-con time (msec)	683 (659, 730)	736 (687, 788)	0.001
Sr-total	-2.9 (-3.7, -2.3)	-1.5 (-2.2, -1.1)	<0.001

Table 1: Comparison of Fontan patients to healthy controls.

Variable	RV N = 24	LV N = 18	p-value
Age (years)	12.8 (10.5, 16.4)	14.6 (8.0, 18.3)	0.8
Male sex (%)	79	53	0.08
Heart rate	77 (66, 87)	72 (67, 80)	0.3
Time from Fontan (years)	8.5 (6.0, 11.9)	9.5 (3.9, 14.1)	0.9
Extra-cardiac non-fenestrated (%)	87%	89%	0.9
GLS (%)	-15.7 (-19.3, -13.1)	-17.0 (-19.8, -14.7)	0.5
εac (%)	-10.0 (-13.7, -6.2)	-9.4 (-12.5, -6.8)	0.7
Time to εac (msec)	186 (166, 209)	179 (166, 212)	0.9
εcon (%)	9.8 (5.7, 15.5)	15.6 (11.2, 8.2)	0.03
Atrial fill time (msec)	456 (420, 509)	421 (354, 465)	0.04
εres (%)	21.5 (17.0, 26.8)	23.4 (20.4, 30.9)	0.17
Fraction passive (%)	54 (31, 69)	64 (54, 70)	0.16
Sr-ac	-1.3 (-2.0, -1.0)	-1.6 (-2.2, -1.2)	0.4
Sr-ac time (msec)	124 (94, 149)	122 (101, 148)	0.9
Sr-res	1.3 (0.9, 1.4)	1.2 (0.9, 1.7)	0.6
Sr-res time (msec)	294 (246, 331)	276 (241, 309)	0.4
Sr-con	-1.3 (-1.9, -1.0)	-1.6 (-2.0, -1.3)	0.2
Sr-con time (msec)	750 (718, 828)	712 (662, 759)	0.02
Sr-total	-1.3 (-1.7, -0.9)	-1.9 (-2.3, -1.3)	0.04

Table 2: Comparison of RV and LV Fontan phenotypes

P1-032

Integrated Sedation Strategy for Obtaining Echocardiograms in Young Pediatric Patients in a High Complexity Echocardiography Lab

Jean Lipinski¹, Kristina Lindsey¹, Leah Bryan², Ritu Sachdeva^{1,2}, Eric Ferguson^{1,2}, Erik Michelfelder^{1,2}, Cyrus Samai^{1,2}, Timothy Slesnick^{1,2}, Timotheus Watson^{1,2}, William Border^{1,2}. ¹Children's Healthcare of Atlanta, Atlanta, GA; ²Emory University School of Medicine, Atlanta, GA

Background: Lack of patient cooperation decreases the diagnostic quality of echocardiograms (echo) in young pediatric patients. Many centers utilize deep sedation and even general anesthesia to perform studies in these patients. However, this is not without risk and results in increased cost and resource utilization. At our center, we developed a strategy where patients aged 1 month to 4 years are scheduled for a sedated echo, but non-sedated strategies are attempted prior to giving sedation. Scanning is performed only by experienced sonographers. The purpose of this study is to examine the effectiveness of our approach that extensively integrates non-sedated techniques, in producing diagnostic quality studies and describe our distractive techniques. **Methods:** Study included patients referred for a sedated echo between January 1, 2017 and December 31, 2018. Medical records were reviewed to obtain age, diagnosis, procedure notes, type of sedation (intranasal or oral midazolam), distraction method (tablet, phone, lighted toy, projected light, music or singing, pacifier or feeding), and scan time. A subset of studies were rated by sonographer and physician as successful or not, based on institutional criteria for image quality (appropriate orientation and technical factors), completeness (all areas seen or attempted), and physician interpretability. **Results:** Study population was 583 patients aged 2 to 48 months with a median age of 12 months. Of these, 136 (23.3%) patients received sedation. Distraction alone was used in 410 (70.3%) patients, both sedation and distraction were used in 130 (22.3%), and 37 (6.3%) patients received no

sedation or distraction. Preoperative patients (n=322) were sedated with similar frequency (22.4%) as non-preoperative (24.5%). The average scan time (minutes) for a complete echo was similar for both sedated (35.3) and non-sedated (34.2) patients. Distraction methods varied by age, with 2-23 month-olds responding to toys, projected light, music, pacifier, and feeding, and 24-48 month-olds responding to toys, tablet or cell phone. In a subset of 90 studies rated for successful imaging, sonographers rated 85 (94.4%) successful, and physicians 89 (98.9%), with 19/90 (21.1%) patients sedated. **Conclusions:** The majority of patients ages 2-48 months referred for echocardiography did not require sedation to complete the study. Use of age-appropriate distraction negated the need for medical sedation in 70.3% of patients yet resulted in diagnostic quality studies. These data support an integrated strategy for sedation of pediatric patients undergoing echocardiography.

P1-033

Severity of Aortic Valve Disease Does Not Impact Echo-Derived Left Ventricular Systolic Deformation Indices Through Young Adulthood: Real Time Analysis During Routine Clinical Studies

Joseph Block¹, Sarah E. Blonsky¹, Matthew W. Buelow¹, Nicholas E. Ebert¹, Evelyn M. Kuhn², Peter C. Frommelt¹. ¹Medical College of Wisconsin, Milwaukee, WI; ²Children's Hospital of Wisconsin, Milwaukee, WI

Background: Standard echocardiographic protocols rely on left ventricular (LV) ejection fraction (EF) and shortening fraction (SF) to assess ventricular function. Commonly, these parameters are preserved even with severe aortic valve disease in children. We assessed LV deformation during routine clinically-indicated echocardiograms using 2D speckle tracking in patients with isolated congenital aortic stenosis (AS) and/or aortic regurgitation (AR). **Methods:** A deformation protocol was performed real-time at the ultrasound machine for studies ordered as part of routine clinical care for patients with AS and/or AR in addition to standard 2D/Doppler imaging. Measures included 2D LV regional and global circumferential strain and strain rate from a short axis view and longitudinal strain and strain rate from an apical view, standard deviation of time to peak systolic circumferential and longitudinal strain, and maximum systolic wall delay to peak strain. Patients were categorized into 4 groups based on severity of aortic valve disease (table), with mild AS defined as a mean gradient <25 mmHg and AR graded by qualitative assessment. Kruskal-Wallis tests were used for overall comparisons and Mann-Whitney tests for 2 group comparisons; a p value of <0.01 was considered significant to adjust for multiple tests. **Results:** 250 patients (mean age = 12.4 years, range 1 month to 28 years) completed the protocol between 12/2014-5/2018. There were no significant differences in any of the circumferential or longitudinal deformation indices between groups based on AS or AR severity. In fact, values were remarkably similar and normal for all groups, even those with moderate-severe AS and/or AR (table). LV EF and SF were also comparable and normal between groups; only indexed LV volumes were different, with larger ventricles in the groups that were defined by moderate-severe AR. **Conclusion:** Both traditional echocardiographic assessments and real-time acquired 2D deformation indices suggest preserved LV systolic function in children and young adults with congenital aortic valve disease, regardless of severity. Although encouraging, these findings imply that these real-time echo-derived indices may lack the fidelity to accurately reflect LV myocardial health in the setting of significant chronic physiologic burdens.

	Mild AS and/or AR	Moderate-severe AS and/or AR	Moderate-severe AS and/or AR	Moderate-severe AS and/or AR	p-value
	N	Mean	SD	95% CI	
Age at Echo	78	10.9	7.2	4.0 - 16.0	0.3
Weight (kg)	78	44.6	27.0	19.7 - 69.5	0.3
BSA (m ²)	78	1.5	0.6	0.8 - 1.7	0.3
LV Global Peak Systolic Circ Strain (%)	78	-28.8	4.3	-31.0 - -26.6	0.0
SD of Time to Peak LV Circ Strain (ms)	78	46.8	32.9	25.9 - 69.7	0.3
Max Wall Delay to Peak LV Circ Strain (ms)	78	121.6	87.2	65.8 - 198.5	0.3
LV Global Peak Circ Strain Rate (1/s)	78	-1.6	0.4	-1.9 - -1.0	0.3
LV Global Peak Systolic Long Strain (%)	78	-19.9	3.5	-17.5 - -22.1	0.3
SD of Time to Peak LV Long Strain (ms)	78	48.1	27.6	28.8 - 67.3	0.3
Max Wall Delay to Peak LV Long Strain (ms)	78	92.8	68.6	50.8 - 130.0	0.3
LV Global Peak Long Strain Rate (1/s)	78	-1.3	0.3	-1.0 - -1.5	0.3
LV Shortening Fraction	78	35.1	3.8	32.0 - 37.8	0.3
LV Ejection Fraction	77	65.2	2.9	62.6 - 68.1	0.3
Indexed LV End Diastolic Volume (ml/BSA ^{1.75})	78	38.4	14.7	27.0 - 50.8	0.3
Indexed LV End Systolic Volume (ml/BSA ^{1.75})	78	20.0	5.6	15.9 - 24.6	0.3

AS:aortic regurgitation; AR:aortic stenosis; BSA:body surface area; circ:circumferential; long:longitudinal; LV:left ventricle; ms:milliseconds; SD:standard deviation. *p<0.05 comparing those groups with mild AS to those with moderate-severe AR

P1-034

Tricuspid Valve Prolapse in Children with Hypoplastic Left Heart Syndrome Patients Requiring Tricuspid Valve Repair is Due to Leaflet Mal-Adaptation, Not Sub-Valve Changes - A Quantitative Three-Dimensional Echocardiography Study

Sachie Shigemitsu¹, Kandice Mah¹, Richard B. Thompson², Justin Grenier², Lily Lin¹, Amal Siltmi¹, Mirza Beigh¹, Neeraj K. Khoo¹, Timothy Colen¹.

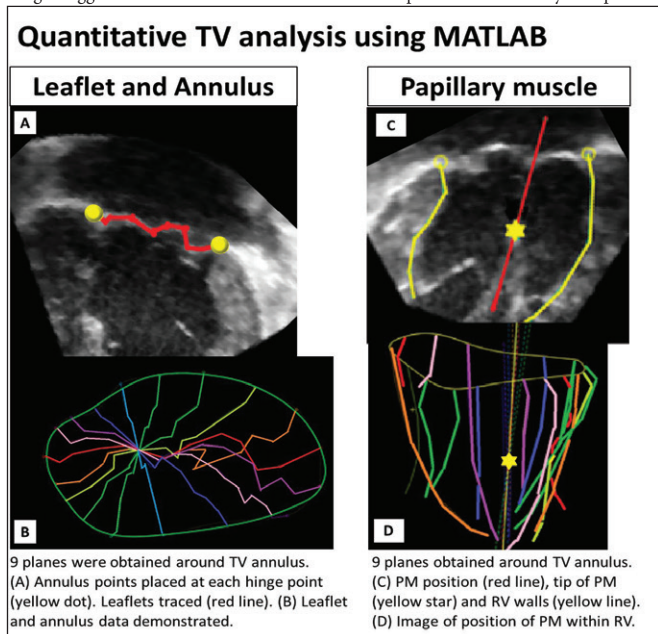
¹Division of Pediatric Cardiology, Department of Pediatrics, Stollery Children's Hospital, University of Alberta, Edmonton, AB, Canada; ²Department of Biomedical Engineering, University of Alberta, Edmonton, AB, Canada

Background: Tricuspid valve regurgitation (TR) is associated with morbidity and mortality in hypoplastic left heart syndrome (HLHS). Over 25% of HLHS patients require tricuspid valve (TV) repair within 10 years, while the mechanism of TR remains poorly understood. This study explores TV remodeling in HLHS requiring surgical repair, using

Poster Session 1 (P1)

Sunday, June 23, 2019

novel quantitative three-dimensional echocardiography (3DE) to further understand the mechanisms of TV failure in HLHS. **Methods:** This case-control study with prospectively acquired 3DE in 72 children with HLHS, 36 children prior to TV repair (group 1) and 36 age- and stage-matched controls with no TV repair and mild or less TR (group 2). All 3DE were analyzed using a specific custom TV software (MATLAB) to quantitate TV annulus and leaflet area (Figure), prolapse and tethering volumes, and bending angle. TV leaflets were segmented into the anterior (AL), septal (SL) and posterior (PL) to measure regional areas and volumes. We also measured position of papillary muscle (PM) and chord length. Variables were indexed by body surface area (BSA), and comparison was performed using t-test with significance at $p < 0.05$. **Results:** Group 1 had larger total annulus (10.3 vs 8.4 cm^2/m^2 , $P < 0.001$) and leaflet (11.7 vs 9.3 cm^2/m^2 , $P = 0.002$) area. SL area (2.66 vs 2.00 cm^2/m^2 , $p = 0.009$) was larger and AL trended to being larger (5.2 vs 4.2 cm^2/m^2 , $P = 0.05$). Group 1 had larger total prolapse volume and for each leaflets (Total leaflet 140 vs 5.8 $\mu\text{l}/\text{m}^2$, $p = 0.002$; AL: 39.4 vs 2.2 $\mu\text{l}/\text{m}^2$, $p = 0.004$; SL: 2.2 vs 0.16 $\mu\text{l}/\text{m}^2$, $p = 0.017$; PL: 2.7 vs 0.12 $\mu\text{l}/\text{m}^2$, $p = 0.032$). No difference in tethering volume for total or each leaflet. Group 1 had greater bending angle (156.6 vs 151.8 degree, $p = 0.034$), hence a flatter annulus. No difference in PM angle and length, nor chord length between the groups. **Conclusion:** Failing TV in children with HLHS had larger annulus and leaflet size, specifically in SL and AL, and greater prolapse of all the leaflets compared to HLHS with competent TV. Despite increased leaflet prolapse, there is no difference in chord or PM length, suggesting that failing TV prolapse is due to leaflet mal-adaptation, rather than chord or PM changes. This novel insight suggests future research into TV leaflet mal/adaptation in HLHS maybe important.



P1-035

Two-Dimensional Speckle Tracking Echocardiographically-Derived Left Ventricular Strain and Strain Rate in Healthy Children: Normal Values with Philips Qlab v10.8

Jamie K. Harrington, Alessandra M. Ferraro, Steve D. Colan, Lynn A. Sleeper, Andrew J. Powell, Adi Adar, Philip T. Levy, David M. Harrild. Boston Children's Hospital, Boston, MA

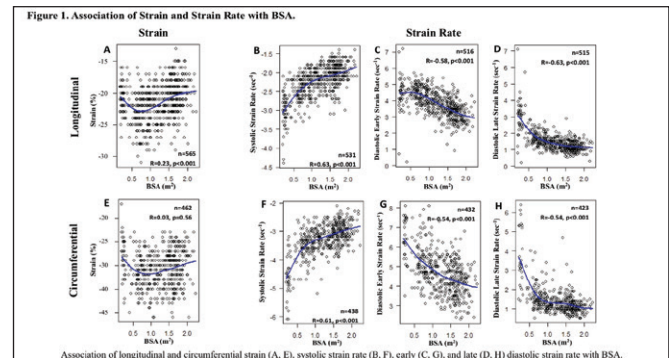
Background: Two-dimensional speckle tracking echocardiographically (2DSTE)-derived deformation parameters are associated with clinical outcomes in children with heart disease. Routine use has been hindered by a lack of normative values and inter-vendor variability. The recent Philips STE platform, QLAB v10.8, incorporates recommendations from the STE Task Force, endorsed by the American Society of Echocardiography, with the goal of reducing inter-vendor variability. Our aim was to determine normal values for left ventricular strain and strain rate in a large cohort of healthy children based on this platform. **Methods:** A database search identified subjects who: 1) were < 21 years of age with structurally and functionally normal hearts, 2) had no conditions with cardiovascular impact, and 3) had transthoracic echocardiographic images suitable for STE analysis. Images were retrospectively analyzed using Philips QLAB v10.8 using apical 4-chamber and mid-ventricular short-axis views. Measurements were: longitudinal and circumferential components of strain (LS, CS), systolic strain rate (LSRs, CSRs), and both early (LSRe, CSRe) and late (LSRa, CSRa) diastolic strain rate. The associations with age and BSA were assessed using Spearman correlation and generalized additive modeling. **Results:** 606 subjects met inclusion criteria (mean age 10.1 ± 5.8 years, range, 0.0 to 19.8 years, 45% female). Strain and strain rate values are shown in Table 1 by age and in Figure 1 by

BSA. All parameters differ by age group and have nonlinear relationships with BSA. The magnitude of all values decreases with increasing age and BSA, except for CS. **Conclusion:** Strain and strain rate parameters are presented from a large cohort of healthy children using 2DSTE from the Philips QLAB v10.8 platform. Strain and strain rate values differ significantly for all age groups. Maturation changes are more pronounced for strain rate compared to strain.

Table 1. Strain and Strain Rate by Age

	<1yr (n=69)	1-5y (n=80)	>5-10y (n=130)	>10-14y (n=130)	>14-18y (n=168)	>18-21y (n=29)	p-values
Longitudinal							
LS (%)	-21 ± 2	-23 ± 3	-23 ± 3	-21 ± 3	-20 ± 3	-20 ± 2	<0.001
LSRs (1/sec)	-2.96 ± 0.49	-2.48 ± 0.32	-2.27 ± 0.29	-2.09 ± 0.34	-2.02 ± 0.31	-2.03 ± 0.28	<0.001
LSRe (1/sec)	4.38 ± 1.18	4.52 ± 0.53	4.16 ± 0.61	3.65 ± 0.72	3.27 ± 0.60	3.25 ± 0.54	<0.001
LSRa (1/sec)	2.98 ± 1.15	1.80 ± 0.39	1.51 ± 0.38	1.27 ± 0.33	1.19 ± 0.32	1.26 ± 0.39	<0.001
Circumferential							
CS (%)	-29 ± 4	-32 ± 4	-32 ± 3	-31 ± 4	-30 ± 4	-29 ± 4	<0.001
CSRs (1/sec)	-4.60 ± 0.75	-3.51 ± 0.47	-3.38 ± 0.38	-3.17 ± 0.48	-3.00 ± 0.37	-2.98 ± 0.33	<0.001
CSRe (1/sec)	6.39 ± 1.12	5.12 ± 0.88	5.01 ± 0.98	4.41 ± 0.95	4.22 ± 0.87	4.02 ± 0.85	<0.001
CSRa (1/sec)	3.58 ± 1.48	1.66 ± 0.61	1.37 ± 0.56	1.32 ± 0.53	1.13 ± 0.41	1.21 ± 0.37	<0.001

LS, longitudinal strain; LSRs, longitudinal systolic strain rate; LSRe, longitudinal early diastolic strain rate; LSRa, longitudinal late diastolic strain rate;
CS, circumferential strain; CSRs, circumferential systolic strain rate; CSRe, circumferential early diastolic strain rate; CSRa, circumferential late diastolic strain rate.



P1-036

Comparison of 2D Speckle Tracking Strain on Echocardiography with Late Gadolinium Enhancement on Cardiac MRI in Children with Myocarditis

Aaron Walsh¹, Jaimin M. Patel², Jason Johnson¹, Ronak Naik¹. ¹University of Tennessee Health Science Center, Memphis, TN; ²University of Mississippi Medical Center, Jackson, MS

Background: Late gadolinium enhancement (LGE) on cardiac MRI (CMR) is being considered a gold standard for the diagnosis of myocarditis. In acute settings, echocardiography provides important insight in overall cardiac function. Role of 2D speckle tracking echocardiographic (2D-STE) longitudinal strain (LS) is unclear in this setting. We chose to evaluate association between LGE positivity in myocarditis with abnormal 2D-STE. **Methods:** Data from 2013-2018 on LGE was collected retrospectively from CMR reports. Echocardiograms performed within one week of CMR were prospectively evaluated to obtain 2D-STE longitudinal strain of left ventricle using 2D Cardiac Performance Analysis module of Tomtec-Arena (Chicago, IL). A univariate analysis was performed comparing Group 1: Positive LGE with Group 2: Negative LGE. A multivariable logistic regression model was then developed to identify variables significantly associated with positive LGE. Sensitivity (Sn) and specificity (Sp) analysis were performed using different cut offs of global longitudinal peak strain (GLPS) values to derive clinical application. A separate logistic regression analysis was performed comparing LGE and abnormal 2D-STE for all myocardial segments. **Results:** Out of 45 patients, 25 were LGE positive and 20 LGE negative. Median age was 16 [14.25-17] vs 12 [10.5-13.5] ($p < 0.001$) respectively. M:F ratio was 3:1 in group 1 compared to 2:1 in group 2. Majority were African-American in both groups (60% vs 80%). GLPS was significantly different in both the groups (-8.98% vs -13.90%, $p < 0.0001$) which remained significant in multivariate logistic regression (OR 1.5 (CI:1.04 - 2.16), $p = 0.02$). Receiver Operating Curve showed GLPS cut off of -10.69% with Sp 81% and Sn 66%. Although highest troponin level was independently associated with Positive LGE (7.11 [1.71-21.43] vs 0.227 [0.10-10.7], $p = 0.006$), the effect did not reach statistical significance in multivariate model (OR 1.17 (CI: 0.99-1.26)) although trend towards positive was observed. Out of 880 myocardial segments, 721 had abnormal longitudinal strain vs 155 LGE positive generating high Sn of 92% but poor Sp of 20%. Abnormal individual segment strain had a significant association with LGE positivity ($p < 0.001$). **Conclusion:** 2D-STE provides a valuable tool to assess myocardial function in acute myocarditis. Lower GLPS values are associated with LGE positivity. We propose the cut off of -11% which has good specificity and reasonable sensitivity to predict LGE positivity. The highest Troponin level is independently associated with LGE positivity.

Poster Session 1 (P1)

Sunday, June 23, 2019

P1-037

Three Dimensional Right Ventricular Global and Regional Strain Predict Outcomes in Pediatric Pulmonary Hypertension

Pei-Ni Jone¹, Nicolas Duchateau², Zhaoxing Pan³, D. Dunbar Ivy¹, Pamela Mocerit⁴. ¹Pediatric Cardiology, Children's Hospital Colorado, University of Colorado School of Medicine, Aurora, CO; ²Creatis, Universite Lyon 1, Lyon, France; ³Biostatistics and Informatics, Colorado School of Public Health, University of Colorado, Denver, CO; ⁴Universite Cote d'Azur, Inria Epione Team, Department of Cardiology, Hôpital Pasteur, CHU de Nice, Nice, France

Background: Right ventricular (RV) function has a key contribution to pediatric pulmonary arterial hypertension (PAH) evaluation. RV deformation progressively worsens and affects survival in adult PAH. RV deformation needs to be assessed using three-dimensional echocardiography (3DE) to evaluate for regional and global values in pediatric PAH. In this study, comparison of 3DE RV myocardial deformation between normal controls, associated PAH with congenital heart disease (APAH-CHD), and idiopathic pulmonary arterial hypertension (IPAH) were assessed and outcomes were evaluated. **Methods:** Fifty controls, 49 APAH-CHD patients, and 45 IPAH patients were evaluated. 3DE RV sequences were analyzed by semi-automated software (TomTec 4D RV function 2.0) and were post-processed to extract global and regional deformation [circumferential, longitudinal, and area strain]. RV is divided in the 4 regions of the septum and free wall (RV inlet, RV outlet, body, and apex). Statistical analyses included the comparison of subgroups based on global and regional deformation, and Cox proportional hazards analysis to evaluate their predictive ability. **Results:** Controls and the two groups of PAH patients had significantly different global and regional deformation ($p < 0.001$). APAH-CHD and IPAH significantly differed in area strain (inlet septum, $p = 0.043$), global circumferential strain ($p < 0.035$), and circumferential strain at the inlet septum $p < 0.023$, apex free wall $p < 0.007$, and inlet free wall $p < 0.030$. Circumferential strain at the RV inflow free wall and circumferential, longitudinal, and area strain at the apex free wall were strong predictors of adverse clinical events (Table 1). **Conclusion:** RV regional and global strain is different in normal controls compared to PAH patients. RV deformation provides novel insights into changes in RV function in pediatric PAH, with regional values emerging as outcome predictors in pediatric PAH.

RV regional and global strain parameters predictors	Hazard Ratio	Lower 95% Wald Confidence Limit	Upper 95% Wald Confidence Limit	Pr > ChiSq
Area Strain (%)				
RV outlet septum	0.983	0.932	1.038	0.5460
RV inlet septum	1.027	0.978	1.078	0.2828
Body septum	1.038	0.997	1.081	0.2715
Apex septum	1.034	0.988	1.083	0.1466
Apex free wall	1.050	1.008	1.095	0.0206
Body free wall	1.031	0.996	1.066	0.0830
RV inlet free wall	1.034	0.992	1.077	0.1129
RV outlet free wall	1.016	0.933	1.107	0.7084
Global	1.044	0.996	1.094	0.0748
Whole Septum	1.043	0.987	1.101	0.1370
Circumferential Strain (%)				
RV outlet septum	0.984	0.929	1.043	0.5932
RV inlet septum	1.035	0.967	1.109	0.3180
Body septum	1.056	0.976	1.144	0.1768
Apex septum	1.059	0.968	1.158	0.2117
Apex free wall	1.100	1.022	1.184	0.0111
Body free wall	1.053	0.996	1.113	0.0686
RV inlet free wall	1.077	1.006	1.158	0.0380
RV outlet free wall	1.075	0.963	1.201	0.1961
Global	1.083	1.000	1.173	0.0508
Whole Septum	1.050	0.958	1.152	0.0256
Longitudinal Strain (%)				
RV outlet septum	1.001	0.918	1.091	0.9858
RV inlet septum	1.034	0.969	1.104	0.3120
Body septum	1.052	0.997	1.111	0.0682
Apex septum	1.054	0.988	1.125	0.1114
Apex free wall	1.081	1.005	1.162	0.0351
Body free wall	1.048	0.982	1.118	0.1565
RV inlet free wall	1.035	0.966	1.109	0.3324
RV outlet free wall	1.006	0.860	1.178	0.9377
Global	1.086	0.994	1.186	0.0680
Whole Septum	1.086	0.998	1.181	0.0546

P1-038

Left Ventricular Strain Normalizes After Balloon Aortic Valvuloplasty in Infants with Congenital Aortic Stenosis

Ashish A. Ankola, Matthew A. Crystal, Mariel E. Turner, Michael P. DiLorenzo, Alejandro J. Torres, Ameer Shah. Morgan Stanley Children's Hospital of New York, Columbia University Medical Center, New York, NY

Background: Severe aortic stenosis (AS) causes significant left ventricular (LV) afterload, LV hypertrophy, and subendocardial ischemia. Despite these alterations, most patients have normal LV ejection fraction. The degree of systolic dysfunction can be assessed using two dimensional speckle tracking echocardiography (2DSTE). We aimed to define changes in LV strain after balloon aortic valvuloplasty (BAV) for infants with AS. **Methods:** Infants < 1 year of age with AS who underwent BAV from 2007-2017 were included. Echocardiograms before/after BAV were retrospectively analyzed with 2DSTE. Paired t-tests and Wilcoxon signed rank tests were used to assess changes in 2DSTE, LV dimensions/function, hemodynamics, and combined outcome of death/repeat intervention post-BAV. **Results:** Twenty-seven patients underwent 29 BAV procedures. Median age at BAV was 29 days (interquartile range 3-52), 70% were male, and 63% had a bicuspid aortic valve. The valve gradient pre-BAV was 47 ± 14 mmHg with an ejection fraction of $64 \pm 10\%$. BAV significantly decreased peak-to-peak gradient across the valve (66 ± 20

to 24 ± 13 mmHg, $p < 0.001$) with no significant difference in aortic insufficiency. Global longitudinal strain (GLS) and longitudinal strain rate significantly improved post-BAV (-17 ± 5 vs. -20 ± 4 , $p = 0.001$; -1.1 ± 0.4 vs. -1.3 ± 0.4 , $p = 0.005$, respectively) with no difference in global circumferential strain. Peak longitudinal strain in the inferoseptal and anterolateral segments was abnormal at the base (-15 ± 6 and -17 ± 5 , respectively) and mid-ventricle (-17 ± 7 and -17 ± 6 , respectively), but normal at the apex (-22 ± 6 and -24 ± 7 , respectively). Peak longitudinal strain in the basal and mid anterolateral segments normalized post-BAV (-17 ± 5 vs. -21 ± 5 , $p < 0.01$; -17 ± 6 vs. -20 ± 5 , $p = 0.01$, respectively). Twenty-six patients had complete follow up. Six (23%) patients had repeat interventions and one (4%) died. These patients had significantly lower pre-BAV GLS compared to the rest (-13 ± 4 vs. -19 ± 4 , $p = 0.004$), but no significant difference in peak-to-peak aortic valve gradient or ejection fraction. **Conclusion:** Longitudinal strain is abnormal in infants with AS and improves to normal levels after BAV. Worse pre-BAV GLS may help identify patients with an increased likelihood of repeat intervention post-procedure.

Left Ventricular Strain and Ejection Fraction Pre and Post Balloon Aortic Valvuloplasty			
	Pre-valvuloplasty	Post-valvuloplasty	P-value
Global Longitudinal Strain	-17.4 (±4.8)	-20.2 (±3.9)	0.001
Longitudinal Strain Rate	-1.1 (±0.4)	-1.3 (±0.4)	0.005
Longitudinal Time to Peak Strain	224 (±31)	209 (±28)	0.01
Global Circumferential Strain	-30.8 (±10)	-31.3 (±8)	0.91
Circumferential Strain Rate	-2.1 (±0.9)	-2.1 (±0.8)	0.48
Circumferential Time to Peak Strain	216 (±32)	211 (±24)	0.75
Ejection Fraction	64.1 (55.2 - 67.9)	67 (59 - 72)	0.04

P1-039

The Fetal Borderline Left Ventricle and Likelihood of a Successful Biventricular Circulation

Kim Haberer¹, Lisa K. Hornberger¹, Angela McBrien¹, Aisling Young², Deborah Fruitman³, Lindsay Mills³, Luke Eckersley¹. ¹University of Alberta, Edmonton, AB, Canada; ²University of British Columbia, Victoria, BC, Canada; ³University of Calgary, Calgary, AB, Canada

Background: Chronic maternal hyperoxia has been proposed to encourage left heart growth in fetuses with borderline left ventricles. However, little evidence exists regarding predictors of successful biventricular (BV) repair or longer term outcomes in these patients. As such we do not yet understand the population that might benefit from hyperoxia therapy. In this study we aimed to establish fetal echocardiographic predictors of a successful BV circulation. **Methods:** We queried the institutional database at the University of Alberta for fetal echocardiograms performed between 2004-2017 with a diagnosis of: hypoplastic left ventricle (LV), coarctation of the aorta, right ventricular (RV)/LV discrepancy and mitral valve (MV) or aortic valve (AV) hypoplasia/stenosis. Inclusion criteria were: 1) patency of mitral and aortic valves 2) LV end diastolic dimension (LVEDD) z score of < -2 and/or a MV or AV annulus z-score of < -2. Exclusion criteria included patients with critical aortic stenosis, conotruncal abnormalities, or atrioventricular septal defects. Studies at 18-26 weeks and 27-37 weeks were analyzed. Postnatally, the type of repair was recorded. Unsuccessful BV repair was defined as univentricular (UV) repair, death, or transplant. **Results:** Of 53 included cases, 37 underwent successful BV repair and 7 did not require surgery (Group 1, n=44). 5 patients underwent UV palliation and 4 died after BV repair (Group 2, n=9). At both early and late fetal echo, a larger MV annulus z-score and right to left shunting at the atrial septum were significantly associated with a successful BV circulation (table 1). At 27-37 weeks' gestation, differences in the LV length z-score and the qualitative adequacy of the LV between the two groups were also significant. Late follow-up was available for 41 patients (mean duration 6 years). There were 2 deaths in those that underwent UV repair. 12 patients with a BV circulation developed at least mild mitral stenosis and 5 patients developed isolated subaortic stenosis. **Conclusions:** A successful BV circulation is common in fetuses with borderline LV. The size of the MV annulus, the direction of flow at the atrial septum, and LV length z score may be important predictors of a successful BV circulation. Long term sequelae in those with BV circulation may include mitral and subaortic stenosis.

Poster Session 1 (P1)

Sunday, June 23, 2019

Table 1: Echocardiographic Measurements at 18-26 and 27-37 weeks' Gestational Age (GA)

GA	Measurement	BV circulation	UV circulation / death	p-value
18 - 26 weeks	Qualitatively adequate LV	21/22 (95%)	1/2 (50%)	0.16
	ASD flow (Right to left / bidirectional)	21/21 (100%)	1/3 (33%)	0.011*
	Antegrade / bidirectional flow in aortic arch	20/21 (95%)	3/3 (100%)	1
	MV z-score (median, range)	-3.0±0.9	-4.6±2.4	0.027*
	AV z-score	-1.5	-1.6	0.89
	LVL z-score (mean, SD)	-1.52±0.24	-1.71±0.76	0.67
27-37 weeks	Qualitatively adequate LV	38/43 (90%)	4/9 (44%)	0.005*
	ASD flow (Right to left / bidirectional)	39/42 (86%)	5/9 (55%)	0.013*
	Antegrade / bidirectional flow in aortic arch	35/40 (88%)	6/9 (67%)	0.15
	MV z-score (median, range)	-3.5±1.4	-1.7±1.5	0.021*
	AV z-score	-1.5±1.2	-1.5±1.7	0.89
	LVL z-score (mean, SD)	-1.4±1.1	-2.4±1.1	0.011*
LVEDD z-score		-2.0±1.1	-2.9±1.1	0.2
		-2.4±1.0	-2.7±0.85	0.32

P1-040

Feasibility and Reproducibility of Left and Right Ventricular Longitudinal Strain Rate in Pediatrics

Doaa M. Aly¹, Sandhya R. Ramlogan², Cliff A. Caldwell¹, Jacklyn M. Steumpler¹, Kayla L. Simpson¹, Rita France¹, Ashley Sherman¹, Stephanie Schmidt¹, Suma Goudar¹, Daniel Forsha¹. ¹Children's Mercy Hospital, Kansas, MO; ²Children's Hospital of Pittsburgh, Pittsburgh, PA

Background: Strain rate (SR) is a measure of cardiac strain per unit time that is widely used in adult imaging. Despite its potential benefits in the evaluation of pediatric heart disease, the wide spread adoption of SR has been challenged by the lack of evidence on reproducibility. The goal of this study is to determine the feasibility, and inter/intravendor reproducibility of vendor default layer peak global SR in the LV and RV of pediatric subjects on two commonly utilized strain platforms. **Methods:** Pediatric subjects (n=53, age 0-16 yr) with normal cardiac structure and either normal ventricular function (n=35) or cardiomyopathy (n=18) were prospectively imaged for three apical LV and one apical RV focused view on the GE Vivid E9 scanner. LV and RV longitudinal global SR was analyzed by GE EchoPAC (GE) and at both acquisition frame rate (TTacq) and compressed frame rate (TT30) by Tomtec. Each vendor's default layer SR (GE mid-myocardial; TT endocardial) was analyzed. Current software versions employing post-EACVI/ASE/Industry Task Force recommendations were utilized. Intervendor reproducibility between GE, TTacq, and TT30 were performed by a single reader on all subjects and intravendor (inter and intrareader) reproducibility was tested on the same platform in 22 random subjects by a blinded second reader. Mean bias, SD, and intra-class correlation coefficient (ICC) were reported. **Results:** Feasibility was measured by the percentage of subjects with adequate strain analysis tracking, and for LV SR was 96% by GE and 100% by TT, while for RV SR was 88% by GE and 85% by TT. Intervendor reproducibility was fair- poor in most comparisons for both ventricles, and was significantly lower than intravendor reproducibility (Table). Intervendor SR agreement was highest in the GE-TT30 comparison (good LV; fair RV). Intravendor (inter and intrareader) reproducibility was good-excellent for both ventricles with higher intrareader reproducibility. **Conclusion:** This study demonstrates high LV and RV SR feasibility by GE and TT in pediatrics regardless of function. Even though biventricular intravendor agreement of SR is reasonably robust for GE and TT, poor intervender agreement remains a relative problem. Accordingly, our results suggest that intervender comparisons of SR should generally not be utilized.

Table:

	LVSR				RVSR			
	N	Bias	SD	ICC	N	Bias	SD	ICC
Intervendor								
GE- TTacq	53	-0.3	0.33	0.48	45	-0.61	0.56	0.04
GE- TT30	53	0.09	0.23	0.70	45	-0.18	0.36	0.59
TTacq-TT30	53	-0.4	0.32	0.36	45	-0.43	0.51	0.20
Intrareader								
GE-GE	20	0.01	0.09	0.95	19	0.01	0.14	0.94
TTacq-TTacq	19	0.03	0.07	0.98	18	-0.03	0.11	0.97
TT30-TT30	19	0.00	0.07	0.97	18	0.00	0.13	0.97
Interreader								
GE-GE	20	0.14	0.16	0.80	19	0.06	0.30	0.76
TTacq-TTacq	19	0.17	0.36	0.67	18	0.29	0.46	0.55
TT30-TT30	19	0.12	0.25	0.60	18	0.12	0.27	0.77

P1-041

Late Left-Sided Heart Obstruction is Associated with Impaired Left Ventricular Function in Children with Surgically Repaired Coarctation of the Aorta or Interrupted Aortic Arch

Taiyu Hayashi, Takahiro Shindo, Yasushi Misaki, Hiroshi Ono. National Center for Child Health and Development, Tokyo, Japan

Background: Although surgical repair of coarctation of the aorta (CoA) or interrupted aortic arch (IAA) is physiologically corrective, recurrent obstruction at the aortic arch or left ventricular outflow tract is not uncommon. This study aimed to evaluate the impact of late left-sided heart obstruction on the left ventricular function in children with surgically repaired CoA and IAA. **Methods:** We included 14 children aged 3-15 years with surgically repaired CoA (n=8) or IAA (n=6), who underwent follow-up echocardiography from January to December 2018. Patients who underwent the Yasui operation were excluded. All but 1 patient had an associated ventricular septal defect. Patients were considered to have left-sided heart obstruction if the peak flow velocity across either the aortic valve or the aortic isthmus exceeded 2.5 m/s. As healthy controls, 30 children without known heart diseases were also included in the study. Echocardiographic measurements including left ventricular ejection fraction (LVEF) computed using the biplane disk summation technique, left ventricular global longitudinal strain (LVGLS), and left atrial strain during the reservoir phase (LASr) were compared between the control group and children with and without left-sided heart obstruction by using the Mann-Whitney U-test. A p-value of <0.05 was considered statistically significant. **Results:** Of 14 patients, 6 had left-sided heart obstruction (5 at the aortic valve, 1 at the aortic isthmus), with a median peak flow velocity of 3.2 (2.6-5.1) m/s. There was no significant difference in age, body surface area, heart rate, systolic blood pressure, and LVEF between the groups. No significant difference in LVGLS and LASr was observed between the controls and children without the obstruction. However, children with left-sided heart obstruction showed significantly worse LVGLS and LASr than the controls. **Conclusion:** Despite a preserved LVEF, late left-sided heart obstruction is associated with impaired left ventricular longitudinal systolic function and diastolic function in children with repaired CoA and IAA. Early re-intervention for left-sided heart obstruction might be beneficial.

Comparisons between children with and without left-sided heart obstruction and the control group

	Control (N=30)	Children without left-sided heart obstruction (N=8)	Children with left-sided heart obstruction (N=6)
Boys	14 (47%)	4 (50%)	1 (17%)
Age at the arch repair (days)	Not applicable	12 (3-59)	10 (3-81)
Age at examination (years)	7.2 (3.1-15.7)	6.7 (3.0-14.9)	7.2 (3.2-12.6)
Body surface area (m ²)	0.85 (0.54-1.83)	0.77 (0.59-1.53)	0.95 (0.46-1.55)
Heart rate (beats/min)	86 (60-115)	83 (66-96)	86 (71-148)
Systolic blood pressure (mmHg)	Not applicable	104 (92-112)	104 (75-118)
LVEF	59% (52%-69%)	57% (53%-58%)	55% (50%-66%)
LVGLS	-21.8% (-28.0% to -17.4%)	-20.2% (-22.0% to -19.4%)	-17.9% (-19.4% to -13.6%)*#
LASr	41.6% (30.0%-60.4%)	36.0% (34.4%-46.1%)	28.4% (23.9%-35.5%)*#

* p < 0.05 compared with control; # p < 0.05 compared with children without left-sided heart obstruction

P1-042

Evolution of Left Ventricular Rotational Mechanics in Infancy and Childhood - Impact of Tetralogy of Fallot Repair on Inherent Rotational Abnormalities

Jennifer Cohen¹, Melanie Tan¹, Berthold Klas², Ira Parness¹, Kenan Stern¹, David Ezon¹, Rajesh Shenoy¹, Miwa Geiger¹, Hari Rajagopal¹, Santosh Uppu¹. ¹Mount Sinai Medical Center, New York, NY; ²TomTec Imaging, Munich, Germany

Background: Impaired left ventricular (LV) rotational myocardial mechanics have been described in children with repaired tetralogy of Fallot (ToF); independent of RV dilation. We aim to assess LV rotational mechanics prior to surgical repair and impact of surgery on systolic and diastolic rotational function. **Methods:** Retrospective single center cohort study in infants with ToF pre and post repair. Inclusion criteria were baseline pre-op transthoracic echocardiogram (TTE) and post-op TTE with optimal LV short-axis basal and apical images. Basal rotation (BR), apical rotation (AR), peak twist (difference between AR and BR), twist rate and untwist rate were analyzed using speckle tracking echocardiography. Baseline and post op comparisons made based on type of surgery -transannular patch (TAP) or valve-sparing (VS) repair. LV end-diastolic eccentricity index and QRS duration were assessed at the time of postop TTE. **Results:** 28 patients (16 TAP, 12 VS) with age at

Poster Session 1 (P1)

Sunday, June 23, 2019

pre-op TTE of 1.9 ± 1.2 mo and at post-op TTE of 1.6 ± 0.6 yrs. Age at surgery was 3.5 ± 1.8 mo, similar between the two groups. Table 1 demonstrates patterns of AR and BR. BR was commonly reversed counterclockwise both pre- and postop. AR directionality was preserved in the majority of the TAP group, but more abnormal in the VS group; unchanged both pre and post-op. There were no statistically significant pre-operative differences in AR and BR between TAP and VS repairs. Postoperatively, AR magnitude (8.0 ± 1.0 vs. $5.6 \pm 1.2^\circ$, $p=0.05$), and peak LV twist (4.6 ± 3.1 vs. $1.1 \pm 2.9^\circ$, $p=0.04$), were higher in the TAP compared to VS repair. There was no difference in twist rate but untwist rate magnitude was higher in TAP group (100 ± 19 vs. 68 ± 11 $^\circ/\text{sec}$, $p=0.045$). QRS duration was similar between TAP and VS repair groups. LV eccentricity index was significantly higher in TAP patients (1.4 ± 0.2 vs. 1.1 ± 0.1 , $p=0.001$). **Conclusions:** Preoperative abnormalities in direction of LV AR and BR were noted in majority of ToF infants. LV AR compensates favorably for abnormal BR and preserves twist especially in those following TAP repair while those with non-dilated RV after VS surgery had decreased AR, twist and untwist rate. LV morphology in those with VS repair may be at increased risk for persistence of abnormal rotational mechanics that can impact diastolic function irrespective of RV dilation.

Table 1: Patterns of basal and apical rotation.

Parameter	Valve-sparing repair (n=16)		Transannular patch repair (n=12)	
	Pre-operative	Post-operative	Pre-operative	Post-operative
Basal rotation				
Normal clockwise	43.8% (7)	50% (8)	25% (3)	41.7% (5)
Reversed counterclockwise	56.2% (9)	50% (8)	75% (9)	58.3% (7)
Change in direction postoperatively				
Normal to reverse		18.8% (3)		16.7% (2)
Reverse to normal		12.5% (2)		0.0% (0)
No change in direction		68.7% (11)		83.3% (10)
Apical rotation				
Normal counterclockwise	68.7% (11)	62.5% (10)	91.7% (11)	83.3% (10)
Reverse clockwise	31.3% (5)	37.5% (6)	8.3% (1)	16.7% (2)
Change in direction postoperatively				
Normal to reverse		31.2% (5)		16.7% (2)
Reverse to normal		25.0% (4)		8.3% (1)
No change		43.8% (7)		75.0% (9)

P1-043

Intranasal Dexmedetomidine Provides Successful and Safe Moderate Sedation for Pediatric Echocardiography in Infants and Uncooperative Young Children—the Ideal Sedative?

David E. Saudek¹, Deborah Walbergh², Peter Bartz¹, Sara Shreve², Amy Schaal¹, Peter Frommelt¹. ¹Medical College of Wisconsin, Milwaukee, WI; ²Children's Hospital of Wisconsin, Milwaukee, WI

Background: Chloral hydrate has been used successfully for pediatric echo sedation; however, it was difficult to administer because of its large volume/bitter taste, and is no longer commercially available. Infants and young children 1-24 months old are routinely sedated for echocardiograms within the Children's Hospital of Wisconsin Echo Lab. With chloral hydrate no longer available, we began using intranasal dexmedetomidine (Dex) in October 2018, administered by cardiology with no anesthesia support. This study compares safety and efficacy of Dex to chloral hydrate in an academic pediatric echo lab with a wide variety of complex congenital heart disease. **Methods:** Chart review was performed comparing patients sedated with Dex for the 3 month period of October through December 2018 with those sedated with chloral hydrate during the prior 12 months. Patients sedated with Dex were given 3 mcg/kg intranasally with an additional 1mcg/kg dose if not adequately sedated within 45 min. Vital signs and sedation score (Ramsay scale) were charted by a dedicated sedation nurse per institutional protocol. Patients were considered sedated when they achieved level 3 (moderate sedation) and sedation completed when they first achieved a level 5 (appropriately responsive). Sedation failure was considered inability to achieve level 3 for a duration that allowed completion of the echo study. **Results:** Results are summarized in Table 1. Chloral hydrate was used in 327 patients and Dex in 113. Patient age, complexity of heart disease, time to achieve level 3 sedation and duration of sedation were similar. A second sedative dose was given more often with Dex than with chloral hydrate, but rates of failed sedation were very low and similar (0.9 vs 2.1%). The average and minimum heart rate and respiratory rate were lower for those receiving Dex, but no intervention or deviation from echo protocol was required. The effects on oxygen saturation were similar. Among those with complex heart disease, only heart rate was lower for those given Dex. **Conclusion:** Sedation with Dex is comparable to chloral hydrate in regards to safety and efficacy for children requiring echocardiography. Consistent with the mechanism of action, patients receiving Dex have a lower heart rate without morbidity. Dex appears to be an ideal drug for pediatric echo sedation.

TABLE 1

Characteristics	Chloral Hydrate (n=327)	Dex (n=113)	p value
Age (months)	9.3	9.5	0.75
Complex Congenital Heart Disease*	26%	28%	0.68
Cyanotic Heart Disease**	8%	11%	0.33
Time to sedation (minutes)	25.4	24.6	0.53
Duration of sedation (minutes)	72.7	69.6	0.26
% Failed sedation (n)	2.1% (7)	0.9% (1)	0.41
Required second med	0%	8%	<0.001
Impact on Vital Signs--All Patients			
Pre-sedation Heart Rate	130.7	132.2	0.41
Average Heart Rate	124	111	<0.001
Minimum Heart Rate	109.3	97	<0.001
Pre-sedation Respiratory Rate	37.5	38.4	0.46
Average Respiratory Rate	34.9	31	<0.001
Minimum Respiratory Rate	25.9	21.1	<0.001
Decrease in O2 Saturation--Baseline to Minimum (%)	3.6	3.2	0.58
% with $\geq 10\%$ drop in O2 saturation	4.6%	4.4%	0.93
Impact on Vital Signs--Complex Congenital Heart Disease	N=86	N=32	
Pre-sedation Heart Rate	128.2	128.6	0.92
Average Heart Rate	120.9	103.4	<0.001
Minimum Heart Rate	107.5	89.4	<0.001
Pre-sedation Respiratory Rate	38.9	38.9	0.67
Average Respiratory Rate	36.1	31.8	0.10
Minimum Respiratory Rate	26.7	22.5	0.07
Decrease in Saturation--Baseline to Minimum (%)	-4.3	-3.9	0.60
% with $\geq 10\%$ drop in O2 saturation	5.8%	9.4%	0.49
Paired t-test or chi squared test performed to compare groups			
* Complex congenital heart disease was defined as condition expected to require surgical intervention with cardiopulmonary bypass during infancy.			
** Cyanotic heart disease defined as baseline saturation <90%			

P1-044

Left Ventricular Dysfunction in Neonatal Ebstein's Anomaly and Tricuspid Valve Dysplasia

Yozo Teramachi¹, Lisa K. Hornberger¹, Lisa Howley², Mary E. van der Velde³, Luke G. Eckersley¹. ¹Fetal & Neonatal Cardiology Program, Division of Cardiology, Department of Pediatrics, Women's & Children Health Research Institute, University of Alberta, Edmonton, AB, Canada; ²Division of Cardiology, Department of Pediatrics, University of Colorado, Denver, CO; ³Division of Cardiology, Department of Pediatrics, University of Michigan, Ann Arbor, MI

Background: Neonates with severe Ebstein's anomaly and tricuspid valve dysplasia (EA/TVD) are often hemodynamically unstable with low systemic perfusion and hypoxia; whereas, this is uncommon in another critical right heart lesion, pulmonary atresia with intact ventricular septum (PAIVS). We have recently demonstrated left ventricular (LV) dysfunction and dyssynchrony to be common in fetal EA/TVVD but not PAIVS. In the current study we sought to explore LV function and mechanics in neonatal EA/TVVD with comparison to PAIVS in the early neonatal period. **Methods:** We identified cases of neonatal EA/TVVD (n=30) and PAIVS (n=17) encountered from 2004-2018. We assessed LV function using 2D, Doppler-derived, longitudinal and circumferential deformation (6-segmental Vector Velocity Imaging) and dyssynchrony indices (standard deviation of time-to-peak, T2PSD) and a novel global dyssynchrony index (DI) in the first 48 hours of life. Results are described as mean \pm standard deviation, or median (95% confidence intervals). **Results:** Gestation at birth was earlier in EA/TVVD than PAIVS (36.4 ± 2.2 weeks vs 38.1 ± 2.4 weeks $p=0.03$). Five cases of EA/TVVD required extra-corporeal membrane oxygenation. 1 EA/TVVD and 1 PAIVS died in the first 30 days. 16 cases in EA/TVVD had antegrade flow from the right ventricle. The table summarizes the findings in EA/IVS with comparison to PAIVS cases. **Conclusion:** LV radial and circumferential deformation is impaired in neonatal EA/TVVD, and there is increased dyssynchrony compared to neonates

Poster Session 1 (P1)

Sunday, June 23, 2019

with PAIVS. Further work will examine the impact of LV mechanics on outcome and requirements for medical support in early life.

Table	EA/TVD (n=30)	PAIVS (n=17)	p-value
LVEF bullet %	57 (51.3-61.4)	60 (56-66)	0.15
LVEF VVI %	54.3 (50.9-56.2)	62.9 (52.5-64.4)	0.06
LV FAC %	41.9 (37.4-48.2)	51.9 (46.2-57.1)	0.0007
LV FAC VVI %	36 (31-40)	44.3 (37.8-46.1)	0.03
CCO L/min	0.81(0.65-0.98)	0.71 (0.53-0.87)	0.5
LV TEI index	0.56 (0.43-0.61)	0.46 (0.4-0.57)	0.86
GLS %	-15.8 (-12.5- -18.1)	-17.4 (-14.6- -19.5)	0.36
GCS %	-15.9 (-11.5 - -18.7)	-24.1 (-20.7- -25.2)	0.0005
LV sphericity	0.6 (0.55-0.64)	0.63 (0.52-0.66)	0.65
LV eccentricity	1.33 (1.19-1.44)	1.04 (1-1.13)	<0.0001
Strain Long DI	0.11 (0.08-0.17)	0.13 (0.06-0.19)	0.78
Strain Radial DI	0.14 (0.06-0.18)	0.05 (0.01-0.07)	0.006
Strain Circum DI	0.17 (0.09-0.27)	0.08 (0.05-0.12)	0.003
Strain Long T2PSD	47.3 (35.6-60.1)	54.7 (48.4-78.1)	0.2
Strain Radial T2PSD	58.5 (45.2-82.7)	33.2 (21.2-62.2)	0.21
Strain Circum T2P SD	60.8 (43.1-86.3)	32 (27.3-43.6)	0.0003

Numbers are described as median (95% confidence intervals).
Abbreviation: CCO; combined cardiac output, DI dyssynchrony index, EF; ejection fraction, FAC; fraction area change, GCS; global circumferential strain, GLS; global longitudinal strain, LV; left ventricular, TEI; tei index, T2PSD; standard deviation of time-to-peak

P1-045

Failure of Current Echocardiographic Scoring Systems to Consistently Predict Successful Early Biventricular Repair in Neonates with Critical Aortic Stenosis and Borderline Left Heart Hypoplasia

Shagun Sachdeva¹, Evelyn Kuhn², Peter C. Frommelt³, Stephanie S. Handler³.
¹Baylor College of Medicine, Houston, TX; ²Children's Hospital of Wisconsin, Milwaukee, WI; ³Medical College of Wisconsin, Milwaukee, WI

Background: Critical aortic stenosis is often associated with variable degrees of hypoplasia of left heart structures. There are several published echo-derived scores to help predict successful biventricular (BiV) vs univentricular (UniV) palliation in these neonates using left heart dimensions and appearance of the left ventricular endocardium. **Methods:** Patients who have undergone initial neonatal aortic valve intervention with the intention of BiV circulation based on expert local opinion were queried from the Children's Hospital of Wisconsin database. Type of initial aortic intervention (valvotomy vs valvuloplasty) and outcome (BiV vs UniV circulation at hospital discharge) were collected. Echocardiographic imaging from their first study prior to either intervention was retrospectively used to compute the following scores - Rhodes, CHSS1, Discriminant, CHSS2 and 2V. **Results:** From 01/1999-12/2017, 68 neonates met inclusion criteria, with a median age at initial echo of 1 day (IQR 0-3 days). Median age at initial intervention was 4 days (IQR 2-10 days) with 33 having balloon valvuloplasty and 35 surgical valvotomy. Successful BiV circulation was maintained in 60/68 patients. Of the remaining 8 patients, 3 had subsequent UniV palliation, 4 died, and 1 underwent heart transplant prior to discharge. None of the binary score predictions of BiV vs UniV (using that score's proposed cut-offs) were significantly associated with the observed outcome. All the scores but the Rhodes predicted successful BiV repair in the majority who maintained BiV circulation. However, a high percentage of those predicted to need UniV palliation had successful BiV repair (89.4% by Rhodes, 79.3% by CHSS 1 score, 85.2% by Discriminant score (Table 1). The 2V score best predicted outcome and agreed with the local approach in majority cases. **Conclusion:** This study highlights the limitations of and need for alternative scoring systems/cut-offs for consistently accurate echocardiographic prediction of early outcome in patients with critical aortic stenosis and borderline left heart hypoplasia.

Table 1: Summary of % successful BiV repair among those with BiV/UniV predicted by the respective scores

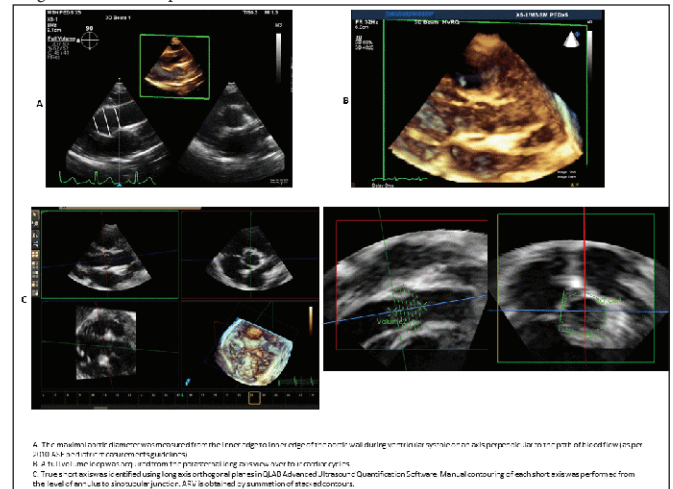
		Rhodes		CHSS-1		Discriminant		CHSS-2		2V	
		BiV Successful		BiV Successful		BiV Successful		BiV Successful		BiV Successful	
		Yes	No	Yes	No	Yes	No	Yes	No	Yes	No
Outcome Predicted	BiV	1	1	37	2	14	0	54	5	60	8
		50.0 %	50.0 %	94.9 %	5.1 %	100.0 %	0.0 %	91.5 %	8.5 %	88.2 %	11.8 %
	UniV	59	7	23	6	46	8	6	3	0	0
		89.4 %	10.6 %	79.3 %	20.7 %	85.2 %	14.8 %	66.7 %	33.3 %		
		60	8	60	8	60	8	60	8	60	8

P1-046

Feasibility and Reproducibility of Three-Dimensional Echocardiography Derived Aortic Root Volumes in Children and Young Adults

Sanjeev M. Gupta¹, Jennifer Cohen¹, Rosalie Castaldo¹, Melanie Tan¹, Jen Yau¹, Santosh Uppu¹, Shubhika Srivastava¹, Hari Rajagopal^{1,2}.
¹Mount Sinai Medical Center, New York, NY; ²South Nassau Community Hospital, New York, NY

Background: Aortic root measurements influence management decisions, yet lack consistency even in published guidelines (depending on age, method and imaging modality). We sought to evaluate the feasibility of measuring aortic root volume (ARV) by three-dimensional echocardiography (3D TTE), and compared the interobserver agreement between ARV and traditional 2D TTE measurements. **Methods:** Thirty consecutive subjects with optimal 3D image data were enrolled (42% male, mean 10 years, range 2 days to 36 years, BSA range 0.21 to 1.81 m²). A 3D-full volume data set was obtained and the true short axis was identified using long axis orthogonal planes in QLAB Advanced Ultrasound Quantification Software. Each short axis image was manually contoured in end systole, from the level of the aortic annulus to the sinotubular junction. ARV was obtained by the summation of these stacked contours. Additionally, traditional 2D TTE aortic root measurements were made at the level of the aortic annulus, root and sinotubular junction in end systole from the inner edge to inner edge of the aortic wall, per 2010 ASE guidelines. All measurements were made by two observers, and interobserver agreement was assessed. **Results:** Mean systolic ARV was 4.3 ± 4.1 mL (0.18-15.1 ml). Interobserver agreement of ARV was excellent (intraclass correlation coefficient [ICC] 0.99; 95% CI 0.97-0.99). Traditional aortic root measurements had an acceptable overall interobserver agreement but with much wider confidence intervals (ICC for annulus, root and sinotubular junction were 0.89, 0.90 and 0.85 respectively). All patients had normal left ventricular volumes and systolic function. **Conclusions:** ARV is feasible by 3D TTE and allows for a reproducible quantification of aortic root size with excellent interobserver agreement. This measurement is simple if the appropriate images are obtained. Utility of this technique in dilated and asymmetric aortic roots needs to be further evaluated. Prospective studies are needed establish accuracy and establish normative data for longitudinal follow up.



A. 3D TTE aortic root volume measurement. B. 2D TTE aortic root measurement. C. 2D TTE aortic root measurements at different levels. Manual contouring of each short axis image performed from the level of the aortic annulus to the sinotubular junction. ARV is obtained by summation of stacked contours.

Poster Session 1 (P1)

Sunday, June 23, 2019

P1-047

Comparison of Right Atrial and Ventricular Strain During Simultaneous Vasoreactivity Testing in Pediatric Pulmonary Hypertension

Courtney Cassidy, Michal Schäfer, Dale Burkett, Dunbar Ivy, Pei-Ni Jone. Children's Hospital Colorado, Aurora, CO

Background: Cardiac catheterization is the gold standard in evaluation of pulmonary hemodynamics in patients with pulmonary hypertension (PH), however, it is invasive. Previous studies have reported right atrial (RA) and right ventricular (RV) strain to be a useful noninvasive tool in evaluation of pediatric PH, as impaired RA function reflects RV dysfunction in PH patients. Evaluation of changes in right heart mechanics during vasoreactivity testing has not been evaluated in pediatric PH. This study evaluated right heart function in PH patients at baseline condition and during vasoreactivity testing with simultaneous invasive hemodynamics. **Methods:** PH patients underwent simultaneous two-dimensional echocardiography and cardiac catheterization at baseline and during acute vasoreactivity testing. RA and RV deformation analysis were performed off-line using TomTec CPA 2.1. RA strain, strain rates, emptying fraction (EF), fractional area change (FAC), and RV global longitudinal strain were measured. A student t-test was performed for comparative analysis. **Results:** 41 PH patients (10.34 ± 5.9 years) were evaluated at baseline condition, 36 of which had vasoreactivity testing performed. No significant differences were observed in right heart function between PH patients at baseline compared to vasoreactivity testing condition (Table 1). Although significant statistical differences were found in invasive hemodynamics between baseline condition and vasoreactivity testing, none of the patients had a 20% decrease in hemodynamics with vasoreactivity testing. **Conclusions:** Right heart mechanics were not altered in pediatric PH patients during vasoreactivity testing, likely due to patient unresponsiveness to vasoreactivity testing. A future study to evaluate a large cohort of patients who are responsive to vasoreactivity testing may be needed to evaluate the changes in right heart mechanics compared to invasive hemodynamics.

	Baseline (n=41)	Challenge (n=36)	P-Value
Atrial EF (%)	51 ± 11	54 ± 9	0.367
Atrial EDV (mL)	14 (10 - 24)	16 (8 - 24)	0.394
Atrial ESV (mL)	34 (21 - 51)	33 (19 - 5)	0.243
HR	81 ± 19	77 ± 16	0.491
e _S = reservoir	33.6 ± 9.2	33.8 ± 8.5	0.942
e _E = conduit	25.2 ± 8.3	25.6 ± 7.3	0.835
e _A = pump	8.9 ± 4.1	8.2 ± 4.0	0.432
SRs	1.4 ± 0.4	1.4 ± 0.4	0.702
SRe	-1.6 ± 0.6	-1.5 ± 0.7	0.728
SRA	-1.1 ± 0.6	-1.0 ± 0.4	0.403
RV GLS	-24.8 ± 3.9	-24.4 ± 3.5	0.625
RV FAC	43 ± 8	43 ± 8	0.912
Cath data			
sPAP (mmHg)	52.0 (40.5 - 64.0)	47.5 (31.0 - 66.8)	< 0.001
mPAP (mmHg)	30.5 (23.5 - 41.8)	27.5 (18.0 - 40.5)	< 0.001
PVRI (WU.m2)	7.2 (3.9 - 10.5)	5.2 (2.3 - 9.2)	< 0.001
SVRI (WU.m2)	15.4 (12.5 - 18.9)	16.6 (12.6 - 18.9)	0.263
CI (L/min/m2)	3.5 ± 0.7	3.5 ± 0.8	0.876
mRAP	6.0 (5.0 - 7.8)	7.0 (5.0 - 8.0)	0.002

CI=cardiac index, EDV= end diastolic volume, ESV= end systolic volume, HR= heart rate, mPAP= mean pulmonary artery pressure, mRAP= mean right atrial pressure, PVRI= pulmonary vascular resistance index, sPAP= systolic pulmonary artery pressure, SRA= late negative strain rate, SRe= early negative strain rate, SRS= peak strain rate, SVRI= systemic vascular resistance index.

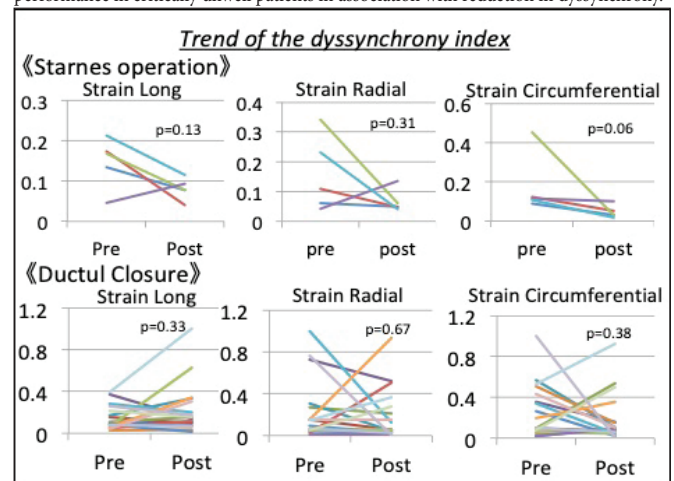
P1-048

Left Ventricular Dysfunction is a Common Feature of Neonatal Ebstein's Anomaly and Tricuspid Valve Dysplasia But Not Pulmonary Atresia with Intact Ventricular Septum

Yozo Teramachi¹, Lisa K. Hornberger¹, Lisa Howley², Mary E. van der Velde³, Luke G. Eckersley¹. ¹Fetal & Neonatal Cardiology Program, Division of Cardiology, Department of Pediatrics, Women's & Children Health Research Institute, University of Alberta, Edmonton, AB, Canada; ²Division of Cardiology, Department of Pediatrics, University of Colorado, Denver, CO; ³Division of Cardiology, Department of Pediatrics, University of Michigan, Ann Arbor, MI

Background: We have recently demonstrated left ventricular (LV) dysfunction and dyssynchrony to be features of fetal and neonatal EA/TVD. Whether LV performance is improved following neonatal intervention is unclear; however, such knowledge would

help in planning medical and surgical management of these often hemodynamically unstable neonates. We sought to investigate the impact of neonatal intervention (ductal closure or right ventricular exclusion/Starnes) on LV performance in EA/TVD. **Methods:** We identified neonates with EA/TVD encountered from 2004-2018 in our institutions. LV function was assessed using 2D, Doppler-derived, deformation (6-segmental Vector Velocity Imaging), dyssynchrony indices (standard deviation of time-to-peak, T2PSD) and a novel global dyssynchrony index (DI - Figure). Data are presented as mean ± standard deviation, or median (95% confidence intervals). Pre and post intervention findings were compared using paired t-test analysis or Wilcoxon test. **Results:** Thirty neonates with EA/TVD were identified of whom 22 had pre and post intervention images that were analyzable. Of the 22, 5 with more severe disease (all cases with pulmonary outflow obstruction) underwent a Starnes procedure and 17 had ductus arteriosus closure as the only management (13 spontaneous, 4 surgical ligation). The LV global function improved after the Starnes procedure (fractional area change Pre 42.8% (32.1-48.2) vs Post 61% (45.9-65) p=0.02; ejection fraction Pre 62.8% (37.6-67) vs Post 70% (40.7-75.2) p=0.07; global circumferential strain Pre -18.7% (-9.13- -22.4) vs Post -32.3% (-24.5- -42) p=0.05) and dyssynchrony decreased (circumferential strain DI Pre 0.12 (0.09- 0.45) vs Post 0.03 (0.02- 0.1) p=0.06). There was no change in LV global function or dyssynchrony after ductal closure. **Conclusion:** The Starnes procedure has a significant acute impact on LV performance in critically unwell patients in association with reduction in dyssynchrony.



P1-049

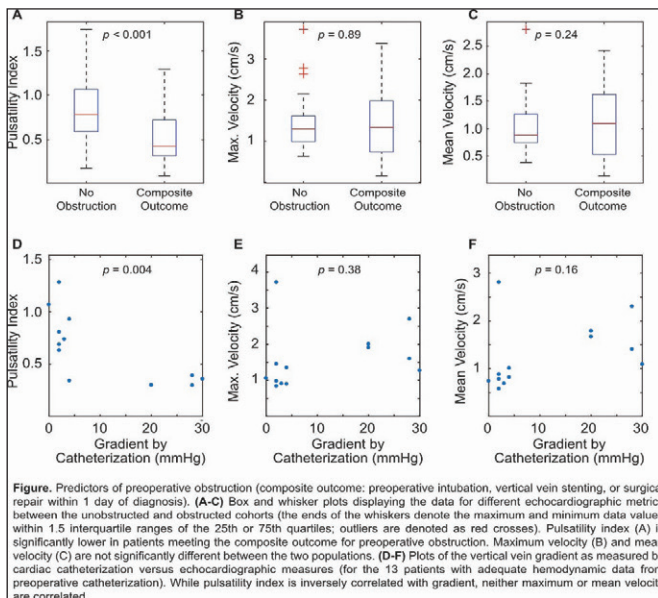
Pulsatility Index Predicts Preoperative Obstruction in Children with Total Anomalous Pulmonary Venous Connection Better Than Other Standard Methods

Brian R. White, Andrew C. Glatz, Christopher E. Mascio, Meryl S. Cohen. The Children's Hospital of Philadelphia, Philadelphia, PA

Background: Preoperative pulmonary venous obstruction in total anomalous pulmonary venous connection (TAPVC) is a major cause of increased morbidity and mortality. However, echocardiographic diagnosis of vertical vein obstruction is often challenging: pulmonary blood flow can vary, especially in single-ventricle heart disease, and the angle of insonation strongly affects Doppler velocities and the use of the modified Bernoulli equation. Pulsatility index, a composite measure of flow, may be a better marker of obstruction. **Methods:** We performed a retrospective review of all patients undergoing repair of TAPVC at our institution from 1/1/06 to 10/23/17, including single-ventricle heart disease. The outcome of interest was preoperative pulmonary venous obstruction defined as a need for preoperative intubation, vertical vein stenting, or urgent surgical repair (within 1 day of diagnosis). Preoperative echocardiograms were reviewed; the spectral Doppler tracing of the vertical vein with the highest maximum velocity was inspected. Pulsatility index was calculated over three beats as (maximum velocity - minimum velocity) / (mean velocity). **Results:** During the study interval, 113 patients underwent TAPVC repair with adequate imaging for analysis. The composite outcome of preoperative obstruction was met by 46 patients (42%). Pulsatility index was lower in preoperatively obstructed patients (0.53 ± 0.28) than in unobstructed patients (0.83 ± 0.35, p<0.001, Fig A); in contrast there were no significant differences in maximum velocity (obstructed: 1.40 ± 0.77 m/s, unobstructed: 1.38 ± 0.52, p=0.89, Fig B) or mean velocity (obstructed: 1.13 ± 0.67 m/s, unobstructed: 1.01 ± 0.40, p=0.24, Fig C). Pulsatility index was inversely correlated with the vertical vein gradient as measured by catheterization (R=-0.73, p=0.004, N=13), whereas maximum velocity (R=0.27, p=0.38) and mean velocity (R=0.41, p=0.16) were not (Fig D-F). Pulsatility index of 0.60 had a sensitivity of 68% and a specificity of 74% for the detection of preoperative obstruction. **Conclusion:** Pulsatility index of the vertical vein is superior to the maximum or mean Doppler velocity for diagnosis of preoperative pulmonary venous obstruction in TAPVC. Future work will focus on reliability and predicting postoperative complications.

Poster Session 1 (P1)

Sunday, June 23, 2019



P1-050

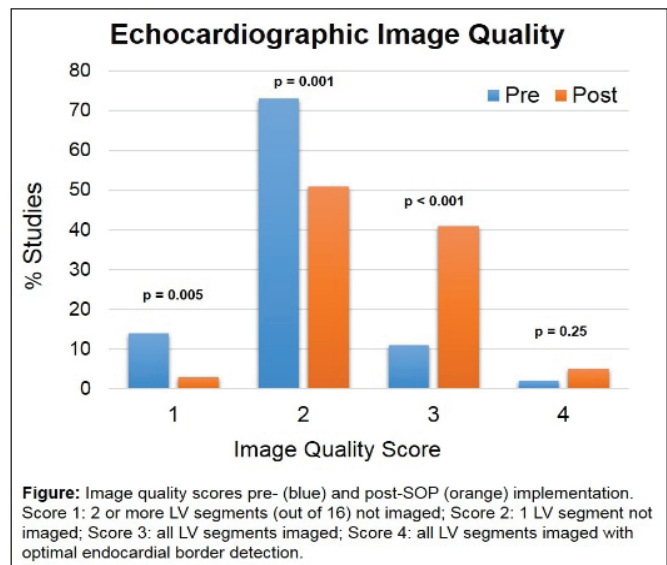
A Cardio-Oncology Imaging Team Improves Ejection Fraction Reliability: A Quality Control Study

Cory Noel¹, Ricardo Pignatelli¹, Hari Tunuguntla¹, Monica Gramatges¹, Nino Rainusso¹, Carolyn Altman¹, Juan Carlos Plana², Robert Loar¹. ¹Texas Children's Hospital/Baylor College of Medicine, Houston, TX; ²Baylor College of Medicine, Houston, TX

Background: Accurate measurement of left ventricular (LV) systolic function by echocardiography is paramount in detection of chemotherapy-induced dysfunction. We hypothesized that limiting the number of imaging operators involved would improve reliability of these measures. **Methods:** A standard operating procedure (SOP) whereby LV measurements were standardized and a cardio-oncology imaging team of 5 sonographers and 6 cardiologists was established 1/2018. The imaging team was made responsible for scanning and interpreting all pediatric oncology patient echocardiograms. In total, 100 consecutive pre-SOP and 100 post-SOP studies (in which all measures of interest were reported) were reviewed. LV end-diastolic dimension (LVEDD), posterior wall thickness (PW), shortening fraction (SF), and ejection fraction by Simpson's biplane (EF) were re-measured by a single blinded reader. Image quality was scored by number of LV segments imaged (range 1-4, 1 worst and 4 best). Inter-observer variability (IOV) pre/post-SOP was assessed with intra-class coefficient (α). Variables were compared with t-test or Chi-square. **Results:** Pre-SOP implementation studies (n = 100) were performed by 27 sonographers and read by 27 cardiologists. Only 13% of studies were graded ≥ 3 . IOV was good for measurement of LVEDD ($\alpha = 0.98$), PW ($\alpha = 0.84$) and SF ($\alpha = 0.85$). IOV for EF was poor ($\alpha = 0.65$). Post-SOP implementation, 92/100 studies were completed by a cardio-oncology team sonographer and cardiologist. Image quality significantly improved (Figure, 46% vs. 13%, $p < 0.001$). IOV for EF also significantly improved ($\alpha = 0.87$, $p < 0.001$), while other measures were similar or marginally improved (Table). The number of patients originally reported with a normal EF, but re-measured $< 55\%$ was decreased (12% vs. 5%, $p = 0.07$). **Conclusion:** Implementation of an imaging protocol by limiting operator involvement improved image quality and reliability of EF measurement. Such practice may lead to improved detection of chemotherapy-induced cardiac dysfunction.

Pre-Implementation			
Variable	Reported	Re-Measured	Alpha
LVEDD (cm)	4.3 ± 0.7	4.4 ± 0.6	0.98 (0.96 – 0.99)
Posterior wall (cm)	0.78 ± 0.17	0.75 ± 0.15	0.84 (0.75 – 0.90)
Shortening fraction (%)	34.7 ± 4.6	32.8 ± 3.4	0.85 (0.50 – 0.93)
Ejection fraction (%)	62.1 ± 5.8	57.9 ± 5.8	0.65 (0.17 – 0.83)
Post-Implementation			
Variable	Reported	Re-Measured	Alpha
LVEDD (cm)	4.2 ± 0.7	4.2 ± 0.7	0.97 (0.96-0.98)
Posterior wall (cm)	0.7 ± 0.2	0.7 ± 0.1	0.87 (0.81-0.92)
Shortening fraction (%)	35.1 ± 4.2	32.8 ± 3.5	0.91 (0.87-0.94)
Ejection fraction (%)	61.2 ± 4.4	58.6 ± 4.7	0.87 (0.81-0.92)

Table: Measures of LV function pre- and post-SOP implementation. IOV assessed with intra-class correlation coefficient (alpha).



P1-051

Evaluation of Right Atrioventricular Function During Exercise in Healthy Youth

Shivani M. Bhatt¹, Michael McBride², Stephen Paridon², Laura Mercer-Rosa². ¹Children's National Medical Center, Washington, DC; ²Children's Hospital of Philadelphia, Philadelphia, PA

Background: There is limited data on right ventricular (RV) diastolic and contractile reserve and right atrial (RA) function during exercise in healthy children. We sought to investigate the changes in RA and RV function from rest to peak exercise and the relationship of these changes with exercise capacity in healthy youth. **Methods:** Subjects presenting for cardiopulmonary exercise test with structurally normal hearts underwent rest and peak exercise research echocardiograms. Peak right atrial longitudinal strain (RALS), RA reservoir volume and RA emptying fraction (RAEF) were used as measures of RA function. Tricuspid myocardial velocities and inflow Doppler (E and A) velocities were used as measures of diastolic function. Peak RV longitudinal strain (RVLS) was used as a measure of systolic function. Exercise test parameters included the percent-predicted maximum oxygen consumption (%mVO₂), percent-predicted maximum work, and oxygen pulse. **Results:** We enrolled 10 patients (age 12.7 ± 1.7 years, 60% female). Tricuspid inflow Doppler peak velocities (E and A) and myocardial velocities (E' and S') increased significantly at peak exercise. There was a significant decrease in the Tricuspid E/A ratio whereas Tricuspid E/E' ratio increased significantly at peak exercise. RA end diastolic volume, RA end systolic volume and RA reservoir volume decreased significantly

Poster Session 1 (P1)

Sunday, June 23, 2019

at peak exercise. There was no significant change in RALS or RAEF at peak exercise. The decrease in Tricuspid E/A ratio from rest to peak exercise and increase in Tricuspid inflow A velocity at peak exercise was associated with greater %mVO₂. There was no association of resting or change in RA measures, Tricuspid myocardial velocities or RVGLS with exercise parameters. RALS was not associated with RV strain at rest or peak exercise (Table). **Conclusions:** In healthy children, at peak exercise, there is augmentation of RV systolic function and RV diastolic function mainly due to increased atrial contraction. A more robust atrial kick is directly associated with better aerobic capacity in normal youth. Our results inform the normal right atrioventricular response to exercise and may provide insight into evaluation of right atrioventricular reserve in disease states.

Echocardiographic Parameters			
	Rest*	Peak*	P-Value
Tricuspid E Velocity (m/s)	0.57 (0.48, 0.64)	0.9 (0.87, 0.94)	0.0004
Tricuspid A Velocity (m/s)	0.29 (0.24, 0.34)	0.96 (0.76, 1.14)	0.0001
E/A Ratio	1.66 (2.12, 2.57)	0.81 (0.96, 1.1)	0.0030
Tricuspid peak E' Velocity (m/s)	0.16 (0.14, 0.17)	0.16 (0.13, 0.18)	0.3569
Tricuspid Peak A' Velocity (m/s)	0.09 (0.08, 0.11)	0.20 (0.15, 0.29)	0.0082
Tricuspid E/E' Ratio	3.865 (2.7, 4.3)	5.78 (4.9, 7.7)	0.0022
Tricuspid S' velocity (m/s)	0.14 (0.14, 0.15)	0.21 (0.18, 0.23)	0.0019
RA end diastolic volume	9.66 (6.98, 11.26)	5.86 (4.36, 8.5)	0.018
RA end systolic volume	34.71 (33.32, 37.68)	21.96 (12.84, 25.17)	0.0004
RA reservoir volume	25.4 (22.83, 29.08)	13.76 (7.82, 19.33)	0.0007
RA emptying fraction	60.75 (55.26, 71.33)	66.15 (60.84, 78.65)	0.173
RALS (%)	64.85 (54.60, 72.57)	53.50 (46.73, 75.25)	0.9466
RVGLS (%)	25.10 (23.18, 27.10)	34.05 (28.18, 38.40)	0.004
RVGLS Rate	1.50 (1.43, 1.70)	3.90 (3.50, 4.35)	0.006
RVFWS(%)	26.15 (23.93, 28.20)	35.45 (30.85, 40.93)	0.002
RVFWS Rate	4.20 (3.50, 4.48)	2.20 (1.65, 3.10)	0.002
Analysis of Exercise Parameters			
Predictor	Outcome	Coefficient#	P-Value
Change in Tricuspid E/A Ratio ^a	Percent-predicted maximum VO ₂	-15 (-26.8, -3.6)	0.020
	Percent predicted maximum Work	-7.5 (-90.6, 75.7)	0.815
	Oxygen Pulse	-0.8(-3, 1.14)	0.404
Tricuspid A inflow velocity (peak exercise)	Percent-predicted maximum VO ₂	50.4 (22.5, 78.4)	0.005
	Percent predicted maximum Work	39.26 (-223, 302)	0.700
	Oxygen Pulse	2.24 (-4.5, 9.03)	0.450

*Results reported as median (IQR)
#Results reported as regression coefficients with 95% Confidence Interval (CI)
^aDifference between Tricuspid E/A ratio peak exercise and Tricuspid E/A ratio rest
P value <0.05 is statistically significant

P1-052

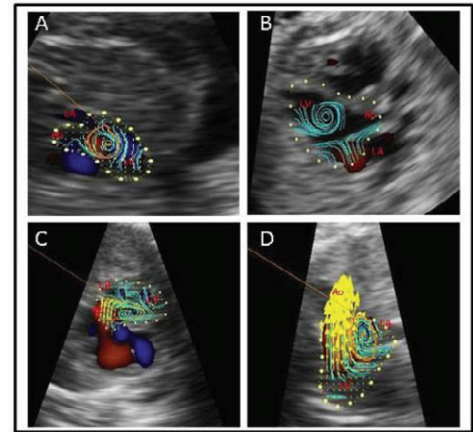
Feasibility and Assessment of Blood Flow and Vortex Formation in the Fetal Heart

Jennifer Cohen, Melanie Tan, Rosalie Castaldo, Jen Lie Yau, Kenan Stern, David Ezon, Hari Rajagopal, Ira Parness, Michele Cafone, Rajesh Shenoy, Santosh Uppu, Miwa Geiger, Shubhika Srivastava. Mount Sinai Medical Center, New York, NY

Background: In vitro fluid dynamic modelling has described vortex formation in the fetal heart. Vortex formation allows for efficient transport of blood volume and can serve as a surrogate to assess diastolic filling. Diastolic filling of the fetal ventricles by inflow and tissue Doppler has demonstrated impaired relaxation and predominant filling in late diastole. We aim to describe feasibility of using vector flow mapping (VFM) to evaluate vortex formation in the fetal heart. **Method:** VFM (Hitachi Aloka) was performed for noninvasive visualization of blood flow velocity vectors from conventional color Doppler fetal echocardiogram images profiling the left ventricular inflow and outflow. Cardiac cycle was marked by mitral and aortic valve opening and closure. We investigated the area, direction and strength of vortices. **Results:** There were 20 fetal echocardiograms with sufficient quality to be analyzed. Median gestational age at time of fetal echocardiogram was 26.5 (range 16-38) weeks. Eighteen of these fetuses had structurally normal hearts and on VFM analysis had streamlined flow directed to the apex in early diastole and a clockwise vortex formation towards the LV outflow in late diastole at the mid ventricular level. Vortex area increased with gestational age; however, vortex strength remained stable throughout gestation. There was one fetus with D-transposition of the great arteries at 38 weeks gestation who had an additional early diastolic clockwise vortex adjacent to the anterior mitral valve. A fetus with heart block was noted to have a clockwise vortex adjacent to the anterior mitral valve during ejection (Figure). **Conclusion:** Visualization and characterization of Vortex by VFM is feasible. The normal fetal LV has a robust late diastolic vortex directing blood to the LV outflow. This is further support of the importance in atrial contraction in contributing to LV diastolic filling. Vortex formation differed from

normal in both D-TGA and CHB, and vortex assessment of various fetal pathologies will likely provide a unique insight into fetal hemodynamics.

Figure: Vortex flow mapping in the normal fetus (A,B) in which there is a late diastolic vortex at the mid-ventricular level directing flow towards the left ventricular outflow. (C) Early diastolic vortex formation in 38 week old fetus with D-transposition of the great arteries. (D) 34 week old fetus with complete heart block with vortex formation during ventricular systole consistent with disordered blood flow pattern in the setting of atrioventricular dyssynchrony LA=left atrium, LV=left ventricle, Ao=aorta.



P1-053

Right Ventricle Function in Children with Dilated Cardiomyopathy Admitted with Heart Failure: Does it Matter?

Gilda Kadiu, Jyothsna Akam Venkata, Pooja Gupta, Robert D. Ross, Sanjeev Aggarwal. Children's Hospital of Michigan, Detroit, MI

BACKGROUND: Dilated Cardiomyopathy (DCM) in children may be associated with death or heart transplant within 5 years of diagnosis in 50% of cases. Right ventricle (RV) dysfunction in adults admitted with heart failure (HF) is associated with a worse prognosis. Our aim was to compare echocardiographic measures of RV function between groups with and without a poor outcome in children with DCM during their initial admission for symptoms of HF. **METHODS:** This was a single center retrospective review of the first echocardiogram diagnostic of DCM during an admission with HF symptoms. Patients with known DCM on medications, those with incomplete echo data, or pericardial effusion were excluded. Echo indices were interpreted by a single reader blinded to clinical data. RV function was assessed by i) TAPSE calculated by 2D methods in apical 4 chamber view, indexed to body surface area (TAPSE index), ii) RV systolic pressure using continuous Doppler from tricuspid valve regurgitation iii) RV fractional area change (FAC) from apical 4 chamber view and iv) ratio of systolic to diastolic time from tricuspid valve regurgitation. The primary outcome was death or heart transplant within a year of presentation. Echo measures were compared between groups with and without the primary outcome using student t-test and Chi-square test. **RESULTS:** The study cohort (n=44) comprised 15 (34%) males, and had a mean (SD) age of 3.2 (4.2) years. ECMO support was required in 14 (32%), left ventricular assist device in 5 (11%), and heart transplant in 17 (39%) patients while 12 (27%) patients died within a year. The cohort had significant RV dysfunction compared to published norms. Mean (SD) RV FAC was 25 (8.8) and abnormal (<35%) in 36/41 (90%), TAPSE index was 1.57 (0.9) and systolic to diastolic ratio was 2.4 (0.62) and abnormal (>1.2) in 100%. Groups with a poor outcome (n=24) and without (n=20) were similar in age and gender. There was no significant difference in RV functional indices between the two groups. **CONCLUSIONS:** The vast majority of children diagnosed with DCM during an admission for symptoms of HF have RV dysfunction, even on the first echocardiogram. However, RV dysfunction, did not predict adverse short terms outcomes unlike the adult DCM experience. Further investigation is needed on prognostic echocardiographic indices in children with severe DCM.

Poster Session 1 (P1)

Sunday, June 23, 2019

Clinical/Demographics Mean (SD) or n%	Death/OHT (n=24)	Survival (n=20)	P value
Age (years)	3.1 (4.4)	2.4 (4.9)	0.65
Gender (male)	10 (42%)	5(25%)	0.32
SBP (mmHg)	82 (15)	86 (13)	0.31
DBP (mmHg)	49 (13)	54 (13)	0.36
Heart rate (bpm)	155 (26)	157 (29)	0.79
TAPSE (cm)	0.72 (0.53)	0.68 (0.35)	0.77
TASPE index (cm)	1.56 (0.98)	1.63 (0.89)	0.79
RVFAC%	24.2 (9.2)	26.2 (8.6)	0.48
S time (sec)	0.29 (0.05)	0.28 (0.06)	0.63
D time (sec)	0.13 (0.03)	0.12 (0.04)	0.63
SD ratio	2.4 (0.69)	2.4 (2.0)	0.97
RVSP	33.9 (8.1)	32.1 (10.2)	0.56
TAPSE/RVSP	4.34 (3.2)	4.4 (2.0)	0.94

P1-054

Prenatal Diagnosis and Assessment of Vascular Rings and Slings by Fetal Echocardiographic, MRI and Genetic Studies: A Large Single Tertiary Care Center Study

Peng Xu¹, Minli Zhao¹, Ting Zhu¹, Jianfang Zhang², Xing Tang³, Jun Li¹, Shuping Ge¹. ¹Ultrasound Department of Xijing Hospital, Xi'an, China; ²Genetics Laboratory of Xijing Hospital, Xi'an, China; ³Radiology Department of Xijing Hospital, Xi'an, China; ⁴St. Christopher's Hospital for Children and Drexel University College of Medicine, Philadelphia, PA

Objectives: Congenital vascular rings and slings (CVRS) have increasingly been diagnosed prenatally by fetal echocardiography (FE), due to the unique window of opportunity to image the tracheal, aortic and ductal arches successfully. **Method:** We reviewed a large cohort of 43987 FEs and related MRI and genetic studies in our institution. In this cohort, 2656 (6.0%) had congenital heart defect (CHD) and 265 (0.6% of all or 10.0% of CHD) fetuses were diagnosed with vascular rings and slings by FE. **Results:** In this study, prenatal FE diagnoses included right aortic arch (RAA) with left ductus arteriosus (n=199, 75.1%), left aortic arch (LAA) with aberrant right subclavian artery (n=41, 15.4%), double aortic arch (DAA)(n=18, 6.8), pulmonary artery sling (n=5, 1.9%), and right aortic arch with double ductus arteriosus (n=2, 0.8%). In this group, 202 (76.2%) cases had simple vascular rings; whereas 63 (23.8%) cases had other associated cardiac defects. There were 45 cases (17.0%) with tracheal compression by FE. Fetal MRI was obtained in 67 cases and 10 (14.9%) had tracheal compression. Chromosomal study was performed for 181 cases, was normal for 177 (97.8%), and showed trisomy 21 for 4 (2.2%). Gene panel study was done for 98, was normal for 89 (90.8%), 22q11 for 4 (4.1%), and undefined or possible benign for 5 (5.1%). For follow-up, 193 cases were delivered, 57 opted for termination of pregnancy, 15 lost for follow-up, and 2 died after birth. **Conclusion:** In this cohort, FE identifies 0.6% of all and 10.0% of CHD fetuses with CVRS prenatally, likely higher than the prevalence of postnatal series, and can evaluate tracheal compression. Fetal MRI provides additional information on the compression of the trachea. Genetic studies can identify chromosomal or gene abnormality in a few patients. An integrated approach can provide a comprehensive assessment of vascular ring for better prognosis and parental counseling.

P1-055

Intraoperative Transesophageal Echocardiography for the Assessment of Residual Atrioventricular Valve Regurgitation in Children: What Does It Tell Us?

Reena M. Ghosh, Matthew A. Jolley, Meryl S. Cohen, Heather Griffis, Christopher E. Mascio, Michael D. Quartermain. Children's Hospital of Philadelphia, Philadelphia, PA

Background: Intraoperative transesophageal echocardiography (iTEE) is standard of care to assess residual valve insufficiency in patients undergoing surgical atrioventricular valve (AVV) repair. However, there are few reports evaluating the correlation between iTEE assessment of residual valve insufficiency and transthoracic echocardiography (TTE) prior to patient discharge. This study aims to assess agreement between iTEE and pre-discharge TTE assessments of residual left AVV regurgitation (AVVR) in children. **Methods:** We performed a single center, retrospective study of patients who underwent left AVV repair as an isolated surgery or as part of an AV canal repair, from 9/1/2015 - 9/1/2017. Exclusion criteria included single ventricle anatomy, AV valve stenosis, mechanical valve replacement or concomitant left sided lesions. The primary outcome was the comparison of left AVVR by iTEE to the pre-discharge TTE. All studies were reviewed by a single reader and degree of AVVR was classified as none/trivial, mild, moderate or severe based on lab criteria. Technical performance of iTEE was deemed "optimal" based on Nyquist and color gain settings. Hemodynamic parameters such as blood pressure, heart rate and left ventricular function were assessed for all cases. **Results:** Of the 57 patients that met our inclusion

criteria 33 (58%) were female, 54 (95%) had an AV canal defect and median age at surgery was 3.9 months. Nine patients (15.8%) had severe left AVVR and required a second bypass run. Post-operative iTEE demonstrated none/trivial left AVVR in 27 patients (47.4%), mild AVVR in 26 (46%) and moderate AVVR in 4 (7.0%). There was 45.6% agreement with the pre-discharge TTE (kappa score 0.15, p-value 0.05). For the 30 patients with non-agreement, 23 (76.7%) had increased grading of regurgitation on pre-discharge TTE. iTEE imaging settings were optimized in 38 (66.7%) patients and agreement in this cohort was 47.4% (kappa score 0.2, p-value 0.12). **Conclusions:** Intraoperative TEE assessment of residual left AV valve insufficiency does not correlate strongly with pre-discharge TTE studies in pediatric patients. The majority of patients with differing AVVR assessment had a higher grade of regurgitation on pre-discharge TTE, which may be related to the different hemodynamic conditions in children when not under anesthesia. iTEE is an important tool in the evaluation of which patients require immediate re-intervention on their valve, but has limitations in regard to predicting the final result.

P1-056

Virtual Reality Three-Dimensional Modeling for Congenital Heart Surgery Planning

Jimmy C. Lu, Gregory J. Ensing, Richard G. Ohye, Jennifer C. Romano, Peter Salsalos, Sonal T. Owens, Thor Thorsson, Sunkyung Yu, Ray Lowery, Ming-Sing Si. University of Michigan, Ann Arbor, MI

Background: Three-dimensional (3D) imaging by echocardiography, computed tomography (CT) and magnetic resonance imaging (MRI) is routine in preoperative evaluation for congenital heart surgery, but standard methods of presentation have variable utility for communication with surgeons. Printed models require significant cost, post-processing and infrastructure. This study aimed to evaluate the impact of virtual reality 3D modeling. **Methods:** This prospective, single-center study included patients undergoing surgical repair of ventricular septal defect (VSD), double outlet right ventricle or atrioventricular valve repair from June - December 2018, with 3D imaging data. Additional diagnoses were included at the surgeons' request. Images were reviewed with the surgeon on traditional platforms: echocardiograms on QLab (Philips, Amsterdam, The Netherlands) and CT and MRI on cvi42 (Circle Cardiovascular Imaging, Calgary, Canada). Images were then reviewed with True 3D (EchoPixel, Santa Clara, CA). Surgeons completed preoperative and postoperative surveys regarding adequacy of imaging, relative utility of the platforms, and change in management or approach. **Results:** In all 20 patients (median 0.8 years old, interquartile range [IQR] 0.3-3.2; median weight 7.9 kg, IQR 5.4-14.3), surgeons felt they had adequate information for operative planning using either platform. Surgeons spent more time with True 3D than traditional methods (median 9 vs 3.5 minutes, p=0.0003). Surgeons strongly agreed that True 3D was worth their time in 16/20 cases (80%, traditional platform 13/20 [65%], p=0.16), and that True 3D provided additional information in 11/20 cases (55%). True 3D led to a change in clinical approach in 2 cases (10%), both with total anomalous pulmonary venous connection (repair or revision). On postoperative surveys, overall satisfaction was similar for the two platforms. There were 2 discrepancies between True 3D data and intraoperative findings, 1 in differentiating the azygos vein from a pulmonary vein, and 1 in evaluating VSD margins in a case with multiple VSDs; in neither case did traditional 3D imaging more clearly delineate the anatomy. In nearly all cases (18/20, 90%), surgeons would choose to review with True 3D for future similar cases. **Conclusion:** Virtual reality 3D modeling shows promise for sharing valuable anatomic details with surgeons. In the majority of cases, surgeons felt the technology was additive for pre-operative planning, and in some cases changed the operative approach. Further study is needed to improve case selection and to evaluate impact on patient outcomes.

P1-057

Intraoperative Echocardiographic Imaging as a Predictor of Early Postoperative Intervention After Superior Cavopulmonary Anastomosis in Children

Richard M. Friesen¹, Sathish M. Chikkabyrappa¹, Fawwaz R. Shaw², Jonathan M. Chen³, Aarti H. Bhat¹. ¹Seattle Children's Hospital, Seattle, WA; ²Emory University, Atlanta, GA; ³Children's Hospital of Philadelphia, Philadelphia, PA

Background: Consensus is lacking on the utility of postoperative transesophageal echocardiography (TEE) in the immediate assessment of superior cavopulmonary anastomosis (SCPA) in children due to known limitations of imaging the superior vena cava (SVC) and branch pulmonary arteries (PA). There is minimal data on predictors for early re-intervention after SCPA despite an estimated 5-12% rate of unanticipated surgical or cardiac catheterization procedure in the same admission. This study aimed to evaluate utility of postoperative imaging in assessing adequacy of SCPA and its ability to predict need for re-intervention or need for surgical revision. **Methods:** Retrospective, single institutional review of contemporary consecutive SCPA cohort (2011-2018). Descriptive data including underlying diagnosis, age and weight at surgery were collected. Intraoperative imaging of SVC, PAs and SCPA included 2D, color and spectral Doppler assessment by TEE as well as epicardial imaging were reviewed. Patients who required reoperation/diagnostic or interventional cardiac catheterization (Group 1) were compared with those who did not require any intervention (Group 2) using paired t test and logistic regression models. **Results:** 101 patients were included, Group 1=25, Group 2=76. SCPA was visualized on color and spectral Doppler (continuous phasic flow) in 100% Group 1

Poster Session 1 (P1)

Sunday, June 23, 2019

and 83% Group 2 patients. Group 1 were significantly younger with lower weight at the time of SCPA compared to Group 2 (Table). Mean gradient by echo through the SCPA was significantly higher in Group 1 than Group 2 (Table). Of the 25 patients who underwent catheterization, 8 subjects underwent intervention on the SCPA itself and their mean SCPA gradient was significantly higher than those who did not require intervention (Table). ROC analysis demonstrated that a mean SCPA gradient by echo of 2.5mmHg had a sensitivity of 98% with a specificity of 50% for requiring early intervention on the SCPA. **Conclusions:** Clinically useful information can almost always be obtained by routine TEE and epicardial imaging immediately after SCPA. Mean gradient across the SCPA was significantly higher in the group that required re-intervention- suggested cut-offs from this data require prospective validation, perhaps in a multi-center collaborative setting.

	Group 1	Group 2	P-value
Mean Age at SCPA (mo)	4.8 ± 1.6	6.7 ± 6.1	0.01*
Weight (kg)	6.5 ± 1.2	7.2 ± 1.8	0.02*
Epicardial Echo Used	40%	13%	0.007*
SCPA Seen by 2D/Color	100%	83%	1.0
SCPA Spectral Doppler	100%	85%	0.06
SCPA Max Velocity (m/s)	0.62 ± 0.4	0.52 ± 0.2	0.21
SCPA Min Velocity (m/s)	0.28 ± 0.2	0.26 ± 0.2	0.69
SCPA Mean Gradient (mmHg)	1.4 ± 1.3	0.8 ± 0.7	0.04*
SCPA Mean Gradient Cath w/ Intervention (mmHg)	2.6 ± 1.2		0.04*
SCPA Mean Gradient Cath w/o Intervention (mmHg)	1.4 ± 1.3		
	Sensitivity	Specificity	AUC
ROC Analysis of Mean Gradient of 2.5mmHg to predict early intervention on SCPA	98%	50%	0.92

Summary table of results. Group 1 = cardiac catheterization and Group 2 = no catheterization. Descriptive statistics along with imaging parameters between groups provided. Sub-analysis of those who underwent catheterization showing differences in mean gradient and ROC cutoff analysis of mean gradient.

P1-058

Intraoperative Coronary Artery Flow Patterns in Patients Undergoing Surgical Correction for Congenital Heart Disease

Conall T. Morgan, Simone Diab, Maria Angeles Vera, Xiaoling Zhang, Kyle Runekles, Grace Reszeinik, Andreea Dragulescu, Osami Honjo, Katherine Taylor, Mark Friedberg, Vitor Guerra, Michael-Alice Moga, Luc Mertens, Cedric Manliot, Lynne E. Nield. *The Hospital for Sick Children, Toronto, ON, Canada*

BACKGROUND: Normative data for intraoperative coronary artery Doppler velocities by transesophageal echo (TEE) in pediatric patients with congenital heart disease (CHD) is lacking. The effect of cardiopulmonary bypass on coronary artery Doppler velocities are unknown. The aim of this prospective study was to compare pre and intra-operative coronary flow velocities in a heterogeneous cohort of children with CHD. **METHODS:** TEE or Epicardial Doppler velocities were obtained of the left anterior descending (LAD), right coronary artery (RCA), left main and circumflex coronaries with qualitative assessment of ventricular function and valvular function both pre cardiopulmonary bypass and intraoperatively. We prospectively recruited 106 patients undergoing surgery for CHD at The Hospital for Sick Children, Toronto from July 2017- June 2018 were included. Those having surgery for coronary artery issues and patients undergoing the Norwood operation were excluded. Patients were grouped as shunt lesions (n=41), right or left heart obstructive lesions (n=38), transposition of the great arteries (TGA) (n=9) and single ventricles (n=18). **RESULTS:** Median age at surgery was 0.8 years (0.5-4.5 years) and median weight at surgery was 7.6kg (5.6-15.3kg). There was a significant change in LAD and RCA peak/mean velocities and peak/mean gradients from pre-bypass to cessation of bypass (Table 1). Flow reversal in the LAD and RCA was observed pre-bypass in 4 patients (4.4%) and 5 patients (5.5%) respectively and in 10 patients (9%) and 14 patients (16%) respectively at the cessation of bypass. There were no deaths. The composite endpoint of ST changes, ECMO or ventricular tachycardia was reached in 6 patients. In multivariable linear regression, in patients with TGA, RCA mean velocity was 19.7cm/sec greater compared with shunt patients (95%CI: 1.79 - 37.6, p=0.03). No significant change in coronary artery peak velocities or Doppler gradients was observed between the groups. LAD and RCA velocities and gradients did not change significantly with age. **CONCLUSION:** Flow velocities, gradients and the presence of flow reversal in the LAD and RCA increase following cardiopulmonary bypass.

Table 1. TEE parameters were for LAD and RCA described before and after surgery

TEE parameter	Pre-operative	Intraoperative	p-value
LAD: Peak velocity of diastolic peak (cm/sec)	51 ± 22	69 ± 26	<0.001
LAD: Mean velocity of diastolic peak (cm/sec)	27 ± 12	40 ± 16	<0.001
LAD: Peak gradient (mmHg)	1.2 ± 1.2	2.3 ± 1.5	<0.001
LAD: Mean gradient (mmHg)	0.4 ± 0.4	0.8 ± 0.7	<0.001
RCA: Peak velocity of diastolic peak (cm/sec)	45 ± 23	67 ± 27	<0.001
RCA: Mean velocity of diastolic peak (cm/sec)	24 ± 11	36 ± 16	<0.001
RCA: Peak gradient (mmHg)	1.1 ± 1.2	2.0 ± 1.4	<0.001
RCA: Mean gradient (mmHg)	0.3 (0.1 - 0.4)	0.6 (0.3 - 0.9)	0.002

P1-059

Does Decreased Aerobic Capacity Correlate with Abnormal Biventricular Function in Patients with Repaired Tetralogy of Fallot?

Jyotsna Akam-Venkata, Preetha Balakrishnan, Yamuna Sanil, James Galas, Chennai Sriam, Sanjeev Aggarwal. *Children's Hospital of Michigan, Detroit, MI*

Background: Patients with repaired Tetralogy of Fallot (rTOF) are at risk of right ventricular and ultimately biventricular dysfunction. Patients with rTOF have decreased aerobic capacity. It is unclear whether the abnormal aerobic capacity correlates with biventricular dysfunction. **Methods:** This is a single center retrospective analysis of patients with rTOF who underwent a cardiopulmonary exercise stress test (CPET) and echocardiogram. Patients with pericardial effusion, arrhythmia and incomplete data were excluded. Echocardiographic parameters of left ventricular (LV) diastolic function (E/A ratio, E/E' ratio at the septal and lateral annulus of the mitral valve, and mitral valve deceleration time-MVDT), LV global function (myocardial performance index-MPI from spectral and tissue Doppler) and right ventricular systolic function (Tricuspid Annular Plane Systolic Excursion-TAPSE by 2D echocardiogram) and TAPSE/ right ventricular systolic pressure-RVSP ratio) were evaluated. Abnormal aerobic capacity was defined as peak oxygen consumption (VO₂max) < 85% predicted on CPET. The demographic and echocardiographic data were analyzed between patients with decreased and normal aerobic capacity using student t-test and Chi-square test (SPSS ver. 22). **Results:** Our cohort of 95 patients consisted of 89 (93.7%) with TOF, 4 (4.2%) with pulmonary atresia and ventricular septal defect and 2 (2.1%) with TOF and absent pulmonary valve. Repair was by placement of a trans-anular patch in 77 (81%) and RV to pulmonary artery conduit in 18 (19%) of patients. The LV diastolic dysfunction indicated by elevated E/A ratio, elevated E/E' ratio at the septal and lateral mitral annulus was present in both groups. Global LV function, based on a prolonged MPI using spectral and tissue Doppler of the mitral valve, was abnormal in all patients with rTOF. RV systolic dysfunction indicated by decreased TAPSE and TAPSE/RVSP ratio was present in all the patients. All abnormalities were found to be similar in patients with normal and decreased aerobic capacity. **Conclusion:** Patients with rTOF have abnormal LV diastolic and global function and abnormal RV systolic function, neither of which seem to be associated with decreased aerobic capacity. Further studies are needed to evaluate the prognostic significance of these findings.

Parameters (mean±SD)	Abnormal Aerobic capacity (n=39)	Normal Aerobic capacity (n=56)	P value
Age at echo (years)	23.08 ± 8.5	20.5 ± 9.2	0.19
Height (cm)	166.6 ± 11	161.9 ± 25.8	0.29
Weight (kg)	67.05 ± 22.09	63.78 ± 22.3	0.49
BSA (m ²)	1.77 ± 0.27	1.69 ± 0.31	0.26
Males (%)	20 (51.2%)	30 (52.6%)	0.19
SBP in mmHg	121 ± 17	119 ± 14	0.72
DBP in mmHg	66 ± 12	67 ± 11	0.81
Heart rate (bpm)	69 ± 18	69 ± 16	0.74
E/A ratio	2.63 ± 2.64	2.22 ± 0.89	0.28
MVDT (sec)	0.139 ± 0.04	0.138 ± 0.04	0.87
E/E' septal annulus MV	12.93 ± 14	9.8 ± 3.07	0.17
E/E' lateral annulus MV	8.05 ± 9.8	5.59 ± 3.52	0.09
LV MPI	0.39 ± 0.28	0.44 ± 0.20	0.34
LV MPI septal annulus MV	0.49 ± 0.34	0.45 ± 0.27	0.59
LV MPI lateral annulus MV	0.43 ± 0.14	0.42 ± 0.13	0.84
RVOT gradient (mmHg)	26 ± 11.9	25.5 ± 11.8	0.89
TAPSE 2D (cm)	1.30 ± 0.48	1.30 ± 0.49	0.9
TAPSE/RVSP (cm/Hg)	0.034 ± 0.15	0.035 ± 0.15	0.76
RVSP (mmHg)	41 ± 11	40 ± 12	0.64

Poster Session 1 (P1)

Sunday, June 23, 2019

P1-060

Fetal and Postnatal Right Ventricular Strain in Hypoplastic Left Heart Syndrome

Carol McFarland¹, Sarah Opsal², Zhining Ou³, Angela Presson³, Nelango Pinto¹, Thomas Miller¹. ¹University of Utah/Primary Children's Hospital, Salt Lake City, UT; ²Primary Children's Hospital, Salt Lake City, UT; ³University of Utah, Salt Lake City, UT

Background: Decreased myocardial function is a poor prognostic factor in hypoplastic left heart syndrome (HLHS). Global longitudinal strain (GLS) correlates with function as measured on MRI and is considered more reproducible and sensitive than other echocardiographic measures of right ventricular (RV) function. While postnatal strain has been shown to correlate with clinical outcomes, there is no data on whether fetal RV strain correlates with either postnatal strain or outcomes in patients with HLHS. **Methods:** A single center, retrospective cohort study of patients with prenatally diagnosed HLHS with fetal echocardiogram between October 2007 and 2013. Subjects with >mild tricuspid regurgitation on fetal echo, anomalous pulmonary venous drainage, restrictive atrial septum and parental decision of comfort care were excluded. Fetal RV GLS and GLS on the first postnatal echocardiogram, prior to surgery, were measured using commercially available Tomtec software. The correlation between GLS at each time point was analyzed. The association of fetal and postnatal GLS with initial hospital length of stay (LOS), right ventricular end diastolic pressure (RVEDP) at pre-Glenn catheterization, and transplant-free survival was evaluated using univariate inverse Gaussian regression, linear regression and Cox proportional hazard regression, respectively. **Results:** Thirty-five subjects met inclusion criteria. The mean fetal strain was -15.6% and the mean postnatal strain was -12.8%. There was no association between fetal strain and postnatal strain (regression coefficient=0.11, p=0.37). There was no association between fetal strain and LOS, RVEDP, or transplant free survival. Four patients underwent transplant and eight patients died, with an average follow up time of 5.8 years. Transplant-free survivors had better RV function as estimated by GLS on post-natal echocardiogram than those that died or were transplanted (-14.0% vs -11.6%, p=0.045), but no difference between the two groups was seen in GLS on fetal echo (-15.0% vs. -15.9%, p=0.6). **Conclusion:** In this small, retrospective cohort we found no correlation between fetal RV GLS and postnatal GLS. While better postnatal, pre-operative strain was associated with transplant-free survival, there was no association between fetal strain and outcomes. While RV myocardial mechanics are important in prognosis in HLHS, variations in the *in utero* environment and peri-natal events may make fetal myocardial mechanics less predictive of later outcomes.

P1-061

Indices of Ventricular Balance in Complete AV Canal Defect are Constant Over Time

Deborah Y. Ho, Brian R. White, Mark A. Fogel, Meryl S. Cohen. The Children's Hospital of Philadelphia, Philadelphia, PA

Background: Determining suitability for biventricular repair in complete atrioventricular canal defect (CAVC) remains clinically challenging. The atrioventricular valve index (AVVI), atrioventricular inflow index (AVII) and the RV/LV inflow angle have been shown to quantify ventricular unbalance in CAVC and aid in surgical decision-making. These indices have been presumed to be constant over time, which has not been previously demonstrated. It is unknown if growth or changes such as right ventricular dilation affect these measures. Inappropriate application could lead to unsuitable assignment to uni-versus biventricular repair, and postoperative morbidity and mortality. **Methods:** We retrospectively reviewed a series of 24 patients with CAVC. Patients were eligible if they had more than one echocardiogram prior to complete repair. Demographic and surgical information was recorded for each patient, as well as the age, weight, and height at the time of each echocardiogram. The modified AVVI, AVII and RV/LV inflow angle in diastole were measured on each study. Characteristics of the two groups were compared using paired sample t-tests. **Results:** 19 patients had biventricular repair and 5 had single ventricle palliation. 5 patients had an initial AVVI of <0.4, but did not all receive univentricular repair. Two patients died, one with univentricular and another with biventricular repair. One patient had arch reconstruction and pulmonary artery banding prior to complete repair. The median length of time between echoes was 83 days (IQR 67, 207). There was no significant change in mean AVVI, which decreased by an average of 1% (CI: -5%, +3%; p=0.6) between time points. Mean RV/LV inflow angle was also consistent over time, decreasing by 0.4° (CI: -7°, 7°; p=0.9). There was a statistically significant but clinically insignificant decrease in mean AVII by 8% (CI: -14%, -3%; p=0.03). **Conclusion:** In this cohort of patients with balanced and right-dominant unbalanced CAVC, there was no significant change in commonly used echo parameters of ventricular balance over time. This suggests that anatomic features in balanced CAVC may not change significantly over time, and thus these indices can be applied to echocardiograms for surgical decision-making regardless of patient age. Further study with a larger cohort is necessary.



Figure 1. Change in weight, RV/LV inflow angle, AVVI and AVII between early (time 1) and follow-up (time 2) echocardiograms.

P1-062

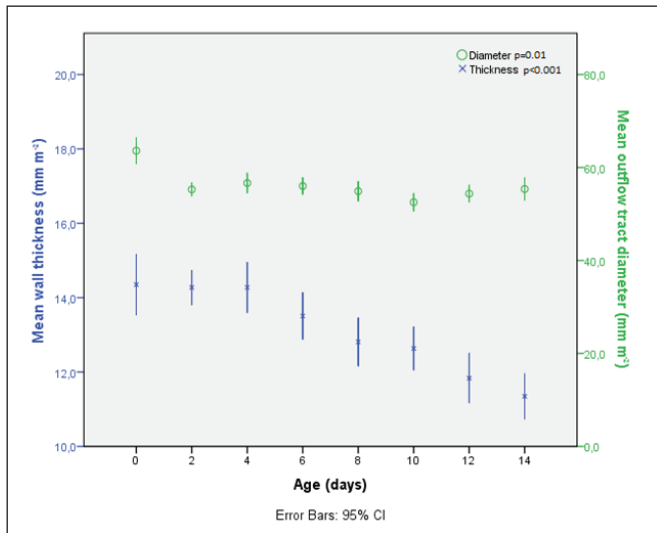
Right Ventricular Remodeling During the First Weeks of Life in Healthy Neonates

Andreas Sando¹, Anne-Sophie Sillesen^{1,2}, Anna Axelsson^{1,2}, Christian Pihl¹, Niels Vejstrup², Kasper Iversen¹, Henning Bundgaard². ¹Department of Cardiology, Copenhagen University Hospital Herlev, Copenhagen, Denmark; ²Department of Cardiology, The Heart Centre, Copenhagen University Hospital Rigshospitalet, Copenhagen, Denmark

Background: The right ventricle (RV) serves as the dominant ventricle in utero. The transition from fetal to post-natal circulation at birth involves marked structural and functional cardiac changes including a large increase in pulmonary blood flow and closure of fetal shunts. Little is known about how the transitional circulation influences RV structure and function in healthy neonates during the first weeks of life. The purpose of this study was to systematically assess RV remodeling in a large, unselected cohort of healthy neonates. **Methods:** Transthoracic echocardiograms of unselected neonates <16 days old and without any signs of structural cardiac abnormalities performed between April 1st, 2016 and August 12th, 2017 were consecutively included from the Copenhagen Baby Heart study (CBHS) until at least 90 neonates per day were included. Left parasternal long-axis RV anterior end-diastolic wall thicknesses and short-axis RV outflow tract end-diastolic diameter were measured offline by one sonographer according to recommendations by the American Society of Echocardiography. RV parameters were corrected for body surface area (BSA). Comparisons were made by T-tests and correlations were computed using univariate linear regression. **Results:** A total of 2,520 echocardiograms were assessed, of which 430 were excluded due to age >15 days (n=290), presence of cardiac abnormality (n=91), or suboptimal parasternal views (n=49). Thus, a total of 2,090 (48% male) were included for analysis. Age, weight, and length at examination were (mean±SD) 7.0±4.7 days, 3.50±0.53 kg, and 52±2 cm, respectively. BSA-corrected mean (95% CI) end-diastolic outflow tract diameter and end-diastolic anterior wall thickness according to age are presented (Figure 1). There was a small age-related reduction in end-diastolic RV outflow tract diameter (r²=0.003, p=0.01) and the BSA-corrected end-diastolic anterior wall thickness decreased by 29% (4.1 mm/m², p<0.001) from birth to day 15. **Conclusion:** RV remodeling during the first 15 days of life in unselected neonates included a small decrease in RV outflow tract diameter and a 29% decrease in anterior wall thickness.

Poster Session 1 (P1)

Sunday, June 23, 2019

Figure 1 Mean (95% CI) BSA-corrected end-diastolic RV anterior wall thickness and end-diastolic RV outflow tract diameter. P-value for correlation.

P1-063

Utility of Echocardiographic Parameters in Diagnosing Elevation of Left Ventricular End-Diastolic Pressure in Heart Transplantation Recipients

Amrit Misra, Swati Sehgal, Jennifer Blake, Sanjeev Aggarwal. Children's Hospital of Michigan, Detroit, MI

BACKGROUND: Pediatric heart transplantation (HT) for the management of end-stage heart failure has shown a marked decline in mortality and morbidity in recent years. However, HT recipients require periodic cardiac catheterization for routine surveillance of rejection and graft dysfunction. Recent studies have found that certain transthoracic echocardiographic parameters, including mitral E wave velocity and E/E' velocity ratio correlate with left ventricular end diastolic pressure (LVEDP). However, the correlation between echocardiographic parameters and catheterization-derived hemodynamics in HT recipients has not been explored. **METHODS:** This is a single center, retrospective chart review of HT patients who had undergone right and left heart catheterization and transthoracic echocardiogram on the same day. Patients with more than one transplant and patients in acute cellular rejection were excluded. LVEDP measurement on cardiac catheterization was used to stratify patients into two groups (< 12 and ≥12 mm Hg) with and without diastolic dysfunction. Echocardiographic parameters including mitral E wave velocity, E wave deceleration time, E' septal wall velocity, E' lateral wall velocity, pulmonary S and D wave velocity, and isovolumetric relaxation time were compared between groups. Statistical analysis consisted of student t-test and Chi-square test (SPSS ver. 22). **RESULTS:** Our cohort included 56 patients with 50% males. The mean (SD) age at the time of echo was 11.6 (5.4) years and the follow up duration after HT was 7.4 (4.3) years. The primary diagnosis for HT was cardiomyopathy in 35 (63%) and congenital heart disease in 21 (37%) subjects. Eleven (19.6%) patients had LV diastolic dysfunction as defined by an LVEDP ≥12 mmHg. The two groups were similar in age, and gender distribution. There were no statistically significant differences between these two groups in the various echocardiographic parameters. **CONCLUSIONS:** Echocardiographic parameters did not discriminate between groups of HT recipients with and without increased LVEDP on cardiac catheterization, suggesting that these measures may not be utilized to predict LVEDP accurately in this population.

Table: Clinical, demographic, and echocardiographic parameters with Diastolic Dysfunction

Parameters (mean ± 1 SD)	LVEDP <12 (n= 45)	LVEDP ≥ 12 (n=11)	p value
Age at the time of study (years)	11.8 ± 5.5	10.8 ± 5.5	0.59
Age at transplant (years)	4.8 ± 5.7	2.2 ± 3.8	0.08
Follow up duration (years)	7.0 ± 4.4	8.6 ± 4.0	0.27
Gender (male)	24 (53%)	4 (36%)	0.25
Height (cm)	142 ± 26	131 ± 27	0.22
Weight (kg)	47.5 ± 24.4	34.2 ± 16.0	0.05
BSA	1.28 ± 0.46	1.01 ± 0.49	0.14
Heart rate (bpm)	94 ± 15	105 ± 21	0.16
E wave velocity	95 ± 18	107 ± 38	0.14
E deceleration time	0.13 ± 0.03	0.12 ± 0.04	0.65
Isovolumetric relaxation time	0.06 ± 0.01	0.05 ± 0.01	0.34
E/E' Septal Ratio	10.5 ± 3.7	11.8 ± 4.1	0.46
E/E' Lateral Ratio	8.4 ± 2.7	10.4 ± 4.1	0.26
Pulmonary vein S wave velocity	46.9 ± 14.3	54.4 ± 21.9	0.49
Pulmonary vein D wave velocity	53.7 ± 12.5	56.9 ± 12.8	0.55

P1-064

Using Simultaneous Multi-Chamber Strain Analysis to Assess the Interchamber Coupling in Patients with Repaired Tetralogy of FallotLing Li¹, Mary Craft¹, Jawad Najdawi¹, Shelby Kutty¹, Berthold Klas², John Cramer¹, David Danford¹. ¹University Of Nebraska Medical Center; Children's Hospital and Medical Center, Omaha, NE; ²TomTec Corp., Unterschleißheim, Germany

Background: The feasibility and reliability of simultaneous multi-chamber myocardial deformation (SMCMD) analysis from the same cardiac cycle has not been fully validated in congenital heart disease. To test the hypothesis that SMCMD can detect strain abnormalities in congenital heart disease, we used 2D echocardiographic speckle tracking to acquire SMCMD in patients with tetralogy of Fallot, and compared the results with those of normal subjects. **Methods:** There were 80 subjects (40 repaired tetralogy of Fallot: age 15.2±9.2, 20 were male; and 40 age and gender matched controls) in whom apical 4-chamber views containing both ventricles and atria in the same sector were available. A single observer performed deformation analysis on all 4 chambers within in the same cardiac cycle (2D CPA, TomTec). The derived endocardial contours and deformation measurements were then exported to ASCII text files. The text files were then imported into a customized Excel (Microsoft Corp., Redmond, WA, USA) spreadsheet for further analysis and structured data management. Deformation indices of right atrium (RA), left atrium (LA), right ventricle (RV) and left ventricle (LV) were computed from the spatiotemporal data. Student t-test was applied to compare measurements between normal and tetralogy of Fallot groups. **Results:** The peak RV, RV free wall, LA and RA global longitudinal strain were all reduced in tetralogy of Fallot compared to controls. The RV/LV, RA/LA, LA/LV and RA/RV strain ratios were lower in tetralogy of Fallot than in controls. Both RV septal and lateral annulus excursion and LV septal annulus excursion were decreased in tetralogy of Fallot relative to controls, whereas LV lateral annulus excursion was no different between groups. RV area, length and mid diameter were larger in tetralogy of Fallot than controls both in the end-diastole and end-systole (**Table**). **Conclusions:** SMCMD is feasible in patients with tetralogy of Fallot, and reveals abnormal strain patterns in both the right and left heart. Technology allowing simultaneous acquisition of strain data from all cardiac chambers may be particularly advantageous in understanding the interchamber coupling in congenital heart disease.

Poster Session 1 (P1)

Sunday, June 23, 2019

		Tetralogy of Fallot (N=40)	Controls (N=40)	p value
Global longitudinal strain (%)	LV	-23.0±2.7	-25.6±2.9	<0.001**
	RV	-24.4±5.0	-30.0±4.2	<0.001**
	RV free wall	-27.8±6.5	-33.3±4.9	<0.001**
	LA	29.2±5.8	36.4±7.3	<0.001**
	RA	28.9±6.7	42.6±9.5	<0.001**
Strain ratio	RV/LV	1.07±0.23	1.17±0.17	0.0360*
	RA/LA	1.01±0.26	1.22±0.31	<0.001**
	LA/LV	1.28±0.24	1.43±0.28	0.0038*
	RA/RV	1.21±0.33	1.51±0.35	<0.001*
Annulus excursion (mm)	LV septal	9.8±2.5	13.1±2.9	<0.001**
	LV lateral	14.1±3.1	15.1±3.1	0.0760
	RV septal	9.6±2.7	14.7±3.6	<0.001**
	RV lateral	13.1±3.4	20.3±4.2	<0.001**
End-diastole	RV area (cm ²)	26.0±9.9	19.7±7.2	0.0020*
	RV length (mm)	82.5±17.4	73.5±15.3	0.0313*
	RV mid diameter (mm)	39.3±7.5	31.2±6.7	<0.001**
End-systole	RV area (cm ²)	16.1±8.9	10.6±4.3	<0.001**
	RV length (mm)	65.9±16.3	53.4±12.6	<0.001**
	RV mid diameter (mm)	30.0±6.8	23.0±5.2	<0.001**
Fractional area change (%)	LV	44.6±4.5	47.4±4.6	0.0238*
	RV	39.7±12.5	46.3±6.0	0.0055*

Parameters (mean±SD)	RVEDVi ≥150 ml/m ² (n=19)	RVEDVi < 150 ml/m ² (n=28)	p value
Age at echo (years)	26.6 ± 10.2	23.1 ± 10.5	0.25
Height (cm)	160.8 ± 40.8	164.5 ± 11	0.29
Weight (kg)	70.84 ± 29.5	65.31 ± 19.3	0.49
BSA (m ²)	1.84 ± 0.35	1.71 ± 0.26	0.26
SBP in mmHg	117.8 ± 10.9	122.5 ± 21.5	0.72
DBP in mmHg	64.8 ± 10.2	67 ± 15.2	0.81
Heart rate (bpm)	70 ± 18	70 ± 13	0.98
E/A ratio	2.86 ± 3.87	2.15 ± 0.87	0.35
MVDT (m sec)	0.131 ± 0.04	0.138 ± 0.04	0.57
E/E' septal annulus MV	14.1 ± 19.03	10.99 ± 3.10	0.46
E/E' lateral annulus MV	8.45 ± 13.2	6.11 ± 3.72	0.38
LV MPI	0.41 ± 0.17	0.38 ± 0.15	0.47
LV MPI septal annulus MV	0.42 ± 0.24	0.47 ± 0.33	0.61
LV MPI lateral annulus MV	0.40 ± 0.07	0.39 ± 0.12	0.84
RVOT gradient (mmHg)	22 ± 5	26.3 ± 11	0.89
TAPSE 2D (cm)	1.10 ± 0.62	1.23 ± 0.42	0.91
TAPSE/RVSP (cm/Hg)	0.034 ± 0.17	0.035 ± 0.13	0.94
RVSP mmHg	38 ± 6	43 ± 12	0.13

P1-066

Fetal Right-Left Discrepancy: Is That Normal?

Allison K. Black¹, Timothy P. Canavan², Jennifer A. Johnson¹, ¹UPMC Children's Hospital of Pittsburgh, Pittsburgh, PA; ²Magee Women's Hospital, Pittsburgh, PA

Background: Prenatal diagnosis of right left (R-L) ventricular size discrepancy has been reported as a marker to predict risk of postnatal coarctation (COA). Assessment of R-L discrepancy has been used in cases of fetal cardiology referral late in pregnancy, when difficulty identifying the aortic arch forces the physician to rely on secondary markers to predict risk of COA. R-L discrepancy can have a high proportion of false positives leading to parental pre-delivery stress and inappropriate uses of resources. In this study, we sought to identify prenatal markers that predict neonatal aortic arch anatomy, to help guide delivery management. **Methods:** Retrospective review from 9/2014 to 10/2018 of all patients diagnosed with fetal R-L discrepancy with concern for COA at a tertiary care referral center. Fetal echocardiogram characteristics were abstracted and correlated with the postnatal aortic arch echocardiogram findings. Fetal measurements including ventricular width, mitral (MV), tricuspid (TV), pulmonary (PV) and aortic valve (AV) annulus diameters were corrected for gestational age using z-scores. These measurements and ratios were compared between patients with and without COA. Logistic regression and Wilcoxon ranked sum testing was used to analyze the data and a p-value of >0.05 was considered statistically significant. **Results:** Thirty-nine patients with R-L discrepancy on fetal echocardiogram were identified. In 30 (77%) fetal patients, COA could not be ruled out, and 9 (23%) fetal pts were diagnosed with COA. Of the 30 pts where COA could not be ruled out, only 4 (13%) had postnatal COA (Table 1). In subset analysis, a lower MV/TV ratio was predictive of COA and patients with a ratio approaching 1 had normal arch anatomy (p=0.022). An aorta to pulmonary valve annulus ratio less than 0.6 as well as an aortic valve Z-score less than -2 were also statistically associated with an increased risk for COA on postnatal echo (both p<0.001). **Conclusion:** Fetal determination of COA by R-L discrepancy continues to be a challenge with a high false positive rate. Practitioners can have a lower index of suspicion for COA in fetuses with similar mitral and tricuspid annular sizes and an aortic valve-pulmonary valve ratio greater than 0.6. Further investigation in a larger cohort is needed to validate these findings.

P1-065

Does Right Ventricular Dilation Correlate with Biventricular Dysfunction in Patients with Repaired Tetralogy of Fallot?

Jyothisna Akam-Venkata, Chennai Sriram, Deemah Mahadin, Pooja Gupta, Sanjeev Aggarwal. Children's Hospital of Michigan/Wayne State University School of Medicine, Detroit, MI

Background: Patients with repaired Tetralogy of Fallot (rTOF) are at risk of chronic right ventricular (RV) volume overload and eventually biventricular dysfunction. Our aim was to compare the echocardiographic indices of biventricular function in rTOF patients with and without RV dilation on magnetic resonance imaging (MRI). **Methods:** This was a single center retrospective analysis of rTOF patients who underwent cardiac MRI and an echocardiogram within a 3 month period. Patients with pericardial effusion, arrhythmia and sub-optimal data were excluded. Echocardiographic indices assessed were a) left ventricular (LV) diastolic function (E/A ratio, E/E' ratio at the septal and lateral annulus of the mitral valve, deceleration time of the mitral valve) b) global function (myocardial performance index MPI using spectral and tissue Doppler) and c) RV systolic function [Tricuspid Annular Plane Systolic Excursion (TAPSE) by 2D echocardiogram and TAPSE/ RVSP right ventricular systolic pressure ratio]. The RV end-diastolic and end-systolic volumes were measured in the end-systolic and end-diastolic phase on steady state free precision (SSFP) cine images acquired in a short axis plane on cMRI using breath hold technique. RV dilation was defined as indexed end-diastolic volume ≥ 150 ml/m². Echocardiographic indices were compared between groups with and without dilated RV using student t-test and Chi-square test. **Results:** The study cohort (n=47) showed evidence of LV diastolic dysfunction, with elevated E/A ratio and elevated E/E' ratio at the septal and lateral mitral annulus as well as global LV dysfunction indicated by increased MPI derived from spectral and tissue Doppler of the septal and lateral annulus of the mitral valve. RV dysfunction was present in all rTOF patients as evidenced by decreased TAPSE and abnormal TAPSE/RVSP ratio. (Table 1) All echocardiographic indices were similar in the 2 group of patients with (n=19) and without (n=28) RV dilation. **Conclusion:** Patients with rTOF have abnormal left ventricular diastolic and global function along with right ventricular systolic dysfunction. However, these functional measures do not correlate with the degree of right ventricular dilation. Further studies are needed to evaluate the determinants of biventricular dysfunction in this population.

Poster Session 1 (P1)

Sunday, June 23, 2019

Table 1:

Fetal and postnatal demographics	Normal (N=26)	Arch Anomaly (N=13)
Gestation age first echo (weeks)	27.5 (±5.7)	30.0 (±6.1)
Gestation age last echo (weeks)	33.2 (±3.3)	32.8 (±3.3)
Mode # fetal echoes	2 (46%)	3 (38%)
Congenital heart disease	14 (54%)	13 (100%)
COA only	0 (0%)	2 (15%)
Interrupted arch and VSD	0 (0%)	2 (15%)
VSD	5 (36%)	2 (15%)
Bicuspid aortic valve (BAV)	1 (7%)	3 (23%)
Left superior vena cava (LSVC)	4 (29%)	0 (0%)
Atrial septal defect	2 (14%)	0 (0%)
BAV with VSD	0 (0%)	1 (8%)
BAV with LSVC	1 (7%)	2 (15%)
BAV with parachute mitral valve	0 (0%)	1 (8%)
Pulmonary stenosis	1 (7%)	0 (0%)
Other fetal findings	6 (20%)	3 (23%)
Genetic syndromes	4 (13%)	1 (8%)
Intrauterine growth restriction	1 (4%)	0 (0)
Fetal anemia	1 (4%)	0 (0)
Delivery hospital		
Main hospital	22 (85%)	11 (85%)
Local hospital	4 (15%)	2 (15%)
Miles from delivery hospital		
Main hospital	62(10-236)	61 (6-140)
Local hospital	10 (3-21)	12 (7-16)
Mode # transthoracic echoes to diagnosis	2 (50%)	1 (69%)

P1-067

Fetal Predictors of Coarctation of the Aorta - Has a Solution Been Found?

Ryan Boggs, Stephanie Philipp, Matthew Gurka, Lindsay Thompson, Rebecca Murcado, Leah Breault, Dalia Lopez-Colon, Himesh Vyas, Jennifer Co-Vu. University of Florida, Gainesville, FL

Background: Although prenatal diagnosis of congenital heart diseases (CHD) via fetal echocardiography (ECHO) has improved outcomes, its ability to accurately diagnose coarctation of the aorta (CoA) remains limited. Multiple studies have sought fetal ECHO predictors of CoA with minimal success. Our study aimed to identify fetal ECHO predictors for CoA in a single cohort of patients. **Methods:** An IRB-approved retrospective review of fetal ECHOs obtained at our institution from 1/2005 to 3/2018 with prenatal suspicion of CoA was performed. ECHOs were blindly analyzed using all previously published fetal ECHO predictors of CoA, which included right and left heart structures and their ratios, aortic isthmus peak systolic velocity, reversed flow in the aortic arch, arch hypoplasia, aortic isthmus/ductus arteriosus angle, ascending aorta (AAo)/descending aorta angle, transverse aorta /descending aorta angle, and the ratio of the aortic arch diameter at the left subclavian artery and left carotid artery to left subclavian artery distance. These parameters were compared between patients with and without a postnatal diagnosis of CoA. The predictive ability of the fetal ECHO values was compared using area under the receiver-operating-characteristic curves (AUC). **Results:** During the study period, 64 fetuses had prenatal suspicion of CoA; postnatally, 15 had and 43 did not have CoA with 6 excluded due to complex CHD. The median gestational age at time of fetal ECHO for both groups was similar (p=0.32). The following fetal ECHO parameters exhibited the strongest ability to predict postnatal CoA (AUC > 0.70): mitral valve Z-score (AUC=0.76), aortic valve Z-score (AUC=0.78), AAo Z-score (AUC=0.75), pulmonary valve/aortic valve diameter (AUC=0.77), and main pulmonary artery/AAo diameter (AUC=0.74). Two parameters with a high specificity and low sensitivity in predicting CoA were flow reversal in the aortic arch (specificity 89%, sensitivity 9%) and an aortic isthmus to ductus arteriosus ratio of <0.5 (specificity 88%, sensitivity 50%). **Conclusion:** This is the first study to analyze all previously published fetal ECHO predictors using a single cohort. While the gold standard for fetal ECHO prediction of postnatal CoA diagnosis remains elusive, the results of our study validate the current practice of using multiple fetal ECHO indices of left sided structures for prediction of postnatal CoA diagnosis. A larger multicenter study is warranted in the further analysis of fetal ECHO measurements and development of a multi-parametric model that can be used as an objective risk assessment for postnatal CoA diagnosis.

P1-100

Correlation of Internal Jugular and Subclavian Vein Diameter Variation on Bedside Ultrasound with Invasive Right Heart Catheterization

Gaurang N. Vaidya, Shahab Ghafghazi. University of Louisville, Louisville, KY

Background: Accurate estimation of fluid status is important in cardiology patients, however, this estimation is often confounded by the body habitus, inaccurate daily input/output charting and inaccurate daily weight measurement. Ultrasound of internal jugular vein (IJV) and subclavian vein (SCV) is comparatively easy skill to acquire for trainees and hospitalists. The study hypothesizes that respiratory variations in IJV/SCV diameters are reliable estimates for the patient's volume status. **Methods:** Patient's scheduled for

right and left heart catheterization were prospectively recruited and portable ultrasound imaging of their IJV and SCV was performed immediately prior to the procedure. Patient was positioned supine and diameter variation noted with resting respiration. Collapsibility was assessed with sniff maneuver. IJV was imaged at the apex of sternocleidomastoid and SCV at the lateral 1/3rd of clavicle. Maximum IJV and SCV diameters were indexed to body surface area (IJV/BSA and SCV/BSA). **Results:** Forty-one patients have been enrolled so far, mean age 58 years, mean BSA 1.94m², right atrial pressure (RA) range 1 - 20mmHg and pulmonary capillary wedge pressure (PCWP) range 4 - 48mmHg. Range of IJV/BSA was 7 - 81 mm/m² and SCV/BSA was 8 - 86 mm/m². SCV could not be imaged in 6 patients. Patients with completely collapsible IJV on sniff maneuver had lower RA pressure (4.8 vs 11.3mmHg, p=0.01) and lower PCWP (12.5 vs 19.6mmHg, p=0.03). Similarly, collapsible SCV had lower RA (5.4 vs 10.6mmHg, p=0.01) and PCWP (11.5 vs 21.2mmHg, p=0.01). Elevated RA pressure (>=10mmHg) patients showed less percent variation in IJV diameter with resting respiration (12 vs 38%, p=0.01) [table 1]. Similarly elevated PCWP >12 mmHg had less percent variation in IJV (16 vs 39%, p=0.01). IJV/BSA positively correlated with left ventricular end-diastolic pressure (R=0.616, p=0.01). **Conclusion:** This ongoing study noted positive correlation between fluid status with IJV and SCV diameters (absolute and respiratory variation).

P1-101

Safety of Echo-Guided Pericardiocentesis with Elevated International Normalized Ratio

Alexander J. Ryu, Garvan Kane, Sorin V. Pislaru, Annap Lekhakul, Jeffrey B. Geske, Sushil A. Luis, Hector I. Michelenia, Vuyisile T. Nkomo, Jeremy J. Thaden, Larry J. Sinak. Mayo Clinic, Rochester, MN

Background: Limited data exist on the safety echo-guided pericardiocentesis in patients with coagulopathy. Existing coagulopathy is generally considered a relative contraindication to pericardiocentesis. **Methods:** We reviewed all pericardiocenteses performed between January 1, 2007 and December 31, 2016 at a single center. Complication rates were compared between cases with international normalized ratio (INR) ≤2.0 and INR >2.0. For cases in which no INR was documented, we assumed the INR to be normal. For cases in which INR was documented, we recorded the value most temporally proximal to the procedure, except in cases where anticoagulation reversal with vitamin K and/or fresh frozen plasma was administered after the pre-procedure INR but prior to pericardiocentesis; in those cases we recorded the lower of the two periprocedural INRs. We paid particular attention to hemorrhagic complications and whether procedures were deemed emergent. We utilized a one-sided, two-proportion Z-test to compare complication rates among INR groups. **Results:** Our review yielded 1197 echo-guided pericardiocenteses performed on 1097 unique patients. Mean age at the time of pericardiocentesis was 62 ± 16 years; 43% of pericardiocenteses were performed on women. INRs ranged from 0.8-8.3. 15 cases had an INR >3.0. The overall complication rate was 1.9%. Among cases with INR ≤ 2.0 (n = 1043), the complication rate was 1.7%, compared to 3.2% in those with INR >2.0 (n = 154, p = 0.09). The hemorrhagic complication rate in cases with INR ≤ 2.0 was 0.7%, compared to 1.9% in those with INR >2.0 (p = 0.04). Overall, 32% of cases were deemed emergent. Excluding emergent cases, hemorrhagic complication rates were 0.3% in the INR ≤ 2.0 group compared to 1.3 % in the INR >2.0 group (p = 0.09). **Conclusion:** Elevated INR is associated with a small, significant increase in hemorrhagic, but not overall, complications in echo-guided pericardiocentesis. Bleeding rates however remain low.

P1-103

Echo in Extracorporeal Membrane Oxygenation

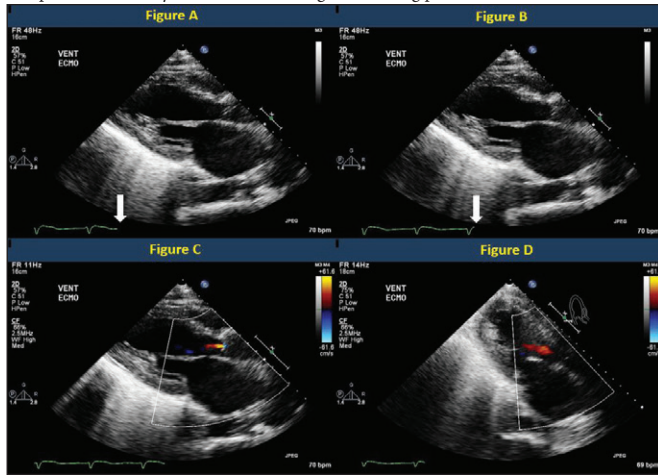
Tal Dulberger¹, Kameswari Maganti¹, David Mehlman^{1,2}. ¹Northwestern Memorial Hospital, Chicago, IL; ²Feinberg School of Medicine, Chicago, IL

Clinical Presentation: A 49-year-old woman with Lupus on chronic steroids who was admitted with diarrhea and vomiting. She was cachectic with recent significant weight loss. Workup revealed acute bilateral deep venous thromboses, and a ventilation-perfusion scan with intermediate probability for pulmonary embolism. She was started on anticoagulation. A few hours later, she was found to be unresponsive. Cardiopulmonary resuscitation was initiated for cardiac arrest due to asystole. Twenty minutes later, Veno Arterial extracorporeal membrane oxygenation (VA ECMO) via right femoral vein/artery was performed at bedside. A transthoracic echo (TTE) was performed to plan an Impella device placement. **Imaging Findings:** TTE demonstrated a mildly dilated left ventricle (LV) with extreme degree of biventricular systolic dysfunction. The mitral valve was immobile in an open position due to tethering from LV enlargement and systolic dysfunction (Figure A, B). No Doppler flow signal is identified across the mitral valve. The aortic valve was also immobile in a closed position with continuous mild aortic regurgitation (Figure C, D). **Role of Imaging in Patient Care:** Echo is an important, readily available tool that can provide a detailed assessment of ventricular and valvular function, presence of intra-cavitary spontaneous echo contrast and thrombus formation. TTE in our patient revealed significant LV dysfunction despite VA ECMO with a need to escalate the therapy for aggressive decompression of LV using an Impella device. **Summary/Discussion Points:** Echo plays a crucial role of ECMO support. It allows evaluation of cardiac chamber size, function, and adequate emptying of the ventricles. In peripheral VA ECMO, the retrograde aortic blood flow competes with stroke volume ejected from the LV. A closed aortic valve will ultimately lead to LV distention and thrombus formation. Additionally, increased

Poster Session 1 (P1)

Sunday, June 23, 2019

afterload can worsen pre-existing aortic regurgitation and LV distension, potentially hindering recovery. At the time of initiation, it can confirm the diagnosis and help choose between VV and VA ECMO. It guides clinicians in the management of these patients. Once the patient is on ECMO, it provides information pertaining to recovery and possible complications. Finally, it is essential during the weaning phase of VA ECMO.



P1-104

Development and Testing of an Online Cardiac Ultrasound Learning Module for Medical Students and Novice Users

Salwa Nihal¹, Terry Li¹, Joshua Durbin², Abbas Rizvi¹, Stephen C. Pang¹, Amer Johri^{1,2}. ¹Department of Biomedical and Molecular Sciences, Queen's University, Kingston, ON, Canada; ²Division of Cardiology, Kingston General Hospital, Kingston, ON, Canada

Background: Advancements in Ultrasound (US) technology have succeeded in the development of more portable, accessible and cost-effective devices such as point-of-care ultrasound (POCUS) that are being used in every specialty of medicine including cardiovascular medicine. Despite the unanimous need of US skills, the integration of US teaching in Canadian medical schools are variable and underdeveloped. This study aimed to develop a novel online learning module that incorporates cadaveric material into cardiac US, and evaluate its effectiveness among first year medical students. **Methods:** Images were created after harvesting of cadaveric hearts, embalming, fixing and finally sectioning to create mirrored images of the views obtained from cardiac US records. Additionally, illustrations with detailed labeling were also added for each of the US view. Ninety-seven first-year medical students from Queen's University School of Medicine participated in this study after completion of their cardiovascular anatomy unit. Students performed a pretest before and a posttest after receiving a presentation of the module. Each test consisted of five cardiac anatomy questions and five US-oriented questions. Results of the pretest and posttest were analyzed by paired t-test using SPSS. Lastly, they completed a survey questionnaire which was used to enumerate their feedback regarding the Module and document their response for implementation of such imaging modalities in the medical curriculum. **Results:** After the learning session, students' overall posttest scores improved to 60% as compared to pretest scores which was 53% with the p-value of < 0.001. Survey questionnaire results revealed that the majority of students (96.9%) showed great desire and enthusiasm towards learning imaging techniques and its integration in the undergraduate medical curriculum. Majority of the students (88.7%) suggested this session was useful and helped them understand the spatial anatomy of the heart. **Conclusion:** The present study demonstrates that early exposure to US learning can be a useful adjunct to teach anatomy in a clinical context to medical students. It can help future clinicians to be better prepared and skilled in using these US devices in their practice.

P1-105

Moderated Poster

Transthoracic Echo Derived Gradients Immediately After SAPIEN S3 Valve Placement do not Correlate with Gradients Measured at 24 Hours and 30 Days Post Transcatheter Aortic Valve Replacement

Peter Auteri, Steven A. Guidera, David G. Boland, Richard Mascolo, Craig Kesack, Jennifer Harrar, James B. McClurken, Joseph S. Auteri, Francis W. Grzywacz. Doylestown Hospital, Doylestown, PA

Background: Transcatheter Aortic Valve Replacement (TAVR) has evolved over the past decade with broader clinical indications for patients with severe aortic stenosis. Transthoracic Echo (TTE) has emerged as the comprehensive tool to analyze the performance, placement and function of these new valves both intra-procedure and post-procedure. Limited data has been reported on intra-procedure TAVR gradients immediately post deployment. **Methods:** From 130 consecutive patients, we retrospectively collected TTE mean aortic valve gradients intra-procedure, Day 1 post-procedure, and Day

30 post-procedure on 23mm, 26mm, and 29mm Edwards Sapien S3 balloon expandable valves. Intra-procedure gradients were obtained post valve deployment immediately after normalization of blood pressure and rhythm. Gradients were obtained via the standard five chamber apical window. Paravalvular aortic regurgitation was assessed via the standard short-axis, three chamber, and five chamber views. **Results:** The patient cohort was 56% male with a mean age of 82.8, STS Score of 5.96%, LVEF of 54.2±12.8% and mean aortic gradient of 44.89±13.80mmHg. All valves were successfully deployed. The intra-procedure mean gradient for all valve sizes was 5.48 ± 2.29mmHg. This result was significantly lower than the Day 1 mean gradient of 12.34 ± 5.08mmHg (p<0.01) and Day 30 mean gradient of 12.58 ± 5.59mmHg (p<0.01). These results were consistent across the 23, 26, and 29mm valve sizes (p<0.01). There was no significant difference in estimated LVEF intra-procedure (55.7 ± 10.9%), Day 1 (56.2±10.8%), or Day 30 (55.9±10.9%). 95% of patients had mild paravalvular aortic regurgitation or less across all groups and time points. 30-day mortality for this cohort was 0%. **Conclusion:** Gradients measured after Sapien S3 valve placement are significantly lower immediately post deployment as compared to Day 1 and Day 30. These results were not related to changes in LVEF or aortic regurgitation, and were not associated with short term mortality. These surprisingly low gradients may result from immediate post-procedure changes in loading conditions or new laminar flow velocity profiles. Intra-procedure TTE derived gradients do not accurately predict gradients measured at one and thirty days post procedure.

Table 1. Mean Aortic Valve Gradients (mAVG) of 23mm, 26mm, 29mm Balloon Expandable Valves Pre-procedure, Intra-procedure Post Deployment, 1 Day, and 30 Day

	23mm	26mm	29mm	All Sizes
Pre-procedure	48.57±12.39 (48)	44.70±15.20 (48)	39.97±12.56 (34)	44.89±13.80 (130)
Intra-procedure	6.18±2.59 (48) *	5.48±2.17 (48) *	4.49±1.61 (34) *	5.48±2.29 (130) *
Day 1	14.06±4.85 (48)	12.52±5.51 (48)	9.66±3.55(34)	12.34±5.08 (130)
Day 30	14.22±4.95 (48)	12.27±6.26 (48)	10.71±4.86 (34)	12.58±5.59 (130)

* (p<0.01) Intra-Op mAVG vs Day 1, and Day 30 across all sizes by paired t-test

P1-106

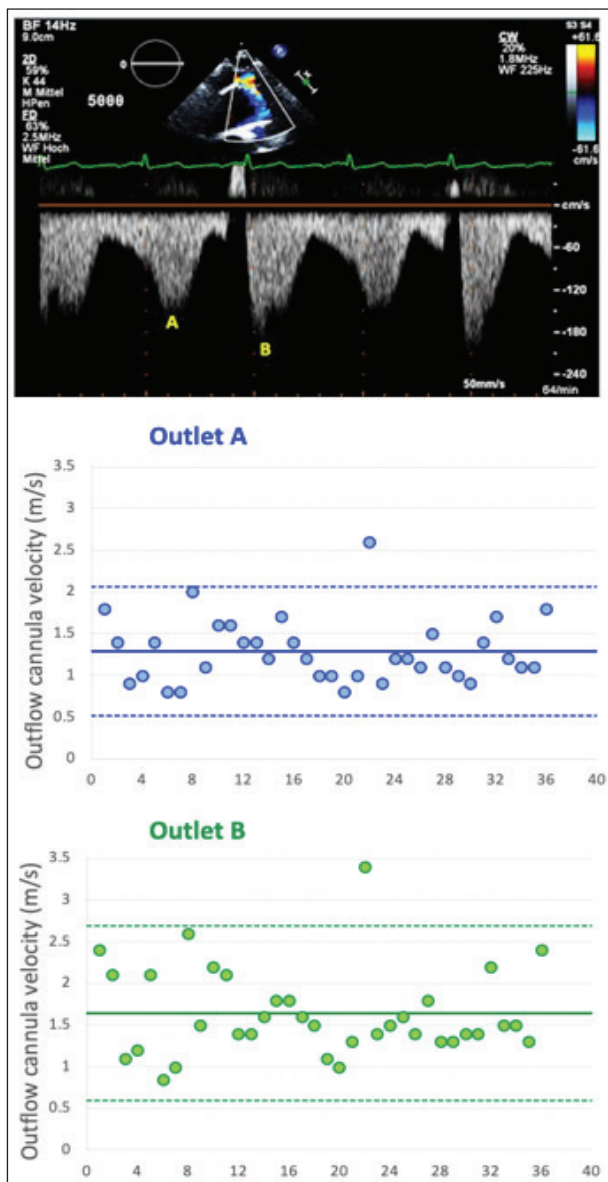
Normal Reference Values of Outflow Cannula Velocities for the New HeartMate III Left Ventricular Assist Device

Eric Kruse, Roberto M. Lang, Victor Mor-Avi, Gabriel Sayer, Takeyoshi Ota, Valluvan Jeevanandam, Nir Uriel, Karima Addetia. University of Chicago, Chicago, IL

Background: Echocardiographic assessment of the left ventricular assist device (LVAD) function includes Doppler interrogation of the outflow tract cannula (OTC). The OTC is anastomosed to the ascending aorta and conducts blood from the LVAD pump to the systemic aorta. Elevated Doppler-derived peak flow velocity in the OTC can signal obstructed flow or cannula malposition. Recently, a new HeartMate III (HMIII) LVAD has been approved for clinical use. There are no cut-off values to identify abnormally high OTC velocities in this type of LVAD. We sought to establish the normal range for OTC velocities for the HMIII. **Methods:** 36 patients with normally functioning HMIII LVADs underwent transthoracic echocardiograms (TTE) with OTC assessment from the right parasternal approach. Continuous wave Doppler peak velocity of the LVAD OTC was measured as native pump flow(A) and post artificial pulse (B) (Figure Left). These patients were used to generate the normal range of OTC velocity (defined as mean±2SD) (Figure Right). **Results:** The outflow Doppler cannula tracing exhibits a distinct bimodal pattern which represents the artificial pulse, which allows for a complete washing of the pump, eliminating stasis as a cause of pump thrombosis. OTC peak velocity for the HMIII LVAD was 1.3±0.4 m/s(A) and 1.6±0.5 m/s(B), with upper reference limits of 2.1 m/s and 2.6 m/s, respectively. **Conclusions:** Since OTC values amongst models of LVADs are different, we hereby report the OTC values for the next generation magnetically levitated HMIII LVAD.

Poster Session 1 (P1)

Sunday, June 23, 2019



P1-107

Initial Echocardiographic Experience with Latest Generation MitraClip XTR

Daniel R. Harland, Tanvir K. Bajwa, Suhail Q. Allaqaband, Bijoy K. Khandheria, Renuka Jain. Aurora Cardiovascular Services, Aurora Sinai/Aurora St. Luke's Medical Centers, Milwaukee, WI

Background: Percutaneous edge-to-edge mitral valve repair (PMVR) using the Abbott MitraClip has become a safe and effective option for inoperable patients with severe mitral regurgitation. In mid-2018, a newer "XTR" version of the clip was made available. We report on our experience, one of the largest in the nation, using the XTR device, particularly how it pertains to intraprocedural echocardiographic imaging. **Methods:** We reviewed records of patients who underwent the XTR procedure. Comprehensive 2D, 3D and 4D transesophageal echocardiography was utilized during the procedure. Echocardiographic complexity of the procedure was estimated with a 4-point scale ranging from routine (1) to very complex (4). Clinical variables were queried from the electronic health record. All echocardiograms were reviewed retrospectively, and characteristics were documented. **Results:** There were 29 patients with severe mitral regurgitation who were deemed inoperable and suited for PMVR with a MitraClip XTR device. Procedural success was 100%. Eighteen of the 29 patients were female (62%). Mitral valve anatomy was deemed complex in 12 (41%) cases. The mean procedure time was 56.8±20.8 min. The XTR device was easily visualized in multiple configurations, and though we noted greater acoustic shadowing with this device, it did not preclude successful deployment. With the new device, successful first-time grasp was achieved in 20 patients (69%). Multiple clips were

deployed in 9 cases (31%). Chordal entanglement was noted in 2 (6%) cases. Following deployment, 27 cases (93%) demonstrated 2+ or less mitral regurgitation. Transesophageal echocardiography was used in all cases; owing to body habitus and acoustic shadowing of the device, transthoracic echocardiography was used in 1 case for post-deployment assessment. **Conclusion:** Our study is one of the first descriptions of echocardiographic characteristics after implantation of the newest generation of the MitraClip XTR device. The XTR shares many echocardiographic characteristics with the earlier generation. Using the new device, we noted easier grasping and successful clinical outcomes despite more acoustic shadowing.

P1-108

Transcatheter Ductal Closure in the Very Low Birth Weight Infant Assisted by Transthoracic Echocardiography: Role and Benefit

Jay Yeh, Andrew Pelech, Frank Ing. UC Davis Health, Sacramento, CA

Background: Transcatheter occlusion of the patent ductus arteriosus (PDA) is the standard of care, but in the fragile, very low birth weight (VLBW) infant this procedure can be challenging. Transthoracic echocardiography (TTE) has been used to assist in this procedure but the role and benefits of intraprocedural TTE are not well defined. **Methods:** We reviewed TTEs performed during PDA occlusion in VLBW infants from 3/18-1/19. PDA dimensions measured by TTE and angiography were compared. Role and impact of TTE to select and determine PDA device position and assessment of flow in branch pulmonary arteries (BPA) and aorta before and after device release were also evaluated. **Results:** 15 VLBW infants (median birth wt. 783 gm, range 485-1429) underwent successful transcatheter PDA occlusion (median wt. at cath 1050 gm, range 755-2540). All pts had successful PDA occlusion using the Micro Vascular Plug (MVP™). Measurements of the PDA by TTE and angiography were comparable. Comparing TTE and angiography measurements, the mean PDA minimum diameter was 0.228 ± 0.054 cm vs. 0.233 ± 0.073 cm ($p = 0.74$), and mean PDA length was 1.079 ± 0.349 cm vs. 1.108 ± 0.284 cm ($p = 0.72$). Bland Altman analysis demonstrated TTE PDA diameter was on average 0.004 cm less than by angiography (95% CI -0.109 to 0.09 cm), with 0.1 cm above or below the TTE PDA diameter not being clinically significant. The two methods of PDA diameter measurements have good clinical interchangeability. Device selection based on TTE measurements were not altered by angiography. TTE evaluation of flow across BPA and aorta during delivery confirmed good flow before and after release, thereby eliminating need for arterial sheath and additional radiation exposure and contrast use. Median fluoroscopy time was 7.7 min (range 5.3 to 17.8 min). Median contrast used was 3.5 ml (range 0.88 to 13.5 ml). Suboptimal device positioning was discovered by TTE during delivery in 4 pts. Successful repositioning of device without additional angiography was possible using TTE. Following device release, there were no pts with significant obstruction across the BPAs and aorta. All pts showed complete PDA occlusion by TTE. **Conclusion:** Intraprocedural TTE serves an important role in transcatheter PDA occlusion in the VLBW infant. PDA measurements by TTE closely approximate those obtained by angiography and device selection based on TTE was not altered following angiography. Real-time TTE information eliminates need for an arterial sheath, minimizes fluoroscopy time and use of contrast, allows for immediate assessment of obstruction, and guidance in device repositioning.

P1-109

Elevated Left Atrial Pressure is Associated with Iatrogenic Atrial Septal Defect Secondary to Transseptal Puncture Following Left Atrial Appendage Closure

Hoang Nguyen, Benita Tjoe. Santa Barbara Cottage Hospital, Santa Barbara, CA

Background: Transseptal puncture is often utilized in interventional cardiology and electrophysiology for procedures requiring left atrial access. This requires the use of large transseptal sheaths that can lead to residual iatrogenic atrial septal defects (iASD). We seek to investigate the incidence of iASDs following placement of left atrial appendage (LAA) closure devices for stroke prevention in patients with nonvalvular atrial fibrillation. We also investigated the association with mean left atrial pressure (mLAP) at the time of implantation. **Methods:** One-hundred twenty seven patients underwent successful implantation of LAA closure devices. A 12F transseptal sheath (14F outer diameter) was used for left atrial access following transseptal puncture. Upon access into the left atrial, mLAP was measured. These patients underwent transesophageal echocardiogram 45 days post-implant to access for peridevice leak. The interatrial septum was also assessed for iASDs. **Results:** Thirty-eight patients (29.9%) were found to have an iASD 45 days following the procedure. Interatrial shunting was predominantly left-to-right when an iASD was present. Mean left atrial pressure was statistically significantly higher in patients with iASDs than without (17.21 ± 5.31 mmHg vs. 15.04 ± 3.39 , $p=0.024$). There was no statistically significant association with age, sex, device size, presence of peridevice leak, or the presence of LAA thrombus. **Conclusion:** Elevated mean left atrial pressure is a predictor of iASD at 45 days following transseptal puncture using a 12F transseptal sheath.

Poster Session 1 (P1)

Sunday, June 23, 2019

P1-110

Short-Term Echocardiographic Outcomes of Patients Undergoing Transcatheter Mitral Valve-in-Valve Replacement

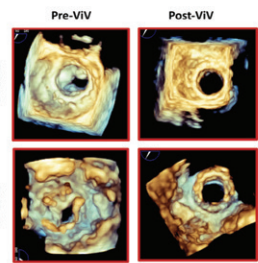
Akhil Narang¹, Amit Pursnani², Michael Salinger², Hyde Russell², Jorge Saucedo², Ted Feldman², Roberto M. Lang³, Mayra Guerrero². ¹Northwestern University, Chicago, IL; ²Northshore University Healthcare, Evanston, IL; ³University of Chicago, Chicago, IL

Background: Transcatheter mitral valve replacement (TMVR) using mitral valve-in-valve (MViV) procedure is a minimally invasive option for patients with failed surgical bioprosthetic mitral valves (MV), who are not considered candidates for repeat standard MV replacement due to high surgical risk. The goal of this study was to evaluate the 30-day (short-term) echocardiographic outcomes in patients undergoing MViV. **Methods:** 30 inoperable patients (age 76±10 years; 65% female) with degenerative bioprosthetic MV disease were enrolled in the MViV arm of the MITRAL trial (Mitral Implantation of TRANscatheter vaLves, NCT 02370511) and underwent transeptal TMVR MViV with a SAPIEN 3 aortic transcatheter heart valve (THV). Assessment included complete baseline transthoracic echocardiogram (TTE), procedural transesophageal echocardiogram (TEE), and 30-day TTE. **Results:** The mean Society of Thoracic Surgeons risk score was 10±7%. Each patient successfully underwent TMVR (Figure). 29/30 patients were alive at 30-day follow-up; one death was non-cardiovascular related. The left ventricular (LV) end-diastolic and end-systolic volumes improved from baseline to 30-day follow-up, while there was no change in LV ejection fraction (EF) (Table 1). The MV leaflet characteristics showed none or trivial central or paravalvular mitral regurgitation at 30-days (Table 2) and improved echocardiographic parameters of mitral stenosis (Table 3). **Conclusion:** In patients undergoing transcatheter MViV, short-term outcomes reveal high procedural success as defined by improved LV volumes, no change in LVEF, no significant residual central or paravalvular regurgitation or mitral stenosis. Future investigations examining the long-term echocardiographic outcomes of MViV are needed.

Table 1: Echocardiographic Parameters			
	Baseline	30 Day	P-Value
LVIDs (cm)	3±0.9	3.3±1.1	0.09
LVIDd (cm)	4.8±0.9	4.9±0.9	0.40
LV PVd (cm)	1.2±0.3	1.0±0.3	0.01
IVSd (cm)	1.2±0.3	1.2±0.3	0.70
LV Mass (gm)	195±111	208±97	0.40
LV EDV (ml)	125±63	112±52	0.01
LV ESV (ml)	60±51	54±42	0.04
LV EF (%)	56±14	55±14	0.87
LA Volume (ES) (ml)	120±52	111±65	0.52
RA Pressure (mm Hg)	8.7±6	5.9±4	0.05
RVPSP (mm Hg)	44±16	33±11	<0.01

Table 3: Mitral Stenosis Parameters			
	Baseline	Post-Procedure	P-Value
MVA (cm ² , PHT)	1.6±0.6	2.0±0.7	0.02
MVA (cm ² , Continuity)	0.9±0.4	1.6±1.0	<0.001
3D MVA (cm ² , TEE)	1.2±0.6	2.7±0.5	<0.001
Peak MV Gradient (mm Hg)	30±11	14±5	<0.001
Mean MV Gradient (mm Hg)	13±7	6±2	<0.001
VTI _{TRAP} /VTI _{LVOT}	4±1	2±1	<0.001

Table 2: Mitral Regurgitation			
	Baseline	30 Day	
Central MR	None/Trivial	40%	100%
	Mild	15%	0%
	Moderate	15%	0%
	Severe	30%	0%
Paravalvular MR	None/Trivial	96%	96%
	Mild	4%	4%
	Moderate	0%	0%
	Severe	0%	0%



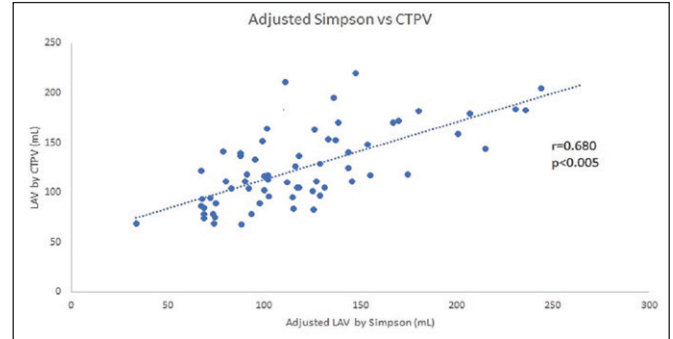
P1-111

Transesophageal Echocardiogram Systematically Underestimates Left Atrial Volume as Compared to Computed Tomography Pulmonary Venogram in Patients Undergoing Atrial Fibrillation Ablation

Vincenzo Trovato, Thura Harfi. The Ohio State University Wexner Medical Center, Columbus, OH

Background: Left Atrial (LA) volume (LAV) is an independent risk factor for cardiovascular disease and mortality. Transesophageal echocardiogram (TEE) is performed in many patients undergoing atrial fibrillation ablation procedure. However, accuracy of LAV measurement from TEE has not been evaluated. Therefore, we sought to investigate the accuracy of LAV by TEE compared to computed tomography pulmonary venogram (CTPV), the gold standard of LAV measurement. **Methods:** LAV from TEE measurements was compared to that obtained from CTPV done on the same day in 70 consecutive patients who underwent atrial fibrillation ablation. The TEE volumes were obtained from 0° and 90° views at end systole using both Simpson's method and area-length method ((LA area_{0°}*LA area_{90°}*0.85)/ LA length_{0°/90°}). LAV on CTPV was calculated via direct volumetric measurement by tracing the LA of the endocardial borders. Mean volume measurements on TEE and CTPV were compared using t test analysis and using Pearson's correlation coefficient. **Results:** The mean LAV measured on TEE was significantly smaller than that measured on CTPV when using Simpson method (61.1mL vs 124.2mL; p <0.005) and area-length method (64.8 mL vs 124.2 mL; p<0.005), respectively. There was no significant difference between the mean volume calculated by Simpson method (60.4 mL) and area-length method (64.8 mL) (p>0.05). TEE underestimated LA volume systematically by 50%. Multiplying the Simpson LAV by a factor of 2 (Adjusted Simpson LAV) resulted in appropriate approximation of the true LAV by CTPV (122.2 vs 124.2; p>0.05), respectively. Figure 1 plots adjusted LAV by Simpson method versus LAV by CTPV and revealed good correlation (r=0.680, p<0.005). **Conclusions:** LAV as measured

by TEE significantly underestimates the true LAV as measured by the gold standard CTPV. Doubling the LAV from TEE results in an appropriate approximation of measurement of true LAV as measured by CTPV.



P1-112

Three-dimensional Transesophageal Echocardiography in Left Atrial Appendage Sizing for Interventional Closure

Dehong Kong, Cuizhen Pan, Xiaochun Zhang, Lili Dong, Xianhong Shu. Zhongshan Hospital, Fudan University, Shanghai, China

Background: Correct sizing of the ostium is a crucial step in left atrial appendage (LAA) occlusion procedures. The aim of the study was to evaluate the value of novel methods based on three-dimensional transesophageal echocardiography (TEE) in LAA sizing. **Methods:** Thirty-two consecutive patients who underwent LAA occlusion and periprocedural transesophageal echocardiography were enrolled. The maximal diameter of the landing zone was measured at four different two-dimensional views (LAADmax2D) and by three-dimensional TEE (LAADmax3D). Perimeter-derived diameter (LAADperi3D) was calculated based on LAA perimeter at the landing zone measured by three-dimensional TEE (LAADperi3D = perimeter/π). The appropriate choice of occluders was confirmed with fluoroscopic criteria. **Results:** LAA was occluded in 31of the patients using the Watchman device with the occluder size of 29.23±3.46mm. Three-dimensional TEE images were successfully acquired and analyzed in 94% of the patients. LAADmax2D, LAADmax3D and LAADperi3D were positively correlated with the device size (r=0.663, 0.601, and 0.900, respectively, P<0.001). The prediction equations for occluder size based on LAADmax2D (occluder size = 0.587 LAADmax2D +14.580) and LAADmax3D (occluder size = 0.92 LAADmax3D +3.683) had the accuracy of 67% (21/31) and 74% (23/31) respectively. The prediction equation for occluder size based on LAADperi3D (occluder size = 0.875 LAADperi3D +6.892) showed the accuracy of 87% (27/31). **Conclusion:** Perimeter-derived diameter based on three-dimensional TEE showed high accuracy in device size decisions in LAA occlusion procedures.

P1-113

Residual Atrial Septal Defect and Significant Device Leak in Left Atrial Appendage Closure Guided by Intracardiac Echocardiography

Edward Chu, Alex Choy, Lori Croft, Srinivas Dukkupati, Vivek Reddy, Martin Goldman. Icahn School of Medicine at Mount Sinai, New York, NY

Background: Transcatheter left atrial appendage (LAA) occlusion guided by intracardiac echocardiography (ICE) has been demonstrated as a safe and feasible intra-procedural alternative to transesophageal echocardiography (TEE), but the approach with ICE requires a larger transeptal orifice size and imaging of the LAA from non-traditional views. It is unclear if ICE-guided LAA occlusion is associated with differences in residual iatrogenic atrial septal defect (ASD) and significant LAA occlusion device leak at short-term follow-up. **Methods:** This retrospective study included all patients who underwent LAA closure with the Watchman device at Mount Sinai Hospital between January 2012 and March 2017, and had a follow-up TEE between 45 days and 6 months after device implant. Transeptal access and device implantation were guided by ICE or TEE. All patients continued anticoagulation for at least 45 days after device implant. Images from the follow-up TEE were reviewed for the primary outcomes of residual ASD and significant device leak > 5mm, and secondary outcomes of device thrombus, device migration, and growth of post-procedural pericardial effusion. **Results:** Of the 166 patients (age 75.3 +/- 1.2 years, male 64%) who underwent successful LAA closure with the Watchman device, transeptal access and device implantation were guided by TEE in 144 patients (87%) and by ICE in 22 patients (13%). On follow-up TEE, there was no significant difference between the TEE and ICE groups in the occurrence of residual ASD (17% vs 23%, p=0.55). There was also no significant difference between the TEE and ICE groups in the occurrence of device thrombus (3% vs. 9%, p=0.18), device migration (1% vs. 0%, p=1.0), and growth of pericardial effusion (4% vs. 0%, p=0.60). **Conclusion:** Implant and device-related complications between ICE and TEE guided LAA occlusion are similar in short-term follow-up. This study further reinforces the safety of ICE as an alternative imaging modality to guide transcatheter LAA closure.

Poster Session 1 (P1)

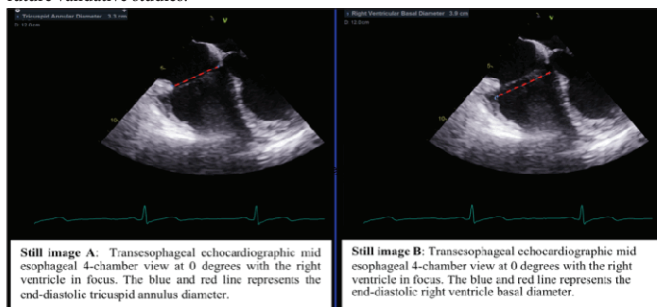
Sunday, June 23, 2019

P1-114

Comparison of 2-Dimensional Transthoracic and Intraoperative Transesophageal Echocardiography in Assessing Tricuspid Valve and Right Ventricular Geometry and Function

Saberio Lo Presti¹, Daniela Urina², Tarek K. Elajami², Ivan A. Arenas³, Orlando Santana³, Steve Xydas⁴, Francesco Nappi⁵, Ana V. Soto³, Christos G. Mihos³. ¹Columbia University Division of Cardiology, Mount Sinai Heart Institute, Miami, FL; ²Department of Internal Medicine, Mount Sinai Medical Center, Miami, FL; ³Echocardiography Laboratory, Columbia University Division of Cardiology, Mount Sinai Heart Institute, Miami, FL; ⁴Columbia University Division of Cardiac Surgery, Mount Sinai Heart Institute, Miami, FL; ⁵Department of Cardiac Surgery, Center Cardiologique du Nord de Saint-Denis, Paris, France

Background: Two-dimensional transesophageal echocardiography (TEE) is utilized to evaluate tricuspid annular (TA), tricuspid valve, and right ventricular (RV) geometry and function at the time of valve surgery. Nevertheless, there is limited data comparing intra-operative TEE with two-dimensional transthoracic (TTE) criteria of right heart dysfunction. The present study aimed to correlate quantitative echocardiographic parameters of TA, tricuspid valve, and RV size and function as assessed by TTE and intra-operative TEE. **Methods:** Fifty-four patients who underwent combined mitral and tricuspid valve surgery were analyzed. TA, tricuspid valve, and RV geometry and function were evaluated at end-diastole in the TTE apical 4-chamber (A4C) and RV inflow views, and TEE mid-esophageal 4-chamber (ME4C) and transgastric RV inflow views. Spearman correlation coefficients (r) were used to test for associations between the respective modalities and variables. **Results:** The mean age was 65 ± 13 years and 61% were female. Tricuspid regurgitation was \geq moderate in all patients, and the etiology was secondary/functional in 89%. The median TAd and RV basal (RvD) diameters in the TTE-A4C view measured 37 mm (interquartile range, IQR, 34-44) and 43 mm (IQR, 40-51), respectively. The TTE-A4C TAd strongly correlated with the TEE-ME4C measurement ($r=0.72$), with a median overestimation of 1 mm (IQR, -2 to 4) by TEE ($p<0.01$). For RvD, the TTE-A4C measurement moderately correlated with the TEE-ME4C view ($r=0.61$), with a median underestimation of -1 mm (IQR, -4 to 3.3) by TEE ($p<0.01$) (Figure). There was no correlation in tricuspid annular plane systolic excursion (TAPSE) when measured by TTE (20 mm, IQR 17-23) and TEE (13 mm, IQR 11-17) ($r=0.22$, $p=0.13$). **Conclusions:** Intra-operative TEE may be a reliable modality for quantitative assessment of TA and RV size. The current findings are best interpreted as hypothesis-generating for future validating studies.



P1-115

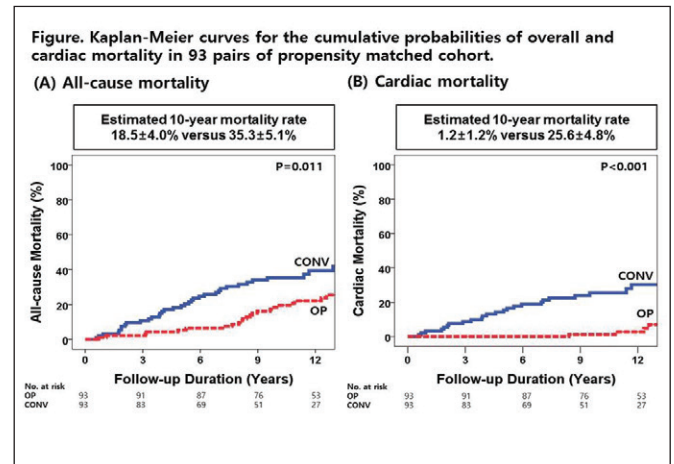
Moderated Poster

Impact of Early Surgery on Long-term Survival in Patients with Asymptomatic Very Severe Aortic Stenosis

Duk-Hyun Kang¹, Dae-Hee Kim¹, Jong-Min Song¹, Kee-Joon Choi¹, Joo-Hee Zo², Seung Woo Park³, Cheol-Hyun Chung¹, Jae-Kwan Song¹, Jae-Won Lee¹. ¹Asan Medical Center, Seoul, Republic of Korea; ²Boramae Hospital, Seoul, Republic of Korea; ³Samsung Medical Center, Seoul, Republic of Korea

Background: The optimal timing of surgical aortic valve replacement (AVR) remains controversial in asymptomatic patients with severe aortic stenosis (AS). This study sought to compare the long-term outcomes of early AVR with a conventional treatment strategy. **Methods:** From 1996 to 2009, 256 asymptomatic patients (125 men; 62 ± 12 years of age) with very severe AS were consecutively enrolled. Very severe AS was defined as critical stenosis in the aortic valve area ≤ 0.75 cm² accompanied by a maximal aortic jet velocity ≥ 4.5 m/s and/or a mean transaortic gradient ≥ 50 mmHg. Early AVR was performed on 119 patients (OP group), whereas conventional management was chosen for 137 patients (CONV group). We compared the endpoints of all-cause mortality and cardiac death between two groups in the overall and propensity score-matched cohort (93 pairs). **Results:** Baseline characteristics were similar between the two groups, but aortic jet velocity and mean transaortic gradient were significantly larger in the OP group ($p<0.01$). The 30-day operative mortality in the OP group was 0.7%. Seventy-four of 137 patients (54.0%) in the CONV group underwent surgical AVR during follow-up. During the median follow-up of 10.9 years, there were 33 deaths (27.7%) including 7 cardiac deaths in the OP group and 56 deaths (40.9%) including 39 cardiac deaths in the CONV group. In the 93 pairs of propensity score-matched cohort, all-cause and cardiac mortality rates were significantly

lower in the OP group (figure) and the OP group had a significantly lower risk of all-cause mortality (HR, 0.54; 95% CI, 0.33-0.88; $p=0.013$) and cardiac mortality (HR, 0.17, 95% CI, 0.07-0.39; $p<0.001$). **Conclusion:** Compared with the conventional treatment, early surgery in asymptomatic patients with very severe AS is associated with improved long-term survival by reducing cardiac mortality. Early surgery can be a therapeutic option to further improve clinical outcomes in asymptomatic patients with very severe AS and low operative risk.



P1-116

Echocardiographic Criteria for Severe Aortic Stenosis Revisited: Insights from a Quarter Century of Data

Deyu Sun¹, Kalie Kebed¹, Victor Mor-Avi¹, Karima Addetia¹, Natasha Markuzon², Roberto M. Lang¹. ¹University of Chicago, Chicago, IL; ²Philips Healthcare, Andover, MA

Background: For optimal interventional planning, it is important to have internally consistent criteria for grading severe aortic stenosis (AS). Prior studies involving small cohorts have demonstrated that the guideline defined values of severe AS of aortic valve maximum velocity (Vmax) =4 m/s and mean gradient (ΔP) =40 mmHg do not consistently correspond to aortic valve area (AVA) =1 cm², but rather to smaller AVAs. Accordingly, we sought to characterize the relationship between Vmax, ΔP , and AVA in a large series of patients with varying degrees of AS, in order to derive hemodynamically consistent cutoff values for these parameters that would better define severe AS with higher statistical confidence. **Methods:** We identified patients with mild to severe AS from our echocardiographic database from 1994 to 2018 (n=988 patients, 2859 studies). Left ventricular systolic function, AVA calculated by the continuity equation, Vmax, and ΔP were extracted. In addition, using ΔP and Vmax, a predicted AVA was derived using the Gorlin equation, assuming a heart rate of 80 bpm, systolic ejection period of 0.33 seconds, and a cardiac output of 6 L/min. **Results:** AVA was plotted against ΔP (Figure 1a) and Vmax (Figure 1b), showing that a substantial number of patients were "discrepant" because they did not consistently meet the guidelines criteria for severe AS, as they were in the lower left quadrants corresponding to AVA ≤ 1 cm² and $\Delta P < 40$ mmHg (n= 480, 19%) and AVA ≤ 1 cm² and Vmax < 4 m/s (n=458, 18%). For the subgroup of patients with reduced ejection fraction (n=249, 455 studies), the incidence of discrepancy was even higher for ΔP and Vmax (Figure 1c and 1d). Based on the curve fits of our data, AVA=1.0 cm² corresponded to $\Delta P=32$ mmHg and Vmax=3.7 m/s. Conversely, $\Delta P=40$ mmHg corresponded to AVA=0.89 cm², and Vmax=4.0 m/s corresponded to AVA=0.92 cm². The predicted Gorlin AVA curve fits based on both ΔP and Vmax yielded smaller AVAs than those seen clinically ($p<0.001$), again demonstrating the hemodynamic inconsistency of the guidelines recommended cutoffs. **Conclusion:** Guidelines recommended cutoff values for ΔP and Vmax correspond to a smaller AVA cutoff than 1 cm², irrespective of systolic function. This provides an inconsistent assessment of AS severity which may fail to deliver clear guidance on the optimal timing of intervention.

Poster Session 1 (P1)

Sunday, June 23, 2019

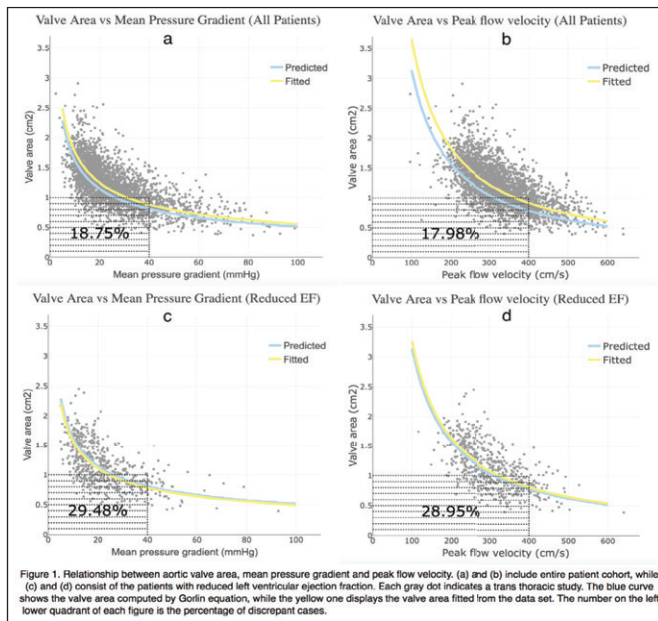


Figure 1. Relationship between aortic valve area, mean pressure gradient and peak flow velocity, (a) and (b) include entire patient cohort, while (c) and (d) consist of the patients with reduced left ventricular ejection fraction. Each gray dot indicates a trans thoracic study. The blue curve shows the valve area computed by Gorlin equation, while the yellow one displays the valve area fitted from the data set. The number on the lower quadrant of each figure is the percentage of discrepant cases.

P1-117

Validation of the 2017 American Society of Echocardiography Criteria for Tricuspid Regurgitation Against Cardiovascular Magnetic Resonance

Yang Zhan¹, Alpna Senapati¹, Pimprapa Vejpongsa¹, Susan Xu², Dipan J. Shah¹, Sherif F. Nagueh¹. ¹Houston Methodist DeBakey Heart & Vascular Center, Houston, TX; ²Houston Methodist Research Institute, Houston, TX

Background: Recommendations for tricuspid regurgitation (TR) severity based on ASE criteria have not been validated against other modalities. We sought to compare echocardiographic indices of TR severity against cardiovascular magnetic resonance (CMR) derived TR regurgitant volume (TR_{RV}) using ASE reported cutoffs: mild <30 mL, moderate 30-44 mL, and severe ≥45 mL. **Methods:** 265 patients with secondary TR underwent CMR and echocardiogram within 60 days (mean 10 ± 14 days). Echocardiographic TR indices included jet area, right atrial area, right ventricle end diastolic area index and fractional area change (FAC), inferior vena cava size, hepatic vein Doppler profile, and CW Doppler contour and density. Quantitative measurements included vena contracta (VC), effective regurgitant orifice area (ERO), and TR_{RV} by PISA. TR_{RV} was calculated using CMR by subtracting pulmonary artery forward flow from right ventricular stroke volume. All analyses were blinded of the other modality's findings. All patients were in sinus rhythm at time of CMR scan. **Results:** There was no difference in BP (P > 0.1), but a small significant difference in heart rate (80±18 vs 77±17, P=0.016) was present between scans. By CMR, there were 165, 49, and 51 patients with mild, moderate, and severe TR, respectively. With worsening TR severity RA and RV volumes increased, whereas LV and volumes decreased. Echocardiographic indices of TR, except for FAC, were significantly different among all groups (p < 0.001). Criteria for mild and severe TR, based on the ASE criteria, show moderate accuracy (AUC 0.57-0.79) (Table 1). Largest AUC was achieved with lower cut-off values for quantitative parameters of severe TR than those in guidelines for VC (0.55 cm, AUC 0.78), ERO (0.27 cm², AUC 0.81), and PISA TR_{RV} (29 mL, AUC 0.77) (Table 2). **Conclusion:** Echocardiographic signals recommended in 2017 ASE guidelines have good accuracy in detecting severe TR quantified by CMR (≥ 45 mL). Lower cutoff values for quantitative indices best detected severe TR as identified by CMR.

Table 1: Accuracy of Individual Echocardiographic Parameters based on ASE criteria for mild and severe TR

Parameter	Sensitivity (%)	Specificity (%)	Area Under Curve
ASE CRITERIA FOR MILD TR			
RV end diastolic area index ≤12.6 mL/m ² (men) and ≤11.5 mL/m ² (women)	59	73	0.66
TR Jet area ≤ 5 cm ²	73	70	0.72
Systolic flow predominance in hepatic veins			
IVC < 2 cm	57	66	0.61
Vena Contracta (cm) < 3 mm	20	95	0.57
TR Effective regurgitant orifice area ≤ 0.20 cm ²	61	86	0.73
TR regurgitant volume (PISA) ≤ 30 mL	80	64	0.72
ASE CRITERIA FOR SEVERE TR			
RV end diastolic area index ≥ 12.7 mL/m ² with normal RV function (FAC ≥ 35%)	40	85	0.62
TR Jet area ≥ 10 cm ²	54	91	0.72
Jet area/Right atrial area ≥ 0.5	26	92	0.59
Systolic flow reversal in hepatic veins			
Inferior vena cava maximum diameter ≥ 2.5 cm	47	85	0.79
CW density (dense similar to inflow)	43	94	0.69
CW contour (triangular)	37	96	0.67
Vena Contracta ≥ 7 mm	67	88	0.77
TR Effective regurgitant orifice area ≥ 0.4 cm ²	71	82	0.77
TR regurgitant volume (PISA) ≥ 45 mL	57	85	0.71

Table 2: Optimal cutoffs of quantitative variables for severe TR based on AUC analysis

Parameter	Sensitivity (%)	Specificity (%)	Area Under Curve
Right atrial maximum volume index ≥ 51 mL/m ²	76	80	0.78
RV end diastolic area index ≥ 12.7 mL/m ²	80	58	0.69
TR Jet area ≥ 7.45 cm ²	72	80	0.76
Jet area/Right atrial area ≥ 0.29	63	74	0.69
Inferior vena cava maximum diameter ≥ 2.15 cm	70	68	0.69
Vena Contracta ≥ 5.5 mm	81	75	0.78
TR Effective regurgitant orifice area ≥ 0.27 cm ²	97	65	0.81
TR regurgitant volume (PISA) ≥ 29 mL	83	72	0.77

P1-118

Right Ventricular Mechanical Pattern in Patients Undergoing Mitral Valve Surgery: Shifting Back and Forth

Marton Tokodi¹, Balint K. Lakatos¹, Erika Kispal¹, Zoltan Toser², Kristof Racsz¹, Adam Soltesz¹, Szabolcs Szigeti¹, Istvan Hartayanszky¹, Endre Nemeth¹, Bela Merkely¹, Attila Kovacs¹. ¹Heart & Vascular Center, Semmelweis University, Budapest, Hungary; ²Argus Cognitive Inc., Dover, DE

Background: Severe mitral regurgitation induces significant changes not only in the left, but also in the right ventricular (RV) morphology and function. The PREPARE-MVR study (Prediction of Early Postoperative Right vEntricular failure in Mitral Valve Replacement/Repair patients) aims to investigate the alterations of RV contraction pattern in patients undergoing MVR and to explore the association of preoperative echocardiographic findings with early postoperative RV failure. **Methods:** We prospectively enrolled 70 patients (62±12 years, 67% males) undergoing open heart MVR. Thirty age and gender matched healthy volunteers served as control group. Transthoracic 3D echocardiography was performed preoperatively and at intensive care unit discharge. Forty-three patients also completed 6 months follow-up. 3D model of the RV was reconstructed and end-diastolic volume index (EDVi) along with RV ejection fraction (RVEF) were calculated. For in-depth analysis of RV mechanics, we decomposed the motion of the RV to compute longitudinal (LEF) and radial ejection fraction (REF). Right heart catheterization was performed to monitor RV stroke work index (RVSWi). **Results:** RV morphology as assessed by EDVi was unaffected by surgery (preoperative vs postoperative; 73±17 vs 71±16 mL, p=NS). RVEF was slightly decreased after MVR (52±6 vs 48±7 %, p<0.05), whereas RV contraction pattern has changed notably. Before MVR, the longitudinal shortening was the main contributor to global systolic function (LEF/RVEF vs REF/RVEF; 0.53±0.10 vs 0.43±0.12; p<0.001), whereas in controls the longitudinal and radial shortening contributed equally to RVEF (0.47±0.07 vs 0.43±0.09; p=NS). Postoperatively, the radial motion became dominant (0.35±0.08 vs 0.47±0.09; p<0.001). However, this shift was only temporary as 6 months later the contraction pattern became similar to controls showing equal contribution of the two components (0.44±0.10 vs 0.42±0.11; p=NS). Preoperative LEF was an independent predictor of postoperative RV failure defined as RVSWi < 300 mmHg* mL/m² or TAPSE < 10 mm (OR=1.16 [1.03-1.35], p<0.05). **Conclusion:** MVR induces significant shift in RV mechanical pattern. Advanced indices of RV mechanics are associated with invasively measured parameters of RV contractility and may predict postoperative RV failure.

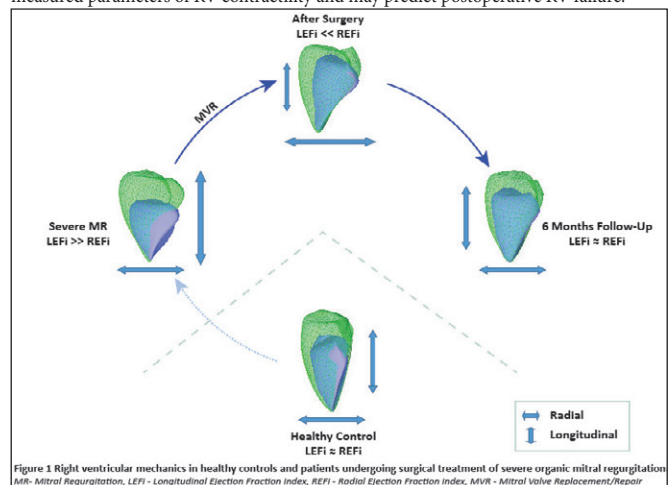


Figure 1 Right ventricular mechanics in healthy controls and patients undergoing surgical treatment of severe organic mitral regurgitation. MR- Mitral Regurgitation, LEFI - Longitudinal Ejection Fraction Index, REFI - Radial Ejection Fraction Index, MVR - Mitral Valve Replacement/Repair

P1-119

Quantitative Assessment of Tricuspid Regurgitation

Yogev Peri, Yan Topilski. Tel Aviv Medical Center, Tel Aviv, Israel

Introduction: The cutoffs for quantitative assessment of TR are not well defined and are based on scant evidence. We assessed tricuspid regurgitation (TR) quantitatively by the proximal isovelocity surface area method (PISA) and performed a long-term outcome analysis in order to find evidence based criteria for classifying TR severity. **Methods:** We enrolled 676 patients (mean age 73.91 ± 13.74 Years; 45 % men) with TR of any cause

Poster Session 1 (P1)

Sunday, June 23, 2019

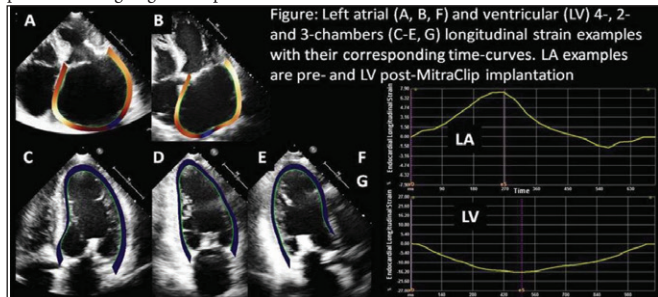
prospectively assessed by the PISA method (regurgitant volume [RVol] 20.47 ± 23 ml per beat; effective regurgitant orifice (ERO) 0.22 ± 0.3 cm²). **Results:** Patients were followed up for all caused mortality. In univariate and multivariate Cox Hazard analysis ERO and Regurgitant Volume were associated with mortality (HR=16.64, P<0.0001; HR = 9.33, P<0.0001 for ERO in univariate and multivariate analysis respectively and for RVol HR=10.09, P<0.0001; HR= 3.65 P=0.0005). To assess thresholds of quantitative parameters we used spline curves (of hazard ratios adjusted for age, EF and pulmonary pressure in the Y axis and ERO or RVol in the X axis, whereby a HR of 1 represents the cohorts mean risk). We found that a cutoff of ERO > 0.38cm² (HR=1.43, P=0.02) and regurgitant volume > 40 ml per beat (HR=1.41, P=0.03) were associated with excess mortality. In nested models RVol was superior to ERO in predicting mortality in TR, in discordance with assessment of mitral regurgitation. In subgroup analysis for patients with systolic dysfunction (EF<50%) vs. preserved function (EF>50%) we found that ERO and RVol were associated with excess mortality only in patients with preserved systolic dysfunction. **Conclusions:** ERO and RVol are independently associated with mortality in TR patients, validating their use in the clinical practice. The cutoffs associated with excess mortality are 0.38cm² for ERO and 40cc for regurgitant volume, similar but not identical to present guidelines. RVol is superior to ERO in assessing survival in TR patients. The role of quantitative assessment in patients with systolic dysfunction is less clear.

P1-120

Left Cardiac Chambers Remodeling by Speckle Tracking Echocardiography in Patients Undergoing Transcatheter Mitral Valve Repair with MitraClip

Diego Medvedofsky, Harish Jarrett, Toby Rogers, Tatsuya Miyoshi, Zuyue Wang, Itzik Ben-Dor, Lowell Saitler, Rebecca Torguson, Ron Waksman, Federico M. Asch. MedStar Washington Hospital Center, Washington, DC

Background: Transcatheter mitral valve repair with MitraClip (MC) improves outcomes in patients with symptomatic severe mitral valve regurgitation (MR) who are inoperable due to high surgical risk. Left atrial (LA) size and function is affected by significant MR. While, left ventricular (LV) ejection fraction (EF) usually worsens after surgical mitral valve surgery, little is known about remodeling post MC and left cardiac chamber's myocardial deformation derived parameters have not been studied in this population. We aimed to assess left cardiac chambers remodeling by speckle tracking echocardiography (STE) derived parameters to better understand changes following MC implant. **Methods:** Consecutive patients with Grade 3+ or 4+ MR who underwent MC implant at our institution between 2014-2017 were included if echocardiograms pre- and 1-2 months post-procedure were available. Baseline and follow-up left cardiac chambers size and function STE (TOMTEC) derived parameters were measured and data was compared (Figure). **Results:** From a total of 67 consecutive patients, 37 had pre- and follow-up echocardiograms available and accordingly were included in this study (79±11 years, 41% female). At baseline 34 patients had grade 4+ and the remaining 3 had grade 3+. At follow-up, in 27 patients the MR degree decreased to ≤2+, and 10 still had ≥3+ MR. While LV end-diastolic and end-systolic volumes (EDV, ESV) did not change (155±63 vs. 146±59ml, p=0.07; 75±42 vs. 76±45ml, p=0.76, respectively) EF, stroke volume (SV) and global longitudinal strain (LS) significantly decreased in magnitude (53±12 vs. 50±13%, p=0.02; 80±29 vs. 70±27ml, p=0.01; -19±4 vs. -17±4.3%, p=0.01, respectively). No significant changes were seen for LA in any parameter: EDV= 94±64 vs. 87±40ml, ESV= 147±77 vs. 141±56ml, EF= 38±13 vs. 39±11%, SV= 53±25 vs. 54±22ml and GLS= -15±5.1 vs. -15±4.4% (p>0.05 for all). **Conclusion:** In patients with grade ≥3+ MR undergoing MC implant, worse LV volumetric and myocardial deformation functional parameters were seen at 1-2 months post-procedure, but no LA remodeling was noted. Future studies with larger populations and longer follow-up are needed to determine the role of LS in assessing patients undergoing MC implant.



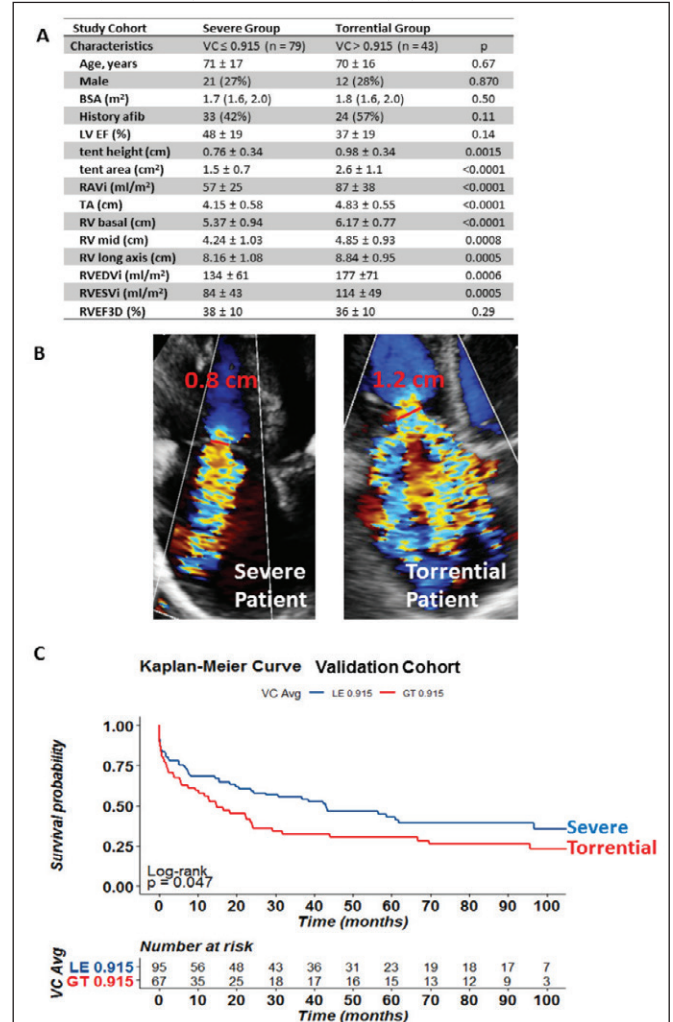
P1-121

Re-Defining Severe Tricuspid Regurgitation: Introducing a New Grade of Torrential Tricuspid Regurgitation Based on Outcomes Data

Kalie Kebed, Karima Addetia, Michael Henry, Megan Yamat, Lynn Weinert, Stephanie A. Besser, Roberto M. Lang. University of Chicago, Chicago, IL

Background: Current guidelines recommend that tricuspid regurgitation (TR) severity be graded into categories of mild, moderate, and severe, following assessment of specific

parameters. Findings from early percutaneous tricuspid intervention trials have shown that the severity of TR frequently far exceeds the current definition of severe. Accordingly, a grading approach that emphasizes outcomes could be useful for the triage of patients with severe TR. We therefore sought to determine whether there exists a subset of patients with severe TR based on current guidelines, who have an increased risk of mortality. **Methods:** Patients with severe TR, defined as vena contracta (VC) ≥0.7 cm, were identified from our echocardiographic database from 2010 to 2018. Patients with primary TR or prosthetic valves were excluded. Demographics and mortality data were obtained from the medical records. Patients were divided into Study (n= 122) and Validation (n=162) cohorts. VC was measured in both the right ventricular (RV) inflow and apical-4 chamber (Fig 1B) views and averaged. For the Study cohort, tricuspid annular (TA), RV end-diastolic (basal, mid, long axis) dimensions, tricuspid leaflet tenting height and area as well as 3D RV volumes (TomTec) were measured from full-volume RV 3D datasets. A K-partition algorithm was used on the Study cohort to derive a mortality-related partition VC value, above which patients were termed Torrential. This VC value was then tested in the Validation cohort using Kaplan-Meier survival analysis. **Results:** In the Study cohort, a partition value of VC >0.915 cm was associated with worse survival, while there were no significant differences in demographic data between the Severe and Torrential groups (Fig 1A). Although TA and RV size in the Torrential group were larger than in the Severe group, RV systolic function was similar (Fig 1A). Importantly, in the Validation cohort there was also increased mortality in the Torrential versus Severe group as defined by the same partition VC value (Fig 1C). **Conclusion:** Among patients traditionally defined as having severe TR, a subset exists with torrential TR, resulting in greater adverse RV remodeling and increased mortality. These patients may derive the greatest benefit from emerging percutaneous therapies.



P1-122

Echocardiographic L-Wave as a Prognostic Indicator in TAVI Patients

Ben Sadeh, Ilan Merdler, Aviram Hochstadt, Ariel Finkelstein, Shmuel Banai, Gad Keren, Yan Topilsky. Tel Aviv Sourasky Medical Center, Tel Aviv, Israel

Introduction: The L wave represents mid-diastolic trans-mitral flow. Its clinical and prognostic value is not completely understood. It is assumed that this wave represents

Poster Session 1 (P1)

Sunday, June 23, 2019

decreased relaxation of the left ventricle and thus diastolic dysfunction. Patients with severe aortic stenosis are prone to left ventricular hypertrophy and diastolic dysfunction. It has been previously shown in this group of patients that Trans-catheter aortic valve replacement (TAVR) induces reverse remodeling and improves diastolic function and prognosis. Our aim was to examine the change in L wave after TAVR and its clinical importance. **Methods:** We examined the clinical and echocardiographic data of 535 patients (mean age 82.58±5.9) undergoing TAVR. The presence and velocity of L-Wave was recorded at baseline and 1 and 6 months post procedure. The impact of the procedure on L-Wave and clinical outcomes were analyzed. **Results:** Patients with L-wave on baseline echocardiography (n=64, 12%) had a smaller stroke volume index by 5.7±2.3ml/m² (p=0.01) and a lower systolic blood pressure by 17.2±6.6mmHg (p=0.01) compared to patients without L wave at baseline echocardiography. In patients with L-wave at baseline, in 31% the L-wave disappeared at 1 month and in 70% at 6 months follow up. In addition, baseline L wave velocity was 34.8±11.5 (cm/s) and decreased significantly at follow up. Patients with L-wave at baseline had higher 3 year mortality post procedure (HR 1.93, 95% CI 1.46-2.54, p<0.001). This was also true for patients with L-wave after 1 month (HR 5.03, CI 3.12-8.08, p<0.001). Multivariate analysis of survival was also statistically significant (p<0.001). **Conclusion:** Post TAVR velocity of L wave decreases significantly and often disappears completely. The presence of L wave before TAVR is an independent risk factor for mortality.

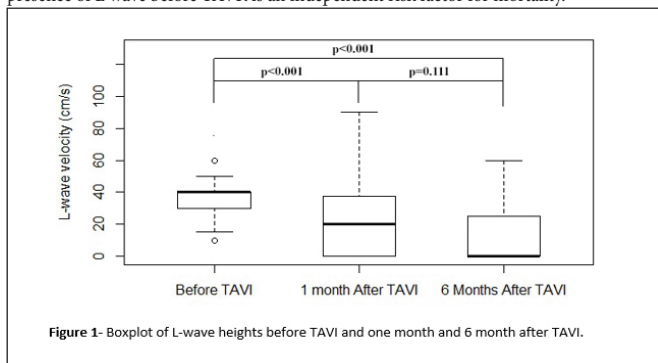


Figure 1- Boxplot of L-wave heights before TAVI and one month and 6 month after TAVI.

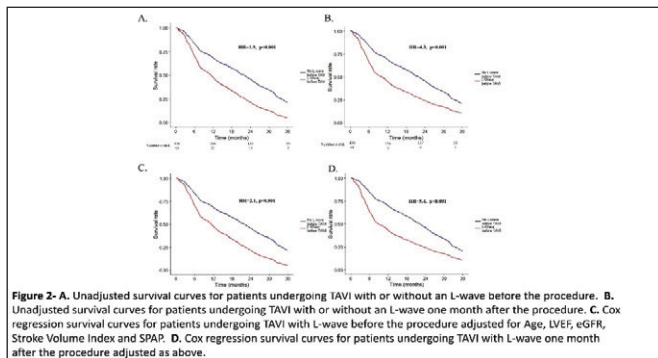


Figure 2- A. Unadjusted survival curves for patients undergoing TAVI with or without an L-wave before the procedure. B. Unadjusted survival curves for patients undergoing TAVI with or without an L-wave one month after the procedure. C. Cox regression survival curves for patients undergoing TAVI with L-wave before the procedure adjusted for Age, LVEF, eGFR, Stroke Volume Index and SPAP. D. Cox regression survival curves for patients undergoing TAVI with L-wave one month after the procedure adjusted as above.

P1-123

Prevalence and Clinical Significance of Tricuspid Regurgitation Following Implantation of Cardiovascular Implantable Electronic Device

Jiwon Seo, Chi Young Shim, Kang-Un Choi, Jah-Yeon Choi, Purevjargal Lkhagvasuren, Geu-Ru Hong, Jong-Won Ha. Division of Cardiology, Severance Cardiovascular Hospital, Yonsei University College of Medicine, Seoul, Republic of Korea

Background: The possibility that cardiovascular implantable electronic device (CIED) could be responsible for tricuspid regurgitation (TR) have been established. However, there are still insufficient data for the prevalence and clinical significance of lead-related TR in patients with CIED. **Methods:** In a single center, CIED registry, 766 patients with permanent pacemaker (PPM) or implantable cardioverter defibrillator (ICD) were retrospectively analyzed. Patients who had not undergone transthoracic echocardiography (TTE) within the previous 90 days of CIED implantation were excluded. Patients who had pre-existing grade 3 or 4 TR, had single atrial lead, or had undergone surgery of tricuspid valve before CIED implantation were excluded. Occurrence of lead-related TR was defined as TR worsened by at least 2 grades on post-implantation TTE during follow-up period. TR severity was graded 0 to 4 on the basis of current guidelines. Cardiovascular outcomes were defined as the composite of cardiovascular death, surgical treatment of tricuspid valve, and hospitalization for heart failure. **Results:** Among 506 patients with PPM and 260 patients with ICD, 523 patients had no TR, 185 patients had grade 1 TR, and 58 patients had grade 2 TR on pre-implantation TTE. During follow-up period (median 664.5 days), significant lead-related TR were occurred in 83 (10.8%) patients and cardiovascular outcomes occurred in 145 patients. In multivariate logistic regression analysis, older age

(RR: 1.02, 95% CI: 1.00-1.05, p=0.0226) and ICD implantation (RR: 2.31, 95% CI: 1.07-5.01, p=0.0328) were independently associated with lead-related TR. In multivariate cox regression analysis, lead-related TR was significantly associated with cardiovascular outcomes (HR: 2.97, 95% CI: 2.01-4.38, p<0.001). **Conclusion:** Lead-related TR in patients with CIED was not uncommon (10.8%). Occurrence of lead-related TR was associated with older age and implantation of ICD. Moreover, lead-related TR was associated with a higher incidence of cardiovascular outcomes including cardiovascular death, surgical treatment of tricuspid valve, and hospitalization for heart failure.

P1-124

Impact of Left Ventricular Longitudinal Function on Prognosis in Patients with Moderate Aortic Stenosis and Preserved Left Ventricular Ejection Fraction

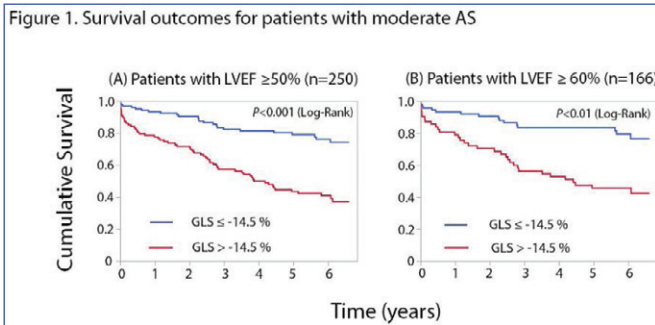
Dan Zhu^{1,2}, Saki Ito¹, William R. Miranda¹, Yuyisile T. Nkomo¹, Sorin V. Pislaru¹, Patricia A. Pellikka¹, Jae K. Oh¹. ¹Mayo Clinic, Rochester, MN; ²Peking University Third Hospital, Peking, China

Background: The management of severe aortic stenosis (AS) has been revolutionized after studies showed efficacy of transcatheter aortic valve replacement (TAVR). In the future indications for TAVR may also be expanded to moderate AS and worse prognosis, such as those with left ventricular dysfunction. We hypothesized that global longitudinal strain (GLS) could discriminate high risk patients among individuals with moderate AS and preserved left ventricular ejection fraction (LVEF). **Methods:** Patients with moderate AS (1< aortic valve area [AVA] ≤1.5cm²) and LVEF ≥50% diagnosed between January-June 2012 were identified. For the assessment of GLS using two-dimensional speckle-tracking strain imaging, conventional apical 2-, 3-, and 4-chamber views were analyzed. Patients were divided in two groups according to the median GLS value for the entire group and all-cause mortality was compared between groups. **Results:** 250 patients were included. Mean age was 72 years, 55% were male, AVA was 1.2±0.2 cm² and LVEF was 62.3±5.6 % (Table 1). Median GLS was -14.5% (IQR: 16.3, 12.7). After a median of 3.8 years, there were 86 deaths. Among patients with LVEF ≥50%, mortality was significantly higher in patients with GLS >-14.5% compared with GLS ≤-14.5% (P<0.001, Fig 1A), even after adjusting for age, male sex and LVEF (P<0.001). Noteworthy, GLS discriminated high risk patients even if in those with an LVEF ≥60% (P<0.01, Fig 1B). **Conclusions:** In patients with moderate AS and preserved LVEF, impaired GLS discriminated high risk patients.

Table 1. Patients characteristics	Total (n=250)	GLS		P
		≤-14.5% (n=139)	>-14.5% (n=111)	
Age, years	71.9±12.4	71.0±12.5	73.5±11.2	0.10
Male sex (%)	138(55)	78 (56)	60(54)	0.74
Hypertension (%)	167(67)	90(65)	77(69)	0.44
Diabetes mellitus (%)	77(31)	35(25)	42(38)	0.03
Coronary artery disease (%)	123(49)	63(45)	60 (54)	0.17
NT-pro BNP, pg/mL	285 (81, 1,337)	165 (61, 420)	711 (194, 3,489)	0.15
AVA, cm ²	1.2±0.2	1.2±0.1	1.2±0.2	0.93
Transaortic peak velocity, m/sec	3.4±0.7	3.4±0.7	3.3±0.7	0.19
Transaortic mean pressure gradient, mmHg	27.1±13.2	28.7±14.6	25.2±11.3	0.40
LVEF, %	62.3±5.6	63.3±5.3	61.1±5.7	< 0.01
Stroke volume index, ml/m ²	50.9±8.8	52.5±8.8	48.9±8.3	< 0.001
LV mass index, g/m ²	103.8±25.7	99.7±22.2	109.0±28.8	< 0.01
Relative wall thickness	0.46±0.08	0.45±0.07	0.46±0.09	0.13
Valvuloarterial impedance, mmHg/mL/m ²	3.2±0.8	3.0±0.5	3.5±0.9	< 0.05
Average E/e'	15 (18.3, 11.3)	13.3 (10, 18)	15.9 (12, 20)	< 0.01

Poster Session 1 (P1)

Sunday, June 23, 2019



P1-125

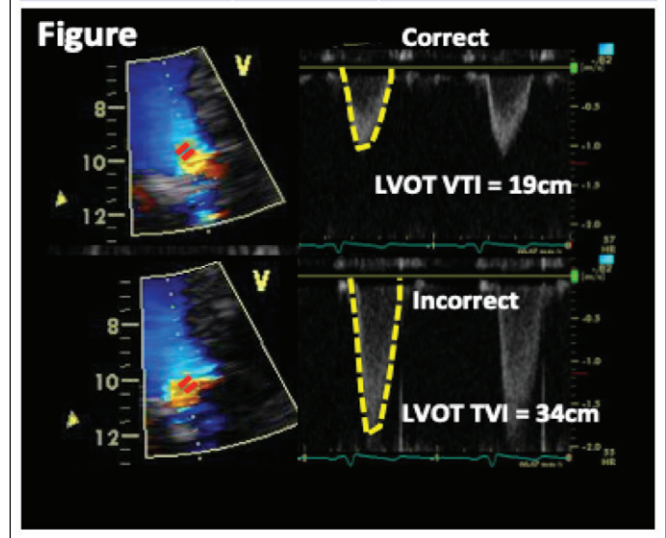
Measurement Errors in the Serial Assessment of Aortic Valve Stenosis Severity

Deyu Sun¹, Kalie Kebed², Karima Addetia², Victor Mor-Avi², Natasha Markuzon³, Roberto M. Lang². ¹Philips Healthcare, Andover, MA; ²University of Chicago, Chicago, IL; ³Philips Healthcare, Andover, MA

Background: The evaluation of aortic stenosis (AS) is routinely performed using the continuity equation from transthoracic echocardiography Doppler data. Traditionally, inaccurate measurements of the left ventricular outflow tract (LVOT) diameter have been considered the common source of error in grading AS. We hypothesized that misplacement of the pulsed Doppler sample volume in the LVOT is an under recognized cause of inaccuracies in aortic valve area (AVA) calculation. We sought to determine which parameters required for the continuity equation (LVOT diameter, LVOT pulsed Doppler velocity time integral (LVOT VTI), aortic valve continuous wave Doppler VTI (AV VTI)) is mostly responsible for errors in clinical practice. **Methods:** We identified patients with mild to severe AS with multiple studies from our echocardiographic database from 1994 to 2018 (n=988 patients, 2859 studies). Patients were excluded if left ventricular systolic function decreased one or more grade between studies. Errors were defined when 1) LVOT diameter changed by more than 2 mm 2) LVOT VTI changed by more than 15% in the absence of a change in LV function 3) AV maximum velocity (Vmax), mean pressure gradient (ΔP) or AV VTI decreased by more than 15% in the absence of a change in LV function relative to the initial study. **Results:** The most common error in the calculation of AVA was in the measurement of the LVOT VTI with 22% of studies having discrepant values. LVOT diameter, AV VTI, AV Vmax and AV ΔP had ≤7% measurement error (Table).

Conclusions: LVOT VTI is a frequent and under recognized source of error in assessing AS, whereas LVOT diameter measurement error is less common. Doppler evaluation of AV (VTI, maximum velocity, and mean pressure gradient) yields a low rate of errors if sampled from multiple transducer positions. More attention should be directed at properly positioning the pulsed Doppler sample volume in the LVOT (Figure) to obtain laminar flow curve with a well defined peak and narrow velocity range to ensure accurate and reproducible assessment of AS.

A	Error Criteria	Measurement Errors n, (mean, 95%CI)
LVOT diameter (mm)	Δ >2mm	130 (4.6%, [3.8%, 5.3%])
LVOT VTI (cm)	Δ >15%	529 (22.0%, [20.4%, 23.5%])
AV V _{max} (m/s)	Δ < -15%	92 (3.2%, [2.6%, 3.9%])
AV VTI (cm)	Δ < -15%	182 (6.4%, [5.5%, 7.3%])
AV ΔP (mmHg)	Δ < -15%	156 (5.5%, [4.6%, 6.3%])



P1-126

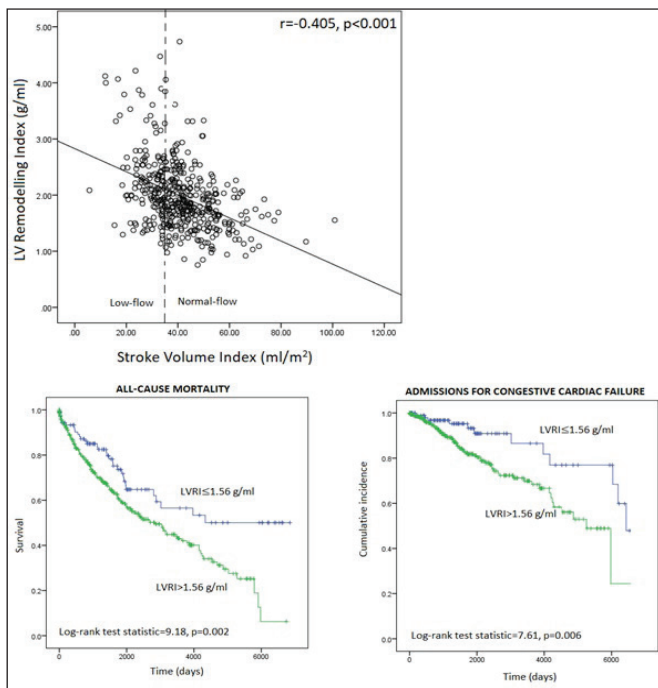
Increased Left Ventricular Remodelling Index in Paradoxical Low-Flow Severe Aortic Stenosis with Preserved Left Ventricular Ejection Fraction Compared to Normal-Flow

Nicholas Ngiam, Nicholas Chew, Hui Wen Sim, Benjamin Yong-Qiang Tan, Ching-Hui Sia, William K.F. Kong, Tiong-Cheng Yeo, Kian Keong Poh. National University Health System, Singapore, Singapore, Singapore

Background: Left ventricular remodelling index (LVRI) has been demonstrated to be able to reliably discriminate between an athlete's heart and pathological LV remodelling. Patients with paradoxical low-flow severe aortic stenosis (LF AS) despite preserved left ventricular ejection fraction (LVEF) appear distinct group from normal-flow (NF) with poorer prognosis, more concentric hypertrophy and smaller LV cavities. We compared LVRI in LF compared to NF AS and examined clinical outcomes. **Methods:** We studied consecutive patients with index echocardiographic diagnosis of severe AS (aortic valve area < 1cm²) with preserved LVEF (>50%). LVRI was determined by the ratio of LV mass to the end-diastolic volume. **Results:** Of the 450 patients studied, 149 (33.1%) were LF. There were no significant differences in baseline clinical profile of patients between LF and NF. LVRI was significantly higher in patients with LF compared to NF (2.27±0.68 vs 1.85±0.53 g/ml, p<0.001). Patients with high LVRI (>1.56 g/ml) had poorer clinical outcomes in terms of mortality (log-rank 9.18, p=0.002) and admissions for cardiac failure (log-rank 7.61, p=0.006). **Conclusion:** Pathological LV remodelling as evidenced by increased LVRI was more common in LF compared to NF AS. Patients with increased LVRI had worse clinical outcomes.

Poster Session 1 (P1)

Sunday, June 23, 2019



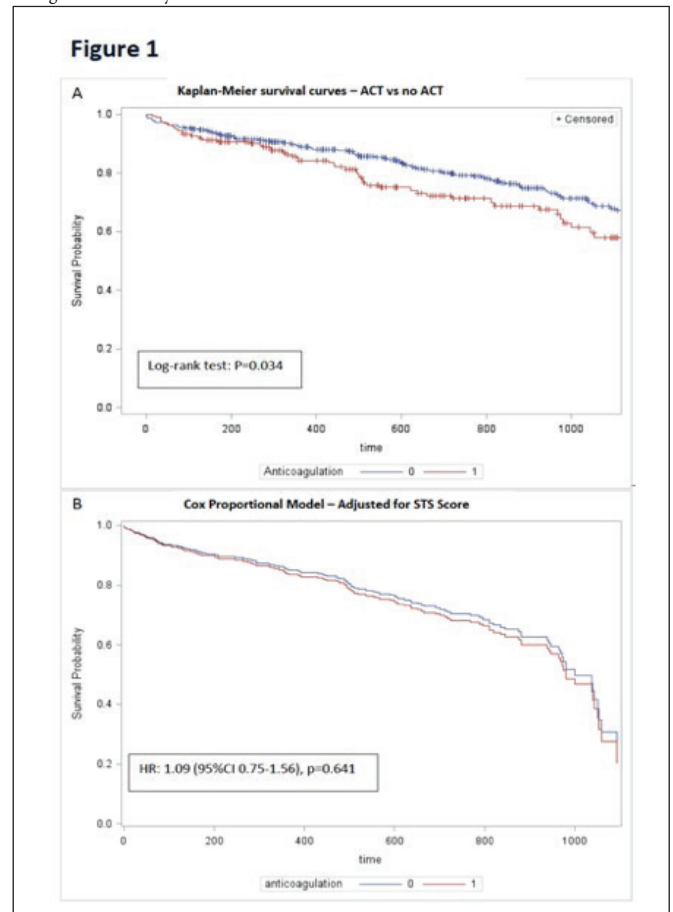
	Low-flow (n=149)	Normal-flow (n=301)	Mean difference/ Odds Ratio (95% CI)	p-value
Age (years)	73.5 (±12.8)	71.0 (±13.1)	2.5 (-0.1 - 5.1)	0.053
Body Mass Index (g/m²)	24.6 (±5.6)	24.7 (±5.3)	-0.1 (-1.2 - 1.1)	0.877
Gender (male)	49 (32.9%)	125 (41.5%)	0.7 (0.5 - 1.1)	0.076
Hypertension	100 (67.1%)	195 (64.8%)	1.1 (0.7 - 1.7)	0.624
Diabetes	57 (38.3%)	100 (33.2%)	1.2 (0.8 - 1.9)	0.295
Hyperlipidaemia	79 (53.0%)	147 (49.0%)	1.2 (0.8 - 1.7)	0.425
Ischaemic heart disease	44 (29.5%)	83 (27.6%)	1.1 (0.7 - 1.7)	0.658
End-diastolic volume (ml)	72.3 (±18.9)	112.6 (±26.3)	-40.2 (-44.9 - -35.5)	<0.001
Left ventricular ejection fraction (%)	66.0 (±7.9)	67.4 (±7.1)	-1.4 (-2.9 - 0.2)	0.077
Left ventricular mass index (g/m²)	99.7 (±33.0)	126.8 (±37.4)	-27.2 (-34.8 - -19.6)	<0.001
Left atrial diameter (mm)	40.0 (±10.2)	41.5 (±8.5)	-1.5 (-3.3 - 0.3)	0.099
Deceleration time (ms)	206.0 (±89.7)	221.3 (±74.9)	-15.3 (-31.8 - 1.2)	0.069
E/A Ratio	0.86 (±0.39)	0.94 (±0.41)	-0.1 (-0.2 - 0.1)	0.070
Peak transaortic velocity (cm/s)	356.8 (±85.8)	383.3 (±95.7)	-26.6 (-44.8 - -8.3)	0.004
Transaortic mean pressure gradient (mmHg)	32.2 (±17.4)	37.1 (±19.9)	-4.9 (-8.6 - -1.1)	0.011
Aortic valve area (cm²)	0.78 (±0.16)	0.79 (±0.17)	0.1 (-0.2 - 0.1)	0.635
Stroke volume index (ml/m²)	28.6 (±5.6)	46.9 (±9.8)	-18.3 (-20.0 - -16.6)	<0.001
Left ventricular remodelling index (LVRI, g/ml)	2.27 (±0.68)	1.85 (±0.53)	0.42 (0.31 - 0.54)	<0.001

P1-127 Long-Term Mortality and Transcatheter Aortic Valve Hemodynamics According to Anticoagulation Therapy

Anthony J. Klappa, Manju Bengaluru Jayanna, Kan Liu. University of Iowa, Iowa City, IA

Background: The number of patients undergoing transcatheter aortic valve replacement (TAVR) is rising. Early valve dysfunction secondary to valve thrombosis and leaflet

motion reduction have important clinical and prognostic sequelae. Post TAVR Doppler echocardiography provides serial assessment of valve hemodynamics and identification of subclinical valve dysfunction. We hypothesize that anticoagulation therapy (ACT) is effective in treating and preventing valve thrombosis and dysfunctional prosthesis. **Methods:** In this retrospective study, we performed a systematic search of our institution's electronic medical record to gather data on 371 consecutive patients who underwent TAVR between December 1, 2011 to February 28, 2016, and included demographics, Society of Thoracic Surgery (STS) risk score, outcomes, and imaging data over a minimum of at least 2 years post-TAVR. Patients alive at discharge with known antithrombotic status were included. Endpoints were all-cause mortality and early valve dysfunction, defined as either an increase in mean gradient ≥ 10 mmHg from baseline or a mean gradient ≥ 20 mmHg if the baseline was < 20 mmHg. Echocardiographic data was obtained from studies performed at follow-up and analysis retaining only patients with complete data were performed. Study population and subgroups were characterized with descriptive statistics. Kaplan-Meier curve and Cox regression model were used for survival time analysis. **Results:** In total, 359 of 371 patients who underwent TAVR met inclusion criteria. Of these, 100 (27.9%) were discharged on ACT. Patients discharged on ACT had a higher STS score compared to those without ACT (6.478 [IQR 4.1-9.2] versus 5.68 [IQR 3.6-8.77] respectively, $p=0.005$). At 3-years follow-up, patients on ACT had a higher mortality than those without ACT (Log-rank test $p=0.034$; Figure 1A). However, when adjusted for STS risk score, survival did not differ between groups (Hazard Ratio 1.09 [CI 0.75-1.56], $p=0.641$; Figure 1B). Additionally, ACT was not associated with a change in mean gradient ($p=0.2391$) nor valve dysfunction ($p=0.796$). **Conclusion:** The comorbidities may be responsible for worse mortality in patients receiving additional ACT after TAVR. ACT did not significantly change valve hemodynamics after TAVR with current echo assessment.



P1-128 Are Normal Mitral and Tricuspid Annuli Measured by 2-D Echocardiography Really Normal?

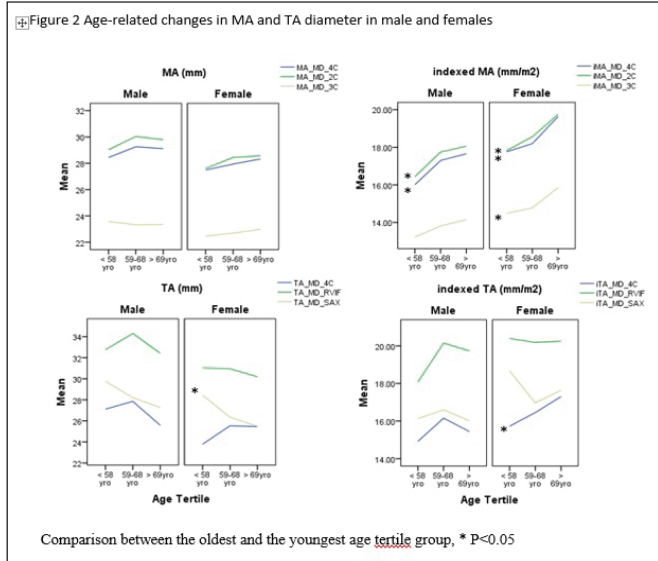
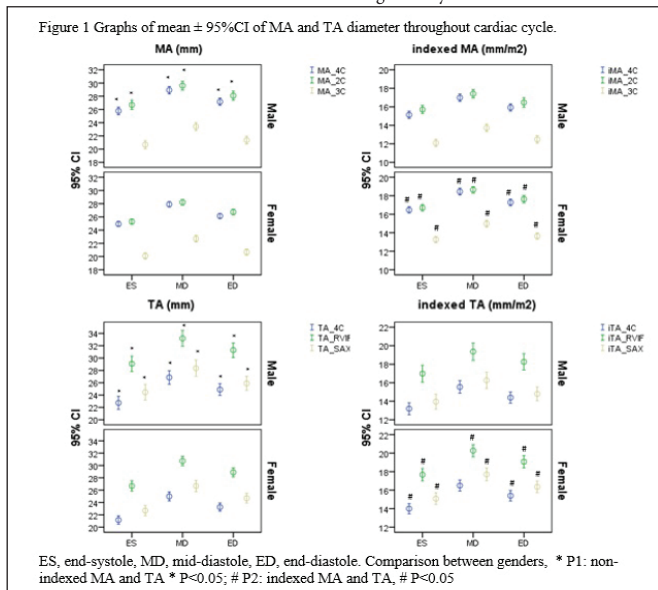
Wen Ruan¹, Nadira Binte Hamid², Abigail Camartin¹, Muh Tyng Teo¹, Wei Ting Foo¹, See Hooi Ewe¹, Zee Ping Ding¹. ¹National Heart Centre Singapore, Singapore, Singapore; ²New York Presbyterian/Columbia University Irving Medical Centre, New York, NY

Background: Mitral annulus (MA) and Tricuspid annulus (TA) diameters play an important role in decision-making in surgical or transcatheter heart valves therapy. Reference values in the guidelines were based on old studies, trans-oesophageal echocardiography, or direct

Poster Session 1 (P1)

Sunday, June 23, 2019

intraoperative measurements. Our aim is to define the normal ranges of TA and MA using routine 2D-trans thoracic echocardiogram (TTE). **Methods:** Retrospective review of TTE studies were performed in National Heart Centre Singapore from Jan to Dec 2016. Patients with symptoms suspected of cardiac etiology and normal echocardiographic findings were included. Patients with more than mild valvular disease, history of cardiovascular risk factors or significant systemic diseases were excluded. MA were measured in the 4-chamber (4C), 2-chamber (2C) and 3-chamber (3C) views, and TA were measured at 4C, right ventricular (RV) inflow and short axis (SA) views. Both MA and TA were measured in end-systole (ES), mid-diastole (MD), end-diastole(ED). ES was measured at the frame before valve opening; MD, at maximal valve opening; and ED, a frame before the valve closure. **Results:** A total of 295 subjects were studied (64±9yrs, 62% female). Figure 1 shows the mean±95% confidence interval of MA and TA diameters (and their indices) in our normal population. Importantly, both MA and TA were largest at MD, when compared with ES or ED (p<0.05). MA was largest at apical 2C, compared to 4C or 3C views; while TA was largest at RV inflow, compared to 4C or SA views (p<0.05). Compared to males, females had smaller non-indexed, but bigger indexed MA and TA diameters. With age, indexed MA gets universal dilatation (p<0.05), although this trend is not observed in tricuspid annulus. (Figure2) **Conclusion:** MA and TA diameter should be measured in mid diastole during maximal valve opening. In view of the complex annular shape, normal 2D reference range should be established with multiple 2-D views with consideration of age, gender and body surface area for accurate assessment of the annuli geometry.



P1-129

Alterations in Left Atrial and Left Ventricular Myocardial Function in Mixed Aortic Valve Disease

Maala Sooriyakanthan¹, Natalie Ho^{1,2}, Geraldine Ong², Howard Leong-Poi², Wendy Tsang¹. ¹Toronto General Hospital, UHN, University of Toronto, Toronto, ON, Canada; ²St. Michael's Hospital, University of Toronto, Toronto, ON, Canada

Background: Patients with mixed aortic valve disease (MAVD; combined moderate or > aortic stenosis (AS) and moderate or > aortic regurgitation) have poorer outcomes compared to those with isolated severe AS. Little is known of the impact of MAVD on left atrial (LA) and left ventricular (LV) myocardial mechanics. We aim to characterize LA and LV myocardial function in MAVD patients. **Methods:** We retrospectively identified 184 patients, 35 moderate MAVD (moderate AS and moderate aortic regurgitation), 40 severe MAVD (severe AS and moderate aortic regurgitation), 33 isolated severe AS, 31 isolated severe aortic regurgitation, and 45 controls, who underwent transthoracic echocardiogram. Simultaneous speckle-tracking longitudinal strain (LS) analysis of the LA and LV were performed on the apical 4-chamber view (EchoInsight, Epsilon) to obtain LV peak LS and LA peak, contractile, and conduit strain. ANOVA with post-hoc Tukey's test was used to compare groups. P<0.05 was considered significant. **Results:** Results are presented in Table 1. Compared to controls, LV peak LS was significantly reduced in moderate MAVD, severe MAVD and severe AS patients. LV peak LS was not significantly different between moderate MAVD and severe AS patients but was significantly lower in the severe MAVD group. Severe aortic regurgitation patients had higher peak LS compared to controls, moderate MAVD, severe MAVD and severe AS patients. LA peak, conduit and contractile strains were significantly reduced in moderate MAVD, severe MAVD and severe AS patients compared to controls and severe aortic regurgitation patients. LA peak and contractile strains were not different between the moderate MAVD, severe MAVD or severe AS groups. However, LA conduit strain was significant reduced in those with severe MAVD compared to the moderate MAVD but not the severe AS group. The severe aortic regurgitation group had preserved LA peak, conduit and contractile strain compared to the other groups. **Conclusion:** Moderate MAVD patients have a reduction in LV and LA myocardial function comparable to isolated severe AS patients. Severe MAVD patients have a greater decline in LV peak LS and LA conduit strain compared to moderate MAVD or severe AS patients. These changes may contribute to the poorer outcomes observed in MAVD patients.

Table 1

	Controls	Moderate MAVD	Severe MAVD	Severe AS	Severe AR
N	45	35	40	33	31
Age, years	66±8	58±22	69±15 [^]	70±12 [^]	55±16 ^{^#}
Female, n(%)	16(36%)	13(37%)	15(38)%	13(39%)	12(39%)
LV EDV indexed, mL/m ²	59±12	88±22*	101±27*	70±17 [#]	146±42 ^{^#}
LV ESV indexed, mL/m ²	30±6	40±10*	47±13*	31±8 [#]	63±21 ^{^#}
LV mass indexed, mg/m ²	73±11	96±19*	112±28 [^]	87±16 [#]	116±24 ^{^#}
LVEF, %	59.6±2.7	54.8±1.9*	53.4±2.0*	55.8±1.8 [#]	56.9±3.1 ^{^#}
LV strain, %	-20.5±1.4	-17.1±1.2*	-15.9±1.3 [^]	-16.8±1.6 ^{^#}	-21.4±1.5 ^{^#}
LV TTP corrected, %	36.6±4.2	37.2±6.7	38.1±6.0	40.6±6.5*	38.4±5.4
LA volume indexed, mL/m ²	31±8	44±19*	48±19*	37±10 [#]	46±19*
LA EF, %	60.8±7.1	47.9±9.4*	42.9±11.8*	45.2±9.3*	55.0±5.8 ^{^#}
LA strain, %	36.8±5.9	28.5±7.1*	26.2±8.6*	27.2±4.5*	34.7±6.8 ^{^#}
Contractile strain, %	-13.6±3.6	-9.2±3.7*	-9.6±4.7*	-10.5±2.2*	-11.7±4.0
Conduit strain, %	-22.7±4.2	-18.8±5.6*	-15.6±4.8 [^]	-16.7±4.4*	-22.6±5.1 ^{^#}
LA TTP corrected, %	42.5±5.7	42.1±7.0	42.5±7.0	46.1±6.7	44.4±6.8
LA:LV peak strain	-1.81±0.31	-1.66±0.39	-1.64±0.47	-1.62±0.27	-1.62±0.31
LA:LV TTP corrected	1.16±0.10	1.14±0.13	1.12±0.09	1.15±0.09	1.16±0.09

TTP corrected = (Time-to-peak strain/R-R)x100%
AR, aortic regurgitation; AS, aortic stenosis; EDV, end-diastolic volume; EF, ejection fraction; ESV, end-systolic volume; LA, left atrium; LV, left ventricle; MAVD, mixed aortic valve disease
*p<0.05 compared to controls, ^p<0.05 compared to moderate MAVD, #p<0.05 compared to severe MAVD, ^#p<0.05 compared to severe AS

PI-130

Identifying the Best Echocardiographic Parameter and Cut Point for Aortic Stenosis Severity Assessment

Giselle Raitz, Zainab Samad, Renato Lopes, Linda Shaw. Duke University, Durham, NC

Background: Age-related calcific aortic stenosis (AS) valve is the most common cause of obstruction of left ventricular outflow in adults. Valve intervention is triggered by symptoms onset and/or left ventricular dysfunction in the presence of severe AS defined by valve anatomy and valve hemodynamics. Guidelines recommend the use of echocardiographic parameters for the evaluation of AS severity. However, there are discrepancies in the current guidelines regarding agreement of different echo parameters and cut-off points to stratify the severity of AS. Most of these cut-offs have been defined using correlational data with cath and outcomes data from old studies. Since there is no true gold standard, choosing

Poster Session 1 (P1)

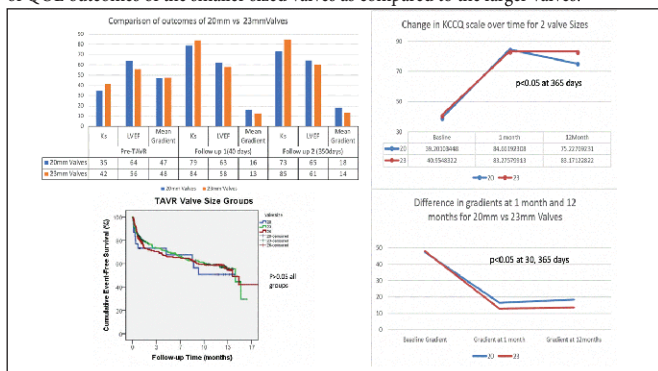
Sunday, June 23, 2019

a cut-off and a parameter that can best dichotomize outcomes presents itself as the best alternative approach. **Methods:** Observational study based on data collected from Duke Echocardiographic Database that searched for patients with AS from Jan 1, 2010 to Dec 31, 2014. Data of 3044 patients were collected prospectively and included into a registry. The inclusion criteria were adult patients >18 years old with diagnostic of stenosis of aortic valve. **Results:** The relationship between unadjusted continuous measures of aortic stenosis - mean aortic valve gradient, aortic valve area (AVA), and peak velocity - and long-term mortality indicates that AVA has a strong association with survival ($p < .0001$) with a decreasing risk as AVA values increase (HR=.622). The peak velocity and mean gradient did not produce a significant relationship with survival ($p=.1371$, $p=.1445$, respectively). The adjusted survival model demonstrated that AVA continues to have a significant association with mortality ($p < .0001$) and mean gradient achieved significance ($p=.0174$). The relationship between AS measures and likelihood of AV intervention within 60 days demonstrated that the best cut-off points were AVA $< 0.6\text{cm}^2$, mean gradient $> 45\text{mmHg}$, and peak velocity $> 4.5\text{m/s}$. All results yielded a highly significant association ($p < .0001$), with good discriminatory ability as evidenced by the c-indices ($\geq .746$). In the adjusted model setting, AVA and mean gradient continued to be significantly associated with AV intervention, but peak velocity was not significant after adjusted for baseline characteristics ($p=.0182$, $p < .0001$, $p=.9189$, respectively). **Conclusions:** While AVA is significant in the 'real world' setting examining survival in the patients without AV intervention, both AVA and mean gradient exhibited a significant association with the referral for AV intervention within 60 days.

P1-131
Size Matter for TAVR

Manik Veer, Mark Doyle, Stephen Bailey, Ramzi Khalil, Victor Farah. Allegheny General Hospital, Pittsburgh, PA

Background: PARTNERS trials helped establish Transcatheter Aortic Valve Replacement (TAVR) as a standard of care for severe aortic stenosis. To understand clinical impacts on quality of life (QOL) post TAVR, the national Transcatheter Valve Therapy (TVT) registry was established. We analyzed our institution's TVT registry data to compare the difference in outcomes of 20mm, 23mm and 26mm valves. **Methods:** 601 consecutive patients who had undergone TAVR ($n=690$) with 20mm ($n=31$), 23mm ($n=301$) and 26mm ($n=269$) valves between May 2012-July 2017 were reviewed. Data was recorded per TVT registry guidelines and follow ups were at 30 days (582/601, 97%) and 365 days (297/420 71%); 70 deceased at <365 days). Clinical parameters and Kansas City Cardiomyopathy Questionnaire scores (Ks) were used to compare the outcomes. **Results:** Baseline average mean gradient (mDP; mmHg) and Ks were 47.7 ± 11.9 and 41.9 ± 26 ($n=331$) for the 20mm and 23mm valves ($p > 0.05$ 20mm vs 23mm). Follow up 20mm vs 23mm valve mDP was 16.4 (27/30) vs 12.9 (284/301) ($p=0.002$) and $18.4(n=14)$ vs $13.5(n=126)$ ($p=0.005$) at 30 and 365 days. Ks was $79.2(27/30)$ vs $84.2(267/302)$ ($p=0.25$) and $73.1(n=13)$ vs $85(n=120)$ ($p=0.04$) at 30 and 365 days. Event rates and mortality between the 3 valves were not significantly different ($p > 0.05$). **Conclusion:** Studies have shown a failure of sustained improvement in QOL post TAVR in some patients. Our cohorts baseline Ks is comparable to data from the national TVT registry. Our patients derived significant benefit from TAVR at 30 days and 365 days. Although our analysis is limited by a small sample of 20mm valve patients, it suggests that mDP are higher at implantation and increase at 365 days for the smaller valve. Patients with 23mm valve had a more sustained improvement in QOL without further increases in mDP at 365 days. Decline of QOL in the 20mm valve subgroup is independent of rehospitalizations. In our experience, extra effort has been made to oversize small transcatheter heart valves when it is deemed feasible. We recommend further review of QOL outcomes of the smaller sized valves as compared to the larger valves.



P1-132

Predictors of Major Adverse Cardiac Events in Asymptomatic Low Gradient Aortic Stenosis with Preserved Ejection

Waleed Al-Darzi, Daniel Kupsky, Abigail Entz, Tamara Roumayah, Crystal Seudeal, Charlotte Burmeister, Karthikeyan Ananthasubramaniam, Henry Ford Hospital, Detroit, MI

Background: Patients with low mean pressure gradient ($< 40\text{mmHg}$) severe aortic stenosis (Aortic valve area $< 1.0\text{cm}^2$) despite preserved ejection fraction ($\geq 50\%$) have had varying outcomes in prior studies. We sought to evaluate what clinical and echocardiographic parameters would help predict major adverse cardiac events (MACE) in these patients. **Methods:** A retrospective data review of patients with asymptomatic low gradient aortic stenosis with preserved ejection fraction was performed. Patients with prior valvuloplasty, surgical aortic valve replacement (SAVR), or transcatheter aortic valve replacement (TAVR) were excluded. Comprehensive demographic, clinical, echocardiographic parameters of 287 patients from January 2014 till December 2015 were obtained. Left ventricular global longitudinal strain (GLS) was able to be measured in 94 patients by using speckle tracking imaging. Composite MACE included congestive heart failure, myocardial infarction, SAVR, TAVR, or death were obtained after the initial echocardiogram date. **Results:** The average age of our studied population is 79.4 years (SD: 13.6). Of them, 67% ($n=63$) are females. Nineteen patients (20%) have atrial fibrillation, 77 patients have hypertension (82%), and 40 patients (43%) have history of coronary artery disease. Baseline echocardiographic parameters include mean aortic valve area of 0.8cm^2 (SD: 0.2) with indexed aortic valve area of $0.5\text{cm}^2/\text{m}^2$ (SD: 0.1). The average of mean pressure gradient is 27.8mmHg (SD: 12.6) and the average stroke volume index (SVi) is $38.6\text{mL}/\text{m}^2$ (SD: 11.5). Sixty-three patients had normal-flow low-gradient severe aortic stenosis (SVi $\geq 34\text{mL}/\text{m}^2$), while 31 patients had paradoxical low-flow low-gradient aortic stenosis (SVi $< 34\text{mL}/\text{m}^2$). Composite outcomes of MACE developed in 58.5% ($n=55$) of the studied population ($n=94$). Independent univariate predictors of MACE were atrial fibrillation (OR, 4.9; 95% CI, 1.3-18.3; $p=0.0174$). Using a multivariate logistic regression, there were higher odds of having MACE among patients with higher mean gradient across aortic valve (OR, 1.1; 95% CI, 1.0-1.1; $p=0.0025$), with lower SVi (OR, 0.9; 95% CI, 0.9-1.0; $p=0.0061$), and with history of atrial fibrillation (OR, 5.3; 95% CI, 1.4-20.6; $p=0.0163$). Valvuloarterial impedance or GLS did not add any independent predictive value for MACE. **Conclusion:** Our single center study of low gradient aortic stenosis patients suggests that commonly used indices such as SVi, mean pressure gradient, and history of atrial fibrillation could best help predict MACE. Larger studies are necessary for further assessment.

P1-133

MitraClip After Failed Surgical Mitral Valve Repair: Echocardiographic Outcomes

Nir Flint, Sam Dawkins, Richard Cheng, Sung-Han Yoon, Takao Morikawa, Jun Yoshida, Atsushi Hayashi, Matthias Raschpichler, Hezzi Shmueli, Moody Makar, Raj Makkar, Saibal Kar, Takahiro Shiota, Robert J. Siegel. Cedars Sinai Medical Center, Los Angeles, CA

Background: Recurrence of mitral regurgitation (MR) after surgical mitral valve repair is not uncommon, especially after anterior or bi-leaflet repair. Compared with an initial surgery, a re-do mitral valve surgery is associated with higher morbidity and mortality, as well as higher rates of mitral valve replacement. Percutaneous mitral valve repair or replacement may be an option for patients with recurrent MR after surgical repair, which are poor surgical candidates or who wish to avoid a second surgery. The MitraClip procedure is the most widely used technique for percutaneous mitral valve repair in both primary and secondary MR. We investigated echocardiographic outcomes before and after MitraClip in a subset of patients which had a previous surgical mitral valve repair. **Methods:** We collected clinical and echocardiographic data of patients with previous surgical mitral valve repair who underwent percutaneous edge-to-edge repair with MitraClip at Cedars-Sinai Medical Center between 2015 - 2018. Pre-procedural, intra-procedural and follow-up echocardiography data were retrospectively analyzed. **Results:** A total of 17 patients (mean age 76 ± 9 , 76% men) underwent a MitraClip procedure following surgical mitral valve repair with annuloplasty. Median time interval between surgery and MitraClip was 3 years (range 0-18). Median echocardiographic follow-up was 32 days (Interquartile range 27-349). One patient died during follow-up. As shown in Table 1, MitraClip resulted in a significant reduction in the degree of MR (88% had mild or less MR during follow-up). A reduction was observed in left ventricular (LV) end-systolic and end-diastolic volumes ($P < 0.001$), pulmonary artery systolic pressure ($P=0.01$) as well as left atrial area ($P=0.055$). There was no significant increase in mitral gradients after MitraClip. Following MitraClip deployment, intraprocedural pulmonary vein flow showed a significant increase in systolic velocities and an increased ratio of systolic to diastolic VTI ($P < 0.001$). **Conclusion:** In patients with recurrence of MR after surgical mitral valve repair at high risk for repeated surgery, MitraClip provides acute and short-term improvement in the severity of MR, as well as a decrease in LV chamber size, pulmonary pressure and degree of tricuspid regurgitation.

Poster Session 1 (P1)

Sunday, June 23, 2019

TABLE 1 Echocardiographic Parameters Before and After MitraClip in Patients with Failed Surgical Mitral Ring

Variable	Pre MitraClip	Post MitraClip	P value
Left Ventricle			
End systolic diameter, cm	3.8 ± 0.9	3.5 ± 1	0.054
End diastolic diameter, cm	5.2 ± 0.7	4.8 ± 0.8	0.004
End systolic volume, ml	56 ± 26	40 ± 23	<0.001
End diastolic volume, ml	115 ± 28	81 ± 33	<0.001
End systolic volume indexed, ml/m ²	28 ± 18	23 ± 14	0.162
Ejection fraction, %	52 ± 17	50 ± 17	0.578
LVOT VTI, cm	15.0 ± 4.8	17.2 ± 1.5	0.234
Mitral Valve			
Mean gradient, mmHg	4.2 ± 1.9	4.7 ± 1.2	0.402
MR grade, n (%)			0.001
+1	0 (0%)	15 (88%)	
+2	0 (0%)	2 (12%)	
≥+3	17 (100%)	0 (0%)	
Left Atrium			
LA area, cm ²	33 ± 10	30 ± 10	0.055
LA volume indexed, ml/m ²	74 ± 34	62 ± 36	0.184
Intra-procedural Pulmonary Vein Pulsed Doppler			
Systolic velocity, cm/s, median (IQR)	17 (12-22)	30 (24-40)	0.003
Diastolic velocity, cm/s, median (IQR)	55 (49-73)	31 (25-40)	<0.001
Systolic VTI, cm, median (IQR)	3.3 (3.0-4.5)	8.8 (5.5-12.7)	<0.001
Diastolic VTI, cm, median (IQR)	12.1 (9.2-14.8)	7.3 (6.2-10.8)	0.018
Systolic VTI/Diastolic VTI ratio	0.19 ± 0.48	1.1 ± 0.6	<0.001
Right Heart Parameters			
PASP	46 ± 12	35 ± 8	0.01
RV diameter, cm	4.4 ± 0.6	4.3 ± 0.7	0.703
IVC diameter, mm	22 ± 4	19 ± 6	0.138
TAPSE, mm	16 ± 4	15 ± 3	0.767
RA area, cm ²	24 ± 6	22 ± 5	0.411
Tricuspid regurgitation ≥Moderate, n (%)	11 (64%)	4 (24%)	0.003

LVOT=left ventricular outflow tract; MR=mitral regurgitation; LA=left atrium; VTI=velocity time integral; IQR=interquartile range; PASP=pulmonary artery systolic pressure; RV=right ventricle; IVC=inferior vena cava; TAPSE=tricuspid annular plane systolic excursion

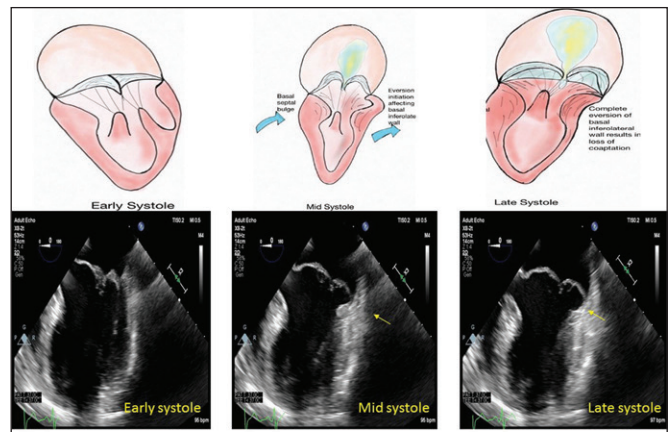


Figure. Mitral valve prolapse with eversion during systolic phase

Parameters	MVP-children (16)	P ¹	Controls (20)	P ¹	MVP-adult (20)
Base/Mid ratio¹					
Inferior	0.77 (0.36-1.07)	0.20	1.05 ± 0.44	<0.001	0.47 ± 0.29
Inferolateral	0.76 (0.49-1.13)	0.016	1.10 ± 0.29	<0.001	0.66 ± 0.40
Base/apex ratio²					
Inferior	0.50 (0.32-0.82)	0.002	0.93 ± 0.25	<0.001	0.35 (0.19-0.71)
Inferolateral	0.81 (0.39-0.93)	0.007	1.13 ± 0.37	<0.001	0.51 ± 0.27
Regional ratio³					
Inferior	0.85 ± 0.41	0.736	0.89 ± 0.16	0.001	0.66 ± 0.23
Global ratio⁴					
	0.72 ± 0.28	0.004	0.95 ± 0.15	<0.001	0.52 ± 0.22

Normally distributed continuous variables are presented as mean ± standard deviation. Non-normally distributed continuous variables are presented as median (inter-quartile range).

MVP, mitral valve prolapse.

¹Ratio of the basal inferior or inferolateral segments to the same segment at the midlevel.

²Ratio of the basal inferior or inferolateral segments to the same segment at the apex level.

³Ratio of average(basal inferior+basal inferolateral)/average the other segments at the base

⁴Ratio of average (basal inferior + basal inferolateral)/average the other segments

¹MVP-children versus controls

²MVP-adult versus controls

P1-134

Central Mitral Regurgitation Caused by End-Systolic Annulo-Ventricular Eversion: A Myocardial Contractility Issue

Mario Castillo-Sang¹, Tarek Alsaied², Cassidy Palmer¹, Vien Truong¹, Brian Kelly¹, Michael Young¹, Gregory Egnaczyk¹, Eugene Chung¹, Justin Tretter², Wojciech Mazur¹. ¹The Christ Hospital, Cincinnati, OH; ²Cincinnati Children's Hospital, Cincinnati, OH

Background: Outward and apical displacement of the left ventricle (LV) base and mitral annulus during systole, atrial displacement of the mitral valve and apparatus with poor coaptation at end-systole leads to central regurgitation. Previously termed in Barlow's as functional bileaflet prolapse, it is best termed end-systolic LV eversion. We postulate this eversion is an annular/LV phenomenon driven by a contraction force gradient from base to apex creating a muscle waist below the base. We aimed to analyze the LV contractility pattern unique to eversion. **Methods:** 36 patients (20 adults and 16 children) had mitral valve prolapse with eversion. Regional circumferential strain (RCS) values were obtained using two-dimensional speckle tracking software (TomTec, Munich, Germany). We compared RCS values and intra-regional patterns of strain between an age-matched [TJ1] control group of 20 healthy adults and the eversion group. We normalized the values by creating a ratio of the basal/mid and basal/apical regions. [TJ2] **Results:** RCS was lower in the basal inferior region of patients with eversion compared to controls (-17.0 ± 8.3 pediatric vs. -26.6 ± 5.7 control, p = 0.001; -13.0 ± 8.0 adult vs. -26.6 ± 5.7 control, p < 0.001). In addition, the basal inferolateral RCS was lower in the eversion group (-19.5 ± 9.8 pediatric vs. -25.9 ± 4.1 control, p = 0.03; -15.1 ± 6.8 adult vs. -25.9 ± 4.1 control, p < 0.001). The basal inferior and basal inferolateral RCS had lowest values compared to other segments (overall p<0.05) in the eversion group. When we normalized the RCS values we found that the basal inferolateral/apical-lateral and basal-inferior/apical inferior ratios were lower in the eversion groups (Table 1). **Conclusions:** End-systolic LV eversion is characterized by weaker contraction in the basal-inferolateral and inferior segments with stronger mid and apical region contraction, leading to outward and apical displacement of the annulus and base. This results in leaflet malcoaptation with end-systolic mitral regurgitation.

P1-135

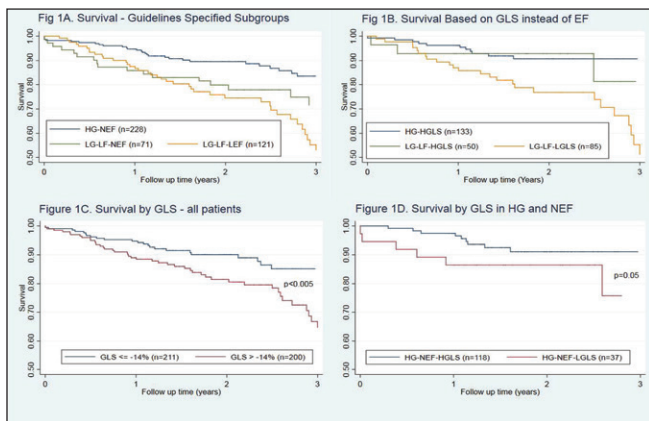
Incremental Prognostic Value of Preoperative Global Longitudinal Strain on Mortality Following Transcatheter Aortic Valve Replacement

Jonas A. Povlsen, Henrik Vase, Vibeke Guldbrand Rasmussen, Kaare Troels Jensen, Christian Juhl Terkelsen, Evald Hoj Christiansen, Ole Norling Mathiassen, Steen Hviitfeldt Poulsen. Department of Cardiology, Aarhus N, Denmark

Background: Prognosis after transcatheter aortic valve replacement (TAVR) is variable. This might depend on preoperative evaluation of myocardial performance by other measurements than ejection fraction (EF). The aim of this study was to investigate the predictive value of preoperative global longitudinal strain (GLS) and the guidelines specified subtypes of aortic stenosis (AS) on mortality following TAVR. **Methods:** We included 511 patients with severe AS who underwent TAVR in the period July 2012 - June 2017. Patients were divided into guideline-specified subgroups based on EF (EF: ≥50 (NEF) or <50% (LEF)), peak gradient (PG: ≥4 (HG) or <4 m/s (LG)) and flow status (stroke volume index (SVI): ≥35 (NF) or <35 ml/min/kg (LF)): (1) HG-NEF (n=228), (2) HG-LEF (n=91), (3) LG-LF-NEF (n=71) and (4) LG-LF-LEF (n=121). We also investigated the effect of replacing EF by GLS in the guideline specified subgroups (GLS ≤-14 (HGLS) and GLS > -14% (LGLS)). **Results:** Mean follow up time was 1033 days. Mean age was 80.2±7.1 years. Median overall survival was 5.3±0.3 years. Comorbidity burden was higher in patients with LF - and LEF status in terms of a higher median plasma creatinine (103 [85;135], p<0.001) and EurologII score (6.1 [3.4;9.6], p<0.001). LG-LF-LEF AS was associated with a significantly worse outcome compared with all other groups (p<0.005, Fig 1A). High gradient status, irrespective of EF (p=0.88), was associated with the best prognosis with a median survival of 5.0±0.5 and 5.5±0.1 years for NEF and LEF, respectively. Overall and in patients with HG-NEF, impaired GLS (>-14%) was associated with poor outcome (Fig. 1B-D). There was a trend towards a poorer prognosis with GLS > -14% in LG-LF-NEF AS (p=0.10). In an univariate analysis impaired GLS > -14% (HR 2.04, p<0.005), LG-LF-LEF status (HR 1.82, p=0.001), PG < 4m/s (HR 1.74, p=0.001) and tricuspid regurgitation gradient > 30 mmHg (HR 1.63, p<0.001) were significant predictors of mortality in contrast to EF, SVI, age, gender and plasma creatinine. GLS > -14% emerged as the only significant outcome predictor in a multivariate analysis (HR 1.93, p<0.05). **Conclusion:** Impaired global longitudinal strain > -14% was the best individual echocardiographic predictor of overall survival in symptomatic severe AS and could identify a subgroup of patients with HG-NEF AS with a worse prognosis.

Poster Session 1 (P1)

Sunday, June 23, 2019



P1-136

Usefulness of Dobutamine Stress Echocardiography in Aortic Valve Regurgitation Patients with Reduced Left Ventricular Systolic Function

Chihiro Saito, Kotaro Arai, Kyomi Ashihara, Nobuhisa Hagiwara. Tokyo Women's Medical University, Tokyo, Japan

Background: The predictor for postoperative reverse remodeling in patients with severe aortic regurgitation (AR) and reduced left ventricular ejection fraction (LVEF) is still unknown. The aim of this study was to perform low-dose dobutamine stress echocardiography (DSE) in patients with severe AR and reduced LVEF and to evaluate the relationship between contractile reserve (CR) and reverse remodeling after surgery. **Methods:** In 32 patients with chronic severe AR and reduced LVEF (LVEF <50%) (mean age was 60 ± 14 years), we performed DSE and assessed CR and examined whether changes in preoperative DSE associated with improvement of postoperative LVEF at 6 months after aortic valve replacement (AVR). **Results:** Before AVR, echocardiographic findings showed LV end-diastolic dimension was 6.6 ± 5.1 cm, LV end-systolic dimension was 5.1 ± 1.3 cm, LVEF 42 ± 8 % at rest. All patients underwent aortic valve surgery. Of 32 patients, 21 patients had EF ≥50% at DSE, and 11 patients had EF <50% at DSE. Of 21 patients with CR, 15 patients (71.4%) had postoperative EF ≥50%. On the other hand, all 11 patients without CR had postoperative EF <50%. Both preoperative EF at rest and during DSE were significantly associated with postoperative EF ≥ 50%, and the receiver operating characteristics (ROC) curve for postoperative EF ≥ 50% indicated the cut-off points as LVEF 44% at rest. Therefore, we further examined 13 patients with EF ≤44% before surgery. The ROC curve for the improvement of postoperative EF indicated the cut-off points as ΔEF 6% during DSE. Of 13 patients, 7 patients had ΔEF ≥6% (with CR) and 6 patients had ΔEF <6% (without CR). Of 7 patients with CR, 6 patients showed improvement of postoperative EF, however, only 1 patients showed improvement of postoperative EF in patients without CR (p=0.03). **Conclusion:** Dobutamine stress echocardiography in patients with severe AR and especially moderately reduced LVEF may be helpful examination for predict postoperative reverse remodeling.

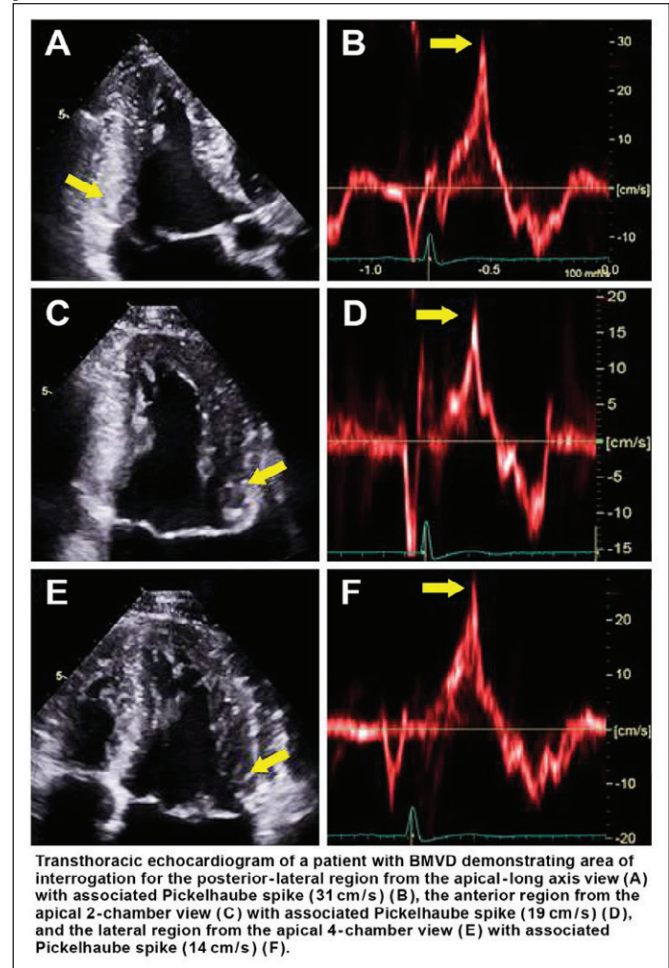
P1-137

Barlow's Bileaflet Myxomatous Mitral Valve Disease: Systematic Search for High Velocity Annular Spike (Pickelhaube)

Denise Ignatowski, McKenzie Schweitzer, Lakshmi Muthukumar, Renuka Jain, Bijoy K Khandheria, A. Jamil Tajik. Aurora Cardiovascular Services, Aurora Sinai/Aurora St. Luke's Medical Centers, Milwaukee, WI

Background: We recently reported a high velocity spiked configuration of the pulsed-wave tissue Doppler signal, the Pickelhaube sign, in patients with Barlow's bileaflet myxomatous mitral valve disease (BMVD). We proposed this signal as one of the high risk markers in BMVD patients for ventricular arrhythmias. The goal of our study was to identify the best location to obtain the highest Pickelhaube spike for BMVD patients. **Method:** A large pulsed-wave tissue Doppler sample volume (5 to 10 mm) was utilized to capture the annular motion at an angle of interrogation as parallel as possible to the Doppler beam. This sample volume was placed at the mitral valve annulus and meticulously tracked towards the basal myocardial segment. We interrogated medial and lateral annuli from the apical four-chamber, posterior and anterior annuli from the apical-two chamber, and posterolateral annulus from the apical-long axis. **Results:** We evaluated 47 BMVD patients (mean age 52 ± 15, 53% female) with a reported Pickelhaube spike. In the first 15 (32%) patients, all five locations were interrogated, and the highest yield was noted in the posterolateral (22 ± 9 cm/sec) and lateral annuli (21 ± 4 cm/sec). In the subsequent 32 (68%) patients, we focused on interrogating the posterolateral and lateral annuli. Of the 32 patients, 19 (59%) patients yielded the highest spike value from the posterolateral annulus (19 ± 6 cm/sec), 5 (15%) from the lateral annulus (13 ± 2 cm/sec), and 1 (3%) from the posterior annulus. There were 7 (22%) patients who shared the same peak value from posterolateral and lateral annulus (14 ± 5 cm/sec). **Conclusion:** In this study, we evaluated multiple

mitral valve annuli in the apical views to determine location of highest Pickelhaube spike. Through this systematic search, we determined that the highest Pickelhaube signal velocity in the majority of patients was found in the posterolateral annulus. This is an important finding for cardiac sonographers as the posterolateral annulus is an unconventional site of interrogation. By focusing on this area, sonographers may help identify high risk BMVD patients.



P1-138

Circumferential Ascending Aortic Strain to Predict Paravalvular Leaks After Transcatheter Aortic Valve Replacement

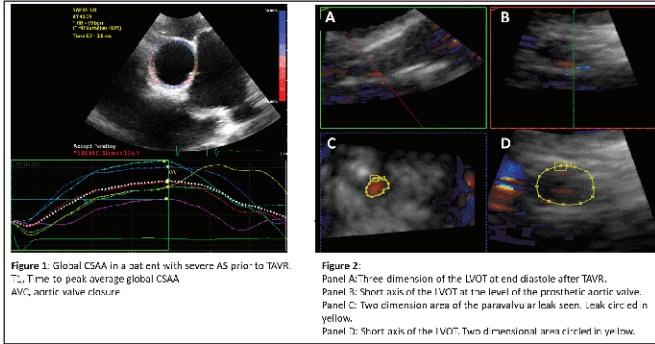
Deepa Raghunathan¹, Jing Zhang², Chunyan Cai², Prakash Balan¹, Simbo Chiadika¹. ¹University of Texas McGovern Medical School Department of Cardiovascular Medicine, Houston, TX; ²University of Texas McGovern Medical School Department for Clinical and Translational Sciences, Houston, TX

Background: Transcatheter aortic valve replacement (TAVR) is a viable option to improve mortality and longevity in patients with severe aortic stenosis (AS) where the risk of surgical replacement is prohibitive. However, paravalvular leak (PVL) is a common and unpredictable complication that worsens mortality when significant. Less compliant aortas may be prone to PVL after TAVR. Strain echocardiography assesses myocardial deformational change of various cardiac structures. We measured circumferential strain of the ascending aorta (CSAA) to determine whether CSAA can predict PVL prior to TAVR. **Methods:** In our tertiary center, we retrospectively compared CSAA in patients with normal aortic valves to CSAA of patients with severe AS before and 24 hours after TAVR. CSAA assessment was performed with a prepackaged software. The peak global strain and time-to-peak global CSAA was measured (Figure 1). Successive CSAA was performed by two blinded readers. To determine PVL in patients after TAVR, the left ventricular outflow tract (LVOT) was acquired in three-dimension. PVL was quantified as the two-dimensional area of regurgitant flow to the short axis area of the LVOT (Figure 2). CSAA and time-to-peak global CSAA were compared in normal aortic valves, and those before and after TAVR. Intraclass correlation (ICC) was calculated based on two-way random effects model to measure the inter-rater reliability. **Results:** 19 patients before and after TAVR was included and 8 had measurable PVL. There was no significant difference between CSAA before or immediately after TAVR (7 ± 4 %, p = 0.48). However, there was

Poster Session 1 (P1)

Sunday, June 23, 2019

a significant difference in the time-to-peak global CSAA before and after TAVR (327 ± 88.3 milliseconds vs. 244 ± 92.9 milliseconds, p = 0.02). In those with PVL, there was no significant difference between CSAA (p=0.64) and time-to-peak global CSAA (p=0.61) prior to TAVR. Inter-observer agreement was strong in CSAA measurements (ICC= 0.95, 95% confidence interval 0.91-0.97). **Conclusion:** Our study shows shortening of the time-to-peak global CSAA in patients with severe AS after TAVR. In patients with PVL, there is no significant difference in the CSAA after TAVR. CSAA changes may occur later as the aorta remodels. Follow up CSAA measurements are essential to determine the utility of this novel modality in TAVR patients.



P1-139

Impact of Transcatheter Aortic Valve Replacement on Left Ventricle Diastolic Function and Remodeling in Patients with Severe Aortic Stenosis and Preserved Left Ventricular Function

Garima Dahiya¹, Andreas Kyvernitakis¹, Aditya A. Joshi¹, Orestis Pappas², Rahul Sinha³, Georgios Lygouris¹, David Lasorda¹, Robert W. Biederman¹, Manreet Kanwar¹, Amresh Raina¹. ¹Allegheny General Hospital, Pittsburgh, PA; ²Jefferson Hospital, Pittsburgh, PA; ³University of Pittsburgh Medical Center, Altoona, PA

Background: Aortic stenosis (AS) is a known cause of left ventricular (LV) hypertrophy and diastolic heart failure. Limited data is available regarding the impact of transcatheter aortic valve replacement (TAVR) on regression of LV hypertrophy and myocardial remodeling. In this study, we sought to investigate the impact of TAVR on diastolic function and LV remodeling by echocardiography, in patients with severe AS and preserved LV systolic function. **Methods:** We reviewed records of patients with severe AS and preserved LV ejection fraction (LVEF) (≥55%), who underwent TAVR in our institution. We studied pre-procedure, within 1 month post-TAVR and 1 year post-TAVR transthoracic echocardiograms and assessed diastolic function parameters based on the 2016 ASE/EACVI guidelines. Patients who had reduced LVEF, a paced rhythm, atrial fibrillation or atrial flutter were excluded from the study. Statistical differences were determined by repeat measures ANOVA and Pearson's Chi Square test using Stata software. **Results:** Of the 342 patients who met the eligibility criteria from the institutional TVT registry, 171 patients were included in the analysis. At 1 year post-TAVR, an improvement in LV diastolic dysfunction was noted (mean grade 1.5 vs 1.28 vs 1.34, baseline, 1 month & 1 year post operatively, p= 0.035). Individual measures of diastolic function such as e' medial, e' lateral, E wave velocity, E/A and E/e' were not seen to change significantly but there was a significant decrease in TR jet velocity (271 vs 248 cm/s, p=0.049). There was also a significant decline in LV mass index (median, 104.35 vs 93; p = 0.006) associated with changes in LV volumetrics, i.e, LV end systolic diameter (29, vs 27; p= 0.009) and LV end diastolic diameter (median, 44 vs 42; p = 0.052). The interventricular septal thickness changed marginally on 1 year follow up (median, 13 vs 12, p= 0.78) while the posterior LV wall thickness stayed the same (median, 11 vs 11, p= 0.28) [table 1]. **Conclusion:** There is an immediate improvement in diastolic dysfunction in patients with severe AS and preserved LV systolic function undergoing TAVR. There is evidence of regression in several LV volumetric parameters suggestive of conceivable reverse LV remodeling. More studies are needed to validate these findings and investigate the impact on morbidity and mortality.

Hemodynamics	Pre-operatively (Median, IQR)	1 month follow up (Median, IQR)	1 year follow up (Median, IQR)	p-value
Systolic blood pressure (mm Hg)	148 (129 - 166)	148.5 (132.5 - 166)	144 (130- 160)	0.152
Diastolic blood pressure (mm Hg)	74 (68-79)	72 (65-80)	74 (67-82)	0.498
Echocardiographic Parameters				
Aortic valve parameters				
Mean AV gradient (mm Hg)	44.4 (40.7- 51.5)	12 (9.1-14.4)	12.6, 9- 16	<0.001
Peak AV gradient (mm Hg)	72.2 (67- 83.9)	21.7 (17.1- 26.7)	23.5 (17- 29.1)	<0.001
Peak AV velocity (cm/s)	423.6 (404.6- 451.6)	232.6 (205- 257.9)	233.5 (202.6-269.4)	<0.001
Diastolic function parameters				
E wave velocity (cm/s)	95.2 (80.8-115.1)	97.9 (80-112)	97.3 (83.3-118.9)	0.256
e' medial (cm/s)	4.4 (4-5.8)	4.9 (4-5.9)	4.85 (4-6.4)	0.593
e' lateral (cm/s)	5.85 (4.6-7)	6 (4.7-7)	6 (4.9-7)	0.441
E/e'	18.53 (13.7- 22.4)	18.08 (14.2- 24.2)	16.66 (14-22.8)	0.262
E/A	0.8 (0.7-1)	0.8 (0.7-1)	0.815 (0.7-1.1)	0.684
Left atrial volume index (mL/m ²)	38.2 (30-45.6)	35 (27.9- 44.3)	36 (27.3- 44.9)	0.102
Tricuspid regurgitation max velocity (cm/s)	271.5 (239.1- 297.3)	248.4 (229.1-282)	252.7 (231.9- 291.5)	0.049
Left ventricle parameters				
LV ejection fraction (%)	65 (60-70)	65 (62-69)	65 (62-69)	0.433
LV Mass Index (g/m ²)	104.35 (85-123.9)	97.45 (79.2- 116.4)	93 (74-115.3)	0.006
LV systolic volume (mL)	26.2 (17.2- 38.4)	26.8 (17-37)	22.6 (15.5-35)	0.378
LV diastolic volume(mL)	76 (60.2-95.7)	73.05 (53.7- 89.7)	69 (54-86)	0.082
LV end systolic diameter (mm)	29 (25-34)	28 (25-32)	27 (23-31)	0.009
LV end diastolic diameter (mm)	44 (39-48)	42 (38-47)	42 (38-47)	0.052
Posterior LV wall thickness (mm)	11 (10-13)	11 (9-13)	11 (9.6-12.8)	0.287
Inter ventricular septal thickness (mm)	13 (11-15)	13 (11-14)	12 (11-14)	0.781

Table 1: Left ventricular and diastolic function variables as seen on transthoracic echocardiography

P1-140

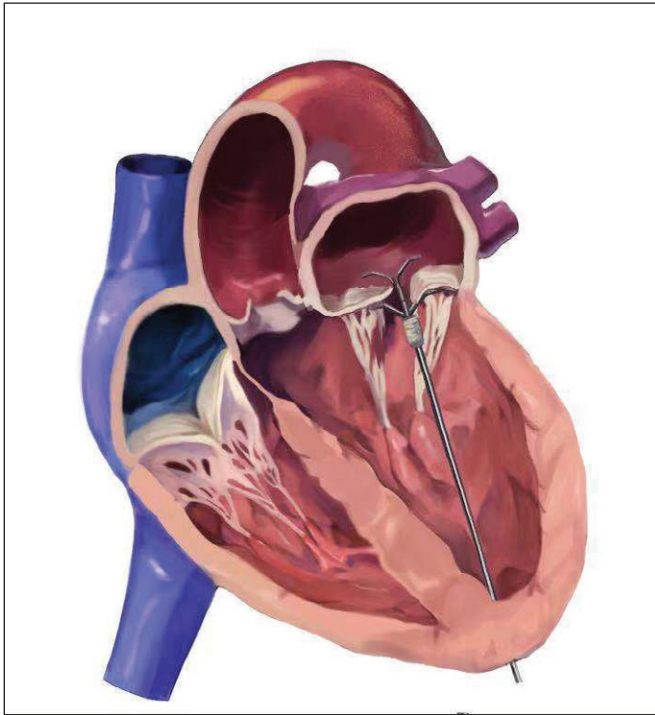
Epicardial Echocardiographic Guidance and Assessment of a Novel, User-friendly, Transcatheter Edge-to-edge Mitral Valve Repair Device in a Porcine Model of Mitral Regurgitation

Z.Y. Ge, C.Z. Pan, Xianhong Shu, W.Z. Pan, D.X. Zhou, H.Y. Chen, L. Wei, J.B. Ge. Zhongshan Hospital, Fudan University, Shanghai, China

Background: The ValveClamp mitral valve repair system (Hanyu Medical Technology, Shanghai, China), has been devised to treat mitral regurgitation (MR) through the transapical route by replicating the edge-to-edge repair surgery. This system encompasses an easily operating leaflet clamp and a smaller-sized delivery system (14F-16F). Epicardial echocardiography is used as the unique imaging modality to guide this procedure. **Methods:** Acute MR was induced in 36 anesthetized porcine subjects by severing the major chordae supporting the corresponding segment of the leaflet. The ValveClamp system was then transapically implanted on the prolapsing segment under epicardial echocardiographic guidance. This guidance protocol consisted of predetermined conventional views and a standardized anatomic-based views. All of the animals were killed 30 days after the procedure to verify proper location of the implanted devices. **Results:** Real-time echocardiography facilitated the deployment of this device. The duration of catheterization ranged from 18-40 min. Cutting the major chordae induced an eccentric MR jet (3+, 27.8%/ 4+, 72.2%) in all of the animals. Echo assessments revealed that the ValveClamp attenuated MR to ≤ 1 in 100% of the pigs, and there is no evidence of mitral valve stenosis. Residual MR was mild in 8 cases (22.2%), trivial in 19 cases (52.8%), and absent in 9 cases (25%). Autopsy demonstrated that 35 of the 36 ValveClamp devices were precisely placed to clip the prolapsing segment of the mitral valve. **Conclusion:** In the present study, the ValveClamp was successfully implanted in all the MR porcine models under epicardial echocardiographic guidance. As the unique imaging modality, it conferred a high success rate and short operation time. **Figures:** Image of X-plane mode showing the procedure of the ValveClamp implantation a and b: There was only slight MR before establishment of the acute MR model. c and d: Cutting the major chordae supporting the A2 segment instantly caused severe MR. e and f: The moment the clamp arms were clamped on the leaflet, MR attenuated substantially (a, c and e: apical 3-chamber view; b, d and f: apical 2-chamber view).

Poster Session 1 (P1)

Sunday, June 23, 2019

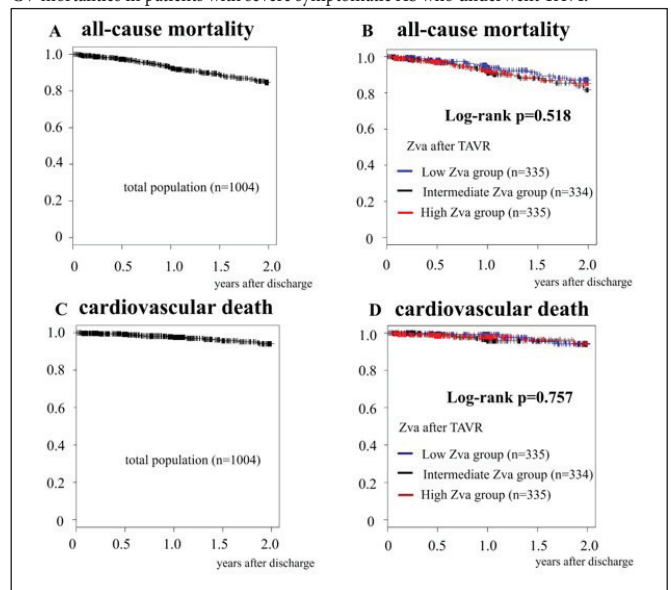


P1-142

Association Between Valvuloarterial Impedance After Transcatheter Aortic Valve Implantation and 2 Year Mortality in Elderly Patients with Severe Symptomatic Aortic Stenosis

Fukuko Nagura¹, Akihisa Kataoka¹, Masahiko Hara², Ken Koizuma¹, Yusuke Watanabe¹, Makoto Nakashima¹, Hirofumi Hioki¹, Hideyuki Kawashima¹, Yugo Nara¹, Shinichi Shirai³, Norio Tada⁴, Motoharu Araki³, Toru Naganuma⁶, Futoshi Yamanaka⁷, Hiroshi Ueno⁸, Minoru Tabata⁹, Mizutani Kazuki¹⁰, Akihiro Higashimori¹¹, Kensuke Takagi¹², Masanori Yamamoto¹³, Kentaro Hayashida¹⁴. ¹Teikyo University Hospital, Itabashi-ku, Japan; ²Shimane University Graduate School of Medicine, Izumo-shi, Japan; ³Kokura Memorial Hospital, Kitakyushu-shi, Japan; ⁴Sendai Kouse Hospital, Sendai-shi, Japan; ⁵Saiseikai Yokohama-City Eastern Hospital, Yokohama-shi, Japan; ⁶New Tokyo Hospital, Matsudo-shi, Japan; ⁷Shonankamakura General Hospital, Kamakura-shi, Japan; ⁸Toyama University Hospital, Toyama-shi, Japan; ⁹Tokyoobay Urayasuichikawa Medical Center, Urayasu-shi, Japan; ¹⁰Osaka City University Hospital, Osaka-shi, Japan; ¹¹Kishiwada Tokusuyukai Hospital, Kishiwada-shi, Japan; ¹²Ogaki Municipal Hospital, Ogaki-shi, Japan; ¹³Nagoya Heart Center, Nagoya-shi, Japan; ¹⁴Keio University Hospital, Shinjuku-ku, Japan

Background: Pre-procedural valvuloarterial impedance (Zva) is considered as a useful predictor of mortality in patients diagnosed with severe aortic stenosis (AS) who undergo transcatheter aortic valve implantation (TAVI). However, the prognostic significance of Zva after TAVI remains unclear. **Purpose:** We aimed to evaluate the prognostic significance of Zva after TAVI. **Methods:** We retrospectively analysed the clinical and echocardiographic data of 1004 consecutive elderly patients (mean age 84±5 years, 27.5% men) who underwent TAVI for severe symptomatic AS. Zva was calculated after TAVI, using Doppler echocardiographic parameters and instantaneous blood pressure measurements. Patients were divided into 3 groups based on tertile values: the high (>3.33 [n=335]), intermediate (2.49-3.33 [n=334]), and the low Zva (<2.49 [n=335]) group. The primary endpoint was the 2-year cumulative all-cause mortality, and the secondary endpoint was 2-year cardiovascular (CV) mortality. **Results:** The estimated 2-year all-cause and CV mortalities using Kaplan-Meier analysis were 16.2% (95% confidence interval (CI) 11.8-20.4), and 2.3% (95% CI 3.2-8.6), respectively. There is no significant intergroup differences in each endpoint (long-rank p=0.518 for all-cause, p=0.757 for CV mortality). Multivariable Cox regression analyses with adjustments of patient characteristics and medications showed that the post-procedural Zva was not associated with both the 2-year all-cause (intermediate vs low: adjusted hazards ratio [aHR]=1.34, 95% CI 0.75-2.40, p=0.316; high vs low: aHR=1.17, 95% CI 0.64-2.16, p=0.613), and the CV mortality (intermediate vs low: aHR=1.50, 95% CI 0.56-4.06, p=0.421; high vs low: aHR=0.25, 95% CI 0.43-3.65, p=0.682). **Conclusion:** Our results suggest that post-procedural Zva were not associated with 2-year all-cause or CV mortalities in patients with severe symptomatic AS who underwent TAVI.



P1-141

Discrepancy of Aortic Valve Area Measurements by Doppler vs. Biplane Measurements in Aortic Valve Stenosis: The Asian Valve Registry

Mai Iwataki¹, Yong-Jin Kim², Seung Woo Park³, Lieng His Ling⁴, Cheuk-Man Yu⁵, Takeshi Hozumi⁶, Hidekazu Tanaka⁷, Chisato Izumi⁸, Jae-Kwan Song⁹, Dae-Won Sohn¹⁰, Yutaka Otsuji¹. ¹University of Occupational and Environmental Health, Kitakyushu-shi, Japan; ²Seoul National University Hospital, South Korea, Seoul, Republic of Korea; ³Samsung Medical Center, Sungkyunkwan University College of Medicine, Seoul, Republic of Korea; ⁴National University Heart Center, National University of Singapore, Singapore, Singapore; ⁵Hong Kong Baptist Hospital, The Chinese University of Hong Kong, Hong Kong, China; ⁶Wakayama Medical University, Wakayama, Japan; ⁷Kobe University Graduate School of Medicine, Kobe-shi, Japan; ⁸Tenri Hospital, Tenri-shi, Japan; ⁹Asan Medical Center Heart Institute, University of Ulsan College of Medicine, Seoul, Republic of Korea; ¹⁰Seoul National University Hospital, Seoul, Republic of Korea

Background: Aortic valve area (AVA) in aortic valve stenosis (AS) is measured by continuity equation utilizing stroke volume (SV) by Doppler or biplane Simpson's method. AVA often show discrepancy due to differences between SV_{Doppler} and SV_{Simpsons}. There are no study demonstrating patients characteristics with large discrepancy. This study investigated data from The Asian Valve Registry that was prospective, multicenter registry of patients with significant AS at 9 centers in Asian countries. **Methods:** In 820 patients with AS (AVA<1.5 cm²), SV_{Doppler} and SV_{Simpsons} were quantified with transthoracic echocardiography. Correlations between (SV_{Doppler} - SV_{Simpsons})/body surface area (BSA) and multiple variables, including age, height, weight, left ventricular end-diastolic diameter index (LVEDDI), left ventricular end-systolic diameter index (LVESDI) and relative wall thickness (RWT) were evaluated. **Results:** 1) SV_{Doppler}/BSA was significantly larger than SV_{Simpsons}/BSA (49±11 vs. 39±11 ml/m², p<0.01) and AVA_{Doppler}/BSA was larger than AVA_{Simpsons}/BSA (0.51±0.15 vs. 0.41±0.14 cm²/m², p<0.01). 2) Increase in (SV_{Doppler} - SV_{Simpsons})/BSA was correlated with increased age (r=0.18, p<0.01), lower height (r= -0.29, p<0.01), reduced LVEDDI and LVESDI (r= -0.09 and -0.15, p<0.01, respectively) and increased RWT (r=0.14, p<0.01). Increased age, lower height, reduced LVEDDI and LVESDI were independent determinant of (SV_{Doppler} - SV_{Simpsons})/BSA by multivariate analysis. **Conclusions:** Both SV and AVA values by Doppler method were significantly larger than those by Simpson's method. This discrepancy was significantly more pronounced with increased age, lower height and reduced LV cavity dimension.

Poster Session 1 (P1)

Sunday, June 23, 2019

P1-143

Assessment of Left Ventricular Diastolic Function After Transcatheter Aortic Valve Implantation in Patients with Aortic Stenosis Based on Two ASE Guidelines

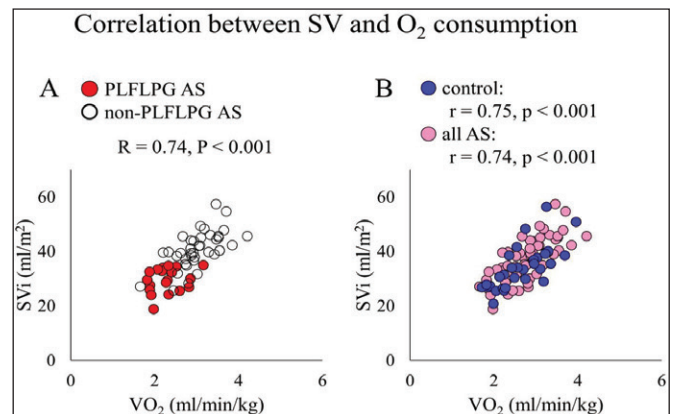
Y. Guo, M. M. Sun, H. Y. Chen, C. C. Dai, D. H. Kong, C. Z. Pan, Xianhong Shu. Zhongshan Hospital, Fudan University, Shanghai, China

Background: Two-dimensional transthoracic echocardiography (TTE) and Doppler imaging are currently the most commonly used for heart function assessment in clinical with good reproducibility. The difference between the previous 2009 and the updated 2016 guidelines for classifications of left ventricular diastolic function (LVDF) and its clinical value remains unexplored. The current study evaluated the change of LVDF in aortic stenosis (AS) patients receiving transcatheter aortic valve implantation (TAVI), and compared the LVDF classification according to the 2009 and 2016 guidelines. **Methods:** Thirty-five AS patients receiving TAVI underwent echocardiography the day before operation (PRE) and at the 3-day (3D), the 1-month (1M) and the 6-month (6M) follow up after TAVI. LVDF was analyzed using 2D, Doppler and tissue doppler imaging to get parameters including E/A, E/E', IVRT, DT, LA area, LAVI and PASP (pulmonary arterial systolic pressure). LVDF classification was respectively evaluated at PRE, 3D, 1M and 6M for each patient and LVDF classification according to the 2009 and 2016 recommendations was compared. **Results:** 1. LA area ($P < 0.001$) and LAVI ($P < 0.008$) were continuously decreased shortly after operation till 6-month follow-up. DT was significantly reduced immediately after TAVI ($P = 0.003$). Improvement of IVRT ($P < 0.007$) and PASP ($P < 0.021$) occurred immediately until 1-month after TAVI while improvement of E/E' ($P = 0.012$) occurred from 3-day to 1-month after TAVI. 2. Forty-four percent (62/140) of LVDF grades by the 2009 recommendations were different from those by the 2016 guidelines. Comparing PRE and 6M, according to 2009 guidelines, 19 patients improved 1 grade, 8 patients improved 2 grade; while according to 2016 guidelines, 9 patients improved 1 grade, 13 patients improved 2 grades, 1 patients improved 3 grades. **Conclusions:** Two-dimensional echocardiography and Doppler imaging could effectively evaluate the change of LVDF in AS patients by echocardiography after TAVI. The degree of LVDF was significantly different between the two 2009 guidelines. Based on 2016 guidelines, more patients experienced an improvement in LVDF classification and can be regarded as favorable results from TAVI.

P1-144

Insights Into the Mechanism of Paradoxical Low Flow-low Pressure Gradient Severe Aortic Stenosis: Its Association with Reduced Oxygen Consumption by the Whole BodyTakeshi Onoue¹, Mai Iwataki¹, Masaru Araki¹, Hideaki Itoh¹, Akihiro Isotani², Hiromi Umeda², Shota Fukuda¹, Yasufumi Nagata³, Yuki Tsuda¹, Yoshihisa Fujino¹, Michiya Hanyu², Kenji Ando², Shinichi Shirai², Masaaki Takeuchi¹, Satoru Saeki¹, Robert A. Levine³, Yutaka Otsuji¹. ¹University of Occupational and Environmental Health, School of Medicine, Kitakyusyu, Japan; ²Kokura Memorial Hospital, Kitakyusyu, Japan; ³Massachusetts General Hospital, Boston, MA

Background: Mechanism of reduced stroke volume index (SVi) in paradoxical low flow-low pressure gradient (PLFLPG) aortic stenosis (AS) remains unclarified. Guyton et al. demonstrated that SVi is determined by whole-body oxygen consumption (VO_2) as opposed to cardiac function in many subjects, including patients with heart disease. We hypothesized that a reduced SVi in PLFLPG AS is associated with reduced whole body VO_2 . This study investigated relationships between VO_2 , SVi and AS severity in patients with AS to examine the association between reduced VO_2 and PLFLPG AS. **Method:** In 59 patients (24 men, mean age 78 ± 7 years) with severe AS ($AVA < 1.0$ cm²), SVi, AS severity and type were evaluated by echocardiography, and VO_2 was measured by the fraction of O_2 in expired gases. Control subjects without AS and cardiac disease included 30 patients (13 men, mean age of 70 ± 6 years). **Results:** The SVi and VO_2 were significantly decreased in 20 patients with PLFLPG AS compared to those in 39 patients with non-PLFLPG AS (30 ± 4 vs 41 ± 7 ml/m² and 2.4 ± 0.5 vs 3.0 ± 0.5 ml/min/kg, $p < 0.01$, respectively). The SVi to VO_2 ratio was not different between PLFLPG AS, non-PLFLPG AS and controls (13.1 ± 2.6 vs 13.5 ± 2.1 vs 13.0 ± 2.2 , n.s.). The SVi was independently correlated with VO_2 ($R = 0.74$, $p < 0.01$) but not with AVA (Fig. A). Control group also showed similar relations compared to patients with AS ($R = 0.75$, $p < 0.01$) (Fig. B). In patients with severe AS, reduced SV was primarily associated with reduced VO_2 by multivariable analysis (Standardized $\beta = 0.68$, $p < 0.01$). Categorized PLFLPG AS was also significantly associated with reduced VO_2 ($p < 0.001$). **Conclusion:** PLFLPG AS is associated with reduced O_2 consumption by the whole body, which offer insights into the mechanism of PLFLPG AS and potential derivation of novel treatments.



P1-145

A Higher Burden of Cardiac Calcification Determined by Echocardiography or Computed Tomography is Associated with a Higher Risk of Permanent Pacemaker Placement After Transcatheter Aortic Valve ReplacementVira I. Ayzembar¹, Cassandra J. Ramm², Siyuan P. Sheng¹, John P. Vavalle².¹University of North Carolina School of Medicine, Chapel Hill, NC;²University of North Carolina Hospitals Department of Cardiology, Chapel Hill, NC

Background: Outcomes of transcatheter aortic valve replacement (TAVR) can be affected by the degree and distribution of cardiac calcification. An echo-based global cardiac calcium score (eCS) has been developed and previously validated. The predictive value of a CT-based global cardiac calcium score (CTCS) on outcomes after TAVR is unknown. Similarly, the relationship between echocardiography and contrasted computed tomography modalities for predicting the global cardiac calcium score has never been evaluated. **Methods:** Consecutive patients at a single academic medical center who received TAVR 11/2014-2/2018 were eligible for inclusion. The eCS and CTCS (range 0-13) were determined using pre-TAVR echocardiograms and contrasted cardiac CT scans by two independent readers. The correlation between eCS and CTCS was assessed using Pearson correlation. The association between eCS and CTCS with post-TAVR complications were analyzed as a continuous, linear variable. **Results:** A total of 154 patients were included. The median age was 82 (IQR 72-86) with 53% being females, 90% with hypertension, 77% with hyperlipidemia, 66% with CAD, and 43% with diabetes. The correlation between eCS and CTCS was $r = 0.76$ ($p < 0.0001$). A one-unit increase in eCS or CTCS was associated with a significant increase in the odds of permanent pacemaker placement (PPM) at 1-2 days after TAVR (eCS - OR 1.76, $p = 0.001$ and CTCS - OR 1.55, $p = 0.005$) and 30 days after TAVR (eCS - OR 1.80, $p = 0.002$ and CTCS - OR 1.51, $p = 0.009$). An increase in eCS or CTCS was not associated with increased odds of left bundle branch block or paravalvular leak after TAVR. **Conclusion:** Both echocardiography and computed tomography are comparable modalities for accessing the cardiac calcium score and appear to be useful in determining which patients are at higher risk of requiring PPM after TAVR. These tools can be easily integrated into the pre-operative risk assessment of patients being evaluated for TAVR.

	Echo-based Ca Score (eCS)		CT-based Ca Score (CTCS)	
	OR (95% CI)	p-value	OR (95% CI)	p-value
1-2d After TAVR				
LBBB	0.97 (0.80, 1.19)	0.785	1.12 (0.94, 1.33)	0.201
PPM	1.79 (1.26, 2.55)	0.001	1.55 (1.14, 2.12)	0.005
Paravalvular Leak ^a	1.08 (0.88, 1.32)	0.456	1.13 (0.94, 1.36)	0.208
30d After TAVR				
LBBB	1.05 (0.69, 1.61)	0.818	0.97 (0.69, 1.36)	0.858
PPM	1.80 (1.25, 2.59)	0.002	1.51 (1.11, 2.05)	0.009
Paravalvular Leak ^a	1.02 (0.82, 1.26)	0.889	0.99 (0.80, 1.22)	0.915

^aModerate/mild leak compared to trace/no leak

Abbreviations: OR, odds ratio; CI, confidence interval; LBBB, left bundle branch block

P1-146

Impact of Aortic Valve Replacement on Mitral Hemodynamics and Mitral Annulus Distension in Mitral StenosisNahoko Kato¹, Ratnasari Padang¹, Cristina Pislaru¹, William R. Miranda¹, Mizuho Hoshina², Kentaro Shibayama², Hiroyuki Watanabe², Kevin Greason¹, Vuyisile T. Nkomo¹, Sorin V. Pislaru¹, Patricia A. Pellikka¹. ¹Mayo Clinic, Rochester, MN; ²Tokyo Bay Uraysu/Ichikawa Medical Center, Uraysu, Japan

Background: Mitral annulus calcification is highly prevalent in patients with aortic stenosis (AS) and can restrict leaflets opening and reduce mitral annulus systolic-diastolic

Poster Session 1 (P1)

Sunday, June 23, 2019

distension (MAD). Reduced cardiac output may underestimate the Doppler-derived mitral valve area (MVA) (continuity equation). We sought to investigate the impact of aortic valve replacement (AVR) on MAD and mitral valve hemodynamics. **Methods:** We retrospectively investigated patients who underwent isolated AVR for severe AS from 2008 to 2015 with MS defined as transmitral gradient by Doppler (TMG) ≥ 4 mmHg. Patients with MS were divided into three groups according to MVA pre and post AVR (MVA_{pre} and MVA_{post}): A (true MS): MVA_{pre} and MVA_{post} ≤ 2.0 cm², B (pseudo MS): MVA_{pre} ≤ 2.0 cm² and MVA_{post} > 2.0 cm², C (no significant MS): MVA_{pre} > 2.0 cm². We assessed the accuracy for identifying group A using MVA_{pre}, TMG, and MAD. **Results:** Of 204 patients with severe AS and MS (age 76 ± 9 years, 42% men, 94% calcific MS), 58 were in group A, 53 in B and 93 in C. Stroke volume pre AVR was smaller in group A and B than C (Table1). Stroke volume increased markedly after AVR in group B. MAD was smaller in group A than C. MVA_{pre} was smaller in group A than B and C. TMG was higher in group A than C. Area under the curve of MVA_{pre} and TMG for identifying group A were higher than MAD (Table 2). MVA_{pre} and TMG were independent predictors of group A (odds ratio [OR] 0.0095, 95%CI 0.0020-0.046, $p < 0.01$ and OR 1.39, 95%CI 1.05-1.85, $p = 0.018$, respectively). **Conclusion:** MAD was the smallest in patients with true MS. However, MVA_{pre} best identified patients with true MS.

	A: True MS	B: Pseudo MS	C: no significant MS	p
SV pre AVR (mL)	82 ± 15	83 ± 16	99 ± 22	< 0.01*
SV post AVR (mL)	82 ± 15	94 ± 20	97 ± 27	< 0.01†
MVA _{pre} (cm ²)	1.6 ± 0.2	1.7 ± 0.2	2.5 ± 0.4	< 0.01‡
MVA _{post} (cm ²)	1.6 ± 0.3	2.5 ± 0.4	2.5 ± 0.7	< 0.01†
TMG (mmHg)	6.1 ± 2.0	5.2 ± 1.4	4.8 ± 1.1	< 0.01†
MAD (mm)	2.3 ± 1.3	2.5 ± 1.0	2.9 ± 1.3	0.021†

Mean ± standard deviation. * $p < 0.05$ group A and B vs. C, † $p < 0.05$ group A vs. B and C, ‡ $p < 0.05$ group A vs. B, B vs. C and A vs. C, § $p < 0.05$ group A vs. C
MS: mitral stenosis, SV: stroke volume, AVR: aortic valve replacement, MVA_{pre}: mitral valve area pre AVR, MVA_{post}: mitral valve area post AVR, TMG: transmitral gradient, MAD: mitral annulus distension (mitral annulus diameter at diastole – mitral annulus diameter at systole)

	AUC	Cutoff value	Sensitivity (%)	Specificity (%)	Accuracy (%)
MVA _{pre}	0.87	1.9 cm ²	93	74	84
TMG	0.70	6 mmHg	50	78	64
MAD	0.58	3 mm	86	27	57

AUC: area under the curve, other abbreviations as Table1.

Table: Peri-procedural and 30-day Mechanical and Conduction Outcomes of Individuals with and without DUST

Variable	DUST+ (N = 55)	DUST- (N = 241)	p-value
Primary composite outcome* – no. (%)	22 (0.4)	116 (48.1)	0.62
Modified primary composite outcome* – no. (%)	4 (7.3)	18 (7.5)	>0.99
Valve Popout – no. (%)	0 (0.0)	12 (5.0)	0.23
Need for Valve Recapture – no. (%)	3 (5.5)	9 (3.7)	0.44
Procedure Aborted – no. (%)	0 (0.0)	1 (0.4)	>0.99
Procedure Converted to Open Surgery – no. (%)	0 (0.0)	0 (0.0)	>0.99
Device Embolization – no. (%)	1 (1.8)	1 (0.4)	0.31
Post-implant Transaortic Mean Gradient (mmHg) – mean (SD)	9.1 (4.6)	10.3 (5.8)	0.21
Contrast Volume (mL) – mean (SD)	149.9 (327.7)	133.4 (103.7)	0.73
Need for Pacemaker Within 30-days – no. (%)	9 (16.4)	41 (17.0)	0.41
Grade of Paravalvular Leak – median (IQR)	1 (0-1)	1 (0-1)	0.86
Post-implantation Arrhythmia by Type – no. (%)			
Atrial Fibrillation	4 (7.3)	11 (4.6)	0.91
Atrial Flutter	0 (0.0)	0 (0.0)	>0.99
Ventricular Tachycardia	0 (0.0)	3 (1.2)	0.57
Accelerated Idioventricular Rhythm	0 (0.0)	1 (0.4)	0.83
Ectopic atrial rhythm	0 (0.0)	1 (0.4)	0.83
New Conduction Disturbance by Type – no. (%)	20 (36.4)	108 (44.8)	0.55
Left Bundle Branch Block	14 (25.5)	59 (24.5)	0.76
Complete Heart Block	8 (14.5)	33 (13.7)	0.75
1 st Degree Atrioventricular Block	0 (0.0)	6 (2.5)	0.32
2 nd Degree Atrioventricular Block	0 (0.0)	2 (0.8)	>0.99
Left Anterior Fascicular Block	0 (0.0)	1 (0.4)	0.83
Intraventricular conduction delay	0 (0.0)	3 (1.2)	0.57
Right Bundle Branch Block	0 (0.0)	2 (0.8)	0.39
Asystole	1 (1.8)	1 (0.4)	0.97

*Includes the composite of valve popout, recapture, aborted procedure, conversion to an open procedure, device embolization, new conduction system disturbance, or need for a pacemaker within 30 days of the procedure. The modified primary composite outcome includes the above conditions, excluding new conduction system disturbance or need for a pacemaker within 30 days

P1-147

The Impact of Discrete Upper Septal Thickness on Outcomes After Transcatheter Aortic Valve Replacement

Nicholas Kiefer¹, Gregory Salber¹, Gordon Burke¹, James Chang¹, Kimberly Guibone¹, Jeffrey Popma¹, Rebecca Hahn², Duane Pinto¹, Jordan Strom¹.
¹Beth Israel Deaconess Medical Center, Boston, MA; ²NewYork-Presbyterian/Columbia University Medical Center, New York City, NY

Background: The role of discrete upper septal hypertrophy (DUST) on pre-procedural transthoracic echocardiogram (TTE) in transcatheter aortic valve replacement (TAVR) is unknown. **Methods:** Medical charts and pre-procedural TTEs of 378 patients who underwent TAVR at Beth Israel Deaconess Medical Center between January 2012 and December 2016 were examined. The association between DUST and the primary composite outcome of valve popout, recapture, embolization, aborted procedure, conversion to open procedure, new conduction disturbance, or need for permanent pacemaker ≤ 30 days post TAVR, was evaluated. Sensitivity analyses were performed varying the definition of DUST. **Results:** Of 296 (78.3%) TAVR patients with interpretable images, 55 (18.6%) had DUST at a median (IQR) of 40 (19-62) days pre-TAVR. Age and sex were similar among those with and without DUST. DUST patients received post-dilation more frequently (DUST+ vs. DUST-: 41.8% vs. 29.9%; $p = 0.04$). A total of 50 (16.9%) individuals received a pacemaker within 30 days, 128 (43.2%) developed a conduction disturbance, and 73 (24.7%) developed a left bundle branch block without differences between groups. DUST was unrelated to the primary outcome on multivariable analysis (adjusted odds ratio DUST+ vs. DUST-: 0.94, 95% CI 0.042-2.11; $p = 0.88$). **Conclusions:** In this convenience sample of TAVR recipients at a large academic medical center, patients with DUST were more likely receive post-dilation. DUST was not associated with procedural or conduction outcomes after TAVR.

P1-148

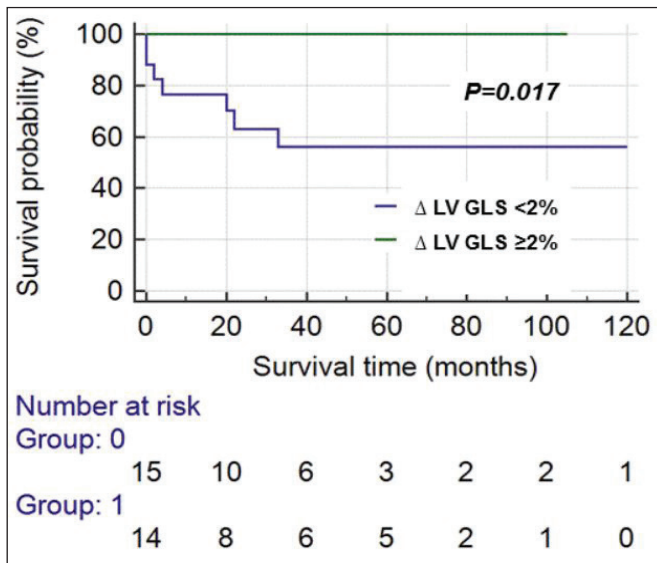
Prognostic Value of Left Ventricular Global Longitudinal Strain During Dobutamine Stress Echocardiography in Patients with Low-flow Low-gradient Severe Aortic Stenosis

Darae Kim¹, Chi Young Shim², Geu-Ru Hong², Jong-Won Ha². ¹Samsung Medical Center, Seoul, Korea, Seoul, Republic of Korea; ²Severance Cardiovascular Hospital, Seoul, Republic of Korea

Background: Contractile reserve (CR) defined with an increase in stroke volume $\geq 20\%$ during dobutamine stress echocardiography (DSE) is a well-known prognosticator in patients with aortic stenosis (AS). However, its clinical significance is often not well applied in the era of transcatheter intervention. Recently, change of left ventricular (LV) longitudinal strain (GLS) has been considered a more sensitive and direct methods for assessing CR. We aimed to investigate if LV GLS during DSE has prognostic value in patients with low flow low gradient (LFLG) severe AS. **Methods:** A total of 38 patients with LFLG severe AS [aortic valve area < 1.0 cm², LVEF $< 40\%$, and mean pressure gradient < 40 mmHg] underwent DSE as part of routine clinical practice. Presence of CR was defined Δ stroke volume $\geq 20\%$ by conventional echocardiography (conventional CR), and Δ [LV GLS] $\geq 2\%$ by speckle tracking imaging during DSE. Clinical risks were evaluated with the EuroScore II. Primary outcome for overall mortality was tracked for 44 months. **Results:** Nineteen (50%) patients underwent surgical aortic valve replacement and 7 (18%) did transcatheter aortic valve replacement. 3-year overall mortality was 26.3%. Patients who survived had similar baseline characteristics to patients who did not survive, except younger age. Patients who survived had significantly higher peak [LV GLS] and Δ [LV GLS] than patients who did not survive (peak [LV GLS] 11.2 ± 4.4 vs. 7.2 ± 1.5 %, $p = 0.001$; Δ [LV GLS] 2.3 ± 1.3 vs. 0.1 ± 1.2 %, $p < 0.001$). In multivariate analyses, Δ [LV GLS] was independently associated with overall mortality (HR 0.432, 95% confidence interval 0.193-0.969, $p = 0.042$), while conventional CR did not show significance. Patients with Δ [LV GLS] $\geq 2\%$ had a better survival compared to those with Δ [LV GLS] $< 2\%$ (log-rank $p = 0.017$, Figure). Δ [LV GLS] had additive predictive values over baseline pressure gradient and EuroScore II for 3-year overall mortality. **Conclusions:** Patient with Δ [LV GLS] $\geq 2\%$ during DSE has a favorable outcome in patients with LFLG severe AS. Novel assessment of CR by Δ [LV GLS] during DSE offers a significantly better prognostic value for patients with LFLG severe AS in the era of transcatheter intervention.

Poster Session 1 (P1)

Sunday, June 23, 2019



P1-149

Practical Application of the Proportionate Versus Disproportionate Mitral Regurgitation Model in a Real-World Setting

Rachel Harris, Nidhi Patel, Patrick Chang, Allan Chen. University of South Florida, Tampa, FL

Clinical Presentation: 57 year old male with stage 4 chronic kidney disease, history of coronary artery disease status post myocardial infarction presented with recent decline in exercise capacity, paroxysmal nocturnal dyspnea, a depressed ejection fraction (EF) from 40% to 30% and significant mitral regurgitation(MR). After maximal medical therapy, decision was made to evaluate patient for percutaneous intervention of the mitral valve. **Imaging Findings:** The patient had a left ventricular (LV) end diastolic dimension (EDD) of 6.81 cm, LV end diastolic volume (EDV) of 360 ml and an indexed LV EDV of 156 ml/m². The LV EF was 31.5% by Simpson's method of disks and severe MR was functional in etiology with an effective regurgitant orifice area of 0.5 cm². **Role of Imaging in Patient Care:** In chronic heart failure patients with functional MR, two recent trials(MITRA-FR and COAPT) emerged with discordant results in long term outcomes. A recent conceptual framework by Grayburn et al. incorporates the degree LV dilatation and EF and postulates that significant MR should be framed by whether the intervention targeted to the mitral valve changes the clinical course of disease. One should determine whether the MR is expected or proportionate, versus unexpected or disproportionate, to the degree of LV enlargement. The model is based on true measurements and have not been compared to two-dimensional echocardiographic data. We apply this model to our patient whose EROA was similar to an expected EROA of ~0.52 cm², as determined by the Gorlin equation, who underwent MitraClip intervention. **Summary/Discussion Points:** Echocardiogram one year post successful placement of 3 MitraClips revealed an LVEF of 27.4%, an LVEDD of 6.94 cm, and an indexed LVEDV of 160ml/m², relatively unchanged from pre-procedure. This case illustrates an example of a patient with a significantly dilated left ventricle with a 'proportionate' degree of severe MR who had no improvement in his left ventricular dimensions or ejection fraction. Conceptually, this framework is intuitive: patients with significant left ventricular remodeling may be less likely to improve. Mitral regurgitation involves a complex anatomic and physiologic process that requires a thoughtful evaluation of both the valve and ventricle for meaningful assessment. Rather than absolute measurements of EROA, consideration of EF and whether MR is 'proportionate' or 'disproportionate' to the LVEDV may better identify subsets of patients that benefit from percutaneous intervention.

P1-150

Clinical and Echocardiographic Characteristics of a Contemporary Cohort of Patients with Bartonella Species Infective Endocarditis

Michael Chetrit, Feihong Ding, Beni Verma, Nabin Shrestha, Steven Gordon, Paul Cremer, Brian Griffin, Bo Xu. Cleveland Clinic, Cleveland, OH

Background: Infective endocarditis (IE) due to *Bartonella species* (sp.) is rare. The echocardiographic characteristics are not well defined. We aimed to investigate the clinical and echocardiographic findings of *Bartonella* sp. IE in the contemporary era. **Methods:** The endocarditis registry and echocardiographic database at our center were retrospectively analyzed to obtain clinical and echocardiographic features of *Bartonella* sp. IE. **Results:** Between 2007 and 2015, there were 11 patients with *Bartonella* sp. IE (54±12 years of age; 100% male; 100% cat exposure) representing <1% (11/1391) of cases in our endocarditis registry. The majority (10, 91%) presented with a subacute (<30 days) blood culture

negative IE. The causative pathogen was *Bartonella henselae* in all cases, diagnosed with 16s rRNA sequencing (9, 81%) and inflammation on pathology. 5 (45%) patients presented with native valve endocarditis (NVE) while 6 (55%) patients presented with prosthetic valve endocarditis (PVE). NVE was associated with a longer time from symptom onset to diagnosis (NVE 200 ±169 days vs. PVE 102±66 days). On echocardiography, NVE showed more valvular destruction and valvular dysfunction, without abscess formation. Conversely, PVE showed less valvular complications, but 3 patients (27%) had aortic root abscess formation. Clinical complications of endocarditis were comparable, including cerebral embolism (2, 18%) and immune mediated glomerulonephritis preceding the diagnosis of endocarditis (3, 27%). 82% were managed surgically (valve replacement: 8, 73%; aorta replacement: 1, 9%), while 18% were managed medically. At a mean follow-up of 28 ±37 months, there were no deaths attributable to endocarditis, or other cardiovascular causes. **Conclusion:** In a contemporary series, NVE due to *Bartonella* sp. was associated with a longer interval to diagnosis, more valvular destruction and subsequent dysfunction on echocardiography, while PVE was associated with a shorter interval to diagnosis, less valvular dysfunction but more aortic root abscess formation. Survival at a mean follow-up of 28 ±37 months was excellent, with no deaths attributable to endocarditis.

Clinical Features		Native Valve Endocarditis (n=5)	Prosthetic Valve Endocarditis (n=6)	p-value
Demographics	Age (mean±SD)	56 ± 11	53 ±12	0.78
	Sex (Male)	5 (100%)	6 (100%)	
	Hypertension	3 (60%)	2 (33%)	0.567
	Diabetes	0 (0%)	0 (0%)	
	Coronary Artery Disease	0 (0%)	3 (50%)	0.132
	Cat exposure	5 (100%)	6 (100%)	
Bacteria Species	<i>Bartonella henselae</i>	5 (100%)	6 (100%)	
Echocardiographic Features		Native Valve Endocarditis (n=5)	Prosthetic Valve Endocarditis (n=6)	p-value
Valve Infected	Aortic	4 (80%)	5 (83%)	1.0
	Mitral	1 (20%)	3 (50%)	0.545
	Aortic and Mitral	0 (0%)	1 (17%)	1.0
Valvular Disease	Myxomatous Valve	1 (20%)		
	Bicuspid Aortic Valve	2 (40%)	2 (33%)	
Vegetation	Location	Non coronary cusp 3 (60%)	Non coronary cusp 1 (17%)	
		Posterior Mitral Leaflet 1 (20%)	Posterior Mitral Leaflet 1 (17%)	
	Size (≤1 cm)	2 (40%)	4 (67%)	0.567
	Size (>1 cm)	2 (40%)	1 (17%)	0.545
	No vegetation present	1 (20%)	1 (17%)	1.0
Valvular Complication	Eccentric Regurgitant Jet	5 (100%)	6 (100%)	
	Valvular Destruction/ Perforation	4 (80%)	2 (33%)	0.242
	Severe Dysfunction	5 (100%)	2 (33%)	0.061
Other Complications	Abscess	0 (0%)	3 (50%)	0.182
	Aortic Graft Infection	1 (20%)	0 (0%)	
Aortopathy	Dilated Aorta	2 (40%)	0 (0%)	0.182

P1-151

The Natural Trajectory of Left Ventricular Systolic Function Post Transcatheter Aortic Valve Implantation

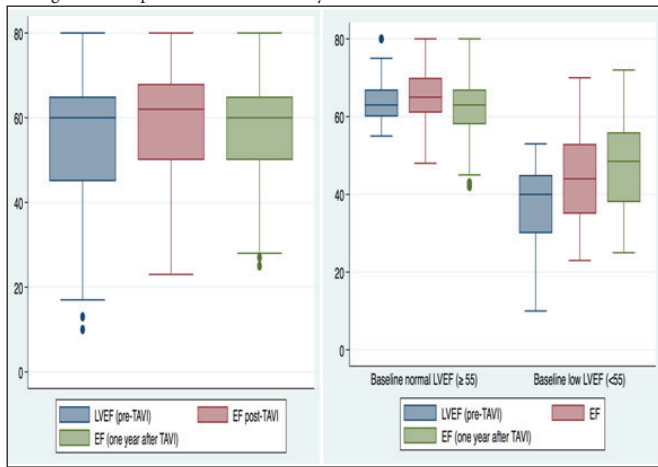
Abdalla Hassan, Cecilia Wong, Anouch Matevossian, Lara Kovell, Colleen Harrington, Gerard Aurigemma. UMass Medical School, Worcester, MA

Background: The long term impact of the transcatheter aortic valve implantation (TAVI) on left ventricular ejection fraction (LVEF) is not clearly identified. We aimed to evaluate the immediate and delayed effect of TAVI on LVEF immediately after and at 1 year post intervention. **Methods:** We queried our institutional TAVI database and identified 238

Poster Session 1 (P1)

Sunday, June 23, 2019

patients who underwent TAVI between January 2014 and December 2016 and had full follow up data up to 1 year post TAVI. Patients were divided into 2 groups; normal and low ejection fraction (EF) patients. We compared the baseline LVEF pre-TAVI to the one immediately after and at 1 year post-TAVI. **Results:** Mean age was 81.9 ± 9.4 years. Males constituted 51.3%. Prior to TAVI, 221 (73.18%) patients had normal EF and 81 (26.82%) had reduced EF. Immediately after TAVI, LVEF improved significantly in both groups; patients with baseline low LVEF (38.7% to 44.0%) and normal LVEF (63.4% to 65.3%) [$p < 0.001$]. At 1 year post-TAVI follow up, only patients with baseline reduced LVEF continued to have significant improvement in their systolic function (38.7% to 47.9%) [$p < 0.001$], while patients with baseline normal LVEF had no significant improvement in their LV systolic function at one year (63.4% to 62.2%) [$p = 0.15$]. **Conclusion:** In patients undergoing TAVI, the LVEF was significantly higher immediately after TAVI regardless of the baseline EF. However, at 1 year post TAVI, only patients with baseline reduced LVEF had significant improvement in their LV systolic function.

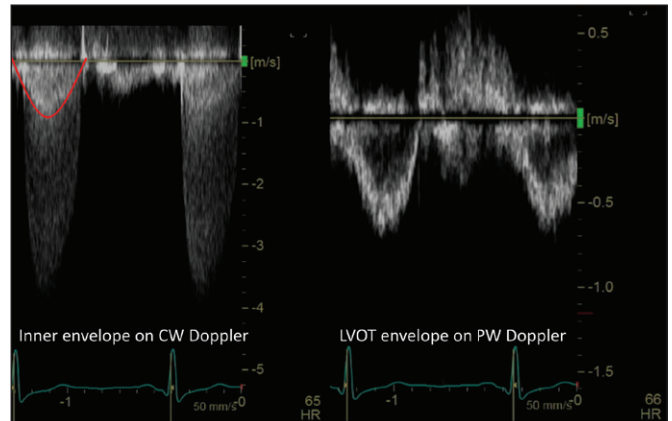


P1-152

Using the Double Envelope Technique to Calculate Aortic Valve Area in Aortic Stenosis

Sanjay Venkatesh, Thelsa T. Weickert, Alan L. Hinderliter, John P. Vavalle, Joseph A. Sivak. University of North Carolina School of Medicine, Department of Medicine, Division of Cardiology, Chapel Hill, NC

Background: The calculation of aortic valve area (AVA) using the continuity equation is traditionally performed by separately measuring left ventricular outflow tract (LVOT) flow using pulsed wave Doppler, and peak aortic valve flow using continuous wave Doppler. There are clinical situations in which the separately measured LVOT velocity profile may not be reliable, such as in irregular rhythms, or when the pulsed wave sample volume is incorrectly positioned. An alternative approach to assess LVOT flow is to treat the inner envelope of the aortic valve continuous wave Doppler signal as representative of the LVOT velocity time integral (VTI) (Figure 1). We examined the accuracy of this double envelope (DE) technique in a cohort of patients with severe aortic stenosis (AS). **Methods:** Pre-procedure echocardiograms of patients with severe native AS who underwent transcatheter aortic valve replacement at our institution from January 2018 to December 2018 were reviewed. Measurements required to calculate AVA and dimensionless index (DI) were collected using traditional and DE approaches. These values were then compared directly to one another using paired Student's t-test. **Results:** Out of the 95 patients included in our study, 35 (37% of overall cohort; mean age= 79.5 ± 6.5 years; mean AS gradient 44 mmHg) had an interpretable inner envelope on continuous wave Doppler through the aortic valve. Compared to the traditional approach, the DE approach overestimated AVA (cm^2) when using VTI (0.73 ± 0.2 vs. 0.80 ± 0.2 , $p = 0.18$) and peak velocity (0.70 ± 0.2 vs. 0.81 ± 0.2 , $p = 0.026$). Compared to the traditional approach, the DE approach also overestimated the DI when using VTI (0.23 ± 0.07 vs. 0.26 ± 0.06 , $p = 0.13$) and peak velocity (0.23 ± 0.07 vs. 0.26 ± 0.07 , $p = 0.021$). **Conclusion:** The DE technique tends to overestimate both AVA and DI by 10-15% compared to direct measurement of the LVOT velocity profile. This slightly overestimated AVA or DI result may be clinically useful in patients where the directly measured LVOT velocity profile is not reliable.



P1-153

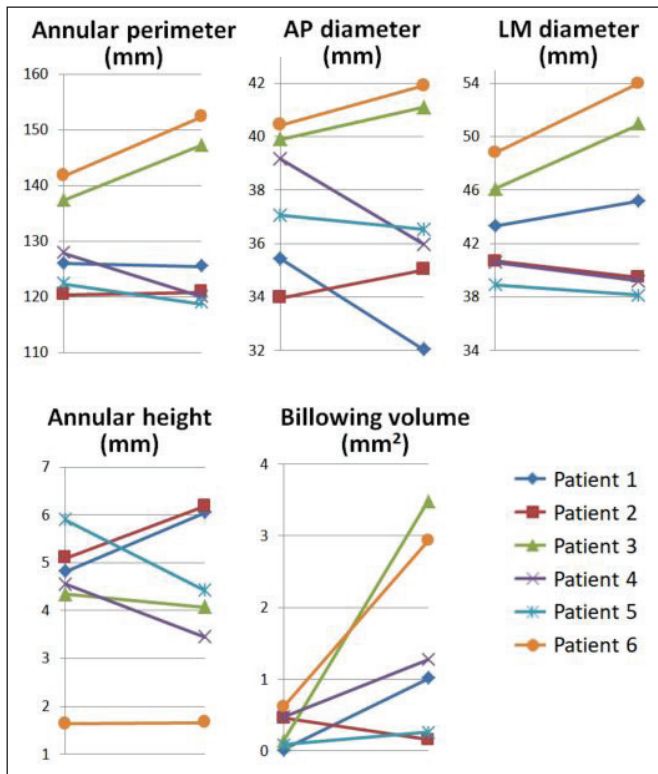
Geometric Change in Mitral Annulus During Systole in Patients with Atrial Functional Mitral Regurgitation

Kikuko Obase, Takashi Miura, Masayuki Takura, Tatsuya Miyanaga, Hiroko Taguchi, Takashi Shimada, Yuichi Tasaki, Shogo Yokose, Shun Nakaji, Ichiro Matsumaru, Kiyoyuki Eishi. Nagasaki University Hospital, Nagasaki, Japan

Background: It has been reported atrial fibrillation (AF) patients with normal left ventricular (LV) function can develop functional mitral regurgitation (MR). Mitral annular dynamics may be associated with the pathogenesis. However, the mechanism is not fully understood. We investigated the geometric change in mitral annulus during systole in AF patients with functional atrial MR. **Methods:** From consecutive 140 patients who underwent mitral repair in our institution, patients with (1) LV remodeling, (2) structural abnormal leaflet, including myxomatous change or ruptured chord (3) sinus rhythm and (4) LV ejection fraction $< 55\%$, were excluded. As the result, 6 patients were identified and studied as atrial functional MR. Using 3D dataset of pre-operative transesophageal echocardiography, perimeter of annulus, annular height, diameters of antero-posterior leaflet (AP) and medial-lateral (LM) direction, and billowing volume were measured at early systole (ES) and late systole (LS). **Results:** Annular perimeter, AP and LM diameter at ES were 129.4 ± 7.1 mm, 38.2 ± 2.6 and 42.6 ± 3.4 mm, respectively. As shown in the figure, annulus perimeter and billowing volume increased from ES to LS in case 3 and 6. In case 4 and 5, on the other hand, annulus decreased in size during systole. In case 1, AP diameter decreased and LM increased from ES to LS. To the contrary, AP increased and LM decreased in case 2. Mean annular height of the 6 cases in ES was 4.6 ± 1.3 mm. **Conclusion:** Geometric change in annulus in atrial functional MR varied. Our results suggest multifactorial mechanism of atrial functional MR and the mechanism possibly can be categorized into several groups. Further investigation is need, because it is essential for optimal surgical treatment, to have deep understanding of the mechanism of regurgitation.

Poster Session 1 (P1)

Sunday, June 23, 2019



P1-154

Performing Transcatheter Aortic Valve Replacement Without Intraoperative Transesophageal Does Not Compromise Patient Safety or Outcomes: A Single Center Experience

Jarrod Betz, Scott Lilly, Konstantinos Dean Boudoulas, Gregory Rushing, Nancy Matre, David Orsinelli. Ohio State University, Columbus, OH

Background: There is a debate concerning the need for general anesthesia (GA) and intraoperative transesophageal echocardiography (iTEE) for transcatheter aortic valve replacement (TAVR). At our institution, we transitioned from a default strategy of GA / iTEE to monitored anesthesia care (MAC) without iTEE in December 2016 as standard for TAVR. **Methods:** We retrospectively compared procedural, valve performance and patient outcomes in the 12 month periods prior to and following this transition, analyzing outcomes amongst patients undergoing TAVR with and without iTEE. **Results:** Among the 218 commercial TAVRs performed in 2016 and 2017, there were 89 patients in the GA / iTEE group and 129 patients in the MAC without iTEE group. The majority of GA / iTEE patients occurred in 2016 prior to the transition of strategy (79/89) with the majority of MAC without TEE patients occurring in 2017 after the transition (121/129). Of note, the patients in the GA / iTEE after the transition generally were receiving GA for another condition (e.g. alternative access). In the no iTEE group pre-transition, most had contraindications to TEE. Device success (73.0% vs 88.4%, $p < 0.01$), contrast volume used (123 vs 81 mL, $p < 0.01$), and procedural time (130 vs 110 min, $p < 0.01$) all favored the MAC without iTEE group. The presence of more than mild paravalvular leak (9.0% vs 4.7%, $p = 0.20$), acute kidney injury (21.3% vs 15.5%, $p = 0.27$), length of stay (5.6 vs 4.5 days, $p = 0.11$) and total adverse events (8.9% vs 7.8%, $p = 0.74$) were similar between the groups. There were differences in the use of self expanding vs balloon expandable valves in the two periods, with increased utilization of the self expanding valves after the transition. **Conclusions:** Our institutional outcomes data suggest TAVR implantation can be performed safely without iTEE guidance. There was no increase in the incidence of negative clinical outcomes or valve performance measures in the absence of iTEE. There was no increase in use of contrast or acute kidney injury incidence. Confounding variables that likely had an impact on outcomes include improving operator experience, newer generation valves, and the implementation of protocols to reduce contrast use. Thus, we cannot conclude MAC without TEE is superior, however this data suggests that in most patients there is no harm by performing TAVR without iTEE.

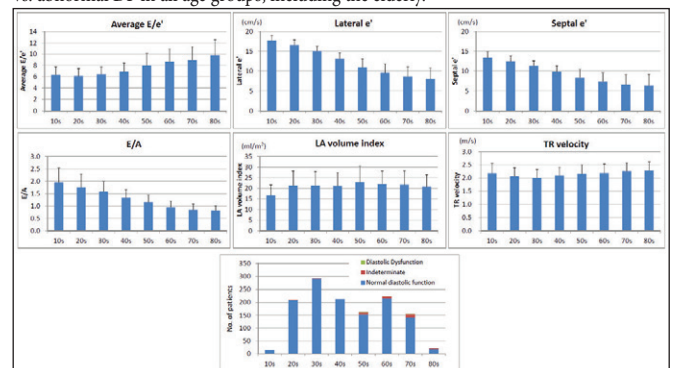
P1-155

Moderated Poster

Echocardiographic Diastolic Function by Age Decades: Results from the World Alliance of Societies of Echocardiography (WASE) Normal Values Study

Tatsuya Miyoshi¹, Karima Addetia², Alexandra Blitz³, Vivekanandan Amuthan⁴, Rodolfo Citro⁵, Masao Daimon⁶, Pedro Gutiérrez-Fajardo⁷, Ravi Kasliwal⁸, James N. Kirkpatrick⁹, Mark J. Monaghan¹⁰, Denisa Muraru¹¹, Kofo O. Ogunyankin¹², Seung Woo Park¹³, Aldo Prado¹⁴, Ana Clara Tude Rodrigues¹⁵, Alexander Rossmann¹⁶, Anita Sadeghpour¹⁷, Gregory Scalia¹⁸, Masaaki Takeuchi¹⁹, Wendy Tsang²⁰, Edwin S. Tuccay²¹, Mei Zhang²², Roberto M. Lang², Federico M. Asch¹. ¹Medstar Health Research Institute, Washington, DC; ²University of Chicago, Chicago, IL; ³TOMTEC Imaging Systems GmbH, Unterschleissheim, Germany; ⁴Jeyalakshmi Heart Center, Madurai, India; ⁵University of Salerno, Salerno, Italy; ⁶The University of Tokyo, Tokyo, Japan; ⁷Hospitales Mac Bernardette, Guadalajara, Mexico; ⁸Medanta Heart Institute, Gurgaon, Haryana, India; ⁹University of Washington, Seattle, WA; ¹⁰King's College Hospital, London, United Kingdom; ¹¹University of Padova, Padova, Italy; ¹²First Cardiology Consultants Hospital, Lagos, Nigeria; ¹³Samsung Medical Center, Seoul, Republic of Korea; ¹⁴Centro Privado de Cardiologia, Tucuman, Argentina; ¹⁵Albert Einstein Hospital, Sao Paulo, Brazil; ¹⁶Rajaie Cardiovascular Medical and Research Center, Echocardiography Research Center, IUMS, Tehran, Islamic Republic of Iran; ¹⁷Genesis Care, Brisbane, Australia; ¹⁸University of Occupational and Environmental Health, Kitakyushu, Japan; ¹⁹Toronto General Hospital, University of Toronto, Toronto, ON, Canada; ²⁰Philippine Heart Center, Quezon City, Philippines; ²¹Qilu Hospital of Shandong University, Jinan, China

Background: American Society of Echocardiography (ASE) guidelines provide recommendation for evaluation of left ventricular (LV) diastolic function (DF), based on cutoff values of four variables. While used worldwide, proposed values and algorithms are predominantly based on data from Caucasian North American and European populations. We aim to test if these values apply to a global population from around the world and evaluate how they change in adults from different age groups. ASE in collaboration with its International Alliance Partners conducted the World Alliance of Societies of Echocardiography (WASE) Normal Values Study to establish and compare normal echocardiographic values in adults across races, ethnicities and countries worldwide. Following ASE 2016 DF guidelines, we describe the change of LV DF parameters by age (decades) and test the algorithms to detect diastolic dysfunction in the entire WASE cohort. **Methods:** WASE Normal Values Study is a multinational, observational, cross-sectional study. The participant countries have enrolled adult individuals free from cardiac, lung and renal diseases evenly distributed among age groups and gender. The following parameters were measured to determine LV DF following the standard ASE protocol: septal and lateral e' , average E/e' , E/A, left atrial volume index (LAVI) and tricuspid regurgitation (TR) velocity. All measurements were analyzed (TOMTEC) following ASE Guidelines. WASE patients were divided according to age by decades. In addition, determination of LV dysfunction was performed using the algorithm for subjects with normal LV ejection fraction. **Results:** As of January 2019, 1291 cases were analyzed. E/A, septal and lateral e' decreased consistently as patients were older. E/e' gradually increased from the 40s, while it was similar in younger groups. There was no significant difference in LAVI. A notable finding is that LV dysfunction was seen in only 3 subjects even if our cohort included many elderly subjects with age over 60 years old. All data is presented in Table. **Conclusions:** Individual parameters used for LV DF evaluation change progressively and consistently as patients get older. Importantly, current guidelines prove useful in distinction of normal vs. abnormal DF in all age groups, including the elderly.



Poster Session 1 (P1)

Sunday, June 23, 2019

P1-156

Left Atrial Myocardial Dysfunction in Patients with Combined Pre- and Post-capillary Pulmonary Hypertension

Sanae Kaga¹, Kazumori Okada¹, Michito Murayama², Taisei Mikami¹, Masahiro Nakabachi³, Shinobu Yokoyama³, Hisao Nishino³, Shingo Tsujinaga⁴, Miwa Sarashina⁴, Hiroyuki Iwano⁴, Toshihisa Anzai⁴. ¹Faculty of Health Sciences, Hokkaido University, Sapporo, Japan; ²Diagnostic Center for Sonography, Hokkaido University Hospital, Sapporo, Japan; ³Division of Clinical Laboratory and Transfusion Medicine, Hokkaido University Hospital, Sapporo, Japan; ⁴Department of Cardiovascular Medicine, Faculty of Medicine and Graduate School of Medicine, Hokkaido University, Sapporo, Japan

Background: Pulmonary hypertension (PH) caused by elevation of left atrial pressure, post-capillary PH, occasionally complicates an increase in pulmonary artery pressure (PAP) in excess of the elevation of pulmonary artery wedge pressure (PAWP), so called as combined pre- and post-capillary PH (CpcPH). Although the presence of CpcPH is reported to worsen the outcome of heart failure, little is known about its pathogenesis. We hypothesized that reduced left atrial function could be associated with the complication of CpcPH in heart failure patients. **Methods:** Transthoracic echocardiography was performed in 57 heart failure patients with post-capillary PH (mean pulmonary PAP ≥ 25 mmHg and mean PAWP >15 mmHg) diagnosed by cardiac catheterization. Left ventricular ejection fraction (LVEF) and indexed left atrial volume (LAVI) were measured by disk method. Early- (E) and late-diastolic (A) transmitral flow velocities and early-diastolic mitral annular velocities (e') were measured using Doppler imaging. Left atrial longitudinal strain during left ventricular systole (LA-Sts) and left atrial contraction (LA-Sta) as well as left ventricular global longitudinal strain (LV-St) were measured in the apical 4-chamber view using speckle-tracking method. Patients with diastolic pressure gradient defined as diastolic PAP minus mean PAWP ≥ 7 mmHg or pulmonary vascular resistance >3 Wood units were classified as CpcPH and those without were classified as isolated post-capillary PH (IpcPH). **Results:** Mean PAP was higher in CpcPH than in IpcPH (38 ± 8 vs 30 ± 5 mmHg, $p < 0.001$) whereas mean PAWP (22 ± 6 vs 24 ± 5 mmHg, NS) was comparable between the groups. LAVI (74 ± 23 vs 68 ± 23 ml/m²), E/A (3.0 ± 1.4 vs 2.3 ± 1.8), and E/e' (15.7 ± 4.4 vs 16.3 ± 8.3) were also comparable between the groups (NS for all). However, CpcPH had significantly larger left ventricular end-diastolic dimension (LVDd) (66 ± 13 vs 57 ± 11 mm, $p < 0.01$), smaller LVEF (28 ± 13 vs $47 \pm 20\%$, $p < 0.001$), LA-Sts (12 ± 5 vs $20 \pm 7\%$, $p < 0.001$), LA-Sta (4 ± 3 vs $8 \pm 3\%$, $p < 0.001$), and LV-St (10 ± 4 vs $15 \pm 6\%$, $p < 0.01$) than IpcPH. Multivariable analysis showed that LA-Sts was the independent determinant of the presence of CpcPH among LVDd, LVEF, LASts, LASta, and LV-St. **Conclusion:** Reduced left atrial function, especially the reservoir function, was associated with complication of CpcPH in heart failure patients with post-capillary PH.

P1-157

Hemodynamic Response to Passive Leg Raise and Its Application in Diastolic Function Evaluation

Anahita Ghorbani, Andre Gabriel, Kathir Balakumaran, Kai Chen. UConn Health Center, Farmington, CT

Background: Passive leg raise (PLR) induces an endogenous fluid challenge via a rapid yet irreversible increase in venous return with resultant augmentation of left ventricular (LV) preload and filling pressures. The aim of our study was to assess hemodynamic response to PLR determined by echocardiography, and its usefulness in diastolic function classification. **Methods:** We prospectively recruited adult patients referred to our lab for outpatient echocardiographic examination. Patients with LV ejection fraction (EF) $< 40\%$ or significant valvular heart disease were excluded. Study protocol was approved by UConn Health Center IRB. All the participants provided written informed consent. Echocardiographic images were obtained in the standard position at baseline and 30 seconds after initiation of PLR. Diastolic function was defined using 2016 ASE Guideline. Echocardiographic parameters were compared pre and post PLR using paired t-test. P value < 0.05 was deemed significant. **Results:** A total of 71 individuals (mean age 62 ± 15 years, 49% women) were included. Mean LVEF (%) was 60 ± 6 . As expected, preload challenge induced by PLR significantly enhanced cardiac output (4.6 ± 0.1 vs 5.6 ± 0.3 L/min, $p = 0.0001$), predominantly driven by an increase in heart rate (69 ± 13 vs 80 ± 23 BPM, $p < 0.0001$). Among all the echocardiographic findings, diastolic parameters appeared to be most sensitive hemodynamic changes after PLR, as evident by increased lateral e' (9.0 ± 2.4 vs 10.5 ± 2.8 cm/s, $p < 0.0001$), decreased E wave deceleration time (220.4 ± 66.2 vs 186.3 ± 51.1 msec, $p < 0.0001$), increased E velocity (83.5 ± 25.3 vs 89.4 ± 27.6 cm/s, $p < 0.01$), and decreased mean E/e' (11.6 ± 4.3 vs 10.9 ± 4.8 , $p < 0.05$). We also observed a distinct hemodynamic response between subgroups of normal and abnormal diastolic function, defined as medial $e' \geq 7$ vs < 7 cm/s. We then applied PLR maneuver to further classify diastolic function categories. Among 28 cases initially classified as indeterminate diastolic function, 1 and 16 were categorized as normal and abnormal diastolic function respectively using post PLR parameters ($p < 0.0001$) (Table). **Conclusion:** Our findings suggest PLR as a maneuver of preload challenge has a significant impact on hemodynamics. Further, PLR may have clinical implication in diagnosis and classification of diastolic dysfunction.

Table. Diastolic function classification pre and post passive leg raise (PLR)

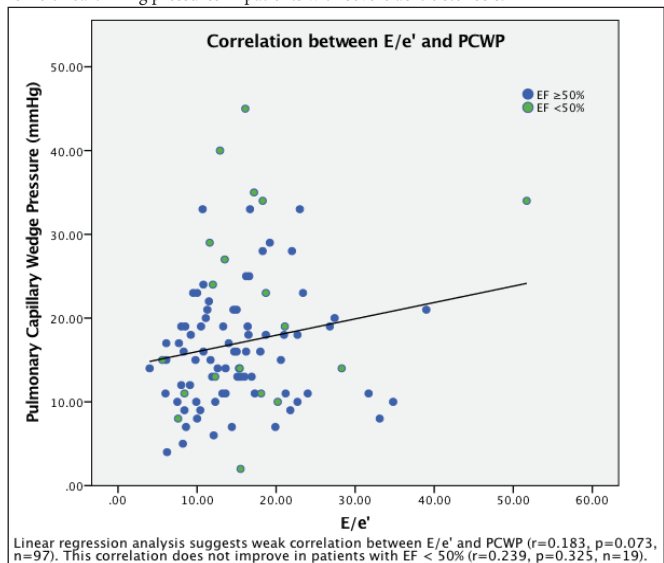
	Diastolic Function Category (n)	Post PLR			Total
		Normal	Abnormal	Indeterminate	
Pre PLR	Normal	15	0	2	17
	Abnormal	2	15	3	20
	Indeterminate	16	1	11	28
	Total	33	16	16	65

P1-158

Tissue Doppler Imaging (E/e') is Weakly Associated with Pulmonary Capillary Wedge Pressure in Patients with Severe Aortic Stenosis

Yoko Kagimoto¹, Natesa G. Pandian², Ayan R. Patel², Andrew R. Weintraub², Jeffrey T. Lyvers¹, Frederick C. Cobey². ¹Massachusetts General Hospital, Boston, MA; ²Tufts Medical Center, Boston, MA

BACKGROUND: While American and European consensus statements advocate employing the ratio of the transmitral E velocity and tissue Doppler early diastolic mitral annular velocity (E/e') in the assessment of left heart filling pressures, a series of recent reports have called into question the reliability of this ratio to predict left atrial pressures in a variety of disease states. We hypothesized that there is a clinically significant correlation between E/e' and pulmonary capillary wedge pressure (PCWP) in patients with severe aortic stenosis. **METHODS:** After institutional IRB approval, we retrospectively re-viewed consecutive patients with severe aortic stenosis who underwent TAVR for severe aortic stenosis. PCWP and E/e' were measured using pulmonary artery catheter and transthoracic echocardiography respectively, during pre-procedural evaluation. As a sub-group analysis, patients were grouped by left ventricular ejection fraction (LVEF) $\geq 50\%$ and LVEF $< 50\%$. Linear regression analysis and one-way ANOVA was used to analyze the data. *A priori* statistical significance set at $p < 0.05$. **RESULTS:** A total of 97 patients met the inclusion criteria. There was a weak correlation between E/e' and PCWP ($r = 0.183$, $p = 0.073$, $n = 97$), although correlation was not statistically significant. This correlation did not improve in patients with LVEF $< 50\%$ ($r = 0.239$, $p = 0.325$, $n = 19$). There was a significant difference in mean PCWP in patients with E/e' less than 8 versus more than 14 by 5.9 mmHg ($p = 0.046$). **CONCLUSIONS:** We did not find clinically relevant relationship between E/e' and PCWP in patients with aortic stenosis. There was a small difference in mean PCWP between patients with E/e' less than 8 versus more than 14. However, the regression analysis demonstrated only a weak correlation between E/e' and PCWP that was not statistically significant. Our results are similar to recent reports that have suggested the limited value of E/e' in predicting left atrial pressures. Caution is warranted when using E/e' as a surrogate for left heart filling pressures in patients with severe aortic stenosis.



Poster Session 1 (P1)

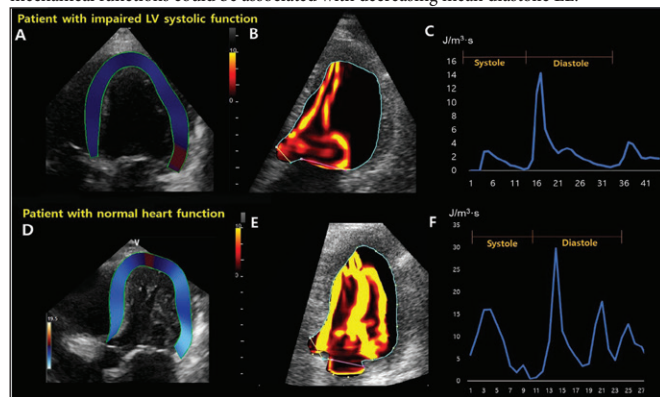
Sunday, June 23, 2019

P1-159

The Association of the Flow Dissipative Energy Loss and Left Ventricular Function in Patients with Heart Failure

Cho Jung Sun^{1,2}, Sirish Shrestha², Muhammad Ashraf², Nobuyuki Kagiyama², Partho P Sengupta². ¹Daejeon St. Mary Hospital, Dae-jeon, Republic of Korea; ²West Virginia University Heart & Vascular Institute, Morgantown, WV

Background: Vortex flow mapping (VFM) as one of the intracardiac flow visualization techniques could allow estimating the flow dissipative energy loss (EL). EL as a quantitative assessment of the left ventricular (LV) intraventricular blood flow could provide insight into LV function. **Methods:** We aimed to investigate the association of EL as hemodynamic function and deformation parameters and conventional echocardiographic parameters as mechanical heart function in patients with heart failure. This cross-sectional study included 240 subjects (54.3 ± 17.4 years) who had a various stage of heart failure. Exclusion criteria were atrial fibrillation, more than moderate valvular heart disease, poor echo images for analysis. **Results:** The patients were divided into two groups which are high global longitudinal strain (GLS) group (n= 198) which was defined as GLS ≤ -15% and low GLS group (n=42) which was defined as GLS > -15%. Enrolled patients underwent conventional echocardiography and two-dimensional speckle tracking echocardiography and VFM. Compared to the two groups, mean systolic and diastolic EL was significantly higher in high GLS group (17.9 ± 16.0 J/m³-s vs. 10.1 ± 9.7 J/m³-s, p < 0.001; 27.6 ± 24.4 J/m³-s vs. 18.8 ± 17.6 J/m³-s, p = 0.009, respectively). Results from multivariate linear regression showed that the lower mean diastolic EL was independently associated with lower LV ejection fraction (EF), LV end-systolic dimension, GLS, and systolic LV strain rate (p < 0.05 for all). Mean systolic EL was associated with LVEF (p < 0.05). **Conclusion:** Heart failure patients with reduced mechanical functions could be associated with decreasing mean diastolic EL.

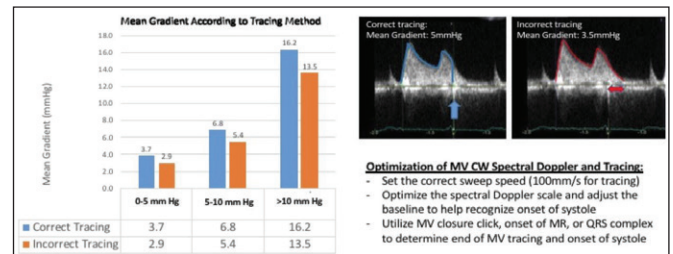


P1-160

Impact of Incorrect Transmitral Doppler Gradient Tracings: Best Practice Guide for Sonographers

Madeline Jankowski, Nadia El-Hangouche, Olga Kisilitsina, Jyothy J. Puthumana, James D. Thomas, Akhil Narang. Northwestern University, Chicago, IL

Background: Transcatheter mitral valve repair/replacement (TMVR) are increasingly performed in patients who have no adequate surgical option for significant mitral regurgitation or stenosis. Patient selection and procedural outcomes typically rely on diastolic mitral valve (MV) gradients to ensure the absence of hemodynamically significant MV stenosis. Tracings of MV gradients is often performed incorrectly - with the most common mistake being extension of the tracing into systolic portion of the cardiac cycle. The purpose of this study was to evaluate the impact of incorrect versus correct Doppler tracings of MV gradients. **Methods:** Consecutive transthoracic echocardiograms whose final report mentioned "mitral stenosis" over a two-month span from a busy academic institution were analyzed. The continuous wave (CW) Doppler tracings of the MV were traced both correctly and incorrectly and the differences were compared. **Results:** A total of 81 patients were included in the analysis. Overall, incorrect tracings resulted in underestimation of the MV gradient by 21%. The difference was highest in patients with correct MV gradients of <5 mm Hg compared to those with gradients >10 mm Hg (22% vs 16%) (Table). Best practices to ensure accurate tracings include: 1) selecting the correct sweep speed of the CW Doppler acquisition, 2) optimizing the spectral Doppler scale and adjust the baseline to recognize onset of systole, and 3) recognizing end diastole and systole onset (Figure). **Conclusions:** Incorrect tracing of MV gradients is not uncommonly observed and can lead to an underestimation of the true gradients. In turn, this may impact decision making for transcatheter interventions in patients with mitral valve disease. Sonographers and procedural echocardiographers should be aware of best practices to ensure accurate measurements of MV gradients.



P1-161

Invasively-Measured versus Echocardiography-Estimated Pulmonary Artery Pressures and Resistance in Young Children: What's the Correlation?

Christiana Tai, Anyir Hsieh, Anita Moon-Grady, Roberta Keller, Hythem Nawaytou. UCSF, San Francisco, CA

Background: Invasive measurements of pulmonary artery pressure (PAP) correlate well with simultaneously acquired echocardiographic estimates of PAP in children but poorly with non-simultaneous echocardiographic estimates of PAP. Therefore, the reliability of non-invasively obtained estimates of pulmonary hypertension in the clinical setting is suspect. We aim to evaluate this discrepancy in the correlations between simultaneous and non-simultaneously acquired echocardiograms and invasively measured PAP and indexed pulmonary vascular resistance (PVRi). **Methods:** We enrolled children less than 72 months of age undergoing cardiac catheterization for pulmonary hypertension evaluation or closure of a patent ductus arteriosus or atrial septal defect. The closest echocardiogram to the catheterization (Non-Sim echo) was analyzed. Another echocardiogram was acquired during catheterization (Sim echo). Correlations between invasively measured PAP and PVRi, and echocardiographic indicators of PAP and PVRi on Non-Sim and Sim echo were evaluated using Spearman correlation test. **Results:** Twenty-six patients, median age 12.1 months (IQR 4.7 - 20.1) undergoing 28 cardiac catheterizations were included. Median duration between Non-Sim and cardiac catheterization was 13 days (IQR 1.55) during which only 4 patients had changes in vasoactive medications. Invasive median systolic PAP was 47mmHg (IQR: 33, 53), median ratio of systolic PAP to left ventricular systolic pressure (sPAP/LVSP) was 0.63 (IQR: 0.46, 0.79) and median PVRi was 3.1WU (IQR: 2.2, 6.4). Tricuspid regurgitant jet peak velocity correlated well with invasive systolic PAP (Non-Sim echo $\rho = 0.82$, $p = 0.04$ / Sim echo $\rho = 0.79$, $p < 0.001$) with a strong correlation between Non-Sim and Sim echo ($\rho = 0.9$, $p = 0.04$). Systolic eccentricity index correlated well with sPAP/LVSP and PVRi (Non-Sim echo $\rho = 0.53$, $p = 0.005$ and $\rho = 0.46$, $p = 0.02$ / Sim echo $\rho = 0.57$, $p = 0.001$ and $\rho = 0.44$, $p = 0.02$) with good correlation between Non-sim and Sim echo ($\rho = 0.68$, $p < 0.001$). Pulmonary artery acceleration time did not correlate with PVRi even after excluding 16 patients with patent ductus arteriosus. **Conclusion:** The strength of the correlations found between invasively measured PAP and PVRi, and specific echocardiographic estimates of PAP and surrogates of PVRi, did not differ between simultaneous and non-simultaneous echocardiograms. In both conditions the correlations were strong to moderate. Clinically obtained echocardiograms, including these specific measurements, can be relied on for screening and possibly grading the severity of pulmonary hypertension.

P1-162

The Determinants of Left Ventricular Energy Loss in Elderly Patients with Preserved Ejection Fraction

Shutaro Futami, Joji Ishikawa, Masuyo Kawano, Chieko Sakurayama, Kazumasa Harada. Tokyo Metropolitan Geriatric Hospital and Institute of Gerontology, Tokyo, Japan

Background: Aging changes the cardiovascular stiffness and structure. These might be associated with increased energy loss of left ventricle. However, the determinants of energy loss are unclear. **Methods:** We stored color Doppler images of the apical three-chamber view with an ultrasound machine, Prosound F75 Premier (Hitachi Aloka, Tokyo, Japan), in 103 hypertensive outpatients with preserved ejection fraction (left ventricular ejection fraction $\geq 50\%$). We measured energy loss (EL) in left ventricle using vector flow mapping system and evaluated determinants of peak EL at early diastolic phase (ED-EL), at late diastolic phase (LD-EL) and at systolic phase (Sys-EL). **Results:** Mean age was 79 ± 7.3 (range 52-97) years (male 43%). Mean ED-EL, LD-EL and Sys-EL were 41.342 ± 46.529 mJ/m/s, 76.430 ± 59.779 mJ/m/s and 38.909 ± 38.244 mJ/m/s. In stepwise regression analysis that included all significant covariates, the determinant of ED-EL was E wave velocity of transmitral flow (unstandardized $\beta = 1.747$; 95%CI 1.157 to 2.337; $p < 0.001$). The determinants of LD-EL were A wave velocity of transmitral flow (unstandardized $\beta = 0.848$; 95%CI 0.135 to 1.560; $p = 0.021$) and peak velocity in left ventricular outflow tract (unstandardized $\beta = 0.569$; 95%CI 0.066 to 1.072; $p = 0.027$). The determinants of Sys-EL were peak velocity in left ventricular outflow tract (unstandardized $\beta = 0.872$; 95%CI 0.595 to 1.150; $p < 0.001$), E wave velocity of transmitral flow (unstandardized $\beta = -0.504$; 95%CI -0.922 to -0.087; $p = 0.019$) and Left ventricular outflow tract diameter (unstandardized

Poster Session 1 (P1)

Sunday, June 23, 2019

$\beta=-4.069$; 95%CI -7.790 to -0.349; $p=0.033$). Even after adjustment for traditional cardiovascular risk factors, ED-EL was significantly related to E wave velocity of transmitral flow; LD-EL was to A wave velocity of transmitral flow and peak velocity in left ventricular outflow tract; and Sys-EL was to peak velocity in left ventricular outflow tract. **Conclusion:** In elderly patients, the EL in left ventricle of diastolic phase could be greater than that of systolic phase. Peak EL in left ventricle at elderly patients was affected by transmitral inflow and left ventricular outflow.

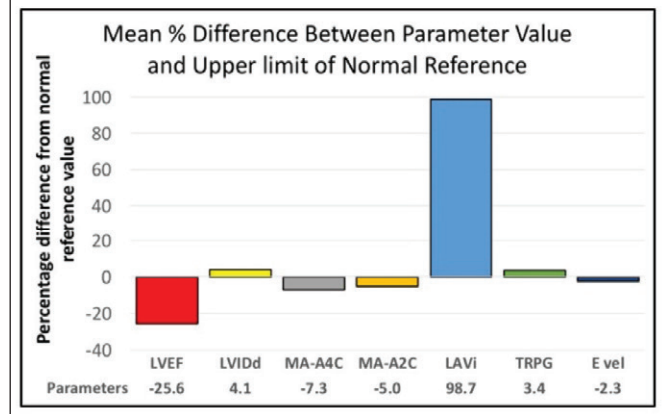
P1-163

Underestimation of Mitral Regurgitation on Transthoracic Echocardiography: The Scope of the Problem and When to be Suspicious

Isla McClelland¹, Kalie Kebed¹, Megan Yamat¹, Deyu Sun², Victor Mor-Avi¹, Roberto M. Lang¹, Karima Addetia¹. ¹University of Chicago, Chicago, IL; ²Philips Healthcare, Andover, MA

Background: As percutaneous procedures for treatment of mitral regurgitation (MR) become more widespread, greater emphasis is being placed on accurate assessment of MR severity. While transesophageal echocardiography (TEE) is regarded as the gold standard for MR assessment, evaluation often begins with a transthoracic study (TTE). However, TTE can underestimate MR severity even if image quality is satisfactory. We sought to determine if there were any characteristics on TTE that were associated with underestimation of MR compared to TEE. **Methods:** We identified 277 TTE studies from our database spanning 1994-2018, which were followed by TEE within 1 month and showed an increase in MR severity by ≥ 2 grades. MR grades were classified as none, mild, mild-moderate, moderate, moderate-severe and severe. Of these, $n=45$ had severe MR on TEE and comprised the study cohort. TTE parameters known to be impacted by worsening MR were measured: left ventricular (LV) end-diastolic diameter (LVIDd), LV ejection fraction (EF), E-wave velocity, mitral annulus dimension in the apical 4- and 3-chamber views (MA-A4C, MA-A2C), left atrial volume index (LAVi), MR jet density (graded from 0 to 3 with 0 being the faintest and 3 the most dense), tricuspid regurgitation peak gradient (TRPG) and MR eccentricity (yes/no). The %difference between the measured value and published upper limit of normal was calculated. Subgroup analysis was performed using those with a grade difference=2 (moderate MR on TTE/severe on TEE $n=21$) and those with grade difference >2 (\leq mild-moderate MR on TTE/severe MR on TEE $n=24$) using t-test to compare between groups. **Results:** Demographics and mean parameter values are reported in the Table. The parameters which were the most abnormal in this cohort were LVEF and LAVi. For the total cohort, LVEF was 25.6 % lower than the lower limit of normal, LAVi was 98% higher than the upper limit of normal, and 64% of patients showed eccentric jets on TTE(Figure). In the subgroup with larger grade discrepancy (>2 grades) between TTE and TEE, LAVi was found to be significantly larger while annulus diameters, LVIDd and MR jet density were not different. **Conclusion:** A large LA volume may be an important factor associated with underestimation of MR from the TTE perspective.

Men (n, %)	26 (58%)
Age (years)	63.0 ± 14
Days between TTE and TEE	9.5 ± 9.5
MR VC (PSL) (cm)	0.5 ± 0.2
LV EF (%)	39.02 ± 17.72
LVIDd (cm)	5.8 ± 1.2
Mitral Annulus diameter (A4ch) (cm)	3.8 ± 0.6
Mitral Annulus diameter (A2ch) (cm)	3.8 ± 0.6
Indexed LA Vol (biplane Simpson)	67.5 ± 27.9
TR gradient (max) (mmHg)	36.3 ± 18.8
Eccentric MR? (n, %)	29 (64%)
MR jet density (0, 1, 2, 3)	1.6 ± 0.8
E (cm/s)	113.1 ± 32.6



P1-164

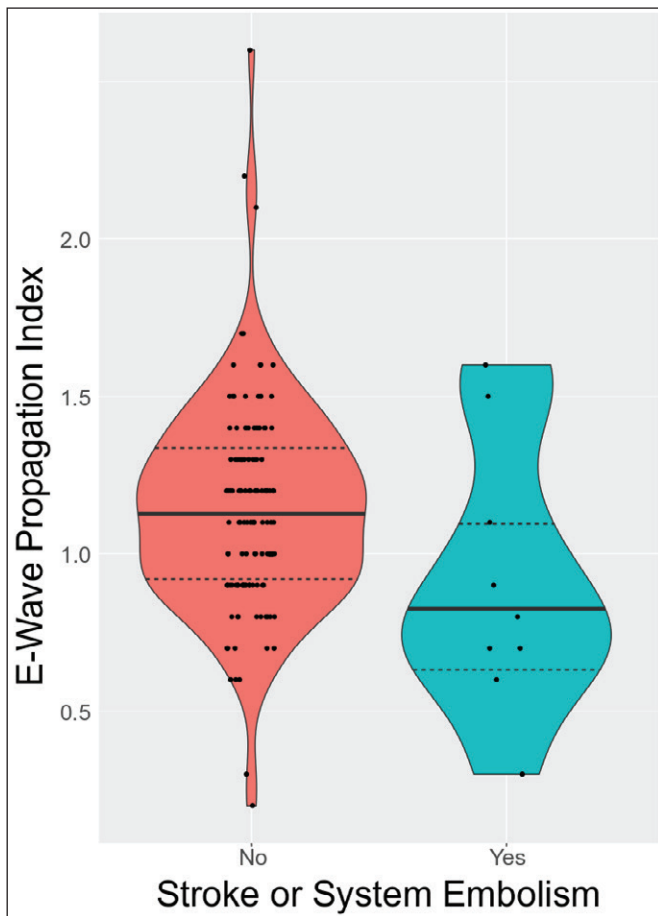
Embolic Risk of Left Ventricular Thrombi Predicted by E-Wave Propagation Index

Austin Robinson¹, Paul Thompson¹, Grayson Eubanks², Christopher Schumann¹, Benjamin Ruth¹, John Dent¹. ¹University of Virginia, Charlottesville, VA; ²University of North Carolina, Chapel Hill, NC

Background: Left ventricular thrombi (LVT) are a complication of myocardial dysfunction, with the potential to embolize. Understanding risk of embolization could guide therapy, but there are few contemporary methods to stratify this risk. E-wave propagation index (EPI), the ratio of mitral E-wave velocity-time integral to LV length, has been demonstrated to be lower in patients with cardiomyopathy and LVT. However, the relationship between EPI and the embolic potential of existing LVT has not been explored. **Methods:** Consecutive patients with echocardiographically-diagnosed LVT at a single center between 2013 and 2018 were reviewed. EPI was measured from the index echocardiogram. Patients were contacted individually to assess outcomes. Embolic events consisted of ischemic stroke or systemic embolism (SSE). Means were compared via a student's t-test. Univariate logistic regression was performed to evaluate EPI as a predictor of SSE. **Results:** We identified 138 patients with LVT, of which there were a total of 9 subsequent SSE (7.0%). The EPI of patients without SSE was 1.142 +/- 0.329, compared to a mean EPI of 0.91 +/- 0.423 in patients with SSE, $p=0.048$. In a univariate logistic regression analysis, EPI was a significant predictor of SSE (OR 0.099, 95% CI 0.010-0.933, $p=0.043$). **Conclusion:** In a single center study of patients with LVT, EPI measured at index echocardiography was a predictor of subsequent embolic risk. These findings suggest that EPI could have merit in a prediction model for embolic risk and that mitral inflow measurements are an important part of an index echocardiogram in new LVT. Further studies with more events to allow for multivariate regression modeling are warranted.

Poster Session 1 (P1)

Sunday, June 23, 2019



P1-165
Ratio of TAPSE to RVSP: A Simple Echo Index for Evaluation of Pulmonary Hypertension in Children with Cardiomyopathy

Marjorie Gayanilo, Deemah Mahadin, Robert D. Ross, Sanjeev Aggarwal.
Children's Hospital of Michigan, Detroit, MI

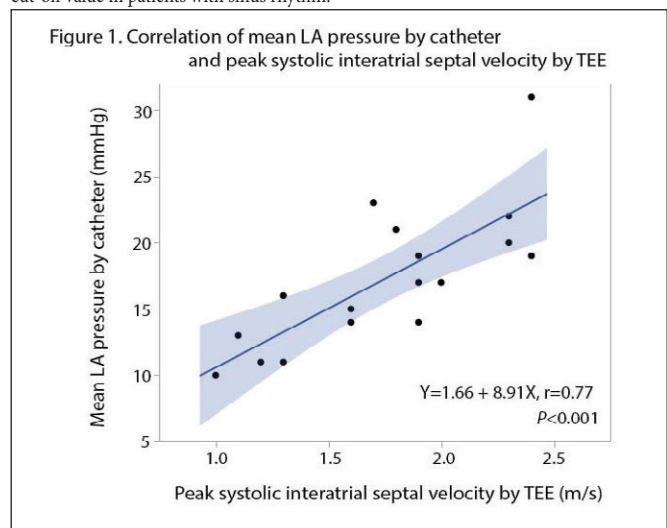
BACKGROUND: Right ventricular dysfunction and pulmonary hypertension are associated with poor outcomes in cardiomyopathy (CM). Pulmonary hypertension is traditionally assessed by direct measurement of pressure and flow during cardiac catheterization (CC). However, CC is invasive and has associated risks. The ratio of tricuspid annular plane systolic excursion (TAPSE) and right ventricular systolic pressure (RVSP) echocardiogram has been shown to be a poor prognostic marker in adults with CM. Our aim was to compare this ratio in children with CM with and without severely increased pulmonary vascular resistance (≥ 6 iWU) on CC. **METHODS:** This was a single center retrospective review of CM patients who had undergone CC within 3 days of an echocardiogram. Patients who had incomplete data, pericardial effusion or were on pulmonary vasodilators were excluded. All measurements were performed by a single reader blinded to clinical and CC data. Echocardiographic measures included i) TAPSE, calculated by 2D methods in apical 4 chamber view and indexed to body surface area ii) RVSP using continuous Doppler from tricuspid valve regurgitation ($4V^2$) with no added atrial pressure, iii) Pulmonary outflow ejection time (PET) and acceleration time (PAT) using Doppler across the pulmonary valve, useful when RVSP can not be estimated due to absence of tricuspid regurgitation. Two groups with pulmonary vascular resistance ≥ 6 iWU and <6 iWU were compared using student t-test and Chi-square test. **RESULTS:** Our study cohort (n=21) included 9 (43%) males, and had a mean (SD) age of 10.2 (7.0) years. The majority [18 (86%)] of patients had dilated CM, while 3 (14%) had restrictive CM. The mean (SD) pulmonary vascular resistance was 3.9 (3.3) iWU, transpulmonary gradient was 10 (6.9), TAPSE was 1.45 (0.67) and indexed TAPSE was 1.6 (1.3). The group (n=6) with pulmonary vascular resistance ≥ 6 iWU had significantly lower TAPSE, pulmonary ejection time and PAT and TAPSE/ RVSP ratio and TAPSE/ PAT ratio, compared to those without severe pulmonary hypertension. **CONCLUSION:** Echocardiographic parameters that combine of right ventricular function, pressures or reduced acceleration times may be useful for assessment of pulmonary hypertension in children with CM. Further exploration of their diagnostic and prognostic utility in CM would be beneficial.

Clinical/Demographics	PVR < 6 iWU (n=15)	PVR ≥ 6 iWU (n=6)	P value
Gender (male)	6(40%)	3(50%)	NS
Age (years)	10.3 (7.6)	10.1 (6.7)	NS
Height (cm)	132 (47)	129 (42)	NS
Weight (kg)	49.0 (37.5)	39.2 (30.7)	NS
BSA (m ²)	1.3 (0.7)	1.2 (0.7)	NS
Heart rate	90 (20)	112 (22)	0.04
TAPSE	1.8 (0.5)	0.7 (0.4)	0.00001
TASPE index	1.97(1.3)	0.68(0.31)	0.03
Pulmonary Ejection Time (msec)	268 (48)	200 (40)	0.00001
PAT (msec)	116 (28)	60 (20)	0.00001
RVSP	22.5 (6)	47.5 (14)	0.00001
TAPSE:RVSP	1.04(0.35)	0.19(0.11)	0.002
TAPSE:PAT	86.5 (29.6)	39.5 (15.6)	0.0001
PAT: Pulmonary Ejection Time	43 (6.3)	29.4(4.5)	0.0001

P1-166
Assessing Left Ventricular Filling Pressure with Doppler Velocities Across a Patent Foramen Ovale

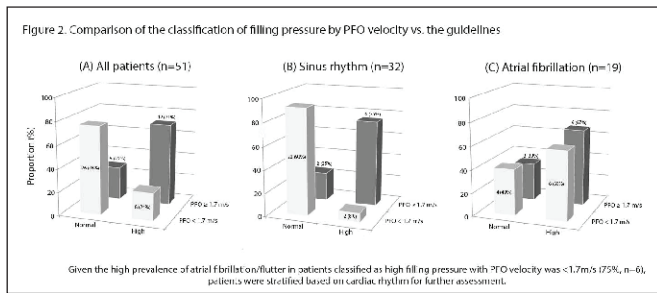
Saki Ito¹, Sumandeep Dhesi², William R. Miranda¹, Jeffrey B. Geske¹, Nandan S. Anavekar¹, Kareem Morant¹, Charanjit S. Rihal¹, Mackram F. Eleid¹, Jae K. Oh¹. ¹Mayo Clinic, Rochester, MN; ²University of British Columbia, Vancouver, BC, Canada

Objectives: To investigate use of Doppler velocities across a patent foramen ovale (PFO) to estimate left ventricular (LV) filling pressure. **Methods:** The best cut-off value of peak interatrial septal velocity across a transeptal puncture site measured by transesophageal echocardiography was determined for estimating high mean left atrial (LA) pressure (≥ 15 mmHg) in 17 patients. The cut-off value was subsequently applied to 67 patients with a PFO undergoing transthoracic echocardiography (TTE) to validate the value of PFO velocity in determining diastolic dysfunction and filling pressure. The peak systolic velocity was chosen as it was assumed that it would be directly proportional to the maximal pressure differences between the LA and right atrium (RA), which occur at the time of v-wave. **Results:** The peak interatrial septal velocities significantly correlated with directly measured mean LA pressures during transcatheter mitral valve procedure (Fig 1. $r=0.77$, $P<.001$). The best cut-off value was 1.7m/s for predicting high LA pressure (AUC 0.91; sensitivity 0.90, specificity 0.86). When this cut-off was applied to patients with TTE, peak PFO velocity ≥ 1.7 m/s correlated with reduced e' , higher E/e' , and higher tricuspid regurgitation velocity ($P<0.01$). LV filling pressure according to the 2016 diastolic guideline was compared with peak PFO velocity in 51 patients. Peak PFO velocity ≥ 1.7 m/s identified 71% (n=12) of patients with high filling pressure based on guidelines and PFO velocity <1.7 m/s identified 76% (n=26) of patients with normal filling pressure (Fig 2A). Of the 24% (n=8) of patients with PFO velocity <1.7 m/s who were classified as having high filling pressure, atrial fibrillation was frequent (75%, n=6). **Conclusions:** A Doppler-derived peak PFO velocity could be valuable in the assessment of LV filling pressure using 1.7m/s as the cut-off value in patients with sinus rhythm.



Poster Session 1 (P1)

Sunday, June 23, 2019



P1-167

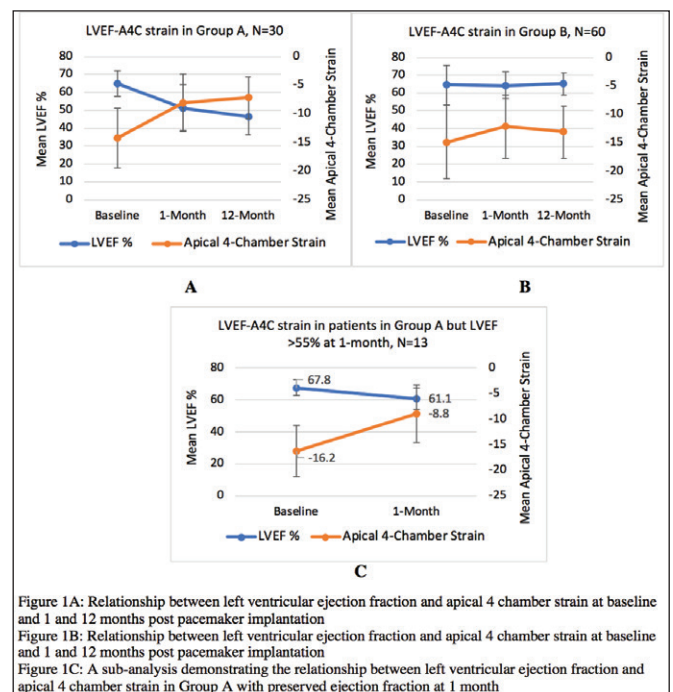
Application of Myocardial Deformation for Early Detection of Pacemaker Induced Cardiomyopathy

Soham Dasgupta¹, Rohit Madani¹, Janet Figueroa², Eric Ferguson¹, William Border¹, Ritu Sachdeva¹, Peter Fischbach¹, Robert Whitehill¹. ¹Children's Healthcare of Atlanta, Atlanta, GA; ²Emory University, Atlanta, GA

Background: Long term right ventricular pacing can cause pacemaker induced cardiomyopathy (PICM). The role of myocardial deformation in identification of left ventricular (LV) dysfunction in pediatric patients with PICM has not been evaluated. We hypothesized that strain imaging will detect cardiac dysfunction prior to decline in LV ejection fraction (LVEF) in pediatric patients with PICM. **Methods:** Study subjects included patients (0-21 years) who had a pacemaker placed between 2011-2017 and had normal LVEF at baseline (prior to pacemaker). Those with a biventricular system or isolated atrial lead, single ventricle, no baseline echo or other etiology for LVEF decline were excluded. Patients were divided into Group A (LVEF < 55% or decline > 10% within 12 months of pacemaker placement) and Group B (LVEF > 55% and decline < 10%). Patient and clinical characteristics including off-line analysis of myocardial deformation using apical 4-chamber strain (A4C) at baseline, and 1 and 12 months following pacemaker implantation were recorded (Table). **Results:** Ninety subjects met the study criteria with 30 in Group A and 60 in Group B with no significant difference in demographics (Table). Pacemaker characteristics were not associated with development of PICM. At 1 and 12 months follow-up, Group A had significantly lower LVEF, higher A4C strain values and EKG QRS duration (Table). While the LVEF and A4C strain were abnormal in Group A as early as 1 month, A4C strain values were not significantly increased in Group B (Fig 1A, B). Patients in Group A with normal LVEF at 1 month (N=13/30, 43%) had significant abnormalities in their A4C strain at that time (Fig 1C). **Conclusion:** Myocardial deformation was abnormal as early as 1 month after pacemaker implantation in those who developed PICM, including 43% of patients in whom LVEF was normal at 1 month. Application of strain imaging during longitudinal follow-up of those with right ventricular pacing may help with early detection of cardiac dysfunction and optimizing timing for a biventricular system.

N (%) or Median (25 th -75 th)	All, N=90	Group A, N=30	Group B, N=60	p-value
Weight, kg	23.3 (11-47.6)	22.9 (5.7-49.8)	23.3 (12.9-46.5)	0.63
Height, cm	125.5 (87-157)	115.5 (63-158)	126 (91.5-155.5)	0.37
Age at placement, months	102 (29.3-166.5)	80.9 (6.9-174.3)	106.3 (39.5-166.2)	0.33
Pacemaker indication				
Congenital CHB	30 (33.3%)	9 (30%)	21 (35%)	0.84
Post-operative	39 (43.3%)	15 (50%)	24 (40%)	
Sick Sinus Syndrome	12 (13.3%)	3 (10%)	9 (15%)	
Other	9 (10%)	3 (10%)	6 (10%)	
Type of Pacemaker				
Single	7 (8%)	1 (3.3%)	6 (10.3%)	0.41
Dual	81 (92%)	29 (96.7%)	52 (89.7%)	
Method of Placement				
Epicardial	62 (68.9%)	23 (76.7%)	39 (65%)	0.26
Transvenous	28 (31.1%)	7 (23.3%)	21 (35%)	
Location of V-Lead				
Apex	52 (68.4%)	20 (74.1%)	32 (65.3%)	0.43
Septum	24 (31.6%)	7 (25.9%)	17 (34.7%)	
Pacing Mode				
DDD	76 (91.6%)	48 (88.9%)	28 (96.6%)	0.41
AAI-DDIR	7 (8.4%)	6 (11.1%)	1 (3.4%)	
Percent Pacing at 12 months				
AS VP	99 (97-100)	100 (100-100)	100 (94-100)	0.08
AP VP	8.5 (1.0-23.0)	18 (1-72)	6 (1-20)	0.24
Baseline				
Apical 4-chamber strain	-15.1 (-17.5, -12.5)	-13.8 (-17.3, -12.1)	-15.4 (-17.9, -12.8)	0.23
LVEF	65.7 (60-70.1)	64.3 (58-70)	66.4 (60-71)	0.44
QRS	82 (72-116)	73 (67-126)	86 (76-112)	0.10
1 month				
Apical 4-chamber strain	-11.4 (-14.3, -7.5)	-8.8 (-11.6, -4.5)	-13.1 (-15.2, -10.2)	<0.001
LVEF	60.7 (55.4-67)	52.1 (46-58.1)	62 (60-68)	<0.001
QRS	142.5 (134-156)	155.5 (143-156)	139 (132-145)	<0.001
12-month				
Apical 4-chamber strain	-11 (-13.8, -7.8)	-6.5 (-9.7, -2.5)	-13.1 (-15.4, -10.4)	<0.001
LVEF	61 (52-66.5)	48.5 (40.4-52)	65.5 (60-68)	<0.001
QRS 12-month	146 (140-156)	156 (145-162)	144 (133.5-156)	0.002

CHB: Complete heart block; AS VP: Atrial Sense Ventricular Paced; AP VP: Atrial Paced Ventricular Paced;
LVEF: Left ventricular ejection fraction



P1-168

Left Atrial Functional Reserve is Impaired Independently from Left Ventricular Remodeling in Lone Paroxysmal Atrial Fibrillation: Lone Atrioopathy Begets Atrial Fibrillation or Vice Versa?

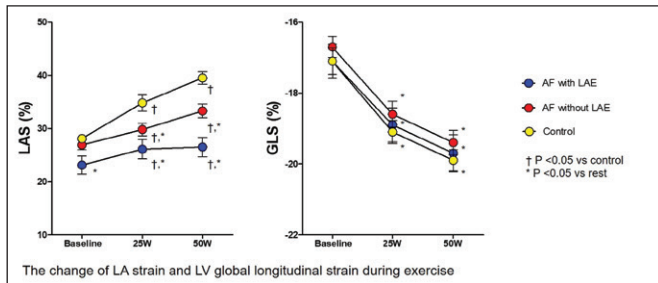
Dong-Hyuck Cho, Hee-Dong Kim, Mi-Na Kim, Jaemin Shim, Jong-Il Choi, Young-Hoon Kim, Wan Joo Shim, Seong-Mi Park. Division of Cardiology, Korea University College of Medicine, Seoul, Republic of Korea

Background: Left atrial (LA) functional and structural remodeling may provoke electrical instability and incident atrial fibrillation (AF). However, it is unclear whether atrial functional impairment is related to AF itself dependently from left ventricular (LV)

Poster Session 1 (P1)

Sunday, June 23, 2019

remodeling in AF. **Method:** A total of 54 patients (age 50±8 yrs) with paroxysmal AF and without structural heart disease and coronary artery disease undergoing ablation and 28 controls were prospectively enrolled. To assess LV and LA function, conventional echocardiography and 2D speckle tracking were performed at rest and during supine bicycle exercise (25W, 3 min increments) in sinus rhythm. AF patients were divided to with LA enlargement (LAE) and without LAE. **Result:** LV global longitudinal strain (GLS) and mitral early diastolic velocity (e') were not different between AF patients and controls, however, LA volume index (LAVI) was higher (P <0.001) and LA strain (LAS) was significantly impaired (25±7 vs. 28±4 %, P=0.03) in AF patients than controls. In AF patients, LV GLS was not different between patients with LAE and without LAE, however, LAVI was larger (P <0.001) and LAS was impaired (27±8 vs. 33±8 %, P=0.003) in patients with LAE. During exercise, in all workloads, LAS and LA function reserve index were lower in AF patients than in controls (5±6 vs. 11±5, P <0.001) (Figure). Whereas, the increment of LV GLS and LV functional reserve were not different between AF patients and controls. In AF patients, LV GLS was similarly increased by low to high workload in both patients with LAE and without LAE. However, the increment of LAS was different; in low workload, LAS was significantly increased in all AF patients, whereas in high workload, LAS was increased only in AF patients without LAE (25W vs. 50W, LAE: 26±8 vs. 27±8 %, P=0.61; without LAE: 30±7 vs. 33±8 %, P <0.001). **Conclusion:** In lone paroxysmal AF, LV function was comparable with control. LA function was impaired not only at rest but also during exercise. Moreover, the impairment of LA functional reserve was more apparent with increment of workload in AF patients with structural remodeling. Atrial functional and structural remodeling may induce lone paroxysmal AF or vice versa which is independent from LV function.



P1-169

«Early» Echocardiographic Response to Cardiac Resynchronization Therapy and Long-Term Mortality in Patients with Congestive Heart Failure

Vadim Kuznetsov, Anna Soldatova, Dmitriy Krinochkin, Tatiana Enina. Tyumen Cardiology Research Center, Tomsk National Research Medical Center, Russian Academy of Science, Tyumen, Russian Federation

Background: The effect of cardiac resynchronization therapy (CRT) can be «early» and «late» but the relationship between time of the best effect and long-term mortality still remains unclear. The purpose of the study was to evaluate clinical, morphological, functional features and mortality in patients with congestive heart failure (CHF) and different time of the best echocardiographic response to CRT. **Materials and Methods:** 122 patients (82.8% men, mean age 54.8±9.6 years) with NYHA functional class III-IV and left ventricular ejection fraction ≤35% were enrolled. At baseline, 1, 3 months and each 6 months after implantation we evaluated clinical and echocardiographic parameters. In 28 patients the best decrease of left ventricular end-systolic volume (LVESV) was achieved up to 3 months (1.1±0.9 months, I group - «early» response) and in 94 patients - after 3 month (22.6±14.9 months, II group - «late» response). Groups did not differ in main clinical characteristics, QRS duration and parameters of mechanical dyssynchrony. **Results:** In II group responders (decrease in LVESV ≥15%) were identified more frequently (90.4% vs 60.7%; p=0.001), all patients with decrease of LVESV ≥30% (super-responders, n=53) had «late» response. During follow-up period (33.2±16.7 months) increase in left ventricular ejection fraction (LVEF) and decrease in LVESV were more evident in patients with «late» response. In Kaplan-Meier analysis mortality in II group was significantly lower (28.6% vs 3.2%; p=0.001). Cox regression showed that LVESV (HR 1.012; 95% CI 1.004-1.021; p=0.005) and the time of the best response (HR 0.131; 95% CI 0.032-0.530; p=0.004) were associated with long-term mortality. **Conclusion:** Patients with «late» response to CRT demonstrate higher rates of responders and super-responders and better dynamics in LVESV and LVEF compared to patients with «early» response. «Early» response and greater LVESV are associated with higher mortality rate. Thus, early clinical and functional improvement should not be used as a marker of the efficacy of CRT in terms of long-term mortality.

P1-170

Variation in Normal Left Atrial Strain Values Between Three Gating Methods

Cassady Palmer¹, Vien Troung¹, Berthold Klas², Sarah Wolking¹, Sherif F. Nagueh³, Wojciech Mazur¹. ¹The Christ Hospital, Cincinnati, OH; ²TomTec Corp., Chicago, IL; ³Houston Methodist Hospital, Houston, TX

Background: There are multiple variables that contribute to the heterogeneity of reported normal left atrial (LA) strain values. Previously reported, ECG may be a misleading method in defining timing for LA strain parameters. The aim of our study was to interrogate the difference in values dependent on defining end-diastole (baseline zero) based on RR gating, PP gating, and volume gating (end-systolic marker set max LA volume and end-diastolic marker set to min LA volume). **Methods:** From a total of 131 prospectively normal healthy volunteers, 30 were excluded secondary to poor image quality. A remaining 101 volunteers (43 male, 58 female; mean age: 42 ± 14 years) had adequate tracking for analysis on Tom Tec with dedicated atrial strain software. LA reservoir, LA conduit, and LA booster strain by 2DSTE were initiated by RR gating, PP gating, and volume gating (LA max and LA min). **Results:** Of 101 cases, 88 (87%) normal volunteers, true LA min occurred prior to onset of QRS. There are significant difference in reported values between these methods across the three components of LA function (overall P < 0.001 for reservoir, conduit and booster function) (Table 1). On Bland-Altman analysis, there was no agreement for LA reservoir strain between RR gating and volume gating (mean difference, 4.6; 95% CI 3.8 to 5.4, p < 0.001), as well as PP gating and volume gating (mean difference, 5.3; 95% CI 4.6 to 5.9, p < 0.001). **Conclusion:** There was variability in left atrial strain values depending how user defined end-diastolic and end-systolic markers. Based on volume defined gating 87% normal volunteers would have decreased values reported if RR or PP gating used.

Left Atrial Function					
	Strain (%)	R-R gating	P-P gating	Volume gating	Overall P value
Reservoir	es	32.08 ± 4.96	31.41 ± 4.79	36.65 ± 6.5	< 0.001
Conduit	ec	21.30 ± 5.33	18.97 ± 5.17	21.93 ± 6.10	< 0.001
Booster pump	ea	10.79 ± 3.43	12.44 ± 2.78	14.73 ± 3.65	< 0.001

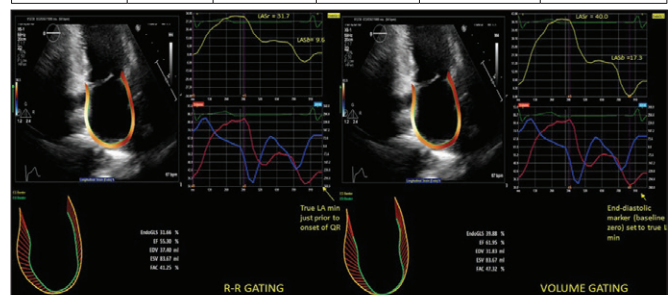


Figure A. LA 2 chamber. Top graph- Strain curve. Bottom graph- Volume curve. True minimum left atrial volume occurs slightly prior to initiation of QRS complex. LASr-Reservoir; LASc-Conduit; LASb-Booster.

P1-171

Left Atrial Function and Strain in Pediatric Hypertrophic Cardiomyopathy

Simone Jhaveri¹, Rukmini Komarlul¹, Doaa Shahbah¹, Manasa Gurumoorthi², Kenneth Zahka¹. ¹Cleveland Clinic Children's, Cleveland, OH; ²Case Western University School of Medicine, Cleveland, OH

Background: Left atrial (LA) strain and volume are early markers of diastolic dysfunction that are associated with arrhythmias and exercise intolerance in adults with hypertrophic cardiomyopathy (HCM). We sought to describe diastolic dysfunction and relation to clinical parameters in pediatric HCM patients. **Methods:** Retrospective chart review of children with HCM who were phenotype-positive (P+) and genotype-positive, phenotype-negative (P-) was performed. LA reservoir strain and contractile strain were measured using speckle tracking echocardiography. LA conduit function, reservoir function and pump function were calculated using LA volumetric analysis. Exercise stress test findings and NT-pro BNP within 1 year of the echocardiogram were reviewed. **Results:** Fifty-nine HCM patients (P+ n=37; P- n=22) and 20 healthy controls were included. Mean age of the cohort was 15.7 years (3-25; 76% male). LA reservoir and conduit function differed between P+ and P- groups. LA strain patterns were significantly lower in P+ as compared to P- patients. LA reservoir strain on 2 chamber view was also lower in P- when compared to controls (40% vs 52%, p=0.001). NT pro BNP (n=15) and arrhythmias (n=3) were not significantly associated with LA strain or function. Higher LA reservoir strain on 4 chamber view correlated with a higher aerobic exercise capacity (n= 40, r= 0.32, p=0.046). **Conclusion:** LA strain and function are significantly lower in P+ patients with HCM in comparison to P- patients. LA reservoir strain was significantly lower in P- HCM patients when compared to healthy controls alluding to subclinical diastolic dysfunction. Lower LA reservoir strain was associated with worsened aerobic exercise capacity.

Poster Session 1 (P1)

Sunday, June 23, 2019

Table 1. Descriptive statistics and comparisons by group

Factor	Genotype positive						Overall p-value
	Phenotype positive (P+, N=37)		phenotype negative (P-, N=22)		Controls (N=20)		
	n	Statistics	n	Statistics	n	Statistics	
Age at ECGIO (yrs), Median (Min, Max)	37	17(3,25) ²³	22	15(10,23) ¹	20	15(7,18) ¹	0.002^a
Sex, No. (%)	37		22		20		0.055 ^c
Male		28(76)		10(45)		14(70)	
BMI, Median (Min, Max)	37	22(15,46)	22	21(15,36)	20	19(14,41)	0.056 ^b
Genotype positive (%)	37	21(57) ²³	22	22(100) ¹³	20	0(0) ¹²	<0.001^c
Age of diagnosis, Median (Min, Max)	36	13(0,20)	22	13(5,19)	0		0.89 ^b
NT pro BNP, Median (Min, Max)	15	314(25,7384)	2	119(87,151)	0		0.45 ^b
ICD placement, No. (%)	37	7(19)	22	0(0)	0		0.039^d
Exercise stress test, No. (%)	37	26(70)	22	14(64)	0		0.77 ^d
VO2/kg, Median (Min, Max)	26	36(14,57)	14	36(27,55)	0		0.55 ^b
Aerobic capacity, Median (Min, Max)	26	10(4,16)	14	10(8,16)	0		0.46 ^b
Exercise capacity, Median (Min, Max)	26	17(4,16)	14	11(9,15)	0		0.81 ^b
LV mass index gm2, Median (Min, Max)	36	64(25,170) ²³	22	39(28,428) ¹	19	36(27,52) ¹	<0.001^c

p-values: a=ANOVA, b=Kruskal-Wallis test, c=Pearson's chi-square test, d=Fisher's Exact test.
For overall p values <0.05, superscripts indicate which pairs of groups differ significantly at a Bonferroni adjusted p value of 0.05/3=0.017.
1: Significantly different from Phenotype positive
2: Significantly different from Genotype positive, phenotype negative
3: Significantly different from Controls

Table 2. Left atrial strain and function: Descriptive statistics and comparisons by group

Factor [Median (Min, Max)]	Genotype positive						Overall p-value
	Phenotype positive (P+, N=37)		phenotype negative (P-, N=22)		Controls (N=20)		
	n	Statistics	n	Statistics	n	Statistics	
LA function							
LA reservoir function (LAVmax-LAVmin)/LAVmin*100	35	133(46,486) ²³	19	170(120,415) ¹	20	200(127,275) ¹	<0.001
LA conduit function (LAVmax-LAVpre-A)/AVmax*100	34	35(17,71) ²³	18	49(32,51) ¹	20	51(36,61) ¹	<0.001
LA contractile function (LAVpre-A-LAVmin)/LAVpre-A*100	34	31(9,51)	18	30(11,69)	20	31(26,50)	0.69
LA strain							
LA reservoir strain (4 ch)	37	27(11,58) ²³	22	38(20,54) ¹	20	44(34,56) ¹	<0.001
LA reservoir strain (2 ch)	32	28(8,58) ²³	18	40(25,65) ¹³	20	57(6,67) ¹²	<0.001
Mean LA reservoir strain (4 and 2 ch)	32	28(10,48) ²³	18	42(26,56) ¹	20	47(22,57) ¹	<0.001
LA contractile strain (4 ch)	32	8(3,23) ²³	20	17(8,17) ¹	20	11(9,61) ¹	0.007

LAVmax maximal LA volume just before the opening of the mitral valve; LAVpre-A LA volume at the onset of P wave on ECG; LAVmin minimal volume at the closure of the mitral valve; ch=chamber
For overall p values <0.05, superscripts indicate which pairs of groups differ significantly, p values based on Kruskal-Wallis test
1: Significantly different from P+
2: Significantly different from P-
3: Significantly different from Controls

Table 3. Spearman Correlation between LA strain and EST variables

Variable	LA strain parameter	N	rho	95% CI	P value
Aerobic capacity	LA reservoir strain 4ch	40	0.32	(0.01,0.63)	0.046
	LA reservoir strain 2 chamber	36	0.12	(-0.23,0.46)	0.50
	Mean LA reservoir strain (2 and 4 ch)	36	0.22	(-0.12,0.56)	0.19
	LA contractile strain	36	0.11	(-0.24,0.45)	0.53
Exercise capacity	LA reservoir strain 4ch	40	0.14	(-0.19,0.46)	0.40
	LA reservoir strain 2 ch	36	0.05	(-0.30,0.39)	0.79
	Mean LA reservoir strain (2 and 4 ch)	36	0.06	(-0.29,0.40)	0.75
	LA contractile strain	36	-0.03	(-0.38,0.32)	0.85
VO2/kg	LA reservoir strain 4ch	40	0.29	(-0.03,0.60)	0.072
	LA reservoir strain 2 ch	36	0.1	(-0.24,0.45)	0.55
	Mean LA reservoir strain (2 and 4 ch)	36	0.2	(-0.14,0.54)	0.25
	LA contractile strain	36	0.03	(-0.32,0.38)	0.87

P1-172

Exercise Stress Doppler Echocardiography in Patients with Non-Valvular Atrial Fibrillation

Muhammad Wajih Ullah, Christina L. Luong, Ratnasari Padang, Jae K. Oh, Patricia A. Pellikka, Robert B. McCully, Garvan C. Kane. Mayo Clinic, Rochester, MN

Background: Atrial fibrillation (AF) is the most common arrhythmia and is associated with advancing age and systemic hypertension, similar to heart failure with preserved ejection fraction. Noninvasive parameters of LV filling pressure (E/e') and pulmonary artery systolic pressure (PASP) by Doppler echocardiography correlate with functional capacity and outcome in sinus rhythm (SR). Their role in AF is less clear. **Methods:** Study subjects were patients who underwent exercise treadmill stress echocardiogram for regional wall motion assessment, Doppler assessment of mitral inflow (E) and early tissue relaxation (e') velocities and pulmonary pressures at rest and immediately following symptom limited exercise. Patients were excluded if they had significant valvular heart disease (defined by moderate or greater stenosis and/or regurgitation of any cardiac valve or previous valve

repair or replacement), congenital heart disease or if they refused to participate in research. Subjects were categorized as those with AF or SR. **Results:** Of a total of 14,937 patients, 310 (2%) were in AF at the time of stress echocardiography. Patients with AF were older (71±10 vs 59±13 years for SR, p<0.001); 22% were female (vs. 44% in SR). While resting BP was similar, resting heart rates were higher in AF than in SR (80±17 vs 73±13 bpm, p<0.0001). AF patients achieved lower workloads (6.4±2.4 METS vs 9.0±2.4 METS for SR, p<0.001) with lower peak double products (22,336±6,677 vs 25,148±5,438, p<0.001). Prevalence of resting (27% vs 10%, p<0.0001) and exercise-induced (37% vs 20%, p<0.0001) regional wall motion abnormalities were higher in AF versus SR. Mean E/e' was higher in AF patients at rest (12±5 vs 9±3, p<0.001) and with exercise (12±5 vs 10±4, p<0.001). E/e' was ≥15 at rest in 20% of AF patients and 6% in SR (p<0.001) and with exercise in 23% of AF patients and 8% of SR patients, p<0.001. PASP was higher in AF than in SR at rest (33±8 mmHg vs 28±6 mmHg, p<0.001) and with exercise (48±12 vs 42±11, p<0.001). E/e' correlated with exercise capacity in both AF and SR with an E/e' cutoff of 11.7 best predictive of an impaired functional capacity (< 5 METS in female and < 7 METS in male). **Conclusions:** AF patients referred for stress echocardiography are older and have a greater prevalence of cardiac disease. Abnormalities of E/e' and RVSP are more prevalent in those with AF and appear to correlate with exercise capacity as in patients with SR.

P1-173

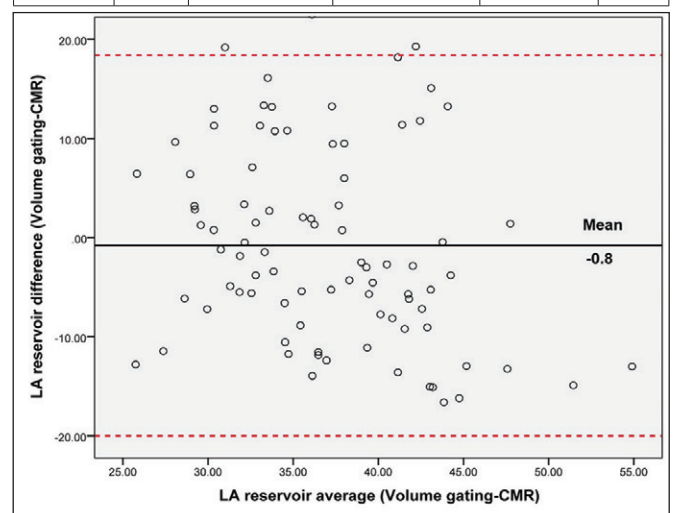
Normal Left Atrial Strain: A Difference Between Two-Dimensional Speckle Tracking Echocardiography and Cardiac Magnetic Resonance

Vien Truong¹, Cassidy Palmer¹, Berthold Klas², Brandy Sheets¹, Sarah Wolking¹, Sherif F. Nagueh³, Wojciech Mazur¹. ¹The Christ Hospital, Cincinnati, OH; ²TomTec Corp., Chicago, IL; ³Houston Methodist Hospital, Houston, TX

Background: The aim of this study was to compare left atrial (LA) two-dimensional speckle tracking (2D STE) triggered by volume gating (end-diastolic marker set to LA min and end-systolic marker set to LA max) to cardiac magnetic resonance (CMR) derived strain. **Methods:** Prospectively from the 131 healthy volunteers enrolled, 87 volunteers (38 male, 49 female; mean age: 42 ± 14 years) had adequate tracking by both modalities. Echocardiogram and CMR exams were both performed within one hour of each other on all volunteers. The reservoir (LASr), conduit (LAScd), and booster (LASct) function were calculated both by using 2D speckle tracking echocardiography (2D STE) and CMR-tissue tracing (CMR-TT). Volume gating (LA max and LA min) was used to initiate 2D STE. Volume gating (LA max and LA min) was used to initiate CMR TT. **Results:** On Bland-Altman analysis, there was agreement between LASr between two methods of volume gating STE and CMR-TT (mean difference, -0.8; 95% CI -2.9 to 1.3, p = 0.45). Conversely, there was not agreement between LAScd between volume gating (mean difference, 2.5; 95% CI 1.6 to 3.4) and CMR. LAScd had no agreement between STE and CMR (P < 0.001). **Conclusion:** Currently, there is no gold standard regarding which modality should be used in assessing left atrial strain. Our study demonstrates a good agreement between LASr using volume gating by both STE and CMR TT. However, consideration of CMR's lower temporal resolution should be considered a limitation in assessing other phases of left atrial strain (LAScd and LASct).

Normal Values of LA strain by 2D STE volume gating and CMR TT volume gating

	Strain (%)	Echo Volume Gating	CMR Volume Gating	Mean Difference	Overall P
Reservoir	es	36.54 ± 6.49	37.33 ± 8.6	-0.8 ± 9.8	0.45
Conduit	ee	21.93 ± 5.89	25.24 ± 7.30	-3.3 ± 7.9	< 0.001
Booster pump	ea	14.61 ± 3.64	12.10 ± 3.59	2.5 ± 4.1	< 0.001



Poster Session 1 (P1)

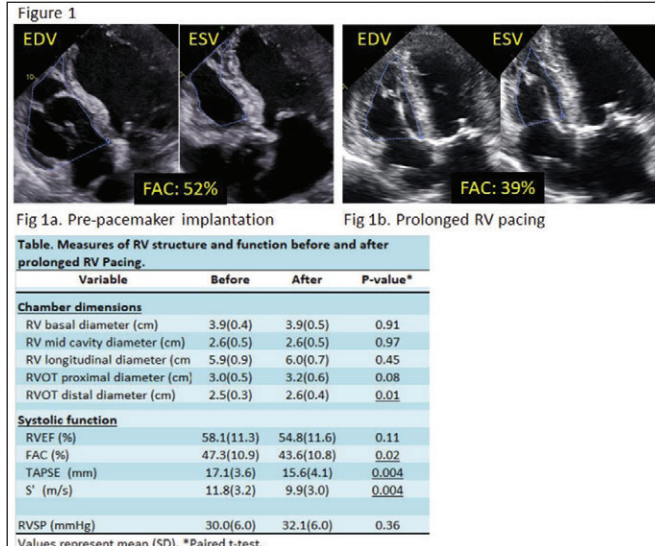
Sunday, June 23, 2019

P1-174

Effects of Prolonged Right Ventricular Pacing on Right Ventricular Structure and Function

Ahmed Zedan, Raftle Fernandez, Christos G. Mlhos, Hakop Hrachian, Ivan A. Arenas. Mount Sinai Medical Center, Miami Beach, FL

Background: Frequent right ventricular (RV) pacing is associated with higher incidence of heart failure. RV pacing can induce changes in regional and global cardiac mechanics which could lead to RV dysfunction. In this study, we aimed to investigate the effects of prolonged RV pacing on RV morphology and function. **Methods:** Patients with a permanent pacemaker and frequent RV pacing (>75%) were eligible. RV function and morphology were evaluated by 2D-echocardiography before and after pacemaker implantation. Primary endpoints were changes in RV size (Basal, mid and longitudinal dimension), right ventricular outflow tract (RVOT) dimensions and RV systolic function evaluated by RV ejection fraction (RVEF), fractional area change (FAC), tricuspid annular systolic excursion (TAPSE) and tissue Doppler-derived tricuspid lateral annular systolic velocity (S'). Paired t-tests were used to compare pre and post echo parameters. **Results:** Thirty-two patients were included. Mean age was 84 years. Nearly 70% were male. The average (SD) pacing rate was 97(5) %. Initial and follow up echographic parameters are depicted in the table. After an average 41 months, RV pacing was associated with an increase in RVOT diameters and a reduction in RV systolic function (decreased in FAC, TAPSE and S'; table). Figure shows an example of FAC before and after prolonged (60 months) of permanent (97%) RV pacing. **Conclusions:** Prolonged frequent RV pacing is associated with changes in RVOT size and a reduction in RV systolic function. The role of RV dysfunction in pacemaker mediated cardiomyopathy deserves further investigation.



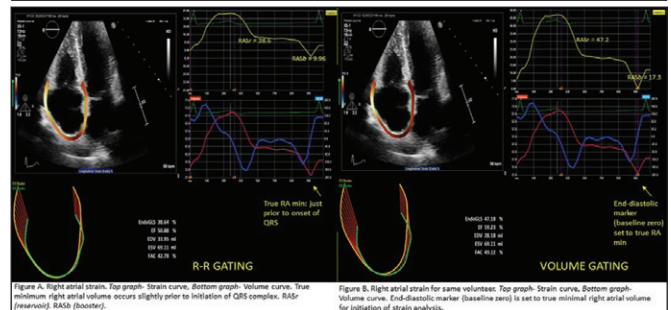
P1-175

Variations in Normal Right Atrial Strain Values Between Three Gating Methods

Cassady Palmer¹, Vien Truong¹, Berthold Klas², Sarah Wolking¹, Sherif F. Nagueh³, Wojciech Mazur¹. ¹The Christ Hospital, Cincinnati, OH; ²TomTec Corp., Chicago, IL; ³Houston Methodist Hospital, Houston, TX

Background: The aim of our study was to interrogate the difference in right atrial strain (RA) values dependent on defining end-diastole (baseline zero) based on RR gating, PP gating, and volume gating (end-systole set to RA max set and end-diastole set to RA min) by 2D speckle tracking echocardiography. **Methods:** Prospectively from the 131 healthy volunteers enrolled, 30 volunteers were excluded secondary to poor image quality. A remaining 101 volunteers (44 male, 57 female; mean age: 42 ± 14 years) had adequate tracking by echocardiography. The reservoir, conduit, and booster function were calculated by strain derived from 2D STE using three methods: RR gating, PP gating, and volume gating. **Results:** Of 101 cases, 65 (64%) normal volunteers, true RA min occurred prior to onset of QRS. The reservoir, conduit and booster function derived from 2D STE using three methods were reported (Table 1). There are significant difference in reported values between these methods across the three components of RA function (P < 0.001 for reservoir, conduit and booster function). **Conclusion:** There was variability in RA strain values depending how user defined end-diastolic and end-systolic markers. The use of RR or PP gating as the initiation of the strain calculation resulted in decreased values compared to volume gating. Volume gating should be used to assess RA strain, as this method captures initiation of strain curve at true RA min.

Right Atrial Function					
	Strain (%)	R-R gating	P-P gating	Volume gating	Overall P value
Reservoir	es	37.7 ± 6.9	35.6 ± 6.6	41.9 ± 9.3	< 0.001
Conduit	ee	26.0 ± 7.1	21.81 ± 6.9	25.4 ± 8.5	< 0.001
Booster pump	ea	11.7 ± 4.4	13.82 ± 3.9	16.6 ± 5.7	< 0.001



P1-176

Evaluation of Left Atrial Volume and Function in Patients with Coronary Slow Flow Phenomenon Using Real-time Three-dimensional Echocardiography

Y. M. Xing, Y. L. Chen, D. H. Kong, C. Z. Pan, Xianhong Shu. Zhongshan Hospital, Fudan University, Shanghai, China

Background: Coronary slow flow phenomenon (CSFP) is a well-recognized clinical entity, characterized by delayed opacification of coronary arteries in the presence of normal coronary angiogram. Although ventricular dysfunction of CSFP has been previously described, the left atrial (LA) alterations has not been fully elucidated. In this study, we aimed to evaluate LA volume and phasic functions using real-time three-dimensional echocardiography (RT3DE) in patients with CSFP. **Methods:** Forty patients with CSFP and 30 controls with normal coronary flow pattern were enrolled in the study. CSFP was diagnosed as thrombolysis in myocardial infarction frame count (TFC) >27 in at least one coronary artery. Comprehensive transthoracic echocardiographic examination and RT3DE for the assessment of LA dynamics were performed in all participants. Indexed LA maximum, minimum, and pre-atrial contraction volumes (LAVi-max, LAVi-min, LAVi-preA) were obtained for every subject, from which the following parameters were calculated as indices of LA function: (i) LA reservoir function: total EF (LATEF) = (LAVi-max - LAVi-min)/LAVi-max×100%; (ii) LA conduit function: passive EF (LAPEF) = (LAVi-max - LAVi-preA)/LAVi-max×100%; (iii) LA booster pump function: active EF (LAAEF) = (LAVi-preA-LAVi-min)/LAVi-preA×100%. **Results:** Conventional echocardiographic parameters, except for isovolumetric relaxation time and transmitral deceleration time, did not differ in the two groups. RT3DE demonstrated higher LA volumes (LAVi-max: 24.07±3.93ml/m² vs. 21.54±4.88ml/m²; LAVi-preA: 16.19±2.94 ml/m² vs. 12.72±2.88 ml/m²; LAVi-min: 9.69±1.73 ml/m² vs. 8.14±1.78 ml/m², all P<0.01) for CSFP patients compared with controls. Furthermore, LA reservoir and conduit function were decreased (LATEF: 59.68±3.72% vs. 61.89±4.24%, P=0.012; LAPEF: 32.74±5.49% vs. 40.69±5.70%, P<0.001), while the booster pump function (LAAEF: 39.89±5.22% vs. 35.45±7.18%, P=0.002) was enhanced in CSFP patients. In addition, the coronary artery mean TFC (mTFC) in CSFP groups was found to be well correlated with LA volumes (r = 0.595 for LAVi-max, r = 0.471 for LAVi-preA and r = 0.463 for LAVi-min, all P < 0.01). **Conclusions:** CSFP was associated with enlarged LA volumes, impaired LA reservoir and conduit function and enhanced contractile function. Evaluation of LA dynamics using RT3DE could facilitate recognition of subtle myocardial alterations related with CSFP.

P1-177

Right Ventricular Strain is a Novel Marker of Left Ventricular Recovery Among Patients with Premature Ventricular Contraction-Induced Cardiomyopathy Undergoing Catheter Ablation

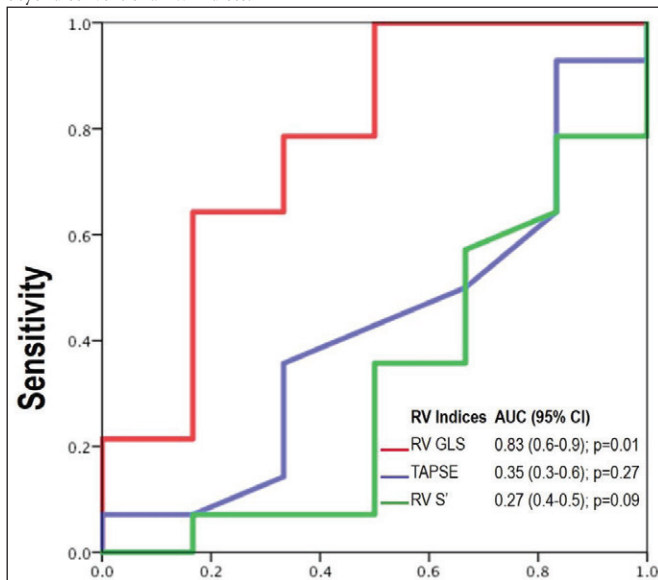
Christiane M. Abouzeid, Maria Chiara Palumbo, Cindy X. You, Brian Yum, James E. Ip, Bruce B. Lerman, Richard B. Devereux, Jonathan W. Weinsaft, Jiwon Kim. Department of Medicine, Weill Cornell Medical College, New York, NY

Background: Premature ventricular contraction (PVC)-induced cardiomyopathy is known to affect left ventricular (LV) systolic function. The prevalence and impact of right ventricular (RV) contractile function on LV functional recovery after catheter ablation is unknown. **Methods:** The population comprised patients with PVC-induced cardiomyopathy who underwent transthoracic echocardiogram (echo) pre- and post-catheter ablation. RV function was quantified on echo using tricuspid annular plane systolic excursion (TAPSE), tricuspid annular systolic velocity (RV S') and RV global longitudinal strain (GLS). RV GLS was quantified on RV focused or 4-chamber view by speckle-tracking echocardiography (TomTEC [Munich, Germany]). **Results:** 20 patients

Poster Session 1 (P1)

Sunday, June 23, 2019

(age: 67±15 yo; M: 50%) with PVC-induced cardiomyopathy were studied. The majority had PVCs originating from the RV outflow tract and LV papillary muscle (35 and 20% respectively). At 2.5±0.8 month follow up, PVC burden substantially decreased (20.1±12.17 vs. 4.93±4.5%; p<0.001) paralleling LV functional improvement after ablation (35±12 vs. 46±13%; p=0.002). Nearly half (45%) of patients demonstrated LV functional recovery (defined as LVEF>50%). Regarding RV parameters, the majority (75%) had RV impairment pre-procedure (RV GLS <20%) with a nearly 5-fold improvement in RV GLS (13.8±3.7 vs. 19.6±4.4%; p<0.001) following catheter ablation. Patients who had LV functional recovery had more robust LV contractile function pre-procedure (LVEF: 42.5±11 vs. 30.0±10%; p=0.02). Regarding RV predictors, whereas impaired RV GLS was strongly associated with persistent LV dysfunction (RV GLS: 12.9±5.4 vs. 18.9±4.5%; p=0.015), conventional RV indices were poor predictors for LV functional recovery (TAPSE: 1.8±0.6 vs. 2.0±0.6 cm; p=0.3 and RV S': 10.5±2.6 vs. 12.4±3.3 cm/s; p=0.2). **Figure 1** illustrates ROC curves for conventional and strain based RV parameters in relation to LV functional response. As shown, RV GLS yields the highest overall diagnostic performance for stratifying LV functional recovery after catheter ablation (AUC: 0.83; p=0.01). **Conclusion:** RV dysfunction quantified via GLS is highly prevalent among patients with PVC-induced cardiomyopathy; RV GLS incrementally improves stratification of LV functional recovery beyond conventional RV indices.



P1-178

The Association of Echocardiographic Measurements of Left Atrial Function by Ischemic Stroke Subtype

Jonathan M. Wong, Stacy Tsai, David Tong, Charlene Chen, Christine Wong, Billy Gao, Michael Ke, Jessica Choe, Ann Bedenk, Julia Fernandes, Susila Patel, Andrew Rosenblatt, Richard E. Shaw, Nobl Barazangi. CPMC, San Francisco, CA

Background: Screening for atrial fibrillation (AF) is critical in the work-up of ischemic stroke. Left atrial (LA) volume enlargement and dysfunction predict both AF and stroke. This study sought to determine which additional measurements of LA function as determined by transthoracic echocardiography (TTE) best discriminated cardioembolic stroke from other stroke etiologies. **Methods:** We retrospectively identified ischemic stroke patients who were consecutively admitted at our institution and underwent TTE within 30 days. Each stroke was "subtyped" by a vascular neurologist according to TOAST criteria. We determined left atrial function by measuring the following TTE volumetric parameters, blinded to stroke etiology: LA volume index (LAVI), LA ejection fraction (LAEF), LA function index (LAFI), LA reservoir function, LA conduit function, LA pump function. Clinical and echocardiographic parameters between stroke subtype were compared using Chi square, Student's t test, and ANOVA and ROC analysis was performed. **Results:** We identified 164 patients who were admitted with ischemic stroke and had a TTE within 30 days of the event, 78% of whom had the TTE after stroke onset. Of the 164 ischemic strokes, 90 were classified as cardioembolic (55%), 25 large artery atherosclerosis (15%), 10 lacunar (6%), and 39 cryptogenic (24%). The mean age was 73 years, 49% male, 77% hypertension, 33% diabetes, 35% smoking history, 34% AF, and 31% received TPA. Compared to patients with other stroke etiologies, patients with cardioembolic stroke had significantly increased LA diameter (mean 4.4 cm, p < 0.001), increased LAVI (mean 47.4 cm³/m², p = 0.002), decreased LAFI (mean 0.16, p < 0.001), decreased LAEF (mean 32.3%, p < 0.001), as well as decreased LA reservoir (p < 0.001), and LA pump function (p = 0.002). Of the different measurements of LA function, LAEF, LA reservoir function, and LAFI best discriminated cardioembolic stroke from other stroke etiology (TABLE). **Conclusion:** Patients admitted with cardioembolic stroke possessed different TTE measures of LA function compared

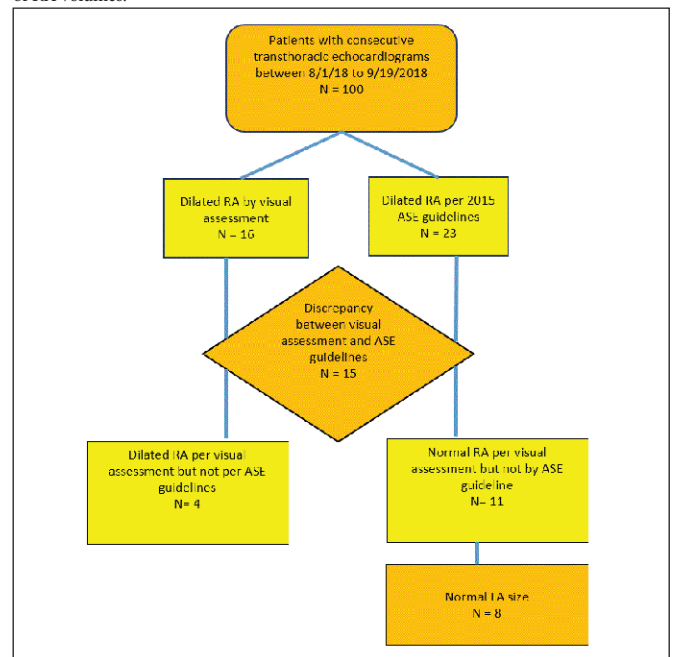
to patients with stroke of other stroke etiologies. More research is needed to determine whether TTE measurements of LA function predict AF in the cryptogenic stroke population, which would potentially help further reduce the burden of recurrent stroke.

P1-179

Can You Trust Your Eyes? The Visual Discrepancy of Right Atrial Assessment

Saurabh Joshi¹, Steve Walling², Kathir Balakumaran¹, Supriya Tigadi¹, Anita Kelsey². ¹University of Connecticut, Farmington, CT; ²Saint Francis Hospital and Medical Center, Hartford, CT

Background: The 2015 American Society of Echocardiography (ASE) chamber quantification guidelines recommends volumetric assessment of right atrial (RA) size using single frame area-length or disk summation technique in a dedicated apical four chamber view. We sought to determine the current day practice of RA measurement by transthoracic echocardiogram (echo) and its correlation with the ASE guidelines. **Methods:** We retrospectively reviewed the first two, daily echoes from 8/1/18 - 9/19/18 performed at an academic city hospital, read by both private and academic cardiologists. We noted RA size, assessment method, and left atrial (LA) size from the official report and retrospectively assessed RA size per ASE recommendation. RA size quantitation methods were assessed for discrepancies and stratified by gender and LA size. **Results:** A total of 100 echoes were reviewed. Patients' mean age was 65 years (50% female). Current day method for RA size assessment was visual estimation in all echoes. RA was interpreted as dilated in 16% of patients by visual assessment. Applying 2015 ASE recommended quantitative method, 23% were dilated. Discrepancy occurred between the two methods for RA size in 15%, which translated into one case of discrepant RA size for every seven echoes interpreted. The majority of discrepancies resulted in an underestimate of RA size by visual assessment compared to ASE guideline (73%). Interestingly, LA size was normal in 73% of these discrepancies, suggesting that normal LA size biased the accurate interpretation of RA size. There was no significant gender difference in the number of discrepant RA measures (14% vs 16% for male and female respectively). **Conclusion:** Our study revealed lack of adoption of the 2015 ASE recommended method for RA size assessment with current day practice of visual assessment. When ASE recommended method of quantitative assessment of RA size is not implemented, visual RA size assessment is likely influenced by adjacent LA size. Accurate RA size assessment is a clinically important reflection of RA pathology or right-sided volume or pressure overload. Lack of adoption of ASE recommended RA size assessment method may reflect increasing time pressures on echo labs. Familiarity with the guidelines should facilitate rapid adoption of guideline directed measurement of RA volumes.



P1-180

Diastolic Dysfunction and Arrhythmia Recurrence After Atrial Fibrillation Ablation

Edward Chu, Alex Choy, Asaf Rabinovitz, William Whang, Vivek Reddy, Martin Goldman. Ichan School of Medicine at Mount Sinai, New York, NY

Background: Chronic cardiopulmonary conditions associated with the development of diastolic dysfunction, such as hypertension, obesity, and obstructive sleep apnea, are also

Poster Session 1 (P1)

Sunday, June 23, 2019

known to contribute to atrial fibrillation (AF) pathogenesis. Successful AF ablation removes the electrical triggers of AF, but does not address the anatomical and mechanical triggers due to underlying diastolic disease. We hypothesize that the presence of residual diastolic dysfunction after AF ablation is associated with the recurrence of atrial arrhythmia. **Methods:** A retrospective review was performed in patients with nonvalvular AF who underwent successful pulmonary vein isolation (PVI) during AF ablation at Mount Sinai Hospital in 2018, and had a transthoracic echocardiogram (TTE) within 90 days after the procedure to assess for the severity of diastolic dysfunction. Diastolic dysfunction and presence of increased left atrial (LA) pressure was evaluated using recent 2016 guidelines from the American Society of Echocardiography. The primary endpoint was the development of atrial arrhythmia, defined as atrial fibrillation, atrial flutter or atrial tachycardia, within the first 6 months after AF ablation. Patients with prior mitral valve intervention, significant mitral valve calcification, and severe valvular disease were excluded from analysis. **Results:** Of the 20 patients (age 62.2 +/- 4.0 years, 65% male, 40% paroxysmal AF) who underwent PVI, 5 (20%) developed arrhythmia recurrence after the procedure. Increased LA size and increased LA pressure (grade II or III diastolic dysfunction) were seen in 5/5 patients who developed recurrence and in 5/15 patients who did not develop recurrence (100% vs 33%, p=0.0325). Individual diastolic parameters, including E/A, E/e', tricuspid regurgitation velocity, and LA volume index were not significantly different between the two groups. Left ventricular systolic function was also not significantly different between those who developed recurrence and those who did not (63% vs 58%, p=0.32). **Conclusion:** In patients who undergo successful AF ablation, those who demonstrate advanced diastolic dysfunction characterized by increased LA size and increased LA pressure are significantly more likely to develop arrhythmia recurrence. This subset of patients would benefit from aggressive management of diastolic dysfunction after successful AF ablation to ensure maintenance of sinus rhythm.

P1-181

Interatrial Appendage Contraction Delay: A Novel Index for Reduced Left Ventricular Ejection Fraction

Jingjing Crystal Huang¹, Colter Wichern², Weimin Jiang¹, Thomas W.R. Smith², Dali Fan². ¹NanJing University of Chinese Medicine, Nanjing, Jiangsu, China; ²University of California, Davis, Department of Cardiology, Sacramento, CA

Background: Normal cardiac depolarization occurs from the right atrium to the left atrium. The difference in timing between the associated contractions of the right and left atrial appendages can be referred to as the interatrial appendage contraction delay (IACD). It can be measured by transesophageal echocardiography (TEE) with pulsed-wave Doppler (PW). In this study, we compared the IACD between patients with a preserved left ventricular (LV) ejection fraction (pEF) and reduced LV ejection fraction (rEF). **Methods:** 101 patients were divided into two groups based on LV ejection fraction of >50% (pEF; n=72) or ≤50% (rEF; n=29). The PW of the emptying flow waves of both the right and left atrial appendages were recorded along with the electrocardiogram triggers. The time intervals from the beginning of the right and left atrial appendage emptying flow waves to the beginning of the correlated QRS complexes (T_{RAA} and T_{LAA}, respectively) were measured (Figure 1). The IACD, defined as T_{RAA}-T_{LAA}, was then compared between patients with pEF and rEF. **Results:** When comparing patients with pEF and rEF (62.90±6.30 vs 41.72±8.69%; p<0.01), IACD was significantly longer in patients with rEF (41.45±15.02 vs 50.55±17.82 msec; p=0.011). Several other traditional predictors of low LV ejection fraction, such as the left atrial volume area-length method (33.25±14.46 vs 41.62±18.07 mL/m²; p=0.027), interventricular septum thickness at end-diastole (1.14±0.27 vs 1.03±0.18 cm; p=0.048), LV posterior wall thickness at end-diastole (1.12±0.27 vs 1.0±0.17 cm; p=0.04), LV internal diameter at end-diastole (4.54±0.77 vs 5.28±0.72 cm; p<0.01), and LV internal diameter at end-systole (2.93±0.67 vs 3.99±0.79 cm; p<0.01) were also significantly different. The remaining parameters were not significantly different between the two groups (Table 1). **Conclusion:** Our study reveals that IACD is prolonged in patients with rEF. This index is quick and easy to measure by way of TEE and may be used in later studies to help further characterize patients with rEF.

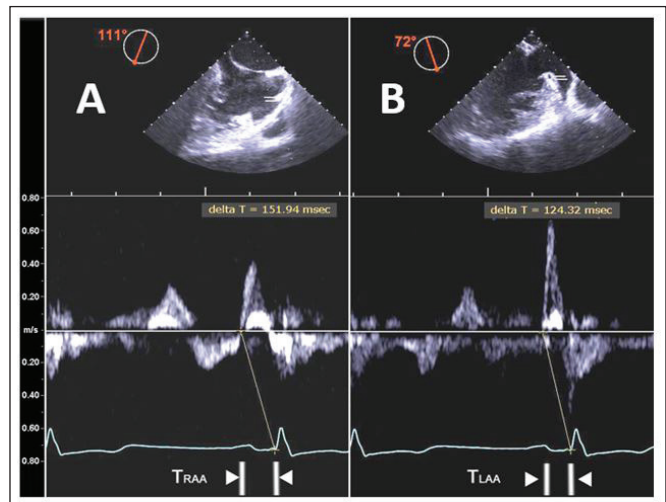


Figure 1. Pulsed-wave Doppler (PW) recordings of the emptying flow waves of the right atrial appendage (A) and left atrial appendage (B). The PW recordings are shown with their respective electrocardiogram triggers. The time interval from the beginning of the emptying flow wave of the right atrial appendage to the beginning of the associated QRS complex was measured (T_{RAA}). The time interval from the beginning of the emptying flow wave of the left atrial appendage to the beginning of the associated QRS complex was also measured (T_{LAA}). Interatrial appendage contraction delay (IACD) was defined as T_{RAA}-T_{LAA}. In this example of a patient with a preserved left ventricular ejection fraction, the IACD is 27.62 milliseconds.

Table 1. Comparing echocardiographic characteristics between patients with preserved left ventricular ejection fraction and patients with reduced left ventricular ejection fraction

Parameter	pEF >50% (n=72)	rEF <50% (n=29)	p-value
LVEF (%)	62.90 ± 6.30	41.72 ± 8.69	<0.01*
IACD (msec)	41.45 ± 15.02	50.55 ± 17.82	0.011*
LA AP 2D (cm)	3.77 ± 0.75	4.06 ± 0.83	0.081
LA Vol A/L (mL/m ²)	33.25 ± 14.46	41.62 ± 18.07	0.027*
LA major A2C (cm)	6.52 ± 7.83	5.80 ± 0.74	0.649
LA major A4C (cm)	6.38 ± 6.22	5.82 ± 1.06	0.648
IVSd (cm)	1.14 ± 0.27	1.03 ± 0.18	0.048*
LVPWd (cm)	1.12 ± 0.27	1.0 ± 0.17	0.040*
LVIDd (cm)	4.54 ± 0.77	5.28 ± 0.72	<0.01*
LVIDs (cm)	2.93 ± 0.67	3.99 ± 0.79	<0.01*
MV PW A Peak (m/s)	0.88 ± 0.42	0.91 ± 0.41	0.781
MV PW E Peak (m/s)	0.95 ± 0.46	1.03 ± 0.34	0.452
E/A Ratio	1.70 ± 0.59	1.36 ± 0.74	0.311
DT (msec)	228.29 ± 85.57	250.62 ± 116.75	0.309
RA 4C ML 2D (cm)	3.99 ± 1.44	3.72 ± 0.73	0.380
RV 4C D2 (cm)	2.74 ± 0.66	2.8 ± 0.71	0.678

*Statistical significance was defined as p<0.05. Preserved left ventricular ejection fraction (pEF); reduced left ventricular ejection fraction (rEF); left ventricular ejection fraction (LVEF); interatrial appendage contraction delay (IACD); left atrium anterior posterior diameter (LA AP 2D); left atrial volume area length method (LA Vol A/L); left atrium area 2-chamber view (LA major A2C); left atrium area 4-chamber view (LA major A4C); interventricular septum thickness at end-diastole (IVSd); left ventricular posterior wall thickness at end-diastole (LVPWd); left ventricular internal diameter at end diastole (LVIDd); left ventricular internal diameter at end-systole (LVIDs); mitral valve pulsed-wave Doppler A-wave peak amplitude (MV PW A Peak); mitral valve pulsed-wave Doppler E-wave peak amplitude (MV PW E Peak); E-wave to A-wave ratio (E/A Ratio); deceleration time (DT); right atrium 4-chamber medial lateral diameter (RA 4C ML 2D); right ventricle 4-chamber medial-lateral diameter (RV 4C D2)

P1-182

Low Intensity Focused Ultrasound Combined with H2O2/PPF-Loaded Acoustic Phase-Change Nanoparticles for Porcine Coronary Artery Embolism Elimination

Nan Jiang, Bo Hu, Sheng Cao, Qing Deng, Qing Zhou, Ruiqiang Guo. Renmin Hospital of Wuhan University, Wuhan, China

Background: Dissolving coronary thrombus effectively and restoring microcirculation is the key to treat acute myocardial infarction (AMI). Based on stable cavitation and 2H2O2=(catalase)2H2O+O2↑ chemical equation, a novel phase-change and oxygen-release contrast agents (hydrogen peroxide solution and perfluoropentane-loaded nanoparticles, H2O2/PPF-loaded NPs) with noninvasive and effective thrombolytic function were used in the treatment for porcine model with acute coronary artery embolism, which **Methods:** H2O2/PPF-loaded NPs were prepared by rotary evaporation and sonication process. After the interventional radiography channel established, pieces of autologous thrombus were injected into distal end of the second diagonal branch of coronary artery by 8F catheter via femoral artery puncture. 12 miniature pigs were randomly divided into four groups. Low intensity focused ultrasound (LIFU) was used to irradiate infarction areas. No other treatments were used in group A. SonoVue microbubbles, H2O2/PPF NPs and t-PA were injected into models through peripheral veins in group B, C and D, accordingly. Coronary artery obstruction and recanalization were observed by DSA before and after treatment. Routine echocardiographic parameters and myocardial contrast echocardiography (MCE) were applied to analyze myocardial motion and perfusion before and after treatments. TTC staining were used to evaluate the infarction range. **Results:**

Poster Session 1 (P1)

Sunday, June 23, 2019

The size of nanoparticles was (437.4 ± 28.6) nm. Cardiac chamber sizes in C and D were both smaller than other groups. Compared with group A and B, ejection fraction was significantly improved in C and D ($P < 0.05$). MCE showed myocardial perfusion in C and D were significant increased. TTC results showed the relative infarcted range of the four groups were $(25.8 \pm 1.8\%)$, $(16.2 \pm 1.9\%)$, $(3.4 \pm 0.7\%)$, $(3.2 \pm 1.8\%)$. It indicated that the infarcted range of C and D were significant decreased ($P < 0.05$), while A and B were not significantly changed. **Conclusions:** PFP phase-change and oxygen-release nanoparticles can effectively dissolve coronary thrombus by stable cavitation under LIFU irradiation, unclog the coronary microcirculation and restore myocardial reperfusion. Also, released O₂ molecules improved local hypoxia environment, which had satisfied therapeutic effect on coronary thrombus elimination.

P1-183

Automated Diagnosis of Ischemic Cardiomyopathy Using Feature-Categorized Vision Method: An Echocardiography Study with Computed Neural Network

Bo Hu¹, Jinsheng Xiao², Hong Tian², Nan Jiang¹, Qing Zhou¹. ¹Renmin Hospital of Wuhan University, Wuhan, China; ²Electronic Information School of Wuhan University, Wuhan, China

Background: Ischemic cardiomyopathy (ICM) leads to regional wall motion abnormality (RWMA) and heart failure (HF), which closely associate with the prognosis of patients with ICM. However, the diagnostic biases in RWMA and HF are almost inevitable in clinical practice, due to image acquisition and reading of echocardiography with different levels of skills and experiences. Thus, it would be helpful for clinical management of ICM using method of automated diagnosis with the improvement of reliability and reproducibility. Thus, we sought to investigate the diagnostic value of feature-categorized vision method from computed neural network, for the establishment of automated diagnosis of ICM. **Methods:** Standard views of left ventricular (LV) long- and short-axes were collected from 101 ICM patients with RWMA and HF at routine echocardiography. RWMA was defined as the wall motion score index (WMSI) ≥ 2 and HF was defined as LV ejection fraction (LVEF) $< 50\%$. WMSI and LVEF were labeled for the patients by the agreement of two experienced cardiologists. In computed neural network, the features of standard views in Dicom data were extracted for categorization using visual geometry group net with multilayer convolution, and for structural segmentation using U-net algorithms. The results of WMSI and LVEF were automatically generated and compared with the labeled data. **Results:** The successful rate of feature extractions and structural segmentations was 98.8% and 97.9%, respectively over all the standard views of ICM patients. The postprocessed 4707 and 1995 images were accepted for WMSI reading and LVEF analysis, respectively. Inter-class correlation coefficient analysis showed that the results of feature-categorized vision method were consistent with the labeled data, for WMSI was 0.92 (95%CI: 0.89-0.96) and LVEF was 0.85 (95%CI: 0.78-0.91). **Conclusions:** Validated using labeled echocardiography data, the feature-categorized vision method of computed neural network has provided accurate diagnosis in regional wall motion abnormality and heart failure for the patients with ischemic cardiomyopathy.

P1-184

The Nucleophilic Gene Delivery System Enhanced the Angiotensin II Gene Transfection Can Reverse Left Ventricular Remodeling in Myocardial Infarction Canines

Sheng Cao, Qing Zhou, Tuantuan Tan, Bo Hu, Nan Jiang, Yijia Wang. Renmin Hospital of Wuhan University, Wuhan, China

Background: This study was conducted to investigate whether the combination of nucleophilic gene delivery system and ultrasound targeted microbubble destruction (UTMD) could improve the transfection efficiency and reverse left ventricular remodeling in myocardial infarction (MI) canines. The nucleophilic gene delivery system was constructed with nuclear localization signal peptide, angiotensin II (AngII) gene and microbubbles to improve the UTMD-mediated gene entering nucleus for transfection and angiogenesis. **Methods:** Thirty dogs were divided into 3 groups (n=10 in each group): control group (MI dogs), non-nucleophilic group (MI dogs with UTMD and non-nucleophilic gene delivery system mediating AngII gene transfection), and nucleophilic group (MI dogs with UTMD and nucleophilic gene delivery system mediating AngII gene transfection). One month later, the size and systolic function of left ventricular were measured by echocardiography. The myocardial contrast echocardiography was performed. CD31 was applied for quantifying capillary density. The AngII, sarcoplasmic reticulum Ca²⁺-ATPase (SERCA2a) and phospholamban (PLB) protein were detected by Western blot. **Results:** The left ventricular end-diastolic dimension and left ventricular end-systolic dimension decreased, and the left ventricular ejection fraction increased in nucleophilic group than these in non-nucleophilic group or control group ($P < 0.05$). The intensity ratio of infarcted region/normal region and the increased rate of intensity by myocardial contrast echocardiography were both higher in nucleophilic group than these in non-nucleophilic group or control group ($P < 0.05$). The immunohistochemistry showed the higher capillary density in nucleophilic group than non-nucleophilic group ($P < 0.05$). The protein relative quantity of AngII and SERCA2a were significantly higher in nucleophilic group, but the PLB was inverse. **Conclusions:** Combination the nucleophilic gene delivery system with UTMD-mediated AngII gene transfection can promote angiogenesis after MI and reverse

left ventricular remodeling. The systolic function of left ventricular may be related to the expression of AngII, SERCA2a and PLB.

P1-185

Early Assessment of Left Ventricular Function by Layer-Specific Strain and Its Relationship to Pulsatile Arterial Load in Patients with Coronary Slow Flow

J. Shi, Y.M. Xing, J.Y. Qian, H.B. Yang, Y. Yan, Q. Li, L.M. Luo, D.H. Kong, C.Z. Pan, Xianhong Shu. Zhongshan Hospital, Fudan University, Shanghai, China

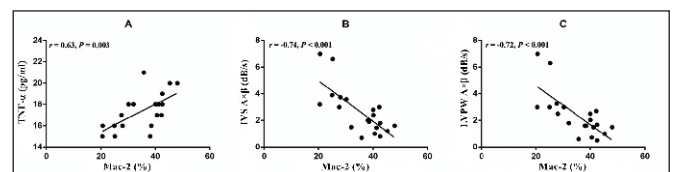
Background: Previous studies reported controversial Left ventricular (LV) function impairment and pathophysiology in patients with coronary slow flow (CSF). Greater arterial load has been shown to increase aortic impedance and endothelial shear stress, potentially affecting coronary anatomy and function. We investigated LV systolic function by a new layer-specific strain technology and assessed the association between pulsatile arterial load and contractility. **Methods and Results:** A total of 70 patients with CSF and 50 controls with normal coronary angiography were included in the study. Layer-specific longitudinal and circumferential strains were assessed from endocardium, mid-myocardium and epicardium (GLS-endo, GLS-mid, GLS-epi and GCS-endo, GCS-mid, GCS-epi) by two-dimensional speckle tracking imaging (2D-STI). Pulsatile arterial load was estimated by indexed arterial compliance (ACI). Layer-specific GLS showed a decreasing gradient from the endocardium to the epicardium in both controls and CSF group. GLS-endo and GLS-mid in CSF group were significantly lower than the control group (all $P < 0.05$). Layer-specific longitudinal strain showed a good correlation with the number of affected coronary arteries (all $P < 0.05$) and the mean thrombolysis in myocardial infarction frame count (TFC) (all $P < 0.05$). ACI was lower in CSF patients ($P = 0.005$) and ACI was correlated negatively with layer-specific GLS (all $P < 0.05$). **Conclusion:** Layer-specific evaluation of the LV provides an understanding of the layer-specific properties of the LV wall and the possible process of the LV impairment in patients with CSF. Greater pulsatile arterial load, as manifested by a lower ACI, is coupled with worse LV longitudinal function in CSF patients.

P1-186

Evaluation of the Effects of Macrophage Infiltration in the Coronary Plaque on the Downstream Myocardial Perfusion in Mice with Adenosine Stress Contrast Echocardiography

Lingying Huang, Youbin Deng, Yibin Wang, Yani Liu, Xinyu Wang. Huazhong University of Science and Technology, Wuhan, China

Background: Previous studies indicated that regional myocardial perfusion mismatched with the coronary artery stenosis severity and inflammation plays important role in both vulnerable plaque and microcirculation perfusion abnormality. This study was designed to explore the effects of macrophage infiltration in the coronary plaque on the downstream myocardial perfusion in Mice. **Methods:** The experimental group consisted of ApoE knockout mice models of the coronary plaque established by feeding with cholesterol-rich diets, and the control group consisted of sex- and age-matched C57BL/6 mice with the same genetic background as ApoE mice. Adenosine stress myocardial contrast echocardiography was performed on all experimental animals. Concentrations of serum interleukin-6 (IL-6) and tumor necrosis factor- α (TNF- α) were determined using mouse enzyme-linked immunosorbent assay kits according to the manufacturer's instructions. The degree of macrophage infiltration in the coronary plaque was evaluated by pathological immunohistochemistry staining. **Results:** The experimental group had a lower left ventricular ejection fraction, and higher serum levels of triglycerides, total cholesterol, high-density lipoprotein, low density lipoprotein, IL-6, and TNF- α than the control group ($P < 0.05$). The values of post-impulse maximal steady-state pixel intensity level (A), rate of contrast replenishment (β), and $A \times \beta$ of the left ventricular myocardium in septal and posterior walls in the experimental group were significantly lower than those in the control group ($P < 0.05$). In the experimental group, the value of the macrophage infiltration found in the plaque of the left main coronary artery correlated positively to the level of serum TNF- α ($r = 0.63$, $P = 0.003$). Although the $A \times \beta$ value of the left ventricular myocardium did not correlated with the coronary artery stenosis severity, it correlated well with the value of the macrophage infiltration in the plaque and the level of serum TNF- α ($r = -0.74$, $P < 0.001$; $r = -0.72$, $P < 0.001$; respectively).



Conclusion: Myocardial perfusion in ApoE knockout mice models of the coronary atherosclerosis was related with degree of macrophage infiltration in the coronary plaque, but not with the degree of coronary artery stenosis severity.

Poster Session 1 (P1)

Sunday, June 23, 2019

P1-187

The Blood Flow Characteristics of Coronary Flow Reserve by Transthoracic Doppler Echocardiography in Patients with Coronary Microvascular Disease

Chenghu Guo, Lijuan Lv, Peixin Lin, Yan Liu, Mingjun Xu, Jichen Pan, Mei Zhang. *The Key Laboratory of Cardiovascular Remodeling and Function Research, Chinese Ministry of Education, Chinese Ministry of Health and Chinese Academy of Medical Sciences, Qilu Hospital of Shandong University, Shandong, Jinan, China*

Background: Multiple cardiovascular risk factors resulted in obstructive coronary artery disease (CAD), but also coronary microvascular disease (CMVD). Exploration of coronary flow characteristics can help deepen the understanding of CMVD. **Methods:** A total of 38 patients with significant coronary ischemic symptom but without CAD (<50% coronary stenosis, measured by coronary artery angiography or coronary computed tomography angiography) performed adenosine stress coronary flow reserve (CFR) by transthoracic Doppler echocardiography. The CFR was the average flow velocity of left anterior descending coronary in diastole during hyperemia (Vh) divided by during rest (Vr). These patients were divided three groups based on the CFR: L group, CFR≤2; M group, 2<CFR≤3; H group, CFR>3. Clinical features, Vh and Vr were compared for three groups. Bivariate correlation analyses were performed to analysis the correlation between Vh, Vr and CFR. **Results:** All patients were performed CFR successfully. The CFR of H group, M group and L group was 4.04±0.98, 2.54±0.22 and 1.74±0.26, respectively (p<0.001). There were significant differences among three groups for age (p=0.037), Vr (p=0.002) and Vh (p<0.001). The Vr of L group was significant higher than H group (p=0.001) and M group (p=0.003), inversely, the Vh of L group lower than H group (p=0.001) and M group (p<0.001). The CFR was inversely correlated with Vr (r=-0.529, p=0.001) and positively with Vh (r=0.55, p<0.001) by bivariate correlation analysis. **Conclusion:** The CFR may be impaired with increased age in patients with CMVD. The early consume of the capacity of flow reserve on rest and the impaired response for stress cause lower CFR and damaged myocardial microcirculation for CMVD patients.

Table 1 Demographic parameters and Doppler coronary flow velocity of the study population

	H group (n=14)	M group (n=17)	L group (n=7)	P value
Demographic parameters				
Age(years)	49±10	56±8	57±7	0.037
Female, n (%)	7(50)	7(41)	4(57)	0.753
Coronary flow velocity				
Vr(m/s)	0.16±0.04	0.17±0.05	0.24±0.05	0.002
Vh(m/s)	0.61±0.15	0.43±0.11	0.41±0.11	<0.001
CFR	4.04±0.98	2.54±0.22	1.74±0.26	<0.001

Vr, average coronary flow velocity in diastole during rest; Vh: average coronary flow velocity in diastole during hyperemia; CFR, coronary flow reserve. Data are presented as mean ± SD or number (percentage).

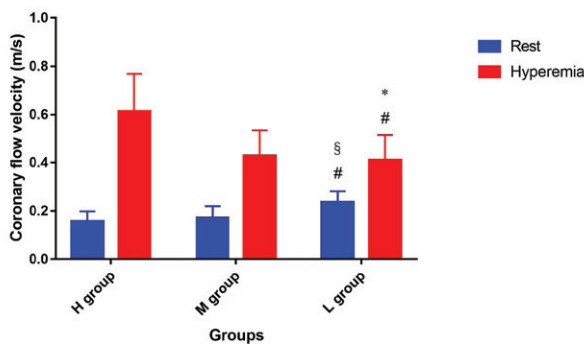


Figure 1 Coronary flow velocity on rest and hyperemia phase among three groups. #, p=0.001 vs H group; §, p=0.003 vs M group; *, p<0.001 vs M group

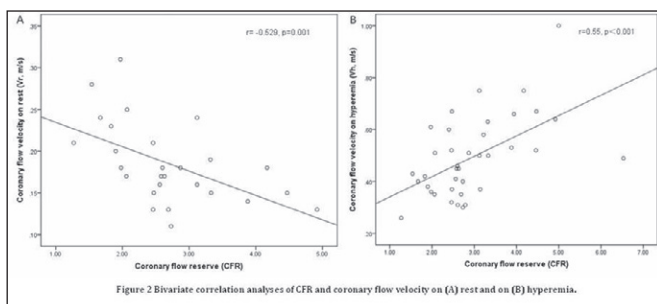


Figure 2 Bivariate correlation analyses of CFR and coronary flow velocity on (A) rest and on (B) hyperemia.

P1-188

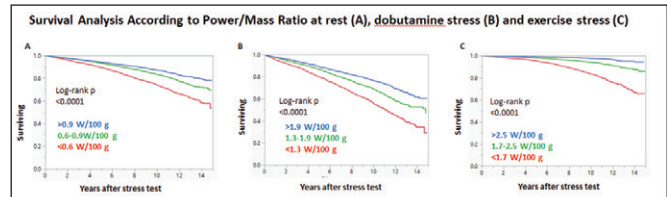
Prognostic Value of Cardiac Power Output in Patients with Normal Left Ventricular Ejection Fraction Referred for Stress Echocardiography

Vidhu Anand, Garvan C. Kane, Sorin V. Pislaru, Rosalyn O. Adigun, Robert B. McCully, Patricia A. Pellikka, Cristina Pislaru. *Mayo Clinic, Rochester, Rochester, MN*

Background: Cardiac power output is a measure of myocardial performance that incorporates both pressure and flow output, however it depends on cardiac mass generating that output. We sought to evaluate the prognostic significance of cardiac power output at peak stress normalized to left ventricular (LV) mass in patients with normal LV ejection fraction (EF >50%). **Methods and Results:** 41,915 patients (age 62 ± 13 years, 46% females) with EF ≥50% and no significant valve disease or right ventricular (RV) dysfunction, undergoing dobutamine (DSE) or exercise (ExSE) stress echocardiography were included (Table). Power/mass at rest and peak stress were calculated as previously described (0.222 x cardiac output x mean blood pressure / LV mass) and expressed in units of Watts/100g myocardium. All-cause mortality was the primary endpoint. Patients were divided into quartiles based on power/mass at rest and peak stress. Patients with higher power/mass were younger, had higher blood pressure and heart rate, lower LV mass, and lower prevalence of prior myocardial infarction, percutaneous or surgical coronary intervention. (Table). During mean follow-up of 4.6±4.2 years, 3677 (8.8%) patients died. Lower power/mass at rest and peak stress were associated with increased mortality (Figure A-C). After adjusting for age, ischemia/infarction on stress test results and diastolic function grade, peak stress power/mass was an independent predictor of mortality and had incremental value (p<0.05) in multivariate models. **Conclusion:** Cardiac power output normalized by LV mass assessed at peak stress is an independent predictor of survival in patients with normal resting EF and no significant valve disease or RV dysfunction.

Table: Baseline characteristics

	All patients (n=41915)	Quartile 1: <0.6 W/100g (n=9929)	Quartile 2-3: 0.6-0.9 W/100g (n=20587)	Quartile 4: >0.9 W/100g (n=11399)	p-value
Age (years)	62±13	65±12	62±13	59±14	<0.0001
Females, n(%)	19440 (46)	2633 (27)	9076 (44)	7731 (68)	<0.0001
Prior myocardial infarction, n(%)	1379 (8)	1379 (14)	1427 (7)	380 (3)	<0.0001
Prior CABG, n(%)	2379 (6)	1114 (11)	1046 (5)	219 (2)	<0.0001
Prior PCI, n(%)	4448 (11)	1807 (18)	2071 (10)	570 (5)	<0.0001
Hypertension, n(%)	24208 (58)	6967 (70)	11664 (57)	5577 (49)	<0.0001
Diabetes mellitus, n(%)	7964 (19)	2559 (26)	3740 (18)	1665 (15)	<0.0001
Left ventricular mass (g)	176±52	217±58	174±43	141±35	<0.0001
Rest heart rate (bpm)	72±13	61±9	70±10	83±12	<0.0001
Rest systolic pressure (mmHg)	132±21	127±20	132±20	137±21	<0.0001
Rest LV stroke volume (mL)	86±15	89±16	87±15	83±14	<0.0001
Peak power/mass (W/100 g)	0.8±0.2	0.5±0.07	0.7±0.08	1.1±0.16	<0.0001



Poster Session 1 (P1)

Sunday, June 23, 2019

P1-189

World-wide Comparison of Echocardiographic Normal Values of Left Ventricular Size and Function in Healthy Adults: Results from the World Alliance of Societies of Echocardiography (WASE) Normal Values Study

Tatsuya Miyoshi¹, Karima Addetia², Alexandra Blitz³, Vivekanandan Amuthan⁴, Eduardo Bossone⁵, Masao Daimon⁶, Pedro Gutierrez-Fajardo⁷, Ravi Kasliwal⁸, James N. Kirkpatrick⁹, Mark J. Monaghan¹⁰, Denisa Muraru¹¹, Kofo O. Ogunyankin¹², Seung Woo Park¹³, Ana Clara Tude Rodrigues¹⁴, Ricardo Ronderos¹⁵, Anita Sadeghpour¹⁶, Gregory Scalia¹⁷, Masaaki Takeuchi¹⁸, Wendy Tsang¹⁹, Edwin S. Tucay²⁰, Mei Zhang²¹, Roberto M. Lang², Federico M. Asch¹. ¹Medstar Health Research Institute, Washington, DC; ²University of Chicago, Chicago, IL; ³TOMTEC Imaging Systems GmbH, Unterschleissheim, Germany; ⁴Jeyalakshmi Heart Center, Madurai, India; ⁵University of Salerno, Salerno, Italy; ⁶The University of Tokyo, Tokyo, Japan; ⁷Hospitales Mac Bernardette, Guadalajara, Mexico; ⁸Medanta Heart Institute, Gurgaon, Haryana, India; ⁹University of Washington, Seattle, WA; ¹⁰King's College Hospital, London, United Kingdom; ¹¹University of Padova, Padova, Italy; ¹²First Cardiology Consultants Hospital, Lagos, Nigeria; ¹³Samsung Medical Center, Seoul, Republic of Korea; ¹⁴Albert Einstein Hospital, Sao Paulo, Brazil; ¹⁵Universidad Nacional de la Plata, Buenos Aires, Argentina; ¹⁶Rajaie Cardiovascular Medical and Research Center, Echocardiography Research Center, IUMS, Tehran, Islamic Republic of Iran; ¹⁷Genesis Care, Brisbane, Australia; ¹⁸University of Occupational and Environmental Health, Kitakyushu, Japan; ¹⁹Toronto General Hospital, University of Toronto, Toronto, ON, Canada; ²⁰Philippine Heart Center, Quezon City, Philippines; ²¹Qilu Hospital of Shandong University, Jinan, China

Background: The American Society of Echocardiography (ASE) chamber quantification guidelines provide normal reference ranges for a variety of parameters. While used worldwide, these values were predominantly obtained from American and European Caucasian populations and may not represent individuals from other regions around the world. Several studies from other individual countries were conducted but they lack uniform acquisition and measurement protocols. Accordingly, ASE in collaboration with its International Alliance Partners conducted the World Alliance of Societies of Echocardiography (WASE) Normal Value Study to establish and compare normal echocardiographic values across races, ethnicities and countries worldwide. We report on similarities and differences in left ventricular (LV) size and function among continents. **Methods:** WASE Normal Values Study is a multinational, observational, cross-sectional study. Individuals free from known cardiac, lung and renal disease were prospectively enrolled with even distribution among age groups and gender. 2 and 3 Dimensional (2D, 3D) datasets were acquired at the enrolling centers, following a standardized WASE protocol. LV internal dimensions and LV mass by liner method, LV volumes, ejection fraction, stroke volume in 2D and 3D images, and peak 2D LV global longitudinal strain were analyzed (TOMTEC) in two core laboratories (each for 2D and 3D) following ASE Guidelines. **Results:** As of January 2019, 1291 cases have been analyzed. All 2D and 3D parameters in LV size and function have significant differences among continents (p < 0.05, ANOVA; Table 1). LV volumes and stroke volume in Asian countries were smaller than those in other regions, even after indexing for body surface area. As expected, LV size in male was larger than that in female. Detailed data by country and for 3D and strain is available for YIA competition. **Conclusions:** The WASE Normal Values Study provides a unique and important set of normal reference values for LV chamber quantification across continents and countries. The results will enable the characterization of diverse populations around the world and provide a novel insight in their similarities and differences.

	Total	North America	Latin America	EU	Africa	East Asia	India	Iran	Dominican	n value
	mean	mean	mean	mean	mean	mean	mean	mean	mean	(ANOVA)
N	1291	149	136	109	104	428	125	138	99	
Age	46 ± 17	51 ± 19	49 ± 17	48 ± 14	50 ± 17	47 ± 18	49 ± 17	47 ± 14	48 ± 18	<0.001
Gender										
Male (n, %)	669 (51.8%)	79 (53.0%)	75 (54.5%)	46 (42.2%)	56 (53.8%)	219 (51.2%)	72 (57.1%)	71 (51.4%)	51 (51.5%)	0.52
Height	167 ± 10	170 ± 10	169 ± 9	170 ± 9	168 ± 9	165 ± 9	169 ± 10	168 ± 9	174 ± 10	<0.001
Weight	68 ± 13	73 ± 13	73 ± 12	67 ± 12	70 ± 12	62 ± 11	62 ± 15	72 ± 12	76 ± 14	<0.001
BSA	1.76 ± 0.22	1.86 ± 0.21	1.84 ± 0.19	1.77 ± 0.19	1.80 ± 0.19	1.67 ± 0.19	1.64 ± 0.24	1.83 ± 0.19	1.90 ± 0.22	<0.001
BMI	24.2 ± 3.5	25.2 ± 3.0	25.4 ± 3.1	23.8 ± 3.9	24.6 ± 3.1	22.6 ± 2.6	24.1 ± 5.1	25.7 ± 3.5	25.1 ± 3.2	<0.001
Systolic BP	121 ± 12	119 ± 12	114 ± 11	121 ± 15	120 ± 12	124 ± 11	122 ± 12	120 ± 11	115 ± 13	<0.001
Diastolic BP	74 ± 9	71 ± 7	75 ± 8	72 ± 10	73 ± 9	75 ± 9	77 ± 8	76 ± 8	68 ± 9	<0.001
LV dimension/volume										
LV DiD (mm)	44 ± 5	46 ± 5	44 ± 5	45 ± 5	46 ± 5	43 ± 5	42 ± 5	44 ± 5	47 ± 6	<0.001
LV DiS (mm)	28 ± 5	29 ± 5	28 ± 5	29 ± 5	28 ± 5	28 ± 4	27 ± 3	29 ± 4	31 ± 4	<0.001
2D LV Mass (g)	109 ± 33	117 ± 33	108 ± 28	103 ± 30	109 ± 31	103 ± 33	95 ± 28	110 ± 31	125 ± 39	<0.001
2D LVEDV (ml)	94 ± 25	102 ± 27	98 ± 25	100 ± 25	97 ± 26	87 ± 21	73 ± 18	95 ± 22	112 ± 27	<0.001
2D LVEF (%)	35 ± 11	38 ± 11	37 ± 10	37 ± 11	36 ± 11	32 ± 9	37 ± 8	35 ± 10	43 ± 11	<0.001
3D LVEDV (ml)	118 ± 35	145 ± 42	125 ± 33	108 ± 32	106 ± 33	112 ± 28	76 ± 21	115 ± 26	130 ± 29	<0.001
3D LVEF (%)	45 ± 16	56 ± 18	47 ± 15	38 ± 14	41 ± 15	42 ± 13	29 ± 8	45 ± 19	49 ± 14	<0.001
Indexed values by BSA										
2D LV Mass Index (g/m ²)	61 ± 15	63 ± 14	58 ± 13	57 ± 13	59 ± 13	65 ± 16	57 ± 12	60 ± 14	66 ± 16	<0.001
2D LVEDV Index (ml/m ²)	53 ± 11	55 ± 12	53 ± 12	56 ± 11	53 ± 11	52 ± 10	45 ± 9	52 ± 10	59 ± 10	<0.001
2D LVEF (%)	19 ± 5	20 ± 5	20 ± 5	21 ± 5	20 ± 5	18 ± 4	16 ± 4	19 ± 4	23 ± 5	<0.001
3D LVEDV Index (ml/m ²)	66 ± 16	78 ± 17	67 ± 18	59 ± 14	52 ± 12	66 ± 13	46 ± 10	63 ± 13	68 ± 11	<0.001
3D LVEF (%)	25 ± 8	30 ± 8	25 ± 8	21 ± 7	20 ± 6	25 ± 7	18 ± 4	24 ± 10	26 ± 6	<0.001
LV Function										
2D LVEF (%)	63 ± 3	63 ± 3	63 ± 2	63 ± 3	63 ± 3	64 ± 3	63 ± 3	63 ± 2	62 ± 3	<0.001
2D LV GLS (%)	-21.2 ± 2.1	-20.5 ± 1.9	-21.1 ± 2.1	-22.2 ± 2.0	-21.4 ± 1.9	-21.2 ± 2.2	-21.8 ± 2.2	-21.4 ± 1.9	-20.7 ± 2.0	<0.001
3D LVEF (%)	62 ± 5	62 ± 4	63 ± 5	65 ± 5	62 ± 4	62 ± 5	61 ± 4	62 ± 5	62 ± 5	0.03
2D LV SV by Doppler (ml)	69 ± 17	77 ± 21	68 ± 15	72 ± 18	65 ± 13	67 ± 14	59 ± 13	71 ± 15	75 ± 18	<0.001
3D LV SV (ml)	73 ± 21	89 ± 25	78 ± 18	70 ± 19	65 ± 20	70 ± 16	47 ± 14	71 ± 17	81 ± 17	<0.001

P1-190

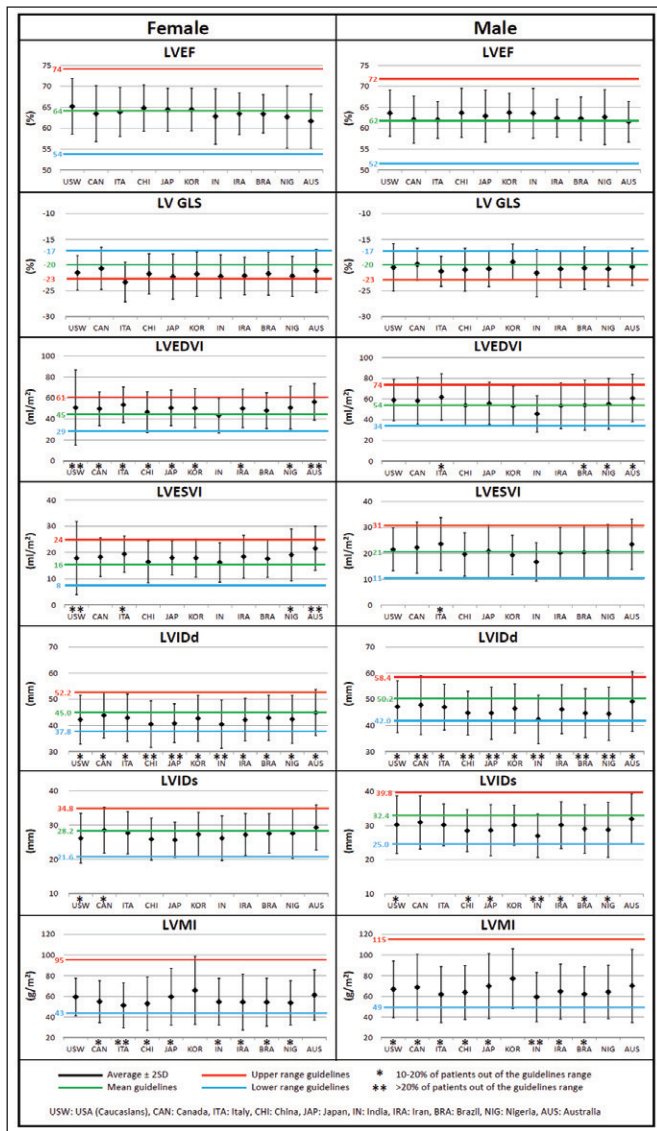
Applicability of Current Reference Values in Different Countries: Results from the World Alliance of Societies of Echocardiography (WASE) Normal Values Study

Tatsuya Miyoshi¹, Karima Addetia², Alexandra Blitz³, Vivekanandan Amuthan⁴, Michael Blankenhagen⁵, Rodolfo Citro⁶, Masao Daimon⁶, Pedro Gutierrez-Fajardo⁷, Ravi Kasliwal⁸, James N. Kirkpatrick⁹, Diego Medvedofsky¹, Mark J. Monaghan¹⁰, Denisa Muraru¹¹, Kofo O. Ogunyankin¹², Seung Woo Park¹³, Ana Clara Tude Rodrigues¹⁴, Ricardo Ronderos¹⁵, Anita Sadeghpour¹⁶, Gregory Scalia¹⁷, Masaaki Takeuchi¹⁸, Wendy Tsang¹⁹, Edwin S. Tucay²⁰, Mei Zhang²¹, Roberto M. Lang², Federico M. Asch¹. ¹Medstar Health Research Institute, Washington, DC; ²University of Chicago, Chicago, IL; ³TOMTEC Imaging Systems GmbH, Unterschleissheim, Germany; ⁴Jeyalakshmi Heart Center, Madurai, India; ⁵University of Salerno, Salerno, Italy; ⁶The University of Tokyo, Tokyo, Japan; ⁷Hospitales Mac Bernardette, Guadalajara, Mexico; ⁸Medanta Heart Institute, Gurgaon, Haryana, India; ⁹University of Washington, Seattle, WA; ¹⁰King's College Hospital, London, United Kingdom; ¹¹University of Padova, Padova, Italy; ¹²First Cardiology Consultants Hospital, Lagos, Nigeria; ¹³Samsung Medical Center, Seoul, Republic of Korea; ¹⁴Albert Einstein Hospital, Sao Paulo, Brazil; ¹⁵Universidad Nacional de la Plata, Buenos Aires, Argentina; ¹⁶Rajaie Cardiovascular Medical and Research Center, Echocardiography Research Center, IUMS, Tehran, Islamic Republic of Iran; ¹⁷Genesis Care, Brisbane, Australia; ¹⁸University of Occupational and Environmental Health, Kitakyushu, Japan; ¹⁹Toronto General Hospital, University of Toronto, Toronto, ON, Canada; ²⁰Philippine Heart Center, Quezon City, Philippines; ²¹Qilu Hospital of Shandong University, Jinan, China

Background: The American Society of Echocardiography (ASE) chamber quantification guidelines provide recommendation for normal reference range for a variety of parameters. While used worldwide, these values were predominantly obtained from Caucasian North American and European populations. We hypothesize normal ranges presented in the Guidelines may not represent chamber size and function worldwide. Accordingly, ASE in collaboration with its International Alliance Partners led the World Alliance of Societies of Echocardiography (WASE) Normal Values Study to establish and compare normal echocardiographic values across races, ethnicities and countries worldwide. In this report, we compare two-dimensional left ventricular (LV) size and function measurements with the reference values recommended by ASE 2015 guidelines. Only patients from the 11 countries with full data analyzed to date are included. **Methods:** WASE Normal Values Study is a multinational, observational, cross-sectional study. Individuals free from known significant cardiac, lung and renal disease were prospectively enrolled. The participant countries have enrolled individuals evenly distributed among age groups and gender. Among others, the following parameters were analyzed following the standard ASE protocol: LV ejection fraction, LV global longitudinal strain, LV volumes and diameters in end-diastole and end-systole, and LV mass. All measurements were analyzed (TOMTEC) at a Core laboratory following ASE Guidelines. Results are being compared with the ASE guidelines normal range values. **Results:** As of January 2019, we have finished analyzing 1174 individuals from 11 countries. The mean ± 2SD for each country, and their comparison against ASE guidelines normal range is shown in the figure. Parameters with 10-20% and >20% of cases falling outside of the guidelines range are marked in the figure (* and ** respectively). While the majority of patients fell within the Guidelines normal range for all parameters, >10 and 20% of cases fell outside of guidelines range, mostly in volume and dimension measurements. **Conclusions:** Populations from the different continents in the WASE study have similarities to the normal ranges recommended in the ASE guidelines. However, small differences with the guidelines and between countries are noted.

Poster Session 1 (P1)

Sunday, June 23, 2019

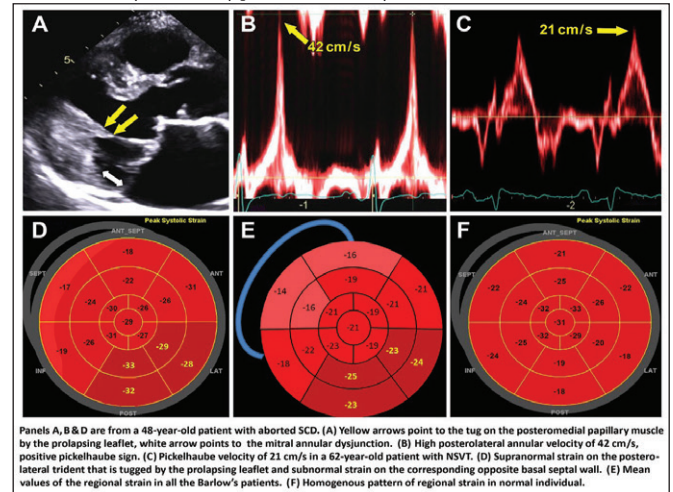


P1-191
Barlow's Myxomatous Bileaflet Mitral Valve Disease: Analysis of Bull's Eye Plot of Global and Regional Myocardial Mechanics

Lakshmi Muthukumar, Arshad Jahangir, Patrycja Galazka, M. Fuad Jan, Renuka Jain, McKenzie Schweitzer, Matt Umland, Bijoy K. Khandheria, A. Jamil Tajik. Aurora Cardiovascular Services, Aurora Sinai/Aurora St. Luke's Medical Centers, Milwaukee, WI

Background: Barlow's myxomatous bileaflet mitral valve disease (BMVD) is a well-known entity but its association with underlying myocardial disease is questionable. We addressed this question by analyzing global and regional myocardial mechanics using the left ventricular (LV) longitudinal strain (LS) bull's eye plot derived from 2D speckle tracking imaging (STI) and tissue annular systolic velocities. **Methods:** Forty-one patients with BMVD were analyzed for ventricular arrhythmias and baseline and clinical characteristics by chart review. Malignant arrhythmia (MA) was defined as sudden cardiac death (SCD), ventricular fibrillation or sustained ventricular tachycardia (VT); non-malignant arrhythmia (NM) as nonsustained VT; and no-arrhythmia (NA) as patients with only premature ventricular contractions. Bull's eye plot of LS derived from STI using GE EchoPAC software and basal lateral and posterolateral tissue annular systolic velocities were analyzed. **Results:** Of 41 patients (mean age 52±14 y; 56% female), 7 had MA, 6 NM and 28 NA. All patients' basal posterior or posterolateral annular tissue systolic velocities had a spiked configuration, the pickelhaube sign. Average pickelhaube velocity in cm/s was 23±7 (MA) vs 15±6 (NM) vs 16±6 (NA). In all patients, a heterogeneous pattern of regional strain was observed compared to the homogenous pattern seen in normal individuals. Mean regional strain in the posterolateral trident, which includes the basal and mid posterior and posterolateral wall segments, was higher (-24±5%) and basal and mid inferoseptal and basal anterosseptal strains were lower (-15±4%) compared to

other segments (-20±5%). **Conclusion:** In BMVD, patient's bull's eye plot offers an at-a-glance view of abnormal LS patterns in segments of the LV myocardium in relation to the prolapsing mitral valve leaflets. Our data demonstrate supranormal strains (>-21%) in the posterolateral trident subtended to the tug by the prolapsing leaflets and subnormal strain (≤18%) in the corresponding opposite basal septal wall segments. Our observations suggest the abnormal heterogeneous myocardial mechanics noted in BMVD may contribute to ventricular arrhythmias and the possibility of identifying high-risk patients by quantifying stretch on the myocardium by pickelhaube velocity and strain values.



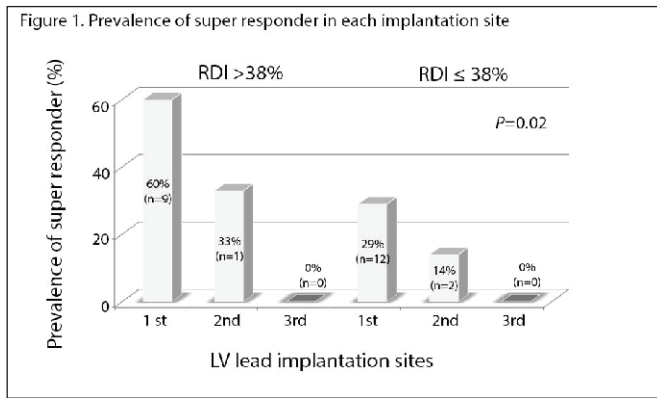
P1-193
The Role of Left Ventricular Radial Discooordination Index in Cardiac Resynchronization Therapy Among Patients with Ischemic Cardiomyopathy - A Sub-Study of the RAISE-CRT Multi-Center Trial

Saki Ito¹, Michael Glikson², Gregory Golovchiner³, Moshe Swissa⁴, Monther Boulus⁵, Raphael Rosso⁶, Aharon Medina⁷, Moti Haim⁸, Paul Friedman¹, Vladimir Khalameizer⁹, Ori Vaturi¹⁰, Nir Shlomo¹¹, Ilan Goldenberg¹¹, Roy Beinart¹⁰, Jae K. Oh¹. ¹Mayo Clinic, Rochester, MN; ²Shaare Zedek Medical Center, Jerusalem, Israel; ³Rabin Medical Center, Petah-Tikva, Israel; ⁴Kaplan Medical Center, Rehovot, Israel; ⁵Rambam Medical Center, Haifa, Israel; ⁶Tel Aviv Medical Center, Tel Aviv, Israel; ⁷Zedek Medical Center, Jerusalem, Israel; ⁸Soroka Medical Center, Beer Sheva, Israel; ⁹Barzilai Medical Center, Askelon, Israel; ¹⁰Sheba Medical Center, Ramat Gan, Israel; ¹¹Association for Clinical Trials, Ramat Gan, Israel

Background: A mid-ventricular radial discooordination index (RDI) (thinning/thickening during ejection) using speckle tracking strain rate has been shown to be predictive for responders of cardiac resynchronization therapy (CRT). However, its role in patients with ischemic cardiomyopathy (ICM) is unclear. **Methods:** Multicenter trial (9 centers in Israel and US) to evaluate the benefit of radial strain guided left ventricular (LV) lead positioning in CRT was conducted in patients with ICM. LV segments according to latest activation without scar were identified by ranking of 6 mid LV segments by time from QRS onset to the latest mechanical activation. Scarred area was defined as peak radial strain <10%. Patients were randomized to two groups: strain guided LV lead implantation vs. conventional techniques (2:1 ratio). In this sub-study, randomization was not taken into consideration. Data analysis was based on the sites actually achieved with the LV lead. RDI was calculated before CRT implantation. LV dyssynchrony was defined as RDI>38%. Super responder was defined as LV end-systolic volume reduction >30% in 6 months. **Results:** In a total of 173 patients (age 69.9±8.4 years, 94% male, LV ejection fraction 30.3±7.2%), RDI was available in 147 patients; 23% (n=34) patients with RDI>38% and 77% (n=113) with RDI≤38%. Patient's characteristics were similar in both groups, but patients with RDI>38% had wider QRS duration and larger LV end-systolic volume (Table 1). Super responders were more frequent in patients with RDI>38% compared to patients with RDI≤38% (48% [n=13] vs 19% [n=17], P<0.01). Super responders were observed more frequently when LV lead was implanted in the 1st recommended site (Figure 1). There were no super responders in the 3rd recommended site regardless of RDI measurements. **Conclusions:** RDI>38% was associated with better LV reverse remodeling response to CRT in patients with ICM. The latest mechanical activation area was shown to be ideal for LV lead implantation regardless of LV dyssynchrony.

Poster Session 1 (P1)

Sunday, June 23, 2019



	All (n=173)	RDI available (n=147)	RDI>38% (n=34, 23%)	RDI<=38% (n=113, 77%)	P
Case	100 (68)	27 (79)	73 (65)	0.10	
Age	69.9±8.4	69.3±10.3	69.9±8.0	0.77	
Male	163 (94)	31 (91)	107 (95)	0.45	
Myocardial infarction	152 (88)	18 (53)	63 (56)	0.77	
6 minutes walk, m	328.1±128.4	330.3±124.8	330.3±131.9	>0.99	
QRS morphology				0.26	
- Left bundle branch block	129 (75)	29 (85)	81 (72)		
- Right bundle branch block	81 (72)	1 (3)	23 (20)		
- Other	30 (17)	4 (12)	9 (8)		
QRS duration, msec	154.7±18.5	160.1±20.7	152.2±17.9	0.05	
LV ejection fraction, %	30.3±7.2	28.2±7.1	30.6±7.0	0.09	
LV end-diastolic volume, ml	287.4±71.7	305.8±83.3	281.8±67.4	0.14	
LV end-systolic volume, ml	203.4±6.7	223.9±79.2	197.5±56.9	0.08	
Stroke volume index, ml/m ²	31.9±9.8	31.5±9.2	32.4±9.7	0.65	
Septal to posterior wall motion delay (M-mode), msec	147.8±85.9	139.1±73.5	149.4±90.9	0.54	
Anteroseptal to posterior time to peak (radial strain), msec	92.7 (36.0-166.7)	129.3 (70.0-207.6)	91.8 (29.9-163.6)	0.04	
RDI, %	24.5 (13.3-35.4)	59.1 (43.8-77.9)	18.2 (11.2-26.5)	-	

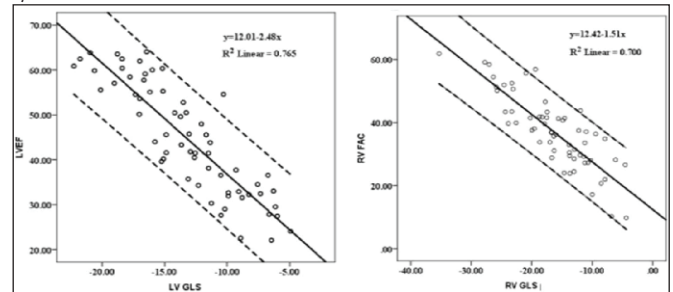
P1-194

Mechanical Improvement After MitraClip Implantation is Associated with Baseline Preserved LVEF and Favorable Volumetric Changes

Wei Chen¹, Andrew Berke², William Chung², Aarsha Gopal², Elena Koss², Jane Cao², Lin Wang². ¹Chinese Academy of Medical Sciences and Peking Union Medical College Hospital, Beijing, China; ²St. Francis Hospital the Heart Center, Roslyn NY, NY

Background: MitraClip implantation is a new option to treat patients with significant mitral regurgitation and high surgical risk. The goal of this study was to evaluate the impact of cardiac mechanics on the cardiac geometry and its association with left ventricular contractility early after MitraClip procedure. **Methods:** Consecutive sixty-three patients (84 ± 5 years old, 48% male) with moderate to severe or severe mitral regurgitation undergoing MitraClip intervention in a single center were included. Volumetric and functional changes were assessed using two-dimensional (2D) transthoracic and speckle-tracking echocardiography (STE) before and 24 hours after procedure. Baseline LV ejection fraction (EF) ≥50% was defined as LV preserved EF group (LVpEF) and LVEF<50% as LV reduced EF group (LVrEF). **Results:** The median age was 84 [interquartile range (IQR): 79-88] years and 48% were men. LV end-diastolic volume were significantly reduced when compared to the baseline [100.36 (IQR: 69.53-146.11) ml vs. 116.43 (IQR: 84.95-155.35) ml, p<0.001]. The reduction, however, was significant among patients with LVpEF [116.86 (IQR: 93.19-148.87) ml vs. 139.09 (IQR: 102.43-191.64) ml, p=0.018], but not among those with LVrEF [134.29 (IQR: 88.67-168.23) ml vs. 134.25 (IQR: 80.74-154.46) ml, p=0.074]. LV global longitudinal strain (GLS) was unchanged after MitraClip procedure, but significantly improved in RV GLS in patients with LVpEF (-14.73% vs. -17.90%, p=0.003). Linear regression analysis revealed significant correlation between GLS changes and

cardiac function improvement in both LV (R²=0.765, p=0.001) and RV (R²=0.700, p=0.001) following MitraClip implantation. **Conclusion:** Baseline preserved LVEF is associated with favorable left heart volume reduction and mechanical improvement. GLS improvement is directly related to cardiac contractility in both left and right ventricles after MitraClip procedure. Further studies are warranted to evaluate whether early intervention could improve clinical outcomes in patients with severe mitral regurgitation and preserved LV systolic function.



P1-195

Left Ventricular Hypertrophy on Echocardiogram in the Era of New Hypertension Guidelines

Chioma Duru¹, Munes Fares¹, Goutham Rao², Carolyn M. Wilhelm¹. ¹Rainbow Babies and Children's Hospital, Cleveland, OH; ²University Hospital, Cleveland, OH

Background: Left ventricular hypertrophy (LVH) is a target end organ injury commonly seen in patients with systemic hypertension (HTN). LVH, a maladaptive response to chronic pressure overload, is an important risk factor for ventricular dysfunction, atrial tachyarrhythmias and sudden death in patients with HTN. Echocardiogram is utilized in pediatric HTN patients to guide medical therapy. In 2017, the American Academy of Pediatrics re-defined LVH as left ventricular mass index (LVMI) > 51 g/m^{2.7} in children older than 8 years of age or LVMI > 115 g per body surface area (BSA) in boys and LVMI > 95 g/BSA in girls. This is a change from the previous quantification chart based on age and gender. The 2017 guidelines shifts the threshold at which more aggressive medical therapy is indicated. The aim of this study was to analyze and highlight the impact of guideline changes in the categorization of patients with diagnosis of hypertensive cardiomyopathy. **Methods:** A single-center retrospective review of pediatric patients age 2-18 years who underwent echocardiogram with indication of systemic HTN from 2014-2017. Collected data included age, sex, BSA, LVMI to g/m^{2.7}, LVMI g/m², BMI, and blood pressure at time of study. Patients with LVH based on historical criteria were identified. The LVMI to g/m^{2.7} and LVMI to g/m² of these patients were re-categorized based on the 2017 AAP guidelines. Patients with congenital heart disease, cardiomyopathy unrelated to HTN and medical conditions that predispose to development of LVH were excluded from the study. Patients with poor image quality and missing data for calculation of LVMI were also excluded. **Results:** 250 patients with systemic HTN between the years 2014-2017 were reviewed. Ninety-nine patients with LVH using historical guidelines were included in this study. There is a male predominance (n = 70) with a median BSA 2.09 (range 0.58-3.01) for the study population. Categorization based on the 2017 guidelines suggest that now only 45 patients (45%) met criteria for diagnosis of LVH. Additionally, it was noted that 37 of these 45 patients (82%) met the diagnostic criteria for severe childhood obesity with a BMI >95% and mostly above 99%. **Conclusion:** The change in LVH guidelines resulted in a marked shift in whether patients met diagnostic criteria for hypertensive cardiomyopathy by echocardiogram and therefore whether intensification of medical therapy was indicated based on target end organ injury. Incidentally, this study also demonstrates that children with severe childhood obesity are at increased risk of developing hypertension and associated cardiovascular sequelae.

P1-196

Determining Factors of Peak Left Atrial Strain in Healthy Individuals

Byung Joo Sun, Jae-Hyeong Park. Chungnam National University Hospital, Daejeon, Republic of Korea

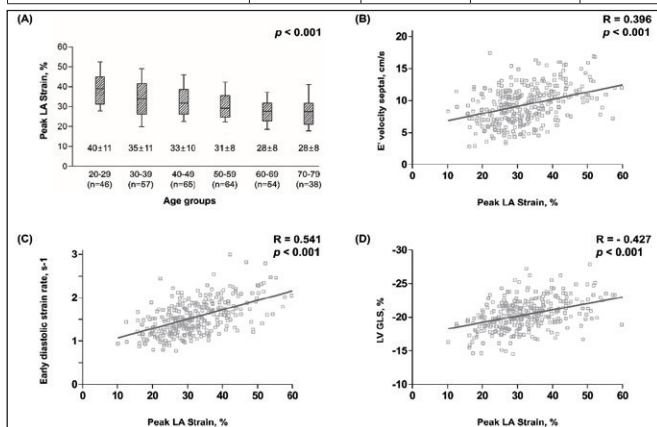
Background: The left atrial (LA) strain assessed by speckle-tracking echocardiography (STE) is a novel parameter of LA function. But, its reference value is not yet established and determining factors for LA strain remain elusive. We aimed to present peak LA strain value in a large-sized, selected group of healthy individuals and to elucidate its determining factors. **Methods:** The present study was a part of the Normal echocardiographic Measurements in Korean population (NORMAL), a prospective nationwide survey from 23 centers in South Korea. We enrolled the 324 subjects (age 49±16 years, 167 females) without history of cardiovascular disease. Using STE, we calculated peak LA strain, left ventricular global longitudinal strain (GLS), and early and late diastolic strain rates (DSR_e and DSR_a, respectively). We presented peak LA strain values in a total and age-groups by decade, and analyzed its association with clinical and echocardiographic parameters. **Results:** Among the total subjects, the mean peak LA strain value was 32±10% (Table).

Poster Session 1 (P1)

Sunday, June 23, 2019

With increasing age, there was a significant trend of decreasing peak LA strain ($p < 0.001$, Figure A). Mitral annular E' velocity, DSR_l and GLS showed significant correlations with peak LA strain (Figure B-D). On multiple linear regression, age ($B = -0.216$, $p < 0.001$), DSR_r ($B = 5.668$, $p = 0.003$), DSR_l ($B = 5.222$, $p = 0.015$) and GLS ($B = -0.966$, $p = 0.002$) showed significant associations with peak LA strain. However, E' velocity did not remain significant after multivariable adjustment. **Conclusion:** Age is an independent determinant for peak LA strain in healthy individuals. STE-derived diastolic strain rate and E' velocity are closely related to LA mechanics. However, conventional parameters including E' velocity could not reflect that.

Clinical and Echocardiographic Parameters				
	Total (n=324)	Male (n=157)	Female (n=167)	P-value
Age, years	49±16	50±16	48±15	0.301
Body surface area, m ²	1.7±0.2	1.8±0.1	1.6±0.1	< 0.001
Systolic blood pressure, mmHg	120±13	123±12	117±13	< 0.001
Diastolic blood pressure, mmHg	72±10	74±10	71±10	0.011
Heart rate, beats/min	68±10	67±10	69±10	0.133
LV mass index, g/m ²	75±14	78±14	71±14	< 0.001
LV end diastolic volume, ml	103±22	113±21	93±17	< 0.001
LV end systolic volume, ml	39±10	43±10	35±9	< 0.001
LV ejection fraction, %	62±4	62±4	63±4	0.162
LA volume index, ml/m ²	27±6	27±6	28±7	0.647
Peak LA strain, %	32±10	30±9	34±10	< 0.001
E velocity, cm/s	69±16	66±15	72±17	0.001
A velocity, cm/s	60±17	60±17	60±16	0.977
E/A ratio	1.2±0.5	1.2±0.4	1.3±0.6	0.030
E' velocity septal, cm/s	9.3±2.9	9.1±2.8	9.5±3.0	0.244
E' velocity lateral, cm/s	12.6±3.7	12.3±3.7	12.8±3.7	0.254
E/E' ratio septal	7.9±2.3	7.7±2.2	8.1±2.4	0.090
E/E' ratio lateral	5.9±1.8	5.7±1.8	6.0±1.8	0.203
Deceleration time, ms	209±38	211±39	207±38	0.303
Isovolumic relaxation time, ms	84±15	84±14	84±16	0.677
Global longitudinal strain, %	-20.4±2.2	-19.5±2.1	-21.2±2.1	< 0.001
Early diastolic strain rate, s ⁻¹	1.6±0.4	1.4±0.3	1.7±0.4	< 0.001
Late diastolic strain rate, s ⁻¹	0.8±0.3	0.8±0.3	0.8±0.3	0.966



P1-197

Normal Ranges of Left Ventricular Strain by Three-Dimensional Speckle-Tracking Echocardiography: A Systematic Review and Meta-Analysis

Vien Truong¹, Hoang Phan², Tam Ngo², Hoang Duong², Khanh Pham², Bao Truong², Tuy Nguyen², Cassidy Palmer¹, Sarah Wolking¹, Michael Young¹, Justin Tretter³, Tarek Alsaied³, Eugene Chung¹, Sherif F. Nagueh⁴, Wojciech Mazur¹. ¹The Christ Hospital Health Network, Cincinnati, OH; ²Pham Ngoc Thach University of Medicine, Ho Chi Minh, Viet Nam; ³Cincinnati Children's Hospital, Cincinnati, OH; ⁴Houston Methodist Hospital, Houston, TX

Background: Establishing normal values and associated variations of three-dimensional speckle-tracking echocardiography (3DSTE)-derived left ventricular (LV) strain is

necessary for accurate interpretation and comparison of measurements. The aims of this study were to perform a meta-analysis of normal ranges of LV global longitudinal strain (GLS), global circumferential strain (GCS), global radial strain (GRS) and global area strain (GAS) measurements derived by 3DSTE and to identify confounding factors that may contribute to variance in reported measures. **Methods:** The authors searched four databases, Pubmed, Scopus, Embase, Cochrane Library, through January 2019 using the key terms "left ventricular/left ventricle/ left ventricles", "strain/deformation/speckle tracking" and "three dimensional/three-dimensional/three-dimension/three dimension/3D". Studies were included if the articles reported LV strain using three-dimensional speckle-tracking echocardiography in healthy normal subjects, either in the control group or comprising the entire study cohort. The weighted mean was estimated by using random effect models with 95% CI. **Results:** The search yielded 895 articles. After abstract and full text screening we included 39 articles with 3,012 patients for meta-analysis. The reported normal mean values of GLS among the studies varied from -23.04% to -15.22% (mean, -19.21%; 95% CI, -22.02% to -18.4%; I²=99.1%), GCS varied from -15.5% to -39.5% (mean, -22.61%; 95% CI, -23.93% to -21.29%; I²=99.6%), and GRS varied from 18.47% to 88.09% (mean, 46.85%; 95% CI, 41.67% to 50.02%; I²=99.8%), GAS varied from -30.51 to -50.80 (mean, -34.91%; 95% CI, -36.64% to -33.18%; I²=99.3%). Software for strain analysis was consistently associated with variations in normal strain values (GLS: $p = 0.06$; GCS: $p < 0.001$; GRS: $p = 0.003$; GAS: $p < 0.001$). **Conclusion:** The normal reference ranges for the four components of left ventricular function are reported. Variations in the normal ranges across studies were associated with software used for strain analysis, emphasizing that this factor should be considered in the interpretation of strain.

P1-198

Changes in Contractile Function Following Transcatheter Aortic Valve Replacement are Influenced by Gender and Baseline EF: Insights from Midwall Stress-Shortening Analysis

Nouran Sorour¹, Ahmed Nagy¹, Bryan Dolan¹, Eugene Chung², Gerald P. Aurigemma¹, Colleen M. Harrington¹. ¹University of Massachusetts, Worcester, MA; ²The Christ Hospital, Cincinnati, OH

Background: Left ventricular (LV) remodeling and changes in ejection fraction (EF) occur post transcatheter aortic valve replacement (TAVR). Patients with severe aortic stenosis (aAS) and a baseline LV ejection fraction <60% have been shown to have a worse prognosis post TAVR, compared with those with EF ≥ 60%. Fractional shortening at the midwall (FSmw) provides better understanding of the changes in contractile function than changes in EF when hypertrophic remodeling is present. While women with aAS appear to have higher prevalence of concentric LV remodeling, it is not clear whether there are gender differences in contractile function, as assessed by FSmw, nor how FSmw changes following TAVR. **Methods:** A total of 436 patients with aAS who underwent TAVR from 2011-2017 were stratified by LVEF <60% and ≥ 60%. They were further stratified according to gender. We compared echo data pre- and 1-year post TAVR: LV mass index (LVMI), relative wall thickness, wall stress (eSS) and FSmw (%). Peak LV pressure was calculated by adding peak aortic velocity to systolic blood pressure to estimate load. Zva was estimated to understand LV and pulsatile load. **Results:** A total of 397 patients were included (45.6% women). Overall, TAVR was associated with LV mass regression: LVMI decreased ($p < 0.05$) in both men and women, but there was only a modest change in relative wall thickness. Changes in FSmw were more closely related to changes in wall stress than Zva: FSmw increasing in men ($p < 0.05$) but decreasing in women. Subgroup analysis demonstrated that almost all of the improvement in FSmw occurred in the group with EF <60% at baseline. **Conclusion:** One-year post TAVR for aAS, both wall stress (eSS) and total ventricular and pulsatile load (Zva) decline. Hypertrophy regresses, but remains concentric in most cases. The overall improvement in contractile function, however, differs significantly by gender, with men showing a dramatic improvement in FSmw, and a reduction in eSS and Zva, but women showing a decrease in FSmw and an increase in eSS. Moreover, the improvement in FSmw in men, and in the group as a whole is driven by the changes in the group with EF <60%. This suggests that this EF value is an important partition value in this population.

Characteristic	Male		Female		Pre vs. 1 year	
	Pre-TAVR	1 year post-TAVR	Pre-TAVR	1 year post-TAVR	Male	Female
Echocardiographic Parameters [mean]						
Gender						
LV mass index (gm/m ²)	118.50	102.82	108.53	90.38	0.00	0.00
Relative wall thickness	0.53	0.49	0.58	0.56	0.10	0.44
LVIDd (mm)	45.12	49.08	49.24	43.52	0.00	0.00
LVIDs (mm)	34.52	32.34	28.82	28.75	0.04	0.95
Valvuloarterial impedance(Zva) (mmHg/mL/m ²)	5.71	5.13	6.35	5.77	0.04	0.05
FS mmW (%)	0.10	0.17	0.20	0.16	0.00	0.06
ESS (gm/cm ²)	155.42	99.76	88.15	100.56	0.00	0.28

Poster Session 1 (P1)

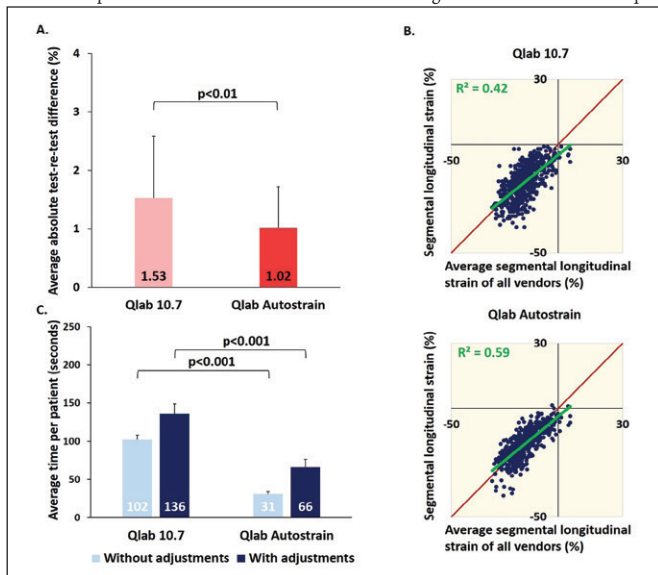
Sunday, June 23, 2019

P1-199

The Impact of Automated Speckle Tracking Analysis on Left Ventricular Longitudinal Strain Measurements

Stéphanie Bézy, Oana Mirea, Serkan Ünlü, Marta Cvijic, Jürgen Duchenne, Jens-Uwe Voigt. University of Leuven, Leuven, Belgium

Background: Global longitudinal strain (GLS) has shown to have an added diagnostic and prognostic value in a wide range of pathologies. For patient follow-up in the clinical routine, fast data processing as well as a good accuracy and reproducibility of strain measurements are essential. The aim of this study was to evaluate how strain measurements and the time of analysis are influenced by a more automated approach to speckle tracking analysis of the left ventricle. **Methods:** 61 patients (56 patients with prior myocardial infarction and 5 healthy volunteers) were retrospectively analysed with the most recent Philips speckle tracking software (QLab Autostrain, AUTO), which provides a fully automated speckle tracking analysis. Global and segmental (SLS) longitudinal strain measurements were obtained from two sets of apical views. Absolute test-re-test variability was calculated to assess the reproducibility of strain measurements. Analysis time was measured from indicating the three image files until the appearance of the strain bull's eye display. Results were compared to data of the previous, semi-manual software (QLab 10.7, MAN) and to the mean measurements of software from 8 other vendors as obtained during a previous inter-vendor study. **Results:** The AUTO strain analysis was feasible in all subjects. The variability of GLS measurements obtained with AUTO was significantly lower than with MAN (1.02 ± 0.70 vs. 1.53 ± 1.06 , $p < 0.01$) (Figure A). SLS obtained with AUTO correlated better to the average of all vendors than SLS obtained with MAN (Figure B). Without manual adjustments, the analysis time for one patient was on average 70% faster with the AUTO software compared to MAN ($p < 0.001$), and 51% faster if manual adjustments were needed ($p < 0.001$) (Figure C). **Conclusion:** The automatic speckle tracking analysis had a positive impact on the reproducibility, accuracy and time efficiency of global and segmental strain analyses. Our data indicate, that continuing efforts of vendors lead to a convergence of speckle tracking analysis results with, at the same time, faster, more accurate and more reproducible results which fosters the increasing routine use of this technique.



P1-200

Discrepant Tricuspid Annular Plane Systolic Excursion and Right Ventricular Ejection Fraction in Pulmonary Arterial Hypertension: Implications for Assessment of Right Ventricular Dysfunction

Abhishek Chaturvedi¹, Mitha Naik¹, Jose Ricardo P.O.², Talha Meeran³, Amresh Raina¹. ¹Allegheny Health Network, Pittsburgh, PA; ²Ascension Borgess Hospital, Kalamazoo, MI; ³Fortis Hospital Mumbai, Mumbai, India

Background: Right ventricular dysfunction (RVD) in pulmonary arterial hypertension (PAH) is associated with functional impairment, hospitalization and mortality. Consequently noninvasive assessment of RVD is critical in appropriate risk stratification. TAPSE is a commonly used and reliable marker of RVD in PAH. However, in some patients, TAPSE appears to be discrepant with other quantitative measures of RV function. We aimed to identify factors which might explain the circumstances in which TAPSE fails to accurately determine RVD in PAH and assess whether alternative metrics of RV function may be more reliable in these situations. **Methods:** We retrospectively analyzed 55 PAH patients who had echocardiograms (TTE), cardiac MRI and right heart catheterization within 3 months. 2 cohorts were identified based on TTE and MRI data: discrepant TAPSE (D-TAPSE) defined as $TAPSE \geq 18$ mm on TTE but $RVEF < 50\%$ on MRI vs non-discrepant TAPSE (ND-TAPSE) and RVEF on MRI. **Results:** The D-TAPSE cohort (N=22) were

similar in age (53 vs 55 yrs, $P=0.29$) to the ND-TAPSE cohort (N=33). D-TAPSE patients had higher TAPSE (21 vs 18 mm, $P=0.009$) but lower RVEF on MRI (40 vs 48%, $P=0.008$). RV diastolic diameter (RVEDD) (49 vs 44 mm, $P=0.01$), and right atrial area (23 vs 18 cm², $P=0.005$) were also significantly higher in D-TAPSE, suggesting that greater right heart dimensions are associated with failure of TAPSE to appropriately identify RVD (Table 1). Interestingly, RV fractional area change (RVFAC) was better able to detect RVD than TAPSE - though RVFAC was not significantly lower in D-TAPSE (27 vs 30%, $P=0.18$), only 1 patient in the D-TAPSE had a normal RVFAC ($>38\%$). Lastly, adjusting TAPSE values for RVEDD improved detection of RVD in the D-TAPSE cohort. Using a TAPSE/RVEDD ratio of 0.5 as a cutoff for detecting RVD, 16/22 patients in the D-TAPSE cohort would have been appropriately characterized as having RVD despite normal 'raw' TAPSE values. **Conclusion:** TAPSE may be discrepant with other metrics of RV function in some PAH patients. This phenomenon is most strongly associated with greater right heart dilatation and may stem from changes in RV geometry that affect single plane measures such as TAPSE as the RV dilates. In PAH patients with significant RV dilatation, use of RVFAC or ratio of TAPSE/RVEDD may better characterize RVD.

Table 1: Comparison of Baseline Characteristics of Pulmonary Arterial Hypertension Patients Based on Discordant and Concordant TAPSE (N=55).

Parameters	Discordant TAPSE (N=22)	Concordant TAPSE (N=33)	P
Demographic parameters			
Age, years	53.1±3.2	55.4±2.7	0.29
Female, %	72.7	84.8	0.27
Body Surface area, m ²	1.9±0.06	1.8±0.04	0.18
Echocardiographic parameters			
Right ventricular ejection fraction, %	39.9±1.8	47.8±2.3	0.008
Tricuspid annular plane systolic excursion (TAPSE), mm	21.1±0.7	17.7±1.0	0.009
Left atrium diameter, mm	34.4±1.8	35.3±1.1	0.32
Left atrium volume index, ml/m ²	27.1±2.9	26.1±1.7	0.38
Left ventricular end diastolic diameter, mm	44.2±1.3	41.5±1.2	0.07
Left ventricular ejection fraction, %	52.3±1.3	63.8±1.3	0.22
Tricuspid regurgitation jet area, cm ²	5.2±0.9	5.3±0.9	0.47
Right ventricular outflow tract acceleration time, ms	78.9±4.1	69.1±4.6	0.07
Peak tricuspid regurgitation gradient, mmHg	64.7±5.5	52.5±4.5	0.06
Mean tricuspid regurgitation gradient, mmHg	39.8±3.8	32.2±2.6	0.048
Estimated right atrial pressure, mmHg	6.3±0.7	6.8±0.7	0.32
Estimated systolic pulmonary artery pressure, mmHg	70.9±6.7	59.5±4.9	0.08
Estimated mean pulmonary arterial pressures, mmHg	46±4	39.3±3.1	0.09
Right atrium area, cm ²	23±1.1	18.4±1.2	0.005
Right atrium area index	12.3±0.7	10±0.6	0.008
Right ventricular end diastolic diameter, mm	49.1±1.7	44±1.5	0.01
Right ventricle end diastolic area, cm ²	28.2±1.3	21.2±1.2	<0.001
Right ventricle end systolic area, cm ²	20.8±1.3	15.3±1.2	0.002
Right ventricle fractional area change (RVFAC), %	26.8±1.8	30.3±2.6	0.16
Ratio of TAPSE/RVEDD	0.44±0.02	0.43±0.03	0.38
Ratio of TAPSE/RVEF	0.55±0.03	0.37±0.01	<0.001
Ratio of TAPSE/RVFC	80±8.2	67.7±5.7	0.11
Right heart catheterization parameters			
Right atrial pressure, mmHg	8.05±0.9	8.2±1.3	0.46
Systolic pulmonary artery pressure, mmHg	73.6±4.1	68.8±3.9	0.21
Diastolic pulmonary artery pressure, mmHg	30.1±1.8	27.4±2.1	0.18
Mean pulmonary artery pressure, mmHg	46.6±2.6	43.8±2.6	0.24
Pulmonary artery wedge pressure, mmHg	9.7±0.7	10.1±1.3	0.4
Pulmonary artery vascular resistance, dynes-sec/cm ⁵	686.3±97	685.1±80	0.5
Systemic vascular resistance, dynes-sec/cm ⁵	1367.2±102	1684.1±121	0.04

All the continuous variables are expressed as mean±SE and categorical variables as frequencies. $P < 0.05$ was considered statistically significant.

P1-201

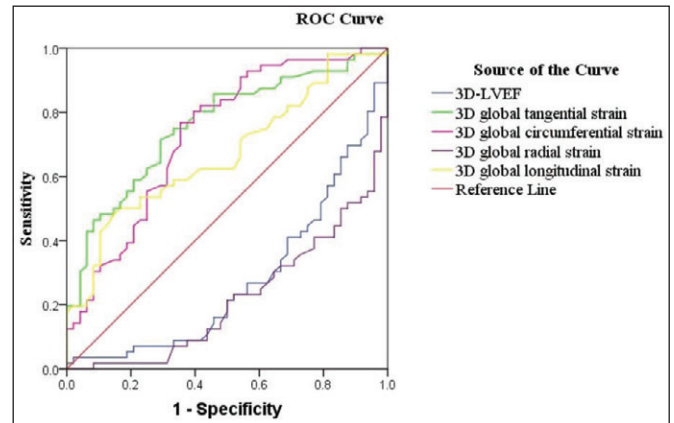
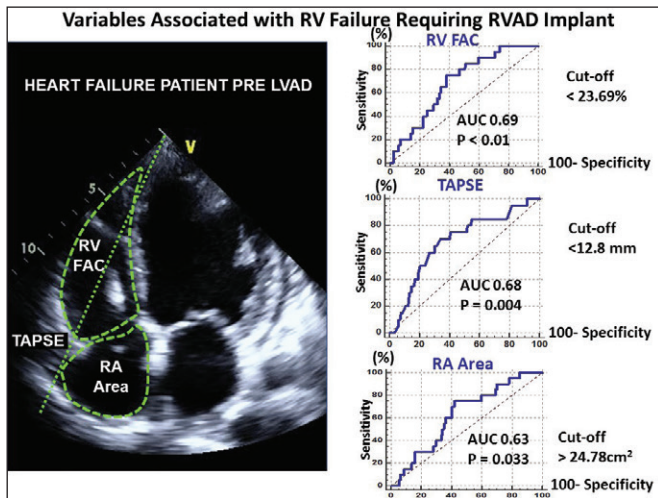
Echocardiographic Markers of Right Ventricular Failure Requiring Right Ventricular Assist Device Support After Left Ventricular Assist Device Implantation in Patients with End-Stage Heart Failure

Yuko Soyama, Maria Karpalioti, David Raymer, Shane LaRue, Britany Dixon, Akinobu Itoh, Justin Vader, John Gorcsan. Washington University in St. Louis, Cardiology Division, St. Louis, MO

Background: Severe right ventricular (RV) failure requiring RV assist device (RVAD) implantation after left ventricular assist device (LVAD) is an important determinant of clinical outcomes. However, it remains difficult clinically to predict severe RV failure requiring RVAD use after LVAD. The objective of this study was to identify echocardiographic variables associated with RV failure requiring RVAD use after LVAD support. **Methods:** We studied 216 patients aged 55±10 years with end-stage HF who underwent continuous-flow LVAD implantation. Baseline echocardiography was performed before LVAD implantation. From the 4-chamber view, we measured RV and RA parameters including RV fractional area change (FAC) and tricuspid annular plane systolic excursion (TAPSE) and RA area. We pre-defined evidence of RV failure as inotropic support > 14 days post LVAD, and severe RV failure as requiring RVAD implantation. **Results:** Of 216 patients, 20 (9%) developed severe RV failure requiring RVAD implantation. RVFAC was measured in 206 patients (95%), TAPSE was measured in 214 patients (98%) and RA area was measured in 202 patients (94%). All 3 parameters were feasible in 200 patients (93%). Receiver operating characteristic (ROC) curves for predicting RVAD use after LVAD implantation were determined (Figures below). RV FAC had the best area under the curve (AUC) (AUC=0.69, $p < 0.01$) for the cut-off values of 23.7%. RV FAC and RA area had the highest sensitivity (75%) in predicting RVAD use ($p=0.004$ and $p=0.033$, respectively). **Conclusions:** RV FAC, TAPSE and RA area are echocardiographic markers of severe RV failure requiring RVAD use after LVAD implantation and have promise for clinical utility.

Poster Session 1 (P1)

Sunday, June 23, 2019



P1-202

Assessment of Left Systolic Functions Using Three Dimensional Speckle-Tracking Echocardiography in Patients with Coronary Slow Flow

Shuo Liu, Yonghuai Wang, Guangyuan Li, Fanxin Kong, Lanting Zhao, Jun Yang, Chunyan Ma. Department of Cardiovascular Ultrasound, First Hospital of China Medical University, China, China

Background: Coronary slow flow (CSF) is characterized by delayed distal vessel opacification in the absence of significant epicardial coronary disease, which is diagnosed by the thrombolysis in myocardial infarction frame count (TFC) during coronary angiography. Current clinical practice tends to underestimate the impact of CSF due to the yet unknown effect on the cardiac function. Therefore, the aim of our study was to evaluate the effects of CSF on left ventricular systolic functions using three dimensional speckle-tracking echocardiography (3D-STE). **Methods:** Seventy-two patients with CSF and fifty age- and sex- matched controls without CSF were enrolled in the study. Three dimensional left ventricular ejection fraction (3D-LVEF), 3D global longitudinal, circumferential, tangential and radial strains were measured by 3D-STE, and the LVEF were measured by two dimensional simpson's method (2D-LVEF) simultaneously. **Result:** Patients with CSF showed significantly lower 3D-LVEF, 3D global longitudinal strain, circumferential strain, tangential strain, and radial strain, but with preserved 2D-LVEF (Table), and a strong correlation was observed between these 3D parameters and the mean TFC. Receiver operating characteristic curve showed lower 3D global longitudinal strain, circumferential strain and tangential strain were the predictor of mean TFC. Furthermore, 3D global tangential strain was the optimal method to detect CSF with the largest area under the curve (area=0.760, $P < 0.001$), and a cutoff value $< -36\%$ predicted CSF with sensitivity 71.4% and specificity 70.8% (Figure). **Conclusion:** The present study demonstrated that CSF lead to a reduction in 3D-LVEF and 3D strain parameters, which indicated that CSF played a notable negative effect on left ventricular systolic functions and should be extensively concerned. 3D-STE may be a useful tool for early detection of left ventricular systolic dysfunction in patients with CSF.

Comparison of left ventricular systolic function parameters between two groups			
Variables	CSFP group(n=72)	Controls group(n=50)	P value
2D-LVEF (%)	62.7±4.1	63.9±4.3	0.189
3D-LVEF (%)	59.3±5.2	63.2±4.3	<0.001
3D global tangential strain (%)	-33.5±4.9	-37.5±3.2	<0.001
3D global circumferential strain (%)	-27.7±4.6	-31.5±4.1	<0.001
3D global radial strain (%)	39.0±5.3	44.2±3.7	<0.001
3D global longitudinal strain (%)	-19.1±4.6	-21.0±2.8	0.013

P1-203

Endurance Exercise in Seniors: Tonic, Toxin or Neither?

Chete M. Eze-Nliam¹, Nelson Schiller B. Schiller², Doug Hayami³, Farzin Ghahghaie², Dwight Bibby², Qi Fang², Greg Marcus¹, Meriam Åström Aneq⁴. ¹Cleveland Clinic, Cleveland, OH; ²University of California, San Francisco, CA; ³Queen Elizabeth II - Halifax Infirmary Site, Halifax, NS, Canada; ⁴Linköpings Universitet, Linköping, Sweden

Background: The beneficial effect of physical activity on the heart function and prevention of cardiovascular heart diseases is established. It is not clear whether the physiological adaptations of the LV to exercise in an older population are associated with deleterious modifications in diastology and ventricular function.. The aim of this study was to analyze ventricular function in older individuals at different levels of exercise training. **Methods:** We included 178 participants at the World Senior Games in St Georges, Utah aged 50 years and above (mean age 68±8yrs, 86 were men; 48%). Three groups were defined based on the type and intensity of sports; low (LIL), moderate (MIL) and high intensity level (HIL). Exclusion criteria were coronary artery disease, atrial fibrillation, valvular heart disease or uncontrolled hypertension. LV and RV size and function were evaluated with an echocardiogram. **Results:** LV deceleration time of inflow through the mitral valve was lower in HIL group (242±54s in LIL, 221±52 s in MIL and 215±58 s in HIL $p = 0.03$). Left atrial volume index (LAVI) was larger in HIL compared to LIL and MIL ($p=0.001$). It remained significantly larger when adjusting for age, gender, heart rate, hypertension and diabetes ($p=0.002$). LV volume was larger in HIL and systolic function was comparable between groups. RV diameter (mm) was larger and the global RV strain (%) was increased in HIL group (35.8±4, LIL; 38.6±5, MIL; 39.2±5, HIL. $p = 0.05$) and (-26.5±5.5, LIL; -24.5±4.4, MIL and -27.0 ± 4.2, HIL, $p= 0.04$). **Conclusion:** LV diastolic filling and RV function were not only preserved but may also be enhanced in senior athletes especially those who participated in high intensity exercise level over long period of time. LV systolic function remained unchanged.

Poster Session 1 (P1)

Sunday, June 23, 2019

Level of Exercise Intensity and Echocardiographic Parameters

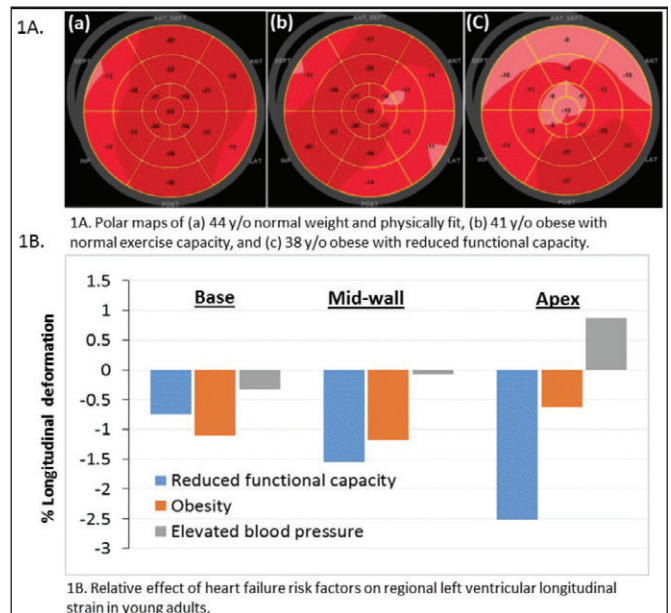
	Sedentary/ Low intensity (Mean±SD,(n))	Moderate intensity (Mean±SD,(n))	High intensity (Mean±SD,(n))	All
Total n	51(29%)	52(29%)	75 (42%)	
MV E (cm/s)	66±11 (49)	69± 12 (49)	68±15 (72)	0.4
MV A (cm/s)	69±15 (49)	73±16 (49)	68±18 (72)	0.3
MV e/a ratio	0.99±0.24 (49)	0.99±0.23 (49)	1.04±0.29 (72)	0.4
MV_dec_time (ms)	242±54 (47)	221±52 (49)	215±58 (71)	0.03*
MV_e ^o _lateral (cm/s)	9.9±2.8 (49)	9.8±2.3 (46)	10.2±3.2 (66)	0.7
E/e ^o _lateral	7.4±2.7 (48)	7.8±2.8 (46)	8.8±8.0 (65)	0.3
MV_e ^o _med (cm/s)	7.5±2.1 (49)	7.6±2.2 (46)	8.0±2.0 (68)	0.3
E/e ^o _med	11.1±11.0 (48)	10.8±9.0 (46)	9.2±10.4 (67)	0.6
LV mass (g/m ²)	70±18 (48)	74±19 (45)	68±15 (49)	0.2
RVID base(mm)	35.8±4.3 (17)	38.6±5.2 (37)	39.2±4.9 (51)	0.047*
RVOT (mm)	34.2±4.2 (17)	35.5±3.8 (37)	35.1±4.3 (49)	0.6
RVEAC (%)	50.6±8.7 (16)	52.4±7.8 (35)	48.9±8.5 (48)	0.17
TAPSE (cm)	20.7±3.3 (16)	21.7±3.4 (37)	22.3±3.4 (47)	0.24
S prime (cm/s)	12.3±1.8 (14)	12.4±1.8 (32)	12.3±1.7 (26)	0.9
RV lat. strain (%)	-26.5±5.5 (17)	-24.5±4.4 (35)	-27.0±4.2 (46)	0.04*
RV strain (%)	-22.5±4.5 (17)	-21.2±3.1 (34)	-22.8±3.9 (46)	0.15
LA volume index (ml/m ²)	32±11 (49)	28±11 (50)	37±17 (72)	0.002*

P1-204

Differential Effect of Lack of Physical Fitness, Obesity and Elevated Blood Pressure on Cardiac Mechanics

Ivan A. Arenas, Juan C. Brenes, Carlos A. Podesta, Jeffrey Lin. Mount Sinai Medical Center, Miami Beach, FL

Alterations in cardiac mechanics occur before the development of heart failure (HF), but it is unclear how risk factors affect regional and/or global mechanics leading to HF. Obesity and high blood pressure have been reported to reduce longitudinal deformation, however, in those studies there was no adjustment by physical fitness. We investigated the independent effect of age, blood pressure (BP), body mass index (BMI) and functional capacity on cardiac mechanics in young adults. **Methods:** 170 healthy adults (25 to 55 y/o) without history of cardiac disease and normal stress echocardiogram were included. Functional capacity was evaluated using a treadmill symptom limited standard Bruce protocol, and number of METs was calculated based on exercise duration. Regional and global left ventricular (LV) strains were measured in resting images by 2D speckle-tracking echocardiography. **Results:** Mean (SD) age was 43(6) years, ~60% were men. Global longitudinal strain (GLS) correlated with BMI ($r = -0.17$; $P=0.02$), diastolic BP ($r = -0.16$; $P=0.03$) and number of METs achieved ($r = 0.16$; $P=0.03$). Age, sex, BMI and number of METs ($P<0.01$) were independently associated with GLS, and there was a linear increase in GLS across quartiles of exercise capacity. The increase in GLS along with exercise capacity was seen in obese or non-obese patients and in those with normal or elevated BP. Apical longitudinal strain (ALS) was a better predictor of functional class compared to mid-wall or basal longitudinal shortening (adjusted r^2 change: 0.16 to 0.2; $P<0.02$). Individuals with reduced physical capacity (e.g. Bottom quartile of exercise capacity) had a greater reduction in ALS, with an apex to base gradient effect (Figure 1B). In contrast, the reduction of GLS related to obesity or elevated BP was greater at the base and mid-wall than at the apex (Figure 1B). Obese individuals with good functional capacity have better apical strain compared to those with decreased exercise tolerance (Figure 1A). **Conclusions:** Obesity and reduced exercise tolerance are independently associated with reduced LV longitudinal shortening. Lack of physical fitness was related to greater reduction in apical shortening while obesity and blood pressure appear to affect more the mid-wall and basal segments, suggesting different pathological mechanisms.



P1-205

Tricuspid Regurgitation Does Not Impact Right Ventricular Contractile Pattern in Pulmonary Arterial Hypertension

Abhishek Chaturvedi¹, Mitha Naik¹, Jose Ricardo P.O.², Talha Meeran³, Amresh Raina¹. ¹Allegheny Health Network, Pittsburgh, PA; ²Ascension Borgess Hospital, Kalamazoo, MI; ³Advanced Heart Failure and Cardiac Transplant, Fortis Hospital, Mumbai, India

Background: Pulmonary arterial hypertension (PAH) is often associated with tricuspid regurgitation (TR) which may lead to right ventricular (RV) remodeling and dysfunction resulting in adverse outcomes. Prior studies have suggested that echocardiographic (TTE) metrics of longitudinal RV contraction such as TAPSE are the afterload response elements of RV function in PAH. We sought to determine whether significant TR, by allowing a low afterload release circuit for the RV, is associated with altered contractile patterns in patients with PAH with a relative increase in longitudinal contraction. **Methods:** We retrospectively analyzed records from 55 PAH patients who had TTE, right heart catheterization and cardiac MRI within 3 months. Patients were divided into two groups: >moderate TR (N=17) versus absent or mild TR (noTR) (N=38) on TTE. Demographic, TTE, MRI and hemodynamic parameters were compared between the groups using STATA 15.0 (StataCorp, College Station, TX). **Results:** Both groups were similar in age (mean age: 52 vs 56 years, $p=0.19$) but predominantly female in the noTR group (59% vs 90%, $p=0.009$). Patients in the TR group were found to have significantly larger right atrial area (25 vs 18 cm², $p<0.001$) and RV end diastolic diameter (53 vs 43 mm, $p<0.001$) compared to the noTR group. In addition, TAPSE, RV fractional area change (RVFAC) and RV ejection fraction on MRI were lower in patients with TR while mean pulmonary artery pressure and pulmonary vascular resistance were higher in TR patients (Table 1). Interestingly, the ratio of TAPSE to RVFAC on TTE and ratio of TAPSE to RV ejection fraction on MRI were similar in groups with and without significant TR. On regression analysis, TR was not associated with the ratio of TAPSE to RVFAC (β , $p: 0.16, 0.3$) and the ratio of TAPSE to RVEF (β , $p: 0.04, 0.75$). **Conclusion:** Our findings suggest that TR does not impact RV contractile pattern in patients with RV dysfunction due to PAH and that TAPSE remains a reliable metric of RV function in PAH patients with moderate or greater TR. Larger studies are needed to confirm our findings.

Poster Session 1 (P1)

Sunday, June 23, 2019

Table 1: Baseline Characteristics of Pulmonary Arterial Hypertension Patients Based on Presence or Absence of Significant Tricuspid Regurgitation (N=55).

Parameters	With TR (N=17)	Without TR (N=38)	P
Demographic parameters			
Age, years	51.7±44.4	55.7±2.2	0.19
Female, %	58.8	89.5	0.009
Body Surface area, m ²	1.8±0.05	1.9±0.04	0.35
Echocardiographic parameters			
Right ventricular ejection fraction, %	37.2±2.4	47.9±1.9	0.0008
Tricuspid annular plane systolic excursion (TAPSE), mm	16.5±1.2	20.3±0.8	0.005
Left atrium diameter, mm	34.7±1.9	35.1±1.1	0.43
Left atrium volume index, mL/m ²	29.2±3.1	25.5±1.7	0.14
Left ventricular end diastolic diameter, mm	41.1±1.4	43.3±1.1	0.12
Left ventricular ejection fraction, %	61.2±2.2	64.1±1.0	0.09
Tricuspid regurgitation jet area, cm ²	8.4±1.2	3.4±0.5	<0.001
Right ventricular outflow tract acceleration time, ms	66.6±6.5	75.8±3.7	0.1
Tricuspid regurgitation velocity, m/s	54.9±34.9	50.8±23.0	0.46
Peak tricuspid regurgitation gradient, mmHg	72.9±5.8	49.7±4.5	0.002
Mean tricuspid regurgitation gradient, mmHg	42.8±3.5	31.5±2.7	0.008
Estimated right atrial pressure, mmHg	7.5±1.0	6.1±0.6	0.11
Estimated systolic pulmonary artery pressure, mmHg	80.4±6.1	55.9±4.7	0.002
Estimated mean pulmonary arterial pressure, mmHg	50.3±3.8	37.8±3.0	0.007
Right atrium area, cm ²	24.8±1.4	18.2±0.9	<0.001
Right atrium area index	13.5±0.8	9.8±0.5	<0.001
Right ventricular end diastolic diameter, mm	53.1±1.8	42.9±1.2	<0.001
Right ventricle end diastolic area, cm ²	27.5±1.6	22.3±1.2	0.008
Right ventricle end systolic area, cm ²	21.4±1.5	15.6±1.1	0.002
Right ventricle fractional area change (RVFAC), %	22.3±2.1	32.0±2.1	0.004
Ratio of TAPSE/RVFE	0.45±0.04	0.44±0.02	0.38
Ratio of TAPSE/RVAFAC	79.2±10.2	68.5±5.1	0.15
Right heart catheterization parameters			
Right atrial pressure, mmHg	10.9±1.7	6.9±0.9	0.02
Systolic pulmonary artery pressure, mmHg	77.3±3.7	67.8±3.8	0.07
Diastolic pulmonary artery pressure, mmHg	34.5±1.9	25.7±1.8	0.002
Mean pulmonary artery pressure, mmHg	51.0±2.4	42.2±2.4	0.01
Pulmonary artery wedge pressure, mmHg	10.1±1.3	9.9±1.0	0.46
Pulmonary artery vascular resistance, dynes-sec/cm ⁵	886.9±121.5	595.5±66.1	0.01
Systemic vascular resistance, dynes/sec/cm ⁵	1884.7±181.2	1404.5±82.5	0.004

All the continuous variables are expressed as mean±SE and categorical variables as frequencies. P<0.05 was considered statistically significant.

P1-206

Right Ventricular Strain Derived from Multiple 2D-Views is a Better Predictor of Cardiovascular Events Compared with Right Ventricular Free Wall Longitudinal Strain

Upasana Jarori, Deborah Green-Hess, Harvey Feigenbaum, Stephen S. Sawada. Indiana University, Indianapolis, IN

Background: Numerous studies have demonstrated the prognostic value of right ventricular (RV) free wall longitudinal strain assessed by 2D speckle tracking, but evaluation is limited to one apical 4-chamber view. We have shown that RV strain can be acquired using multiple 2D-views. This study compared the prognostic value of multi-view RV strain to RV free wall longitudinal strain (FWS). **Methods:** GE Vivid echocardiographs were used to acquire images in 3 views of the RV in 106 subjects (mean age 56 yrs, 60 % male) with variable RV systolic function and EF>40%. The RV focused apical 4-chamber (4C) view imaged the septum and RV free wall, the apically tilted medially angulated long axis (LAX) view imaged the anterior and inferior walls and the short axis (SAX) view at the aortic valve level imaged the RV outflow tract. 2D strain was processed using a semi-automated software program. For each subject, RV-FWS was calculated as the average of the basal, mid and apical free wall segments and global RV strain was calculated as the weighted average of the 3 views (4C and LAX with 6 segments, SAX with 4 segments). Subjects were followed for cardiovascular (CV) events (cardiac death, cardiac arrest, cardiogenic shock, heart failure and malignant arrhythmias). SPSS was used for Cox regression and ROC analysis. **Results:** 106 subjects with mean global RV strain of -17.9 ± 4.6 and RV-FWS of -20.2 ± 7 were followed for 19 ± 17 months. On Cox regression analysis, significant univariate predictors of events were history of coronary artery disease (p = 0.01), hypertension (p = 0.01), right atrial area (p<0.001), RV outflow tract diameter (p = 0.03), RV basal diameter (p<0.001), global RV strain (p<0.001) and RV-FWS (p<0.001). Age, gender, ejection fraction and type 2 diabetes mellitus were not predictors. On subsequent multivariate analysis, RV basal diameter ($\chi^2 = 30$), global RV strain ($\chi^2 = 24.7$) and h/o CAD ($\chi^2 = 7.9$) emerged as independent predictor of events. RV-FWS ($\chi^2 = 10.8$) was not an independent predictor of events. ROC analysis revealed that global RV strain had an area under the curve of 0.801 (95% CI: 0.708 - 0.894) with optimal cutoff value of -17.5% (Sensitivity 81%, Specificity 67%), while RV-FWS had an area under the curve of 0.729 (95% CI: 0.627 - 0.832) with optimal cutoff value of -19.3 % (Sensitivity 69%, Specificity 65%). **Conclusion:** Global RV strain derived from multiple views is an independent predictor of cardiovascular events while RV free wall longitudinal strain is not. Global RV strain is better at risk stratifying subjects with various levels of RV systolic function when compared to RV-FWS.

P1-207

Left Atrial Remodeling May Precede Measurable Changes in Diastolic Function Variables Among TAVR Patients: A Serial Echocardiographic Study

Colleen M. Harrington¹, Rohit Malhotra¹, Nouran Sorour¹, Ahmed Nagy¹, Eugene Chung², Gerald P. Aurigemma¹. ¹University of Massachusetts, Worcester, MA; ²The Christ Hospital, Cincinnati, OH

Background: Transcatheter aortic valve replacement (TAVR) has been shown to improve outcome and relieve symptoms in severe AS. The mechanism has been assumed to include improved cardiac systolic and diastolic function due to afterload reduction. Our aim was to study the change in cardiac function following TAVR, with special emphasis on reduction in diastolic dysfunction (DD). **Methods:** We analyzed standard early (E) and late (A) mitral inflow velocities, tissue Doppler e', and left atrial volume index (LAVi) before and 1 year following TAVR. 142 patients with complete data were included in the final analysis; we excluded pts with atrial fibrillation and mitral annular calcification, as these confound diagnosis of DD. **Results:** (Table) Except for LAVi and peak A, there was very little change in mean values or grade of DD. Surprisingly, at 1 year there was little change in ejection fraction (EF). **Conclusion:** At 1 year following successful TAVR, there was a strong signal that diastolic function improved, namely that LA size decreased and LA contractile function increased. However, this was not immediately obvious from the grade of diastolic dysfunction or the individual parameters, e.g. E/e'. These data suggest that improvements in functional status and outcome from TAVR may not be reflected by current approaches to diastolic function grading, or may not be apparent at 1 year following the procedure

Parameter	Pre TAVR (Mean)	One year post TAVR (Mean)	P value
Left ventricular ejection fraction	49.8 %	49.1%	0.46
Left atrial Volume Index	47.2 mL/m ²	44.1 mL/m ²	0.043
Peak A velocity	99.3 cm/s	105.5 cm/s	0.02
Peak E velocity	102.2 cm/s	101.1 cm/s	0.69
Average E/e'	20.8	21.05	0.814
Peak TR velocity	3.0 m/s	2.95 m/s	
Isovolumic contraction time	97.1 ms	100.4 ms	0.56
Isovolumic relaxation time	90.1 ms	93.6 ms	0.57
Mean aortic valve gradient	46.5 mm Hg	10.7 mm Hg	0.00
LV Mass Index	99 g/m ²	114 g/m ²	0.0007
Normal diastolic function	5	5	-
Grade 1 diastolic dysfunction	16	16	-
Grade 2 diastolic dysfunction	54	60	-
Grade 3 diastolic dysfunction	11	7	-

P1-208

Echocardiographic Evaluation of Athletes' Heart in Male and Female Soccer Players

Giorgio Galanti¹, Melissa Orlandi¹, Benedetta Tosi¹, Gianni Pedrizzetti², Loira Toncelli¹. ¹Università degli Studi di Firenze, Florence, Italy; ²Università degli Studi di Trieste, Trieste, Italy

BACKGROUND: Echocardiography and strain analysis can show not only morphological but also functional changes in athletes' heart secondary to training. We aimed to assess gender differences in cardiac remodeling of elite male and female soccer players before seasonal training; athletes were homogenous for lifestyle, load and type of training. We also studied its temporal progression in male athletes over a regular season. **METHODS:** A cross-sectional study examined gender differences in cardiac remodeling of 55 professional soccer players compared to 39 paired controls at baseline conditions. A 6-month longitudinal study aimed to assess the impact of training on athletes' heart of 17 male players. Athletes were examined with 2D and speckle tracking echocardiography before and during the regular season. **RESULTS:** All subjects showed values within the normal range. Male and female athletes showed a significant increase, compared to controls, of wall thickness (WT: 10.44±0.96 vs 9.29±0.66, p<0.001; 8.78±0.84 vs 8.29±0.57, p=0.04), indexed cardiac mass (iCM: 95.93±14.62 vs 82.82±9.73, p<0.001; 123.67±21.97 vs 98.62±11.82, p<0.001), and ejection fraction (EF; 60.69±5.59 vs 56.68±3.54, p=0.01; 62.06±6.33 vs 57.32±5.52, p=0.02); male athletes showed a significant increase in left ventricular diastolic volume (122.50 ±21.41 vs 102.99±22.08; p<0.001), while female athletes had higher global longitudinal strain (GLS) compared to female controls (-26.52±4.1 vs -23.5±2.8, p=0.01) and global male study population. No significant differences were observed in right ventricle remodeling and GLS. Multiple linear regression showed a correlation between both sex and training, and cardiac remodeling. Athletes followed up for 6-month showed significant reduction in EF (60.69±5.59 vs 55.59±7.20, p=0.005) and in GLS (-24.27±3.4 vs -20.78±2.21, p<0.001) compared to basal measurements, but no significant differences in WT, iCM and ventricular volumes. **CONCLUSIONS:** Cardiac remodeling in athletes is a balanced physiological phenomenon occurring in both sexes and is more pronounced in males; however, women seem to have higher GLS independently of training. Seasonal training is associated with normal cardiac function, increased mass and volumes, and reduced EF and GLS. These findings suggest that exercise-induced cardiac remodeling is complex and classic cardiac hypertrophy is not the only feature happening; athlete's heart adapts to exercise decreasing basal function to be more efficient during effort.

Poster Session 1 (P1)

Sunday, June 23, 2019

P1-209

A New Normal? Defining Cardiomechanical Properties in Theoretical Models, Echocardiograms, and MRI

Vinayak Kumar, Chaitanya Rao, Armando Manduca, Nandan Anavekar. Mayo Clinic, Rochester, MN

Background: The current understanding of myocardial contractility is limited, especially regarding the material properties of myocardium. The myocardium is assumed to be incompressible, though recent evidence indicates that the myocardial volume in systole (MV_s) and diastole (MV_d) are different. The reasons for this difference in MV are unclear. Notably, this has never been rigorously studied in a prospective cohort of patients without cardiac risk factors. **Methods:** Part 1: The standard literature values for strain and myocardial dimensions were applied to two mathematical models of the left ventricle (LV) to calculate MV_s and MV_d. The two models are 1) the standard truncated ellipsoid model of the LV, and 2) a new truncated ellipsoid model with a thin apex that more accurately models LV anatomy. Part 2: A prospectively derived cohort of patients after 2010 with no cardiac risk factors at Mayo Clinic obtained transthoracic echocardiogram (TTE) and/or cardiac MRI. Age, gender, and imaging reports were used to calculate MV_s and MV_d. JMP[®] was used to perform statistical analysis. **Results:** Part 1: In both mathematical models, MV_s/MV_d ≠ 1, reinforcing that myocardial volume varies throughout the cardiac cycle. Part 2: 101 patients were recruited to receive cardiac MRI, 51 of whom also agreed to obtain TTE. Age and gender were similar between the two populations. MV_s/MV_d was significantly different when comparing cardiac MRI (mean 0.8644, SD 0.044) vs TTE (mean 0.7903, SD 0.0647). In comparing the male and female populations for cardiac MRI data, the mean age is similar at 39 years but the mean MV_s/MV_d is smaller in females than males (0.8547 vs 0.8787, p=0.003). In comparing the male and female populations for TTE data, the mean age is similar at 40 years but the mean MV_s/MV_d is smaller in males than females (0.7655 vs 0.8038, p=0.041). This disparate gender difference was preserved in subgroup analysis of patients who received both MRI and TTE. In both imaging modalities, there was minimal correlation of MV_s/MV_d with age. **Conclusion:** These results indicate that contrary to what the literature assumes, the myocardium is compressible. As such, the standard practice of measuring cardiac dimensions in diastole alone incompletely captures cardiac physiology. The results also indicate that normal hearts in both cardiac MRI and TTE have MV_s/MV_d < 1 and that age is not associated with MV_s/MV_d, with unclear gender association. MV_s and MV_d should be studied in pathologic hearts to determine whether this index can characterize cardiac function and predict outcomes. *Abbreviations: standard deviation (SD)*

P1-210

Assessment of Right Ventricular Function Using Comprehensive Eighteen-Segment Echocardiographic Strain Analysis in Patients Undergoing Left Ventricular Assist Devices

Michael Yaoyao Yin, Stephen Ishihara, Brandon Sullivan, Thomas Anderson, Anna Catino, Stephen H. McKellar, Antigone Koliopoulou, Josef Stehlik, James C. Fang, Craig H. Selzman, Stavros Drakos, Omar Wever-Pinzon. University of Utah, Salt Lake City, UT

Background: Acute right ventricular failure (RVF) is a frequent complication after implantation of left ventricular assist devices (LVAD). Prior studies have assessed various RV echocardiographic parameters as potential predictors of post-LVAD RVF, including peak longitudinal strain of the RV lateral wall from single four-chamber view, although no strong associations have been found. Knowing the differential contribution of each RV segment to RV function, we sought to use a novel three-view, eighteen-segment strain analysis to evaluate specific RV segments in patients undergoing LVAD implantation. **Methods:** LVAD candidates were prospectively enrolled and echocardiograms were performed immediately before LVAD implant. Images of modified RV 4-chamber, 2-chamber and 3-chamber views were obtained, and strain analysis was performed on eighteen RV segments (Figure 1). RVF was defined as the need for RV assist devices, inotropes for >14 days or pulmonary vasodilator for >48 hours post-LVAD. Baseline clinical characteristics and 2-D, 3-D and strain echocardiographic parameters were compared between patients with and without post-LVAD RVF. **Results:** Fourteen patients were enrolled, of whom ten developed RVF post-LVAD. There were no significant differences in the baseline clinical characteristics, 2-D and 3-D echocardiographic parameters, or RV peak global longitudinal strains between patients with and without post-LVAD RVF. Patients without RVF had significantly higher peak strain in the basal and mid segments of the anterior, lateral and posterior free walls, while there were no differences between the groups in septal segments (Table 1). **Conclusion:** Longitudinal RV strain, using a comprehensive 18-segment approach was able to discriminate patients with and without RVF after LVAD implant. Further assessment with a larger number of patients is warranted.

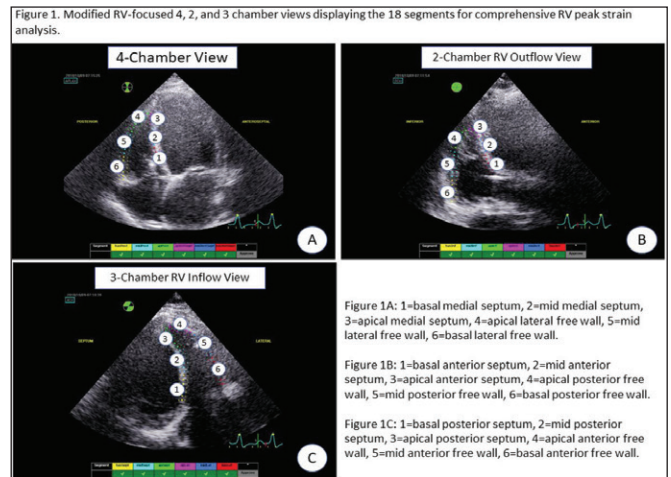


Table 1. Comparison of RV echocardiographic parameters between patients with and without RVF.

	Right Ventricular Failure (n=10)	No Right Ventricular Failure (n=4)	P-value
Pre-LVAD 3-D RV Echo Parameters			
3-D RV ESV (ml)	77.83 ± 22.92	79.10 ± 10.04	0.74
3-D RV EDV (ml)	111.83 ± 26.46	121.45 ± 0.78	0.99
3-D RVEF (%)	30.39 ± 10.99	34.69 ± 8.49	0.51
Pre-LVAD RV Strain Parameters (%)			
RV GLS	-7.11 ± 3.39	-10.58 ± 2.35	0.12
Basal Medial Septum	-4.43 ± 0.22	-7.75 ± 4.35	0.22
Mid Medial Septum	-2.70 ± 3.80	-5.00 ± 6.38	0.72
Apical Medial Septum	-2.60 ± 5.08	3.75 ± 13.22	0.15
Basal Lateral FW	-8.70 ± 6.90	-21.50 ± 1.73	0.007
Mid Lateral FW	-9.20 ± 5.82	-20.50 ± 3.31	0.007
Apical Lateral FW	-7.30 ± 5.42	-10.25 ± 9.91	0.48
Basal Posterior Septum	-4.30 ± 3.06	-8.50 ± 2.38	0.02
Mid Posterior Septum	-4.20 ± 2.34	-5.75 ± 1.89	0.32
Apical Posterior Septum	-4.50 ± 6.94	-2.75 ± 14.95	0.40
Basal Anterior FW	-4.30 ± 6.68	-23.00 ± 8.04	0.006
Mid Anterior FW	-6.00 ± 5.41	-14.25 ± 6.75	0.05
Apical Anterior FW	-7.10 ± 7.16	-3.75 ± 8.96	0.39
Basal Anterior Septum	-2.30 ± 6.57	-7.25 ± 7.93	0.32
Mid Anterior Septum	-4.90 ± 4.58	-3.00 ± 8.28	0.62
Apical Anterior Septum	7.00 ± 5.00	4.50 ± 8.35	0.02
Basal Posterior FW	-2.60 ± 8.33	-18.75 ± 3.77	0.005
Mid Posterior FW	-4.70 ± 7.93	-17.00 ± 3.55	0.007
Apical Posterior FW	-8.60 ± 3.27	-11.75 ± 6.02	0.35

Continuous variables are expressed as mean (standard deviation). Categorical variables are expressed as n (%). Parameters with significant differences are displayed in red. ESV, end systolic volume; EDV, end diastolic volume; FW, free wall; GLS, global longitudinal strain; RVEF, right ventricular ejection fraction.

P1-211

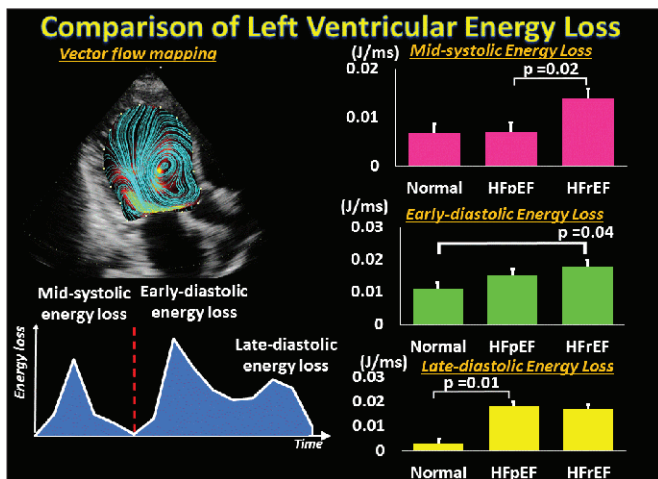
Comparison of Left Ventricular Energy Loss Assessed by Vector Flow Mapping in Heart Failure Patients with Reduced and Preserved Ejection Fraction

Yuko Soyama¹, Nobuyuki Kagiya¹, Masataka Sugahara², Maria Karpmpalioti¹, Justin Vader¹, John Gorcsan¹. ¹Washington University in St. Louis, St. Louis, MO; ²Hoshigaoka Medical Center, Hirakata, Japan

Background: Vector Flow Mapping (VFM) assessment of left ventricular (LV) energy loss is a novel means to assess LV flow dynamics non-invasively. Heart failure (HF) is classified clinically by LV ejection fraction: HF with preserved ejection fraction (HFpEF) and HF with reduced ejection fraction (HFrEF). Little is known about LV energy loss in patients with HFpEF compared with those with HFrEF. We aimed to compare LV energy loss in HFpEF and HFrEF patients. **Methods:** We studied 86 subjects; 47 HF patients and 39 normal subjects. HF was categorized as HFpEF (LVEF > 50%) or HFrEF (LVEF ≤ 35%). LV energy loss was assessed from the apical long axis view using VFM (PROSOUND F75 Premier CV Hitachi Corp). Three peaks of energy loss in the cardiac cycle were quantified as mid-systolic, early-diastolic and late-diastolic peak energy loss. Also, we measured LV global longitudinal strain (GLS) using the speckle tracking method. **Results:** VFM was feasible in all subjects. There were 35 HFrEF patients (EF=23.7±12.1%, GLS=-5.25±2.0%), 12 HFpEF patients (EF=9.9±6.9%, GLS=-2.4±4.3%) and 39 normal subjects (EF=66.6±4.6%, GLS=18.5±1.4%). The mid-systolic energy loss in HFrEF patients was significantly larger than in normal control or HFpEF (0.014±0.012, 0.0068±0.0034, 0.0070±0.0048 J/ms, p=0.02). Early-diastolic energy loss in normal controls, HFpEF and HFrEF were 0.011±0.009, 0.015±0.008 and 0.018±0.014 J/ms, respectively (p=0.04). Late-diastolic energy loss was significantly higher in both HFpEF and HFrEF than in normal controls (0.018±0.016, 0.017±0.0009 and 0.003±0.001 J/ms, p=0.01). **Conclusions:** Mid-systolic energy loss was larger in HFrEF patients than normal controls or HFpEF patients. Late-diastolic energy loss was significantly higher in both HFpEF and HFrEF patients than in normal controls. VFM has potential to enhance understanding of HF with reduced and preserved EF.

Poster Session 1 (P1)

Sunday, June 23, 2019



P1-212

Comparison of Three-Dimensional Speckle-Tracking Echocardiography and Cardiac Magnetic Resonance Feature Tracking for Evaluation of Left Ventricular Volumes and Function

Ming-dan Deng, Hong Tang. West China Hospital of Sichuan University, Chengdu, China

Background: Three-dimensional speckle-tracking echocardiography (3DSTE) becomes feasible recently. However, values of 3DSTE parameters varies among vendors and software, and data related to its validation was limited. This study aimed to assess the accuracy of 3DSTE by comparing to cardiac magnetic resonance feature tracking (CMRFT) for evaluation of left ventricular volumes and function. **Methods:** 93 out of 121 patients with various heart diseases were successfully enrolled. Echocardiography and CMR were performed on the same day. The values of left ventricular volumes, EF, global longitudinal strain (GLS), global circumferential strain (GCS) and global radial strain (GRS) were calculated off-line using EchoPAC software for 3DSTE and cvi42 software for CMRFT. Inter-technique comparisons included linear regression and Bland-Altman methods. **Results:** An excellent correlation was found between 3DSTE and CMRFT for the measurement of left ventricular volumes ($r, 0.97$) and EF ($r, 0.93$), but 3DSTE provided smaller LV volumes estimates (bias \pm SD, -13 ± 20.5) and slightly higher EF estimated (bias \pm SD, $4\pm 6.6\%$). For myocardial deformation, the parameter with the highest correlation was GCS ($r, 0.86$), followed by GLS ($r, 0.85$) and GRS ($r, 0.80$). Relatively small bias and narrow limits of agreement were found in GLS and GCS (bias \pm SD, $-1.2\pm 2.9\%$ and $1.2\pm 3.3\%$ respectively). But value of GRS was greater in 3DSTE compared to CMRFT (bias \pm SD, $9.6\pm 10.1\%$). **Conclusion:** Although left ventricular volumes are underestimated and GRS is overestimated by 3DSTE, the high correlation of EF, GLS and GCS between 3DSTE and CMRFT makes 3DSTE a useful tool for the evaluation of left ventricular function in patients.

P1-213

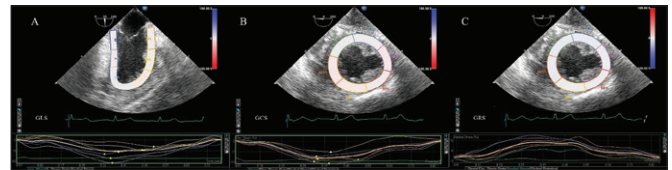
Effect of Pericardial Incision on Left Ventricular Morphology and Deformation in Patients During Coronary Artery Bypass Graft

Lanting Zhao. Department of Cardiovascular Ultrasound, First Hospital of China Medical University, Shenyang, Liaoning, China

Background: Accurate assessment of left ventricular (LV) systolic function is essential in patients after coronary artery bypass graft (CABG). Deformation parameters including global strain and twist obtained by two dimensional speckle tracking echocardiography could provide a complete assessment of LV systolic function and detect subtle systolic dysfunction. Pericardium plays an important role in maintaining cardiac motion, however, whether the incised pericardium without suturing during CABG could influence LV deformation is unclear. In this study, we sought to investigate the effect of pericardial incision on LV morphology and deformation in patients during CABG. **Methods:** Intraoperative transesophageal echocardiography was conducted in 18 patients during elective CABG before and after pericardial incision in 5 minutes. LV longitudinal and mid-cavity transversal diameters, sphericity index, relative wall thickness, volumes and ejection fraction were measured. LV global longitudinal (GLS), circumferential (GCS) and radial strain (GRS), and twist obtained by two dimensional speckle tracking echocardiography were measured (Figure). **Results:** After pericardial incision, LV mid-cavity transversal diameters increased while sphericity index decreased ($P<0.001$), and relative wall thickness increased ($P<0.05$) immediately. Meanwhile, GLS and GCS were significantly reduced, while GRS had a notable increased ($P<0.001$). LV twist significantly decreased ($P<0.001$) simultaneously, however, LV volumes and ejection fraction remained unchanged (Table). **Conclusions:** Pericardial incision lead to LV morphology immediately transformed from ellipsoid to round. Meanwhile, LV deformation altered with a decrease of longitudinal and

circumferential shortening while an increase of radial thickening, and a depressed twist despite unchanged ejection fraction. Therefore, the altered deformation parameters may probably not reflect the real LV systolic function in patients after CABG.

Changes in LV morphology and systolic function before and after pericardial incision			
Variable	Before pericardial incision (n=18)	After pericardial incision (n=18)	P value
LV longitudinal diameter (mm)	70.67 \pm 5.52	69.38 \pm 8.92	0.186
LV mid-cavity transversal diameter (mm)	38.67 \pm 3.79	43.33 \pm 4.22	0.000
LV sphericity index	1.84 \pm 0.14	1.60 \pm 0.13	0.000
Relative wall thickness (cm)	0.35 \pm 0.06	0.38 \pm 0.08	0.020
LV end-diastolic volume (ml)	106.78 \pm 29.33	108.11 \pm 29.22	0.178
LV end-systolic volume (ml)	46.83 \pm 19.83	48.39 \pm 19.72	0.295
LV stroke volume (ml)	59.94 \pm 11.45	59.72 \pm 13.19	0.883
LV ejection fraction (%)	57.34 \pm 6.24	56.29 \pm 7.26	0.387
Global longitudinal strain (%)	-16.49 \pm 3.14	-10.86 \pm 3.28	0.000
Global circumferential strain (%)	-22.72 \pm 5.63	-18.05 \pm 6.05	0.000
Global radial strain (%)	17.99 \pm 6.01	24.23 \pm 7.55	0.000
Twist($^{\circ}$)	9.10 \pm 3.55	4.02 \pm 1.91	0.000



P1-214

Prognostic Impact of Left Ventricular Diastolic Dysfunction in Subjects with Reserved and Reduced Ejection Fraction

Lin Wang, Jonathan Weber, Michael Passick, Jane J. Cao. St. Francis Hospital the Heart Center, Roslyn, NY

Introduction: Left ventricular (LV) diastolic dysfunction (DD) is an important cause of mortality and heart failure (HF) in patients with preserved ejection fraction (LVEF). It remains unclear if there is prognostic impact of LVDD in patients with reduced ejection fraction (EF). **Methods:** Study subjects were selected from a research study where consecutive patients had undergone echocardiography (echo) at a single center (2007-2015). LVDD was assessed by echo following the algorithm from the latest ASE guidelines. Preserved LVEF was defined as having EF $\geq 50\%$ and reduced EF as having EF $< 50\%$. Those subjects with normal EF and normal diastolic function were served as controls. Cox proportional hazards models were utilized to estimate the hazards of a composite outcome that included all-cause mortality obtained from the National Death Index and hospitalized HF from medical records. Demographic and medical history covariates were included for confounding control in the models. **Results:** A total of 500 subjects were included who were 66% male and were a mean age of 55 \pm 16 years. During an average follow up of 2.6 \pm 2.8 years (up to 12 years) 112 events occurred including 42 deaths and 70 patients hospitalized for HF. In a multivariate Cox proportional hazard model adjusting for age, gender, body surface area, smoking history, presence of hypertension, coronary artery disease, diabetes and hyperlipidemia, there was significantly increased risk of composite outcome among DD patients with preserved and reduced EF with the hazard ratio of 4.3 (95% CI 2.1 to 5.7) and 7.4 (CI 4.0 to 13.9), respectively. Moreover, among those with reduced EF advanced DD (grade II and III) was associated with greater risk of adverse outcomes than mild DD (grade I) in excess of 4.0 times (CI 2.3 to 6.8). **Conclusions:** LV diastolic dysfunction defined by the latest ASE guidelines is associated with significantly increased risk of mortality and hospitalized HF not only in patients with preserved LVEF but of greater risk in patients with reduced LVEF. In addition, among patients with reduced LVEF diastolic function of advanced grade is associated with worse outcome than mild grade. Our findings suggest characterizing diastolic dysfunction is valuable in prognostication of patients with reduced LVEF.

Poster Session 1 (P1)

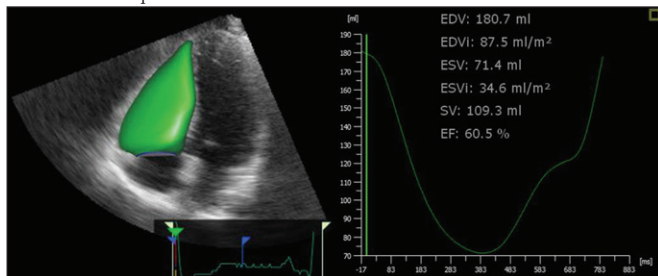
Sunday, June 23, 2019

P1-215

Machine Learning Based 3D Echocardiographic Automated Quantification of Right Ventricular Size and Function: Validation Against Cardiac Magnetic Resonance

Davide Genovese¹, Nina Rashedi¹, Lynn Weinert¹, Akhil Narang¹, Karima Addetia¹, Amit R. Patel¹, David Prater², Alexandra Gonçalves², Victor Mor-Avi¹, Roberto M. Lang¹. ¹University of Chicago, Chicago, IL; ²Philips Healthcare, Andover, MA

Background: Three-dimensional echocardiography (3DE) allows accurate and reproducible measurements of right ventricular (RV) size and function. However, widespread implementation of 3DE in routine clinical practice is limited because the existing software packages are relatively time-consuming and skill-demanding. The aim of this study was to test the accuracy and reproducibility of new machine-learning (ML) based, fully automated software for 3D quantification of RV size and function. **Methods:** Fifty-six unselected patients with a wide range of RV size and function and image quality, referred for clinically indicated cardiac magnetic resonance (CMR) imaging, underwent a transthoracic 3DE exam on the same day. End-systolic and end-diastolic RV volumes (ESV, EDV) and ejection fraction (EF) were measured using the ML-based algorithm and compared to CMR reference values using Bland-Altman and linear regression analyses. **Results:** The automatic approach was accurate in 32% patients with analysis time of 15±1 sec. Endocardial contour editing was necessary after the automated post-processing in the remaining 68% patients, prolonging analysis time to 114±71 sec. RV volumes and EF measurements were accurate in comparison to CMR reference (biases: EDV: -25.6±21.1 ml; ESV: -7.4±16 ml; EF: -3.3±5.2%) and showed excellent reproducibility (coefficient of variations <7% and intraclass correlation coefficient ≥0.95 for all measurements). **Conclusion:** The new ML-based 3DE algorithm provided accurate and reproducible automated RV volume and EF measurements in one-third of unselected patients without any boundary editing. In the remaining patients, editing required <2 minutes on average and resulted in accurate measurements. This approach provides a promising solution for fast and accurate quantification of RV size and function.



P1-216

Right Ventricular Long Axis Deformation (RVLAD): A Novel Marker for Quantifying Function

Vlad Radulescu¹, Nicholas Chan¹, Kevin F. Kennedy², Robert Faigen¹, Andrew Scatola¹, Gaurav Rao¹, Ewelina Kuzawinski¹, Lauren Finkelstein¹, Erica Chung¹, Justine Carneglia¹, Bani M. Azari¹, Sonia Henry¹. ¹Northwell Health, Manhasset, NY; ²Mid America Heart Institute, Kansas, MO

Background: Echocardiographic evaluation of right ventricular (RV) function continues to be challenging due to incomplete visualization of the RV free wall and cardiac translational motion. Therefore, we designed a novel method of quantification using transthoracic echocardiography (TTE) called right ventricular long axis deformation (RVLAD). This measure of RV function evaluates longitudinal shortening of RV from base to apex, independent of free wall and translational motion. The aim of this study was to validate this novel method. **Methods:** RVLAD measures were performed retrospectively on post-image acquisition of 80 TTEs, using standard views, performed on patients referred for routine TTE. Following image acquisition, the RV apex and RV lateral tricuspid annulus were identified in the RV focused view. A linear strain line was drawn between these 2 points, which were speckle tracked through the cardiac cycle, resulting in a RVLAD value. We used Philips EPIC 7c aCMQ 1.85 exclusively for consistency in strain analysis. Each study was independently reviewed by three board certified readers. RVLAD was compared to the consensus of three accepted measurements of RV function: TAPSE, S', and visual qualitative assessment. Continuous variables were compared using a Student's T-test, while categorical variables were compared using chi-square or Fisher's exact test. This study was approved by our institutional IRB. **Results:** 80 studies were analyzed with TAPSE, S', and RV visual assessment, 70 demonstrated normal RV function and 10 abnormal RV function. RVLAD measurements were compared to these standard RV measurements. A ROC analysis was performed comparing RVLAD to agreement of three standard measures. This yielded an RVLAD cutoff of less than 11.98% as indicative of abnormal right ventricular function with a sensitivity of 100% and a specificity of 92.9%. The area under the ROC curve for RVLAD was 0.98. **Conclusion:** RV assessment with RVLAD demonstrated excellent ability to discern normal from abnormal RV function when compared to validated methods. The use of RVLAD offers numerous potential advantages. The RVLAD does not depend

on high quality definition of the lateral RV free wall and is not affected by chest wall and cardiac translational motion. This is because with RVLAD, RV excursion between two landmarks (RV apex and RV lateral tricuspid annulus) are assessed independent of probe location. This also suggests RVLAD may be valid for non-standard views in challenging patients and in tranesophageal echocardiography. Future studies are aimed at validating the RVLAD in these situations.

P1-217

Evaluation of Immediate Effects on Cardiac Synchrony and Contraction at Different Pacing Sites by Echocardiography

Y.N. Wang, H.Y. Chen, M.R. Zhu, X.Y. Chen, Y.G. Su, Xianhong Shu. Zhongshan Hospital, Fudan University, Shanghai, China

Background: Electrical pacing is the most common therapy for patients with bradyarrhythmia and cardiac conduction dysfunction. Traditional pacing sites including right ventricular apex (RVA), right ventricular outflow tract (RVOT) and ventricular septum (VS) were reported to cause ventricular asynchrony. His bundle (HIS) pacing and left bundle branch (LBB) pacing are new pacing modes regarded as more physiological. This study aimed to compare immediate effect on cardiac synchrony and contraction when pacing at different sites using echocardiography in order to explore an optimal pacing method. **Methods:** Twelve patients required pacing therapy were enrolled. During pacemaker implantation, a pacing lead was placed at RVA, RVOT, VS, HIS, LBB in sequence with a 10-min washing interval. Electrocardiogram and echocardiography images were recorded before (PRE) and immediate after pacing. Left ventricular (LV) volumes and ejection fraction (EF) were obtained. Inter-ventricular mechanical difference (IVMD) was measured. Strains, time intervals between the onset of QRS and the peak strains of LV segments and their deviations (PSD) were analyzed. **Results:** 1. Pacing at traditional sites (RVOT, RVA, VS) led to an immediate prolongation of QRS duration and a tendency of longer IVMD, among which RVA and VS pacing produced a deteriorated LVEF and PSD. 2. QRS duration didn't change significantly after HIS or LBB pacing. However, the pre-ejection time of LV was decreased and resulted in a shorter IVMD with LBB pacing. Immediate IVMDs of different pacing sites were significantly different. IVMDs of LBB and HIS pacing were comparably the shortest, and IVMDs of RVA pacing were the longest. **Conclusion:** Pacing at conventional sites, especially at RVA, leads to an immediately deteriorated electric and mechanical synchronism and weakened left ventricular contraction. LBB and HIS pacing best maintains the physiological electric activation and contraction pattern. It suggests that LBB and HIS pacing might be superior to conventional pacing sites.

P1-218

Evaluation of Three-Dimensional Cardiac Mechanics in Chagas Disease

Viviane T. Hotta^{1,2}, Maria Cristina Donadio Abduch¹, Marcelo Luiz Campos Vieira¹, Barbara Maria Ianni¹, Charles Mady¹, Edimar Alcides Bocchi¹. ¹Heart Institute/University of Sao Paulo Medical School, Sao Paulo, Brazil; ²Fleury Medicina e Saúde, Sao Paulo, Brazil

Background: Chagas disease (CD) is an endemic infectious illness that still remains a great economic burden. New techniques like three-dimensional speckle tracking (3D STE) may play a role in the evaluation of CD. The present study aims to address the feasibility of 3D STE in patients with CD. **Methods:** Seventy-two consecutive patients with CD underwent clinical, electrocardiographic and echocardiographic evaluation. The exclusion criteria were age < 18 or beyond 75-years old, systemic arterial hypertension, diabetes mellitus, hypothyroidism, renal or hepatic failure, atrial fibrillation or arrhythmias, coronary artery disease, pacemakers' users, pregnancy and chronic obstructive pulmonary disease. Comprehensive conventional (2DE) and three-dimensional echocardiography (3DE) were performed according to joint recommendations from the American Society of Echocardiography. **Results:** Seventy-two patients were recruited and enrolled in three groups: Group 1 (G1), patients with left ventricular ejection fraction (LVEF) < 0.35 (N=22); Group 2 (G2), 0.35 > LVEF < 0.55 (N=22); Group 3 (G3), LVEF > 0.55 (N= 28). Gender distribution, mean age, anthropometric variables and risk factors were similar between the groups. 2D STE feasibility was 99.5, 99% and 100% in G1, G2 and G3, respectively. 3D Longitudinal strain feasibility was 93%, 89% e 88% in G1, G2 and G3 respectively. Interobserver and intraobserver variabilities for longitudinal parameters were 8% and 10%, and 4% and 7% for 2D and 3D analysis, respectively. For the 3D STE analysis, the lowest interobserver variability was 5% (Area strain) and the highest was 15% (Circumferential strain). Area strain (5%) and Radial strain (5%) had the lowest intraobserver variability and circumferential and longitudinal strain the highest (7%). 3D Global longitudinal strain were lower in G1 in comparison to G2 and G3 (p=0.002; p<0.001). 3D Global circumferential strain were lower in G1 and G2 in comparison to G3 (p<0.001; p=0.024, respectively). 3D Global radial strain were lower in G1 in comparison to G2 and G3 (p=0.026; p< 0.001, respectively). 3D Area strain were lower in G1 in comparison to G2 and G3 (p=0.011; p< 0.001, respectively). **Conclusions:** 3D STE in patients with CD appears to be an accurate, reproducible and promising method in the presence of normal or reduced LVEF, despite the presence of severe LV dilation and dysfunction or apical abnormalities. However, 3D STE needs further development and refinement for application in clinical practice and its ultimate usefulness still remains to be defined.

Poster Session 1 (P1)

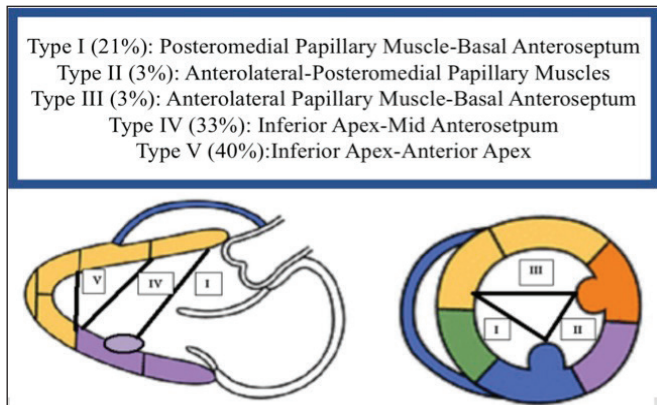
Sunday, June 23, 2019

P1-219

Role of Left Ventricular False Tendons in the Development of Adverse Ventricular Remodeling and Secondary Mitral Regurgitation After Myocardial Infarction

Saberio Lo Presti¹, Diego Lugo², Jorge Perez², Ben Johns Vadasser¹, Esteban Escobar³, Sofia A. Horvath⁴, Christos G. Mihos⁴. ¹Columbia University Division of Cardiology, Mount Sinai Heart Institute, Miami, FL; ²Department of Internal Medicine, Mount Sinai Medical Center, Miami, FL; ³Coronary Care Unit, Columbia University Division of Cardiology, Mount Sinai Heart Institute, Miami, FL; ⁴Echocardiography Laboratory, Columbia University Division of Cardiology, Mount Sinai Heart Institute, Miami, FL

Background: Left ventricular (LV) false tendons are fibromuscular bands arising from, and attaching to, the trabeculated LV endocardium or papillary muscles. The study aim was to test the hypothesis that LV false tendons, via a possible 'constraint' mechanism, attenuate adverse ventricular remodeling and secondary mitral regurgitation after myocardial infarction. **Methods:** Seventy-one patients admitted to the Coronary Care Unit following an ST-elevation (N=63) or non-ST-elevation (N=8) myocardial infarction were analyzed. All had a baseline echocardiogram and at least one follow-up study performed after revascularization. Patients were compared based on the presence of LV false tendons versus without. Chi-square analysis, Student t-test, and Mann Whitney U-test were used for the statistical analyses. **Results:** A total of 29 patients (41%) had LV false tendons. The mean age (64 ± 13 vs. 66 ± 13 years, $p=0.67$) and LV ejection fraction (41 ± 14 vs. $39 \pm 15\%$; $p=0.45$) were similar between the LV false tendon and no false tendon groups. The most common morphologic types of LV false tendons were IV and V (figure). At follow-up, there was no significant difference in adverse chamber remodeling amongst the LV false tendon versus no false tendon group (1.1 ± 0.9 vs. 0.9 ± 0.7 years, $p=0.3$) when assessed by: $\geq 10\%$ decrease in the relative LV ejection fraction (39% vs. 26% , $p=0.83$); $\geq 10\%$ increase in the LV end diastolic diameter index (41% vs. 41% , $p=1.0$); and, $\geq 10\%$ in the LV mass index (48% vs. 41% , $p=0.68$). Finally, there was no difference in the prevalence of moderate or greater secondary mitral regurgitation at follow-up (17% vs. 10% , $p=0.5$), or when patients were stratified according to LV tendon morphology or ischemic territory affected. **Conclusions:** The presence of LV false tendons appears to be a benign anatomic variant, and does not impact LV remodeling or secondary mitral regurgitation after myocardial infarction.



P1-220

Value of Global Longitudinal Strain as a Surrogate Marker of Myocardial Fibrosis Assessed by Late Gadolinium Enhancement by Magnetic Resonance Imaging in Patients with Nonischemic Cardiomyopathy

Takeshi Hozumi, Shingo Ota, Takahiro Nishi, Kazushi Takemoto, Teruaki Wada, Naoki Maniwa, Manabu Kashiwagi, Kunihiko Shimamura, Yasutsugu Shiono, Akio Kuroi, Yoshiki Matsuo, Hironori Kitabata, Yasushi Ino, Takashi Kubo, Atsushi Tanaka, Takashi Akasaka. Wakayama Medical University, Wakayama, Japan

Background: Previous studies have reported the presence of late gadolinium enhancement by cardiovascular magnetic resonance (CMR-LGE) suggesting myocardial fibrosis is useful as prognostic index in patients with nonischemic cardiomyopathy (NICM). Left ventricular (LV) global longitudinal strain by speckle-tracking echocardiography (STE-GLS) suggesting myocardial damage may be used for the detection of CMR-LGE in patients with NICM. The purpose of this study was to investigate the value of STE-GLS in detection of myocardial fibrosis assessed by CMR-LGE in patients with NICM. **Methods:** The study population consisted of 50 patients with NICM who underwent both STE and CMR. STE-GLS was evaluated from 3 apical views using STE analysis software (EchoPAC, GE). Presence of CMR-LGE (Intera Achieva, Philips), LV end-diastolic and end-systolic volume index (LVEDVI, LVESVI), LV ejection fraction (LVEF), E/A, E/e', LV atrial volume index (LAVI), and STE-GLS from 3 apical views were evaluated in the study patients. **Results:** In 41 (82%) of 50 patients, STE-GLS was successfully analyzed while CMR-LGE in all the

patients. Thus, the final study population consisted of 41 patients in whom both CMR and GLS analysis were successful. The patients were divided into two groups; 18 patients with CMR-LGE (Group-A) and 23 without CMR-LGE (Group-B). There were no significant differences in LVEDVI, LVESVI, LVEF, E/A, E/e', and LAVI between Group-A and Group-B (109 ± 6 vs 113 ± 7 ml/m², 78 ± 22 vs 82 ± 27 ml/m², 28 ± 6 vs $29 \pm 7\%$, 1.3 ± 1.1 vs 1.2 ± 0.8 , 11.3 ± 3.7 vs 11.7 ± 5.9 , and 50 ± 23 vs 49 ± 14 ml/m²). STE-GLS in Group-A was significantly reduced compared with Group-B (-7.6 ± 3.0 vs $-9.9 \pm 3.2\%$, $p=0.01$). According to ROC curve, $|\text{STE-GLS}| < 7.9\%$ was the best threshold value for identifying the presence of LGE (sensitivity 78%, specificity 70%, AUC 0.71). **Conclusions:** The present results showed that STE-GLS was useful for detection of myocardial fibrosis assessed by CMR-LGE in patients with NICM. It suggests that STE-GLS may be used as a screening marker to select the candidate for CMR examination to confirm myocardial fibrosis by LGE-CMR in patients with NICM.

P1-221

Diastolic Mechanics Differ Between Stress Cardiomyopathy and Acute Left Anterior Descending Myocardial Infarction

Colleen M. Harrington, Mark O'Connor, Timothy Fitzgibbons, Gerald P. Aurigemma. University of Massachusetts, Worcester, MA

Background: Stress cardiomyopathy (SCM) is a prevalent but poorly understood disease. There is incomplete knowledge concerning systolic and diastolic mechanics, nor, to date, are there measures which reliably distinguish SCM from acute LAD territory MI at presentation. Accordingly, we sought to identify acute differences between SCM and LAD MI, which can be distinguished by comprehensive echocardiography (echo). **Methods:** 67 women, 25 with apical variant SCM, 19 with LAD MI, and 23 control subjects with no obstructive coronary disease were studied. All had transthoracic echo and coronary angiography with left heart catheterization within 48 h of presentation. Echo data (systolic and diastolic function, global longitudinal strain (GLS, %)), and invasive hemodynamics were compared. **Results:** Echo diastolic function indices were abnormal, and paralleled invasive left ventricular end diastolic pressures (LVEDP) in both groups. However, there were no differences between SCM and LAD MI in any echo measurement. Invasive pre-atrial contraction pressures (pre-A) were lower in SCM than LAD MI (Table). **Conclusion:** Women with acute SCM cannot be distinguished from LAD MI by LVEF, GLS, or diastolic function on echo. Both exhibit markedly elevated LVEDP, but pre-A pressures are systematically lower in SCM, suggesting diastolic mechanics differs between the groups, and that atrial systole is of particular importance in maintaining preload in the acute setting.

	SCM		LAD STEMI		No CAD Controls		P Value
Number of Pts	25		19		23		
	Mean	SD	Mean	SD	Mean	SD	SCM vs. STEMI
E Velocity (m/s)	0.8	0.3	0.7	0.2	0.8	0.2	0.18
A Velocity (m/s)	0.8	0.3	0.7	0.2	0.7	0.2	0.18
E/A	1.1	0.5	1.0	0.4	1.2	0.4	0.86
E/E'	15.8	6.5	13.2	4.8	9.3	3.3	0.22
LAVI (ml/m ²)	34.8	10.1	29.2	9.1	24.4	6.8	0.11
LVEF (%)	40.5	12.6	39.9	11.5	61.9	4.1	0.98
GLS (%)	-9.0	4.4	-6.7	6.5	-17.6	6.8	0.41
PRE A (mmHg)	13.6	5.2	19.4	5.3	8.4	6.2	0.0032*
LVEDP (mmHg)	23.0	6.2	27.1	7.5	14.0	7.6	0.16

Statistical analysis performed using ANOVA, with Tukey HSD Post Hoc Test (Asterisk denotes statistical significance at $p < 0.05$.)

P1-222

Prognostic Value of Right Ventricular Three-Dimensional Speckle-Tracking Strain in Pulmonary Hypertension: Superiority of Longitudinal Strain Over Circumferential and Radial Strain

Yuman Li^{1,2}, Mengmei Li^{1,2}, Lei Li^{1,2}, Li Zhang^{1,2}, Qing Lv^{1,2}, Jing Wang^{1,2}, Yali Yang^{1,2}, Mingxing Xie^{1,2}. ¹Department of Ultrasound, Union Hospital, Tongji Medical College, Huazhong University of Science and Technology, Wuhan, China; ²Hubei Key Laboratory of Molecular Imaging, Wuhan, China

Aims: Right ventricular (RV) dysfunction is a predictor of adverse outcomes in patients with pulmonary hypertension (PH). Three-dimensional speckle tracking echocardiography (3D-STE) has been increasingly used to quantify RV function, but we do not know which 3D-STE parameters provide the most important clinical information. The purpose of our study was to investigate whether RV longitudinal strain (LS) provided a better estimation of RV systolic performance and prognostic information. **Methods:** 60 patients with PH and 35 normal controls were enrolled in our study. RV LS, circumferential strain (CS), radial strain (RS) were calculated by 3D-STE. RV volumes and ejection fraction (EF) were obtained from cardiac magnetic resonance (CMR) imaging. **Results:** Patients with moderate and severe PH had decreased RVEF compared with controls. Our findings revealed that LS showed significant reduction in mild PH patients; whereas CS and RS were decreased in moderate and severe PH patients. Patients with severe PH exhibited

Poster Session 1 (P1)

Sunday, June 23, 2019

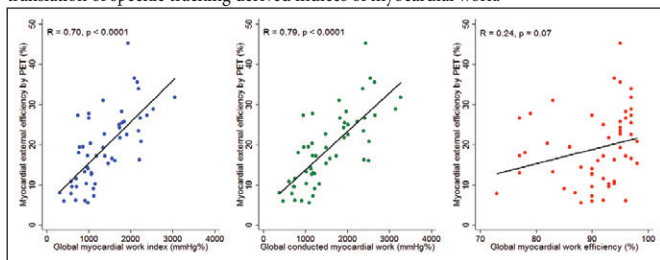
reduced RV LS, RS and CS compared with patients with mild PH. RV LS had a better correlation with CMR-derived RVEF, and 6-min walking distance, pulmonary vascular resistance and pulmonary artery systolic pressure than CS and RS. Only LS improved 6 months after medical treatment. RV LS (hazard ratio [HR]: 1.186; 95% confidence interval [CI]: 1.017 to 1.383; $p=0.029$) and RVEF (HR: 0.878; 95% CI: 0.779 to 0.989; $p=0.033$) were independent predictors of unfavorable clinical outcomes. **Conclusions:** Patients with PH show decreased RV strain. LS best correlates with CMR-derived RVEF, hemodynamic parameters and exercise capacity, and provides prognostic information.

P1-223

Speckle Tracking Derived Myocardial Work Indices Strongly Correlates with Myocardial External Efficiency by ¹¹C-acetate Positron Emission Tomography in Cardiac Amyloid Patients

Tor S. Clemmensen¹, Jens Sørensen^{1,2}, Fabian Mikkelsen¹, Hans Eiskjær¹, Sara Rosengren², Lars P. Tolbod¹, Hendrik J. Harms¹, Sven-Olof Granstam², Frank A. Flachkampff¹, Steen H. Poulsen¹. ¹Aarhus University Hospital, Aarhus, Denmark; ²Uppsala University Hospital, Uppsala, Sweden

Background: The mechanoenergetic coupling is calculated by ¹¹C-acetate positron emission tomography (PET) as myocardial external efficiency (MEE_{pet}), which reflects the ratio of left ventricular external stroke work and the energy equivalent of myocardial oxygen consumption. Recently, speckle tracking echocardiography has demonstrated a potential to evaluate myocardial work index (MW_{ECHO}), global conducted myocardial work (GCW_{ECHO}) and myocardial work efficiency (MWE_{ECHO}). The present study aimed to evaluate the relation between PET derived MEE_{pet} and speckle tracking derived GCW_{ECHO} , MW_{ECHO} and MWE_{ECHO} . **Methods:** We included 54 subjects from Aarhus University Hospital, Denmark and Uppsala University Hospital, Sweden. These subjects comprised 36 patients with cardiac amyloidosis, 12 healthy subjects and 6 subjects with myocardial hypertrophy without amyloid. All subjects underwent comprehensive echocardiographic evaluation and ¹¹C-acetate PET. **Results:** Patients with CA had lower GCW_{ECHO} and MW_{ECHO} than healthy subject and hypertrophic subjects (GCW_{ECHO} : 1186±468 mmHg% versus 2407±306 mmHg% and 2068±708 mmHg%, $p<0.0001$; MW_{ECHO} : 1044±390 mmHg% versus 2091±307 mmHg% and 1741±783 mmHg%, $p<0.0001$). MWE_{ECHO} was lower in CA patients than healthy subjects (89±6% versus 96±1%, $p<0.001$) whereas no difference was observed between CA patients and hypertrophic subjects ($p=0.86$). In cardiac amyloidosis patients a significantly lower MEE_{pet} was found as compared to healthy subjects and hypertrophic subjects (15±6% versus 28±8% and 26±7%, $p<0.0001$). We found a strong correlation between MW_{ECHO} and MEE_{pet} ($\beta_1=48$, 95% CI (34-61), $p<0.0001$) and an even stronger correlation between GCW_{ECHO} and MEE_{pet} ($\beta_1=59$, 95% CI (45-74), $p<0.0001$, Figure 1. No significant relation was observed between MWE_{ECHO} and MEE_{pet} ($\beta_1=0.18$, 95% CI (-0.01-0.37), $p=0.07$). **Conclusion:** The speckle tracking derived measures of myocardial work (MW_{ECHO} and GCW_{ECHO}) are significantly decreased in patients with CA as compared to controls. Both MW_{ECHO} and GCW_{ECHO} were significantly correlated to the PET-derived myocardial external efficiency whereas we found no significant relation between MEE_{pet} and MWE_{ECHO} . This work further supports the clinical translation of speckle tracking derived indices of myocardial work.



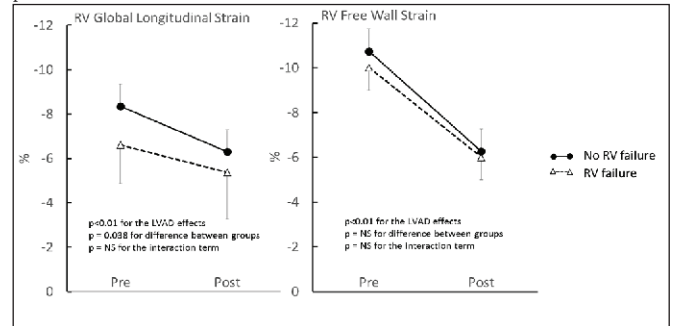
P1-224

Right Ventricular Mechanics in Patients Undergoing Left Ventricular Assist Device Therapy: Clinical Impact and Correlation with Pulmonary Artery Pulsatility Index

Nicolas Isaza, Matthew Gonzalez, Chonyang Albert, Richard A. Grimm, Antonio L. Perez, Edward G. Soltesz, Michael Z. Tong, Jerry D. Estep, Zoran B. Popovic, Brian P. Griffin, Bo Xu. Cleveland Clinic Foundation, Cleveland, OH

Introduction: Early Right ventricular failure (RVF) is a common complication after left ventricular assist device (LVAD) implantation, contributing to early mortality. Pulmonary artery pulsatility index (PAPi) is a hemodynamic predictor of early RVF post LVAD. The role of pre and post-operative RV strain in patients undergoing LVAD therapy has not been well studied. Additionally, the relationship between PAPi and RV mechanics is unknown. **Methods:** 51 patients undergoing LVAD implantation at our center (between 2004 and 2017), who had transthoracic echocardiograms before and after surgery, and PAPi measurements pre-operatively were retrospectively analyzed. RV mechanics (global longitudinal strain [GLS]; and free wall strain [FWS]) were calculated. Additionally, a

correlation analysis between RV mechanics and PAPi was performed. **Results:** 9 out of 51 patients (17.6%) had a diagnosis of early RV failure. Figure 1 shows the RV mechanics in the two groups (early RV failure vs. no early RV failure). Both GLS and FWS significantly worsened following LVAD implant in both groups ($p<0.01$). Nonetheless, RV GLS before and after LVAD was better in patients without RV failure ($p=0.038$). PAPi was significantly lower in the RV failure group (3.06 ± 2.61 vs. 7.26 ± 3.60 , $p<0.01$) and it was found to have a moderate correlation with RV FWS after LVAD implantation ($R=0.41$). **Conclusion:** LVAD implantation resulted in global reduction of RV strain parameters, even among patients without apparent early RV failure, supporting the presence of a subclinical degree of RV dysfunction following LVAD. A lower RV GLS pre and post LVAD implantation translated into clinical and hemodynamic RV failure post-LVAD. The addition of RV strain parameters to PAPi may shed more light in understanding who is at risk for early RVF post-LVAD.

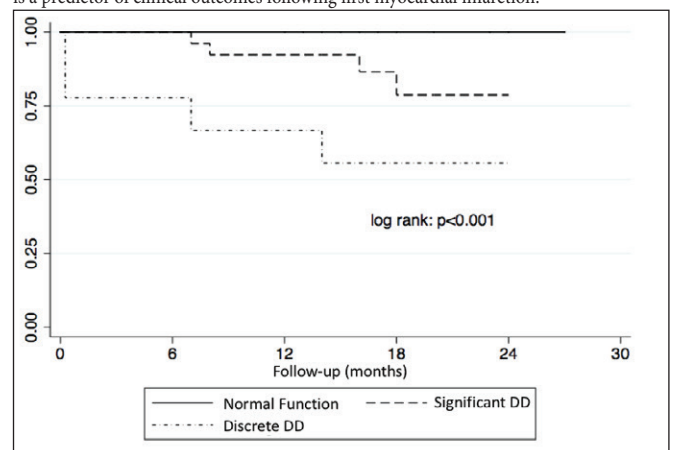


P1-225

Prognosis Value of Diastolic Dysfunction Assessed Using 2016 ASE Guidelines Following First Myocardial Infarction

Vanessa Bordin, Gustavo Gavazzoni Blume, Thyago Proença De Moraes, Leonardo Piazza, Natália Boing Salvatti, Isabela Pedroza Vieira, Luka David Lechinewski, José Carlos Moura Jorge, Vitória Lea Nuevo Miguel. Santa Casa de Misericórdia de Curitiba, Curitiba, Brazil

Background: Recently the American Society of Echocardiography recommended a simplified approach for assessing diastolic function. Although readily incorporate to clinical practice, prospective studies assessing its value are lacking in the current literature. The aim of this study was to assess the prognostic value of significant diastolic dysfunction (DD) assessed using the algorithm recommended in the 2016 American Society of Echocardiography and European Association of Cardiovascular Imaging guidelines in patients with first myocardial infarction. **Methods:** Seventy one consecutive patients with first ever myocardial infarction were included. Doppler echocardiography was performed within 24 hours of admission in all patients. Significant DD was defined as grade 2 or 3 DD. The primary outcome measure was composite major adverse cardiovascular events (MACEs), comprising death, myocardial infarction and heart failure. **Results:** At the mid-follow-up of 16.1 months, 14% of the patients had advanced DD, where 44.4% of these patients died due to cardiovascular reasons, and two deaths occurred in the first week. There were no deaths in the group without diastolic dysfunction. In the Kaplan-Meier analysis, DD was a strong predictor of MACEs (log rank = $p < 0.001$). **Conclusions:** Significant DD assessed using the 2016 American Society of Echocardiography guidelines is a predictor of clinical outcomes following first myocardial infarction.



Poster Session 1 (P1)

Sunday, June 23, 2019

P1-226

Correlation of Exercise Intensity and Right Ventricular Remodeling Among Filipino Marathon Runners

Debbie Lynn A. Udarbe, Arnold S. de Guzman, Harold C. Sunga, Angeles University Foundation Medical Center, Angeles City, Philippines

Background: It has been suggested that excessive endurance exercise could have possible dose-dependent risks. This study sought to delve into that by correlating the level of physical activity in the development of right ventricular remodeling demonstrated as a change in right ventricular indices during stress echocardiography among Filipino marathon runners. **Methods:** Active marathon runners are recruited with normal stress echo with main outcome measures, before and during active exercise (at least 85% of Maximum Predicted Heart Rate) of Right Ventricular (RV) indices using tricuspid annular systolic excursion (TAPSE), fractional area change (FAC), RV S'm, RV e', RV a', and RV e'/a' and correlated to level of physical activity. **Results:** It was found out that in a total of 100 marathon runners, distance ran per week is significantly associated with RV a' and TAPSE at rest and peak exercise ($p < 0.05$). Specifically, for every one km increase in distance ran per week, there is a 0.0005 decrease in RV a' and a 0.006 increase in TAPSE at rest; and for every one km increase in distance ran per week, there is a 0.001 decrease in RV a' a 0.009 increase in TAPSE. The number of years running was found to be significantly associated with RV S'm' and TAPSE during peak exercise ($p < 0.05$). For every additional year of running, there is a 0.001 increase in RV S' at peak exercise and a 0.039 increase in TAPSE. Greater cumulative distance across years of running was found to be significantly associated with RV a' and trans annular plane TAPSE at rest ($p < 0.05$); showing that for every one km increase in distance ran across years, there is a 0.00004 decrease in RV a', but with a 0.0007 increase in TAPSE. During Peak exercise, there is also a significant association between greater distance covered across years of running and TAPSE ($p < 0.05$), particularly, for every one km increase in distance ran across years, there is a 0.001 increase in TAPSE. **Conclusion:** The study was able to demonstrate that running experience is inversely related to RV a'. Hence, majority of the blood during the filling of the right ventricle is less dependent in the late phase of the right atrial contribution. Moreover, the blood volume is directly related to the increase in RV S'm and TAPSE whereby it is expected to increase during exercise secondary to increase in contractility and compliance. These findings and the long standing effect on the right ventricle may lead to remodeling of the chamber, and subtle changes may start in their diastolic parameters.

P1-227

Insight Into Recovery Process of Damaged Myocardium in Dilated or Secondary Cardiomyopathy in Children - an Assessment by Two-dimensional Strain

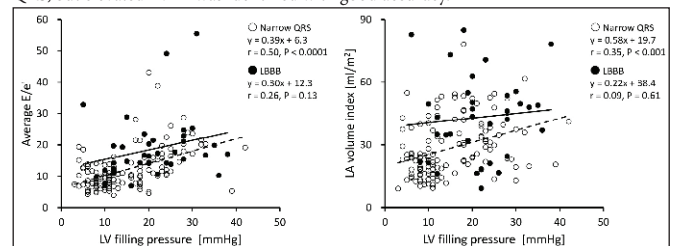
Kazuya Sanada, Jr., Shizuoka Children's Hospital, Shizuoka, Japan

Background: Idiopathic dilated cardiomyopathy (IDCM) in children is relatively responsive to medication. Also, secondary cardiomyopathy (SDCM) caused by afterload mismatch due to coarctation of aorta (CoA) is also reversible in majority of cases by interventions at appropriate timing. However, there are paucity of data regarding the myocardial recovery processes assessed by two-dimensional (2D) strain. We hypothesized that the recovery process of the myocardium might be different according to the underlying pathologies. The objective of this study is to clarify how strain pattern changes during recovery process in IDCM and SDCM in children. **Methods:** Eleven patients (age; mean 2.2 ± 4.2 years old) diagnosed as IDCM (Group I: 4 cases) and SDCM (Group S: 7 cases) from 2009 to 2018, were enrolled in this retrospective study. The 1st echo after admission for group I and the postoperative 1st echo for group S were set as the starting points for recovery process. The end point of recovery process was when it fulfills the following all criteria: LV-ejection fraction $> 55\%$; LV end-diastolic dimension $< 120\%$ of Normal; BNP < 20 pg/ml. Strain were analyzed at 4 time points: (1) starting point of recovery process; (2) end of intensive care; (3) at discharge; (4) end point of recovery. The LV strain analyses were made off-line using 2D Cardiac Performance Analysis (TOMTEC). Global longitudinal strain (GLS), Global circumferential strain (GCS), Global radial strain (GRS) were analyzed on parasternal and apical views, and they were converted to Z-score, which based on the data of normal children. **Results:** The time period from (1) to (4) was significantly longer in group I [I: 53.0 ± 35.6 (days); S: 18.7 ± 14.4 ($p < 0.05$)]. Analysis time point (1): GLS [I: $z = -5.08 \pm 1.85$; S: $z = -4.73 \pm 0.77$ (NS)]; GCS [I: $z = -4.57 \pm 0.81$; S: $z = -4.62 \pm 1.11$ (NS)]; GRS [I: $z = -2.32 \pm 0.44$; S: $z = -1.55 \pm 0.80$ (NS)]. GRS was higher than GLS or GCS ($p < 0.05$) in both groups. Analysis time point (4): GLS [I: $z = -1.63 \pm 1.38$; S: $z = -2.77 \pm 1.17$ (NS)]; GCS [I: $z = -0.62 \pm 0.49$; S: $z = -1.37 \pm 1.48$ (NS)]; GRS [I: $z = -0.34 \pm 0.32$; S: $z = -0.43 \pm 0.70$ (NS)]. GRS was higher than GLS ($p < 0.05$) in group S. The proportions of cases with strain-z < 2 were: GLS: 5/11 (45.4%); GCS: 2/11 (18.2%); and GRS: 0/11 (0%) at end point of recovery (4). **Conclusion:** The recovery process of the myocardium shows same pattern in IDCM and SDCM, and its order was as follows: GRS \Rightarrow GCS \Rightarrow GLS. However, although the all patients show normal GRS at the end of recovery, half of the patients still show significantly reduced GLS. Myocardial injury in children showed same recovery pattern regardless of the cause.

P1-228

Estimation of Left Ventricular Filling Pressure in Left Bundle Branch Block: Limitations of Echocardiographic MarkersKasumi Masuda¹, John M. Aalen², Oyvind Senstad Andersen², Magnus Reinsfelt Krogh³, Hans Henrik Odland³, Espen W. Remme², Sherif F. Nagueh⁴, Satoshi Nakatani¹, Marie Stugaard¹, Otto Armin Smiseth². ¹Osaka University Graduate School of Medicine, Suita, Japan; ²Oslo University Hospital, Institute for Surgical Research, Oslo, Norway; ³Oslo University Hospital, Oslo, Norway; ⁴Houston Methodist Hospital, Houston, TX

Background: Estimation of left ventricular (LV) filling pressure (LVFP) by echocardiography is more challenging in patients with left bundle branch block (LBBB) than in patients with narrow QRS. **Aim of the study:** To investigate how LBBB modifies indices of LVFP. **Methods:** We studied 39 patients with LV failure and LBBB or LBBB type of electrical activation due to right ventricular (RV) pacing. They were compared to 132 patients with LV failure and narrow QRS. Diastolic function was evaluated by echocardiography and measurements included mitral annular velocities (e'), mitral early filling velocity (E) and left atrial (LA) volume indexed to body surface area. We calculated E/e' using the average of septal and lateral e'. Pulmonary capillary wedge or LV pre-A pressure was measured as LVFP. **Results:** In patients with narrow QRS there was as expected, a significant correlation between E/e' average and LVFP (Figure - left panel). In patients with LBBB, however, there was no significant correlation between E/e' average and LVFP. However, when average E/e' exceeded 14, 53 of 62 patients had elevated LVFP (> 12 mmHg) and accuracy was 74%. As shown in the Figure (right panel) there was as a significant correlation between LA volume index and LVFP for patients with narrow QRS. For patients with LBBB, however, there was wide scatter in the relationship and no significant correlation. When comparing LBBB and narrow QRS patients, LA volume index in LBBB patients was markedly larger and showed more variability, 43 ± 20 and 28 ± 14 ml/m², respectively. **Conclusion:** In patients with LBBB or RV pacing the LA volume index did not reflect LVFP. Average E/e' showed more variability in LBBB than in narrow QRS, but elevated LVFP was identified with good accuracy.



P1-229

Fetal Cardiac Function in Left-sided Congenital Heart Disease: A Speckle-Tracking Echocardiographic Study

ZhiLing Luo, Li Li, Yan Shen, Yunnan Fuwai Cardiovascular Hospital, Kunming, China

Background: The aim of this study was to assess the biventricular systolic and diastolic function in fetuses with left-sided congenital heart disease, using a comprehensive cardiac functional assessment and exploring the role of speckle-tracking to assess myocardial deformation. **Methods:** A cross-sectional study was conducted in 61 fetuses, including 20 fetuses with left-sided congenital heart disease (6 fetuses with hypoplastic left ventricle, 14 fetuses with well-developed left ventricle) and 41 matched healthy fetuses. Maternal baseline characteristics, standard fetoplacental Doppler indices, and conventional echocardiographic and myocardial deformation parameters were prospectively collected. **Results:** 6 fetuses with hypoplastic left ventricle had a significantly lower ejection fraction (EF), fractional shortening (FS), Global longitudinal peak systolic strain (LPSS), systolic strain rate (SSR), early diastolic strain rate (SRe) and late diastolic strain rate (SRa) of the left ventricle (EF: $39.73 \pm 10.95\%$ vs $71.42 \pm 5.94\%$, $p < .01$; FS: $17.42 \pm 5.45\%$ vs $37.21 \pm 4.28\%$, $p < .01$; LPSS: $-10.08 \pm 2.97\%$ vs $-26.79 \pm 3.22\%$, $p < .01$; SSR: -0.95 ± 0.18 vs -2.56 ± 0.43 1/sec, $p < .01$; SRe 0.79 ± 0.43 vs 2.46 ± 0.61 1/sec, $p < .01$; SRa 0.80 ± 0.17 vs 2.39 ± 0.81 1/sec, $p < .01$). And no effect modification was demonstrated on deformation analysis of right ventricle. Deformation analysis demonstrated a lower LPSS, SSR, SRe and SRa for the left ventricle in 14 fetuses with well-developed left ventricle (LPSS: $-21.55 \pm 6.85\%$ vs $-26.79 \pm 3.22\%$, $p < .05$; SSR: -1.94 ± 0.73 vs -2.56 ± 0.43 1/sec, $p < .05$; SRe 1.70 ± 0.57 vs 2.46 ± 0.61 1/sec, $p < .01$; SRa 1.62 ± 0.82 vs 2.39 ± 0.81 1/sec, $p < .01$). However no effect modification was demonstrated on EF and FS of left ventricle. In contrast, all measurements of right ventricle did not show any statistical difference regarding deformation parameters compared to healthy controls. **Conclusion:** Fetuses with left-sided congenital heart disease present signs of left ventricular systolic and diastolic dysfunction by deformation analysis. In contrast, all measurements of right ventricle did not show any statistical difference regarding deformation parameters. Two-dimensional speckle-tracking could offer an additional benefit over conventional echocardiography to detect subclinical unfavorable changes in myocardial function in this population.

Poster Session 2 (P2)

Monday, June 24, 2019

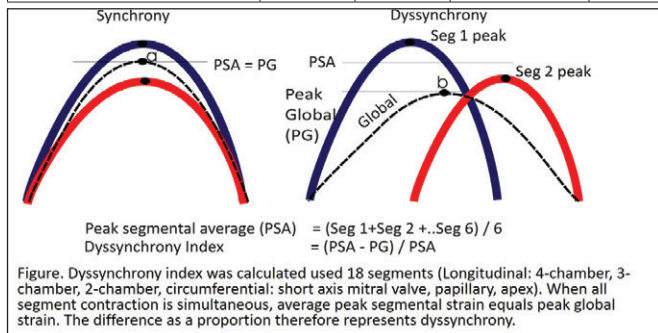
P1-230

A Novel Index of Dyssynchrony Outperforms Other Measures During RV Pacing in Pediatric Patients

Mirza Beigh, Ganesh Gnanappa, Joseph Atallah, Michal Kantoch, Carolina Escudero, Sachie Shigemitsu, Luke G. Eckersley. Division of Cardiology, Stollery Children's Hospital and University of Alberta, Edmonton, AB, Canada

Background: Electromechanical dyssynchrony is common in pediatric patients with cardiomyopathies and congenital heart disease and impairs cardiac output. Current echocardiography measures are laborious, angle-dependent and poorly predict response to resynchronization. We developed a novel strain imaging based dyssynchrony index (DI) found to be effective in detecting fetal LV dyssynchrony. This study aims to validate the DI in children with transient pacing-induced LV dyssynchrony in the electrophysiology (EP) laboratory. **Methods:** We prospectively recruited seven children aged 6.9 to 15.7 years with normal cardiac anatomy undergoing EP study for ablation of supraventricular tachycardia. After successfully ablation a baseline echocardiogram was performed. The RV apex was then paced at 10bpm above baseline to induce LV dyssynchrony, and echocardiogram repeated. Conventional analysis included LV output by Doppler continuity equation, Simpson's biplane LV ejection fraction and septal-posterior wall motion delay (SPWMD). Speckle tracking imaging for global longitudinal and circumferential strain (LS, CIRC), and segmental strain to calculate 18 segment time to peak longitudinal and circumferential strain standard deviations (T2PSD) and DI (Figure). Student t-test was used for comparison, significance p<0.05. **Results:** RV pacing successfully induced LV dyssynchrony evidenced by increased ECG QRS duration and impaired LV systolic function (reduced peak global LS, CircS, ejection fraction and stroke volume) (Table). Although SPWMD was not different during pacing induced LV dyssynchrony, both longitudinal and circumferential DI were increased, while LS T2PSD was increased but not CIRC T2PSD. **Conclusion:** Right ventricular pacing successfully induced clinical LV dyssynchrony resulting in impaired LV global function. The strain imaging derived novel dyssynchrony index increased appropriately with LV dyssynchrony and was more sensitive than SPWMD and more consistent than segmental strain T2PSD.

	Baseline	Paced	Percent change	p-value
QRS duration	88±9	133±20	36%	0.001
Stroke volume (ml)	52±14	36±10	-31%	0.05
Cardiac Index (L/min/m2)	3.11±0.61	2.61±0.6	-16%	0.15
LVEF (%)	52±5	47±2	-10%	0.02
Peak global Long strain (%)	-15.7±2.2	-11.1±3.3	-29%	0.01
Peak global Circ. Strain (%)	-15.2±3.2	-9.8±4.2	-36%	0.02
SPWMD Long Axis (ms)	61±76	113±85	85%	0.25
SPWMD Short Axis (ms)	72±94	112±94	56%	0.49
Global LS DI	0.05±0.03	0.13±0.06	160%	0.03
LS T2P (ms)	386±19	371±24	-4%	0.28
LS T2PSD (ms)	39±9	72±26	85%	0.02
GLOBAL CircS DI	0.12±0.07	0.29±0.16	142%	0.02
Circ. T2P (ms)	354±43	376±46	6%	0.39
Circ.T2PSD (ms)	92±22	106±43	15%	0.50



POSTER SESSION 2 (P2)

Presented Monday, June 24, 9:00 AM-4:00 PM

Value of Echocardiography (Quality and Cost) / Outcomes / Comparative Effectiveness

P2-01 through P2-026

3D Echocardiography
P2-027 through P2-051

Diseases of the Aorta / Vascular Disease
P2-052 through P2-064

New Technology
P2-065 through P2-093

Artificial Intelligence / Machine Learning
P2-094 through P2-106

Contrast Echocardiography
P2-107 through P2-121

Echocardiography in Systemic Disease (DM, HTN, Obesity) / Pericardial Disease / Primary Myocardial Disease
P2-122 through P2-151

Clinical Cases: Adult Patients
P2-152 through P2-229

P2-001

Prevalence of Clinically Important Abnormalities Found on Transthoracic Echocardiograms Ordered for Finding of Heart Murmur Found on Physical Exam

Isla McClelland, Victor Mor-Avi, Roberto M. Lang, R. Parker Ward. University of Chicago, Chicago, IL

Background: A heart murmur (HM) found on physical examination is a common indication for transthoracic echocardiography (TTE). Current ACC/AHA guidelines recommend TTE, and Appropriate Use Criteria (AUC) deem TTE appropriate in the initial evaluation of any patient with murmur and a "reasonable suspicion" of valvular or structural heart disease. However, the prevalence of clinically important TTE abnormalities in patients referred for HM has not been reported, and clinical factors that predict important TTE abnormalities in patients with HM are unknown. We sought to define the prevalence of clinically important TTE abnormalities in patients with HM referred for TTE. **Methods:** We reviewed 350 consecutive patients (aged 18 years and older) referred for initial TTE with an indication of HM to University of Chicago Echocardiography Laboratories. Clinical details that contributed to the referral for TTE, AUC designation, and TTE findings were recorded. Composite endpoints of "Any TTE Abnormality" and "Any Major TTE Abnormality", defined as those prompting immediate or short term (<1 year) treatment or follow up (e.g. moderate or severe valvular heart disease, significant structural disease/LVOT obstruction), were noted. **Results:** Among patients referred to TTE for indication of HM, 23% had a "Major TTE abnormality" and 39% had a completely normal TTE. Severe valvular disease (stenosis or regurgitation) was present in 4%. No worse than mild valvular disease, which AUC would suggest no follow up needed in the absence of new symptoms for ≥3 years was present in 41%. Review of additional clinical factors (e.g. murmur characteristics, signs or symptoms) supported a "reasonable suspicion" of heart disease, and thus were Appropriate by the AUC in 82% of studies, with 11% found to be "Rarely Appropriate". Among "Appropriate studies", 25% had a "Major TTE Abnormality" and 32% had completely normal TTE. Among "Rarely Appropriate" studies, no Major TTE abnormalities were found, and 73% of TTEs were completely normal. **Conclusions:** There is a low prevalence of clinically important TTE abnormalities in patients referred for initial TTE for the indication of HM found on physical examination, and completely normal TTEs in this group are common. AUC based on supporting clinical factors effectively stratify the likelihood of finding major abnormalities on TTE, with "Rarely Appropriate" TTEs identifying patients very unlikely to have any significant TTE abnormalities. Further study to define the clinical factors most predictive of important TTE abnormalities in patients referred for the indication of HM is warranted.

Poster Session 2 (P2)

Monday, June 24, 2019

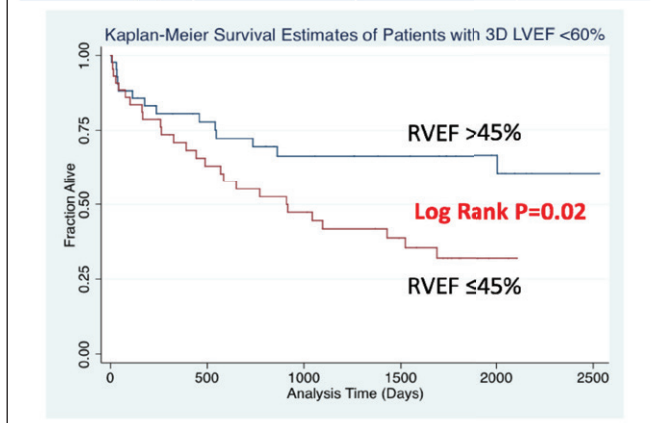
P2-002

Value of 3D versus 2D Echocardiographic Parameters of Right Ventricular Function in Predicting Mortality

Akhil Narang¹, Kanako Kishiki², Lynn Weinert², Francesco Maffessanti², Diego Medvedofsky², Victor Mor-Avi², Karima Addetia², ¹Northwestern University, Chicago, IL; ²University of Chicago, Chicago, IL

Background: Conventional 2D echocardiographic (2DE) parameters of right ventricular (RV) function, such as fractional area change (FAC), tricuspid annular plane systolic excursion (TAPSE), and free wall strain (FWS) correlate with outcomes. In this study we sought to determine (1) which 2DE RV parameter best predicts mortality, (2) whether 3D echocardiographic (3DE) parameters, such as RV ejection fraction (EF), are superior to 2D parameters in predicting mortality, and (3) whether there is incremental value of RV parameters over left ventricular (LV) function in predicting mortality. **Methods:** We retrospectively studied 204 consecutive inpatients and outpatients (excluding those with severe pulmonary hypertension, tricuspid valve intervention, or pacemakers) (58±18 years, 53% female) who underwent echocardiography over two years, and had transthoracic 2DE and 3DE full-volume datasets of both ventricles. FAC, TAPSE and FWS were measured from RV-focused views, while RVEF and LVEF were measured from the 3DE datasets using commercial software (TomTec). Mortality was determined from the medical records and social security death index. Univariate and multivariate Cox proportional hazard models were used to identify parameters independently associated with mortality. Survival analysis was then performed for these parameters for the two quantiles of LVEF to determine whether they would provide incremental value over 3D LVEF for predicting mortality. **Results:** During the mean follow-up of 3±2 years, 66 (32%) patients died. All 2DE parameters and 3D RVEF were significantly different between survivors and non-survivors in univariate analysis. In a multivariate model, RVEF was the only parameter independently associated with mortality (Table). In patients with LVEF <60% (median of the sample), RVEF with a cutoff of <45% (guideline cut-off for normal versus abnormal 3D RVEF) provided incremental value in predicting mortality (P=0.02), while in patients with LVEF >60%, it did not add incremental value (p=0.12) (Figure). **Conclusion:** Among conventional 2DE and 3DE indices of RV function (FAC, TAPSE, or FWS), only RVEF was independently associated with mortality. Furthermore, our data indicate that 3D RVEF may incrementally predict mortality in patients with reduced LV function.

Parameter	Survivors	Non-Survivors	P-Value (Multivariate Model)
FAC (%)	0.45 ± 0.11	0.41 ± 0.12	0.39
TAPSE (mm)	2.0 ± 0.6	1.8 ± 0.6	0.32
FWS (%)	-22 ± 7	-19 ± 6	0.43
3D RVEF (%)	47 ± 12	43 ± 11	0.037



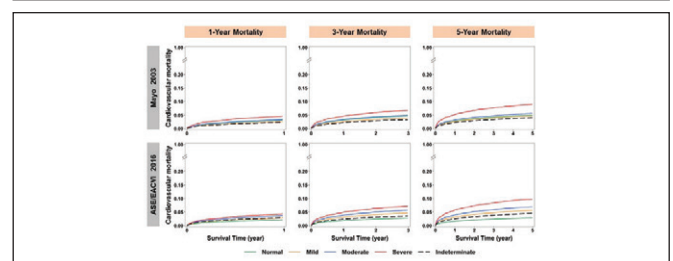
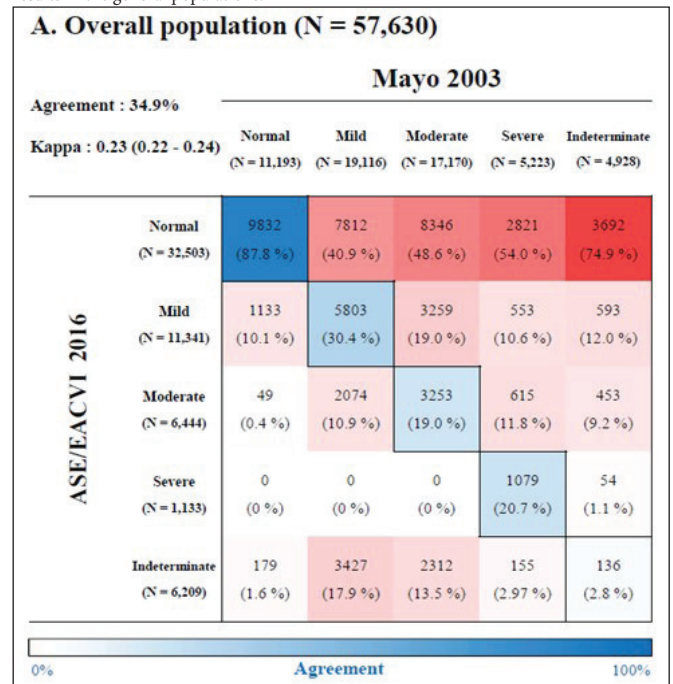
P2-003

Validation and Comparison of Diastolic Functional Assessments for Cardiovascular Mortality

Hsin-Yueh Liang. China Medical University Hospital, Taichung City, Taiwan

Background: Despite several echocardiographic diagnostic algorithms having been proposed, consensus on a standardized diastolic dysfunction (DD) classification framework remains controversial. The aim of the present study was to validate and compare the prognostic performance of the conventional DD diagnostic algorithm (Mayo 2003) and the American Society of Echocardiography and the European Association of Cardiovascular Imaging 2016 algorithm (ASE/EACVI 2016) for predicting cardiovascular (CV) mortality in a large hospital-based cohort. **Methods:** A prospective cohort of 57 630 adult patients who underwent clinically indicated echocardiographic studies at a tertiary medical center from 2008 to 2016 were enrolled. Classification concordance between Mayo 2003 and ASE/

EACVI 2016 and prediction performance comparison of 3-year CV mortality incidence were analyzed according to Harrell's C-statistics and the net reclassification index (NRI) using the Meta-Analysis Global Group in Chronic Heart Failure (MAGGIC) risk equation as reference. **Results:** The most notable discrepancy in DD classification between Mayo 2003 and ASE/EACVI 2016 appeared in the "normal" category, where the numbers of normal classification were mostly tripled by ASE/EACVI 2016 (Fig1). The absolute number of patients correctly reclassified by ASE/EACVI 2016 was 23 181 patients, corresponding to 42% of absolute NRI. Impaired left ventricular ejection fraction and DD conferred mutually independent excess risks of CV mortality. The dose-response effects of DD on CV mortality were more evident using ASE/EACVI 2016 (Fig 2). The discrimination performance for CV mortality, quantified using Harrell's C-statistics after adding DD classification based on either Mayo 2003 or ASE/EACVI 2016 into the MAGGIC risk equation, was not significantly improved. **Conclusions:** Compared with Mayo 2003 DD classification, ASE/EACVI 2016 is more generalizable to predict CV death. Future research should verify our results in the general populations.



P2-004

An Educational Strategy to Improve the Acquisition of 3D Left Ventricular Ejection Fraction by Cardiac Sonographers

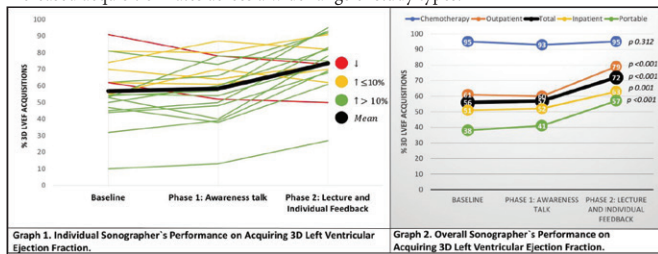
Maria Camila Trejo-Paredes¹, Edith Lilianna Posada-Martinez¹, Xochitl Arely Ortiz-Leon¹, Peter Flueckiger², Karen Bachand³, Yi-Hwa Liu¹, Lissa Sugeng¹, Robert L. McNamara¹. ¹Yale University, New Haven, CT; ²Piedmont Healthcare, Atlanta, GA; ³Yale New Haven Hospital, New Haven, CT

Background: Left ventricular ejection fraction (LVEF) has a crucial role in determining prognosis and therapeutic decision making in numerous cardiovascular conditions. Per protocol at our echo lab, 3D echocardiography is the preferred one for LVEF assessment; however, acquisition rates amongst sonographers are low and vary significantly. We aimed to improve sonographers' acquisition rates and decrease variability by implementing different educational strategies. **Methods:** This observational prospective study targeted cardiac sonographers at a single academic tertiary center. We reviewed all complete transthoracic echocardiograms and excluded studies that used an ultrasound enhancement agent. Initially, we assessed baseline performance over 6 months. Subsequently, we assessed performance during two consecutive phases. Phase 1 was for 6 months after the sonographers attended an awareness talk showing baseline performance but no individual feedback. Phase 2 was for 45 days after the sonographers attended a lecture

Poster Session 2 (P2)

Monday, June 24, 2019

on the significance of 3D-LVEF and received individual feedback on their 3D LVEF acquisition performance during the baseline period and Phase 1. **Results:** At baseline, there was not only low 3D-LVEF acquisition rate (56%) but also significant variability among sonographers (range 10-91%). Overall sonographer 3D-LVEF acquisition in Phase 1 showed no improvement from baseline (absolute difference +1.3% CI -1.3 - +3.1, $p=0.415$). However, Phase 2 showed significant overall improvement (absolute difference +15.6% CI 12 - 19, $p<0.001$) and decrease in variability; the differences between the maximal and minimum 3D LVEF acquisition rates were 81% at baseline and 68% in phase 2 (Graph 1). The subgroup of portable studies represented the lowest performance with rates of 38% at baseline, increasing to 57% in Phase 2. The subgroup of chemotherapy outpatients represented an ideal scenario for 3D LVEF use, with consistent rates above 91% (Graph 2). **Conclusions:** Despite a lab quality improvement initiative aimed at increasing use of 3DE for LVEF, acquisition rates remained low when only a general report of lab performance was presented to the sonographers. However, specific personalized feedback to sonographers increased acquisition rates across a wide range of study types.



P2-005

Prognostic Value of Layer-Specific Global and Regional Longitudinal Strain in Patients with Non-ST Elevated Acute Coronary Syndrome

Chong Liu, Jia-wei Tian. Department of Ultrasound, Second Affiliated Hospital of Harbin Medical University, Harbin, China

Background: Layer-specific strain echocardiography has been proven to be a powerful method for predicting coronary artery stenotic degree in patients with non-ST elevated acute coronary syndrome (NSTEMI-ACS). However, its prognostic efficacy in these patients has not been established. The aim of our study is to investigate the prognostic value of layer global longitudinal strain (GLS) and territorial longitudinal strain (TLS) related to ischemic area in predicting cardiac events following NSTEMI-ACS patients with preserved left ventricular ejection fraction (LVEF). **Methods:** One hundred and seven consecutive NSTEMI-ACS patients underwent successful percutaneous coronary intervention (PCI) were enrolled. Transthoracic two-dimensional echocardiography examinations were performed within 48h of admission (before PCI). Any episodes of clinical cardiac events of re-infarction and/or revascularization, ventricular arrhythmias, hospitalization for heart failure, and died for all-cause were recorded with a median follow-up time of 29.7 (26.3 - 32.6) months. **Results:** During follow-up, 27 patients (25.2%) developed the clinical cardiac events. GLS and TLS for three myocardial layers were reduced in patients with cardiac events, as endocardial GLS (-19.3 ± 1.6% vs. -21.7 ± 1.6%, $P < 0.001$), endocardial TLS (-17.8 ± 2.0% vs. -21.0 ± 1.8%, $P < 0.001$). TLS and GLS in the endocardium or mid-myocardium showed higher accuracy than that in epicardium for detection of patients with cardiac events (P all < 0.05). In univariate and multivariate Cox regressions including clinical baseline characteristics, sex, hypertension and diabetes mellitus were all associated with the high risk of developing the cardiac events (baseline model $\chi^2 = 25.6$). The addition of wall motion score index, LVEF, global and regional layer longitudinal strain parameters to baseline model showed the increased predictive power, yet endocardial TLS (Hazard ratio, 2.06 (1.63 - 2.61); $P < 0.001$) presented the greatest incremental prognostic information in model power ($\chi^2 = 62.0$, $P < 0.001$). **Conclusion:** In NSTEMI-ACS patients with preserved LVEF, global and regional longitudinal myocardial deformation defined as layer GLS and TLS assessed before PCI were all independent predictors of cardiac events. Especially, endocardial TLS added the most significant incremental prognostic value over baseline clinical parameter to identify at high risk of developing cardiac events to earlier guide whether the additional treatments are needed.

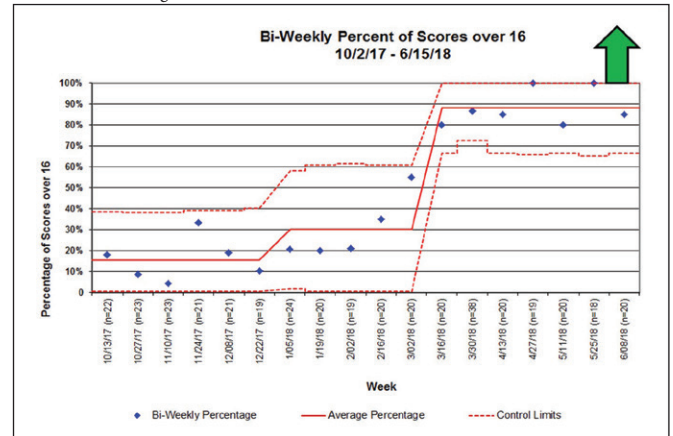
P2-006

Using Quality Improvement Methodology to Standardize Doppler Acquisition in a Pediatric Cardiology Echocardiography Lab

Eunice Hahn, Nikki Duncan, Angela Statile, James Brown, Garick Hill, Christopher Statile. Cincinnati Children's Hospital Medical Center, Cincinnati, OH

Background: A review of our echocardiography laboratory practices demonstrated a variable assessment of Doppler interrogation of heart valves, leading to difficulties in comparison over time and ambiguity in the accuracy of the measurement. Nationally, quality metrics in echocardiography have been promoted. We sought to use quality improvement methodology to achieve measurable improvement in Doppler acquisition. **Methods:** A standardized protocol for Doppler acquisition was developed and translated into a 20-point scoring system. Tracking was conducted via random assessment of two first-

time, normal studies per day, if available. A baseline was established over a 4 month period. Interventions were then conducted over a 4 month time period including standardizing the process for acquisition, education, visual tracking, and individual feedback. **Results:** In total, 407 studies were analyzed (n=162 pre- and n=245 post-interventions). The percentage of studies with a goal Doppler score of 16 or higher pre-intervention was 17%. The median score was 13. Over a 4 month intervention period, the median score improved to 18.1 with 85% of studies achieving goal scores (Figure 1). Special-cause variation occurred after distribution of the protocol with educational meetings with further improvement after increased awareness and feedback regarding Doppler acquisition. **Conclusion:** Significant improvement in valvar assessment is possible with the use of a measurable scoring system and a concrete goal of incorporating 20 areas of Doppler assessment. Future goals include implementation of this assessment in all abnormal studies, thereby developing consistency in assessment throughout the lab.



P2-007

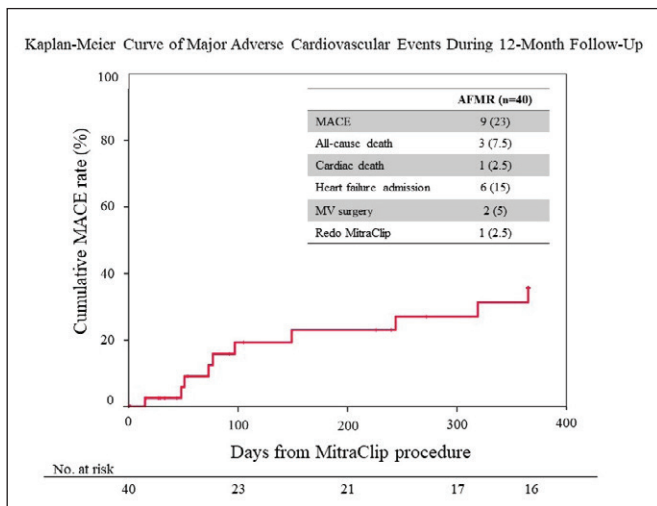
Clinical Outcome after MitraClip in Patients with Functional Mitral Regurgitation Due to Atrial Fibrillation

Jun Yoshida, Hiroki Ikenaga, Takafumi Nagaura, Nir Flint, Florian Rader, Robert Siegel, Saibal Kar, Takahiro Shiota. Cedars Sinai Medical Center, Los Angeles, CA

Background: Chronic atrial fibrillation with subsequent mitral annular dilatation and mitral leaflets malcoaptation is a recognized etiology of functional mitral regurgitation (FMR). The outcomes of patients with atrial fibrillation (AF) induced functional mitral regurgitation (AFMR), undergoing MitraClip has not been reported. **Methods:** Patients with FMR grade ≥ 3 and AF without left ventricular (LV) dysfunction or dilatation who underwent MitraClip at Cedars-Sinai Medical Center were included in the study. Echocardiographic and clinical data at baseline, 1-day and 12-months after MitraClip were retrospectively analyzed. Major adverse cardiovascular events (MACE) were defined as the combination of all-cause death, heart failure hospitalization, mitral valve surgery and re-do MitraClip. **Results:** 40 patients (mean age 80 ± 11 , 48% men) were included in the analysis. Baseline echocardiographic characteristics showed left atrial dilatation (median left atrial volume index of 87 ml/m^2). Median LV end-diastolic volume index was 62 ml/m^2 ; LV end-systolic volume index was 25 ml/m^2 ; LV ejection fraction was 58%, systolic pulmonary artery pressure was 47 mmHg , and BNP was 362 pg/ml . All patients had NYHA functional class III/IV at baseline. Twelve months post MitraClip, a significant improvement was observed in functional class, with only 28% of patients in NYHA III/IV compared with 100% prior to the procedure ($P < 0.001$). The rate of patients with MR grade ≥ 3 decreased from 100% at baseline to 14% at 1-day and 16% at 12-months follow-up ($p < 0.001$, respectively). However, compared with early (1-day) residual MR, the prevalence of MR ≥ 3 was increased at 12-months ($p=0.001$). During 12-months follow-up (median 263 days, Interquartile range [45-731]), MACE occurred in 9 (23%) patients (Figure 1) and was mainly attributed to hospitalization from heart failure (6 patients). Three patients died from any cause including 1 (2.5%) cardiac death. 3 (7.5%) patients needed mitral valve surgery or re-do MitraClip. **Conclusion:** In patients with FMR secondary to atrial fibrillation, MitraClip showed significant reduction in MR severity as well as improved functional capacity during mid-term follow-up.

Poster Session 2 (P2)

Monday, June 24, 2019



P2-008

Pediatric Echo Lab Study Acuity: A Novel Approach to Benchmarking

Tammy Lane Churchill, Ann E. Perkins, Shahryar Chowdhury, Carolyn L. Taylor. Medical University of South Carolina, Charleston, SC

Background: There is a scarcity of national benchmarking data regarding pediatric sonographer time management and resource utilization. Our pediatric echocardiography laboratory was faced with the need to produce data that quantified 1) our need for hospital resources dedicated to sonographer training and staffing and 2) the complexity of our pediatric imaging workload. To reach these goals, we implemented a system to track study acuity (SA). The objective was to create a system that quantified sonographer workload in a pediatric echo lab at an academic surgical center that could be used to guide staffing objectives and highlight training needs. **Methods:** Echocardiograms were rated as either low SA or high SA. High SA was based on the need for prolonged study time, complex congenital heart disease, and teaching or sonographer partnered echos. Specifically, high SA categories were defined as: 1) pre-operative 2) sedated 3) teaching fellow / junior sonographer or transesophageal echo assist 4) new complex congenital heart disease 5) catheterization lab studies (pre or intra-procedural) 6) Complete and/or discharge echos performed in the cardiac intensive care or stepdown unit and 7) fetal echos. Over 18 months (July 1, 2017 - December 31, 2018) sonographers recorded SA daily for all echos they performed. SA category data was compared between fiscal year 2018 (July 2017- June 2018) versus the first half of fiscal year 2019 (July 2018-December 2018). **Results:** In fiscal year 2018, number of high SA echos compared to the total number of echos performed was 2343 of 9806 (24%). In the first half of fiscal year 2019, the proportion of high SA echos increased (1519 of 5217 (29%)), $p < 0.05$. The 3 SA categories responsible for the highest utilization were discharge / ICU complete echos (37%), teaching and TEE assist (36%) and Cath lab (15%) associated studies. **Conclusion:** SA collection is a novel approach for collecting benchmarking data specific to the workload in pediatric echo labs. At our pediatric cardiac surgical center, high SA echos comprise at least ¼ of the total echos performed. We also showed that the proportion of high SA echos increased over time. This data can be used to advocate for resources, staffing needs and the time needed for training pediatric sonographers and fellows. SA is promising tool for multi-center collaboration to assess appropriate study time allotment, correlating SA to surgical volume and complexity, echocardiography billing and physician relative value units (RVUs).

P2-009

The Long-Term Progression of Mitral and Tricuspid Regurgitation on Echocardiography

Jordan B. Strom, Patrick Hyland, Yuansong Zhao, Changyu Shen, Lawrence J. Markson, Warren J. Manning. Beth Israel Deaconess Medical Center, Boston, MA

Introduction: While transthoracic echocardiography (TTE) is frequently performed for surveillance of mitral regurgitation (MR) and tricuspid regurgitation (TR), limited data exist on rates of long-term disease progression. **Methods:** Structured report data from 220,135 consecutive TTEs (118,647 patients) at Beth Israel Deaconess Medical Center, adjudicated by board certified faculty echocardiographers, were linked to death information from the Social Security Death Master File, 1/26/2000-12/31/2017. MR and TR were semiquantitatively graded (0+, 1+, 2+, 3+, 4+). Those with mitral or tricuspid valve annuloplasty or prostheses and those with only one echocardiogram during this period were excluded. Using the Kaplan-Meier method, the median and interquartile time to MR or TR progression were determined, adjusted for the competing risk of death, censoring at the end of the follow-up period. **Results:** A total of 187,902 TTEs on 108,168 individuals demonstrated $\geq 1+$ MR and 155,701 TTEs on 95,702 individuals demonstrated $\geq 1+$ TR.

Of those with ≥ 2 TTEs with MR/TR data, 5,379 (9.5%) with MR and 3,630 (10%) with TR had disease progression (Table). The median (IQR) time between TTEs was 412 days (85-1050). Patients with more significant MR and TR had a higher prevalence of mitral valve prolapse, were older, and had lower left ventricular ejection fractions ($p < 0.001$ for all). Pulmonary artery systolic pressure increased with severity of MR and TR ($p < 0.001$). The median (IQR) time in days for progression decreased with increasing regurgitant severity and was similar for MR and TR (MR: 414 [58-1330] days for 0 to 1+, 913 [230-2265] for 1 to 2+, 620 [128-1493] for 2 to 3+, and 457 [87-966] for 3 to 4+; TR: 422 [76-1225] days for 0 to 1+, 1022 [285-2158] for 1 to 2+, 625 [163-1601] for 2 to 3+, and 460 [107-1104] for 3 to 4+). Of those with 1+ MR or TR at baseline, 84.6% of those with MR and 86.8% of those with TR did not progress over the 18-year period. **Conclusions:** For patients with MR/TR, there is a progressive decline in the interval to progress to the next severity stage. Of those with baseline 1+ MR/TR, the vast majority have no disease progression. Further research on predictors of progression and the cost effectiveness of time intervals for surveillance echocardiography is warranted.

Table: Time to Progression of Mitral and Tricuspid Regurgitation

Time to Progression of Mitral Regurgitation		
Transition (N = 5379)	Frequency (%)	Median (IQR) Time to Progression, Days*
No transition (N = 29,554)		
0+ to 0+	1111 (3.2)	842 (112-2175)
0+ to 1+	1181 (3.4)	414 (58-1330)
0+ to 2+	23 (0.07)	520 (138-3384)
0+ to 3+†	6 (0.02)	239 (11-568)
1+ to 1+	27156 (77.7)	1144 (317-2546)
1+ to 2+	2732 (7.8)	913 (231-2266)
1+ to 3+	610 (1.7)	1038 (257-2346)
1+ to 4+	105 (0.3)	1039 (275-2122)
2+ to 2+	864 (2.5)	636 (108-1685)
2+ to 3+	769 (2.2)	582 (181-1615)
2+ to 4+	130 (0.4)	582 (181-1615)
3+ to 3+	316 (0.9)	448 (89-1321)
3+ to 4+	322 (0.9)	457 (87-966)
4+ to 4+	107 (0.3)	313 (50-932)
Time to Progression of Tricuspid Regurgitation		
Transition (N = 3630)	Frequency (%)	Median (IQR) Time to Progression, Days*
No transition (N = 23,896)		
0+ to 0+	228 (0.8)	1053 (245-2174)
0+ to 1+	253 (0.9)	422 (76-1225)
0+ to 2+‡	10 (0.04)	873 (174-1148)
1+ to 1+	22926 (83.3)	1158 (351-2453)
1+ to 2+	2129 (7.7)	1022 (285-2158)
1+ to 3+	600 (2.2)	1015 (313-2179)
1+ to 4+	118 (0.4)	1009 (184-2296)
2+ to 2+	532 (1.9)	621 (126-1597)
2+ to 3+	597 (2.2)	625 (163-1601)
2+ to 4+	107 (0.4)	566 (134-1546)
3+ to 3+	210 (0.8)	479 (76-1254)
3+ to 4+	190 (0.7)	460 (107-1104)
4+ to 4+	62 (0.2)	260 (29-963)

*For those who did not have progression (e.g. 0+ to 0+, 1+ to 1+), this represents the median (IQR) time of observation. †One patient had progression of MR from 0 to 4+ in 391 days. ‡One patient had progression of TR from 0+ to 3+ in 1582 days and one patient had progression of TR from 0 to 4+ in 71 days.

P2-010

The Unintended Impact of Indexation of Echo Measurements in People of Non-Caucasian Ethnicity

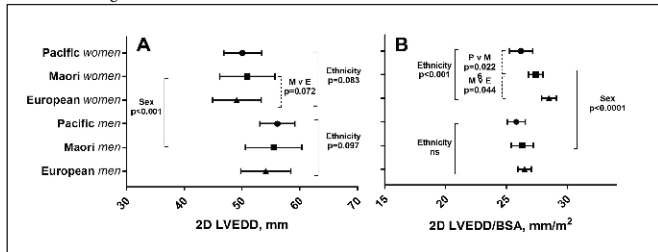
Gillian Whalley^{1,2}, Allannah Harrington^{3,2}, Andrew Kerr³, Jonathan Christiansen⁴, Bettina Ikanasio⁵, Arun Deo², Greg Gamble⁶, Sue Crengle¹.
¹University of Otago, Dunedin, New Zealand; ²Unitec Institute of Technology, Auckland, New Zealand; ³Middlemore Hospital, Auckland, New Zealand; ⁴North Shore Hospital, Auckland, New Zealand; ⁵Auckland University of Technology, Auckland, New Zealand; ⁶University of Auckland, Auckland, New Zealand

Background: Guidelines recommend indexing measurements to BSA. Despite increasing evidence that reference ranges differ by ethnicity (likely related to differences in fat free mass (FFM)), current ASE/EACVI guidelines (derived from mostly Caucasians) do not account for ethnicity. Indigenous New Zealanders, or Māori, and migrant Pacific peoples have high rates of CVD, but they also have higher FFM than the Caucasian population. We hypothesized that Māori or Pacific peoples will have larger hearts and that the upper and lower centiles of echocardiographic reference ranges will be different in Māori and Pacific peoples compared to European New Zealanders. We also evaluated the impact of indexing LVEDD. **Method:** A targeted population cohort of 263 adults (18-50yrs) who identified as Māori (N=71), Pacific (N=53) or European (N=139). Participants were healthy; no history of CVD, diabetes, hypertension & no CV medications. Diabetes (random glucose) and significant hyperlipidemia (random total cholesterol) were excluded using point of care testing. Body composition was assessed using Tanita scales. Echos were analysed by a single observer blinded to all other data. Quantile regression was used to identify the upper and lower limit of normal (ULN and LNN). ANOVA to identify differences between sexes and the ethnic groups. **Results:** Men had larger LVEDD in all groups and Māori and Pacific cohorts had bigger LVEDD than the European cohort in both sexes. Indexing to BSA, did not eliminate these differences and in fact resulted in higher ULN for the European

Poster Session 2 (P2)

Monday, June 24, 2019

cohort. **Conclusion:** Applying the current ASE/EACVI reference ranges in this population will over-diagnose cardiac enlargement. Conversely, when measurements are indexed to BSA, unintentional bias is introduced that systematically disadvantages Māori and Pacific patients, who have the highest CVD risk. Unique reference ranges for all ethnic groups are required in order to optimally detect and manage CVD in different populations, especially for those at highest risk.



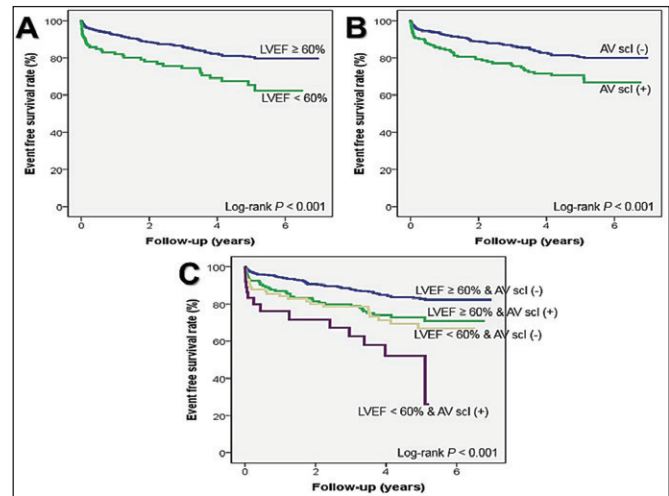
LVEDD and LVEDD/BSA by sex and ethnicity									
Variable	Maori Men	Pacific Men	European Men	Maori Women	Pacific Women	European Women	ANOVA	ANOVA	ANOVA
N	28	27	65	43	26	74	sex	ethnicity	interaction
LVEDD	55.5 ± 4.9	56.1 ± 3.0	54.1 ± 4.4	50.9 ± 4.8	50.1 ± 3.3	49.1 ± 4.2	<0.0001	0.0142	0.7062
LVEDD/BSA	26.3 ± 2.4	25.8 ± 1.9	26.5 ± 2.2	27.4 ± 2.0	26.2 ± 2.4	28.5 ± 2.6	0.0003	0.0003	0.0930

P2-011

Echocardiographic Parameters Determining Cardiovascular Outcomes in Patients After Acute Ischemic Stroke

Joo-Hee Zo, Sr.¹, Hack-Lyoun Kim, Sr.¹, Jae-Sung Lim, Sr.². ¹Boramae Medical Center, Seoul, Republic of Korea; ²Hallym University Sacred Heart Hospital, Anyang, Republic of Korea

Background: Few data are available on the prognostic impact of echocardiographic parameters in patients with acute ischemic stroke (AIS). The aim of this study was to evaluate the prognostic significance of echocardiographic parameters in patients with AIS. **Methods:** A total of 900 patients with AIS who underwent transthoracic echocardiography (TTE) (72.6 ± 12.0 years and 60% male) were retrospectively reviewed. Composite events including all-cause mortality, non-fatal stroke, non-fatal myocardial infarction, and coronary revascularization were assessed during clinical follow-up. **Results:** During a median follow-up of 3.1 years (interquartile range, 0.6-5.1 years), there were 151 (16.8%) composite events. Univariable analyses showed that low left ventricular ejection fraction (LVEF) (< 50%), increased peak tricuspid regurgitation (TR) velocity (> 2.8 m/s) and aortic valve (AV) sclerosis were associated with composite events (P < 0.05 for each). In the multivariable analyses after controlling for potential confounders, LVEF < 60% (hazard ratio [HR], 1.77; 95% confidence interval [CI], 1.19-2.62; P = 0.004) and AV sclerosis (HR, 1.57; 95% CI, 1.10-2.22; P = 0.012) were independent prognostic factors associated with composite events. Multivariable analysis showed that HR for composite events gradually increased according to LVEF and AV sclerosis: HR was 2.6-fold higher in the highest-risk group than in the lowest group (P = 0.003). Additional information of AV sclerosis and LVEF to clinical factors further increased the predictive power of composite events (global chi-square, from 69 to 77, P < 0.001). **Conclusions:** In patients with AIS, reduced LVEF and the presence of AV sclerosis predicts the future vascular events. Patients with AIS exhibiting reduced LVEF and AV sclerosis may benefit from aggressive secondary prevention.



P2-012

The Natural History of Aortic Stenosis: Influence of Age, Gender, Left Ventricular Function and Severity of Aortic Stenosis

Kalie Kebed¹, Deyu Sun², Karima Addetia¹, Victor Mor-Avi¹, Natasha Markuzon², Roberto M. Lang¹. ¹University of Chicago, Chicago, IL; ²Philips Healthcare, Andover, MA

Background: Prior aortic stenosis (AS) studies on the yearly progression of aortic valve area (AVA) were performed on small cohorts of patients. These studies provided little information on the influence of gender, age, left ventricular (LV) systolic function, or baseline severity on AVA progression. In this study, we aimed to characterize the progression of AVA (ΔAVA) on a large population of patients with varying degrees of AS and the influence of demographic and baseline echocardiographic factors. **Methods:** We identified 916 patients with mild to severe AS with more than one study from our database from 1994 to 2018 (total of 2547 studies). Age, gender, LV systolic function, and AVA calculated by the continuity equation were extracted for subgroup analysis. Annual rates of ΔAVA were determined by a linear-mixed effects model (β slope) and were compared using t-test. **Results:** The median patient age at the time of the initial echocardiogram was 75 years, and 44% were male. The rate of progression of AS was -0.062±0.003 cm²/year. This rate was not influenced by age or LV function, but was more rapid in men compared to women. There was an inverse relationship between initial severity of AS and progression rate (Table 1). **Conclusions:** The ΔAVA in AS in this large study suggests a lower decline than previously reported in smaller studies. This knowledge of the temporal progression and gender differences should provide clinical information on the expected interval before intervention is needed for severe AS.

		n	ΔAVA (cm ² /year)	
			Annual rate of change (β)	P-value
All patients		916	-0.062±0.003	
Age	Age ≥75yr	468	-0.057±0.004	0.08
	Age <75yr	448	-0.066±0.004	
Gender	Male	404	-0.068±0.004	0.03
	Female	512	-0.057±0.003	
AVA	Mild (>1.5cm ²)	292	-0.082±0.004 (*)	<0.001 (* vs ^)
	Moderate (1.0-1.5cm ²)	466	-0.057±0.003 (^)	
	Severe (<1.0cm ²)	158	-0.023±0.008 (+)	
LV Function	Normal	773	-0.061±0.003	0.29
	Reduced	143	-0.069±0.008	

P2-013

Leftward Posterior Deviation of Atrial Septum Primum Predicts Morbidity in Patients with Hypoplastic Left Heart Syndrome

Kamalvir Gill¹, Leo Lopez², Thomas Taylor¹, Juan Carlos Muniz¹. ¹Nicklaus Children's Hospital, Miami, FL; ²Lucile Packard Children's Hospital, Palo Alto, CA

Background: Leftward posterior deviation of atrial septum primum (LDSP) occurs <64% of neonates with hypoplastic left heart syndrome (HLHS), but there are no reports of its impact on outcomes. We reviewed the prevalence of LDSP and its correlation with outcomes in our study population. **Methods:** Neonates with HLHS managed at our institution between 2001 and 2018 were retrospectively evaluated. Demographic and clinical data obtained during the initial hospital admission were collected. The prevalence of LDSP was determined. Deviation was measured in subcostal short and long axis views on all LDSP patients by 2 independent observers (Fig 1). A deviation index (DI)

Poster Session 2 (P2)

Monday, June 24, 2019

= [(theoretical-functional left atrial area)/ theoretical area] was calculated for each view and averaged. **Results:** LDSP was seen in 57/94 (61%) HLHS patients. When comparing patients with and without LDSP, there was no significant difference in gestational age, birth weight, length of stay, and mortality (Table 1). Patients with LDSP had an increased incidence of unplanned reoperations, postoperative catheterizations and infections. After adjusting for gestational age, birth weight, HLHS subtype, and type of surgery, the presence of LDSP predicted reoperation (Odds Ratio (OR) = 3.6, $p < .01$), catheterization (OR = 2.7, $p = .05$), and infection (OR= 3.4, $p < .05$), but not cardiac arrest ($p = .2$), nor need for mechanical circulatory support ($p = .1$). The DI predicted higher risk for complications, including reoperation (DI $\geq .17$), catheterization (DI $\geq .07$), and infection (DI $\geq .12$). There was excellent interobserver Intra-Class Correlation reliability of the DI ($ICC_{\text{absolute-agreement}} = .82$ and $ICC_{\text{consistency}} = .90$). **Conclusion:** HLHS patients with LDSP has a higher prevalence of postoperative morbidity, and the DI is predictive of adverse events. Preoperative echocardiographic evaluation of LDSP may be helpful in risk stratification and counseling.

Table 1: Clinical Data

Complication	No Deviation (n=37)	Deviation (n= 57)	p-value
Mortality	11 (30%)	10 (18%)	0.17
Median LOS	25	30	0.33
Cardiac Arrest	3 (8%)	11 (19%)	0.14
Mechanical Circulatory Support	5 (14%)	14 (25%)	0.19
Unplanned Reoperation	8 (21%)	28 (49%)	<0.01
Postoperative Cardiac Catheterization	7 (19%)	22 (39%)	<0.05
Pacemaker Placement	0	0	1
Arrhythmia Requiring Cardioversion	4 (11%)	7 (12%)	0.83
Stroke	1 (3%)	0	0.39
Seizure	2 (5%)	2 (4%)	0.66
Intracranial Hemorrhage	4 (11%)	6 (11%)	0.97
Dialysis	3 (8%)	4 (7%)	0.84
Chylothorax	1 (3%)	1 (2%)	0.76
Paralyzed Diaphragm	0	3 (5%)	0.28
Reintubation	7 (19%)	12 (21%)	0.8
Infection/Sepsis	5 (14%)	19 (33%)	<0.05
Necrotizing Enterocolitis	1 (3%)	4 (7%)	0.36
Pericardial Effusion requiring drainage	1 (3%)	3 (5%)	0.55
Transfer for transplant	0	3 (5%)	0.28

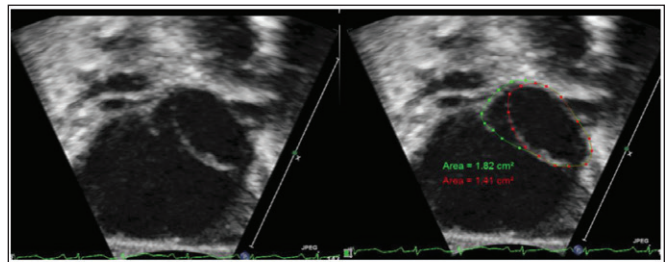


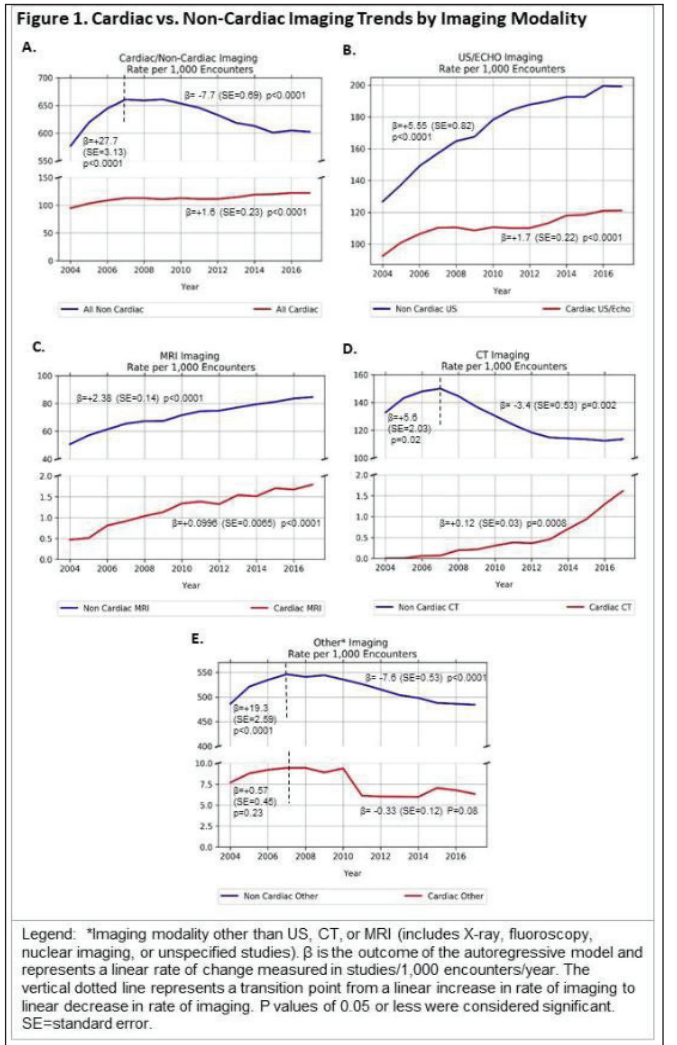
Fig. 1. Calculation of the Deviation Index (DI): The functional left atrium (red, 1.41 cm²) is defined as the area of the left atrium bounded by deviated septum primum. The anatomic left atrium (green, 1.82 cm²) is the theoretical left atrial area if septum primum were not deviated. DI = [(anatomic – functional) / anatomic] = 0.23. A larger DI value reflects a larger amount of deviation. RA = right atrium. LA = left atrium. LDSP = leftward deviated septum primum.

P2-014 Contemporary Use and Temporal Trends in Utilization of Imaging in Pediatric Hospitals: A Pediatric Health Information Service Database Analysis from 2004 to 2017

Shae Anderson¹, Janet Figueroa², Courtney E. McCracken², Timothy C. Slesnick¹, William Border¹, Ritu Sachdeva¹. ¹Emory University/CHOA, Atlanta, GA; ²Emory University, Atlanta, GA

Background: Concern exists over the growth in cardiac imaging and related expenditures in adults. There is no such data for pediatric patients. We sought to determine temporal

trends in the use of non-invasive cardiac imaging and compare these with non-cardiac imaging using the Pediatric Health Information Service (PHIS) database. **Methods:** Data from pediatric inpatient encounters (encntrs) from Jan 2004-Dec 2017 at 35 children's hospitals were extracted from the PHIS database. Temporal trends in the use of non-invasive cardiac and non-cardiac imaging including ultrasound (US), magnetic resonance imaging (MRI), computerized tomography (CT), and others (X-Ray, fluoroscopy, and nuclear imaging) were studied. Autoregressive models assessed linear trends. **Results:** A total of 5,869,335 encntrs over 14 years were analyzed (median=166,209 encntrs /center). At the end of 2017, 61.7% encntrs had an imaging study (60.4% non-cardiac and 11.9% cardiac—11.8% echo, 0.2% cardiac MRI and 0.2% cardiac CT). Overall inpatient imaging use based on rate per 1,000 patient encounters rose linearly until 2007 (+28.2 studies/1,000 encntrs/yr from 2004-2007) then declined linearly (-7.2 studies/1,000 encntrs/yr from 2008-2017). Non-cardiac imaging trends mirrored overall imaging trends, peaking in 2007 (+27.7 studies/1,000 encntrs/yr from 2004-2007 then -7.7 studies/1,000 encntrs/yr from 2008-2017); however throughout the entire study period there was an increase in cardiac imaging (Fig 1A). Cardiac and non-cardiac US and MRI use increased over time (Fig 1B,C). Unlike non-cardiac CT use, which peaked in 2007 and then declined, cardiac CT use increased linearly (Fig 1D). Use of "other" non-cardiac imaging also peaked in 2007 and then declined, whereas no significant trends were seen for "other" cardiac imaging (Fig 1E). **Conclusions:** Overall there has been steady linear growth in cardiac imaging for pediatric inpatients, unlike non-cardiac imaging. However, cardiac imaging continues to comprise a small fraction of inpatient imaging. While trends in cardiac and non-cardiac US and MRI are uniformly increasing, the use of cardiac CT is rising faster than other modalities, unlike non-cardiac CT. Further investigation is underway to evaluate patient and center characteristics associated with these trends.



Legend: *Imaging modality other than US, CT, or MRI (includes X-ray, fluoroscopy, nuclear imaging, or unspecified studies). β is the outcome of the autoregressive model and represents a linear rate of change measured in studies/1,000 encounters/year. The vertical dotted line represents a transition point from a linear increase in rate of imaging to linear decrease in rate of imaging. P values of 0.05 or less were considered significant. SE=standard error.

Poster Session 2 (P2)

Monday, June 24, 2019

P2-015

Standardization of Assessment of Image Quality on Transthoracic Echocardiograms: A Quality Study in the Echo Lab

Denise Ignatowski, Brianna Johnson, Rachael Esenberg, Adil Wani, Renuka Jain, Bijoy K. Khandheria. Aurora Cardiovascular Services, Aurora Sinai/ Aurora St. Luke's Medical Centers, Milwaukee, WI

Background: Image quality is reported on all echocardiograms and is part of the national standard for a complete report; yet there is no standard criteria. As part of a quality study, we evaluated current practice for image quality assessment and investigated a standardized assessment tool. **Methods:** We surveyed sonographers, soliciting comments on how they determine image quality. We then de-identified 100 transthoracic echocardiograms. A team of 4 experienced sonographers was asked to classify 25 of these echocardiograms into five categories: Excellent, Good, Fair, Poor, and Technically Difficult. Two sonographers were then provided a defined protocol for grading image quality and asked to reassess 50 echocardiograms using this scale. **Results:** Seventeen sonographers responded to initial survey. Sonographers reported using multiple criteria - 3 overlapping criteria were most common: image clarity (n=12), ability to answer clinical question (n=11), and difficulty obtaining images due to patient factors (n=4). During initial review of 100 echocardiograms, there was modest correlation ($r = 0.574, p < 0.001$) between review and initial sonographer assessment. After introduction of tool (Table), the correlation between 2 sonographers improved significantly and was very strong ($r = 0.80, p < 0.001$). **Conclusion:** Although image quality on echocardiograms is a requirement on all reports, there are currently no guidelines for grading image quality. In our laboratory, each sonographer had a unique method for assessing image quality, using an overlap of three factors. The introduction of standard criteria for image quality assessment greatly improved correlation between sonographers. With standardized image quality guidelines, we can begin to relate the level of image quality to the amount of information available to interpret and we look forward to expanding this tool as part of improving quality in echocardiography laboratories.

1	Excellent	All cardiac structures are clearly visualized Valve structures and all valve leaflets are clearly visualized All segments of LV endocardium well visualized Well defined Doppler signals No artifacts are present
2	Good	All cardiac structures are clearly visualized Valve structures and all valve leaflets are well visualized All segments of endocardium well visualized Defined Doppler signals Artifacts, if present, do not hinder visualization of key structures
3	Fair	All cardiac structures are visualized, some imaging planes are off-axis Valve structures are visualized, but not clearly Left ventricular endocardial definition adequate for EF evaluation Defined Doppler signals Artifacts are present which hinder visualization of key structures
4	Poor	All cardiac structures are not visualized Valve structures are not well visualized Left ventricular endocardial definition is inadequate for EF evaluation Unable to acquire accurate Doppler signals due to off-axis views or lack of optimization Artifacts are present which hinder visualization of key structures
5	Technically Difficult	One or more imaging windows is unavailable for assessment Critical cardiac structures and valves are not well visualized Left ventricular endocardial definition, even with contrast use, is suboptimal Unable to acquire accurate Doppler signals Severe artifacts are present

P2-016

Impact of Collaborative and Consensus Based Quality Improvement Bundle on Measurement Variability and Imaging Quality of Routine Surveillance Echocardiograms in Children Receiving Cardiotoxic Chemotherapy

Aarti H. Bhat, Kathryn Whitlock, James Nelson, Joey Goulding, Abigail Cone, Ray-Ann Queen, Michele Clouse, Arti Desai. Seattle Children's Hospital, Seattle, WA

Background: Awareness and concern for long-term cardiac dysfunction in childhood cancer survivors is increasing as is the importance of echocardiography (echo) based surveillance in this group. Accurate measurements of left ventricular (LV) wall thickness, dimension and systolic function are critical to early detection of changes leading to appropriate management modifications. We sought to develop and implement a quality improvement (QI) intervention to: (1) decrease measurement variability; (2) increase image acquisition completeness and (3) improvement technical adequacy of echos performed as part of standard care. **Methods:** Education intervention implemented in a tertiary academic children's hospital's echo lab included development of an imaging protocol, checklist and multiple collaborative sessions to develop consensus around precise measurement techniques based on standard recommendations. Post-intervention retrospective review of measurement variability, acquisition completeness and technical adequacy was performed by random selection of echos by a group of sonographers and physicians blinded to the original report. LV dimensions and fractional shortening (FS) were measured on M-mode, ejection fraction (EF) by biplane Simpson's method. Aggregate measures were used to calculate x-bar control chart limits, absolute deviations in measurements compared using exact nonparametric tests. Acquisition completeness and technical adequacy were compared in a generalized linear mixed model adjusted for duplicate reads, expressed as a percentage. **Results:** 128 echos on patients under 18 years of age were reviewed by nine experienced over-readers and compared with original reads before and after intervention along with assessment of study completeness and quality. LV wall and systolic function measurement variability was mostly stable over the entire study period (Table). Completeness of acquisition remained unchanged at 92% and technical adequacy improved from 56% to 69%. **Conclusions:** Robust pre-intervention imaging and measurement technique precluded observable improvements but lead to better understanding of common pitfalls and challenges within the echocardiography lab and confidence in measurement practices, particularly as they apply to this high-risk group of patients.

Measurement	Pre-intervention		Post-intervention		P Value
	Mean ^a	(95% CI)	Mean ^a	(95% CI)	
IVS(d)	0.08	(0.06, 0.10)	0.09	(0.08, 0.11)	0.27
LVID(d)	0.14	(0.11, 0.17)	0.12	(0.10, 0.15)	0.37
PW(d)	0.09	(0.07, 0.11)	0.09	(0.07, 0.11)	0.83
IVS(s)	0.10	(0.08, 0.13)	0.14	(0.12, 0.17)	0.04
LVID(s)	0.11	(0.08, 0.13)	0.12	(0.10, 0.15)	0.46
PW(s)	0.10	(0.08, 0.13)	0.12	(0.09, 0.14)	0.41
FS	2.30	(1.73, 2.86)	2.72	(2.19, 3.26)	0.28
EF	4.35	(3.39, 5.31)	4.54	(3.63, 5.44)	0.78

Abbreviations: IVSD(d) = left ventricular interventricular septum, diastole; LVID(d) = left ventricular internal dimension, diastole; PW(d) = left ventricular posterior wall, diastole; IVS(s) = left ventricular interventricular septum, systole; LVID(s) = left ventricular internal dimension, systole; PW(s) = left ventricular posterior wall systole; FS = fractional shortening; EF = ejection fraction.

^a Value represents the mean absolute deviation of each original measurement from the average of over-reader measurements for each study (in mm for all LV dimensions and in % for FS and EF).

P2-017

Off-Axis Imaging of the Left Ventricular Outflow Tract by Two-Dimensional Echocardiography Leads to Underestimation of Aortic Valve Area

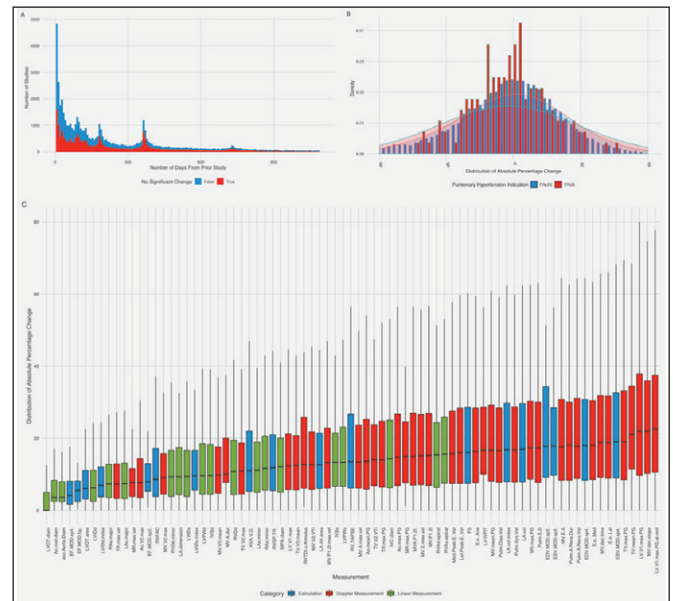
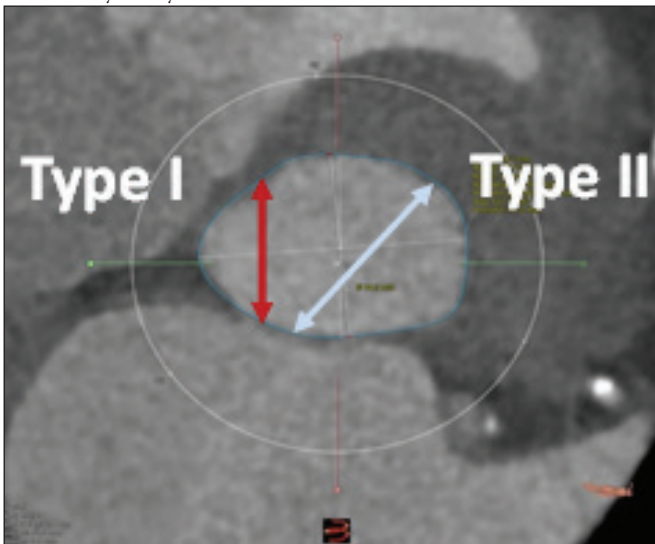
Li Zhou, Charles W. Craver, Min Pu. Wake Forest University Baptist Medical Center, Winston Salem, NC

Background: Accurate calculation of aortic valve area (AVA) is essential for diagnosis of severe aortic stenosis. The greatest potential source of error in the calculation of AVA by continuity equation is left ventricular outflow tract (LVOT) diameter, as it is squared to calculate LVOT area. It has been long recognized that the LVOT area is under-calculated by echocardiography (echo) due to an oval geometry. We hypothesized that the off-axis imaging of LVOT by echo could also be a source of error for underestimation of LVOT area. In order to verify the hypothesis, we conducted a head-to-head comparison of LVOT measurements by traditional two-dimensional (2D) echocardiography and multi-detector computed tomography (CT). **Methods:** Standardized 2D echo and CT images were obtained in 48 patients. The major and minor axes of the LVOT were measured 5 mm below the aortic annulus by cardiac CT using 3mensio Structural Heart software (Pie

Poster Session 2 (P2)

Monday, June 24, 2019

Medical Imaging, Netherlands). The LVOT diameter was also measured in the parasternal long-axis view at 5 mm below the aortic valve by echo. We classified the off-axis imaging into two types (Figure). Type I is the LVOT diameter measured by echo was less than the minor axis by CT, while Type II is the LVOT diameter measured by echo was greater than the minor axis, but less than the major axis by CT. **Results:** The major and minor axes of LVOT measured by CT were 25.9 ± 3.7 mm and 20.7 ± 3.2 mm, respectively. The LVOT diameter by echo was 20.0 ± 2.7 mm. Twenty-seven patients (56%) were found to have Type I off-axis (LVOT 19.5 ± 2.7 mm by echo vs. 22.0 ± 3.1 mm by CT, $p < 0.01$) and 21 patients (44%) had Type II off-axis (20.5 ± 2.6 mm by echo vs. the minor axis 18.7 ± 2.9 mm and the major axis 26.3 ± 2.0 by CT, $p < 0.01$). Clearly, Type I off-axis error resulted in significant underestimation of LVOT area, and thus led to a smaller AVA. **Conclusion:** The off-axis imaging of LVOT by 2D echo was common and Type I off-axis could result in a significant under-calculation of AVA. Routine use of biplane during 2D echo to bisect the LVOT may identify and reduce the error.



P2-018

Defining 'No Significant Change': Standard Error of Standard Echocardiogram Measurements

David Ouyang, Stanford University, Menlo Park, CA

Introduction: Comparison statements in reports highlight clinically relevant changes between imaging studies. While there is no formal definition of 'no significant change', this statement suggests that variation from the study to the prior study is within the measurement error of each measurement or are not clinically significant. The precision of any measurement depends on biological variability, variation across practitioners, and inherent variation of the measurement. Previous efforts to determine the precision of echocardiogram measurements are confounded by observation bias, and there has been no large-scale assessment during typical clinical practice of an accredited echocardiography lab. **Methods:** From a corpus of 127,886 reports from routine echocardiography studies from 2004 to 2018 at a large academic medical center, we identified 25,915 studies reported as having no significant change compared to a prior study. Quantitative measurements from each study was extracted and a distribution of the percent change from prior study was obtained from 535,651 direct pairwise comparisons. The indication for study was identified to assess its influence on measurement precision. **Results:** We identified 58,337 echocardiogram studies with a prior study for comparison, of which 25,915 (44.4%) studies were reported as having no significant change. The likelihood of having no significant change did not correlate with time between studies. In these studies, linear measurements had less variance than Doppler measurements ($p < 0.001$). Clinically relevant measurements (such as ascending aortic root diameter for patients with Marfan's syndrome and right ventricular systolic pressure for patients with pulmonary hypertension) had less variance than the same measurement when measured as part of a routine study ($p < 0.001$ for both, F-test for variance). **Discussion:** No significant change is a common but not well-defined term in imaging studies. This study retrospectively estimates the standard error of conventional echocardiogram measurements by comparing consecutive studies without change. Inter-reader variation is highlighted by differences in precision based on indication of study. The relative precision of each measurement varied by type of measurement and likely the attention placed on the measurement.

P2-019

Association of Echocardiography Use and Inpatient Mortality in Patients with Septic Shock - Insights from National Inpatient Sample

Abhishek Chaturvedi¹, Parul Chandrika², Muhammad Salman Faisal¹, Manreet Kanwar¹, Raymond Benza¹, Amresh Raina¹. ¹Allegheny Health Network, Pittsburgh, PA; ²East Carolina University, Greenville, NC

Background: Patients with septic shock (SS) often have significant cardiovascular comorbidities and sepsis can itself induce myocardial dysfunction which can contribute to poor outcomes. Transthoracic echocardiography (TTE) is a readily available, noninvasive means to assess cardiac structure, function and hemodynamics. We sought to determine whether use of TTE is associated with lower mortality in patients with SS using 2014 National Inpatient Sample (NIS) database. **Methods:** NIS is the largest all-payer inpatient care database and represents a random, 20% stratified sample of all inpatient hospitalizations from 46 states, representing >97% of the total US population. Patients with diagnosis of SS and use of TTE were identified using the ICD9 diagnosis code 785.52 and procedure code 88.72 respectively. Neonates and those with hospitalizations lasting <24 hour were excluded to counter bias created by critically ill patients in whom a fatal outcome occurred without sufficient lead time to obtain TTE. Demographics, comorbidities, and inpatient mortality (IM) were compared between TTE vs noTTE groups. **Results:** Amongst 35.4 million weighted hospitalizations in 2014, 443685 SS patients were identified (mean age 65.3 years, 51% male). Only 6.5% of SS patients underwent TTE during their hospitalization. Patients who had TTE had a significantly higher burden of heart failure, valvular and pulmonary disease, hypertension, complicated diabetes, renal failure, fluid and electrolyte imbalance, and history of drug abuse (Table 1). However, IM was actually lower in the TTE group (30% vs 31.5%; $p=0.02$). On multivariate regression analysis, TTE was found to be associated with lower odds of IM in SS even after adjustment for age, gender, race, Elixhauser comorbidities, income and insurance status [OR(CI): 0.92 (0.86-0.98) ; $P=0.009$]. **Conclusions:** Our findings suggest that use of TTE is associated with decreased odds of mortality in SS patients. This may be secondary to the information provided by TTE that assists physicians in hemodynamic monitoring, risk stratification and management decisions for use of fluids and vasopressors.

Poster Session 2 (P2)

Monday, June 24, 2019

Table 1: Comparison Of Baseline Characteristics And Mortality Between Patients Who Underwent TTE Versus Those Who Did Not Undergo TTE In Septic Shock (N=443685).

Parameters	TTE (N=28045)	No TTE (N=415640)	P
Demographics			
Age, years	64.0±0.2	65.4±0.1	<0.001
Males, %	54.5	51.2	<0.001
Elixhauser comorbidities			
Congestive Heart Failure, %	39.5	28.2	<0.001
Valvular heart disease, %	18.8	7.4	<0.001
Pulmonary circulation disorder, %	14.1	8	<0.001
Peripheral vascular disease, %	12	10.6	0.001
Hypertension, %	56.4	53.6	<0.001
Paralysis, %	6.5	7.3	0.02
Other neurological disorder, %	10.2	11.9	<0.001
Chronic pulmonary disease, %	24.6	26.3	0.005
Diabetes without complications, %	23.5	23.7	0.68
Diabetes with complications, %	7.4	6.1	<0.001
Hypothyroidism, %	12.5	13.4	0.04
Renal failure	31	27.3	<0.001
Liver disease, %	9.7	9	0.09
Chronic peptic ulcer disease, %	0.1	0.1	0.7
HIV and AIDS, %	0.8	0.6	0.26
Lymphoma, %	2.4	2.4	0.94
Metastatic cancer, %	4.3	6.5	<0.001
Solid tumor without metastasis, %	3.2	4.5	<0.001
Rheumatoid arthritis/Collagen vascular disease, %	3.7	3.7	0.96
Coagulation deficiency, %	25.2	21.2	<0.001
Obesity, %	15.2	13.2	<0.001
Weight loss, %	26.8	25.1	0.006
Fluid and electrolyte disorder	76	73.2	<0.001
Blood loss anemia, %	1.4	1.5	0.42
Deficiency anemia, %	33.9	33.2	0.23
Alcohol abuse, %	6.6	6.4	0.48
Drug abuse, %	6.4	3.8	<0.001
Psychoses, %	4.9	4.9	0.9
Depression, %	8.7	10	0.002
Outcome Measures			
Mortality, %	30	31.5	0.02

Values are reported as mean for continuous variables. Categorical variables are represented in frequencies. Between group comparisons were performed using Student's t-test for continuous variables and by using chi-squared test for Categorical variables. p<0.05 considered for statistical significance.

P2-020

A Standardized Imaging Protocol Improves Quality and Reduces Practice Variability in Echocardiographic Assessment of Ventricular Function by First-Year Pediatric Cardiology Fellows

Brian R. White, Deborah Y. Ho, Lindsay S. Rogers, Shobha S. Natarajan. *The Children's Hospital of Philadelphia, Philadelphia, PA*

Background: Teaching pediatric cardiology fellows to perform and interpret transthoracic echocardiograms (TTEs) is one of the most important components of fellowship. A common type of TTE performed independently by first-year fellows is the acute inpatient assessment of ventricular function. Therefore, as part of our efforts to continuously improve education, we created a standardized TTE imaging protocol for this focused assessment. We present results of implementing this protocol with the goal of reducing unnecessary practice variation in TTE images acquired and methods used for quantitative assessment. **Methods:** For our educational intervention, first-year fellows starting in 2018 were given a standard protocol to assess function with a quick-reference card. Pre-intervention baseline data of existing practice variability were obtained from review of fellow-imaged TTEs from October through January of fellowship years 2015-2017. Post-intervention data were collected from fellow-imaged TTEs from 10/1/18-1/31/19. TTEs were eligible for inclusion if they were (1) assessments of ventricular function or pericardial effusion and (2) performed by first-year fellows without sonographer supervision. Exclusion criteria were (1) early study termination due to patient instability or (2) mechanical circulatory support. While all studies were reviewed for demographic reporting completeness, TTEs on patients with univentricular or unrepaired biventricular congenital heart disease were excluded from image evaluation. **Results:** A total of 292 TTEs met inclusion criteria (227 before and 65 after the protocol intervention). A full image review was performed on 128 TTEs (80 pre- and 48 post-intervention). Results are summarized in the Table. Documentation of systemic blood pressure measurements was more complete after the protocol introduction. The protocol also led to more complete subcostal evaluations and increased quantitative evaluations of function. However, omission of some views remains common. **Conclusion:** There is unintended practice variability amongst independent first-year pediatric cardiology fellows, which can be mitigated with the use of a standardized imaging protocol. Reducing continued practice variation will be a focus of future educational efforts and quality improvement.

First-year fellow compliance with the transthoracic echocardiography ventricular function protocol

Demo-graphic Criteria	Pre-Intervention (N=227)	Post-Intervention (N=65)	p-value				
Notate Weight	98%	100%	0.28				
Notate Height	85%	94%	0.06				
Notate Blood Pressure	89%	97%	0.04				
Subcostal Views	Pre-Intervention (N=80)	Post-Intervention (N=48)	p-value		Pre-Intervention (N=80)	Post-Intervention (N=48)	p-value
Any	92%	94%	0.61				
Effusion Sweep	90%	94%	0.46				
Frontal or LAO Sweep	51%	69%	0.05	Color Doppler of the Atrial Septum	16%	23%	0.35
Spectral Doppler of the Descending Aorta	26%	50%	0.006				
Apical Views	Pre-Intervention (N=80)	Post-Intervention (N=48)	p-value		Pre-Intervention (N=80)	Post-Intervention (N=48)	p-value
Any	99%	100%	0.44				
Four-Chamber View	94%	96%	0.62	Two-Chamber View	38%	67%	0.001
Simpsons' Four-Chamber	43%	67%	0.008	Simpsons' Two-Chamber	25%	50%	0.004
Four-Chamber Complete Sweep	51%	54%	0.75				
TAPSE	50%	79%	0.001				
Tricuspid Valve Color Doppler	79%	85%	0.35	Tricuspid Valve Spectral Doppler	74%	83%	0.21
Mitral Valve Color Doppler	86%	90%	0.58	Mitral Valve Spectral Doppler	76%	81%	0.51
Left Ventricular Outflow Tract	45%	54%	0.32	Left Ventricular Outflow Tract Color Doppler	59%	69%	0.26
Parasternal Long and Short Axis	Pre-Intervention (N=80)	Post-Intervention (N=48)	p-value		Pre-Intervention (N=80)	Post-Intervention (N=48)	p-value
Any Long Axis	80%	81%	0.86				
Left Ventricular Long Axis	66%	73%	0.43	Long Axis Complete Sweep	54%	42%	0.19
Any Short Axis	94%	92%	0.66				
Short Axis, Base	31%	50%	0.03	Short Axis Complete Sweep	65%	71%	0.50
Short Axis, Mid-Ventricular	88%	85%	0.74	M-Mode for Shortening Fraction	82%	81%	>0.99
Right Ventricular Outflow Tract Color Doppler	40%	54%	0.12				

P2-021

Improving Quality of Transesophageal Echocardiographic Examination for Patients with Atrial Fibrillation Using an Automated Protocol

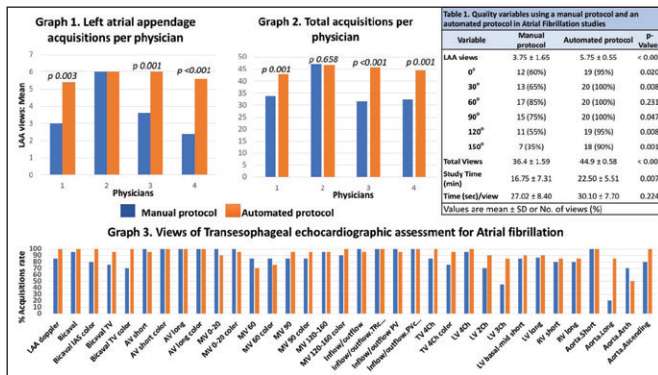
Maria Camila Trejo-Paredes¹, Roy Arjoon², Edith Lilitana Posada-Martinez¹, Xochitl Arely Ortiz-Leon¹, Ashley Brogan², Peter Flueckiger³, Ben A. Lin¹, Robert L. McNamara¹, Lissa Sugeng¹. ¹Yale University, New Haven, CT; ²University of Pennsylvania, Philadelphia, PA; ³Piedmont Healthcare, Atlanta, GA

Background: Variability in transesophageal echocardiographic examinations (TEE) may lead to diagnostic dilemmas and additional testing. Maintaining TEE quality across echocardiographic laboratories is difficult even with Intersocietal Accreditation Commission (IAC) guidelines. Our aim was to improve TEE quality using an automated TEE protocol in patients undergoing TEE with an indication of atrial fibrillation (AF).

Poster Session 2 (P2)

Monday, June 24, 2019

Methods: A retrospective review of TEE studies for AF using a manual TEE protocol performed by 4 physicians on a Phillips iE33 (Philips Healthcare, Andover, MA) was done. Each attempt at imaging a cardiac structure was noted along with the time/study. TEE quality was defined as complete assessment of the left atrial appendage (LAA) as per our echolab protocol (includes 6 views: at 0, 30, 60, 90, 120 and 150 degrees), and overall protocol completeness (48 views). Our quality improvement strategy included: presentation of the variability found on the initial retrospective review to the TEE operators and implementation of an automated TEE protocol on the EpiQ 7C (Philips Healthcare). Our automated TEE protocol followed the IAC guidelines for TEE image acquisition. We reassessed TEE quality 1 year after implementation. **Results:** The effect of an automated TEE protocol demonstrated improvement in the number of acquisitions for LAA assessment at different angles ($p < 0.001$) and an increase in the overall number of TEE image acquisitions ($p < 0.001$). The automated protocol required a longer study time ($p < 0.007$), but there was no significant difference in the time/view ($p = 0.224$) (Table 1). All physicians had a more complete LAA evaluation (Graph 1) and improved study completeness (Graph 2-3), particularly inclusion of the bicuspid tricuspid valve color, left ventricle 3 chambers, aorta long axis and ascending aorta ($p < 0.05$). **Conclusion:** An automated TEE protocol improves adherence to IAC guidelines for TEE and enables a more complete study without significantly lowering physician efficiency. These findings may aid with a more standard and consistent approach to TEE imaging across operators and locations. Future studies are warranted to determine if this improvement in quality results in an increased diagnostic or prognostic value of TEE for this subset of patients.



Baseline Characteristics				
Overall N= 985	eSVR tertile 1	eSVR tertile 2	eSVR tertile 3	P value
eSVR 6.4 ± 1.6	4.8 ± 0.5	6.2 ± 0.4	8.2 ± 1.3	<0.0001
SBP (mmHg)	122 ± 16	133 ± 17	144 ± 23	<0.0001
DBP (mmHg)	70 ± 10	75 ± 10	80 ± 12	<0.0001
Age (years)	66 ± 10	66 ± 11	68 ± 11	0.038
Male	75%	82%	88%	<0.0001
Hypertension	67%	69%	76%	0.035
Myocardial infarction	51 %	58%	53%	0.13
LVOT VTI (cm)	26 ± 4	21 ± 3	18 ± 3	<0.0001

Results				
Outcomes	eSVR tertile 1 Reference	eSVR tertile 2 HR (95% C I)	eSVR tertile 3 HR (95% C I)	P value
All cause mortality	Reference	1.1 (0.8, 1.6)	1.6 (1.1, 2.3)	0.012
Heart Failure	Reference	1.4 (0.9, 2.4)	1.9 (1.1, 3.3)	0.029
Myocardial Infarction	Reference	1.4 (0.8, 2.4)	1.3 (0.7, 2.5)	0.49
Cardiovascular mortality	Reference	1.3 (0.5, 3.3)	3.3 (1.3, 8.9)	0.016
Combined outcomes	Reference	1.6 (1.1, 2.2)	2.1 (1.8, 2.9)	<0.001

P2-022

Doppler Derived Systemic Vascular Resistance Predicts Cardio-Vascular Outcomes in Hypertension

Bhaskar Arora, Qizhi Fang, Dwight Bibby, Nelson Schiller. UCSF Medical Center, San Francisco, CA

Background: Blood pressure depends on the interaction between volume and resistance. This interaction can be expressed as systemic vascular resistance (SVR). Since SVR is a basic expression of afterload, we investigated the relationship of SVR derived by echocardiography (eSVR) with cardiovascular outcomes and all-cause mortality in a cohort of patients with stable coronary artery disease. Noninvasive SVR is calculated using the ratio of mitral regurgitation velocity (MR Vmax) and left ventricular outflow tract time velocity integral (LVOT VTI) and correlates well with right heart catheterization derived SVR. We, herein, propose a modification of above calculation by substituting systolic blood pressure (SBP) for MR Vmax. eSVR can therefore be readily obtained at bedside and it's use as a guide to therapy may be explored. **Methods:** The data from 985 subjects with established coronary artery disease in the Heart and Soul study formed the study cohort. We performed retrospective analysis of this prospectively obtained data and calculated eSVR using SBP, obtained at the time of the echocardiography, and LVOT VTI. Baseline characteristics of the Heart and Soul study population have been previously published. The cohort was divided into 3 groups based on the distribution of eSVR. Multi variate adjusted linear regression models were used to examine the relationship of eSVR with composite outcome of myocardial infarction, heart failure, stroke, cardiovascular death and all-cause mortality. **Result:** shown as a table. **Conclusion:** eSVR in the highest tertile was predictive of adverse cardiovascular outcomes. eSVR can be readily obtained using noninvasive data and could be a potential target of treatment. These are hypothesis generating results which call for further research.

P2-023

Impact of a New Echocardiography Orientation Course on Number and Quality of Echocardiograms Performed by First-Year Pediatric Cardiology Fellows

Jie Tang, Jarrett Linder, Valerie Capone, Deborah Ho, Jill Savla, Brian White, Heather Griffiths, Antara Mondal, Michael O'Byrne, Michael Quartermain, Lindsay Rogers. The Children's Hospital of Philadelphia, Philadelphia, PA

Background: At many centers, cardiology fellows are responsible for performing inpatient transthoracic echocardiograms (TTEs) while on call. Most fellows enter training without prior TTE experience, creating demand for rapid acquisition of imaging skills. In July 2018, we implemented a new, intensive echocardiography orientation course for incoming cardiology fellows at our program. The course emphasized hands-on TTE learning, including 6 sessions of 2-on-1 instruction with an advanced fellow, using healthy child volunteers. We investigate the impact of the course on quality and quantity of TTEs performed during the first 6 months of fellowship, as compared to previous classes of fellows who did not receive orientation. **Methods:** After orientation, the number of TTEs performed by the entering fellowship class of 2018 (n = 6 fellows) were counted through the first 6 months of training. Total daytime and nighttime/on-call TTEs were tracked, and TTEs were noted to be independent or assisted. TTE numbers were compared with those of 4 previous classes of fellows who started training in 2014 through 2017 (n = 25 fellows, 6-7 fellows per class). An expert-reviewed grading rubric focused on image optimization was used to assign numeric image quality scores to TTEs performed by the entering classes of 2017 and 2018; possible scores ranged 0 to 39. 45 randomly-chosen TTEs were reviewed from each class by a blinded reviewer. Scores were compared between the 2 classes. **Results:** Based upon their night float/call schedules and daytime TTE rotations, fellows pre- and post-orientation had similar opportunities for imaging. Post-orientation, the average number of TTEs performed per fellow during the first 6 months of training increased from 79.3 to 101.8 (p = 0.090). This increase was attributed to increased daytime TTEs (46.5 to 76.5 per fellow; p = 0.045), the majority of which were performed with assistance. No difference was observed in the number of nighttime/on call TTEs or independent TTEs performed. TTEs performed by fellows who received orientation scored significantly higher in image quality, with an average score of 29.1 out of 39, compared to 27.0 scored by fellows who did not receive orientation (p = 0.016). **Conclusion:** Fellows who participated in a focused echocardiography orientation course performed significantly more daytime and higher quality studies, compared to a historical cohort who spent comparable time on TTE rotations and on call. Future goals should be focused on promoting independence and confidence through this course, and empowering fellows to complete independent TTEs early in their training.

Poster Session 2 (P2)

Monday, June 24, 2019

P2-024

Severity of Coexistent Mitral Regurgitation and Predictors of Improvement After Transcatheter Aortic Valve Replacement

Joan Ava Kaye R. Tiu, Fabio Enrique B. Posas, Ofelia N. Valencia, Ma. Helga F. Sta. Maria. St. Luke's Medical Center Global City, Taguig, Philippines

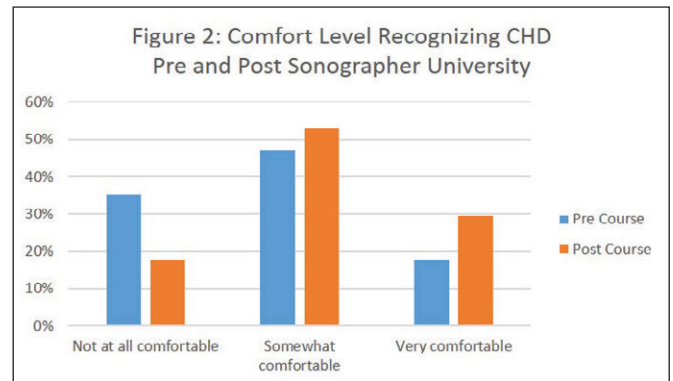
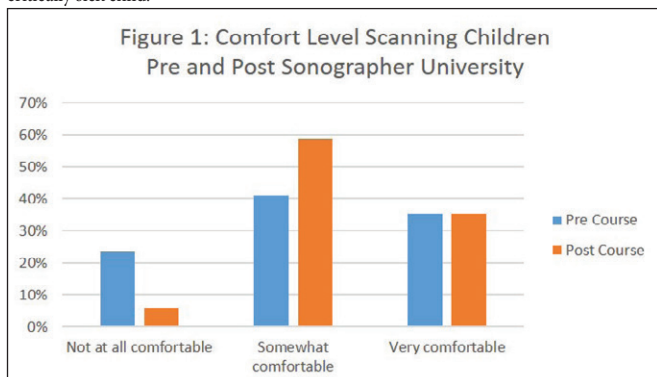
Background: Many patients with severe symptomatic aortic stenosis (AS) have concomitant mitral regurgitation (MR). Echocardiography plays a key role in identifying prognostic factors of MR improvement after transcatheter aortic valve replacement (TAVR). **Objective:** To assess the severity of coexistent MR and the predictors of its improvement after TAVR. **Method:** Out of 117 patients in a single-center TAVR registry, 57 patients fulfilled the inclusion criteria. Baseline transthoracic echocardiogram (TTE), follow-up study <1 week and >1 month post-TAVR were reviewed. Off-line analysis of TTE images was performed to assess the severity of coexistent MR (using vena contracta width and jet area/left atrial area %) and identify the predictors of its improvement. **Results:** There was significant improvement in MR severity post-TAVR; the mean MR vena contracta width pre-TAVR of 0.34±0.14 cm improved to 0.18±0.13 cm <1 week and 0.19±0.39 >1 month post-TAVR (p value <0.05); the mean MR jet area/LA area% pre-TAVR of 0.19±0.08 improved to 0.09±0.07 <1 week and 0.07 >1 month post-TAVR (p value <0.05). The degree of MR improved in 56% of patients <1 week and 87% of patients >1 month post-TAVR. Better functional capacity was correlated with MR improvement post-TAVR (correlation coefficient of 0.266 <1 week and 0.265 >1 month post-TAVR, p value <0.05). Normal mitral annular diameter, absence of extensive mitral annular calcification, improved aortic valve (AVA) and decreased transaortic mean gradient (p value <0.05) were independent predictors of improvement of coexistent MR in patients with severe symptomatic severe AS. **Conclusion:** MR significantly improved after TAVR with improvement of AVA and mean gradient as independent predictors. Other predictors include better functional capacity, normal mitral annular diameter and absence of extensive mitral annular calcification. TAVR performed on these patients resulted in significant reduction of MR.

P2-025

Sonographer University: Improving Adult Sonographer Comfort in Scanning Children With Critical Congenital Heart Disease in Remote Areas of Oregon and Washington

Lindsay Hamilton-Scott, Christina Ronai, Jennifer E. Huang, Erin J. Madriago. OHSU, Portland, OR

Background: Children with critical congenital heart disease (CCHD) often present with life-threatening illness to their local hospitals in remote areas. Adult focused sonographers perform echocardiograms in an effort to identify disease, yet feel uncomfortable performing studies on children with CCHD. Although performing complete pediatric echocardiograms requires significant training, remote locations necessitate sonographers with limited experience to look for CCHD in children. **Methods:** We created a two day course, Sonographer University (SU) to improve adult sonographer comfort in scanning children and recognizing CCHD. Efficacy of SU was evaluated through surveys assessing comfort and qualitative evaluation pre and post course. SU consisted of a series of lectures, multi-media simulated case studies, roundtable discussion, an interactive cardiac pathology station and a full day of hands-on scanning of 20 volunteer pediatric patients (8 months to 16 years) with either normal hearts or disease. Topics included an overview of critical congenital heart lesions, crucial views for each defect, pitfalls to imaging children, and how to get help when needed. **Results:** 44 people attended from Washington and Oregon. 65.7% responded that they are asked to scan children either occasionally or frequently. Comfort level scanning children in general and comfort recognizing CCHD improved substantially after SU (figure 1 and 2). Qualitative evaluation was overall excellent, and 89% of respondents stated they would repeat the course. The group qualitatively felt the course had improved their skills, knowledge and confidence with scanning children. **Conclusion:** In remote areas, children with CCHD may require immediate echocardiographic evaluation from sonographers reluctant to do so. With the help of SU, sonographers had improved comfort recognizing CCHD, improved confidence in performing a pediatric echocardiogram and improved knowledge surrounding when and how to get help in a critically sick child.



P2-026

Evaluation of Diagnostic Accuracy of Dipyridamole Stress Echocardiography for Cardiac Allograft Vasculopathy in Heart Transplantation

Gustavo Gavazzoni Blume, Rafael Petracca Pistori, Thyago Proença de Moraes, José Carlos Moura Jorge, Lidia Ana Zytynski Moura, Marcelly Gimenes Bonatto, Paulo Ricardo Francozi Gois, Leonardo Piazza, Vanessa Bordin, Márcia Olandoski. Santa Casa Hospital, Curitiba, Brazil

Background: Cardiac transplant recipients still have had high morbidity and mortality in the subsequent years after transplantation, mainly by cardiac allograft vasculopathy (CAV). It is essential to develop ways to diagnose early CAV, at least hemodynamically significant coronary stenosis, for preventing allograft failure and mortality. There is lack of data about the role of Dipyridamole Stress Echocardiography (DiSE) for CAV diagnosis. Few studies published with this intention are dated to 1990s and demonstrated similar diagnostic accuracy for CAV when compared with Dobutamine Stress Echocardiography (DoSE) studies from this century. The objective of this study was to evaluate the diagnostic accuracy of DiSE for CAV, the first using the current International Society of Heart and Lung Transplantation CAV recommended nomenclature of 2010. **Methods:** A cross-sectional, unicentric study was done with cardiac allograft recipients accompanied at Cardiac Transplant Service of the Santa Casa Hospital of Curitiba, Paraná state, Brazil. Twenty seven patients were submitted to DiSE and invasive coronary angiography (ICA). The diagnostic accuracy of DiSE was calculated by comparing its results with the ICA results, the latter considering the gold-standard method for CAV diagnosis. The mean interval between DiSE and ICA considering all 27 patients was 40.4 days. **Results:** DiSE results demonstrated sensitivity 28.6%, specificity 95%, positive predictive value 66.7% and negative predictive value 79.2% for CAV diagnosis. Considering only patients with CAV 2 and 3, the values were 33.3%, 95.2%, 66.7% and 83.3%, respectively. Excluding the only patient with myocardial bridge and considering only patients with CAV 2 and 3, the values were 33.3%, 100%, 100% and 83.3%. **Conclusion:** This study revealed low sensitivity, high specificity, and reasonable positive and negative predictive values of DiSE for CAV diagnosis, similar to previous studies that evaluated DiSE and DoSE in CAV scenario. Both DiSE and DoSE are not considered good options for CAV screening; however, DiSE is an easy-to-perform, apparently safe, well-tolerated method, and its applicability should not be neglected in CAV scenario. Further major, prospective studies are needed to evaluate the true utility of DiSE in the follow-up of transplanted patients.

Dipyridamole Stress Echocardiography	Invasive Coronary Angiography	
	Negative	Positive
Negative	19 (95% specificity)	5
Positive	1	2 (28.6% sensitivity)
Total	20	7

P2-027

Moderated Poster

Feasibility of 3D Printing Aortic Root Model by Three-Dimensional Transesophageal Echocardiography Data: A Preliminary Study

Wanwan Song, Qing Zhou, Yuanting Yang, Hongning Song, Bo Hu, Ruiqiang Guo, Jun Xia, Xinping Min. Renmin Hospital of Wuhan University, Wuhan, China

Background: Transcatheter aortic valve replacement (TAVR) has been introduced to China since 2010. After numerous clinical practice, it is about to enter a stage of rapid improvement in Chinese medical system. A large base and a high proportion (about 40%) patients with severe bicuspid aortic valve (BAV) stenosis in TAVR which is the Chinese characteristics. According to a new generation of valves in TAVR for BAV and China's existing experience, the result is not inferior to the tricuspid aortic valve, but it

Poster Session 2 (P2)

Monday, June 24, 2019

need more accurate preoperative image evaluation and Strategy formulation. Aortic root (AoR) 3D printing to printed patient-specific 3D models is a promising technique that may have applications in this field. **Methods:** Fifteen patients with BAV who underwent surgical aortic valve replacement (SAVR) were enrolled in this study and record the intra-operative replacement sizing by Edwards Lifesciences. Three-Dimensional Transesophageal Echocardiography (3D-TEE) were performed pre-operation. Complete and clear AoR volumetric data were collected and imported it into the Mimics and 3-Matic to make 3D AoR digital mould then save as STL file. 3D printer print the AoR mould by using polyvinyl alcohol (PVA), and infused with silicone material. Dissolve PVA in water to obtain the soft and translucent AoR 3D model(3D-M). Measure the aortic annulus' Area, perimeter (Peri), maximal diameter (D max) and minimal diameter (D min) of 3D-TEE,3D-M and replacement respectively; and calculate the mean diameter (D mean) of the 3D-M. Matched data from different measurements were analyzed with T-test, Bland-Altman plot and Pearson correlation. **Results:** No significant differences were found among the measurements of 3D-TEE and replacement ($P = 0.27$). The measurements of the 3D-TEE are slightly smaller than 3D-M ($P < 0.05$) and a high correlation of D mean with the size of replacement ($r = 0.97$, $P < 0.001$). The Bland-Altman scatter plot shows that the Area, Peri, D max, and D min measurements of the aortic annulus are within the consistency threshold. **Conclusion:** 3D-TEE can be used as another image data source to 3D printed AoR-M and 3D printing of aortic root can offer reliable BAV patient-specific information to be used in the pre-operative planning of SAVR or TAVI.

P2-028

Worldwide Normal Values for Left and Right Ventricular Size and Function Using 3D Echocardiography: First Report from the World Alliance of Societies of Echocardiography (WASE) Normal Values Study

Karima Addetia¹, Tatsuya Miyoshi², Alexandra Blitz³, Vivekanandan Amuthan⁴, Rodolfo Citro⁵, Masao Daimon⁶, Pedro Gutierrez-Fajardo⁷, Ravi Kasliwal⁸, James N. Kirkpatrick⁹, Mark J. Monaghan¹⁰, Denisa Muraru¹¹, Kofo O. Ogunyankin¹², Seung Woo Park¹³, Aldo Prado¹⁴, Ana Clara Tude Rodrigues¹⁵, Anita Sadeghpour¹⁶, Gregory Scali¹⁷, Daniel Stapf¹⁸, Masaaki Takeuchi¹⁹, Wendy Tsang²⁰, Edwin S. Tucay²⁰, Mei Zhang²¹, Federico M. Asch², Roberto M. Lang¹. ¹University of Chicago, Chicago, IL; ²MedStar Health Research Institute, Washington, DC; ³TOMTEC Imaging Systems GmbH, Unterschleißheim, Germany; ⁴Jeyalakshmi Heart Center, Madurai, India; ⁵University of Salerno, Salerno, Italy; ⁶The University of Tokyo, Tokyo, Japan; ⁷Hospitales Mac Bernardette, Guadalaajara, Mexico; ⁸Medanta Heart Institute, Gurgaon, Haryana, India; ⁹University of Washington, Seattle, WA; ¹⁰King's College Hospital, London, United Kingdom; ¹¹University of Padova, Padova, Italy; ¹²First Cardiology Consultants Hospital, Lagos, Nigeria; ¹³Samsung Medical Center, Seoul, Republic of Korea; ¹⁴Centro Privado de Cardiologia, Tucumán, Argentina; ¹⁵Albert Einstein Hospital, Sao Paulo, Brazil; ¹⁶Rajaie Cardiovascular Medical and Research Center, Echocardiography research center, IUMS, Tehran, Islamic Republic of Iran; ¹⁷Genesis Care, Brisbane, Australia; ¹⁸University of Occupational and Environmental Health, Kitakyushu, Japan; ¹⁹Toronto General Hospital, University of Toronto, Toronto, ON, Canada; ²⁰Philippine Heart Center, Quezon City, Philippines; ²¹Qilu Hospital of Shandong University, Jinan, China

Background: Echocardiography is the most widely used imaging technique to assess cardiac chamber size and function. Current normative reference values are largely based on Caucasian populations from North America and Europe. The World Alliance of Societies of Echocardiography (WASE) study was designed to evaluate normal subjects from around the world to generate universal global reference ranges. In this study we sought to assess the worldwide feasibility of 3D echocardiographic acquisitions (3DE) of the left and right ventricles (LV, RV) and report size and function measurements on the first round of enrolled subjects. **Methods:** WASE is a worldwide prospective, observational, cross-sectional study. Healthy subjects free of cardiac, lung and renal disease were prospectively enrolled from 19 centers in 15 countries including 6 continents. 3D full-volume datasets of the LV and RV were obtained separately and stored to allow offline analysis (Tomtec). Analyses were completed by the Core lab. LV and RV measurements included end-diastolic and end-systolic volumes (EDV, ESV) and ejection fraction (EF). Results were categorized by gender and age groups (18-40, 41-65 and >65 years). 3D datasets were deemed adequate for analysis if all walls were visible in the dynamic dataset. Groupwise comparisons were performed by one-way ANOVA and only when significant inter-group differences were detected, pairwise comparison was performed. P-values were adjusted by Bonferroni method. Significance level is 0.05. **Results:** Analysis was attempted on 1,200 LV and RV datasets. Adequate datasets for 3D analysis were more commonly acquired for the LV than the RV (870 (73%) vs. 756 (63%), respectively). From these, preliminary normal reference ranges are being reported (Table). Overall, men have significantly larger LV and RV EDV, ESV and lower LV and RV EF than women ($p < 0.05$). Within age groups EDV and ESV decrease progressively with each older age group. See Table for comparisons. Interestingly, overall, while LV EF increases with age, RV EF decreases with age. **Conclusions:** Despite guideline emphasis on 3D echocardiography for the assessment of LV/RV volumes, acquisition of adequate 3D datasets worldwide remains highly variable. Age and gender must be taken into consideration when interpreting LV and RV volumes and EF ranges.

		LV			RV				
		n	EDVI (ml/m ²)	EF (%)	ESVI (ml/m ²)	n	EDVI (ml/m ²)	EF (%)	ESVI (ml/m ²)
All	18-40	333	70.43±16.57a	61.0±11.97a	27.01±7.6a	340	61.59±23.33a	55.85±16.28a	27.54±12.29a
	41-65	326	64.21±14.46b	62.32±5.35a	24.23±7.15b	293	58.04±21.92a	54.1±6.18b	26.68±10.35ab
	65+	131	59.98±15.41c	63.52±5.74b	21.92±7.29c	123	50.51±16.47b	52.14±6.63c	24.33±9.17b
All	840	66.39±16.08	62.29±4.87	25.16±7.60	756	58.41±22.11	54.57±5.43	26.68±11.32	
Male	18-40	207	72.11±13.61a†	60.95±3.58a†	28.30±8.19a†	192	64.6±25.92a†	54.23±5.53a†	29.87±13.6a†
	41-65	196	65.69±15.64b	61.19±5.82a†	25.58±7.95b†	148	61.23±24.00a†	53.29±5.73a†	28.61±11.5ab†
	65+	61	60.89±17.34b	62.55±4.47a	23.01±8.79b	57	51.3±17.65b	51.18±7.01b	24.98±9.13b
All	433	68.09±17.8†	61.26±4.8†	26.52±8.38†	397	61.14±24.53†	53.45±5.91†	28.7±12.35†	
Female	18-40	176	68.45±13.56a†	62.92±4.15a†	25.51±6.54a†	140	57.07±10.04a†	57.94±6.59a†	24.52±9.59a†
	41-65	130	62.68±13b	63.48±4.55a†	22.9±5.94b†	145	54.78±19.12ab†	54.92±6.53b†	24.7±9.79a†
	65+	71	59.21±13.63b	64.34±5.86a	21.01±5.52b	66	49.83±15.49b	52.36±6.22b	23.77±9.63a
All	437	64.57±13.8†	63.39±4.66†	23.71±6.37†	359	55.06±18.53†	55.8±6.76†	24.46±9.38†	

With n one of the three groups ("All", "Male", "Female"), comparison results were denoted by letter "a", "b", "c". Comparisons are made between age groups (adjacent cells). An "a" near the value for age group "18-40" will another "a" near age group "41-65" denotes that the two values are not significantly different. However if "b" is found near the value for the "41-65" age group then the two values are significantly different. Cells of a column with no common letters, i.e. "a", "b" and "c" are significantly different. The cross group two-sided comparisons, i.e. male vs female of the same age group, were performed by two-sided t test. Significant difference of each age group ("18-40", "41-65", "65+", and "All") was denoted by †, ‡, #, †, #, respectively. If there is no label, then there is no significant difference between groups.

P2-029

Sex Differences Associated with Higher Cumulative BMI from Early Adulthood to Middle Age and Left Atrial Remodeling by Three-Dimensional Speckle Tracking Echocardiography: The Coronary Artery Risk Development in Young Adults (CARDIA) Study

Henrique Doria de Vasconcellos^{1,2}, Aisha Betoko¹, Luisa A. Ciuffo¹, Henrique M. Turim³, Bharat Ambale-Venkatesh⁴, Jared P. Reis⁴, Norrina Allen⁵, Donald M. Lloyd-Jones⁵, Laura Colangelo⁶, Pamela J. Schreiner⁶, Cora E. Lewis⁷, Stephen Sidney⁸, Christopher Cox⁹, Samuel S. Gidding⁹, Joao A.C. Lima¹. ¹Johns Hopkins, Baltimore, MD; ²Federal University of Vale do Sao Francisco / School of Medicine, Recife, Brazil; ³University of Sao Paulo, Ribeirao, Brazil; ⁴National Heart, Lung, and Blood Institute, Bethesda, MD; ⁵Northwestern University, Chicago, IL; ⁶University of Minnesota, Minneapolis, MN; ⁷University of Alabama, Birmingham, AL; ⁸Kaiser Permanent, Oakland, CA; ⁹Nemours Cardiac Center, Wilmington, DE

Background: Although higher body mass index (BMI) has been associated with cardiac dysfunction, the relationship between obesity and left atrial (LA) structure and function is not entirely understood. We examined the association of greater cumulative BMI with left atrial adverse remodeling using three-dimensional speckle tracking echocardiography (3D STE). **Methods:** CARDIA is a community-based cohort study initiated in 1985-86 of black and white men and women aged 18-30 years at baseline from 4 US fields centers. Eight re-examinations have been performed to date. 2,144 participants who had satisfactory image quality on the 3D STE analysis at the year-30 examination and with BMI measurements during the follow-up period were included in this study. Cumulative BMI was defined by summing the product of BMI in kg/m² measured in each visit and the subsequent years until the next BMI was obtained over 30 years of follow-up. 3D STE-derived LA parameters were: maximum, minimum, and pre-atrial contraction volumes (Vmax, Vmin, and VpreA); total, passive and active emptying fraction (tEF, pEF, and aEF), maximum systolic longitudinal strain (LSmax), and longitudinal early and late diastolic strain rates (LSre and LSra). Multivariable linear regression analyses stratified by gender assessed the relationship between cumulative BMI and LA structure/ function, adjusting for demographics and traditional cardiovascular (CV) risk factors (Table 1). **Results:** Mean age was 55 ± 3.6 years, 54.8% (n=1,168) women, 46.6% (n=995) African American. As shown in Table 1, greater cumulative BMI was independently associated with higher 3D LA volumes indices: Vmax ($\beta_m = 0.20$ / $\beta_w = 0.16$, $p < .001$), Vmin ($\beta_m = 0.22$, $p < .001$ / $\beta_w = 0.09$, $p = .005$) and VpreA ($\beta_m = -0.23$ / $\beta_w = 0.15$, $p < .001$) in both men and women; with lower 3D LA longitudinal deformation: LSmax ($\beta_m = -0.12$, $p = .002$), LSre ($\beta_m = 0.10$, $p = 0.011$), LSra ($\beta_m = 0.08$, $p = .031$) in men; and with higher 3D LA emptying fractions: total EF ($\beta_w = 0.07$, $p = .029$), active EF ($\beta_w = 0.10$, $p = .006$) in women. **Conclusion:** This study showed that while greater cumulative BMI from early adulthood throughout middle age was associated with higher LA volumes in both genders, differences were found for LA function, with lower LA longitudinal deformation in men and higher possible compensatory reservoir and active LA function in women.

Poster Session 2 (P2)

Monday, June 24, 2019

Table 3: Association between cumulative BMI and LA 3D Echo parameters

3D LA Echo Parameters ^a	Model 1				Model 2			
	Men		Women		Men		Women	
	β	P-value	β	P-value	β	P-value	β	P-value
3D LA Vmax, mL/m ²	0.17	<0.001	0.16	<0.001	0.20	<0.001	0.16	<0.001
3D LA Vmin, mL/m ² ^b	0.15	<0.001	0.09	0.006	0.22	<0.001	0.09	0.005
3D LA VpreA, mL/m ² ^b	0.18	<0.001	0.15	<0.001	0.23	<0.001	0.15	<0.001
3D LA total EF, % ^b	0.02	0.603	0.09	0.005	-0.05	0.215	0.07	0.029
3D LA passive EF, %	-0.02	0.589	-0.02	0.631	-0.05	0.626	-0.004	0.915
3D LA active EF, %	0.03	0.459	0.11	0.001	-0.03	0.427	0.10	0.006
3D LSmax ^b , %	-0.13	<0.001	0.001	0.977	-0.12	0.002	-0.003	0.938
3D LASre ^b , sec ⁻¹	0.12	0.001	0.02	0.474	0.10	0.011	0.01	0.796
3D LASra ^b sec ⁻¹	0.05	0.142	-0.05	0.44	0.08	0.031	-0.05	0.112

The multivariable linear regression model is showing coefficients per 117.7 kg/m² in men and per 175.1 kg/m² in women x years for cumulative BMI and P-values.
Model 1: Adjusted for age and race at year 3D examination.
Model 2: Model 1 + adjusted for heart rate, education level, physical activity, systolic blood pressure, smoking, diabetes, alcohol intake, low-density lipoprotein cholesterol, and high-density lipoprotein cholesterol at year 3D examination.
^a Abbreviations: 3D, three-dimensional; LA, left atrial; EF, ejection fraction; Vmax, maximum LA volume; Vmin, minimum LA volume; VpreA, pre-atrial contraction LA volume; LSmax, LA global longitudinal strain; LASre, LA first negative diastolic strain rate peak; LASra, LA second negative diastolic strain rate peak.
^b Sex-specific statistically significant interactions in the full adjusted model.

P2-030

Echocardiographic Measurements in Normal Chinese Adults Focusing on Three-dimensional Echocardiography: A Prospective, Nationwide, and Multicenter Study

Ying-Bin Wang¹, Yu Zhang¹, Gui-Hua Yao², Hong Tang³, Li-Xin Chen⁴, Li-Xue Yin⁵, Tian-Gang Zhu⁶, Jian-Jun Yuan⁷, Wei Han⁸, Jun Yang⁹, Xian-Hong Shu¹⁰, Ya Yang¹¹, Yu-Lin Wei¹², Yan-Li Guo¹³, Wei-Dong Ren¹⁴, Dong-Mei Gao¹⁵, Gui-Lin Lu¹⁶, Ji Wu¹⁷, Hong-Ning Yin¹⁸, Yu-Ming Mu¹⁹, Jia-Wei Tian²⁰, Xiao-Jing Ma²¹, Hao Wang²², Jing Yao²³, Li-Jun Yuan²⁴, Hong-Yan Dai²⁵, Xian-Chuan Ding²⁶, Jin-Feng Xu¹, Mei Zhang¹, Yun Zhang¹. ¹Qilu Hospital of Shandong University, Jinan, China; ²Qilu Hospital of Shandong University, Qingdao, China; ³West China Hospital, Sichuan University, Sichuan, China; ⁴Shenzhen People's Hospital/The Second Clinical Medical College of Jinan University, Shenzhen, China; ⁵Electronic Science and Technology University of China, The Affiliated Sichuan Provincial People's Hospital, Sichuan Sheng, China; ⁶Peking University People's Hospital, Beijing Shi, China; ⁷Henan Provincial People's Hospital, Henan Sheng, China; ⁸The First Affiliated Hospital of Harbin Medical University, Heilongjiang Sheng, China; ⁹The First Affiliated Hospital of China Medical University, Shenyang, China; ¹⁰Zhongshan Hospital, Fudan University, Shanghai Shi, China; ¹¹Beijing Anzhen Hospital, Capital Medical University, Beijing Shi, China; ¹²Sun Yat-sen Memorial Hospital, Sun Yat-sen University, Guangdong Sheng, China; ¹³The First Hospital Affiliated to Army Medical University (Southwest Hospital), Chongqing, China; ¹⁴Shengjing Hospital of China Medical University, Liaoning Sheng, China; ¹⁵China-Japan Union Hospital of Jilin University, Jilin Sheng, China; ¹⁶The First Affiliated Hospital of the Medical College, Shihezi University, Xinjiang, China; ¹⁷The First Affiliated Hospital of Guangxi Medical University, Zhuangzuzhiqu, China; ¹⁸The Second Hospital of Hebei Medical University, Hebei, China; ¹⁹The First Affiliated Hospital of Xinjiang Medical University, Urumqi, China; ²⁰The Second Affiliated Hospital of Harbin Medical University, Heilongjiang Sheng, China; ²¹Wuhan Asia Heart Hospital, Hubei Sheng, China; ²²Fuwai Hospital/Chinese Academy of Medical Sciences, Beijing, China; ²³Jiangsu Province Hospital, Jiangsu Sheng, China; ²⁴Tangdu Hospital of Air Force Medical University of PLA, Shaanxi, China; ²⁵Qingdao Municipal Hospital, Shandong Sheng, China; ²⁶Yan'an Hospital Affiliated to Kunming Medical University, Yunnan Sheng, China

Background: Currently three-dimensional echocardiography (3DE) technologies have been widely used in evaluating the features of cardiac chamber. However, the reference values of 3DE for Chinese have not been established yet. The aim of this study (Echocardiographic Measurements in Normal Chinese Adults-2, EMINCA2) was to establish normal values of echocardiographic measurements of the 3DE in a nationwide, population-based cohort of healthy Han Chinese adults. **Methods:** In EMINCA2, a total of 945 healthy Han Chinese volunteers aged 18 to 89 years were screened at 28 collaborating laboratories throughout China. Full-volume 3DE images were stored and sent to a core laboratory for offline analysis. Two professional analysts completed the analysis respectively in this laboratory by using the software of EchoPAC and QLAB, with double blind method. The data were divided into groups by gender (male, female) and age (18-44, 45-59 and 60-89). Comparisons were performed by one-way ANOVA and T-test. P-values were adjusted by Bonferroni method. Significance level is P<0.05. **Results:** A total of 710 qualified healthy subjects (mean age, 49.72 ± 17.56 years; 337 men) were ultimately enrolled in EMINCA2 so far. The indicator values of each group were described in the Table. On the whole, the value of 3D End-Diastolic Volume (3D-EDV), 3D End-Systolic Volume (3D-ESV) are significantly larger in male than in female, and these values are significantly larger in young group (18-44) than in other two groups (45-59, 60-89) (p<0.05). While, for the value of 3D Ejection Fraction (3D-EF), the young women are significantly larger than young men (p<0.05), the impacts of gender and age are not significantly in people over 44 years old. The details can be found in the Table **Conclusions:** Normal reference values of 3DE were established for the first time in a nationwide, population-based cohort of healthy Han Chinese adults. From EMICA2, we suggested that reference values stratified

of 3D-EDV and 3D-ESV should be established among all age groups and gender; for 3D-EF, stratified reference values should be used in young people (from 18 to 44), while a unified reference value can be used in other adults.

		n	3D-EDV (ml/m ²)	3D-ESV (ml/m ²)	3D-EF (%)
male	18-44	146	86.46±13.29a#	36.45±9.325a#	58.33±7.88a#
	45-59	88	81.82±14.67b^	32.49±8.303b^	60.74±7.20b
	60-89	103	74.08±16.85c*	29.06±8.365c*	60.80±6.73b
	all	337	82.45±15.47**	33.71±9.391**	59.54±7.54
female	18-44	164	74.45±14.63a#	28.96±7.439a#	61.22±7.07a#
	45-59	109	65.87±16.62b^	25.27±8.007b^	61.79±6.86a
	60-89	100	64.10±15.18c*	24.97±7.963b*	61.89±6.88a
	All	373	70.03±16.00**	27.18±7.869**	61.40±6.99
total	18-44	310	80.23±15.29a	32.63±9.332a	59.74±7.83a
	45-59	197	73.28±17.75b	26.66±8.915b	61.29±7.05b
	60-89	203	69.16±16.81c	27.04±8.370c	61.32±6.78b
all	710	75.96±16.94	30.32±9.276	60.58±7.34	

Inter-group (named "male", "female" and "total") comparison results were denoted by letter "a", "b", "c", two subgroups with the same letter (i.e. "male 45-59 3D-EF" and "male 60-89 3D-EF") means there is significantly statistic different, two subgroups with different letters (i.e. "male 18-44 3D-EF" and "male 45-59 3D-EF") means there is no significantly statistic different. The group wise comparison results, i.e. male vs female at the same age, were noted by "#", "a", "ab", "b*" ("18-44", "45-59", "60-89", "all") respectively. The symbol means there is significantly statistic different.

P2-031

Are There Differences in 3D LV and RV Size and Function Parameters Between Populations Around the World? First Report from the World Alliance of Societies of Echocardiography (WASE) Normal Values Study

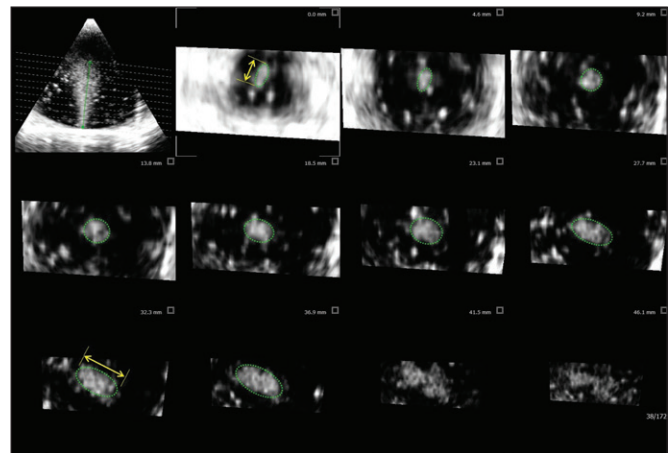
Karima Addetia¹, Tatsuya Miyoshi², Alexandra Blitz³, Vivekanandan Amuthan⁴, Rodolfo Citro⁵, Masao Daimon⁶, Pedro Gutierrez-Fajardo⁷, Ravi Kasliwal⁸, James N. Kirkpatrick⁹, Mark J. Monaghan¹⁰, Denisa Muraru¹¹, Kofo O. Ogumyankin¹², Seung Woo Park¹³, Ana Clara Tude Rodrigues¹⁴, Ricardo Ronderos¹⁵, Anita Sadeghpour¹⁶, Gregory Scalia¹⁷, Masaaki Takeuchi¹⁸, Wendy Tsang¹⁹, Edwin S. Tucay²⁰, Mei Zhang²¹, Federico M. Asch², Roberto M. Lang¹. ¹University of Chicago, Chicago, IL; ²MedStar Health Research Institute, Washington, DC; ³TOMTEC Imaging Systems GmbH, Unterschleißheim, Germany; ⁴Jeyalakshmi Heart Center, Madurai, India; ⁵University of Salerno, Salerno, Italy; ⁶The University of Tokyo, Tokyo, Japan; ⁷Hospitales Mac Bernardette, Guadalajara, Mexico; ⁸Medanta Heart Institute, Gurgaon, Haryana, India; ⁹University of Washington, Seattle, WA; ¹⁰King's College Hospital, London, United Kingdom; ¹¹University of Padova, Padova, Italy; ¹²First Cardiology Consultants Hospital, Lagos, Nigeria; ¹³Samsung Medical Center, Seoul, Republic of Korea; ¹⁴Albert Einstein Hospital, Sao Paulo, Brazil; ¹⁵Universidad Nacional de la Plata, Buenos Aires, Argentina; ¹⁶Rajaie Cardiovascular Medical and Research Center, Echocardiography research center, IUMS, Tehran, Islamic Republic of Iran; ¹⁷Genesis Care, Brisbane, Australia; ¹⁸University of Occupational and Environmental Health, Kitakyushu, Japan; ¹⁹Toronto General Hospital, University of Toronto, Toronto, ON, Canada; ²⁰Philippine Heart Center, Quezon City, Philippines; ²¹Qilu Hospital of Shandong University, Jinan, China

Background: Normative reference values for echocardiography reported in the guidelines are largely based on data obtained from North America and European subjects. However, multiple studies have suggested that there might be differences in normal values between populations around the world. The World Alliance of Societies of Echocardiography (WASE) study is a cross-sectional study of healthy subjects prospectively enrolled from 19 centers in 15 countries and 6 continents in which enrollees were free of cardiac, lung and renal disease. The study was designed to obtain universal global reference ranges for both 2D (2DE) and 3D (3DE) echocardiographic data to determine if differences in echocardiographic measurements exist between different ethnicities. In this preliminary report we sought to determine whether differences exist in 3D size and function of the left and right ventricles (LV, RV) between Caucasian (North America, Australia and Latin America (CAU)) and Asian population (Japan, South Korea and China (ASIA)). **Methods:** 3D full-volume datasets of the LV and RV were obtained as part of the WASE echocardiographic protocol and stored offline to allow Core Lab analysis (Tomtec). LV and RV measurements included end-diastolic and end-systolic volumes (EDV, ESV) and ejection fraction (EF). Subject BSA, gender and age were recorded and reported. 3D datasets were deemed adequate for analysis if all walls were visible in the dynamic dataset. Measurements acquired in CAU and ASIA subjects were compared using two-tailed t-test. **Results:** To date 3D LV analysis has been completed for 283 CAU and 364 ASIA subjects (Table). ASIA subjects had significantly lower BSA than CAU subjects. ASIA subjects had smaller LV and RV volumes when compared with their CAU counterparts with similar LV EF and lower RV EF (all p-values <0.05). These differences occurred despite indexing to BSA. **Conclusions:** These preliminary results appear to suggest that normal reference values for 3D volumes and EF are population specific.

Poster Session 2 (P2)

Monday, June 24, 2019

	North America, Latin America, Australia (CAU)		Japan, South Korea, China (ASIA)		T-TEST (2-tailed)
	N = 283		N = 364		
	N	MEAN ± SD	N	MEAN ± SD	P value
Demographics					
Age (years)	283	46 ± 16	364	44 ± 16	0.291
Male (n, %)	283	142 (50%)	364	186 (51%)	NS
BSA (m ²)	283	1.9 ± 0.2	364	1.7 ± 0.2	< 0.001
Left ventricle					
EDV (ml)	277	137 ± 38	349	113 ± 28	< 0.001
EDVI (ml/m ²)	277	72 ± 18	349	67 ± 13	< 0.001
EF (%)	277	62 ± 4	349	63 ± 5	0.218
ESV (ml)	277	52 ± 17	349	43 ± 14	< 0.001
ESVI (ml/m ²)	277	28 ± 8	349	25 ± 7	< 0.001
SV (mL)	277	84 ± 23	349	70 ± 16	< 0.001
Right ventricle					
EDV (ml)	259	123 ± 54	304	93 ± 33	< 0.001
EDVI (ml/m ²)	259	64 ± 25	304	55 ± 18	< 0.001
EF (%)	259	56 ± 6	304	54 ± 7	< 0.001
ESV (ml)	259	55 ± 27	304	44 ± 19	< 0.001
ESVI (ml/m ²)	259	29 ± 13	304	26 ± 10	0.003
SV (mL)	259	68 ± 29	304	49 ± 17	< 0.001



P2-033
Deterioration of Global Tangential Strain by Three-dimensional Echocardiography is a Predictor of Unfavorable Outcomes in Patients with Cardiac Resynchronization Therapy

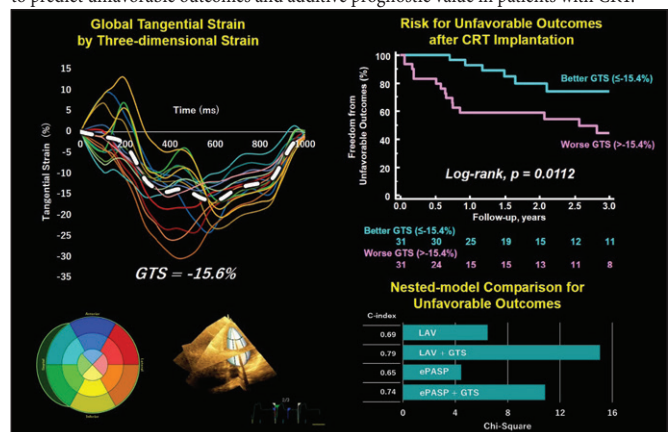
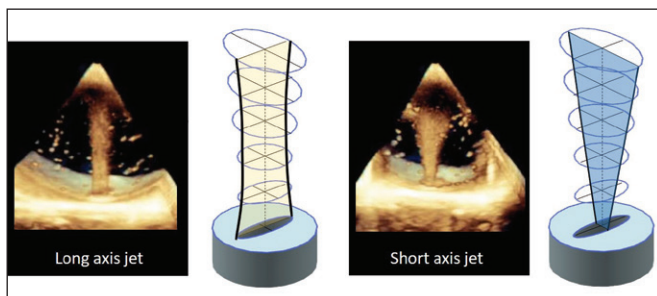
Masataka Sugahara, Kenki Ashida, Hideyuki Kishima, Akiko Goda, Takanao Mine, Masaharu Ishihara, Tohru Masuyama. Cardiovascular Division, Department of Internal Medicine, Hyogo College of Medicine, Nishinomiya, Japan

Background: Speckle tracking method by two-dimensional echo has been reported as a useful predictive marker after cardiac resynchronization therapy (CRT). However, global left ventricular (LV) function has a three-dimensional (3D) characteristic which integrates with LV contraction and scar burden. Therefore, we hypothesized that 3D strain is associated with unfavorable outcomes in patients with CRT. **Methods:** We studied 62 candidates of CRT implantation from a single center according to current clinical guidelines. All patients received baseline routine echo study with 3D dataset which was suitable for strain analysis using vendor independent software. We measured global tangential strain (GTS), global longitudinal strain (GLS) by 3D echocardiography (3DE). We tracked unfavorable outcomes which predefined as death, hospitalization due to worsening HF for 3 years after CRT implantation. **Results:** The predefined combined endpoint occurred in 21 patients (34%) over 3 years out of 62 patients aged 68±11 years with 160±26 ms of QRS duration and 29±7% LV ejection fraction. The median GTS was -15.4%. Although GLS was not predictive, GTS greater than -15.4% had high probability of unfavorable outcomes over 3 years (Log-rank, p = 0.0122). In univariate Cox analysis, GTS, left atrial volume (LAV) and estimated pulmonary artery systolic pressure (ePASP) were significantly associated with unfavorable outcomes [GTS: hazard ratio (HR) = 1.23, 95% confidence interval (CI) = 1.07-1.43, p = 0.0022; LAV, HR = 1.02, 95%CI = 1.00-1.04, p = 0.011; ePASP, HR = 1.05, 95%CI = 1.00-1.09, p = 0.0347]. An addition of GTS improved the predictive power of routine echo predictors (LAV, ePASP) by the bivariate Cox analysis (p = 0.0005, and p = 0.0044, respectively). **Conclusion:** Baseline GTS by 3DE has potential to predict unfavorable outcomes and additive prognostic value in patients with CRT.

P2-032
Twisting Elliptical Jets

Nadia El Hangouche, Jeesoo Lee, Michael Markl, James Thomas. Northwestern Memorial Hospital, Chicago, IL

Background: Assessment of regurgitant severity can use the width of the vena contracta and the spatial extent of the regurgitant jet in the receiving chamber by color Doppler. For a circular regurgitant orifice, the jet spreads symmetrically from the orifice. However, regurgitant orifices are often elliptical, as in functional mitral regurgitation (FMR), from which jet propagation is not well understood. We sought to assess the near field propagation of a jet emanating from an elliptical planar orifice simulating FMR. **Methods:** We generated gravity-driven water flow between two chambers with an elliptical orifice (4 x 13 mm in diameter) in the partitioning wall. Optison™ was added to enhance the jet. On multiple runs, Philips Epiq and GE E95 echocardiographs were used to acquire 2D and 3D B-mode and color Doppler datasets to discern the 3D morphology of the jet. Datasets were processed with Tomtec multiplanar tool to slice the jet perpendicular to its propagation axis every 4.6 mm to define the cross-sectional shape. **Results:** Figure 1 illustrates the jet in 3D imaged from the orifice long axis (first 2 panels) and short-axis (last 2 panels) perspectives. The jet consistently spread out more from the short axis cut than the long axis, which actually showed convergence over about 2 cm of propagation downstream before diverging. Transverse slices along the jet (Figure 2) clearly show that the jet shape aligns with the orifice long-axis at the origin (yellow arrows), becoming circular about 1 cm downstream, and reverses its orientation by 90° so the long-axis of the jet cross-section actually aligns with the orifice short-axis at ~3 cm. Such axis-switching is predicted by differential interaction of the jet with traveling vortices. **Conclusion:** The downstream progression of an elliptical jet is marked by the switching of its geometrical axes which can have important consequences on the vena contracta measurement site and the spatial extent of the jet in the receiving chamber imaged by 2D echocardiography.



Poster Session 2 (P2)

Monday, June 24, 2019

P2-034

Three-Dimensional Assessment of Right and Left Ventricle Volumes and Strain with Pectus Excavatum Repair: An Intraoperative Transesophageal Echocardiographic Study

Venkata Siva Krishna Kumar Pulivarthi, Dawn E. Jaroszewski, Michael Gotway, Tasneem Z. Naqvi. Mayo Clinic Hospital, Phoenix, AZ

Background: Pectus excavatum (PE) deformity can cause cardiac compression. We have shown the beneficial effects of PE bar insertion (Nuss) surgery on right and left ventricular (RV & LV) function by 2D echo. We present findings on effects of Nuss surgery on RV geometry, LV and RV volumes and strain by 3-D echocardiography. **Methods:** Intraoperative 4-6 beat 3D full volume loops were acquired for the LV and RV by transesophageal echocardiography (Philips IE33 ultrasound) pre- and post-bar insertion & pre- and post-bar removal from 2017-2019. Images were analyzed offline using TomTec software. Twenty-five patients (29.7±10.5 yrs, inspiratory Haller index 4.13±0.76; male 60%) had 3D RV and 28 patients (32±10.5 yrs, inspiratory HI: 4.16±0.7, male 61%) had 3D LV images pre and post bar insertion. Three patients (27±3.6 yrs, inspiratory Haller index 3.6±0.86; male 100%) had 3D RV and eight patients (29±8.5 yrs, inspiratory HI: 4±1, male 75%) had 3D LV images pre- and post-bar removal surgery 3 years after initial Nuss surgery. Paired Student t-test was performed on pre and post data sets. **Results:** PE surgery improved 3D RV volume, RVEF, Basal (RVDd base) & mid RV diameter (RVDd mid) and RV free wall longitudinal strain (RVLS %) (Figure 1). Significant improvement occurred in 3D LV volumes, EF, LV global longitudinal strain (LVGLS%), peak LV strains [tangential (TS), radial (RS) and longitudinal strain (LS)] after bar insertion (Table 1). No significant change in any of these parameters was seen post bar removal (p=NS for all). **Conclusion:** Our findings demonstrate the acute beneficial effect of cardiac decompression in patients who undergo PE surgery. 3D echocardiography can demonstrate changes in LV and RV chamber volume and in LV and RV strain in patients undergoing PE repair surgery.

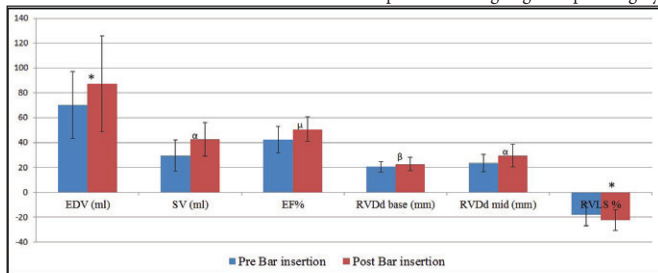


Figure 1: Effect of Pectus Excavatum Surgery (Bar Insertion) on Right Ventricular Volume, Size and Free Wall Speckle Tracking Longitudinal Strain. EDV: End diastolic volume; EF: Ejection fraction; SV: Stroke volume; RVDd: Right ventricular diastolic diameter; RVLS: Right ventricular longitudinal strain. *p-value<0.01, **p-value<0.0001, ***p-value<0.001.

Variable	Bar insertion @Left ventricle (N= 28)			Bar removal @Left ventricle (N= 8)		
	Pre bar insertion Mean±SD	Post bar insertion Mean±SD	p-value	Pre bar removal Mean±SD	Post bar removal Mean±SD	p-value
HR (bpm)	66.4±10.2	71.89±12.15	0.033	67.5±9.72	64.5±12.52	0.14
SBP	109.68±17	108.7±16.9	0.43	111.6±11.7	95.8±9.2	0.008
DBP	63.8±9.4	58.6±8.4	0.026	66.3±11.9	56.7±5.4	0.038
Frame rate	29.1±6.5	30.35±5.31	0.1	28.12±5.43	28.3±6.92	0.42
EDV (ml)	86.1±32	81.56±26.71	0.15	77.96±23.35	81.28±24.6	0.26
ESV (ml)	44.5±23.2	37.46±16.77	0.014	34.13±12.8	36.45±11.11	0.22
SV (ml)	41.6±11.8	44.1±11.83	0.12	43.8±11.72	44.85±13.88	0.37
EF %	50.1±8.6	55.43±7.54	0.0013	56.62±5.27	55.18±2.92	0.26
GLS %	-11.5±5.4	-15.8±5	0.0031	-17.35±11.8	-14.58±4.18	0.19
GCS %	-22±5.9	-25.8±7.68	0.3	-26.12±3.95	-25.25±1.82	0.31
CO (in ml)	2720.33±751.55	3127.14±862	0.011	2969.5±952.42	2825.12±745.57	0.29
Peak Global PTS	-25.6±7.52	-29.34±6.87	0.029	-32.28±4.52	-31±2.72	0.25
Peak Global CS	-20±6.94	-21.47±7.9	0.21	-24.53±3.19	-25±2	0.39
Peak Global RS	25.95±8.37	30.46±8.52	0.026	33.57±7.12	32.31±5.11	0.36
Peak Global LS	-11.54±5.08	-15.29±4.99	0.006	-15.68±6.58	-13.76±4.61	0.27

Table 1: Effect of Pectus Excavatum Surgery (Bar Insertion) on Left Ventricular Volume and Speckle Tracking Strain Compared to Control (Bar Removal) HR-Heart rate; SBP-Systolic Blood pressure; DBP-Diastolic blood pressure; EDV-End diastolic volume; ESV-End systolic volume; SV-Stroke volume; EF-Ejection fraction; GLS-Global longitudinal strain; GCS-Global circumferential strain; CO-Cardiac output; PTS-Principal tangential strain; CS-Circumferential strain; RS-Radial strain; LS-Longitudinal strain

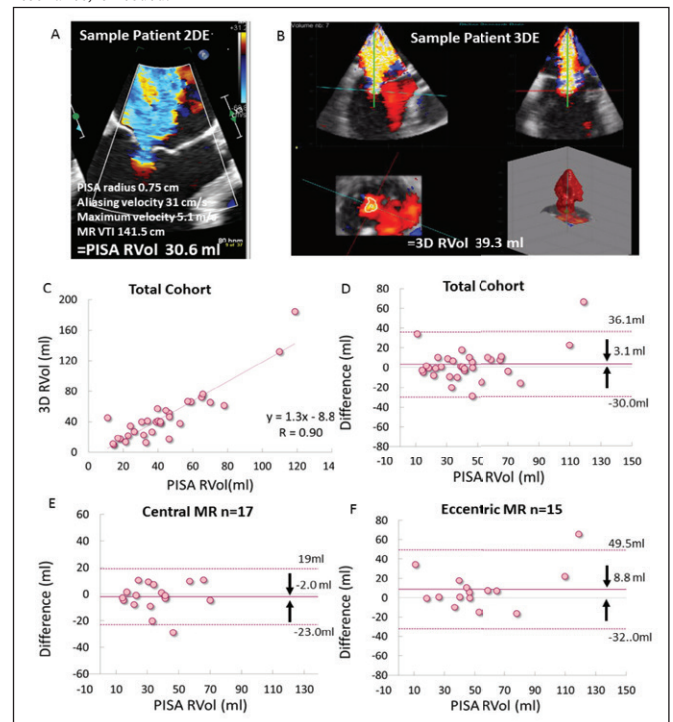
P2-035

Novel Transesophageal Echocardiographic Quantification of Mitral Regurgitation Using Three-Dimensional Color Doppler Method

Kalie Kebed¹, Jimmy Su², Karima Addetia¹, Odile Bonnefous², Stephane Allaire², Megan Yamat¹, Eric Kruse¹, Alexandra Goncalves², Roberto M. Lang¹. ¹University of Chicago, Chicago, IL; ²Philips Healthcare, Andover, MA

Background: Two-dimensional echocardiography (2DE) proximal isovelocity surface area (PISA) derived regurgitant volume (RVol) is the primary quantitative imaging-based technique for the assessment of mitral regurgitation (MR). RVol requires adequate acquisition of the PISA shell and proper alignment of the MR Doppler jet, which may be difficult in eccentric jets leading to underestimation. In this study, we sought to validate a new three-dimensional echocardiography (3DE) method based on B-mode and color Doppler ultrasound data to quantify MR RVol. **Methods:** Patients (n=36) referred for clinical transesophageal echocardiogram (TEE) to evaluate MR severity underwent imaging

of the mitral valve with quantification of MR (RVol) by standard 2DE PISA (Fig 1A), as well as 3DE full-volume (frame rate >20 Hz) color Doppler acquisitions (Philips Epic X8-2t) which included the area of flow convergence, the mitral annulus and a portion of the MR jet in the left atrium. The datasets were analyzed offline using a new 3DE method (Philips software prototype), which uses the combined 3DE and color data together to provide an automatic, quantitative measure of RVol. An estimate of the RVol is then automatically obtained over the cardiac cycle (Fig 1B). Comparisons of RVol between 2DE and 3DE were done using Bland-Altman analysis. **Results:** The 3D measurements were feasible in 32/36 patients. A good correlation was noted between RVol derived from 2DE PISA and 3DE color Doppler with r=0.90 (Fig 1C); a bias of 3.1±16.9 ml (Fig 1D) and 95% limits of agreement (LOA) =±33.7 ml [-30 ml and 36.1 ml]. Of note, there was a considerably better correlation in patients with central MR jets (n=17; 53%) with a lower bias -2.0±10.7 ml and tighter LOAs (Fig 1E) compared to those with eccentric MR jets (n=15; 47%) with a bias of 8.8±20.1 (Fig 1F). **Conclusion:** A novel 3DE color Doppler method to quantify RVol is feasible and shows good agreement with 2DE PISA, especially in patients with central MR. As expected, in patients with eccentric MR, where 2DE PISA is less reliable and may underestimate RVol, the new 3DE method provided more discordant results with larger RVol. This suggests that the 3DE method may overcome the 2DE PISA limitations, but further validation against an independent reference standard, such as cardiac magnetic resonance, is needed.



P2-036

Characteristics, Associated Cardiovascular Abnormalities and Clinical Outcomes of Congenital Sinus of Valsalva Aneurysm: A Single Center 7-year Experience

Shuang Liu, Limin Zhang, Ru Li, Chunyan Ma, Jun Yang. First Hospital of China Medical University, Shenyang, China

Background: Congenital sinus of Valsalva aneurysm (CSVA) is a rare congenital cardiac anomaly. This study sought to determine CSVA frequency in a large echocardiography database, to characterize associated cardiovascular abnormalities, and to describe long-term outcomes. **Methods:** Thirty-nine patients (mean ± SD age, 41.0 ± 18.5 years with a range of 4 to 80 years at the time of the index diagnosis; female sex, 53.8%) received a diagnosis of CSVA from a total of 525815 echocardiograms from the First Hospital of China Medical University between January 1, 2011, and June 1, 2018 (frequency, 0.007%). **Results:** The majority of CSVA was type I (38.5%) or type II (28.2%) (Sakakibara classification) 23 (59.0%) were ruptured while 41% were unruptured. 38.5% CSVA patients are associated with ventricular septal defect (VSD), and 23.1% was subarterial VSD, which predominately presented that in type I. 9 (23.1%) patients had mild or greater aortic regurgitation (AR). Infective endocarditis (IE) affected predominantly in aortic and/or tricuspid valve in 5 (12.8%) patients. Besides VSD and AR, obstruction of terminal space, arrhythmia, myocardial infarction can be found in unruptured patients. Moreover, type IV had a high incidence of rupture. Three-dimensional (3-D) echocardiography provided a more vivid CSVA anatomic structure and relationships among the intracardiac structure to help define the associated anomalies. During a mean ± SD follow-up of 4.12 ± 2.41 years (range, 0.20-7.41 years), overall survival for the entire cohort was 94.1%. **Conclusions:** Cardiac

Poster Session 2 (P2)

Monday, June 24, 2019

abnormalities were relatively common in patients with CSVA. 3D echocardiography should be commended in the diagnosis of CSVA, and long-term survival of CSVA was excellent.

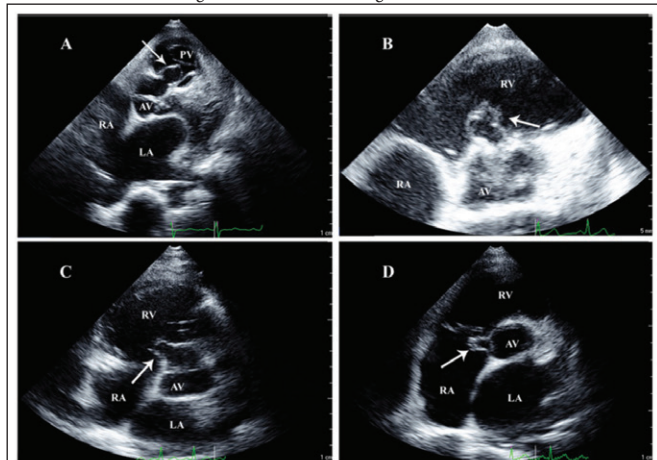


Figure 1. Congenital sinus of Valsalva aneurysm classification recommended by Sakakibara in accordance with originate site (Arrows). A, Type I, aneurysm originate from the left part of right coronary sinus. B, Type II, aneurysm originates from the central part of right coronary sinus. C, Type III, Aneurysm originates in the right part of the right coronary sinus. D, Type IV, aneurysm originates in the non-coronary sinus. LA, left atrium; RA, right atrium; RV, right ventricle; AV, aortic valve; PV, pulmonary valve.

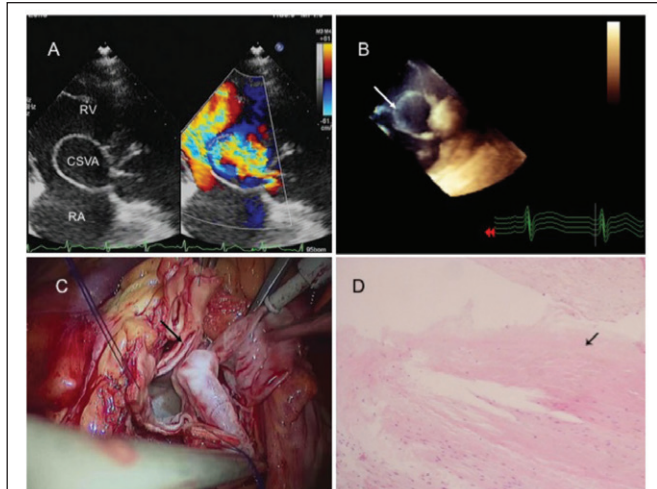


Figure 2. A, Transesophageal echocardiography demonstrated the large aneurysm, however the orifice was missed. B, 3D echocardiography showed the aneurysm protruded to right heart with a rupture orifice (arrow) that was confirmed by surgery (C). D, Aneurysm specimens revealed medial degeneration with fibroplastic proliferation in one patient (arrow). CSVA, Congenital sinus of Valsalva aneurysm; RA, right atrium; RV, right ventricle

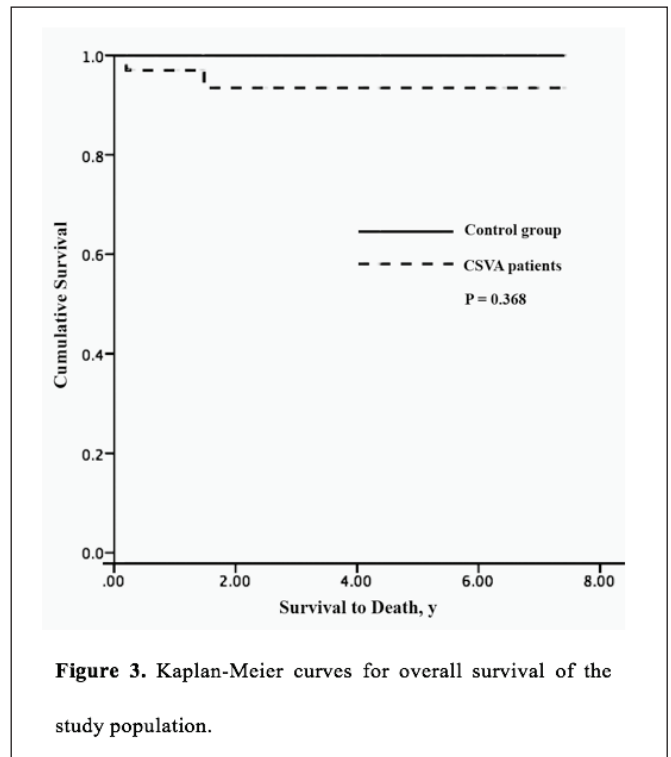


Figure 3. Kaplan-Meier curves for overall survival of the study population.

P2-037

Characterization of Non-P2 Mitral Regurgitation Using Real-Time Three-Dimensional Transesophageal Echocardiography

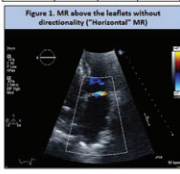
Edith L. Posada-Martinez¹, Xochitl A. Ortiz-Leon¹, Maria C. Trejo-Paredes¹, Juan B. Ivey-Miranda¹, Ben A. Lin¹, Robert L. McNamara¹, Njeri Thande¹, Bernardo Lombo¹, Jose A. Arias-Godinez², Lissa Sugeng¹. ¹Yale University, New Haven, CT; ²National Institute of Cardiology, Mexico City, Mexico

Background: The jet and hemodynamic characteristics of mitral regurgitation (MR) due to P2 scallop flail or prolapse have been described using two (2D) and three-dimensional transesophageal echocardiography (3DTEE); however, less is known about MR due to pathology of the other scallops (nonP2) which tends to be very eccentric. We aim to characterize non P2 MR, according to the affected scallop, with 2D transthoracic (2DTTE) echocardiography and 3D TEE. **Methods:** This retrospective study included patients who had severe degenerative MR on TEE performed from October 2015-December 2018 and had a 2DTTE within 6 months. Two investigators independently reanalyzed 2D TTE and 2D-3D TEE images to characterize the MR jet based on the affected scallops. “Horizontal” MR was defined as a jet above the leaflets without any directionality. We also reviewed the agreement between TEE and intraoperative findings of the leaflet abnormality. **Results:** We included 50 patients with severe MR, 62% were males and mean age was 68 ± 15 years. One third had atrial fibrillation. On TTE, the mean LVEF was 63 ± 9% and the mean left atrial volume was 52 ± 17 ml/m². On TEE, the most and least affected segments were P2 (28%) and A1 (2%), respectively. The medians of effective regurgitant orifice area and regurgitant volume were 0.52 cm² and 74 ml, respectively. However, only 67% of non-P2 cases had flow reversal in at least 1 of 4 pulmonary veins compared with 93% in P2 cases. On TTE, the E velocity was <1.2 m/s in 56% vs. 38% (non-P2 and P2, respectively). Moreover, 2 patients (7%) had E/A<1 in non-P2 MR while all were >1 in P2. Regarding to the direction of the flow on TTE, a “horizontal” jet was more frequently identified when the affected scallops were A2, A3 and P3. As expected, A1 jets were directed posteriorly, P1 and P2 anterior or anteroseptally. However, the direction of the jet was more heterogeneous in mixed scallops and bileaflet. Most patients underwent MV surgery (64%), and agreement between the TEE and the operative findings was 92% (Kappa 0.89, p<0.001). **Conclusion:** 3D TEE provides essential details about MR jet direction and severity. “Horizontal” MR on TTE may herald severe MR when evaluated on TEE and most frequently involves the A2, A3, or P3 scallops. This study highlights specific characteristics of non P2 MR not well described previously.

Poster Session 2 (P2)

Monday, June 24, 2019

Table 1. Characteristics of Mitral Regurgitation parameters based on affected scallop									
n=50	A1 n=12 (24%)	A2 n=16 (32%)	A3 n=12 (24%)	P1 n=12 (24%)	P2 n=14 (28%)	P3 n=12 (24%)	Anterior mixed n=9 (18%)	Posterior mixed n=8 (16%)	Situated n=8 (16%)
3D TEE Color									
NOTE: Flow Direction	Posterior (100%)	Posterior (100%)	Posterior (100%)	Anterior (100%)	Anterior (14 (28%))	Anterior (5 (8%))	Posterior (5 (50%))	Anterior (3 (38%))	Central (4 (50%))
Clock face	3 to 6	6	6 to 9	12 to 3	12	9 to 12	3 to 9	9 to 3	-
TEE Flow Direction	Posterior (100%)	Horizontal (67%)	Horizontal (100%)	Anterior (100%)	Anterior (100%)	Horizontal (30%)	Horizontal (100%)	Horizontal (100%)	Central (33%)
Transcatheter aortic valve replacement									
E Vel (m/s)	1.04	1.39	1.10	1.43	1.33	0.91	0.98	1.02	1.18
A Vel (m/s)	0.45	0.85	0.90	1.22	0.70	0.90	0.51	0.79	0.90
E/A ratio	2.3	1.3	1.2	1.1	1.6	1.1	2.5	1.2	1.4
Transesophageal echocardiogram									
MR vel (m/s)	5.9	5.1	5.8	5.8	4.8	5.6	3.7	5.4	5.3
MR VTI (cm)	153	158	167	190	128	136	96	80	169
EROA (cm ²)	0.46	0.41	0.68	0.53	1.05	0.8	0.48	0.47	0.56
Reg Vol (ml)	71	67	100	129	136	134	96	57	68
LAA volume (ml)	0.34	0.39	0.52	0.15	0.28	0.52	0.44	0.46	0.47
Reg flow PV (%)	0 (7.8%)	2 (100%)	1 (50%)	13 (93%)	1 (50%)	4 (80%)	2 (50%)	4 (50%)	0



functional class. **Results:** At the baseline, the ratio LVAV/LVEDV negatively correlated with the LVEF ($r=-0.905$, $P<0.05$). After SVR, LVEDV, LVESV and NYHA functional class decreased while LVEF increased ($P<0.05$). We found a negative correlation between LVAV/LVEDV and Δ LVEF ($r=-0.835$, $P<0.05$), Δ LVESV ($r=-0.721$, $P<0.05$). 75% patients had cardiac improvement. Receiver-operating characteristic curve analysis yielded cut-off values of LVAV/LVEDV <25% best associated with cardiac function improvement, area under the curve was 0.82 ($P<0.05$). **Conclusions:** the ratio LVAV/LVEDV can predict cardiac function improvement after SVR in LVA patients. RT-3DE might be a useful means to evaluate LVA volume.

P2-040

Improving 3D Full Volume Dataset Acquisition to Support Ejection Fraction Estimation in a High Volume Pediatric Echocardiography Laboratory: a Quality Improvement Initiative

Ashley Warta, Tyler Johnson, Laura Kuzava, Alison Samrany, Hollie Carron, Rita France, Janelle Noel-Macdonnell, Anitha Parthiban, Hayley S. Hancock. Children's Mercy Kansas City, Kansas City, MO

Background: Echocardiography (echo) is widely used to assess ventricular size and ejection fraction (EF), however accuracy and reproducibility of measurements are affected by subject, operator, and equipment factors. Ejection fraction estimation by 3D echo does not make geometric assumptions and has been shown to be more reliable and reproducible than 2D echo; however, sonographer experience is variable and a learning curve is involved. We hypothesized that the quality of 3D full volume (FV) acquisitions by sonographers, and the percentage of analyzable 3D FV datasets could be improved by implementing a quality improvement (QI) initiative comprised of systematic training/testing phases. **Methods:** Sonographers attended a general education session on 3D image acquisition, and acquired 5 3D FV datasets each (phase I). Datasets were scored by four 3D expert readers. The overall score included an acquisition score (imaging window, gain, depth, and plane score components) and whether or not a dataset was analyzable (maximum score=25). Baseline Phase I was followed by a second education session (individual training for sonographers with lower scores [phase II]), a 3D FV analysis workshop session (phase III), and a review session of 3D FV analysis (phase IV). Sonographers provided 5 datasets for feedback/scoring following each session. To assess for improvement, sonographer scores, overall lab scores, and percentage of analyzable datasets were tracked. **Results:** Eighteen pediatric sonographers participated (5 no 3D experience, 4 beginner, 2 advanced beginner, 4 intermediate, and 3 advanced). Median scores and % analyzable datasets (interquartile range) for each phase is shown in Table 1. Although there were no significant differences in the median overall scores or acquisition scores through the phases, the percentage of analyzable 3D FV datasets increased from phase I and II to phase III, and was sustained in phase IV. A significant change in the percentage of analyzable datasets was seen from phase II to phases III and IV ($p=0.0044$ and $p=0.0158$, respectively). **Conclusion:** We successfully implemented a QI initiative for improving image acquisition of 3D FV datasets. Continuous QI cycles of testing, scoring, and education resulted in a quantifiable improvement in the percentage of analyzable 3D FV datasets for 3D EF.

Variable	Phase I	Phase II	Phase III	Phase IV
Total Overall Score	20 (17, 21)	19 (13, 21)	21 (19, 22)	20 (15, 23)
Acquisition Score	16.5 (15, 18)	17 (11, 18)	17 (16, 19)	16.5 (14, 18)
Percent Analyzable	60% (40%, 80%)	40% (20%, 60%)	60% (60%, 80%), significant change compared to phase II, $p=0.0044$	80% (40%, 100%), significant change compared to phase II, $p=0.0158$

P2-038

The Normal Biventricular Function in the Transplanted Heart by Three-Dimensional Speckle-Tracking Echocardiography

Wei Sun^{1,2}, Chun Wu^{1,2}, Shuangshuang Zhu^{1,2}, Li Zhang^{1,2}, Mingxing Xie^{1,2}. ¹Department of Ultrasound, Union Hospital, Tongji Medical College, HUST, Wuhan, China; ²Hubei Province Key Laboratory of Molecular Imaging, Wuhan, China

Background: Speckle-tracking echocardiography (STE) was a promising noninvasive technique to monitor acute rejection in heart transplantation (HT) patients. To our knowledge, the studies about the feasibility and accuracy of three-dimensional (3D) STE to evaluate the biventricular function in transplanted heart comparison with cardiac magnetic resonance (CMR), and the normal biventricular function assessed by 3DSTE of HT patients has yet to be studied. Therefore, the objectives of the study were 1. to testify the feasibility and accuracy of 3DSTE to evaluate the biventricular function in HT patients in comparison with CMR; 2. to explore the normal biventricular function in clinically stable patients at 1 year after HT using 3DSTE. **Methods:** Protocol 1 enrolled 38 HT patients who experienced 3DSTE and CMR examination within 24h. Protocol 2, 3DSTE data were compared between 46 clinically stable patients at 1 year after HT and 46 healthy controls. **Results:** Protocol 1, the ventricular ejection fraction (EF) derived from 3DSTE had an excellent accuracy comparison with the corresponding value of CMR: LVEF ($r=0.96$, $LOA = -0.5\pm3.7\%$), RVEF ($r=0.95$, $LOA=0.5\pm4.5\%$). Left ventricular (LV) global longitudinal strain (GLS), LV global circumferential strain (GCS) were significantly correlated with standard CMR-LVEF ($r=0.85$, $r=0.93$, respectively, $p<0.01$). Right ventricular (RV) free wall longitudinal strain (FWLS) were also correlated well with standard CMR-RVEF ($r=0.74$, $p<0.01$). Protocol 2, compared with healthy controls, lower 3D LVEF and RVEF were observed in HT patients ($p<0.01$), but these two values were still within normal range. 3D LVGLS, LVGCS, RV FWLS and LV twist were significantly reduced in transplanted heart, whereas LV systolic dyssynchrony index (SDI) was increased. And the LV global performance index (GPI) was also reduced. Moreover, the strain values were good for differentiating between these two groups, the cutoff value of -19.3% for the LVGLS had 94% accuracy and the cutoff value of -21.4% for the RV FWLS had 90% accuracy. **Conclusion:** Our study demonstrated that 3DSTE had a high sensitivity and accuracy to evaluate biventricular function in HT patients. For clinically stable and healthy patients at 1 year after HT, although their LVEF and RVEF within the normal range, their myocardial mechanical function was impaired. Exploring the specifically normal bi-ventricular function of HT patients by 3DSTE is essential during follow-up studies.

P2-039

The Volume Ratio of Aneurysm and Left Ventricle by Real-time Three Dimensional Echocardiography Predicting Cardiac Function Improvement to Surgical Ventricular Reconstruction in Patients with Left Ventricular Aneurysm

Yanxiang Zhou, Qing Zhou, Jinling Chen, Ruiqiang Guo. Renmin Hospital of Wuhan University, Wuhan, China

Background: Surgical ventricular reconstruction (SVR) can reverse adverse ventricular remodeling resulting from left ventricular aneurysm (LVA) and improve cardiac function. However, the operative procedures associate with high perioperative morbidity and mortality rates. Thus, predicting cardiac function improvement after SVR is crucial because it can help identify patients who might benefit from SVR. The aim of the study was to detect whether the ratio of left ventricular aneurysm volume (LVAV) and left ventricular end-diastolic volume (LVEDV) assessed by real-time 3D echocardiography (RT-3DE) could predict cardiac function improvement of patients with LVA in response to SVR. **Methods:** 60 patients with LVA underwent RT-3DE to obtain data on left ventricular ejection fraction (LVEF), LVEDV, left ventricular end-systolic volume (LVESV), and LVAV. All patients underwent clinical and echocardiographic assessments at baseline and at 12 months after SVR. Relative increase in the LV ejection fraction (LVEF) was defined as Δ LVEF and relative decrease in LV end-systolic volume (LVESV) was defined as Δ LVESV. Cardiac function improvement was defined as Δ LVESV>15%, Δ LVEF>20% or reduction in NYHA

P2-041

Intra- and Inter-vendor Variability of Quantitative 3D Mitral Valve Modeling Software

Didem Oguz, Eleid Mackram, Sunil Mankad, Sorin Pislaru, Joseph Maalouf, Vuyisile Nkomo, Jae K. Oh, Jeremy Thaden. Mayo Clinic, Rochester, MN

Background: We aimed to investigate the intra-vendor and inter-vendor variability of two different quantitative 3D (3 dimensional) mitral valve modeling software platforms. **Methods:** Volumetric datasets of twenty-four patients with mixed/secondary mitral regurgitation who underwent 3D transcatheter aortic valve replacement (TAVR) were analyzed with two different quantitative mitral valve modeling software programs (MVN, Philips Healthcare; 4D MV Assessment, TomTec Imaging Systems). Bland-altman and intraclass correlation coefficient were used to assess agreement between the two software platforms. **Results:** Pre-procedural 3D echocardiographic data of the two software platforms are shown in the Table. Between the software packages, linear correlation for anteroposterior diameter was $r=0.82$ ($p<0.0001$), anterolateral-posteromedial diameter was $r=0.77$ ($p<0.0001$), annulus height was $r=0.63$ ($p=0.0009$), 3D circumference was $r=0.88$ ($p<0.0001$), tenting height was $r=0.74$ ($p<0.0001$), and

Poster Session 2 (P2)

Monday, June 24, 2019

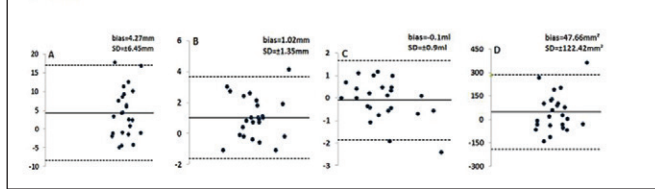
tenting volume was $r=0.84$ ($p<0.0001$). **Conclusion:** Currently available and validated 3D mitral valve modeling software packages provide a quantitative analysis of complex mitral valve anatomy. Many parameters show good reproducibility within and between different software platforms. However, others show significant variability highlighting the need for improved standardization in this new era of quantitation.

Table: Pre-procedural 3D echocardiographic data of two softwares

All patients(n=24)	MVN(QLab)	ICC of MVN(QLab) measurements	4D MV Assessment	ICC of 4D MV Assessment measurements	ICC of QLab vs 4D MV Assessment
AL-PM (mm)	39.9±4.8	0.90(0.78-0.96)	40.0±4.1	0.86(0.69-0.94)	0.76(0.52-0.89)
AP (mm)	35.7±4.4	0.91(0.81-0.96)	34.9±3.9	0.93(0.85-0.97)	0.82(0.63-0.92)
Annular Height (mm)	6±1.6	0.84(0.66-0.93)	5.0±1.5	0.78(0.56-0.90)	0.63(0.31-0.82)
3D Circumference (mm)	127.7±13.2	0.94(0.87-0.98)	123.5±12.4	0.93(0.84-0.97)	0.87(0.73-0.94)
Ellipticity (%)	111.3±9.7	0.67(0.37-0.84)	115.1±7.8	0.53(0.17-0.76)	0.17(-0.24-0.53)
Annular 2D Area (mm ²)	1198.5±263.1	0.95(0.88-0.98)	1150.8±234	0.94(0.87-0.97)	0.88(0.74-0.95)
Ant Leaf 3D Area (mm ²)	844.3±206.5	0.89(0.76-0.95)	710.3±175.4	0.89(0.77-0.95)	0.79(0.57-0.90)
Post Leaf 3D Area (mm ²)	350.3±152	0.60(0.27-0.81)	585.6±137.6	0.85(0.69-0.93)	0.64(0.33-0.83)
Anterior Leaflet Length	29.4±5.2	0.90(0.79-0.96)	26.1±4.5	0.73(0.49-0.88)	0.74(0.48-0.88)
Posterior Leaflet Length	15.8±2.9	0.35(-0.05-0.66)	12.6±2.4	0.63(0.30-0.82)	0.59(0.25-0.8)
Tenting Volume (ml)	2.3±1.2	0.89(0.75-0.95)	2.5±1.6	0.93(0.84-0.97)	0.81(0.60-0.92)
Tenting Height (mm)	6.8±2.3	0.88(0.75-0.95)	6.3±2.4	0.84(0.67-0.93)	0.73(0.47-0.88)
Anterior Leaflet Angle (°)	17.7±9.8	0.44(0.06-0.71)	14.6±5.6	0.79(0.57-0.9)	0.73(0.47-0.88)
Posterior Leaflet Angle (°)	33.2±11.3	0.68(0.39-0.85)	31.3±10.6	0.63(0.31-0.82)	0.59(0.25-0.80)
Nonplanar Angle (°)	129.1±16.7	0.77(0.54-0.89)	156.4±8.5	0.69(0.40-0.85)	0.28(-0.13-0.61)
Aorto-mitral angle (°)	125.5±9.5	0.12(-0.29-0.49)	123.8±7.7	-0.007(-0.4-0.39)	-0.16(-0.52-0.26)
CC diameter (mm)	21.7±5.1	0.45(0.06-0.72)	39.4±3.9	0.83(0.64-0.92)	0.40(0.009-0.69)

AL-PM: Anterolateral-posteromedial, Ant Leaf 3D Area: Anterior Leaflet 3D Area, AL-Posterior, CC diameter: Commissure to commissure diameter, 4D: 4 dimensional, ICC: Intraclass correlation coefficient, MV: Mitral valve, Post Leaf 3D Area: Posterior Leaflet 3D Area.

Figure: Comparison of MVN(QLab) and 4D MV assessment(TomTec) softwares by using Bland-altman analyses. A:3D Circumference, B:Annulus height, C:Tenting Volume, D:Annular 2D area



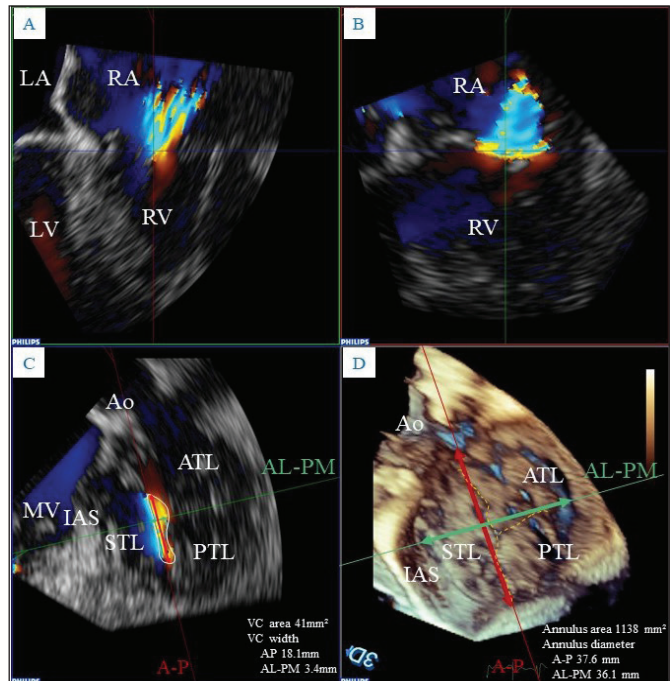
P2-042

Vena Contracta in Functional Tricuspid Regurgitation Caused by Atrial Fibrillation: A Real-Time Color Doppler Three-Dimensional Transesophageal Echocardiography Study

Jun Yoshida, Takahiro Shiota. Cedars Sinai Medical Center, Los Angeles, CA

Background: The aims of this study were to investigate the characteristics and determinants of 3-dimensional (3D) vena contracta (VC) in functional tricuspid regurgitation (TR) caused by atrial fibrillation (AF). **Methods:** Two-dimensional transthoracic and 3D transesophageal (TEE) echocardiography with color Doppler capability were performed in 28 patients having various degrees of functional TR due to AF. No organic tricuspid valve dysfunction or other valvular disease, right / left ventricular dilatation, dysfunction or pulmonary hypertension was found in these patients. 3D tricuspid annular area and its anteroposterior (A-P) and anterolateral-posteromedial (AL-PM) diameters, tethering angles of each tricuspid leaflets, 3D-VC area, 3D-VC widths parallel to A-P and AL-PM direction at mid-systole were measured. **Results:** Clinical and echocardiographic characteristics of 28 patients are shown in Table 1. In all patients, 3D-VC shape was ellipsoidal and identified along the septal leaflet (Figure, panel C), not between anterior and posterior leaflet. 3D-VC area was correlated with tricuspid annular area ($p=0.001$). Though both A-P and AL-PM 3D-VC width were correlated with 3D-VC area, median A-P 3D-VC width was larger than AL-PM 3D-VC width (15.5 vs. 3.5 mm, $p<0.001$). A-P annular diameter had correlation with both A-P and AL-PM 3D-VC widths whereas AL-PM annular diameter didn't. Multivariate analysis showed that only A-P annular diameter independently determined the 3D-VC area ≥ 37 mm² ($p=0.046$) which were the cut off for moderate TR. Receiver operating characteristic curve showed that the optimal cut-off value of A-P annular diameter for predicting the 3D-VC area ≥ 37 mm² was 22 mm/m². **Conclusion:** In patients with functional TR caused solely by AF, the 3D-VC had an ellipsoidal shape that extended toward A-P direction along septal leaflet with enlargement of tricuspid annulus. A-P annular diameter of 22 mm/m² was the only independent determinant of 3D-VC area ≥ 37 mm² which indicated \geq moderate TR.

Clinical and echocardiographic characteristics of patients with functional TR caused by AF	
	Functional TR caused by AF n=28
Clinical characteristics	
Age, y	82 [72-85]
Female sex	19 (68)
Body surface area, m ²	1.85[1.57-1.97]
2D transthoracic echocardiography	
Left ventricular ejection fraction, %	59[55-66]
Right ventricular fractional area change, %	46.0 [41.4-54.3]
Tricuspid annular plane systolic excursion, mm	16.2 [13.6-20.4]
Systolic pulmonary artery pressure, mmHg	38.7 [30.2-47.3]
Tricuspid regurgitation vena contracta, mm	5.7 [3.8-7.0]
Tricuspid regurgitation jet area, cm ²	6.5 [2.3-9.8]
3D transesophageal echocardiography	
Tricuspid annulus at mid-systole	
AL-PM diameter, mm/m ²	20.6 [18.9-24.3]
A-P diameter, mm/ m ²	20.7 [17.6-23.0]
Annular area, mm ² /m ²	646.1 [524.6-765.0]
Tricuspid valve tenting volume, ml	0.7 [0.3-1.5]
Tethering angle of septal leaflet, °	6.3 [1.8-9.1]
Tethering angle of anterior leaflet, °	6.8 [4.9-10.4]
Tethering angle of posterior leaflet, °	6.7 [4.3-10.4]
3D-vena contracta area, mm ²	46 [23-55]
AL-PM 3D-vena contracta width, mm	15.5 [9.1-20.5]
A-P 3D-vena contracta width, mm	3.5 [2.8-4.6]



P2-043

Role of 3-Dimensional Trans-Esophageal Echocardiography in Assessing Angulation of Outflow Graft Anastomosis of Ventricular Assist Device

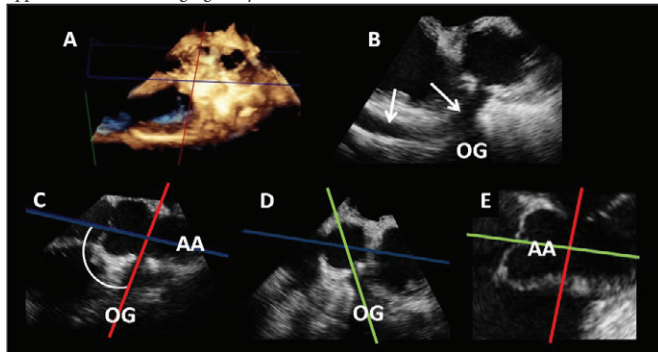
Neha Gupta, Steve Goldstein, Patrick Bering, Ezequiel Molina, Samer Najjar, Jonathan Grinstein, Rebecca Torguson, Ron Waksman, Federico M. Asch, Preetham Kumar, Diego Medvedofsky. Washington Hospital Center/ Georgetown University, Washington, DC

Background: In heart failure patients supported with ventricular assist device (VAD), the angulation at the anastomosis between the outflow graft (OG) and ascending aorta (AA) has been linked to development of aortic regurgitation, where a more acute angle is potentially preferred as it would avoid the development of aortic regurgitation. Currently,

Poster Session 2 (P2)

Monday, June 24, 2019

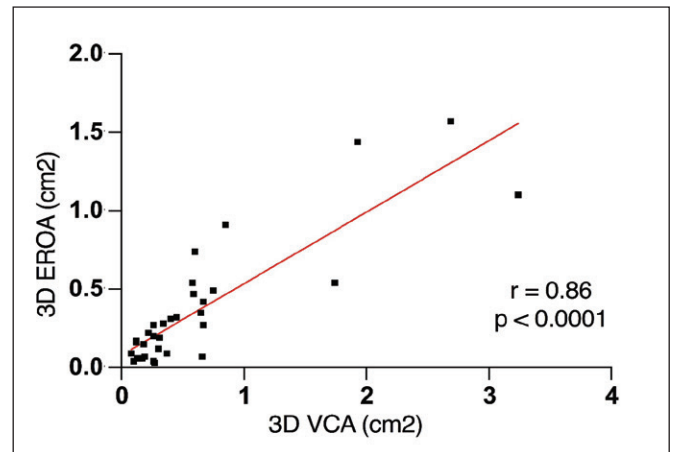
no universal surgical technique exists for OG connection to the AA. 3-Dimensional (3D) trans-esophageal echocardiography (TEE) has the potential to assess the angulation of OG anastomosis to AA. We aimed to evaluate the feasibility of 3D TEE to determine the angle at the anastomosis between the OG and AA in VAD patients. **Methods:** 3D TEE datasets of the AA at the OG insertion level were acquired in 16 consecutive patients during VAD implantation (Figure, panels A-B). Offline multi-planar reconstruction analyses (3DQ, Philips) were performed to measure the angle between the long axis of the OG (Figure, C) and the long axis of the AA at the level of the anastomosis. Orthogonal views of the OG long axes were determined to find its correct orientation (Figure, C red axis, D green axis, E). The angle between the AA and OG at the anastomosis was measured manually in a reconstructed mid-esophageal long-axis view of the aortic valve, as it is the most common view used to assess aortic regurgitation in VAD patients (Figure, B). The frame selected was early systole by electrocardiogram. **Results:** 16 patients were enrolled, and one patient was excluded due to poor image quality. 3D analysis was performed in 15 patients (94% feasibility): 53±10 years, 38% women, 62% HeartWare, 38% HeartMate 3 and 75% non-ischemic cardiomyopathy, and the measured angle was 79±18° (range 48° to 108°). Sixty nine percent of the cases were found to have an acute angle (<90°) at the anastomosis between OG and AA. **Conclusion:** 3D-TEE imaging of the angulation between of the AA and OG at the level of the anastomosis is feasible. This approach could potentially guide surgeons during VAD implantation to achieve a more favorable angle associated with less aortic regurgitation. Further investigation is needed to better understand clinical applications of this imaging analysis.



P2-044
A Novel Three-Dimensional Volumetric Method to Quantify Tricuspid Regurgitation: Comparison with Flow Convergence Methods and Three-Dimensional Vena Contracta Area

Y. Liu, B.Q. Chen, Q. Li, L.L. Dong, Xianhong Shu. Zhongshan Hospital, Fudan University, Shanghai, China

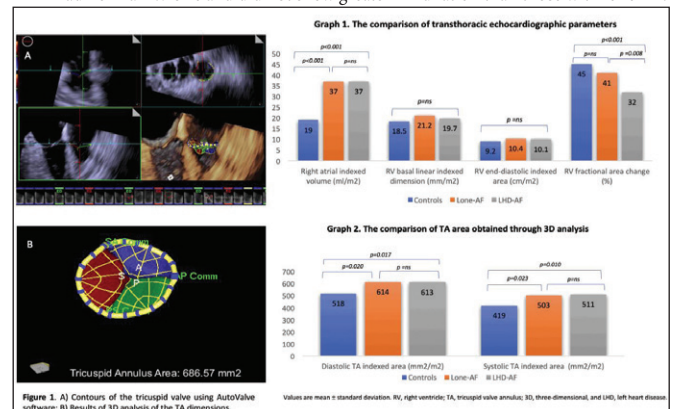
Background: Theoretically, tricuspid regurgitation (TR) can be quantified by subtracting pulmonary stroke volume from right ventricle stroke volume. The aim of this study was to examine the feasibility of the novel volumetric method combining three-dimensional (3D) right ventricle stroke volume and two-dimensional (2D) right ventricular outflow tract forward stroke volume, its correlation with other quantitative echocardiographic parameters of TR, and its ability to detect severe TR. **Methods:** Forty patients with more-than-mild TR in the absence of pulmonary regurgitation or intracardiac shunt prospectively underwent 2D and 3D transthoracic echocardiography. Single-beat non-breathhold 3D data sets of the right ventricle and 3D color data sets of TR were obtained. 2D evaluation of TR severity included averaged vena contracta width from two orthogonal planes and effective regurgitant orifice area (EROA) and regurgitant volume derived from flow convergence method. 3D regurgitant volume was calculated through subtracting the right ventricular outflow tract forward stroke volume from the right ventricular stroke volume, where the outflow tract cross-sectional area was derived from single-view measured diameter, and 3D EROA was then derived by dividing the regurgitant volume with the velocity-time integral of TR. 3D vena contracta area (VCA) was obtained by direct planimetry. **Results:** Thirty-three patients were included in the final analysis. 3D regurgitant volume and EROA correlated well with 3D VCA ($r = 0.79, P < .0001$ and $r = 0.86, P < .0001$) and 2D EROA ($r = 0.87, P < .0001$ and $r = 0.92, P < .0001$) and moderately with averaged vena contracta width ($r = 0.76, P < .0001$ and $r = 0.78, P < .0001$). 3D EROA showed a better agreement (95% limits of agreement from -1.14 to 0.62 cm²) than did 2D EROA (95% limits of agreement from -1.12 to 0.78 cm²) in Bland-Altman analysis against 3D VCA. Receiver operator characteristic curve suggested the best cutoff value for severe TR by 3D EROA was 0.30 cm² (sensitivity: 88%; specificity: 100%). **Conclusions:** 3D volumetric quantitation is feasible in the majority of patients with more-than-mild TR. 3D EROA is a robust parameter for quantification of TR, showing high correlation with other quantitative measurements. 3D EROA has good cutoff accuracy in detecting severe TR.



P2-045
Understanding Tricuspid Valve Remodeling in Atrial Fibrillation Using Three-Dimensional Echocardiography

Xochitl A. Ortiz-Leon¹, Edith L. Posada-Martinez¹, Maria C. Trejo-Paredes¹, Juan B. Ivey-Miranda¹, Helene Houle², Jason Pereira³, Ian Crandall³, Eileen Bouman³, Paul Da Silva³, Alyssa Brooks³, Christine Gerard³, Ben A. Lin¹, Robert L. McNamara¹, Bernardo Lombo¹, Farid Jaababaie¹, Michael Fucci¹, Elise Meoli¹, Jose A. Arias-Godinez⁴, Lissa Sugeng¹. ¹Yale University, New Haven, CT; ²Siemens Healthineers, Mountain View, CA; ³Yale New Haven Hospital, New Haven, CT; ⁴National Institute of Cardiology, Mexico, Mexico

Background: Three-dimensional (3D) echocardiography is uniquely and accurately able to assess the dimensions of the tricuspid valve annulus (TA). It has been proposed that long-standing atrial fibrillation (AF) causes right atrial and TA dilation as well as tricuspid leaflet malcoaptation and severe functional tricuspid regurgitation. Our aim was to characterize the TA remodeling in patients with AF using a novel 3D custom automated software. **Methods:** 43 patients underwent clinically indicated transesophageal and transthoracic echocardiography. 15 patients with AF and structural heart disease or left ventricle dysfunction constituted the left heart disease (LHD)-AF group, 13 patients with AF without any structural heart disease and normal left ventricular function formed the lone-AF group and 15 patients with normal left and right ventricular function and normal sinus rhythm comprised the control group. 3D data sets obtained in the mid esophageal 4-chamber right ventricle (RV) focused view were analyzed off-line to obtain TA area, maximal and minimum diameters, and total perimeter in end-diastole and end-systole using AutoValve software (version 2.2.2, Siemens), figure 1. Three measurements were averaged in AF patients. **Results:** All 43 patients were analyzed, the average age was 60±14 years, 58% were men. Only 14% (n=6) had moderate or severe tricuspid regurgitation. The mean left ventricular ejection fraction was 42±11% in LHD-AF group. In both AF groups, the RV size was normal and the right atrium was dilated without difference between lone-AF group and LHD-AF group (graph 1). The RV fractional area change was normal in lone-AF group while decreased in LHD-AF group. The systolic pulmonary artery pressure was elevated in all AF patients. TA dimensions were largest in diastole. All TA measurements were significantly larger in AF groups than controls but when indexed to body surface area, diameters and perimeter were not significant. There was no difference in any indexed TA parameter between lone-AF and LHD-AF groups (graph 2). **Conclusion:** Using a novel AutoValve software, we found that lone-AF affects TA remodeling by increasing its area, this could be explained partly by the right atrial dilatation; unexpectedly patients with LHD had normal RV size and did not show greater TA dilation than those with lone-AF.



Poster Session 2 (P2)

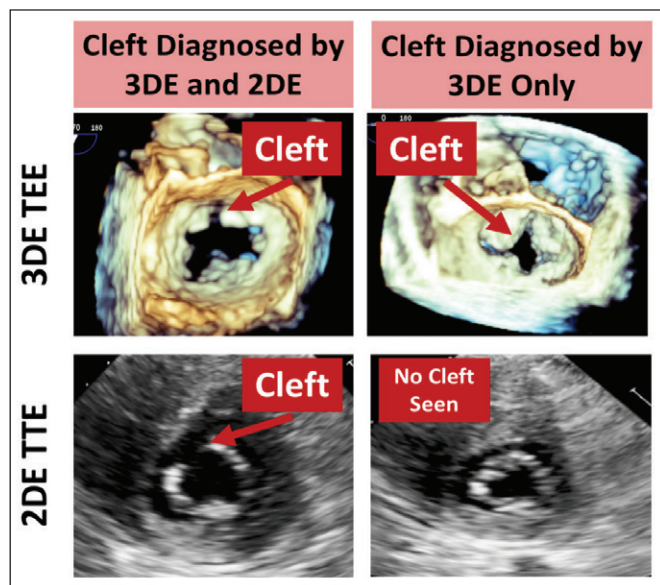
Monday, June 24, 2019

P2-046

Incremental Value of 3D Over 2D Echocardiography in Diagnosing Cleft Mitral Valve

Akhil Narang¹, Karima Addetia², Lynn Weinert², Megan Yamat², Victor Mor-Avi², Roberto M. Lang². ¹Northwestern University, Chicago, IL; ²University of Chicago, Chicago, IL

Background: Three-dimensional echocardiography (3DE) has enabled unparalleled visualization of the mitral valve (MV) and detailed understanding of the mechanisms of mitral regurgitation (MR). Recently it has been shown that 3DE aids in the diagnosis of isolated cleft MV in patients with unexplained significant MR referred for transesophageal echocardiography (TEE). The incremental value of 3DE compared to 2DE for the diagnosis of MV is not known. The purpose of this study was to determine the diagnostic accuracy of cleft MV using 2DE compared to 3DE. **Methods:** We retrospectively studied 20 consecutive patients with significant MR due to isolated cleft MV diagnosed by 3D TEE (iE33 or EPIQ 7, Philips). 3DE acquisitions were then compared to 2D transthoracic (TTE) short-axis acquisitions of the MV. A cleft MV was defined on 3DE as a leaflet gap reaching the annulus throughout the cardiac cycle or on 2DE when a gap in leaflet was observed in the short-axis view. **Results:** Of the 20 patients with cleft MV diagnosed on 3DE, 15 were located on the anterior leaflet, while 5 were located on the posterior leaflet. Cleft MV was identified in only 6/20 (30%) of patients using 2DE acquisitions. The location of the leaflet gap on 2DE matched the location of the cleft noted by 3DE in all these cases. In the remaining 14/20 cases, a cleft was not appreciated on 2DE. **Conclusion:** In patients with significant MR, 3DE is an important tool to aid in detecting pathologies such as cleft. 2DE is often unable to detect cleft mitral valve disease while 3DE adds incremental diagnostic value. 3DE should be used routinely in patients with unexplained significant MR.



P2-047

Incremental Value of Right Parasternal Transthoracic Echocardiographic Examination Over the Left Parasternal Approach in Assessing Ascending Aorta Size. Additional Benefit of Three-Dimensional Echocardiography

Raziye E. Akdogan¹, Swetha Srialluri¹, Ming C. Hsiung², Navin C. Nanda¹, Mahmoud G.A. Abdelsalam¹, Hanan Fadala¹. ¹University of Alabama Birmingham, Birmingham, AL; ²Cheng Hsin General Hospital, Taipei, Taiwan

Background: Although two-dimensional right parasternal transthoracic echocardiographic examination (2DRPE) was described a long time ago, it has not been used extensively in clinical practice. The aim of the present study was to assess the incremental value of 2DRPE over two-dimensional left parasternal transthoracic echocardiographic examination (2DLPE) in evaluating the size of ascending aorta (AA) in adult patients (pts) and also determine if live/real-time three-dimensional (3D) RPE provided any additional benefit over 2DRPE. **Methods:** Two groups of unselected consecutive pts were examined by 2DLPE, 2DRPE, and 3DRPE. The AA was successfully imaged by 2D and 3D RPE in 39/65 (60%) pts in the first group (24 males, mean age 63.2 years), and 48/76 (63%) pts in the second group (28 males, mean age 64 years). **Results:** The maximum length of AA visualized by 2DRPE (5.24 ± 0.82 cm) was larger than 2DLPE (3.69 ± 1.05 cm) in 82/87(94%) pts ($p < 0.001$). The AA length was larger than 5.6cm (normal anatomic length) in 26/87(30%) pts by 2DRPE and none by 2DLPE. Both the maximum AA inner luminal width and leading-edge to leading-edge width by 2DRPE (3.73 ± 0.55 cm and 3.92 ± 0.54 cm, respectively) were greater than 2DLPE (3.45 ± 0.56 and 3.67 ± 0.56 , respectively, $p < 0.001$). The AA leading-edge to leading-edge width was larger than 4.5 cm in 11/87(12%)

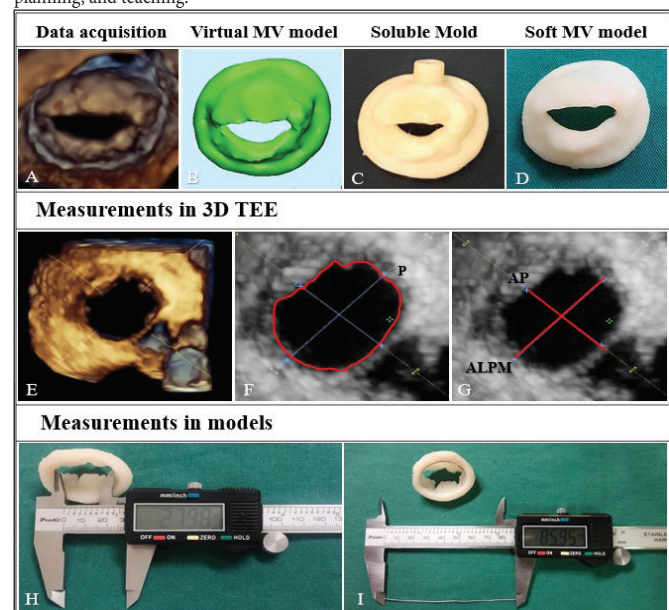
pts by 2DRPE as compared to 7/87(8%) pts by 2DLPE. Similar to computed tomography scan and magnetic resonance imaging where the mid AA width is often taken at the level of the right pulmonary artery, mid AA width could also be taken at this level by 2DRPE in 79/87(91%) pts since this landmark was visualized during 2DRPE. However, this vessel could be visualized in only 2/87 (2%) pts with 2DLPE. 3DRPE conferred additional benefit over 2DRPE. The maximal AA length by 3DRPE was larger than 2DRPE in 48/87(55%) pts and the maximal inner lumen and leading edge to leading edge widths were larger in 54 /87(62%) and 66/87(76%) pts, respectively. **Conclusion:** Our preliminary study demonstrates significant incremental value of 2DRPE over 2DLPE in the assessment of AA. 3DRPE confers an additional advantage over 2DRPE.

P2-048

Feasibility of Mitral Valve Model Made by Three-Dimensional Printing Based on Echocardiographic Data

Yuanting Yang, Qing Zhou, Hongning Song, Sikai Chen, Hao Wang, Wanwan Song. Renmin Hospital of Wuhan University, Wuhan, China

Background: We aims to explore the feasibility of using transesophageal 3D echocardiography (3D-TEE) data to generate 3D patient-specific models of mitral valve (MV). **Methods:** A retrospective study was performed in 22 patients, including 5 cases with normal mitral valve, 7 cases with mitral valve stenosis, 10 cases with mitral valve prolapse. 3D-TEE volumetric data of 22 patients were acquired (Fig1A) and postprocessed to create virtual MV model (Fig1B), and then the soft MV models (Fig1D) were made by injecting silicone to the soluble molds (Fig1C). Measurements of the MV annulus antero-posterior (AP) diameters, anterolateral and posteromedial (ALPM) diameters, perimeter (P), and MV opening width (W) obtained from the 3D echo data set (Fig1E-G) were compared with those performed on the 3D models using a caliper (Fig1H-I), from which the absolute difference of the measurements between 3D models and the 3D echo data were calculated. **Results:** 3D-TEE volumetric data were successfully postprocessed and made as 3D MV models in all patients. The differences of the MV parameters measured using the 3D models were not significant from those measured on the 3D echo data ($P > 0.05$ for all). It showed little absolute difference in value of the MV parameters between the 3D models and the 3D-TEE images. **Conclusion:** The MV models made by 3D-TEE and 3D printing technique is feasible with highly conserved fidelity. This technique has the potential for rapid integration into clinical practice to assist with decision-making, surgical planning, and teaching.



Poster Session 2 (P2)

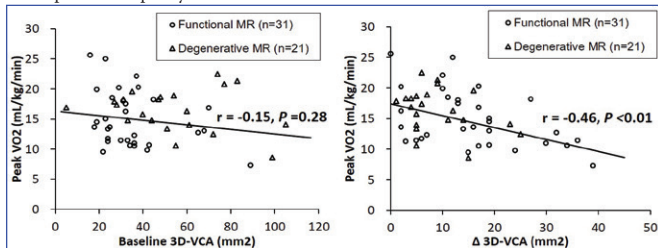
Monday, June 24, 2019

P2-049

Determinants and Clinical Impact of Exercise-Induced Mitral Regurgitation in Patients with Heart Failure: A Three-Dimensional Transesophageal Echocardiography Study Using Handgrip Exercise

Yu Harada, Hiroto Utsunomiya, Kanako Izumi, Hitoshi Susawa, Mirai Kinoshita, Kiho Itakura, Takayuki Hidaka, Yasuki Kihara. Hiroshima University Hospital, Hiroshima, Japan

Background: The three-dimensional (3D) vena contracta area (VCA), measured using color 3D transesophageal echocardiography (TEE), is well known as an accurate parameter for the severity of mitral regurgitation (MR). However, a routine TEE examination is conducted at rest, and it is not unusual that there is a discrepancy between the severity of MR at rest and the symptoms of patients with heart failure. The aims of this study were (1) to investigate the increase in 3DVCA (Δ 3DVCA) by using isometric hand-grip exercise during 3D-TEE, (2) to compare baseline and Δ 3DVCA with effort intolerance, (3) to evaluate the mitral valve (MV) geometrical effects of hand-grip exercise and its association with Δ 3DVCA. **Methods:** Sixty-seven symptomatic patients with moderate to severe MR (degenerative, n=36; functional, n=31) were prospectively enrolled between May 2017 and January 2019. Using 3D-TEE and dedicated software, 3D MV parameters (anterior-posterior and anterolateral-posteromedial diameters, annular area, annular height, tenting height and volume, prolapse height and volume, and 3DVCA) were measured at baseline and after 3-minute handgrip exercise. Δ 3DVCA was calculated as the difference between baseline 3DVCA and handgrip 3DVCA. **Results:** Baseline 3DVCA was significantly larger in the degenerative MR group (49.1 ± 21.2 mm² in degenerative vs. 35.1 ± 17.0 mm² in functional, $P < 0.001$). During handgrip exercise, the 3DVCA increased significantly in both MR groups, but a larger Δ 3DVCA was observed in patients with functional MR (7.6 ± 1.4 vs. 15.8 ± 1.5 mm², $P < 0.001$). In the fifty-two patients we could assess for effort tolerance, Δ 3DVCA was more strongly correlated with effort intolerance than baseline 3DVCA ($r = -0.46$, $P < 0.01$; Figure). Multivariate analyses of Δ 3DVCA revealed several differences between two groups. In functional MR, tenting height and baseline 3DVCA were associated with Δ 3DVCA ($P = 0.0123$ and $P = 0.0329$, respectively). Meanwhile, in degenerative MR, prolapse volume and baseline 3DVCA were associated with Δ 3DVCA ($P < 0.0001$ and $P = 0.005$, respectively). **Conclusions:** This 3D-TEE study showed determinants and clinical impact of exercise-induced MR on effort tolerance in symptomatic patients with MR, and highlighted the need for comprehensive diagnostic workup and multiplicity of the treatment of MR.

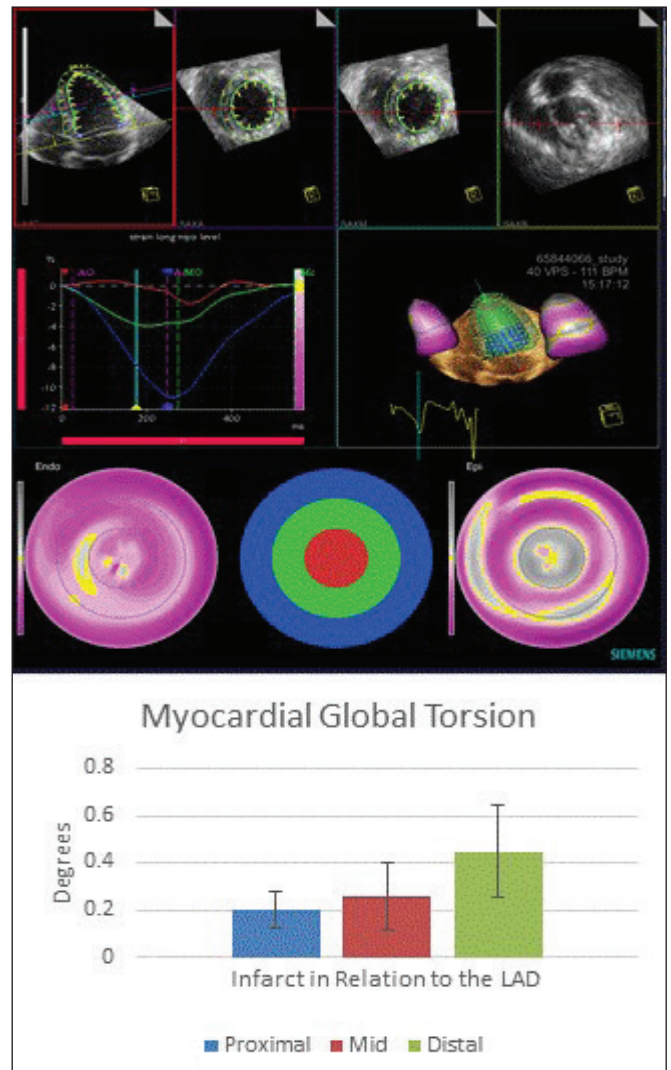


P2-050

Three-Dimensional Speckle Tracking Echocardiography Derived Global Torsion Can Estimate the Extent of Myocardial Ischemia

Muhammad Ashraf¹, Priyanka Vachhani², Kacie Amacher², David J. Sahn². ¹WVU, Morgantown, WV; ²OHSU, Portland, OR

Background: Left Ventricular (LV) torsion is suggested a useful index of dynamic heart function. **Methods:** Eight open-chest pigs were subjected to increasing myocardial ischemia by successively occluding the left anterior descending artery (LAD) at 3 different levels from distal to mid and proximal levels, with images obtained at baseline and at each level of occlusion. High resolution 3D full volume images were acquired with using 4Z1 probe on Siemens Acuson SC 2000 ultrasound system, and analyzed to determine global torsion (GT). **Results:** Increasing the extent of myocardial ischemia with proximal LAD occlusion correspondingly decreased the average GT significantly ($0.203^\circ \pm 0.0779$), as compared with distal occlusion ($0.448^\circ \pm 0.006$), $P < 0.05$. **Conclusions:** Three-dimensional speckle tracking based assessment of global torsion is feasible to evaluate the extent of myocardial ischemia.



P2-051

Impact of Calcification on Three-Dimensional Transesophageal Echocardiography Aortic Annulus Sizing

Mohammed T. Essa, Yeunjung Kim, David Hur, Lissa Sugeng. Yale School of Medicine, New Haven, CT

Background: Transcatheter aortic valve replacement (TAVR) primarily uses cardiac computed tomography (CCT) for aortic valve sizing. Previous studies have shown three-dimensional transesophageal echocardiography (3D TEE) has good correlation with CCT sizing and is an alternative imaging modality. However, the impact of calcification in aortic annulus (AA) sizing is not well understood. Our goal was to understand the impact of AA calcification on 3D TEE versus CCT sizing. **Methods:** Patients who underwent TAVR at our institution between 2015-2018 were retrospectively enrolled. TAVR planning and valve sizing were done with CCT, 3D TEE and automated software (eSie Valve, Siemens Healthineers, Mountain View, CA) were used to calculate AA and aortic valve calcium was estimated (Syngo Calcium scoring software, Siemens, Forchheim, Germany). The prosthetic aortic valve size chosen for TAVR were considered as gold standard measurements for comparison. The fidelity of measurements between CCT and Siemens automated 3D measurements on TEE was assessed using intraclass correlation coefficient. **Results:** 54 patients mean age 78.9 ± 8.2 , 48.2% females with severe symptomatic aortic stenosis (AS) were enrolled. The mean time between TEE and CT was 3.5 days. 51 patients successfully underwent CCT and TEE measurements of AA with area, perimeter, minor and major diameters. All measured values were significantly correlated with and without adjustment for valvular calcium score, $p < 0.05$. On the evaluation of Agatston score and calcium volume, higher calcium score and volume did not decrease agreement (by intraclass correlation coefficient) between CT and TEE measurements (Table 1). Nearly half of patients had all measurements within range of chosen valve by both modalities, however, unlike TEE, MDCT tended to overestimate parameters (Table 2). Pts with low calcium score (AU < 2006) tended to all be classified correctly by TEE. In high calcium

Poster Session 2 (P2)

Monday, June 24, 2019

score (AU > 3894) MDCT tended to have all parameters within range of chosen valve. **Conclusion:** Both CT and TEE provided high fidelity measurements with little inter- and intra-observer variation and provide confidence in both modalities even with significant aortic valve annular calcification.

Table 1. Intraclass correlation coefficient of MDCT and TEE measurements by aortic valve calcium score

Aortic valve calcium score range (mean)*	Aortic annulus area	Aortic annulus perimeter	Major diameter	Minor diameter
0-2006 (1333)	0.67	0.48	0.45	0.58
2007 - 3071 (2446)	0.83	0.83	0.6	0.71
3072 - 3893 (3419)	0.82	0.78	0.56	0.71
≥3894 (5465)	0.84	0.76	0.6	0.86
*Agutston unit (AU)				

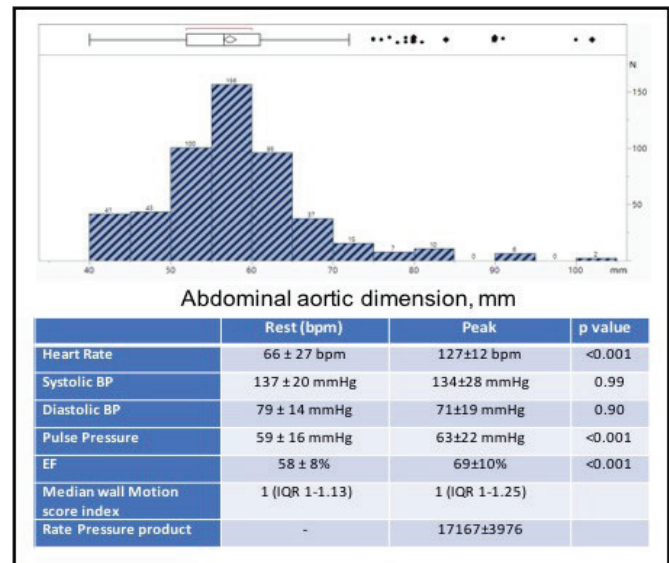
Table 2. Percentage of modality sizing falling within the range of chosen valve.

	Modality			
	3D TEE		MDCT	
All measurements within range of chosen valve*	51%		46%	
Measurements outside range of chosen valve*	Underestimation (26%)	Overestimation (24%)	Underestimation (12%)	Overestimation (42%)
We used standard sizing provided by respective companies*				

P2-052 Moderated Poster Feasibility and Safety of Dobutamine Stress Echocardiography in Patients with Abdominal Aortic Aneurysms: 5 Year Single Center Experience

Hilal Olgun Kucuk, Garvan C. Kane, Patricia A. Pellikka, Peter C. Spittell, Robert B. McCully, Brandon M. Wiley. Mayo Clinic, Rochester, MN

Background: Dobutamine stress echocardiography (DSE) is frequently used for preoperative cardiac risk stratification in patients with vascular aneurysms. Hemodynamic effects of dobutamine infusion may increase shear stress across aneurysm wall and potentially lead to rupture. **Methods:** Among 1513 patients with vascular aneurysms who underwent DSE during a 5-year period between May 2018 and January 2013; 512 patients with abdominal aortic aneurysm (AAA) were identified. In 2 patients, DSE was deferred secondary to concern for rupture risk due to aneurysm size (80 mm and 90 mm) and nuclear stress testing was performed instead. **Results:** The mean age was 73.8±8 years; 77% were male. Of the cohort, 38% had previous CAD; 81% had hypertension (HT) and 9.5 % had a pre-stress LVEF below 45%. The mean diameter of the AAA was 57±9 mm (range 40-102mm); 33.5% of the patients had AAA greater than 60 mm (Figure 1). The average daily per patient rupture risk, based on aneurysm size, was 0.03 ± 0.03% for a cumulative daily risk of rupture of one of the cohort of 15%. Overall DSE was tolerated well; in 496 patients the study was terminated either due to achievement of target heart rate or peak dose of dobutamine & atropine. 0.1% patients developed side effect resulting in early termination of the study (5 significant HT, 5 severe symptoms, 2 significant hypotension, 1 supraventricular arrhythmia and 1 ventricular arrhythmia), rates similar to patients without AAA. Mean peak administered dobutamine dose was 34±7 µg/kg/min. Atropine was used to achieve target heart rate in 62% patients. Target heart rate was achieved in 458 (89%) patients (Table 1). 61.9% of the patients had a normal DSE whereas 22.6% developed ischemia. No patients had cardiac arrest, hemodynamic instability or acute MI as a result of DSE. However, 1 patient (76 years old male with an enlarging 80 mm infrarenal AAA and previous coronary artery bypass surgery, peripheral artery disease and HT) underwent an apparent uncomplicated DSE. However, within two hours of being dismissed from the stress laboratory, he had aneurysm rupture and died. **Conclusion:** DSE overall appears low risk in a cohort of AAA patients with an estimated cumulative daily rupture risk of 15%. However, 1 patient with a very large AAA (0.2% of the overall cohort) had rupture and died within hours of DSE.



P2-053 Impact of High Baseline Left Ventricular Filling Pressure on Transcatheter Aortic Valve Replacement Outcomes

Vien T. Truong¹, Wojciech Mazur¹, Gregory F. Egnaczyk¹, Dean J. Kereiakes¹, Ian J. Sarembock¹, Joseph K. Choo¹, Satya Shreenivas¹, Sherif F. Nagueh², Eugene S. Chung¹. ¹The Christ Hospital Health Network, Cincinnati, OH; ²Methodist DeBakey Heart and Vascular Center, Houston Methodist Hospital, Houston, TX

Background: Left ventricular filling pressure (LVFP) has been demonstrated to be a major predictor of poor cardiovascular outcomes. However, estimation of LVFP in aortic stenosis (AS) patients is limited by the high prevalence of significant mitral annular calcification (MAC). The aim of this study was to investigate the effect of transcatheter aortic valve replacement on LVFP and the relationship of LVFP to mortality and hospitalization. **Methods:** This a single center retrospective study of 140 consecutive patients in sinus rhythm with significant MAC who underwent TAVR for severe AS from May 2011 to June 2015. Mean follow up duration was 3.06 ± 1.48 years (minimum 2.4 years, maximum 6.5 years). Diastolic function was assessed using recently proposed criteria by Abudiyab et al for those with significant MAC. High LVFP was defined as a mitral E/A ratio more than 1.8 or ratio of 0.8 to 1.8 and isovolumic relaxation time less than 80ms. **Results:** At baseline, the proportion of patients with high LVFP was 40.7%, similar to one month (39.7%, p=0.86). However, the proportion of patients with high LVFP was significantly decreased at 1 year when compared to those at baseline (26.9% vs. 40.7%, p = 0.02). Multivariate analysis showed that high LVFP at baseline significantly increased risk of all-cause mortality compared to patients with normal LVFP (HR: 2.84; 95% CI, 1.33-6.05; p = 0.007). **Conclusion:** High baseline LVFP was associated with a significantly increased all-cause mortality and LVFP does not improve in the short term, but at 1 year post TAVR.

P2-054 The Rotational Position of the Aortic Root is Associated with Aortic Dilation in Turner Syndrome

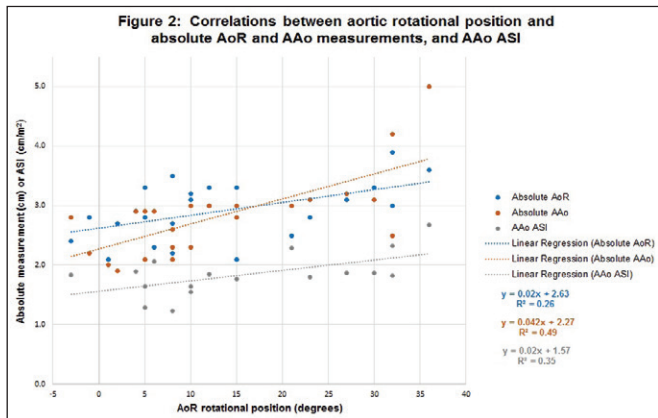
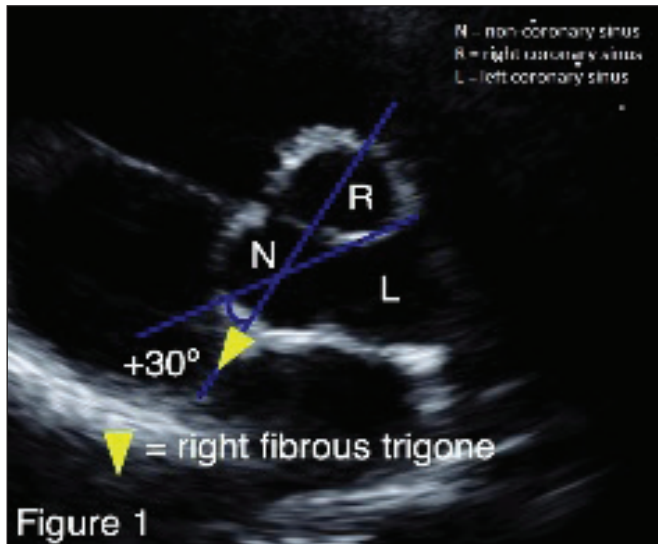
Colleen Pater, Amy Shikany, Laura Riley, Lisa J. Martin, Iris Gutmark-Little, Philippe F. Backeljauw, Nicole M. Brown, Justin T. Tretter. Cincinnati Children's Hospital Medical Center, Cincinnati, OH

Background: Progressive aortic dilation is common in Turner syndrome (TS), risk factors of which are poorly understood. We recently reported variation in the aortic root (AoR) rotational position relative to the left ventricular base in normal subjects, which correlates to variability in myocardial versus fibrous support of the AoR. We aimed to assess the relationship between AoR rotational position and aortic dimensions in a TS cohort. **Methods:** TS patients with trisinate roots (trileaflet or bileaflet valves) and aortopathy were included. Aortic dimensions were measured from their most recent transthoracic echocardiogram on parasternal long axis views. Turner-specific Z-scores (TSZ) were determined in patients birth to 15 years old, and aortic size index (ASI) in patients older than 15 years. The AoR rotational angle was measured in the parasternal short axis plane in diastole, focusing on the center of the non-coronary sinus relative to the right fibrous trigone (Figure 1). **Results:** 24 patients with TS were included (age 40.5 ± 11.9 years). The mean AoR dimension was 2.9 ± 0.5 cm (TSZ 0.03 ± 1.1, ASI 1.90 ± 0.23 cm/m²) and ascending aorta (AAo) dimension was 2.8 ± 0.7 cm (TSZ 0.45 ± 1.14, ASI 1.85 ± 0.36 cm/m²). The mean rotational position angle of the AoR was +13.3 ± 11.4 degrees. There was a positive correlation between a more clockwise rotational position of the AoR with both the

Poster Session 2 (P2)

Monday, June 24, 2019

absolute AoR ($r^2 = 0.26, p=0.01$) and the absolute AAO ($r^2 = 0.49, p<0.001$) measurements. There was no correlation with the AoR TSZ or ASI, or the AAO TSZ. There was also a positive correlation with the AAO ASI ($r^2 = 0.35, p = 0.01$) (Figure 2). **Conclusion:** There is an association between clockwise rotational position of the AoR and increased aortic dimensions in TS patients. Prior investigations suggest that the rotational position of the AoR is primarily determined during development, implying that the AoR position precedes the aortic dilation seen in this study. This suggests that the AoR rotational position may be a risk factor for progression of aortic dilation in TS.

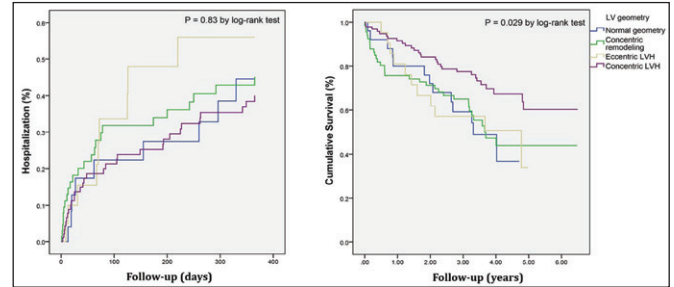


P2-055
Transcatheter Aortic Valve Replacement and Left Ventricular Geometry: Survival and Gender Differences

Vien Truong¹, Wojciech Mazur¹, John Broderick¹, Gregory F. Egnaczyk¹, Dean J. Kereiakes¹, Ian J. Sarembok¹, Joseph K. Choo¹, Satya Shreenivas¹, Sherif F. Nagueh², Cheryl Bartone¹, Brian Volz¹, Eugene S. Chung¹. ¹The Christ Hospital Health Network, Cincinnati, OH; ²Methodist DeBakey Heart and Vascular Center, Houston Methodist Hospital, Houston, TX

Background: The aim of study is to assess the relationship between baseline left ventricular (LV) geometry and outcomes after Transcatheter Aortic Valve Replacement (TAVR). **Methods:** This is a retrospective analysis of 265 consecutive patients who underwent TAVR for severe AS, between May 2011 and May 2015, under the approval of the Institutional Review Board of the Christ Hospital, Cincinnati, OH. A total of 206 patients were eligible for inclusion after 49 patients were excluded due to inadequate echocardiography data at the baseline. Patients had baseline LV geometry classified as 1) concentric hypertrophy, 2) eccentric hypertrophy, 3) concentric remodeling or 4) normal. **Results:** Distribution of baseline LV geometry differed between male and female patients ($X^2 = 16.83, P = 0.001$) but not at 1 month ($X^2 = 2.56, P = 0.47$) or 1 year ($X^2 = 5.68, P = 0.13$). After TAVR, a majority of concentric hypertrophy patients evolved to concentric remodeling. Survival differed across LV geometry groups at 1 year ($\chi^2(3) = 8.108, P = 0.044, \text{log-rank test.}$) and at 6.5 years ($\chi^2(3) = 9.023, p = 0.029, \text{log-rank test.}$) Compared to patients with concentric hypertrophy, patients with normal geometry (hazard ratio [HR]: 2.25; 95% confidence interval [CI], 1.12-4.54; $p = 0.023$) and concentric remodeling (HR: 1.89; 95% CI, 1.12-3.17; $p = 0.016$) had higher rates of all-cause mortality. **Conclusion:** Baseline concentric

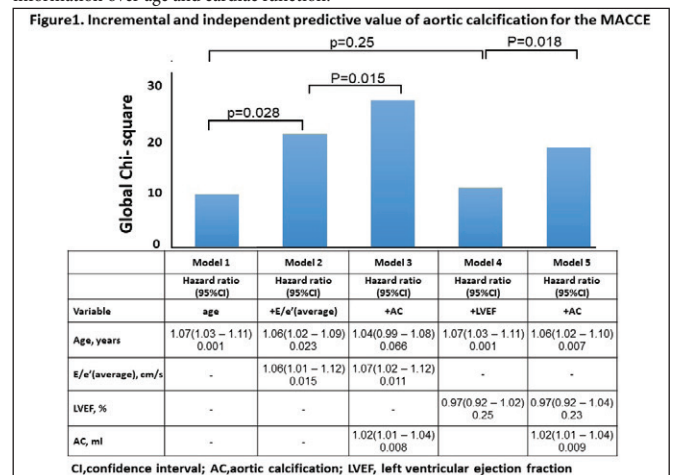
hypertrophy confers a survival advantage after TAVR. Although baseline patterns of LV geometry appear gender specific (women demonstrating more concentric hypertrophy), this difference resolves after TAVR.



P2-057
Aortic Calcification Has Independent and Incremental Prognostic Value Over Cardiac Function for Cardiovascular Event in Patients with Preserved Ejection Fraction

Hidemi Sorimachi¹, Tomonari Harada¹, Kuniko Yoshida¹, Toshimitsu Kato¹, Masaru Obokata¹, Masahiko Kurabayashi¹, Kazuaki Negishi². ¹Gunma University Graduate School of Medicine, Maebashi, Japan; ²University of Sydney, NSW, Australia

Background: It is suggested that aortic calcification is an important predictor of cardiovascular morbidity and mortality, irrespective of traditional coronary risk factors. However, the mechanism underlying the relationship between aortic calcification and cardiovascular events remains unknown. We aimed to determine whether aortic calcification is an independent predictor of cardiovascular outcomes, and to elucidate incremental prognostic utility of aortic calcification over the models with age and systolic or diastolic function. **Methods and Results:** We retrospectively reviewed the records of 485 patients (median age, 71±13 years; 288males) who underwent clinically-indicated computed tomography and echocardiography at our hospital between October 2012 and July 2014. The calcification volume at the aortic wall was assessed as any area $\geq 1 \text{ mm}^2$ with attenuation ≥ 200 Hounsfield units. The median aortic calcification volume was 9.9 mL (25th and 75th percentile, 2.6, 21.1). We assessed E/e' as diastolic function and LVEF as systolic function. Primary endpoint was major adverse cardiac and cerebrovascular events (MACCE). During a median follow-up of 959 days, 30 MACCE occurred. AC volume was significantly larger in patients who developed MACCE than those who did not ($p=0.003$). In multivariable analysis, AC was independently associated with MACCE after adjusting for age and E/e' (HR, 1.02; 95% CI, 1.01-1.04; $p=0.008$) or LVEF (HR, 1.02; 95% CI, 1.01-1.04; $p=0.009$). Furthermore, the AC significantly improved predictive value over age and cardiac function. **Conclusions:** AC provided independent and incremental prognostic information over age and cardiac function.



Poster Session 2 (P2)

Monday, June 24, 2019

P2-058

Vascular Outcomes of a Pregnancy Complicated by Preeclampsia

Logan C. Barr¹, Jessica Pudwell², Julia E. Herr³, Amer Johri³, Graeme N. Smith⁴. ¹Queen's University, Kingston, ON, Canada; ²Department of Obstetrics & Gynecology, Kingston General Hospital, Kingston, ON, Canada; ³Department of Medicine, Queen's University, Cardiovascular Imaging Network at Queen's, Kingston, ON, Canada; ⁴Department of Obstetrics & Gynaecology, Kingston General Hospital, Kingston, ON, Canada

Background: Preeclampsia (PE) is a hypertensive complication of pregnancy that is a major cause of maternal morbidity and mortality. However, PE is also associated with an elevated lifetime risk for cardiovascular disease through poorly understood mechanisms. We hypothesize that postpartum microvascular endothelial dysfunction associated with PE may predate macrovascular disease. **Methods:** Healthy women with previous PE (n=27) and normotensive controls (n=16) between 6 months and 5 years postpartum have been recruited. Recruitment is ongoing. Microvascular vasodilation in the right volar forearm was assessed using laser speckle contrast imaging (LSCI) (moorFLPI-2, Moor Instruments Inc, Axminster, UK) with stepwise iontophoresis of 1% acetylcholine and sodium nitroprusside solutions (20 μ A, 50 μ A, and 2 applications each of 100 μ A and 120 μ A) using an iontophoresis controller (MIC2, Moor Instruments Ltd, Axminster, UK). Macrovascular indicators of cardiovascular health were assessed with a two-dimensional carotid ultrasound scan on both left and right carotid arteries (GE Healthcare, Wisconsin, USA), quantifying carotid intima-media thickness (CIMT), plaque burden, and carotid strain. **Results:** Systolic and diastolic blood pressures were not significantly different between groups. Formerly preeclamptic participants had significantly higher body mass index (p=0.01). Vasodilation significantly increased with iontophoretic dose among both groups compared to the lowest dose (p<0.05). 2-way ANOVA did not identify significant differences between subject groups in endothelium-dependent, nor endothelium-independent vasodilation to stepwise iontophoresis. However, formerly preeclamptic women had significantly higher endothelium-dependent vasodilation when using a linear fixed-effect model controlling for the number of weeks postpartum (p=.044). There were no significant differences between subject groups with respect to most measures of CIMT, plaque burden, and carotid strain. However, far wall circumferential strain was higher among normotensive participants (p=.03). **Conclusions:** A pregnancy complicated by PE is associated with changes in microvascular vasodilatory function, but not macrovascular indicators of cardiovascular health, in the early postpartum period. These findings corroborate our hypothesis that microvascular changes predate large-vessel indicators of dysfunction. Further study would identify the precise relationship of PE to postpartum microvascular aberrations and the mechanistic changes that account for our preliminary findings.

P2-059

Circumferential Ascending Aortic Strain in Healthy Adults Aged 24 to 75 Years

J. Shi, YS Wang, WP Zhao, Xianhong Shu. Zhongshan Hospital, Fudan University, Shanghai, China

Background: Two-dimensional speckle-tracking echocardiography (2D-STE) for the measurement of circumferential ascending thoracic aortic strain (CAAS) in healthy adults is not elucidated. We aimed to establish normal adult STE-derived CAAS and to evaluate associations with age, gender and other physiologic parameters. **Methods:** One hundred eighty-one healthy subjects aged 24-75 were prospectively gathered and examined with two-dimensional echocardiography. The global peak CAAS was the parameter used, and an average of six segments of arterial wall deformation was calculated. The corrected CAAS was calculated as the global CAAS/pulse pressure (PP). Aortic stiffness (β 2) index was assessed according to $\ln(\text{Ps/Pd})/\text{CAAS}$. **Results:** We included 171 healthy subjects (age 44.3 \pm 10.9 years, 50% female, CAAS16.0 \pm 6.9%). The CAAS was independently predicted by age (β =0.387, P<0.001), and gender (β =-2.701, P=0.001). The corrected CAAS was independently predicted by age (β =-0.009, P<0.001), SAC (β =-0.206, P<0.001) and gender (β =-0.068, P=0.001). The β 2 index was independently predicted by age (β =0.136, P<0.001), and PP (β =0.059, P=0.007). **Conclusion:** CAAS using 2D-STE can be performed on a clinical basis and may become an important method for the assessment of aortic mechanical parameter. Age, gender and LV afterload-related variables were the most important determinants of 2D-STE global CAAS. Therefore, these factors should be taken into account for strain interpretation in clinical practice.

P2-060

Comparison of Exercise Blood Pressure Gradients and Echocardiographic Doppler Gradients in Coarctation of the Aorta

Amanda M. McIntosh, Julie C. Fernie, Sonali Patel, Bruce Landeck, II, Christopher M. Rausch. Children's Hospital Colorado/University of Colorado, Aurora, CO

Background: Coarctation of the aorta requires surveillance throughout the lifespan after repair due to potential for development of aortic aneurysm, hypertension, and residual coarctation. Previous studies have shown that exercise arm-leg blood pressure (BP) gradients are associated with residual coarctation when compared to direct gradients

measured by invasive catheterization. Echocardiography has also been used to evaluate for residual or recurrent coarctation and is used more routinely than catheterization or other imaging modalities in clinical surveillance of patients with coarctation of the aorta. To our knowledge, no study has compared exercise arm-leg BP gradients with echo Doppler measurements in the descending aorta following repair of coarctation of the aorta. We predict that exercise arm-leg BP gradients will correlate with echo Doppler gradients. **Methods:** We performed retrospective comparison of 264 cardiopulmonary exercise tests (CPETs) completed by 234 patients with coarctation of the aorta aged 5 to 43 years between January 1, 2011 and December 31, 2017. Systolic exercise arm-leg BP gradients taken at peak exercise were compared with Doppler gradients measured by resting transthoracic echos performed within one year of the CPET. **Results:** The median age at the time of CPET was 14.8 years and 68.6% of subjects were male. 53.4% of patients had surgical end to end anastomosis repair at a median age of 1 month (IQR=0.24-16.44). 52.7% of patients had hypertension. The median exercise systolic arm-leg BP gradient was 2 mmHg (IQR=-18-20) and at rest was -6 mmHg (IQR=-15-5). The median echo peak coarctation gradient calculated using the full modified Bernoulli equation was 9.95 mmHg (IQR=3.29-19.17). The correlation between exercise arm-leg systolic BP gradient and echo coarctation gradient was weak [$r=0.375$, (0.25-0.49); p<0.0001]. **Conclusion:** Exercise arm-leg systolic BP gradients only weakly correlated with resting echo Doppler gradients in patients following repair of coarctation of the aorta. Although both tests are routinely used for clinical surveillance following repair, clinicians should use caution when comparing exercise arm-leg BP gradients with echo gradients in follow-up of patients with repaired coarctation of the aorta.

P2-061

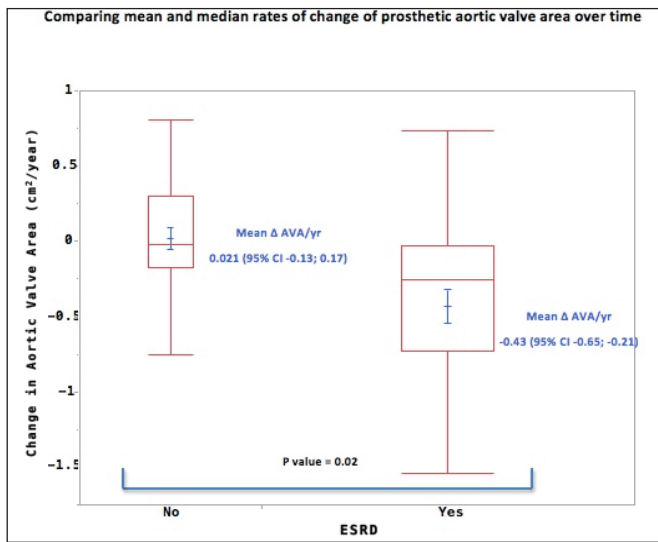
The Rate of Failure of Bioprosthetic Aortic Valves in Patients with ESRD

Megha Penmetsa, Karl Richardson. Wake Forest Baptist Medical Center, Winston-Salem, NC

Background: The prevalence of aortic stenosis increases with age. The advent of transcatheter aortic valve procedures has allowed replacement in a more elderly, frail, and comorbid population. Patients with end-stage renal disease (ESRD) may be more likely to have aortic valve replacement with a bioprosthetic valve. It has been shown that there is rapid progression of aortic stenosis in patients with ESRD, but there are few published modern reports investigating the impact of renal disease on the rate of failure of these devices. The purpose of this study is to evaluate the rate of failure of bioprosthetic valves in patients with ESRD compared to patients with normal renal function. **Methods:** Our institution's electronic medical record was queried to identify patients with bioprosthetic aortic valves and at least two transthoracic echocardiograms (TTEs) 6 or more months apart. Patients with ESRD and a bioprosthetic valve were compared to a random sample of 21 similar patients with normal renal function. TTE imaging and Doppler data were abstracted to calculate changes in aortic valve area (AVA) and peak gradient over time. Results were analyzed using a Kruskal-Wallis one-way ANOVA analysis. **Results:** Data from 66 medical charts (45 ESRD, 21 normal renal function) were included. Cohorts were similar in age, gender and type of bioprosthetic valve. The calculated aortic valve area in patients with ESRD declined at 0.43 (95% CI -0.66, -0.21) cm^2/year compared to an essentially stable 0.021 (95% CI -0.13, 0.17) cm^2/year (p = 0.02) in patients with normal renal function (Figure 1). The change in peak gradient was 6.77 mmHg/year compared to -0.64 mmHg/year (p = 0.06) for the ESRD and normal renal function groups, respectively. **Conclusion:** We were able to further understand the impact of ESRD on the rate of change of the bioprosthetic aortic valve in a modern cohort. Our results confirm limited available data regarding an accelerated rate of failure of bioprosthetic valves, and our results serve to more effectively quantify this rate of change. This data may inform discussions regarding risks and benefits of aortic valve replacement in patients with ESRD and further illustrates that ESRD is an important risk factor to consider when determining which valve type to use in patients requiring aortic valve replacement.

Poster Session 2 (P2)

Monday, June 24, 2019



P2-062

Ultrasound Ultrafast Imaging of the Carotid Artery Pulse Wave Velocity: Is the Surrogate of Regional Artery Stiffness

Lingyun Fang^{1,2}, Dan Zhang^{1,2}, Feixiang Xiang^{1,2}, Yue Song^{1,2}, Mingxing Xie^{1,2}, Jing Wang^{1,2}. ¹Department of Ultrasound, Union Hospital, Tongji Medical College, HUST, Wuhan, China; ²Hubei Key Laboratory of Molecular Imaging, Wuhan, China

Background: Cardiovascular diseases (CVDs) are the leading causes of death in the world and responsible for over 17.7 million deaths annually. Arterial stiffness could be a strongest predictor for coronary heart disease and stroke. Pulsed wave velocity(PWV) is “the most hallowed and still probably the best” measure of arterial stiffness and closely related to the processing of arteriosclerosis. Techniques to measure PWV present limitations. There are based on the mathematical model calculation, or need special instruments and required a fairly high level of technical expertise. A new ultrasound-based technique, Ultrasound Ultrafast imaging could noninvasive assessment of regional carotid artery stiffness. The imaging system has a very high frame rates over than 2000 frames per second, and could quickly obtain the PWV propagate along the carotid artery. The objective is to detect the PWV in elder Humans carotid artery in vivo. Determine the feasibility and accuracy to assess artery stiffness by Ultrasound Ultrafast imaging. Confirm the relationship between the local carotid artery PWV and the stiffness of the systemic vessels. **Methods:** Ultrasound Ultrafast imaging was performed and obtain the velocity propagate along the left common carotid arteries of fifty-nine (n = 59) healthy volunteers. Including the PWV at the beginning of the systole and at the ending of the systole, P_{BS} PWV, P_{ES} PWV, the mean PWV (mPWV) were calculated. E-Tracking technology in measuring artery elasticity modulus (PWV β) and cardio-ankle vascular index(CAVI) were calculated in all subjects. The correlation between parameters derived from Ultrasound Ultrafast imaging and elastic modulus were analyzed. Indicate artery elasticity and the impact of modifying factors such as BMI, age and hypertension. **Results:** (1) The success rate of first obtain the P_{BS} PWV were 94.2% and 90.8%, which required a median overall duration of 73s. (2) mPWV were significant positively correlated with PWV β and CAVI (r=0.68, P<0.01, r=0.48, P<0.05). BMI, age and hypertension were also positively correlated with PWV. (3) The mPWV have a good repeatability and conformity. Interobserver and intraobserver variabilities were 4.2% and 3.6 % respectively. **Conclusion:** The elasticity of carotid artery is an integral part of the global arterial elasticity. Ultrasound Ultrafast imaging is a reliable method to assess the regional carotid artery stiffness. The technique can directly and quickly measure PWV of local vessels, with high repeatability and provides a new method for clinical early assessment artery elasticity.

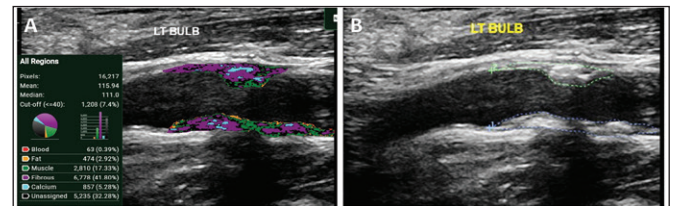
P2-063

IntelliPlaque: A Novel, Automated Grayscale Analysis of Carotid Artery Plaque to Predict Risk in Patients Presenting to the Emergency Department with Chest Pain

Winnie Chan, Marie-France Héu, Julia E. Herr, Steven Brooks, Nicole O’Callaghan, Dathan Liblik, Amer Johri. Queen’s University, Kingston, ON, Canada

Background: Vulnerable atherosclerotic plaque is composed of inflammatory, calcified, lipid or neovascularized tissue components. Such differential tissue characteristics within an individual lesion may be evaluated by ultrasound using grayscale pixel distribution analysis (PDA). The HEART Score is a clinical decision tool used in the emergency department (ED) to predict cardiovascular (CV) outcomes in patients presenting with chest pain. Our

objective was to determine whether carotid plaque composition by a novel automated PDA method correlated with the HEART Score and high sensitivity troponin (hsTn) in the ED. **Methods:** Focused carotid ultrasound was performed in 213 patients presenting to the ED with chest pain suspicious for coronary ischemia. Total plaque area was summed from the long axis view of both the left and right carotid bulbs (Fig. 1B). Plaque composition by PDA was assessed using a novel, rapid, semi-automated software (IntelliPlaque™, Fig. 1A) using grayscale ranges of 0-4 (blood), 8-26 (fat), 41-76 (muscle), 112-196 (fibrous), and 211-255 (calcium). The number of pixels falling within each grayscale range was divided by the total number of plaque pixels, reported as a percentage (%), and averaged for both sides. Spearman’s rho was used to evaluate the correlation between plaque characteristics (total plaque area and plaque composition) and the HEART score. Wilcoxon-Mann-Whitney two sample test was used to compare plaque area and composition with hsTn.



Results: Plaque area increased with HEART score (rho = 0.43; p<0.0001) and was higher in patients with a positive hsTn (56.0 mm² vs 43.6 mm²; p=0.03). PDA of plaque revealed that higher % calcium composition correlated with higher HEART scores (rho = 0.18; p=0.01) and the % calcium composition was higher in patients with a positive hsTn (0.63% vs 0.31%; p=0.02). **Conclusion:** Plaque area and % calcium correlated with the HEART Score and positive hsTn. These findings suggest a role for plaque characterization as an early imaging biomarker predictive of CV risk in patients with a presenting complaint of chest pain with ischemic features. A further study to correlate plaque composition with 30-day outcomes is currently underway and has the potential to significantly enhance risk stratification of one of the most common reasons for presentation to the ED.

P2-064

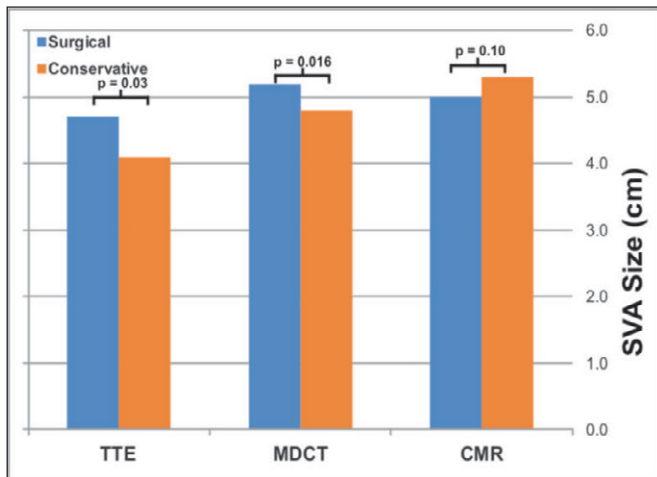
Echocardiographic Assessment of Sinus of Valsalva Aneurysms: Comparison with Computed Tomography and Cardiac Magnetic Resonance

Bo Xu¹, Jorge Betancor², Carlos Godoy Rivas³, Serge Harb¹, Scott D. Flamm⁴, L Leonardo Rodriguez¹, Brian P. Griffin¹. ¹Section of Cardiovascular Imaging, Heart and Vascular Institute, Cleveland Clinic, Cleveland, OH; ²Aventura Hospital and Medical Center, Miami, FL; ³Department of Internal Medicine, Cleveland Clinic, Cleveland, OH; ⁴Imaging, and Heart and Vascular Institutes, Cleveland Clinic, Cleveland, OH

Background: Sinus of Valsalva aneurysms (SVAs) are rare. We investigated the echocardiographic assessment of SVAs, compared to multidetector cardiac computed tomography (MDCT) and cardiac magnetic resonance (CMR). **Methods:** Patients diagnosed with SVAs at our center over a 20-year period (January 1997 to June 2017) were retrospectively analyzed. **Results:** There were 103 patients (mean age: 56 years; male: 69%). 78 patients (76%) presented with non-ruptured SVAs, and 23 (22%) with ruptured SVAs (of whom, 91.3% were treated surgically). The mean durations of follow-up were 4.0 years in the surgical group, and 4.8 years for the conservative group. 76 patients (74%) underwent surgery. The only in-hospital death was related to endocarditis. Transthoracic echocardiography (TTE) was the first-line imaging investigation: 100% (surgical group) and 96% (conservative group). Additional imaging studies included: 1. transesophageal echocardiography (TEE): 94.7% (surgical group) vs. 37% (conservative group), p < 0.05; 2. MDCT: 61.8% (surgical group) vs. 37% (conservative group); 3. CMR: 22.4% (surgical group) vs. 14.8% (conservative group). At diagnosis, the maximum sinus-to-sinus aortic root diameters were: 4.7 ± 1.0 cm (surgical group) vs. 4.1 ± 1.0 cm (conservative group) by TTE, p=0.03; 5.2 ± 1.1 cm (surgical group) vs. 4.8 ± 1.1 cm (conservative group) by MDCT, p = 0.016; and 5.0 ± 1.0 cm (surgical group) vs. 5.3 ± 1.3 cm (conservative group) by CMR, p = 0.10. **Conclusion:** In a contemporary 20-year cohort, TTE was the first-line imaging investigation for assessing SVAs. Additional imaging (TEE, MDCT and CMR) were more frequently utilized for patients undergoing surgery for SVAs. The outcomes of patients with SVAs managed in a pathway incorporating multimodality cardiac imaging, led by echocardiography, were excellent.

Poster Session 2 (P2)

Monday, June 24, 2019

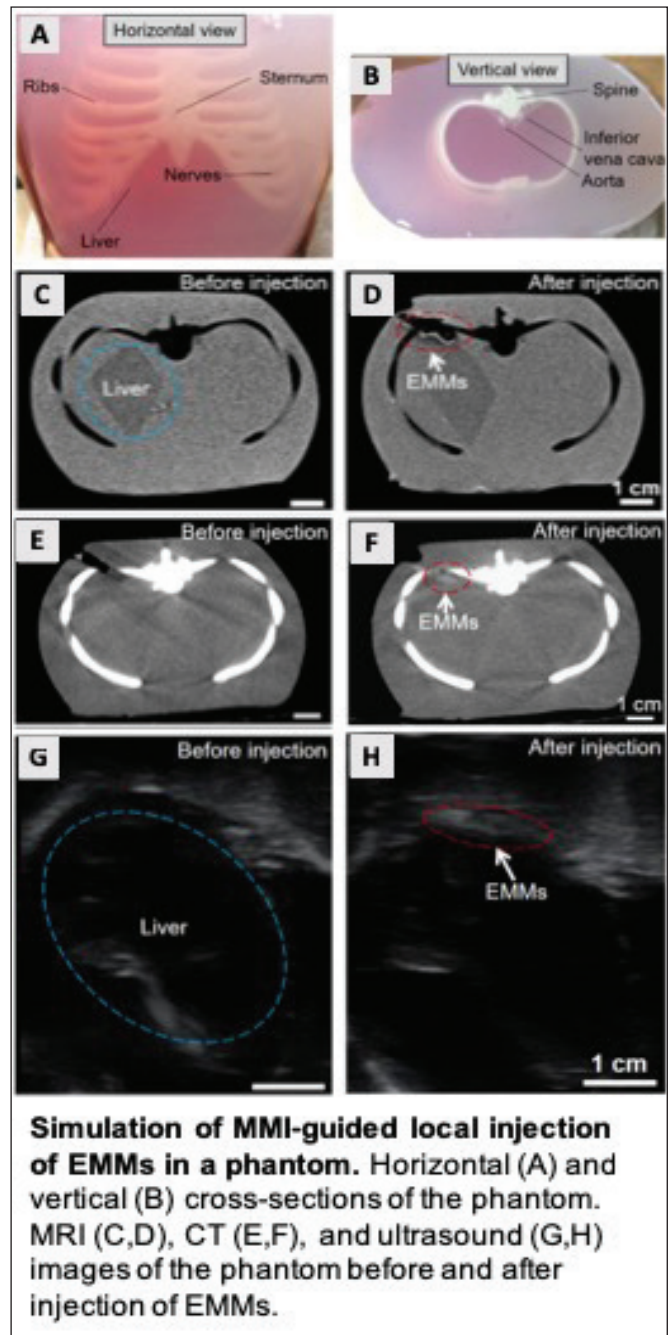


P2-065

Novel Concepts in Theranostics: Magnetic Nanoparticle Embedding Within Ultrasound Contrast Drug Carriers Allows Guidance by Multi-modality Imaging

Wenwei Huang¹, Lanxi Chen¹, Christie Boswell-Patterson², Junyun Tang¹, Yan Li¹, Jianhua Zhou¹, Amer Johri². ¹Sun Yat-sen University, Guangzhou, China; ²Cardiovascular Imaging Network at Queen's University, Kingston, ON, Canada

Background: Theranostic use of contrast enhanced ultrasound can both guide drug delivery and control the rate of drug release. Previously we reported on the creation of a novel ultrasonic contrast agent consisting of an eccentric aqueous core and an elastic polydimethylsiloxane (PDMS) shell. We demonstrated that these microcapsules could be loaded with drug and then stimulated with external ultrasonic stimuli to 'burst' and release drug at a specific site, in a controlled manner. However, accurate localization of such ultrasound agents remains a challenge if echogenicity is identical to surrounding tissue. To investigate the use of complementary multi-modality imaging (MMI) to solve this problem, we embedded magnetic nanoparticles within the PDMS shell, making eccentric magnetic microcapsules (EMMs). Our **objective** was to determine whether magnetic EMMs could be accurately and simultaneously visualized by ultrasound, magnetic resonance imaging (MRI) and computed tomography (CT). **Methods:** EMMs were prepared on a three-phase microfluidic device. The morphology and structure of the EMMs were confirmed by scanning electron microscopy (SEM, JSM-6010LA). MRI (Siemens), CT (GE Healthcare) and ultrasound (Mindray) were used to visualize the EMs. To simulate MMI-guided local injection of the EMMs, we prepared a phantom consisting of: agarose to mimic liver and soft tissue, a skeletal model to mimic bone, and PVC to mimic vessels. We then imaged the EMMs using all 3 modalities following their injection into the phantom. **Results:** After injection, the EMMs were successfully visualized by MRI, CT, and ultrasound (Figure 1). However, it remained difficult to distinguish the magnetic EMs from bony tissue using MRI, from the soft tissues in CT images, and from the surrounding sham tissues under ultrasound, likely due to artifact. Nevertheless, the integration of MRI, CT and ultrasound, allowed us to track EMMs during injection more precisely than could have been accomplished by one modality alone. **Conclusions:** Our findings suggest the potential for ultrasonic theranostic agent guidance by MMI. Further work is required to assess toxicity and clearance of such modified particles, however our study provides an important proof-of-concept for drug carrier guidance and delivery enhanced by multi-modality imaging.



P2-066

Moderated Poster

High-Definition Blood Flow Imaging in Assessment of Left Ventricular Function: Comparisons with Cardiac Magnetic Resonance Imaging and Contrast Echocardiography

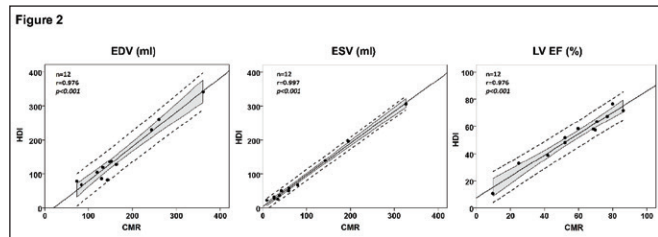
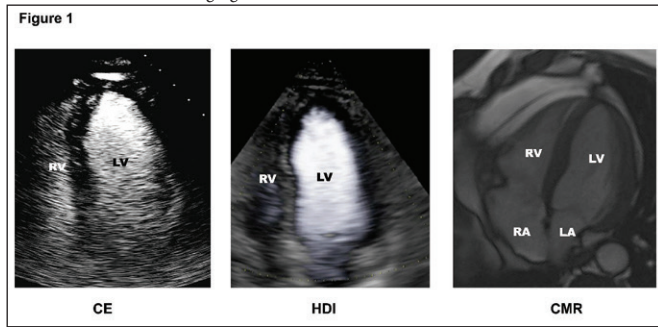
Masood Ahmad, Geru Wu, Luba Frank, Tianrong Xie, Meneleo M. Dimaano. University of Texas, Galveston, TX

Background: We recently reported the efficacy of High-Definition blood flow imaging (HDI-Arietta 70, Hitachi Healthcare) in assessment of left ventricular (LV) volumes/function and demonstrated the results are comparable to those obtained by contrast echocardiography (CE). The present study further validated the HDI technique in assessment of LV function by simultaneous comparisons with CE and Cardiac Magnetic Resonance imaging (CMR). **Methods:** Twelve patients (age range 25-79 yrs.) with limited baseline echocardiographic images had measurements of LV end diastolic volume (EDV, ml), end systolic volume (ESV, ml), and ejection fraction (EF, %) by CE, HDI, and CMR. (Figure 1, 4 chamber views by CE, HDI, and CMR, LV=left ventricle, RV=right ventricle, LA=left atrium, RA=right atrium). **Results:** Measurements of EDV, ESV, and EF correlated well by the three imaging techniques with correlation coefficients (r) ranging

Poster Session 2 (P2)

Monday, June 24, 2019

from 0.97 to 0.99 in comparisons between HDI and CMR (Figure 2), and from 0.94 to 0.96 in comparisons between CE and CMR. The limits of agreement for the inter-methods comparisons by Bland-Altman analysis (mean \pm 1.96 SD) between HDI and CMR for LVEF, EDV, and ESV were $5.02 \pm 12.5\%$, 19.87 ± 36.4 ml and 2.51 ± 17.21 ml respectively, and between CE and CMR, $1.91 \pm 11.92\%$, 22.48 ± 53.84 ml, and 9 ± 46.55 ml respectively. **Conclusions:** Assessment of LV size and function by High-Definition Blood Flow imaging correlated well with CMR. Using CMR as the gold standard, the agreements in measurements of LV volumes were slightly superior for High-Definition Blood Flow imaging compared to contrast echocardiography. In measurements of LV ejection fraction, contrast echocardiography showed slightly less mean difference when compared to High-Definition Blood Flow imaging.

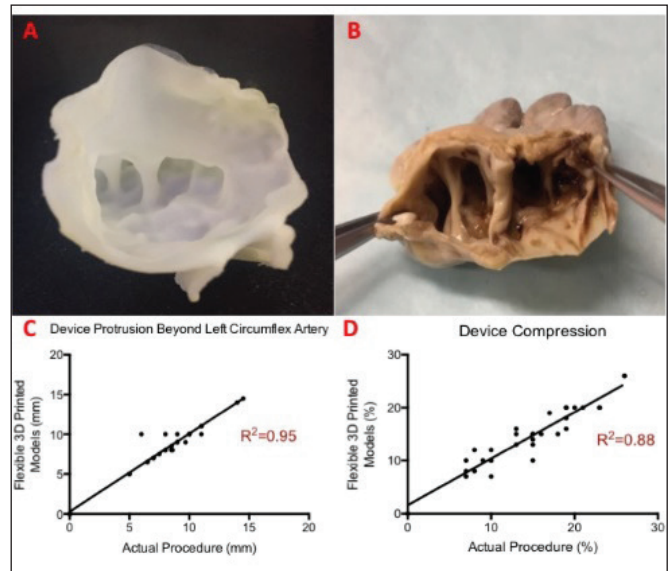


P2-067

Echocardiography-Based Three-Dimensional Printing for Sizing and Positioning of Percutaneous Left Atrial Appendage Occluder Device

Yiting Fan¹, Martin Leong^{1,2}, Marco Chow^{1,2}, Ka-Wai Kwok², Alex P. Lee¹.
¹Prince of Wales Hospital, The Chinese University of Hong Kong, Hong Kong, China; ²Mechanical Engineering, University of Hong Kong, Hong Kong, China

Background: Accurate sizing and positioning of percutaneous left atrial appendage (LAA) occlusion (LAAO) device underscores the importance of understanding LAA anatomy and tissue-device interaction. 3D printing using tissue-mimicking materials allows creation of patient-specific models for simulation of interventional procedure. We aim to evaluate the accuracy of LAAO device sizing and positioning on 3D-printed LAA models. **Methods:** 3D transesophageal echocardiography (TEE) datasets of 57 patients (age=72 \pm 9, 39 men) undergoing LAAO [WATCHMAN (n=32); Amulet device (n=25)] were converted to physical LAA models by 3D printing (Connex 3; Stratasys) using flexible materials (Agilus Clear; Stratasys). Device size, position, and compression on the printed models were compared with that observed in the actual procedure. **Results:** 3D printing was feasible in all subjects. The maximal (24.2 \pm 3.3mm vs. 23.9 \pm 3.3mm), minimal LAA orifice diameters (19.4 \pm 4.4mm vs. 19.2 \pm 3.2mm), and LAA depth (27.7 \pm 6.4mm vs. 27.1 \pm 6.1mm) were similar when measured on 3D datasets and printed models (all p=NS). Printed models recreated pectinate muscles of surgical specimens accurately (Fig. A & B). Device testing accurately determined optimal device size in all patients (100%), in contrast to only 71% by 3D TEE (p<0.05). Device shoulder protrusion beyond LAA ostium (r²=0.95) and device compression (r²=0.88) in the simulated procedure correlated closely with the actual procedure (both p=NS) (Fig. C & D). **Conclusion:** Echocardiography-derived 3D printed models provides incremental information on LAA anatomy and tissue-device interaction that may allow more accurate device sizing and positioning than conventional 2D/3D imaging guidance.



P2-068

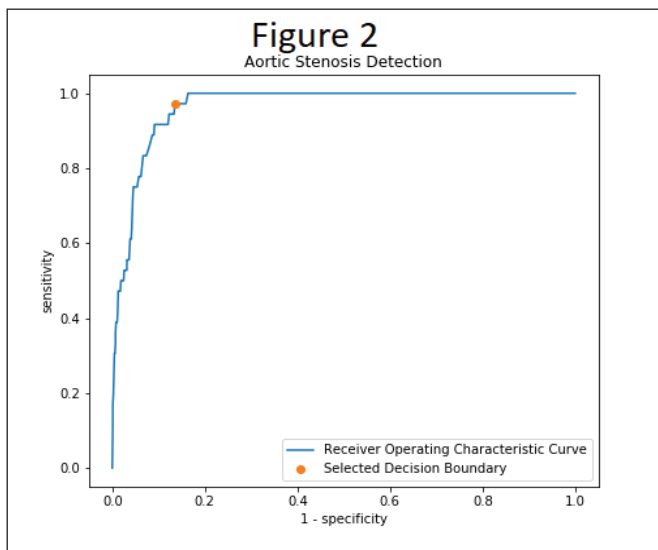
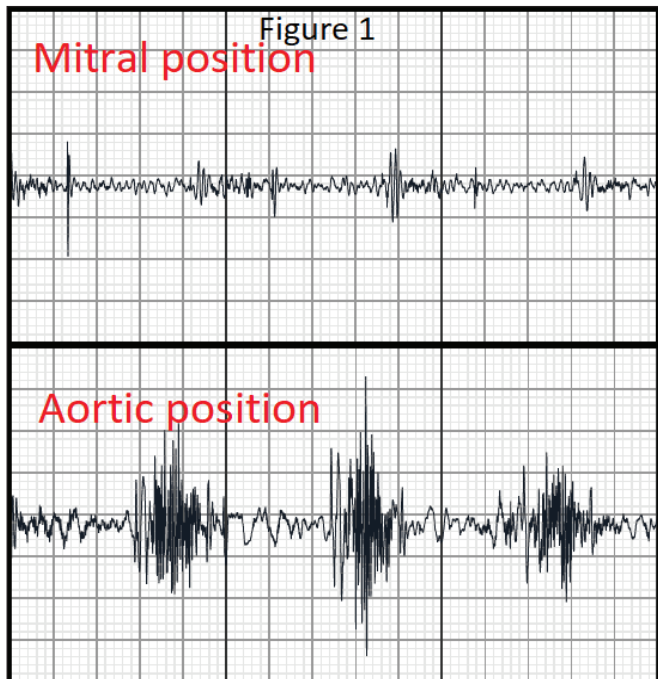
Handheld Wireless Digital Phonocardiography for Machine Learning-Based Detection of Aortic Stenosis

Brent E. White¹, Jason H. Paek¹, Steve L. Pham², John Maidens², Patrick M. McCarthy¹, James D. Thomas¹. ¹Northwestern Memorial Hospital, Chicago, IL; ²Eko Devices, Inc., Berkeley, CA

Background: Aortic stenosis (AS) is a common disease which can be detected as a murmur on auscultation, but studies show that up to 80% of new primary care physicians do not detect AS murmurs which are confirmed by transthoracic echocardiography (TTE). The FDA-approved Eko CORE device is a digital stethoscope wirelessly paired with the Eko Mobile application to allow recording and analysis of phonocardiograms (PCG). These PCG data drive a machine learning-based detection algorithm to identify clinically significant AS, validated by TTE, as part of the ongoing Phono- and Electrocardiogram Assisted Detection of Valvular Disease (PEA-Valve) Study. **Methods:** Patients undergoing TTE at Northwestern Medicine underwent PCG recording by the Eko CORE device. Recordings 15 seconds long were obtained at four standard auscultation positions. A TensorFlow-based machine learning algorithm assessed the presence or absence of murmur with dominant localization to the right upper sternal border indicating clinically significant AS, defined as moderate or greater on TTE (Figure 1). **Results:** To date, 161 patients with 639 recordings have been enrolled, with 14 patients (8.7%) found to have significant AS on TTE. The receiver-operating characteristic curve had an area of 0.964, yielding a sensitivity of 97.2% (95% CI, 84.7-99.5%) and a specificity of 86.4% (95% CI, 84.0-88.7%) for the detection of AS (Figure 2). **Conclusion:** PCG assessment using the Eko CORE device and machine learning interpretation is a fast and effective method to screen for significant AS and should be validated in a primary care setting, which may lead to more appropriate referrals for echo.

Poster Session 2 (P2)

Monday, June 24, 2019



P2-069
Planning Structural Heart Interventions: Comparison of Measurements Made on Volume Rendered 3D Virtual Reality Models Versus Conventional 3D Software

Niklas Hitschrich¹, Akhil Narang², Georg Schummers¹, Karima Addetia³, David Hitschrich¹, Victor Mor-Avi³, Bernhard Mumm¹, Roberto M. Lang³.
¹TOMTEC, Unterschleissheim, Germany; ²Northwestern University, Chicago, IL; ³University of Chicago, Chicago, IL

Background: Accurate measurements of cardiac structures, particularly valves, are critical for planning valvular interventions. Three-dimensional echocardiography (3DE) is time consuming because measurements require expertise with multiplanar reconstruction (MPR) to manipulate 3D datasets and knowledge of specialized software. We have developed a workflow to create dynamic, volume rendered virtual reality (VR) models from 3DE datasets and a VR environment that enables intuitive manipulation and measurements of cardiac structures while reducing the need for prior experience. The purpose of this study was to compare the time, accuracy and variability of measurements made with conventional software (TOMTEC 4D Cardio-View™) to those made on VR models in the VR environment. **Methods:** Datasets from 30 patients who underwent a clinical 3D transesophageal echocardiogram (TEE) to evaluate aortic valve (AV) or mitral valve (MV) pathology were used in this study (15 datasets each). Each dataset was converted into a 3D VR model using the novel algorithm. Blinded measurements independently performed

by three users (ranging from novice to experienced) were made using conventional MPR and the custom VR environment using headsets and hand controllers. Common clinical measurements of the AV (left ventricular outflow tract (LVOT) diameter, AV area) and MV (anterior-posterior (A-P) and anteromedial-posterolateral (AM-PL) diameters and MV annular circumference) were performed. **Results:** All (30/30) TEE datasets were successfully converted and loaded into the novel VR environment in under 2 minutes. Measurements made in VR of all AV and MV parameters had lower variability than the same measurements performed using conventional software (Table). Furthermore, the times required to perform measurements in VR was shorter than the times using conventional software (Table). **Conclusion:** This is the first study to demonstrate that measurements made on VR models obtained from 3DE datasets have lower variability and are faster than those made using conventional methodology. Using a VR environment to analyze and measure 3DE-based models is a promising new tool to plan and guide structural interventions that offers the advantage of true 3D visualization and interaction.

Intraobserver Variability n = 15 for each measurement		4D CARDIO-VIEW™ Bias ± LOA (%)	Virtual Reality Bias ± LOA (%)
MV	A-P Diameter (cm)	1.4 ± 13.4	-0.7 ± 9.3
	AL-PM Diameter (cm)	3.0 ± 17.0	0.3 ± 9.2
	Annul Circumference (cm)	-0.1 ± 13.4	-2.4 ± 8.0
	Annular Area (cm ²)	-0.1 ± 23.8	-4.0 ± 16.7
AV	LVOT Diameter (cm)	-0.1 ± 16.1	-0.8 ± 8.5
	Area Circumference (cm)	-3.4 ± 8.3	0.8 ± 8.6
	Area (cm ²)	-7.0 ± 14.6	0.4 ± 14.1

Mean Measurement Time Each MV: n = 135 (VR) Each AV: n = 105 (VR) n = 45 (CV) n = 30 (CV)		4D CARDIO-VIEW™ Mean Time (s)	Virtual Reality Mean Time (s)
MV	A-P Diameter (cm)	96.4	48.1
	AL-PM Diameter (cm)	32.7	18.9
	Annulus Circumference (cm)	77.0	65.1
	Annular Area (cm ²)	77.0	65.1
AV	LVOT Diameter (cm)	75.6	83.5
	Area Circumference (cm)	80.8	69.3
	Area (cm ²)	80.8	69.3

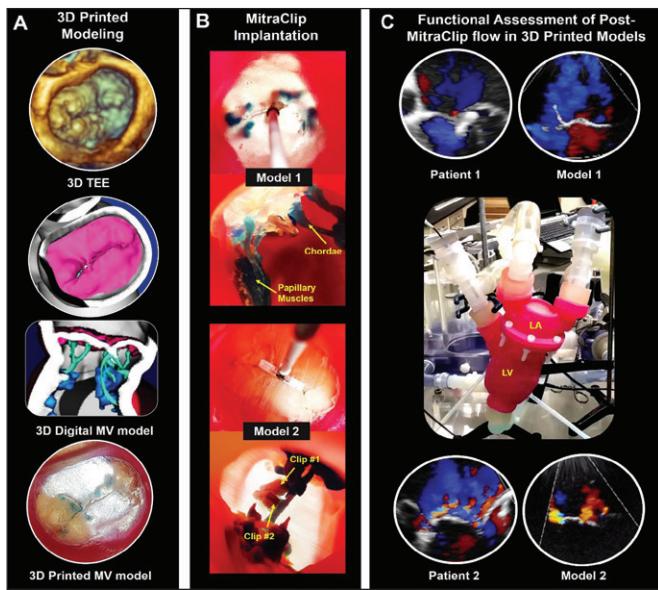
P2-070
Functional 3D Printed Modeling of the Mitral Apparatus for MitraClip Intervention

Marija Vukicevic¹, Kinan Carlos El-Tallawi¹, Clara I. Angulo¹, Stefano Filippini¹, Eleonora Avenatti², Colin M. Barker¹, Stephen H. Little¹.
¹Houston Methodist Hospital, Houston, TX; ²Cardiovascular Research Foundation, New York, NY

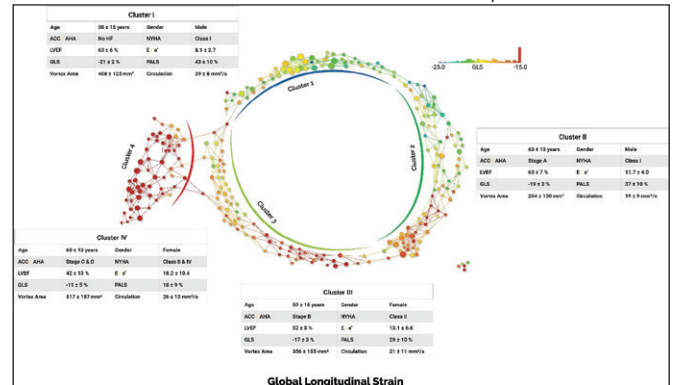
Background: The MitraClip procedure is a catheter-based treatment for patients with severe mitral regurgitation (MR) and prohibitive surgical risks. The evaluation of multi-jet residual MR after MitraClip can be challenging. We sought to test if 3D printed models could be useful tools for the assessment of post-MitraClip hemodynamic conditions. **Methods:** En-face and long-axis 3D transesophageal echocardiographic (TEE) imaging datasets (systole) were used for the reconstruction of five patient-specific MV apparatus models. MitraClip devices were implanted in all five multi-material 3D printed MV models and each post-MitraClip construct was coupled into a flow loop and subjected to the patient-specific systolic hemodynamic condition. Post-MitraClip geometry and residual MR was evaluated using echocardiographic imaging and standard flow measurements. **Results:** Five functional patient-specific, multi-material 3D printed models of the MV apparatus and left ventricle (LV), including chordae, papillary muscles and left ventricle outflow tract were generated using a co-registration technique (Figure A). Each anatomical element was printed of different materials with appropriate mechanical properties suitable to mimic native valve tissue behavior. Selected 3D print materials for the leaflets and chordae were flexible enough for implantation of MitraClip devices as demonstrated in two specific patients (Figure B). Color Doppler images captured from models compared favorably to actual patient post-MitraClip implantation images (Figure C). Residual MR in the models with single or multiple MitraClip devices was quantified. The measurements showed a significant reduction of MR (up to 77%) within the tested models. This finding corresponded well to the actual MR reduction observed in the patients (Figure C). **Conclusion:** Functional MV apparatus models can be accurately reconstructed using 3D echocardiographic images. 3D printed models can be used for the benchtop implantation of MitraClip devices and resemble the clinical deployment. When subjected to patient-specific hemodynamic conditions, 3D printed models with implanted MitraClip devices are suitable for mimicking the realistic residual MR found in specific patients and allow for the in vitro assessment of MR after MitraClip deployment.

Poster Session 2 (P2)

Monday, June 24, 2019



the value of a novel patient similarity network using topological data analysis (TDA) for integrating multidimensional echocardiographic data to identify relatively homogenous patient subgroups with similar clinical presentations. **Methods:** Total 297 patients (55.4 ± 17.4 years) underwent conventional two-dimensional (2-D) echocardiography and Doppler-based measurements enriched with 2D speckle tracking and vector flow mapping for integrating multiple parameters of left ventricular (LV) structure and function. Total forty two echocardiographic variables were integrated to create similarity networks using TDA. The patient groups were compared for clinical stages of cardiac disease and occurrence of short-term major adverse cardiac and cerebrovascular events (MACCE). **Results:** The TDA model integrated multiple echocardiographic variables and resulted into the formation of a loop with continuous changes in LV geometry and function. After defining four clusters in the TDA model (I-IV), patients in each cluster showed distinctive clinical presentation based on ACC/AHA heart failure stage and occurrence of MACCE. In particular, cluster IV had higher prevalence of stage C heart failure [KNI] (59%, p<0.001) and NYHA III or IV (61%, p<0.001), higher incidence of MACCE (p<0.001) compared to patients in the remaining three clusters. **Conclusion:** TDA can fuse multidimensional parameters of echocardiography for identifying distinct cardiac phenogroups in terms of clinical characteristics, cardiac structure and function, hemodynamics and outcomes.



P2-071

Improving the Efficiency of Healthcare Delivery with Digital Health Technologies in the ASE Foundation Community Health Outreach Imaging and Cardiovascular Examinations (CHOICE) Program: A Cluster Randomized Trial

Sirish Shrestha¹, Sanjeev Bhavnani², Grace Casacalang-Verzosa¹, Muhammad Khalil¹, Ritu Thamman³, Jay Patel¹, Anand Desai¹, Rohan Shah¹, Lan Hu¹, Marco Piccirilli¹, Muhammad Ashraf¹, Partho P. Sengupta¹. ¹West Virginia University Hospitals, Morgantown, WV; ²Scripps Clinic, San Diego, CA; ³University of Pittsburgh School of Medicine, Pittsburgh, PA

Background: Screening for acute and chronic diseases with new digital health technologies represent promising methods to diagnose common cardiac diseases in resource-limited areas; however, the impact of technology-based care on provider referral and downstream testing has not been rigorously evaluated. We compared conventional clinical assessment with technology-first assessments used as clinical decision-support tools to understand the incremental value of digital health devices in clinical diagnoses, referrals, resource utilization, and perceived quality of care. **Method:** Patients were enrolled in a cluster randomized study at 4 cardiac outreach centers randomized to either standard care or to digital health assessments. Psychological well-being, lifestyles and habits, risk factors, and user experiences were measured using onsite and follow-up surveys. In the technology arm, point of care tests included smartphone enabled pocket ultrasound and electrocardiogram, and wireless connected vital sign devices were provided at the patient visit. **Results:** Total 374 individuals (median age: 61 [21 - 85] years) were enrolled, with patients stratified to standard-of-care arm (n = 187) and technology-enabled care (n = 187). Compared to standard-care, treating physicians using digital health devices at the point-of-care demonstrated greater diagnostic certainty for conditions including myocardial ischemia (24 % vs 13%, p = 0.030), heart failure (17% vs 3%, p < 0.001), atrial fibrillation (15% vs 3%, p < 0.001), and pulmonary embolism (3% vs 0%, p = 0.012). Significantly more number of patients in the technology-arm were recommended for appropriate testing (20% vs 8%, p = 0.002) and follow-up visits (27% vs 15%, p = 0.011). Although there were no significant differences in patient's experience between the groups, patients in the technology arm expressed greater confidence when physicians explained and discussed their results with them (98% vs 72%, p < 0.001). **Conclusions:** An intervention of technology-enabled care with digital health devices used at the point-of-care in ambulatory settings improves physician diagnostic certainty for clinical decision making. This may prove to be an effective strategy to reduce the number of downstream tests and referrals in resource constrained environments.

P2-072

Network Tomography for Integrating Features and Similarities of Multiparametric Echocardiographic Data

Cho Jung Sun^{1,2}, Sirish Shrestha², Muhammad Ashraf¹, Nobuyuki Kagiyama², Yasir Abdul Ghaffar², Irfan Zeb², Partho P. Sengupta². ¹Daejeon St. Mary Hospital, Dae-jeon, Republic of Korea; ²West Virginia University Heart & Vascular Institute, Morgantown, WV

Background: Network-based approaches for precision medicine take advantage of computational methods that support integration of heterogeneous data to support clustering and subgroup identification, eventually leading to tailored therapies. We assessed

P2-073

Association of LA Reservoir Strain and ATTR Cardiomyopathy in Patients with LV Hypertrophy

Andrea C. Furlani, Waddy Gonzalez, Faraj Kargoli, Mohammed Makkiya, Mark Travin, Cynthia C. Taub. Montefiore Medical Center, Bronx, NY

Background: The cardiac involvement of transthyretin-related amyloidosis (ATTR) is associated with atrial (especially interatrial septum) and ventricular amyloid deposits, often leading to decreased left ventricular (LV) function and increased left atrial (LA) pressure. We aim to evaluate the left atrial strain in patients with suspected TTR cardiac amyloidosis and its association with the diagnosis. We hypothesized that atrial amyloid deposits in ATTR patients would lead to greater impairment of LA strain when compared to other causes of LV hypertrophy. **Methods:** LA and LV strain were retrospectively analyzed by echocardiography (Tom Tec Imaging systems, Germany) from a cohort of LV hypertrophy and heart failure patients (n=61), who underwent technetium 99m-pyrophosphate (Tc-PYP) nuclear scintigraphy due to suspicion for ATTR cardiomyopathy. Furthermore, the cohort was divided into two groups based on their nuclear test results. Apical 4 and 2 chamber views were used for assessment of atrial global longitudinal strain (LAGLS), measured at the end of the reservoir phase. Apical 4, 2 and 3 chamber views were used for left ventricula global longitudinal strain (LVGLS) analysis. Continuous and categorical data are presented as means and frequencies, respectively. Comparisons between means were performed using student t-test. Categorical data were compared with Fisher Exact test. **Results:** There were 29 patients with positive 99m Tc-PYP test (n=29) vs. 32 with negative test. Baseline characteristics were different between groups (Table), being LAGLS impaired in all patients. LV end-diastolic volume (LVEDV) and LV ejection fraction (LVEF) were significantly smaller on the amyloid group. In our fully adjusted model (LVEF, LVGLS, gender, age and atrial fibrillation), we found significant difference in the interatrial septal strain between groups. **Conclusion:** Interatrial longitudinal septal strain is significantly lower in patients with positive (Tc-PYP) nuclear scintigraphy compared with those with negative study. This data suggests that amyloid deposits indeed cause localized impairment of LA mechanics. Although reduced LA reservoir strain (LAGLS) is associated with ATTR cardiomyopathy in patients with LV hypertrophy and heart failure, this parameter is essentially dependent on the LV function.

Poster Session 2 (P2)

Monday, June 24, 2019

Tc-PYP nuclear scintigraphy				
Demographics	total	-	+	p Value
Age, mean (years)	74 ± 11	69±11	80±7	<0.0001
Gender				
Female, n (%)		14 (44)	8 (28)	0.1892
AFib, n (%)		21 (66)	16 (55)	0.404
Echocardiography				
LVEDV	114 ± 44	131 ± 49	96 ± 31	0.0016
LVESV	65 ± 35	72 ± 40	59 ± 26	0.1515
LVEF (%)	44 ± 14	48 ± 14	40 ± 12	0.017
LVGLS	-11 ± 5	-13 ± 5	-7.9 ± 3.4	0.0002
LAGLS	13 ± 8	16 ± 10	10 ± 6	0.0112
IALS	10 ± 7	13 ± 8	6 ± 4.8	0.0001

AFib = atrial fibrillation; LVEDV = left ventricular end-diastolic volume; LVESV = left ventricular end-systolic volume; LVEF = left ventricular ejection fraction; LVGLS = left ventricular global longitudinal strain; LAGLS = left atrial global longitudinal strain; IALS = interatrial septal longitudinal strain.

P2-074

Validation of Acoustoelectric Cardiac Imaging in Swine Model: Toward Real-time, High Resolution Electroanatomic Mapping in Humans

Alexander Alvarez, Cameron Wilhite, Chet Preston, Andres Barragan, Russell S. Witte. University of Arizona, Tucson, AZ

Background: Arrhythmias account for high morbidity and mortality in the United States. While electrocardiography (ECG) can diagnose arrhythmias, it lacks spatial resolution to delineate local arrhythmias like reentry circuits. Acoustoelectric Cardiac Imaging (ACI) is a novel electroanatomic mapping (EAM) technology with submillimeter resolution, allowing for identification of abnormalities undetectable on ECG. ACI, based on the acoustoelectric (AE) effect, combines ultrasound (US) with recording electrodes to detect interaction signals proportional to local cardiac currents. 3D images over time can be generated by electronically steering the US beam in the heart. ACI may also be combined with pulse echo US to reveal cardiac anatomy. The goal of this study was to validate ACI in a large animal model by demonstrating accurate mapping of the cardiac activation wave. **Methods:** An open-chest swine model (n=6) was used. After thoracotomy, a twenty-electrode EAM lasso catheter or sixteen-electrode surface grid array (4mm spacing) was placed on ventricular epicardium to record both low frequency ($\leq 10\text{ kHz}$) electrograms and high frequency ($\geq 100\text{ kHz}$) AE potentials. One of two US probes - a 2.5 MHz linear array (Philips P4-1) or custom 0.6 MHz 2D matrix array - were placed above the electrodes and acoustically coupled to the ventricle. US was pulsed at 6 kHz while scanning the beam, and AE signals detected on the electrodes were amplified, filtered, digitized, and processed to produce activation wave images. Pulse echo US was also collected to identify cardiac structures and motion. **Results:** As seen in the figure, preliminary data suggests that electrophysiology maps obtained with the surface grid array on the right ventricle demonstrate propagation of cardiac depolarization and repolarization after apical pacing. In addition, in multiple beam positions, M-mode AE images demonstrate signals at ~60mm (in the myocardium) that are time-locked with the peak of low frequency electrograms with an SNR greater than 1. **Conclusion:** This work provided initial validation of ACI as a technique that can detect cardiac activation in an *in vivo* large animal model with sub-millimeter resolution. As such, ACI has potential to serve as a noninvasive, high resolution modality for mapping reentry circuits.

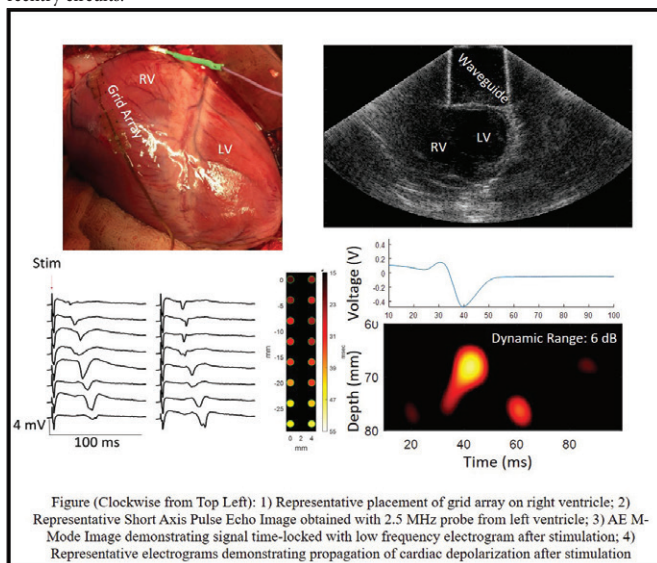


Figure (Clockwise from Top Left): 1) Representative placement of grid array on right ventricle; 2) Representative Short Axis Pulse Echo Image obtained with 2.5 MHz probe from left ventricle; 3) AE M-Mode Image demonstrating signal time-locked with low frequency electrogram after stimulation; 4) Representative electrograms demonstrating propagation of cardiac depolarization after stimulation

P2-075

Efficient and Effective Left Atrial Appendage Evaluation Using the MicroTEE Transducer

Alberta H. Yen, Cindy Wang, David H. Liang. Stanford University, Stanford, CA

Background: Transesophageal echocardiography (TEE) is the modality of choice for evaluation of the left atrial appendage (LAA) for thrombus. These procedures are usually performed under moderate sedation prior to elective procedures such as atrial fibrillation ablation, however sedation poses the risk of circulatory and respiratory complications requiring post-procedural monitoring which limits TEE exams and utilizes nursing resources. A smaller transducer with comparable image quality could allow for studies without moderate sedation, less patient discomfort, and quicker procedure times to create a more efficient lab. **Methods:** Focused LAA studies were performed in eligible patients undergoing elective atrial fibrillation ablation or LAA occlusion (Watchman) procedures using a Philips EPIQ ultrasound machine and the S8-3t MicroTEE transducer (Philips, Andover, MA), a miniaturized multiplane transducer measuring 7.5 x 5.5 mm at the tip and 5.2 mm in diameter in the shaft. All examinations were assessed for procedural success, image quality, and study duration, measured as time from patient consent to discharge from the lab. To determine feasibility and efficiency of a no-sedation protocol, a subset of 32 patients was consented to undergo TEE evaluation with topical application of 2% viscous lidocaine to the oropharynx. These patients were assessed for procedural discomfort (scale 0-10) and desire to undergo a no-sedation MicroTEE procedure in the future. **Results:** 45 patients (mean age 67 years, range 43-89) had a LAA evaluation using the MicroTEE transducer. 95.6% of studies were successful, resulting in interpretable and sufficient image quality to evaluate for thrombus. The two failed studies were due to failure to intubate with excessive gag reflex. Thrombus was identified in two patients. Patients rated an average discomfort level of 2.3 out of 10. Study time was significantly reduced in patients not receiving sedation (average 24.8 minutes compared to 78.6 minutes in patients receiving sedation, $P < 3 \times 10^{-6}$). **Conclusion:** Focused LAA studies can be successfully and efficiently performed without moderate sedation using a MicroTEE transducer, producing sufficient image quality to evaluate for thrombus and LAA function. Patients perceived the MicroTEE transducer and no-sedation protocol favorably and reported a low degree of discomfort. There was a significant reduction in study duration. The MicroTEE transducer may therefore be considered for use in focused LAA evaluations in a no-sedation protocol that is more time and resource efficient to the lab and minimizes patient discomfort.

P2-076

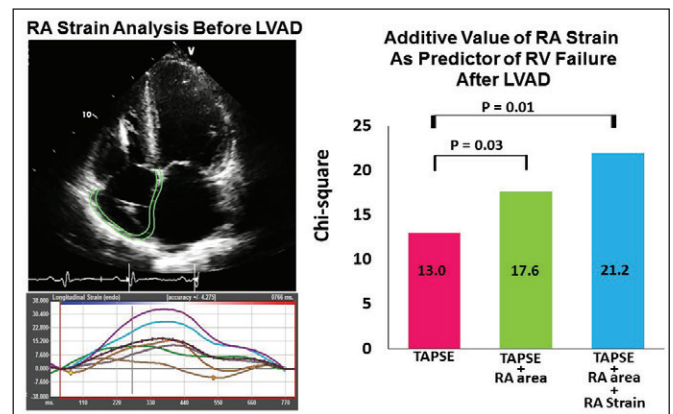
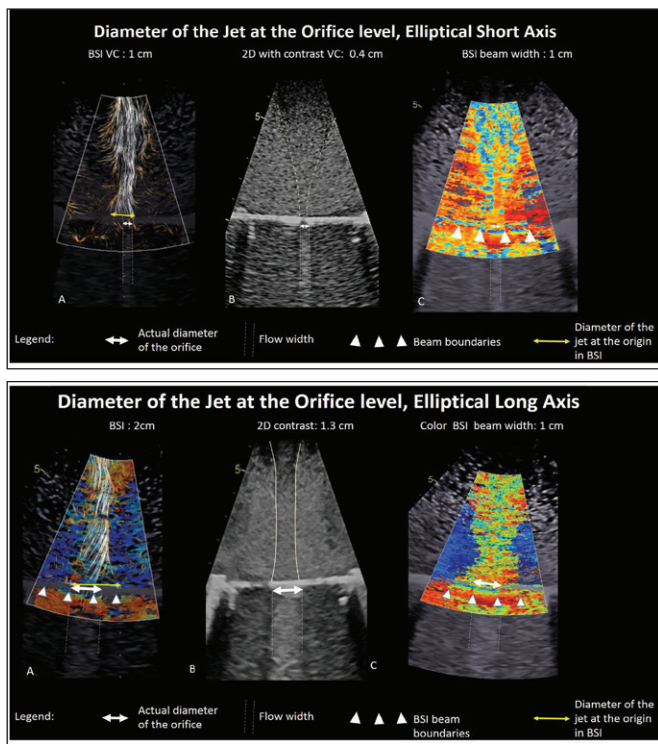
Vena Contracta by Blood Speckle Tracking Imaging, It is Ready for Clinical Use?

Nadia El Hangouche, Jeessoo Lee, Michael Markl, James Thomas. Northwestern Memorial Hospital, Chicago, IL

Background: Blood speckle tracking imaging (BSI) is an innovative technique that is based on tracking small clusters of blood cells to yield velocity in two dimensions. It requires a very high frame rate (400 to 600 fps) due to the high speed of the moving targets. Results are displayed as velocity vectors of the tracked blood speckles. We investigated the feasibility of using the velocity vectors obtained from BSI in order to measure the vena contracta of a flow through a known orifice. **Methods:** We measured vena contracta of the flow created by a hydrostatic flow generator using an elliptical orifice with known diameters (4 x 13 mm). The orifice was imaged in long and short axis in order to simulate two diameters. Fluid consisted of water and OPTISON™. We used a GE Vivid E95 echo machine and a pediatric probe (6s). We used 2D, color Doppler, and blood speckle tracking imaging to assess the diameter of the jet at the exit of the orifice. Flow velocities tested were: 1.7m/s, 2.6 m/s, 3.2m/s as measured by continuous Doppler. **Results:** BSI measured values of the orifice flow diameter predictably overestimated the known dimensions of the orifice, driven mainly by the width of the sparse ultrasound beams needed for the high frame rate (~14 pulses per frame each about 1cm wide at the orifice depth). If the orifice was intersected by 2 beams, as in figure 2, where the flow was imaged in the long axis of the ellipse, the VC by BSI was the additive diameter of the 2 beams. **Conclusion:** Blood speckle tracking imaging is a promising novel technology that enables visualization of the flow pattern by means of 2D velocity vectors. However the beam width artifact limits its use for vena contracta measurement.

Poster Session 2 (P2)

Monday, June 24, 2019



P2-077

Right Atrial Strain as Additive Predictor of Right Ventricular Failure After Left Ventricular Assist Device Implantation

Maria Karmpalioti, Yuko Soyama, David Raymer, Shane LaRue, Brittany Dixon, Akinobu Itoh, Justin Vader, John Gorcsan, III. Washington University in St. Louis, St Louis, MO

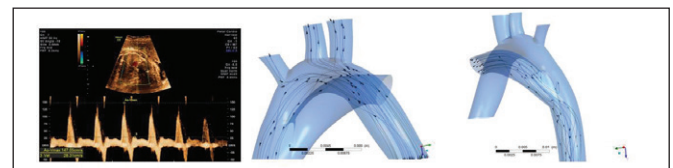
Background: Right ventricular (RV) failure after left ventricular assist device (LVAD) in patients with end stage heart failure (HF) is of significant clinical importance. Although various predictors of RV failure after LVAD have been attempted in the past, prediction of RV failure remains challenging. Our objective was to test the hypothesis that the new approach of right atrial (RA) strain imaging is additive to routine measures of tricuspid annular plane excursion (TAPSE) and RA area as predictors of RV failure post LVAD. **Methods:** We studied 214 HF patients aged 58 ± 10 yrs who received continuous-flow LVAD by baseline pre-operative echocardiography. RV failure after LVAD was defined as need for RV assist device (RVAD) or at least 14 days of inotropic therapy, as previously described. Maximal RA area and TAPSE were quantified from the apical 4-chamber view. RA peak global longitudinal strain (RAGLS) was determined from the apical 4-chamber view using speckle tracking echocardiography (TomTec, Corp.). **Results:** Of 214 LVAD patients, 74 (34%) had evidence of RV failure post operatively. Patients with RV failure as compared to others had significant lower TAPSE (12.7 ± 4.1 cm vs. 15.3 ± 4.4 cm, $p < 0.001$), and larger RA area (26.0 ± 7.3 cm² vs 22.9 ± 7.5 cm², $p=0.005$). RA strain was feasible in 176 (82%). Peak RA strain was also significantly lower in LVAD patients with subsequent RV failure: 10.3 ± 6.7 % vs 15.3 ± 9 %, $p < 0.001$. compared with the others. Using ROC analysis for RV failure, TAPSE had 51.3% sensitivity, and 73.6% specificity ($p < 0.001$, AUC=0.656), RA area had 74.6% sensitivity, and 51.9% specificity ($p = 0.001$, AUC=0.628) and peak RA strain had 66.7% sensitivity, and 63% specificity ($p < 0.001$, AUC=0.671), respectively. Using Chi-Squared analysis, RA strain was additive to TAPSE and RA area in predicting RV failure ($p=0.01$). **Conclusions:** RA strain, when feasible by speckle tracking echocardiography, was additive in being associated with RV failure in HF patients post LVAD and has promise for clinical usefulness.

P2-078

Retrograde Flow in Aortic Isthmus in Fetuses with Congenital Heart Defects and Computer Flow Dynamic Modeling

Zhuo Chen¹, Shen Lin², Amy Throckmorton³, Jiancheng Han¹, Yang Xu¹, Shuping Ge¹, Yihua He¹. ¹Beijing Anzhen Hospital, Beijing, China; ²Shenzhen Second People's Hospital, Shenzhen, China; ³BioCirc Research Laboratory, School of Biomedical Engineering, Science and Health Systems, Drexel University, Philadelphia, PA; ⁴The Heart Center, St. Christopher's Hospital for Children/Drexel University College of Medicine, Philadelphia, PA

Background and Objectives: Retrograde flow (RF) in the aortic isthmus is frequently observed in fetuses in various hemodynamic states including congenital heart defects (CHD). This study sought to: 1) establish the association between this observation and variables of CHD by fetal echocardiography (FE); and 2) to computer flow dynamic (CFD) model to probe the causes and mechanisms underlying this observation. **Methods:** A total of 256 (gestational age (GA) 26.3 ± 9.8 weeks) fetuses with CHD and 168 (GA: 25.8 ± 10.3 weeks) with normal FE were examined from January, 2011 to May, 2016. The study group was divided into: 1) no RF, 2) end systolic RF, end diastolic RF, systolic RF, diastolic RF, and systolic and diastolic RF sub-groups (Figure A). GA, cerebroplacental ratio (CPR) of pulsatility index (PI) in middle cerebral and umbilical arteries, cardiothoracic area ratio (CTR), left and right atrial dimensions (LA/RA), left and right ventricular dimensions (LV/RV), aortic and pulmonary artery dimensions (AO/PA), and aortic isthmus and ductal arch dimensions (AI/DA), velocity ratio of aorta and pulmonary artery (AO/Pav), aortic isthmus and ductal arch in systolic (AI/DVs) and diastolic (AI/DVd). Using principal component analysis (PCA), the component score coefficient matrix and optional variance percent (OVP) was calculated by PCA and the RF pattern was simulated by CFD (Figure B). **Results:** RF modeling by CFD was feasible (Figure B). Component analysis by PCA showed that four types of variables were associated with RF: 1) Structural variables contribute 23.7% OVP, including LV/RV, LA/ RA, AO/PA, and IS/DA; 2) Resistance variables 16.8% OVP, i.e. CPR; 3) Growth variables 12.2% OVP, i.e. GA and CTR; and 4) Velocity variables 10.9% OVP, i.e. AO/Pav, AI/DVd. **Conclusions:** Retrograde flow in the aortic isthmus is associated with structural, resistance, growth, and velocity variables in fetal circulation in various CHD and normal 3rd trimester pregnancies. Simulation and modeling by CFD is feasible and may be useful to understand the causes and mechanisms of retrograde flow and its utility in diagnosis and prognosis in CHD.



P2-079

Experimental Study on the Accuracy of Ultrasonic-CT Multimodality Cardiac Image Fusion Technology

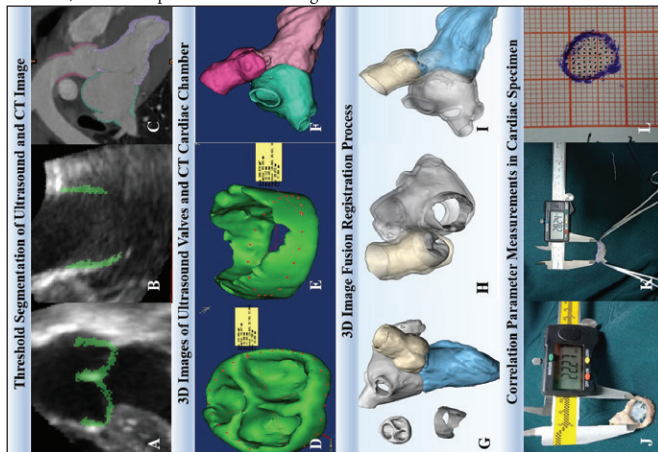
Sikai Chen, Qing Zhou, Yanxiang Zhou, Yuanting Yang. Renmin Hospital of Wuhan University, Wuhan, China

Background: To explore the feasibility of ultrasound-CT cardiac imaging fusion through animal experiments, to check the accuracy of image fusion image registration, and to provide data support for multimodal cardiac imaging fusion methodological research. **Methods:** Six male beagle dogs weighing 10.2 ± 0.3 kg. After the anesthesia of the experimental animals, cardiac CT enhancement images were acquired using a 256-row Revolution CT produced by GE. The thoracic surgery was performed at the animal surgery center, and the mitral and aortic valve volume images were collected from the surface

Poster Session 2 (P2)

Monday, June 24, 2019

of the heart using the GE Vivid E9 transesophageal 3D volume probe 6VT-D. Cardiac specimens were fixed using formalin and measured for relevant parameters. Ultrasound and CT images were subject to threshold segmentation and 3D reconstruction using Mimics 19.0 and 3-Matic 11.0 software, and the ultrasound valve images were registered to the corresponding positions of the CT heart chamber of registration point fusion to obtain a multimodal fusion heart image. Measurement parameters: AP, ALPM, circumference and area of mitral annulus, percentage of anterior and posterior valvular annulus, maximum diameter of anterior and posterior annulus to left ventricular apex; circumference and area of aortic annulus, three semilunar valves account for the percentage of the annulus, the maximum diameter of the AVO to the left ventricular apex, and the angle between the aortic valve and the mitral annulus. **Results:** There were no significant differences in the measurement parameters between the mitral annulus and the aortic annulus. The difference between the anterior and posterior mitral apical and left ventricular apex fusion images and specimens was 2.5 ± 0.7 mm, 2.2 ± 0.4 mm, 2.9 ± 0.8 mm. The difference between the aortic valve and the mitral annulus plane was $3.2 \pm 1.1^\circ$. **Conclusion:** Ultrasound-CT multimodal image fusion technology is feasible, and ultrasound valve image fusion registration is accurate, which can provide medical images with more clinical information.



P2-080

Tissue-Tracking Mitral Annular Displacement in Single Four-Chamber View Can be Used as a Simple Index of Left Ventricular Longitudinal Deformation

Takahiro Nishi, Takeshi Hozumi, Kazushi Takemoto, Teruaki Wada, Naoki Maniwa, Manabu Kashiwagi, Kumihiro Shimamura, Yasutsugu Shiono, Akio Kuroi, Yoshiki Matsuo, Hironori Kitabata, Yasushi Ino, Takashi Kubo, Atsushi Tanaka, Takashi Akasaka. Department of Cardiovascular Medicine, Wakayama Medical University, Wakayama, Japan

Background: Noninvasive assessment of left ventricular (LV) deformation using global longitudinal strain (GLS) has prognostic value in patients with and without preserved ejection fraction (EF). Application of speckle-tracking technology to the mitral annulus provides rapid and easy assessment of both septal and lateral mitral annular displacement (TMAD) and mid-point of mitral annular line in apical four-chamber view (AP4), which may be used as a simple index of LV deformation (Figure). Thus, we attempted to examine whether TMAD can be used as a simple index of LV longitudinal deformation in patients with and without preserved EF. **Methods:** The study population consists of 65 patients without segmental wall motion abnormality, significant valvular diseases, and arrhythmia in whom both TMAD and GLS were successfully measured. We estimated GLS from 3 apical views (AP4, apical 2-chamber and apical longitudinal views) and TMAD from AP4. TMAD was automatically and quickly evaluated as the base-to-apex displacement of septal (TMADsep), lateral (TMADlat), and mid-point of annular line (TMADmid) (Figure). The percentage of M-TMAD to LV length from the mid-point of mitral annulus to the apex at end-diastole (%TMADmid) was also calculated. We compared each TMAD values with GLS values by linear regression analysis, and analyzed TMAD values by ROC curve to detect decreased LV longitudinal deformation ($|GLS| < 12.0\%$). **Results:** There were good correlations between each TMAD index and $|GLS|$ values (TMADsep:r=0.79, TMADlat:r=0.83, TMADmid:r=0.84, %TMADmid:r=0.87). According to ROC curve, the best cut-off value for each TMAD index in determining LV longitudinal deformation was shown in Table. **Conclusions:** TMAD in only AP4 which is rapidly evaluated can be used as a simple index of LV longitudinal deformation.

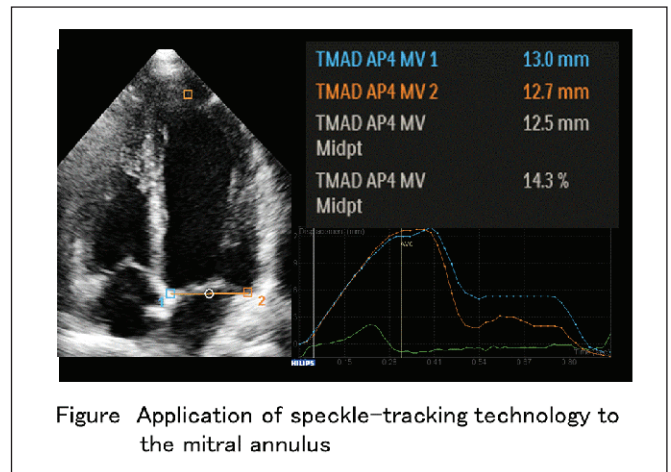


Figure Application of speckle-tracking technology to the mitral annulus

	sensitivity	specificity	cut-off value	AUC
TMADsep	0.8846	0.9211	6.4(mm)	0.9352
TMADlat	0.9231	0.7895	8.0(mm)	0.9378
TMADmid	0.9615	0.8158	7.8(mm)	0.9433
%TMADmid	1	0.8158	9.5(%)	0.9529

Table the sensitivity, specificity, cut-off value, and AUC for each TMAD index in determining LV longitudinal deformation

P2-081

Measurement of Ultrasound Induced Changes in Strain within Murine Myocardium Using Speckle Tracking Echocardiography

Ankur Chaudhury¹, Austin Wanek², Harpreet Singh³, Andrew Kohut⁴. ¹Drexel University College of Medicine, Philadelphia, PA; ²University of Cincinnati, Cincinnati, OH; ³Ohio State University Medical Center, Columbus, OH; ⁴University of Pennsylvania Health System, Philadelphia, PA

Background: Speckle tracking software is a powerful tool which enables the user to measure strain patterns using echocardiography images. We used the Vevo 2100 Imaging System (FUJIFILM VisualSonics) and VEVO Strain software (FUJIFILM VisualSonics) to acquire images, measure and analyze changes in strain patterns within the murine myocardium when subjected to high intensity focused ultrasound, an increasingly explored modality with a variety of potential medical applications. **Methods:** Ultrasound pulses were generated by amplifying an alternating voltage from a function generator into a custom 2.5MHz focused transducer able to generate pressures in excess of 800 kPa at its focal point. The probe surface was positioned 7.7cm from the left anterolateral chest wall, in a columned standoff filled with coupling gel. These pulses were targeted at the anterior surface of the left ventricle in 30 sedated mice. A microcontroller was used to synchronize the pulses to 3 different periods within the cardiac cycle - early, mid, and late diastole. Using speckle tracking software, echo images were analyzed to obtain global longitudinal strain (GLS) in the endocardial and epicardial regions. **Results:** Statistically significant ($p < 0.05$, two tailed t-test with equal variance) changes in GLS were observed in all three time periods. In the early diastolic group (n=6 native vs n=5 augmented beats), the anterior apical endocardium and anterior mid epicardium experienced significant increase in strain with ultrasound augmentation. In the mid diastolic group (n=13 native vs n=13 augmented), the anterior apical and posterior mid regions of the epicardium experienced significant strain increase. Finally, in the late diastolic group (n=9 native vs n=7 augmented), the anterior apical and anterior mid regions of the epicardium experienced significant strain increase. Although not significant, the regions adjacent to the apex showed a trend of increased strain in all three sets of experiments; conversely, the basilar region tended to experience a decrease in strain. **Conclusion:** Increases in GLS were significant and seen to be most prominent nearest to the apical region in all three sets of experiments. This observation, along with the trend of decreased strain in the basilar region, seem to indicate that when the ultrasound

Poster Session 2 (P2)

Monday, June 24, 2019

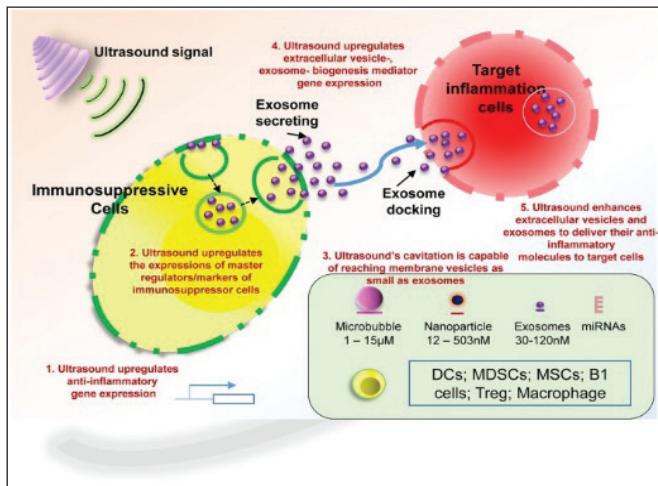
pulse strikes the anterior surface of the ventricle, it induces a torque like effect, with the apex acting as the hinge point. By our assessment, this is the first demonstration of ultrasound-induced augmentation in the global longitudinal strain (GLS) pattern of the left ventricle in a small animal model.

P2-082

Low-Intensity Ultrasound Sonoporation-Induced Cardiovascular Anti-Inflammatory Effects are Mediated by Several New Mechanisms Including Gene Induction, Immunosuppressor Cell Promotion, and Enhancement of Exosome Biogenesis and Docking

Qian Yang, Xijing Hospital, Xi'an, China

Background: Low-intensity ultrasound (LIUS) was shown to be beneficial in cardiovascular mitigating inflammation and facilitating tissue repair in various pathologies. Determination of the molecular mechanisms underlying the anti-inflammatory effects of LIUS allows to optimize this technique as a therapy for the treatment of malignancies and aseptic inflammatory disorders. **Methods:** We conducted cutting-edge database mining approaches to determine the anti-inflammatory mechanisms exerted by LIUS. **Results:** Our data revealed following interesting findings: (1) LIUS anti-inflammatory effects are mediated by upregulating anti-inflammatory gene expression; (2) LIUS induces the upregulation of the markers and master regulators of immunosuppressor cells including MDSCs (myeloid-derived suppressor cells), MSCs (mesenchymal stem cells), B1-B cells and Treg (regulatory T cells); (3) LIUS not only can be used as a therapeutic approach to deliver drugs packed in various structures such as nanobeads, nanospheres, polymer microspheres, and liposomes, but also can make use of natural membrane vesicles as small as exosomes derived from immunosuppressor cells as a novel mechanism to fulfill its anti-inflammatory effects; (4) LIUS upregulates the expression of extracellular vesicle/exosome biogenesis mediators and docking mediators; (5) Exosome-carried anti-inflammatory cytokines and anti-inflammatory microRNAs inhibit inflammation of target cells via multiple shared and specific pathways, suggesting exosome-mediated anti-inflammatory effect of LIUS feasible; and (6) LIUS-mediated physical effects on tissues may activate specific cellular sensors that activate downstream transcription factors and signaling pathways. **Conclusions:** Our results have provided novel insights into the mechanisms underlying anti-inflammatory effects of LIUS and have provided guidance for the development of future novel therapeutic LIUS for cardiovascular inflammatory disorders, tissue regeneration and tissue repair.



P2-083

Comparison of Synchrony and Deformation Between Left Bundle Branch Pacing and His Bundle Pacing Using Two-Dimensional Speckle Tracking Echocardiography

Y.F. Cheng, H.Y. Chen, M.R. Zhu, X.Y. Chen, Y.G. Su, Xianhong Shu, Zhongshan Hospital, Fudan University, Shanghai, China

Background: Although his bundle pacing (HBP) and Left bundle branch block (LBBB) can achieve physiological electrical activation of the ventricles. However, its effects on ventricular synchronism and contraction function remains unknown. The current study is aimed to compare the echocardiographic characteristics between HBP and LBBP. **Methods:** Forty-six pacing-indicated patients were prospectively enrolled. Twenty-nine patients underwent LBBP (17 male patients, 69.6±13.7yrs, LBBP group) and 17 patients underwent HBP (13 male patients, 70.4±14.7yrs, HBP group). LBBP was achieved by trans-septal method in the basal ventricular septum. Left ventricular end diastolic volume (LVEDV), left ventricular end systolic volume (LVESV), left ventricular ejection fraction (LVEF), and tricuspid annulus plane systolic excursion (TAPSE) were obtained. Strains and time to peak strains of right ventricular free wall and 16 left ventricle segments were analyzed using two-dimensional speckle tracking echocardiography (2D STE). The standard deviation of

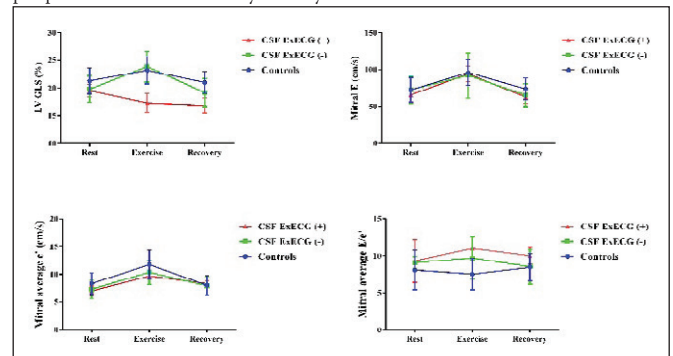
time to peak strains of 16 left ventricular segments was calculated as PSD. **Results:** 1. There was no significant difference of all the parameter between the two groups at baseline. QRS duration, LVEDV, LVESV, LVEF and TAPSE are not significantly different between the two groups at 6-month follow-up. 2. Compared to the baseline, time to peak longitudinal strain (TTPS) of apical septum, apical lateral wall were shortened after 6 months of HBP, while they didn't change significantly after 6 months of LBBP. After pacemaker implantation, the LBBP group had a delayed TTPS of apical septum, apical lateral wall and basal RV free wall than the HBP group (all $p < 0.05$). However, PSD was comparable between the two groups ($p > 0.05$). 3. Compared to the baseline, global left ventricular longitudinal strain (LVGLS) and longitudinal strain of RV free wall (RVLS) were deteriorated after 6 months of HBP, while they were preserved in the LBBP group. After 6-month pacing, LVGLS and RVLS were significantly stronger in the LBBP group than those in the HBP group. (LVGLS, $-16.10 \pm 3.75\%$ vs. $-13.18 \pm 4.11\%$; RVLS, $-17.50 \pm 5.46\%$ vs. $-13.70 \pm 4.35\%$, both $p < 0.05$). **Conclusion:** Patients received LBBP had a comparable left ventricular synchronism and a better myocardial contraction compared to patients with HBP. LBBP may be a promising alternative pacing strategy. Two-dimensional STE is more sensitive than conventional echocardiography in assessing cardiac synchrony and segmental deformation.

P2-084

Value of Treadmill Exercise Echocardiography Combined with Stress Electrocardiography for Stratification of Left Ventricular Systolic and Diastolic Function in Patients with Coronary Slow Flow

Yonghuai Wang, Jinyang Li, Shuang Liu, Lixin Mu, Guangyuan Li, Cuiting Zhao, Hang Yu, Jun Yang, Chunyan Ma, First Hospital of China Medical University, Shenyang, China

Background: Coronary slow flow (CSF) is an angiographic entity characterized by delayed coronary opacification in the absence of evident obstructive lesion in the epicardial coronary artery. CSF patients may have a diverse spectrum of clinical presentation, such as rest angina, exercise angina or mixed angina, and exhibit different results with exercise stress electrocardiography (ExECG). However, how the LV function in CSF patients varies during exercise is still not precisely known. This study aimed to evaluate LV systolic and diastolic function during exercise in CSF patients and investigate the value of treadmill exercise echocardiography combined with ExECG for the stratification of LV function. **Methods:** Fifty patients with CSF and 43 age- and sex-matched controls without CSF were enrolled in the study. Diagnosis of CSF was made by TIMI frame count. All patients were performed ExECG, treadmill exercise stress echocardiography and two-dimensional speckle-tracking analysis. Metabolic equivalents (METs) during exercise were recorded. LV systolic and diastolic functions were evaluated at rest, peak exercise and recovery phase. **Results:** All CSF patients and controls reached 85% of maximal predicted heart rate. And METs were lower in CSF patients than controls (10.78 ± 2.09 vs. 12.16 ± 1.63 , $p = 0.009$). In total, positive ExECG was found in 12 CSF patients (24%) but not in controls. At rest, LV global longitudinal strain (GLS) decreased and mitral average E/e' increased in the CSF patients than controls, but there were no difference between CSF patients with positive ExECG and negative ExECG. During exercise, CSF patients with negative ExECG had significantly increased LV GLS and decreased mitral average E/e' , but CSF patients with positive ExECG had significantly decreased LV GLS and increased mitral average E/e' (Figure). **Conclusions:** Although CSF patients had impaired LV diastolic and systolic function at rest, CSF patients with negative ExECG exhibited favourable LV function during exercise. Therefore, the CSF patients with negative ExECG may be motivated and encouraged to take appropriate exercise. This is a preliminary study and some larger prospective studies are necessary to verify these results.



Poster Session 2 (P2)

Monday, June 24, 2019

P2-085

Determination of LV Volume and Ejection Fraction with a Novel 3D Knowledge Reconstruction Technique in Comparison with Contrast Echocardiography Measurements

Stephen Pylypchuk, Harald Becher, Jonathan D. Windram, Mazankowski Heart Institute, Edmonton, AB, Canada

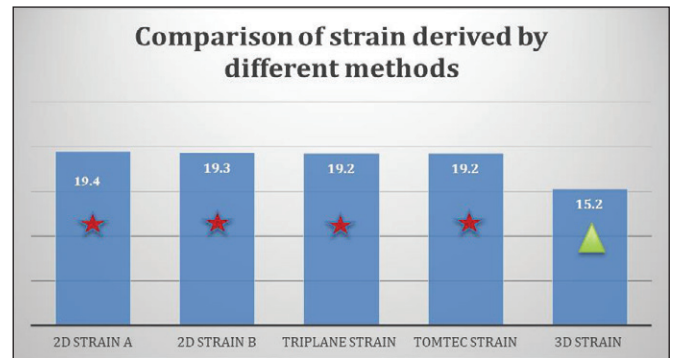
Background: Three dimensional contrast imaging remains the gold standard of left ventricular (LV) volume and ejection fraction (EF) assessment by echocardiography. Ultrasonographic enhancing agents pose a small risk of anaphylactic reaction however as well as necessitating prolonged image acquisition as compared to non-contrast studies adding to healthcare costs. The Ventripoint system, is a new technique that allows for three dimensional assessment of LV volumes and EF without the need for ultrasonographic enhancing agents thereby reducing risk to the patient and echo lab spending. Our aim was to assess reliability of the Ventripoint system knowledge based reconstruction software in assessing LV measurements in comparison to contrast echocardiography. **Methods:** Two dimensional transthoracic echocardiographic images were obtained from the parasternal and apical windows using a Philips EPIQ ultrasound machine with a standard Philips S5-1 probe. A magnetic field generator with the addition of a magnetic field localizer system attached to the ultrasound probe was used to collect data on the position and orientation of the receiver. Spatial orientation data was then analyzed using the Ventripoint knowledge based reconstruction software to develop a three dimensional framework of the left ventricle from which LV volumes and ejection fraction were obtained. These measurements were then compared to LV volumes and EF obtained by contrast echocardiography which were measured by biplane method of disks using bolus Definity contrast to optimize the endocardial definition. Correlation and mean differences between LV end-diastolic volume (LVEDV), LV end-systolic volume (LVESV) and EF measured by the Ventripoint system were compared to contrast echocardiography using the Pearson's method and t-test, respectively. **Results:** We present preliminary data on this novel technique in 16 patients. There was no significant difference in the mean LVEF between the Ventripoint assessment (45 +/- 11 %) and contrast echocardiography (45 +/- 15%) by contrast echocardiography. There was correlation of EF between the two methods (P=0.014). In addition no significant difference was noted in either the LVEDV (150 +/- 35 ml and 153 +/- 35 ml) or the LVESV (81 +/- 27 ml and 86 +/- 37 ml) between the two methods. **Conclusion:** The use of the Ventripoint knowledge based reconstruction technique revealed no significant differences in the measurement of ventricular volumes or EF in comparison to contrast echocardiography measurements.

P2-086

Reliability of Speckle-Tracking Echocardiography

Inga Vaitenas, Kameswari Maganti, Menhel Kinno, Bernadette Wodzinski, Northwestern Memorial Hospital, Chicago, IL

Introduction: The advent of speckle tracking Echo (STE) provided an-angle independent method for the assessment of myocardial mechanics. Left ventricular (LV) global longitudinal strain (GLS) is becoming a widely acceptable parameter for the detection of early LV systolic dysfunction in different clinical scenarios. **Aim:** This study sought to assess for differences in GLS values using different acquisition methods: conventional 2-dimensional (2D) at 2 different time points approximately 2 minutes apart, real-time triplane (3P), using vendor independent software, and 3-dimensional (3D)echo derived GLS. **Hypothesis:** We hypothesize that there will be no significant difference in the GLS obtained by the different acquisition methods. **Methods:** We analyzed 216 (average age 53.6 ± 16 years, 58 % females) consecutive patients undergoing a clinically indicated echo. Cine loops from 3 standard apical views (4-chamber, 2-chamber, and apical long-axis) were recorded using gray-scale harmonic imaging and saved in raw data format (Vivid E95, General Electric Health Care, Milwaukee, WI) for 2D, and 3P. Images for 2D and 3P were obtained at a frame rate of 50 to 70 per second. During 3D imaging, the pyramidal scan volume was focused on the LV volume and the data sets were acquired during a single breath hold. All the digital loops were saved for off-line analysis (EchoPac 12.0). These values were then compared values derived by vendor independent software (TomTec-Arena). Analysis of variance (ANOVA) was used test the difference between the 5 methods' means and followed by pair-wise student's t test. **Results:** The mean ± SD for LV ejection fraction for the whole cohort was 60 ± 6.4%. The mean ± SD of GLS for 2D (A and B), 3T, vendor independent software, and 3D methods are depicted in the figure. There was no statistically significant difference between 2D A, 2D B, 3P, and TomTec derived values. However, there was a statistically significant difference between the 2D and 3D methodologies. **Conclusion:** The LV GLS is a reliable method for assessment of LV function when measured either by 2D, 3P or 3D methods. The values of LV GLS obtained by 2D, 3P and using independent vendor software methodologies are similar. LV GLS obtained by 3D gives significantly lower values than the ones obtained by 2D or 3P and, therefore, these values are not interchangeable.



P2-087

Development and Initial Clinical Experience with an Electronic Critical Findings Alert for Echocardiographic Studies

Jason D'Souza, Kyle Lehenbauer, Jesse Cantu, Bethany A. Austin, Michael L. Main, Saint Luke's Mid America Heart Institute, Kansas City, MO

Background: Echocardiographic critical findings must be promptly reported to clinicians by the interpreting physician. There is a need for a vendor independent electronic medical record alert system, which could be triggered by the echocardiographic reader at the time of report finalization to facilitate communication to relevant care team members. **Methods:** We developed an electronic critical findings alert using the Synapse Cardiovascular echocardiographic reporting system (FUJIFILM Medical System, Stamford CT) and the Epic electronic medical record (Verona, WI). A drop down menu was added to the Synapse Cardiovascular IMPRESSION label on the echo report templates. If the reading physician selects "Yes" from the dropdown, a discrete data value worded "New critical echo findings available for this patient" is added to an OBX segment in the outbound HL7 message (ORU) to EPIC. Synapse generates the ORU when the report is finalized by the reading physician. The OBX segment is in a format that is accepted by the incoming Epic Bridges interface. An LRR record name "ECHO CRITICAL" is listed in OBX 3.1. This LRR record was created in EPIC and is used to map the echo critical discrete value to the patient chart when attached to an order. When the critical findings discrete data posts to the patient chart, it triggers a Best Practice Advisory (BPA). This BPA appears as a banner message in Epic to notify users entering the patient's chart of a critical finding on the echo report. The BPA continues to appear when the chart is accessed, until an advanced practice provider or physician on the care team electronically acknowledges it. **Results:** Between 12/10/2018 and 1/28/2019, the critical findings alert was triggered by the interpreting physician 105 times. Severe and potentially life threatening diagnoses included intracardiac thrombus (13%), new large pericardial effusion (6%), right ventricular strain indicating possible pulmonary embolus (5%), vegetation (2%), cardiac tamponade (2%), aortic dissection (2%), severe mitral regurgitation as a complication of myocardial infarction (1%), ascending aortic aneurysm (1%), and prosthetic valve thrombosis (1%). While the electronically triggered diagnoses ranged in clinical severity, one third of the identified studies represented severe and potentially life threatening diagnoses that required immediate action. **Conclusion:** We describe development and initial clinical experience with an electronic critical findings alert for echocardiographic studies. These methods may be applicable to many other healthcare systems.

P2-088

Impact of Frame Rate on Left Ventricular and Atrial Longitudinal Strain Values in Vendor Independent Two-Dimensional Speckle Tracking Echocardiography Software

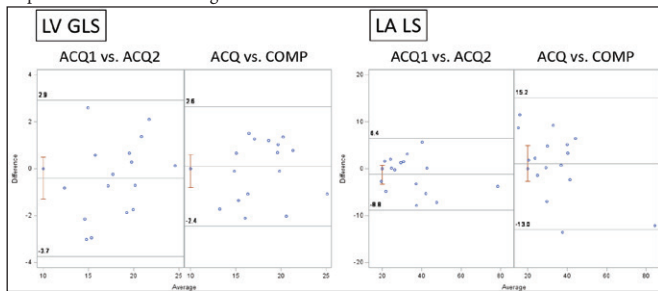
Tatsuya Miyoshi, Diego Medvedofsky, Sameer Desale, Federico M. Asch, Medstar Health Research Institute, Washington, DC

Background: Left ventricular and atrial (LV, LA) longitudinal strain (LS) analyses are increasingly used to detect and predict subclinical myocardial change in various diseases. American Society of Echocardiography consensus statement recommends higher frame rate in two-dimensional (2D) speckle tracking echocardiography and many studies used images at over 50 frames/second. However, echocardiographic images are frequently saved at compressed frame rate (30 frames/second) to save network drive capacity, even if they were acquired at higher frame rate. Therefore, we aimed to evaluate variability of LV and LA LS at different acquisition and compressed frame rates. **Methods:** Twenty patients with various backgrounds were randomly selected. Four patients were excluded due to poor image quality. Accordingly, sixteen patients were analyzed. 2D images were exported with two different settings: the first (ACQ) keeping the acquisition frame rate (50-60 frames/sec), the second set of images (COMP) were saved at compressed frame rate (30 frames/sec). Peak LV global (GLS, from three apical views) and LA LS in four-chamber view were measured with vendor independent software (TOMTEC). Images were measured at ACQ frame rate twice for intraobserver variability analysis and also calculated the averaged values. Comparisons included intraobserver variability of the difference between ACQ and

Poster Session 2 (P2)

Monday, June 24, 2019

the value at COMP frame rate, determined by coefficients of variation and t-test. **Results:** Intraobserver variability analysis showed no significant mean difference between two ACQ measurements for both LV GLS and LA LS. Comparison between ACQ and COMP also showed no significant mean difference in LV GLS and LA LS. Intraobserver coefficients of variation for LV GLS and comparison between ACQ and COMP were 6.6 and 4.9, while for LA LS were 8.0 and 14.6, respectively. The difference of coefficient variation for LA LS was significant ($p=0.03$), while that for LV GLS was not ($p=0.28$). Bland-Altman analysis is presented in the figure. **Conclusions:** LV GLS had high reproducibility using COMP frame rate while that of LA GLS was lower. These findings suggest LA LS is more affected by different frame rates than LV GLS. Further investigation is needed to assess the clinical implications of these findings.



P2-089

The Value of Echocardiography in Optimizing Multi-point Pacing Parameters for Improving Cardiac Resynchronization Therapy Response
M.R. Zhu, H.Y. Chen, Y.N. Wang, J.F. Wang, Xianhong Shu. Zhongshan Hospital, Fudan University, Shanghai, China

Objectives: To evaluate the value of echocardiography in optimizing multi-point pacing (MPP) parameters for improving cardiac resynchronization therapy (CRT) response. **Methods:** Ten healthy adult Beagle underwent left bundle branch ablation followed by rapid atrial pacing to induce dyssynchronized heart failure (DHF) animal model. After implantation of MPP-CRT, an acute pacing protocol including three configurations was performed: (1) default setting (FDS) configuration: use minimal delays (5 ms) as LV latest-excitation site (LV1)—earliest-excitation site (LV2) delay and LV2—right ventricular (RV) delay; (2) electro-cardio optimization (ELEC-OPT) configuration: measure the electro-sensing delay time of latest-activation point (LV1) (RLD) and the earliest-activation point (LV2) (RED) under single RV pacing, and then program (RLD-RED)/2 as LV1—LV2 delay and RED/2 as LV2—RV; (3) echocardiography optimization configuration (ECHO-OPT): first, identify the respective corresponding myocardial segment of the RV and 4 LV electrodes by single electrode pacing, and then find the earliest-contraction (minimum time to peak longitudinal strain (TpLS)) segment using speckle tracking imaging; secondly, analyze the speckle tracking echocardiography before CRT and identify the 5 segmental TpLS corresponding RV electrode (RV-TpLS) and 4 LV electrodes. Of 4 LV segments, measure the TpLS of latest-contraction segment (LV-TpLS_{max}) and earliest-contraction segment (LV-TpLS_{min}). Finally, program (LV-TpLS_{max})-(LV-TpLS_{min}) as the LV1—LV2 delay and (LV-TpLS_{min})-RV as LV2—RV delay. **Results:** Compared with normal beagle, myocardial contractility of DHF beagle model was significantly reduced, which demonstrated by a significant reduction of LVEF (Normal vs. DHF: $64 \pm 1.4\%$ vs. $30 \pm 0.5\%$, $P<0.05$) and LV global longitudinal peak strain (GLPS) (Normal vs. DHF: $-12.3 \pm 0.4\%$ vs. $-5.15 \pm 1.8\%$, $P<0.05$), as well as a significant LV dyssynchrony (PSD) (Normal vs. DHF: 36 ± 1.4 ms vs. 77 ± 14.1 ms, $P<0.05$). Cardiac function was improved to varying degree in three MPP configurations with different pacing parameters programmed. Besides, among FDS, ELEC-OPT and ECHO-OPT configuration, there was a gradually increasing tendency in LVEF and GLPS, and a gradually decreasing tendency of PSD (FDS vs. ELEC-OPT vs. ECHO-OPT: 78 ± 33.9 ms vs. 50.5 ± 3.5 ms vs. 48 ± 1.4 ms, $P>0.05$). **Conclusions:** The ECHO-OPT configuration tends to be superior to FDS and ELEC-OPT in improving acute myocardial contractility and dyssynchrony. Echocardiography has a potential in improving CRT response.

P2-090

Quantitative Analysis of Intraventricular Blood Flow Dynamics Using a New Technique

Eun Kyoung Kim, Seung Woo Park. Samsung Medical Center, Seoul, Republic of Korea

Background: Although studies on intraventricular blood flow dynamics have been conducted continuously, its clinical applications have been hampered by a limited vendor, complex software, long processing time and the absence of objective parameters. Recently, we suggested Doppler Analyzer which a novel method visualizing intracardiac blood flow patterns and enables quantification of flow dynamics with 2-dimensional (2D) and color Doppler data using conventional echocardiography. Here, we tried to investigate the relation between the conventional parameters reflecting LV systolic function and new parameters reflecting intraventricular flow dynamics. **Methods:** We got the conventional

color Doppler and 2D images at the apical 3 chamber view during three cardiac cycles. By tracing LV wall using commercially available software (EchoPAC System, General Electric), LV wall position and velocity data were acquired. Using the digitalized software named as 'Doppler Analyzer', we visualized overall velocity field within the LV cavity and calculated 'Circulation Strength' and 'Energy Dissipation' which means dynamic force of blood flow and attenuation of dynamic fluid energy, respectively. Calculation formulas were as follows; Circulation Strength = $\int_A \mu((\delta V_x)/\delta y - (\delta V_y)/\delta x - (\delta V_x)/\delta y) dA$, Energy Dissipation = $\int_A \mu((\delta V_x)/\delta y - (\delta V_y)/\delta x)^2 dA$. **Results:** We analyzed 76 patients (44 male, 56.4 ± 15.0 years), 53 of whom had normal cardiac function (Group A) and 23 of whom had left ventricular dysfunction (Group B). Median duration of measurements was 3 (IQR, 2-5) minutes per person. There were significant differences of LV ejection fraction ($65.6 \pm 5.1\%$ vs. $32.6 \pm 11.0\%$, $p<0.001$) and LV global longitudinal strain (-19.6 ± 2.8 vs. $-9.3 \pm 4.0\%$, $p<0.001$) between two groups. Compared to Group A, Group B had lower Circulation Strength during diastole ($(9.1 \pm 3.0) \times 10^{-3}$ vs. $(4.9 \pm 3.5) \times 10^{-3}$, $p<0.001$) and systole phase ($(3.6 \pm 2.2) \times 10^{-3}$ vs. $(2.9 \pm 2.6) \times 10^{-3}$, $p=0.282$). Among three parameters that reflect blood flow dynamics within the LV cavity, Circulation Strength during diastole was significantly correlated with LVEF (correlation coefficient, $r=0.548$, $p<0.001$) and strain value ($r=-0.634$, $p<0.001$). **Conclusion:** Using conventional echo data, we could quantify intraventricular flow dynamics and derive objective parameters, Circulation Strength and Energy Dissipation. Circulation Strength during the LV filling period was significantly correlated with LVEF and strain. To confirm the clinical implication of the above parameter, clinical validation study in various disease entities is currently being processed.

P2-091

Vector Flow Mapping Analysis of Left Ventricular Wall Shear Stress in Healthy Adult Volunteers

Li Ping Dong, Jia Wei Tian. The Second Affiliated Hospital of Harbin Medical University, Harbin City, Heilongjiang Province, China

Background: Vector flow mapping (VFM), a new technique to study the characteristics of intracardiac hemodynamics, is increasing in popularity. Energy loss (EL) and vortex, the parameters of VFM, are described in detail in many articles. But wall shear stress (WSS), as a new parameter, has not been elaborated in detail and studied in depth. This study examined use of new VFM for assessment of left ventricular (LV) WSS in healthy adults at different stages of cardiac cycle. **Methods:** Analysis WSS in 50 healthy volunteers using VFM, including the observation of the relationship among WSS of different segments of the LV at the same stage and change regulation of WSS of different segments of LV at different stages of the same cardiac cycle. **Results:** 1. the relationship among WSS of different segments of the LV at the same stage: In P1, P2 and P3 period, the relationship among three segments of the absolute value of WSS of anterior septum, posterior septum and anterior wall of the LV. In P5, P6 and P7 period, the relationship among three segments of the absolute value of WSS of lateral, posterior and inferior walls of the LV: basal segment > middle segment > apical segment, the difference was statistically significant ($p < 0.05$). 2. change regulation of WSS of different segments of LV at different stages of the same cardiac cycle: In p1-p2-p3 period, the absolute values of WSS in basal and middle segments of anterior septum, posterior septum and anterior wall: Increasing first and then decreasing. In P2 period, the absolute value of WSS in basal segment of anterior septum was the largest. In P3 period, the absolute value of WSS in middle segment of anterior wall was the smallest. In p4-p5-p6-p7 period, the absolute value of WSS in the basal and middle segments of lateral wall, posterior wall and inferior wall: Increasing-decreasing-increasing trend. In P5 period, the absolute value of WSS in basal segment of inferior wall was the largest. In P6 period, the absolute value of WSS in middle segment of lateral wall was the smallest. The change rate distribution is consistent with the basal segment > the middle segment. The difference was statistically significant ($p < 0.05$). **Conclusions:** VFM technique can be used to quantitatively evaluate the relationship among WSS of different segments of the LV at the same stage and change regulation of WSS of different segments of LV at different stages of the same cardiac cycle.

P2-092

Initial Clinical Experience with Mixed Reality Interactive Visualization of Three-Dimensional Echocardiographic Datasets During Percutaneous Interventions

Jaroslav Kasprzak¹, Mateusz Kierepka², Jan Z. Peruga¹, Bartosz Machura², Maciej Stanuch², Adriana Zlahoda-Huzior², Jakub I. Kasprzak², Katarzyna Wdowiak-Okrojek¹, Piotr Lipiec¹. ¹Dept. of Cardiology, Medical Univ. Lodz, Lodz, Poland; ²MedApp SA, Krakow, Poland

Background: Echocardiographic three-dimensional (3D) datasets acquired from transesophageal (TEE) window are commonly used as procedural aid during percutaneous cardiac interventions. We hypothesized that innovative mixed reality display can be integrated with procedural workflow to improve 3D perception and navigation in 3DTEE datasets. **Methods:** 3DTEE datasets were acquired before, during and after the completion of intracardiac procedures in 6 patients (LAMBRE LAAO, PMBV, 2 ASD occlusions and 2 PFO occlusions); 24 Cartesian DICOM files were used to test the feasibility of mixed reality, head-mounted device overlying holographic image of cardiac data onto real-world viewing by the interventional or imaging operator. A dedicated software pathway was used for files conversion, real-time Wi-Fi streaming of 3D rendering from PC to device

Poster Session 2 (P2)

Monday, June 24, 2019

and manipulation of spatial data during the procedures. In one case real-time streaming of raw 3DTEE data was obtained during the study. Custom viewer was used to perform volume rendering and adjustment (cropping, transparency and shading control). **Results:** 3D TEE was performed in all 6 patients (4 women, age 40-83). Twenty four selected, cardinal 3DTEE datasets were successfully transferred and displayed in mixed reality head-mounted device as a holographic image overlying the real world view. The analysis was performed both before and during the procedure and compared with flatscreen 2-D display of the echocardiograph. In one case, real-time data transfer was successfully tested during mitral balloon commissurotomy. The quality of visualization was good without diagnostic content loss in all (100%) datasets. Volume rendered views were tested with a selection of transfer functions, filters and intensity widow settings. The quality of display was judged comparable to current 2-D volume-rendering on commercial workstations. Beside the target structures additional details were clearly seen including fenestrations of defect and significant prominent Eustachian valve and earlier intracardiac implants. Touchless user interface was judged convenient for easy intraprocedural optimization of views. **Conclusions:** Mixed reality display using a commercially available head-mounted device can be successfully integrated with intracardiac percutaneous procedures with benefit of touchless image control and unobstructed real world viewing, thus showing superiority over virtual or enhanced reality solutions. Expected progress includes integrating color flow data and optimization of real-time streaming.

P2-093

The VVI Ventricular Function Assessment in Second-Third Trimester Fetus with Tricuspid Regurgitation

Liu Hong^{1,2}, Haiyan Cao^{1,2}, Li Zhang^{1,2}, Qingchang Chen^{1,2}, Mingxing Xie^{1,2}.
¹Department of Ultrasound, Union Hospital, Tongji Medical College, HUST, Wuhan, China; ²Hubei Key Laboratory of Molecular Imaging, Wuhan, China

Objective: To evaluate the changes of ventricular function in second-third trimester fetus with tricuspid regurgitation by velocity vector imaging (VVI). **Methods:** The fetus include in this study diagnosed as tricuspid regurgitation during January 2014 to August 2017 in the Union Hospital of HUST. They were divided in: group A-mild tricuspid regurgitation, group B- severe tricuspid regurgitation. The control group included 36 normal fetuses in the same period. To evaluate the global ventricular motion of the group A, B and the control group by VVI. The following parameters of the left and right ventricular were obtain by manual tracing endocardial at the end of ventricular diastolic in four-chamber view: the global systolic longitudinal velocity (GLVs), the global diastolic longitudinal velocity (GLVd), the global systolic longitudinal strain rate (GLSRs), the global diastolic longitudinal strain rate (GLSRd) and the global longitudinal strain (GLS). The differences of baseline and parameters between groups A, B and the control group were analyzed. **Results:** 1.Comparison of general data: There were no significant differences among the group A, B and the control group ($P > 0.05$). 2. Comparison of right ventricular parameters: There were significant differences among the group A, B and the control group in terms of the right ventricular GLVs, GLVd, GLS, GLSRs and GLSRd ($P < 0.01$); there were significant differences between the group B and the control group in terms of the right ventricular GLVs, GLVd, GLS, GLSRs and GLSRd ($P < 0.01$). 3. Left ventricle parameter comparison (ANOVA analysis): There were significant differences between group A and B in terms of the left ventricle GLVs, GLVd, GLS, GLSRs and GLSRd ($P < 0.01$); There were significant differences between group B and the control group in terms of the GLVs, GLVd, GLS, GLSRs and GLSRd ($P < 0.01$). **Conclusion:** The ventricular function is significantly different among the fetus diagnosed as mild/severe tricuspid regurgitation and normal, the ventricular systolic and diastolic function is obviously impaired. There were no significant differences between the mild tricuspid regurgitation fetus and control in terms of the ventricular function index, which means mild tricuspid regurgitation did not cause fetal ventricular function damage. The qualitative and quantitative measurements of prenatal fetal tricuspid regurgitation is beneficial to evaluate the effects of cardiac structure, activity and rhythm, which helps to predict the prognosis, guide clinical practices, and give recommendations of good birth and good care.

P2-094

Evaluation of a Deep-Learning Algorithm Designed to Aid Novice Scanners in Obtaining Diagnostic Quality Echocardiograms

Akhil Narang¹, Ha Hong², Ching Hsieh², Ali Chaudhry², Sara Guttas², Alan S. Pearlman³, Neil J. Weissman⁴, James D. Thomas¹. ¹Northwestern University, Chicago, IL; ²Bay Labs, Inc., San Francisco, CA; ³University of Washington, Seattle, WA; ⁴MedStar, Washington, DC

Background: Transthoracic echocardiography (TTE) is the most widely used cardiac imaging modality but usually requires highly-trained sonographers to acquire diagnostic images. A newly developed investigational device utilizing deep-learning model (EchoGPS, Bay Labs) is the first of its kind to combine real-time image quality assessment with adaptive anatomic guidance on transducer maneuvers to allow individuals with limited echocardiography training to acquire 10 standard TTE views. The goal of this study was to compare the diagnostic quality of echocardiograms obtained by registered nurses (RN) with limited training (<4 hours) using EchoGPS to the images obtained by a trained cardiac sonographer. **Methods:** The EchoGPS deep-learning model provides real-time visual feedback and guidance during image acquisition in order to optimize the quality of

10 standard parasternal, apical, and subcostal B-mode TTE views. 16 volunteers (median age 50 years, 56% male, 25% with BMI >30) underwent a limited TTE performed by 4 RNs without prior experience in echocardiography other than orientation to the software. An experienced registered cardiac sonographer also scanned the subjects. Five level 3 echocardiographers, blinded to subject and scanner, independently evaluated whether each set of 10 clips was sufficient to evaluate qualitative parameters related to the left and right ventricle; left atrium; mitral, tricuspid, and aortic valves; and inferior vena cava (IVC). **Results:** Qualitative assessments were deemed feasible in a high percentage of patient studies for the majority of cardiac structures evaluated whether imaged by the sonographer or the RNs, with the exception of the IVC (Table). The EchoGPS model guided acquisition of each of the 10 echocardiographic views in all 64 exams (median time of 3:16 minutes/view). **Conclusion:** This feasibility study is the first to show that a deep-learning based model may facilitate medical personnel with very minimal training in echocardiography in obtaining diagnostic-quality echocardiograms. This technology may be able to facilitate access to TTE in settings with limited resources and also in clinical settings where immediate interrogation of cardiac chamber size and function is required.

Clinical Parameter	RN Diagnostic Confidence	Sonographer Diagnostic Confidence
LV Size	98%	100%
LV Function	98%	100%
RV Size	92%	100%
RV Function	92%	93%
LA Size	95%	100%
Pericardial Effusion	98%	100%
All Valves	84%	93%
Aortic Valve	94%	100%
Mitral Valve	97%	100%
Tricuspid Valve	86%	93%
IVC Size	58%	73%

P2-095

Automated Echocardiographic Quantification of Left Ventricular Ejection Fraction Without Volume Measurements Using a Machine Learning Algorithm Mimicking a Human Expert

Federico M. Asch¹, Nicolas Poilvert², Theodore Abraham³, Madeline Jankowski⁴, Jayne Cleve⁵, Mike Adams², Nathanael Romano², Ha Hong², Victor Mor-Avi⁶, Roberto M. Lang⁶. ¹MedStar Health Research Institute, Washington, DC; ²Bay Labs, San Francisco, CA; ³University of California, San Francisco, CA; ⁴Northwestern Memorial Hospital, Chicago, IL; ⁵Duke University Medical Center, Chapel Hill, NC; ⁶University of Chicago, Chicago, IL

Background: Echocardiographic quantification of left ventricular (LV) ejection fraction (EF) relies on either manual or automated identification of endocardial boundaries followed by standard calculation of model-based end-systolic and end-diastolic LV volumes. Recent developments in artificial intelligence resulted in computer algorithms that allow near automated detection of endocardial boundaries and measurement of LV volumes and function. However, boundary identification is still prone to errors limiting accuracy in certain patients. We hypothesized that a fully automated machine learning algorithm could be developed, which circumvents border detection and instead estimates the degree of ventricular contraction, similar to a human expert trained on tens of thousands of images. This study was designed to test the feasibility and accuracy of this approach. **Methods:** Machine learning algorithm was developed and trained on a database of >50,000 echocardiographic studies, including multiple apical 2- and 4-chamber views, to automatically estimate LVEF (AutoEF, BayLabs). Testing was performed on an independent group of 99 unselected patients, whose automated EF values were compared to reference values obtained by averaging measurements by 3 experts using conventional volume-based technique. Inter-technique agreement was assessed using linear regression and Bland-Altman analysis of bias and limits of agreement (LOA). Consistency was assessed by mean absolute deviation (MAD) among automated estimates based on different combinations of apical views. Finally, sensitivity and specificity of detecting of EF<35% was calculated. These metrics were compared side-by-side against the same reference standard to those obtained from conventional EF measurements by clinical readers. **Results:** Automated estimation of LVEF was feasible in all 99 patients. AutoEF values showed high consistency (MAD=2.9%) and excellent agreement with the reference values: $r=0.94$, $bias=1.0\%$, $LOA=\pm 11.8\%$, with sensitivity 0.91 and specificity 0.93 for detection of EF<35%. This was similar to clinicians' measurements: $r=0.94$, $bias=1.4\%$, $LOA=\pm 13.4\%$, sensitivity 0.93, specificity 0.87. **Conclusions:** Machine learning algorithm for volume-independent LVEF estimation is highly feasible and similar in accuracy to conventional volume-based measurements, when compared to reference values provided by an expert panel.

Poster Session 2 (P2)

Monday, June 24, 2019

P2-096

Artificial Intelligence for Assessment of Regional Wall Motion Abnormality from Echocardiographic Images

Kenya Kusunose, Takashi Abe, Akihiro Haga, Hirotsugu Yamada, Masafumi Harada, Masataka Sata. Tokushima University Hospital, Tokushima, Japan

Background: An effective intervention for reduction of misreading of regional wall motion abnormalities (RWMAs) is needed. The aim of this study was to evaluate whether a deep convolutional neural network (DCNN) could detect RWMAs and differentiate groups of coronary infarction territories from conventional 2-dimensional echocardiographic images compared with cardiologist/sonographer or resident readers. We hypothesized that a DCNN trained with echocardiographic images may provide improved detection of RWMAs in the clinical setting. **Methods:** A total of 300 patients with history of myocardial infarction were enrolled. In this cohort, 100 each had infarctions of the left anterior descending branch (LAD), left circumflex branch (LCX), and right coronary artery (RCA). The age-matched 100 control patients with normal wall motion were selected from our database. Each case contained cardiac ultrasound images from short axis views at end-diastolic, mid-systolic and end-systolic phases. After 100 steps of training, diagnostic accuracies were calculated on the test set. We independently trained 10 versions of the same model, and performed ensemble predictions with them. **Results:** For detection of the presence of wall motion abnormality, the area under the receiver-characteristic curve (AUC) by deep learning algorithm was similar to that by cardiologist/sonographer readers (0.99 vs. 0.98, $p=0.15$), and significantly higher than the AUC by resident readers (0.99 vs. 0.90, $p=0.002$). For detection of territories of wall motion abnormality, the AUC by the deep learning algorithm was similar to the AUC by cardiologist/sonographer readers (0.97 vs. 0.95, $p=0.61$) and significantly higher than the AUC by resident readers (0.97 vs. 0.83, $p=0.003$). **Conclusion:** Our results support the possibility of DCNN use for automated diagnosis of RWMAs in the field of echocardiography.

P2-097

Unsupervised Cluster Analysis of Aortic Stenosis Patients Reveals Distinct Population with Different Phenotypes and Outcomes

Soongu Kwak¹, Yunhwan Lee², In-Chang Hwang³, Jun-Bean Park¹, Yeonyee E. Yoon³, Hyung-Kwan Kim¹, Yong-Jin Kim¹, Goo-yeong Cho³, Dae-Won Sohn¹, Sungho Won², Seung-Pyo Lee¹. ¹Seoul National University Hospital, Seoul, Republic of Korea; ²Seoul National University, Seoul, Republic of Korea; ³Seoul National University Bundang Hospital, Seongnam-si, Republic of Korea

Background: The clinical course of aortic stenosis (AS) patients may be heterogeneous considering the complex interactions between the patients' comorbidities and the cardiac dysfunctions as well as the stenotic valve itself. We aimed to explore whether unsupervised clustering analysis of moderate or severe AS patients can identify distinct subgroups with different prognostic significances. **Methods:** This study included a derivation cohort of 398 newly diagnosed moderate to severe AS patients prospectively enrolled between 2013 and 2016 (mean age 71±10 years, 55% male, 53% severe AS). A comprehensive dataset regarding demographics, laboratory, and echocardiography parameters (32 continuous variables) were used for the unsupervised clustering. Phenotypes and adverse clinical outcomes were compared between the clusters. The findings of the derivation cohort were validated using a separate validation cohort (n=262). Cardiac mortality was defined as sudden cardiac arrest, death from heart failure or myocardial infarction, and death related to aortic valve replacement. **Results:** Three clusters were identified, each presenting markedly different features. Cluster 1 (n=60) was predominantly associated with cardiac dysfunction, i.e., significantly lower left ventricular ejection fraction, cluster 2 (n=86) consisted of predominantly elderly with more comorbidities especially end-stage renal disease, whereas cluster 3 (n=252) demonstrated neither decompensated heart function nor comorbidities. The adverse outcomes significantly differed by the clusters where cluster 2 demonstrated the highest all-cause mortality during a median follow-up of 2.4 years (mortality rate: 13.3% vs. 19.8% vs. 6.0% for cluster 1, 2, and 3; $P<0.001$ by log-rank test). The cause of mortality significantly differed between each clusters with cluster 1 being most strongly associated with cardiac mortality (adjusted hazard ratio [HR], 7.61; 95% confidence interval [CI] 2.08-27.9; $P=0.002$), whereas cluster 2 had a significantly higher risk of non-cardiac mortality (adjusted HR, 1.76; 95% CI 1.07-2.89; $P=0.024$), each compared to cluster 3. The phenotypes and association of clusters with specific outcomes were reproduced in the validation cohort. **Conclusions:** Unsupervised clustering analysis of AS patients revealed three distinct subgroups that presented distinct phenotypes and outcomes. The result provides a new perspective in the categorization of AS patients regarding comorbidities and cardiac dysfunction beyond the aortic valve and its association with outcome.

P2-098

Machine Learning Algorithm of Noninvasive Cardiac Imaging for Classification of Cardiac Mass

Seo-Young Lee, Taehoon Ko, Seung-Pyo Lee. Seoul National University Hospital, Seoul, Republic of Korea

Background: Cardiac tumors are rare and therefore, the correct diagnosis may be difficult solely with the echocardiographic characteristics. We hypothesized machine-learning (ML)

algorithms based on simple echocardiographic features of tumors may help classify the cardiac tumors correctly. **Methods:** 254 consecutive patients (46.6% male; 57.13±15.57 years old) who underwent transthoracic echocardiography (TTE) within 1 month of either transcatheter biopsy or surgical excision of the mass and had a definite pathologic diagnosis of the target mass were included. The patient's clinical data and 11 key TTE image features (Table) were recorded by a single independent observer. We derived classification algorithms based on 6 ML methods (Table) using data from the derivation cohort (n=177) and tested the performance of each algorithm using a separate validation cohort (n=77). We compared each algorithm's performance in classifying the cardiac masses into 4 groups: primary malignancy, secondary malignancy, myxoma, non-myxoma benign mass. We also tested the performance of algorithms with an independent human expert. The classification performance was scored with the area-under-the receiver operating characteristic curve (AUC). **Results:** The AUC for each classifier algorithm ranged between 0.74 and 0.96. Of the 6 ML models, the extreme-gradient boosting (XGBoost) model showed the best AUC. Compared with the human expert, the XGBoost model showed higher classifying accuracy (85.7% versus 76.6%) and higher performance on the ROC curve (Figure). The support vector machine and logistic regression model showed a similar performance compared with the human expert. **Conclusion:** Our results suggest that the performance of cardiac tumor classifying algorithms using various ML are similar to or may even be better than a human expert. The ML algorithms may help guide the decision of cardiac mass classification.

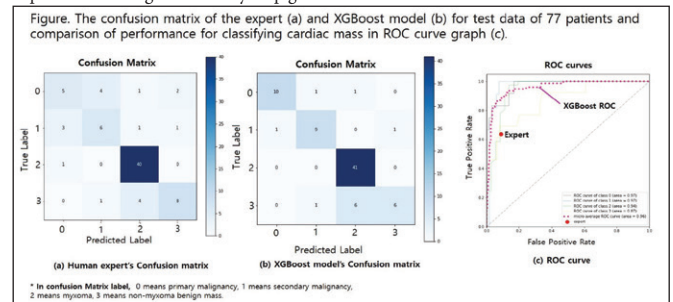


Table. 11 Key echocardiographic features and 6 machine learning methods used for this analysis--

Key echocardiographic features--	Machine learning methods used for analysis--
1. Cardiac mass location--	1. Decision tree--
2. Cardiac mass echogenicity; heterogeneous or homogenous--	
3. Cardiac mass mobility; hypermobile or immobile--	2. Random forest--
4. Valvular destruction or valve attachment of mass--	
5. Flow obstruction due to cardiac mass--	3. Neural network--
6. Invasion to adjacent structure or cardiac chamber wall of mass--	
7. Pericardium extension of cardiac mass--	4. Logistic regression--
8. Multifocal lesion--	
9. Thrombus attached to cardiac mass surface--	5. Support vector machine--
10. Pericardial effusion--	
11. Tamponade feature in echocardiography due to cardiac mass or Pericardial effusion--	6. Extreme-gradient boosting (XGBoost)--

P2-099

Validation of a Novel Artificial Intelligence Left Ventricular Ejection Fraction Quantification Software (LVivoEF by DIA®) by Cardiac MRI

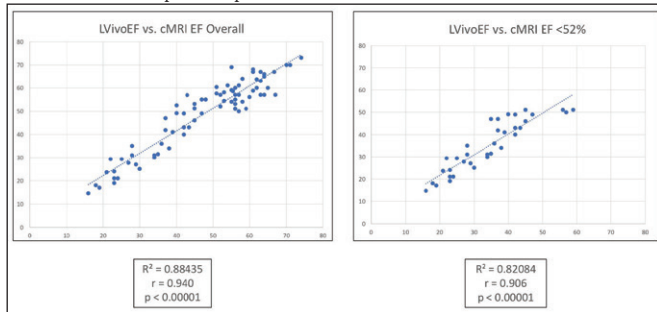
Rajeev Samtani¹, Solomon Bienstock¹, Steve Liao¹, Usman Baber¹, Arieh Greenbaum², Lori Croft¹, Eric Stern¹, Martin Goldman¹. ¹Jcahn School of Medicine at Mount Sinai, NY, NY; ²Montefiore Medical Center, NY, NY

Background: The diagnosis of left ventricular (LV) function and ejection fraction (EF) is the most frequently requested transthoracic echo (TTE) diagnosis, but its quantification can be patient habitus, machine, sonographer, and interpreter dependent. Application of a rapid, on-line artificial intelligence technology to quantify LVEF would remove reader subjectivity and would be an invaluable tool for improving TTE interpretation. Our study aims to determine if artificial intelligence with LVivoEF by DIA® (which can be run across several electronic platforms), correlates well with Cardiac Magnetic Resonance Imaging (cMRI) LVEF, as the gold standard. **Methods:** We performed a retrospective single center study of 76 patients (pts) who underwent both routine TTE and cMRI within 6 months with no interval cardiac intervention or clinical event. Pts 4-chamber LVEF's were analyzed by a novel artificial intelligence software, LVivoEF by DIA®, which provides fully automated LV analysis and generates LVEF through pattern recognition, machine learning, and image processing algorithms for automated detection and tracking displaying the endocardial border as an overlay on the moving image. Using linear regression and chi square, the DIA 4-chamber EF's were compared to the cMRI EFs. **Results:** There were 76 patients (59% male, mean age 54.3 years, range 20-88 years), mean LVEF by cMRI was 48.6%, range 14.6 to 73.0%. Using the ASE classification, 42 had a normal EF (>51%), 14 had mildly abnormal (41-51%), 8 moderately abnormal (30-40%), and 13 severely abnormal EF's (<30%) by their cMRI. The correlation between LVivoEF and cMRI derived EF for all pts was $R^2=0.890$ ($p<0.00001$), and for those with abnormal cMRI EF (<52%), $R^2=0.821$ ($p<0.00001$) (Figure). LVivoEF also accurately separated EF ≤40% and >40%, $\chi^2=51.1$, $p<0.00001$. **Conclusion:** Compared to cMRI as the gold standard, LVivoEF AI software provides accurate LVEF over a wide range of cardiac function. By providing the endocardial border overlay on the moving images, LVivoEF facilitates immediate confirmation by the reader of its accuracy. The strong correlation between LVivoEF AI may expedite more

Poster Session 2 (P2)

Monday, June 24, 2019

accurate TTE LVEF quantification, particularly in pts with low EF's in whom accuracy has clinical and therapeutic implications.



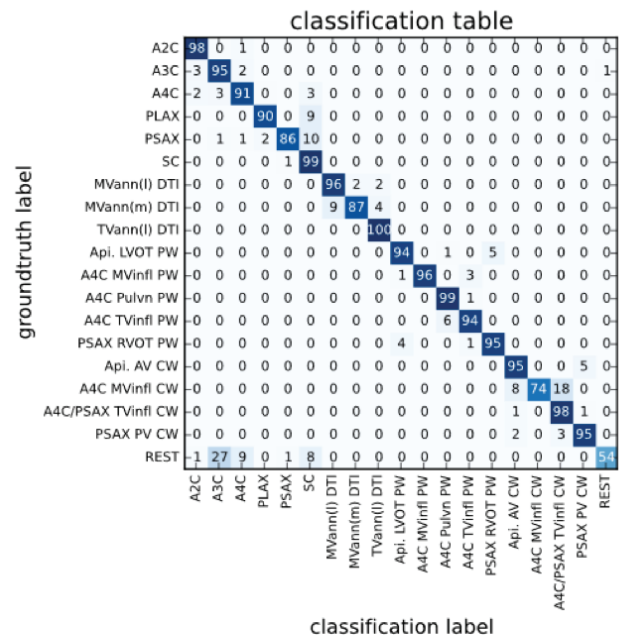
P2-100

Computer Identification of Standard Echocardiographic Views Using a Convolutional Neural Network

Kalie Kebed¹, Davide Genovese¹, Tatsuya Miyoshi², Karima Addetia¹, Marcus Schreckenber³, Alexandra Blitz³, Sabrina Zörnack³, Vivekanandan Amuthan⁴, Rodolfo Citro⁵, Masao Daimon⁶, Pedro Gutiérrez-Fajardo⁷, Ravi Kasliwal⁸, James N. Kirkpatrick⁹, Mark J. Monaghan¹⁰, Denisa Muraru¹¹, Kofo O. Ogunyankin¹², Seung Woo Park¹³, Ana Clara Tude Rodrigues¹⁴, Ricardo Ronderos¹⁵, Anita Sadeghpour¹⁶, Gregory Scalia¹⁷, Masaaki Takeuchi¹⁸, Wendy Tsang¹⁹, Edwin S. Tucay²⁰, Mei Zhang²¹, Federico M. Asch², Roberto M. Lang¹. ¹University of Chicago, Chicago, IL; ²MedStar Health Research Institute, Washington, DC; ³TOMTEC Imaging Systems GmbH, Unterschleissheim, Germany; ⁴Jeyalakshmi Heart Center, Madurai, India; ⁵University of Salerno, Salerno, Italy; ⁶The University of Tokyo, Tokyo, Japan; ⁷Hospitales Mac Bernardette, Guadalajara, Mexico; ⁸Medanta Heart Institute, Gurgaon, Haryana, India; ⁹University of Washington, Seattle, WA; ¹⁰King's College Hospital, London, United Kingdom; ¹¹University of Padova, Padova, Italy; ¹²First Cardiology Consultants Hospital, Lagos, Nigeria; ¹³Samsung Medical Center, Seoul, Republic of Korea; ¹⁴Albert Einstein Hospital, Sao Paulo, Brazil; ¹⁵Universidad Nacional de la Plata, Buenos Aires, Argentina; ¹⁶Rajaie Cardiovascular Medical and Research Center, Echocardiography Research Center, IUMS, Tehran, Islamic Republic of Iran; ¹⁷Genesis Care, Brisbane, Australia; ¹⁸University of Occupational and Environmental Health, Kitakyushu, Japan; ¹⁹Toronto General Hospital, University of Toronto, Toronto, ON, Canada; ²⁰Philippine Heart Center, Quezon City, Philippines; ²¹Qilu Hospital of Shandong University, Jinan, China

Introduction: Deep learning has shown great promise in helping experts with still image-based diagnosis in radiology. To date, this technique has not been widely applied to echocardiography because a typical study consists of multiple image loops, still images and Doppler recordings acquired from different transducer positions. Computer identification of the echocardiographic views is the first step towards automated measurement and interpretation of echocardiograms. Accordingly, the aim of this study was to train and then test a convolutional neural network (CNN) to identify the different echocardiographic views and recordings. **Methods:** A training and test set of over 250,000 images (>600 studies) and a validation set of over 80,000 images (200 studies) were used to train a CNN to recognize 18 echocardiographic views, 6 from 2D (digital loops and still images) and 12 tissue Doppler (DTI), pulsed wave Doppler (PW) and continuous-wave Doppler (CW). Training images included a variable spectrum of zoom, depth, focus, sector width, gain, and image quality. These images were labelled by an observer and inputted into the CNN to build the library of echocardiographic views and recordings. Subsequently, on the validation set, the CNN was instructed to identify the views and recordings and stacks the images according to the echocardiographic feature to be interpreted: LV dimension/systolic function, LV diastolic function, RV and RA dimensions/function, Valves (Mitral, Aortic, Tricuspid, Pulmonary) and Pericardium. The results of the automated identification were compared to the ground truth provided by an expert reader. **Results:** Automated classification of views by the trained CNN took an average of 0.87 sec per study. The CNN was able to identify and sort by stacks the heterogeneous input of images achieving an overall accuracy of 91.1%. 2D views were recognized correctly with an accuracy of 90.3%, while DTI, CW, PW, which always appeared as still images, had a 94.4% accuracy (Figure 1). Identification of images resulted in a correct stack composition in 99.0% (Table 1). **Conclusion:** CNN was able to quickly and mostly accurately identify all views from 2D echocardiographic studies, which is the required step prior to automated segmentation, measurements and interpretation.

Figure 1. Classification Accuracy on Validation Pool [%]



Reading Stack	Studies with complete stack
LV Dimension / Systolic Function	99.5%
LV Diastolic Function	100%
RV/RA Dimensions/Function	99.0%
Mitral Valve	99.8%
Aortic Valve	96.0%
Tricuspid Valve	99.4%
Pulmonary Valve	98.4%
Pericardium	100%

Table 1. Probability of Complete Reading Stacks

P2-101

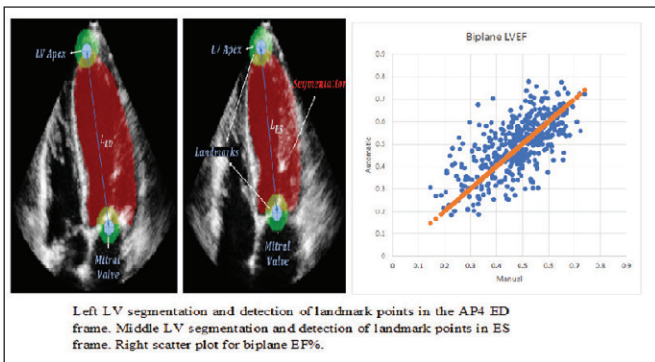
Assessment of Left Ventricular Ejection Fraction the Present and Future

Hany Y.A. Girgis, Mohammad Jafari, Zhibin Liao, Robert Rohling, Kenneth Gin, Purang Abolmaesumi, Teresa S.M. Tsang. University of British Columbia, Vancouver, BC, Canada

Background: The most commonly used echocardiographic technique for assessment of left ventricular ejection fraction (LVEF) is the modified Simpson's technique. However, this technique is time-consuming, tedious, and lacks reproducibility, and precision. **Objectives:** We hypothesized that advances in machine learning, a popular subdiscipline of artificial intelligence could enable building a fully automated and accurate echocardiographic technique for assessment of the LVEF. **Methods:** The machine learning model was evaluated on a dataset of 427 patients. Each patient has a pair of apical two-chamber (AP2) and apical four-chamber (AP4) views, resulting in a total of more than 40,000 echo frames. A computationally efficient multi-task deep fully convolutional network was proposed for LV segmentation and landmark detection in AP2 and AP4 views. Segmentation performance was assessed by using the Intersection over Union metric (IoU) or Dice score ranges from 0% to 100%. **Results:** When compared to a Level III echocardiographer's LVEF assessment, the 427 patients dataset machine learning EF (MLEF) had a mean Dice score of 92% for LV segmentation, a mean Euclidean distance of 2.85 pixels for LV landmark detection, 6.2% median absolute error and 7.9 % mean absolute error for biplane LVEF estimation. **Conclusion:** Machine learning analysis allowed an efficient and automated estimation of biplane LVEF compared to an expert-level assessment.

Poster Session 2 (P2)

Monday, June 24, 2019



P2-102

Artificial Intelligence Tools for Postinfarction Myocardial Recovery Prediction Based on Analysis of Echocardiographic Myocardial Texture

Blazej W. Michalski¹, Slawomir Skonieczka², Michal Strzelecki², Michal Simiera¹, Ewa Szymczyk¹, Paulina Wejner-Mik¹, Piotr Lipiec¹, Karina Wierzbowska-Drabik¹, Jaroslaw Kasprzak¹. ¹Dept. of Cardiology, Medical Univ. Lodz, Lodz, Poland; ²Institute of Electronics, Lodz Univ. of Technology, Lodz, Poland

Background: Left ventricular (LV) function recovery carries prognostic significance after myocardial infarction (MI) but is difficult to predict. We applied artificial intelligence (AI) to analyze myocardial texture for predicting long-term recovery of the left ventricle from unenhanced and contrast-enhanced myocardial images acquired 7 days after reperfused ST-elevation MI. **Methods:** Apical echocardiographic views (native or contrast-enhanced with iv Sonovue imaged with Contrast Perfusion Sequence, CPS) were recorded in 61 pts (19 females, age 59.7±11.9) with first ST-elevation MI treated with successful primary percutaneous coronary intervention. A custom software (MaZDa 4.6) was used for texture analysis. Briefly, 299 image features were calculated for defined regions of interest in each image (including 9 features from histogram, 6 from gradient matrix, 20 from run length matrix, 220 from co-occurrence matrix, and 44 from wavelet transform). Up to 10 most reproducible parameters were selected based on low variation and, later, Fisher criterion with minimization of classification error along with average correlation coefficient. AI approaches used to analyze textures included Multilayer perceptron neural network -MLP, support vector machines -SVM, and Adaptive Boosting algorithm AdaBoost. Recovery parameters were defined as: improvement of LV wall motion score index (WMSI), absence of remodeling defined as >8% increase in LV end-diastolic volume (LVEDV) and improvement >5% of LV ejection fraction % after 1 year. **Results:** Tested approaches had similar effectiveness for predicting regional and local LV function evolution after one year. Results for native grayscale and red component of CPS myocardial perfusion images were comparable. Rates of accurate prediction are shown in the table, with best result for WMSI prediction. **Conclusions:** Texture analysis with artificial intelligence tools can be applied to echocardiograms recorded 7 days after reperfused ST-elevation MI to predict recovery of myocardial function. Accuracy for predicting regional WMSI improvement was superior to prognosing LVEDV or EF change. Performance of different tools was similar both in native and contrast enhanced images.

Accuracy of 1-yr predictions of LV function change									
	ΔWMSI			ΔEF			ΔLVEDV		
	native grey	con-trast red	con-trast grey	native grey	con-trast red	con-trast grey	native grey	con-trast red	con-trast grey
Adaptive Boosting	78%	79%	78%	64%	54%	59%	61%	60%	60%
Neural network	77%	79%	78%	63%	63%	58%	62%	59%	60%
Support vector machine	77%	79%	78%	64%	65%	63%	61%	60%	58%

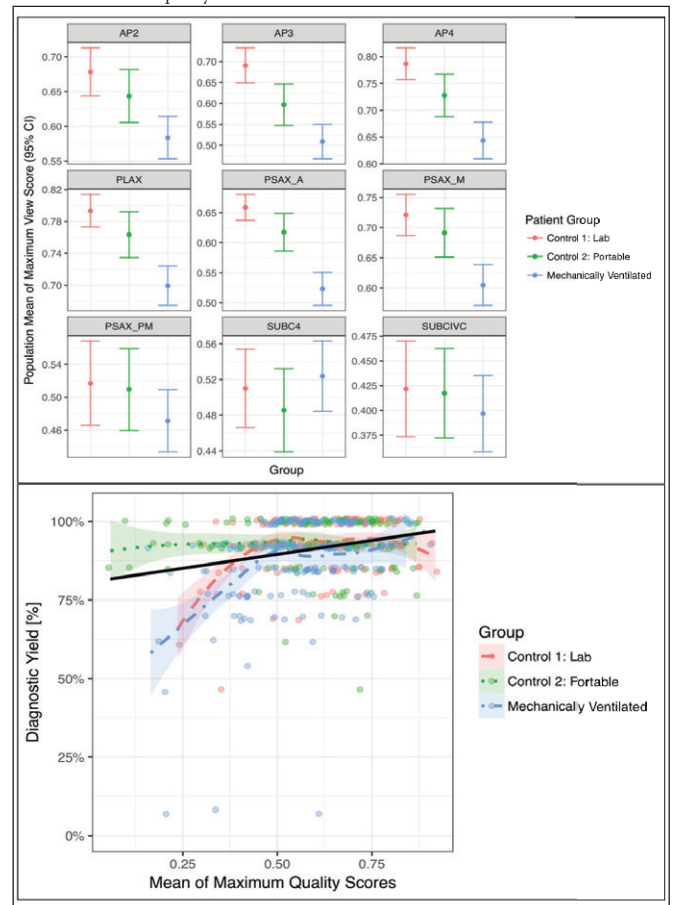
P2-103

Machine Learning Derived Video Quality Analysis and Diagnostic Yield of Transthoracic Echocardiograms

Christina L. Luong¹, Zhibin Liao¹, Amir Abdi¹, Hany Girgis¹, Robert Rohling¹, Kenneth Gin¹, John Jue¹, Darwin Yeung¹, Elena Szefer², Darby Thompson², Michael Tsang¹, Pui Kee Lee¹, Parvathy Nair¹, Purang Abolmaesumi¹, Teresa S.M. Tsang¹. ¹University of British Columbia, Vancouver, BC, Canada; ²Emmes Canada, Burnaby, BC, Canada

Background: This study evaluated the application of a machine learning model for automated video quality scoring of transthoracic echo (TTE) to three clinical groups.

Our objectives were: 1) Use machine learning for video quality analysis, 2) Establish the diagnostic yield of TTE by clinical group, and 3) Determine the relationship of machine learning video quality and diagnostic yield. **Methods:** A machine learning model was used to analyze TTE video clips from 3 matched cohorts for image quality scoring of nine standard views. Case TTEs were comprehensive studies in mechanically ventilated patients between 01/01/2010-12/31/2015. For each case TTE, there were two matched spontaneously breathing controls (Control 1: Inpatients scanned in the lab and Control 2: Portable ward studies). We report the overall mean maximum and view specific video quality scores. Diagnostic yield was calculated as the reported proportion of 12 standard parameters from the clinical database. An inverse probability weighted regression model was fit to determine the relationship between machine learning quality score and diagnostic yield. **Results:** 175 mechanically ventilated TTEs were included with 350 Controls (175 Control 1: Lab and 175 Control 2: Portable). The machine learning model analyzed 14,086 videos for quality. The overall mean maximum video quality score was significantly lower for mechanically ventilated TTEs (0.55 [95% CI 0.54, 0.56]) versus 0.61 (95% CI 0.59, 0.62) for Control 1: Lab and 0.64 (95% CI 0.63, 0.66) for Control 2: Portable; p= 0.002. Furthermore, mechanically ventilated TTEs were of lower diagnostic yield with fewer reported parameters. An inverse probability weighted linear regression model for the relationship of video quality and diagnostic yield of TTE demonstrate that higher video quality score is positively associated with diagnostic yield (Figure, black line). **Conclusion:** mechanically ventilated TTEs were of inferior quality and diagnostic yield compared to spontaneously breathing controls. Machine learning analysis allowed for efficient estimation of video quality not feasible with manual assessment.



P2-104

Artificial Intelligence for Visual Assessment of Left Ventricular Systolic Function in Patients with a Wide Range of Ejection Fraction

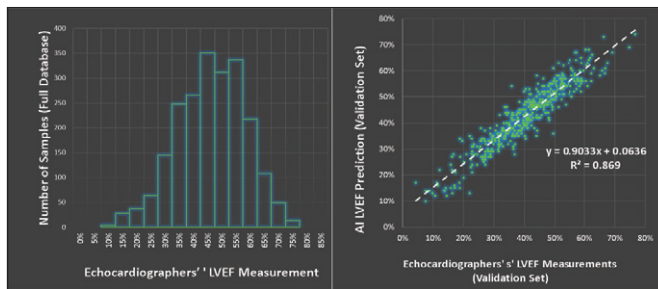
Delaram Behnami¹, Hany Y.A. Girgis^{2,3}, Christina Luong^{2,3}, Dale Hawley³, Robert Rohling¹, Kenneth Gin², Purang Abolmaesumi¹, Teresa Tsang^{2,3}. ¹Department of Electrical and Computer Engineering, University of British Columbia, Vancouver, BC, Canada; ²Division of Cardiology, University of British Columbia, Vancouver, BC, Canada; ³Vancouver Coastal Health, Vancouver, BC, Canada

Background: While echocardiography (echo) plays a vital role in the diagnosis of cardiovascular diseases, interpretation remains largely dependent on the expertise of the echocardiographer. Recent advances in artificial intelligence (AI) have proven powerful in analysis of complex medical data, such as echo. In this retrospective study, we investigate

Poster Session 2 (P2)

Monday, June 24, 2019

the feasibility of utilizing AI for estimation of left ventricular ejection fraction (LVEF). Of note, our method attempts to imitate the experienced echocardiographers' visual estimation of LVEF, which is independent of measurements of left ventricular dimensions or volume. **Methods:** An echo database was obtained from Vancouver Coastal Health, containing 2,181 exams, acquired within the period of 1/1/2010 to 31/12/2015. In a supervised learning framework, a deep neural network was trained to analyze apical four-chamber (A4C) and two-chamber (A2C) cine loops from patients with a wide range of LVEF and predict their LVEF (see Fig. 1, left for data distribution). The neural network consisted of three-dimensional convolutional layers which help extract relevant spatio-temporal features from cine loops and dense layers which then map these features to the expert-annotated LVEF. LVEF was labeled based on expert echocardiographers' reporting of the LVEF in the clinical database. The training data consisted of 1,751 echocardiographic studies, each including 15 frames extracted from A2C and A4C cine loops. The remaining 430 echocardiographic studies were used to validate the model. **Results:** Using the proposed approach, a root-mean-square error of 5.15% and R-squared (R^2) score of 0.869 were achieved (see correlation results in Fig. 1, right). In terms of qualitative predictions, normalized classification accuracies of 95%, 99%, 95%, and 96% were obtained for severe LV dysfunction ($LVEF \leq 20\%$), moderate LV dysfunction ($20\% < LVEF \leq 40\%$), mild LV dysfunction ($40\% < LVEF \leq 55\%$), and normal LV function ($55\% < LVEF < 80\%$), respectively. **Conclusion:** We demonstrated that AI-based video analysis can be reliably used to replicate experienced echocardiographers' visual assessment and estimate the echocardiographic LVEF. Future work is planned to further validate the presented method for use in a clinical setting.



P2-105

Artificial Intelligence Application for Assessing Point-of-Care Ultrasound Image Quality

Andrea Fung, Nathaniel Moulson, Shane Balthazaar, Hany Girgis, Nathan Van Woudenberg, Purang Abolmaesumi, Christina Luong, Ken Gin, John Jue, Michael Y.C. Tsang, Parvathy Nair, Teresa S.M. Tsang. University of British Columbia, Vancouver, BC, Canada

Comparison	ANOVA Analysis	Accuracy (for correctly identified images)
Subjective vs. A.I. Software Scoring of Cart-based Images	F(8,395) = 12.694, p<0.0001	73.54%
Objective vs. A.I. Software Scoring of Cart-based Images	F(8,395) = 12.618, p<0.0001	70.18%
Objective vs. A.I. Software Scoring of POCUS Images	F(8,395) = 10.006, p<0.0001	72.4%
Subjective vs. A.I. Software Scoring of POCUS Images	F(8,395) = 8.008, p<0.0001	77.40%

Background: A rapidly growing number of healthcare providers are integrating point-of-care ultrasound (POCUS) into clinical practice. As echocardiography is highly operator-dependent, concern exists that novice users of cardiac POCUS will acquire and interpret low quality images, affecting diagnostic accuracy and treatment decisions. We seek to address this issue by applying a novel Artificial Intelligence (A.I.) software that provides real-time quality feedback, guiding users in acquiring high quality images. Our objectives are: 1) to evaluate the accuracy of our A.I. software for assessing image quality compared to expert analysis (Level III Echocardiographer); and 2) to evaluate the accuracy of our quality assessment A.I. software applied to POCUS images compared to cart-based images. **Methods:** Patients were enrolled prospectively. Nine standard views were acquired from both cart-based machines and POCUS devices. Acquired images were randomized and received an objective and subjective image quality score by a Level III echocardiographer. Scoring systems were previously developed and validated methods, based on an adapted 4-point subjective rating of percent endocardial border visibility and an objective scoring method for assessing novice user image acquisition in POCUS. Images were then assessed for quality by the A.I. software, which uses a multi-layered network to extract relevant features and temporal dependencies. The network was trained on 17,400 quality-labelled cines. **Results:** Image data from 53 participants (2118 images) across 9 standard echo views show that overall mean accuracy of A.I. software scores, in comparison to both subjective

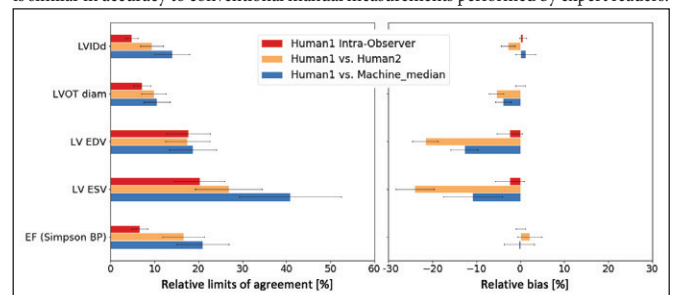
and objective expert scores, was higher in POCUS than cart-based image analysis (Table 1). Assuming normality of data, the A.I. software produced significantly lower quality scores across all views compared to expert scoring methods, as all 95% confidence intervals were above zero (Table 1). These results were consistent, regardless of false view classification by the A.I. software. **Conclusion:** While the A.I. software consistently underestimated image quality across all views for both POCUS and cart-based image analysis, it shows moderate accuracy for assessing image quality with maximal accuracy achieved in the extreme quality ranges of data.

P2-106

Application of Machine Learning to Two-Dimensional Echocardiographic Chamber Dimension and Function Measurements

Karima Addeia¹, Tatsuya Miyoshi², Kalie Kebed¹, Marcus Schreckenberg³, Alexandra Blitz³, Hendrik Wiebe³, Vivekanandan Amuthan⁴, Rodolfo Citro⁵, Masao Daimon⁶, Pedro Gutiérrez-Fajardo⁷, Ravi Kasliwal⁸, James N. Kirkpatrick⁹, Mark J. Monaghan¹⁰, Denisa Muraru¹¹, Kofo O. Ogonyankin¹², Seung Woo Park¹³, Ana Clara Tude Rodrigues¹⁴, Ricardo Ronderos¹⁵, Anita Sadeghpour¹⁶, Gregory Scalia¹⁷, Masaaki Takeuchi¹⁸, Wendy Tsang¹⁹, Edwin S. Tucay²⁰, Mei Zhang²¹, Federico M. Asch², Roberto M. Lang¹. ¹University of Chicago, Chicago, IL; ²MedStar Health Research Institute, Washington, DC; ³TOMTEC Imaging Systems GmbH, Unterschleissheim, Germany; ⁴Jeyalakshmi Heart Center, Madurai, India; ⁵University of Salerno, Salerno, Italy; ⁶The University of Tokyo, Tokyo, Japan; ⁷Hospitales Mac Bernardette, Guadalajara, Mexico; ⁸Medanta Heart Institute, Gurgaon, Haryana, India; ⁹University of Washington, Seattle, WA; ¹⁰King's College Hospital, London, United Kingdom; ¹¹University of Padova, Padova, Italy; ¹²First Cardiology Consultants Hospital, Lagos, Nigeria; ¹³Samsung Medical Center, Seoul, Republic of Korea; ¹⁴Albert Einstein Hospital, Sao Paulo, Brazil; ¹⁵Universidad Nacional de la Plata, Buenos Aires, Argentina; ¹⁶Rajaie Cardiovascular Medical and Research Center, Echocardiography Research Center, IUMS, Tehran, Islamic Republic of Iran; ¹⁷Genesis Care, Brisbane, Australia; ¹⁸University of Occupational and Environmental Health, Kitakyushu, Japan; ¹⁹Toronto General Hospital, University of Toronto, Toronto, ON, Canada; ²⁰Philippine Heart Center, Quezon City, Philippines; ²¹Qilu Hospital of Shandong University, Jinan, China

Background: Echocardiographic measurements of cardiac chamber size and function show wide inter- and intra-observer variability, largely because they are performed by different operators using different cardiac cycles and visual identification of boundaries in images that have a wide range of zoom, depth, focus, and image quality. To date, artificial intelligence algorithms have not been widely applied to 2D echocardiography. We hypothesized that a fully automated machine-learning algorithm would quantify chamber dimensions and function similarly to an expert trained reader, but faster and with less variability. **Methods:** A machine-learning algorithm was developed and trained on a database of >600 normal echocardiographic studies, to measure left ventricular (LV) end-diastolic dimension (LVIDd), LV outflow tract diameter (LVOT diam), LV end-diastolic and end-systolic volumes (EDV, ESV), and biplane ejection fraction (EF). Testing was performed on an independent group of 30 normal subjects and values compared to reference values obtained by a human expert using guideline-based manual measurement techniques. The reader repeated the measurements after 1 month to assess intra-observer variability. A 2nd independent reader performed the measurements to assess inter-observer variability. The human observers were allowed to choose the cardiac cycle in which to make measurements. The machine-learning algorithm was designed to make measurements in all available cardiac cycles and provide a median value. For each parameter, Bland-Altman analysis was used to calculate bias and 95% limits of agreement between the machine-learning algorithm and the expert reader 1 (both normalized by the mean of the two readers). These agreement metrics were compared to those of the inter- and intra-observer human readings. **Results:** Machine-learning measurements showed high consistency and excellent agreement with the expert reference, as reflected by a smaller bias than between the two human readers, but with wider limits of agreement (Figure), red for intra- and orange for inter-observer variability, and blue for machine learning). **Conclusions:** Machine learning algorithm for 2D echocardiographic chamber quantitation is similar in accuracy to conventional manual measurements performed by expert readers.



Poster Session 2 (P2)

Monday, June 24, 2019

P2-107

Real-Time Myocardial Perfusion Echocardiography with an Ultrasound Enhancing Agent for the Assessment of Coronary Allograft Vasculopathy in Children and Young Adult Heart Transplant Patients

Runqing Huang¹, Steven C. Greenway², Sharon L. Mulvagh³, Nowell M. Fine², Jason H. Anderson¹, Mary J. Hepinstall¹, Shalon A. Maxson¹, Paul J. Morrisette¹, Jenna M. Severson¹, Jonathan N. Johnson¹. ¹Mayo Clinic, Rochester, MN; ²The University of Calgary, Calgary, AB, Canada; ³Dalhousie University, Halifax, NS, Canada

Background: Cardiac allograft vasculopathy (CAV) is a major adverse prognostic factor for heart transplant (HT) recipients. Currently, invasive coronary angiography (ICA) is the gold standard for the detection of CAV but it lacks sensitivity for early microvascular changes and cumulative radiation exposure is of concern. Real-time myocardial perfusion echocardiography (RTMPE) is a non-invasive, non-ionizing alternative to assess cardiac and microvascular function. The objectives of this study were to determine the feasibility of RTMPE to detect CAV in young HT recipients. **Methods:** HT patients undergoing annual surveillance with ICA were recruited to undergo RTMPE using dobutamine stress and contrast agent Definity (Lantheus). Regional wall motion abnormalities (RWMA) and myocardial contrast perfusion (MP) were qualitatively assessed. Average myocardial blood flow (MBF, ml/min/g) at rest and peak stress was quantified using QLAB software (Philips). Myocardial blood flow reserve (MBFR) was defined as the ratio of peak to rest MBF. **Results:** A total of 36 patients from two centers were enrolled (Table 1). Of these, 13 patients also underwent intravascular ultrasound (IVUS) during ICA. We identified 5 patients with CAV by ICA and/or IVUS, two with obstructive disease and three with mild CAV. There were no serious adverse events related to RTMPE. RWMA were assessed in all patients. MP was assessed in 32 patients. MBFR quantification was feasible in 20 patients. MP and/or RWMA were present in 6 patients, two of whom had obstructive CAV and one had mild CAV. Patients with CAV had significantly lower MBFR than those without (2.04 ± 0.19 vs. 3.65 ± 1.70). Median MBFR was 2.71. Total cholesterol and low-density lipoprotein were observed to be higher in patients with MBFR < 2.71 (157±31 vs. 138±25, p < 0.04 and 85±23 vs. 65±16, p<0.03, respectively). **Conclusions:** These initial data demonstrate the novel application of dobutamine stress RTMPE using ultrasound enhancing agents to safely assess CAV in children and young adults. Further assessment is warranted to determine if this technique could provide an alternative noninvasive approach to current invasive standard of care.

Table 1. Patient characteristics.

	All Patients (n=36)	Patients with CAV (n=5)	Patients without CAV (n=31)	P
Male (n, %)	21 (58)	2 (40)	19 (61)	0.37
Age (years)	14 ± 5	20 ± 5	13 ± 4	0.005
Years post-transplant	7 ± 4	10 ± 5	7 ± 4	0.10
Transplant indication				
Cardiomyopathy	21 (58)	2 (40)	19 (61)	0.37
Congenital heart disease	15 (42)	3 (60)	13 (39)	0.37
Prior treated rejection	10 (36)	1 (20)	9 (29)	0.67
Diabetes	3 (8)	2 (40)	1 (3)	0.02
Hypertension	5 (14)	1 (20)	4 (13)	0.68
Hypercholesterolemia	5 (14)	1 (20)	4 (13)	0.68
Renal insufficiency	9 (25)	1 (20)	8 (26)	0.77
Statins treatment	20 (56)	2 (40)	18 (58)	0.45
MBFR	3.41 ± 1.67	2.04 ± 0.19	3.65 ± 1.70	0.002

P2-108

Effect of Diagnostic Intermittent High Mechanical Index Impulses on Global Longitudinal Strain in Patients with Normal versus Abnormal Systolic Function

Arif Albulushi, Joan Olson, Feng Xie, Ahmed Aboeta, Thomas Porter. University of Nebraska Medical Center, Omaha, NE

Background: Intermittent high mechanical index (MI) impulses from a transthoracic ultrasound transducer are recommended for regional wall motion (RWM) delineation and detection of myocardial perfusion following an intravenous administration of ultrasound enhancing agents (UEAs). High MI impulses >1.0 have also been shown to augment microvascular blood flow via a purinergic signaling pathway, but their effects on left ventricular (LV) myocardial function are unknown. **Objective:** We sought to determine the effect of transthoracic diagnostic high MI impulses on LV mechanics when utilized with UEAs to analyze RWM in patients with normal vs. abnormal systolic function. **Methods:** Thirty five patients referred for analysis of RWM were prospectively randomly assigned to very low MI (<0.2) imaging with intermittent high MI impulses (Group 1) vs. very low MI imaging alone (Group 2) during apical imaging (4,2, and 3 chamber). All imaging was performed during a 3% Definity (Lantheus Medical) infusion. High MI impulses were applied for five frames (1.8 MHz, 1.0-1.1 MI) intermittently in each apical window (two applications/view). Regional and global (GLS) longitudinal strain were measured at baseline prior to UEA administration and at five and 10 minute intervals after UEA administration and clearance from the blood pool. Patients with normal LV ejection fraction (LVEF)>50% were compared to those with abnormal LVEF in each Group. **Results:** Mean age was 61 ± 12 years. 18 patients (13 normal LVEF, 5 abnormal LVEF) were randomized to Group 1 and 17 (12 normal LVEF, 5 abnormal LVEF) randomized to Group

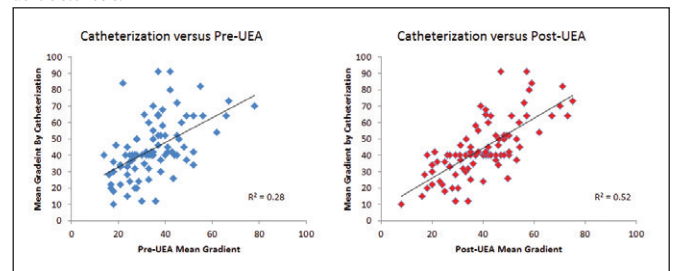
2 (no high MI impulses). There were no differences between Groups with respect to age, gender, or cardiac risk factors. GLS increased at five (p<0.05) and 10 (p<0.0001) minutes in Group 1 patients but did not change in Group 2 patients at these time intervals. The increase in GLS in Group 1 high MI patients was especially pronounced in those with a low LVEF (35±8% increase in GLS in patients with low LVEF group versus 9±9% increase in normal LVEF group, p<0.001). **Conclusion:** Intermittent transthoracic high MI impulses applied during a commercially available UEA infusion significantly improve LV mechanics for up to 10 minutes after completion of imaging. This increase is most marked in patients with depressed LV systolic function, and therefore may be a therapeutic application in patients with ischemic or non-ischemic cardiomyopathies.

P2-109

The Effect of Ultrasound Enhancing Agents on Transaortic Doppler Measurement in Severe Aortic Stenosis

Daniel Musikantow, Rajeev Samtani, Solomon Bienstock, Asaf Rabinovitz, Martin Goldman, Lori Croft. Icahn School of Medicine at Mount Sinai, New York, NY

Background: Echocardiography (echo) is the primary diagnostic modality for the diagnosis and quantification of aortic stenosis (AS). Because clinical decisions are based on the echo measurements, it is essential that the assessment of AS peak and mean gradients are accurate. The use of ultrasound enhancing agents (UEAs) has become an integral component of an echo exam and is recommended for the quantification of left ventricular volumes, ejection fraction and regional wall motion. UEAs are also frequently used to enhance the signal during Doppler analysis however little is known about their effect on the measured velocities. **Methods:** In a single center, we performed a retrospective analysis of 290 echocardiograms using UEAs in patients with severe AS, defined as a valve area < 1.0cm². Peak and mean Doppler gradients were individually traced and measured before and after infusion of UEA. When available, mean transaortic gradients from catheterization were compared against the values obtained from echo-Doppler interrogation. **Results:** Duplicate studies of patients, patients with atrial fibrillation and those without post-UEA Doppler images were excluded from the study. 195 studies remained available for analysis, 92 of whom had gradients available from catheterization. The peak velocity recorded by continuous wave Doppler increased from an average of 3.65 ± .65 m/s to 3.90 ± .79 m/s (P<.001) with UEA enhancement. Mean gradient also increased from an average of 33.7 ± 13.4 mmHg to 39 ± 15.6mmHg (P<.001). Of the 135 patients with initial peak transaortic velocities < 4m/s, 38 patients (28%) reached a peak velocity of ≥ 4m/s with use of UEAs. The values obtained with UEA echocardiography correlated better with mean gradients obtained by catheterization compared to pre-UEA images (R² = .51 versus .28, P < .05). **Conclusion:** UEAs enhance the visualization of Doppler signal. This results in significantly higher measured velocities across the aortic valve and allows for categorization of patients with previously discordant metrics of AS severity. Furthermore, post-UEA measurements demonstrate improved correlation with invasive hemodynamics. Further studies are needed to analyze the effects of UEA in other Doppler measurements and in those without severe aortic stenosis.



P2-110

Fully Automated Echocardiographic Artificial Intelligence Software Could Replace Contrast Agents for Improving Accuracy of Left Ventricular Ejection Fraction Quantification

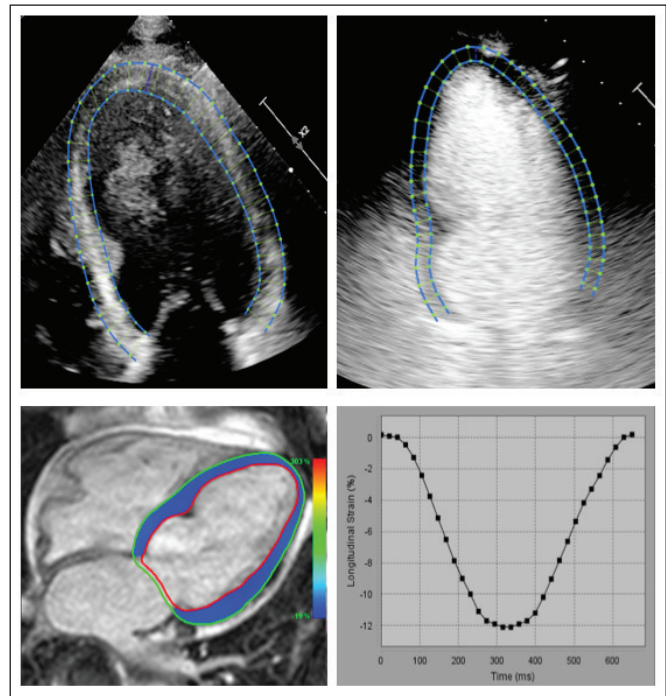
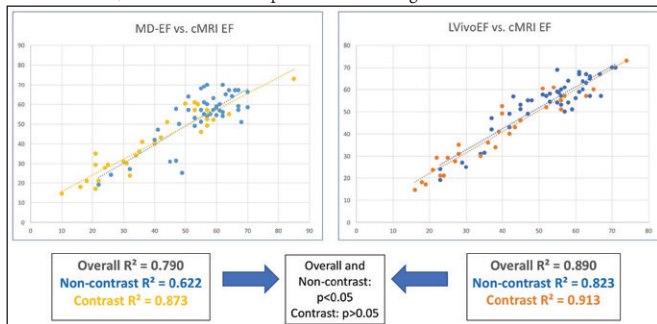
Solomon Bienstock, Rajeev Samtani, Steve Liao, Usman Baber, Lori Croft, Eric Stern, Martin Goldman. Icahn School of Medicine at Mount Sinai, NY, NY

Background: Transthoracic echocardiography (TTE) plays an integral role in the diagnosis and management of cardiac disease. However, quantitative analysis of left ventricular ejection fraction (LVEF) is labor intensive, time consuming, and frequently subjective with wide inter and intra-observer variability. Ultrasound contrast agents can improve LVEF analysis, but cost and IV administration limit their use. We sought to determine if LVEF calculated by an artificial intelligence (AI) software (LVivoEF by DIA*) is more accurate than the physicians' measurement (MD-EF), using cardiac MRI (cMRI) as the gold standard. **Methods:** This is a retrospective single center study of 76 patients (pts) who underwent both routine TTE and cMRI within 6 months with no interval cardiac intervention or clinical event. Pts' 4-chamber EF's were analyzed using LVivoEF by DIA*, AI software quantification that uses pattern recognition, machine learning, and image processing algorithm for automated detection and tracking of the LV endocardial border

Poster Session 2 (P2)

Monday, June 24, 2019

to determine LVEF. Using linear regression and the Fisher r to z transformation, AI generated EF's were compared to the EF by cMRI and physician read EF (MD-EF), for both contrast and non-contrast studies. **Results:** We studied 76 patients (59% M, 41% F, mean age 54.3 years, range 20-88 years), mean LVEF by cMRI was 48.6, range 14.6 to 73.0. Using the ASE definitions for EF: 42 had a normal EF (>51%), 14 mildly abnormal EF's (41-51%), and 21 moderate-severe abnormal EF's (<40%). For all pts, there was a stronger correlation between LVivoEF and cMRI derived EF ($R^2=0.890$) than by MD-EF ($R^2=0.790$) ($p=0.036$). Importantly, in non-contrast studies compared to cMRI, LVivoEF ($R^2=0.823$) was significantly better than MD-EF ($R^2=0.622$) ($p=0.039$), while for contrast studies, LVivoEF ($R^2=0.913$) and MD-EF ($R^2=0.873$) were similar ($p=0.453$) (Figure). **Conclusion:** Compared to cMRI, LVivoEF AI was more accurate than physician measured LVEF's overall and for TTE's without contrast and was similar to MD-EF for contrast enhanced studies. Thus, LVivoEF AI could standardize accurate TTE quantification of LVEF without the added time, IV insertion and expense of contrast agents.



P2-111

Contrast-Enhanced Echocardiographic Measurement of Longitudinal Strain: Accuracy and Its Relationship with Image Quality

Ilya Karagodin, Davide Genovese, Eric Kruse, Amit R. Patel, Nina Rashedi, Roberto M. Lang, Victor Mor-Avi. University of Chicago, Chicago, IL

Background: The importance of left ventricular (LV) global longitudinal strain (GLS) is increasingly recognized in a variety of clinical scenarios. However, in a subset of patients with poor image quality, GLS measurement is difficult or impossible without the use of contrast enhancement. Recently, we demonstrated the feasibility of contrast-enhanced GLS measurements. We sought to determine whether contrast enhancement improves (1) the accuracy of GLS measurements against cardiac magnetic resonance (CMR) reference, and (2) their reproducibility compared to non-enhanced GLS. Additionally, we evaluated the dependence of accuracy and reproducibility on image quality. **Methods:** We prospectively enrolled 25 patients undergoing clinically indicated CMR imaging who consequently underwent transthoracic echocardiography (TTE) with and without low-dose contrast injection of Optison (1 mL Optison/3 mL saline IV, GE Healthcare). GLS was measured from both non-contrast and contrast images using speckle tracking software (Epsilon Imaging). These measurements were compared to each other and to CMR reference values obtained using feature tracking software (SuiteHEART, Neosoft). Inter-technique comparisons included linear regression and Bland Altman analyses. Repeated measurements in a randomly selected subgroup of 15 patients were used to assess inter-observer variability using intra-class correlation (ICC). **Results:** Contrast-enhanced GLS was in close agreement with non-enhanced GLS measurements ($r = 0.96$; bias: $0.0 \pm 1.2\%$). Reproducibility of contrast-enhanced GLS was better than non-enhanced GLS (ICC = 0.94 vs. 0.90). Also, the agreement between contrast-enhanced GLS and CMR ($r = 0.83$; bias: $0.8 \pm 2.3\%$) was better than for non-enhanced GLS ($r = 0.75$; bias: $0.9 \pm 2.6\%$). In 12/25 patients with suboptimal TTE images that rendered GLS difficult to measure, contrast-enhanced GLS showed better agreement with CMR than non-enhanced GLS ($r = 0.88$ vs. 0.84), and also higher reproducibility (ICC = 0.98 vs. 0.93). **Conclusions:** We found that contrast-enhanced TTE images can be used to accurately and reproducibly measure GLS, resulting in good agreement with CMR, even in patients with suboptimal acoustic windows. This approach may aid in the assessment of LV function in this patient population.

P2-112

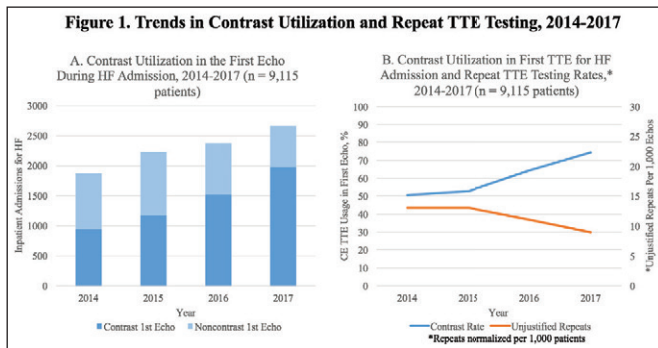
Routine Use of Contrast at Admission Transthoracic Echocardiogram for Heart Failure Reduces the Rate of Repeat Echocardiograms During Index Admission: Observational Data from 9,115 Patients

Katherine C. Lee^{1,2}, Shizhen Liu¹, Patrick Callahan¹, Theresa Green¹, Terika Jarrett¹, Kenneth S. Edwards¹, Mani Vannan¹. ¹Piedmont Heart Institute, Atlanta, GA; ²Georgia Institute of Technology, Atlanta, GA

Background: Heart Failure (HF) is the 4th most common cause for all admission to US hospitals, and it is the most common reason for inpatient TTE. We developed a disease-based contrast use protocol for all patients receiving TTE for HF admission at our echo lab, irrespective of image quality. The goal of this retrospective analysis of the database was to evaluate the impact of this disease-based contrast protocol for HF admission on the number of repeat TTEs and LOS for an index HF admission. **Methods:** 9,115 admissions (between 2014 and 2017) to PAH (5,337 men; mean age 67.6 ± 15.0 years) were identified as HF or HF-related admissions. Inclusion criteria included HF symptoms and ICD-10-CM coding for HF. All patients received at least one TTE during admission. Patients were separated into those who received Definity[®] in the first TTE (contrast group) and those who did not (non-contrast group). Repeat TTEs were classified as justified if performed for concrete clinical indications (details in manuscript). All other repeat TTEs were classified as unjustified. **Results:** HF admissions to PAH increased from 1,867 in 2014 to 2,655 in 2017, totaling 9,115 admissions ($n = 5,600$ contrast group, 3,515 non-contrast group). Of these, 927 patients had repeat TTE testing ($n = 505$ contrast group, 422 non-contrast group), which was considered justified in 823 patients. Thus, 104 patients had unjustified repeat TTEs, of which 80 belonged to the non-contrast group (76.7%) and 24 belonged to the contrast group. Also, overall contrast usage in the first echo increased from 50.4% in 2014 to 74.3% in 2017 (Figure 1A), and the rate of unjustified repeats decreased 30.7% from 13 to 9 per 1,000 echos (Figure 1B). Across all 9,115 admissions, the rates of unjustified repeat TTE were 2.3% and 4% (non-contrast and contrast groups, respectively), with patients in the contrast group receiving fewer echos per admission ($n = 9,115$, $p < 0.05$). Thus, patients who did not get contrast in the first TTE were five times as likely to have an unjustified repeat TTE during an admission for HF. **Conclusions:** Thus, routine use of contrast in the first TTE for HF significantly decreases repeat TTE testing during an index HF admission. This trend was seen even when baseline contrast usage was high. This may also have implications for LOS for HF (data being finalized) and cost savings.

Poster Session 2 (P2)

Monday, June 24, 2019

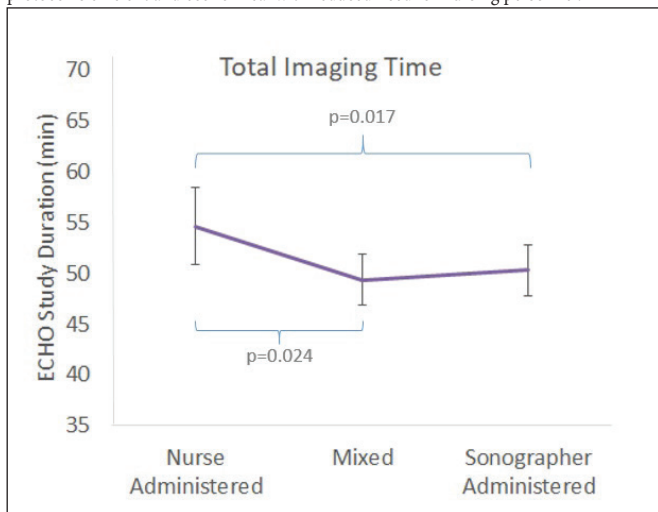


P2-113

Optimizing Contrast Enhanced Echocardiography by Employing a Sonographer Administered Intravenous Line and Echo Enhancement Protocol

Courtney R. Usry, Satoshi R. Shin, Rosco Gore. San Antonio Military Medical Center; Fort Sam Houston, TX

Background: Up to 20% of echocardiograms obtained are suboptimal, leading to further downstream testing. Contrast enhanced echocardiography is endorsed for use by the American Society of Echocardiography (ASE) when 2 or more adjacent wall segments are not well visualized. However, varied institutional protocols limit such use due to increased study time and personnel needed to obtain such imaging. **Methods:** We aimed to evaluate if intravenous (IV) line placement and contrast administration by sonographers led to decreased time to complete outpatient echocardiography exams when compared to having a nurse perform both. Sonographers received a one-day training on the techniques for contrast administration and for IV placement. Baseline completion times utilizing the nurse administered protocol were taken from March 2015 to June 2015. Sonographers who had completed training began administration of contrast after a nurse placed the IV in a mixed protocol. After a three month familiarization period, data on study duration was recorded. Sonographers were then trained to place an IV line and after a familiarization phase, data collection was performed for the sonographer administered protocol. The study duration times from the three groups were compared. **Results:** A total of 232 patients were included for analysis (47 patients in the nurse administered protocol, 85 patients in the mixed protocol, and 100 patients in the sonographer administered protocol). The time spent obtaining contrast enhanced imaging was not significantly different between the groups ($p = 0.116$). There was a significant difference in time spent to complete each echocardiogram when comparing the mixed protocol at 49.4 ± 11.4 minutes, and the nurse administered protocol at 54.6 ± 12.9 minutes ($p = 0.024$). Also, the difference in time spent to complete each exam was shorter with the sonographer administered protocol (50.3 ± 12.6 minutes) in comparison to the nurse administered protocol ($p = 0.017$). **Conclusion:** Utilizing a protocol that allows the sonographer to administer echo contrast reduced the study time by approximately 5 minutes. Allowing the sonographer to also place the IV did not significantly increase study time. This indicates that a sonographer driven protocol is efficient and economical with reduced need for nursing personnel.



P2-114

Impact of Contrast Echocardiography on Clinical Outcomes in Critically Ill Patients

Michael L. Main¹, Rao Fu², Jake Gundrum², Cesare Orlandi³, Nancy M. Allen LaPointe⁴, Sharon Mulvagh⁵. ¹Saint Luke's Mid America Heart Institute, Kansas City, MO; ²Premier Applied Sciences, Premier Inc., Charlotte, NC; ³Lantheus Medical Imaging, Billerica, MA; ⁴Premier Applied Sciences, Premier, Inc., Charlotte, NC; ⁵Dalhousie University, Halifax, NS, Canada

Background: Ultrasound contrast agents (UCAs) improve image quality in patients with baseline technically difficult studies. Limited data suggests UCA use is associated with changes in subsequent clinical management and lower mortality in intensive care unit (ICU) patients. We conducted a retrospective observational study to determine if contrast echocardiography (versus non-contrast echocardiography) is associated with differences in length of stay, subsequent resource utilization, and patient management in the ICU setting. **Methods:** The Premier Healthcare Database (Charlotte, NC) was analyzed to identify ICU patients receiving DEFINITY[®] vs. no use of contrast during the initial rest transthoracic echo (TTE). The primary outcomes of interest were subsequent TTE and transesophageal echocardiography (TEE) during the index hospitalization, and ICU length of stay (LOS). Prior to comparing outcomes between the DEFINITY[®] and no-contrast cohorts, propensity scoring was used to statistically model treatment selection to minimize selection bias. Patient, clinical, index visit and hospital characteristics were included in a logistic regression model to generate propensity score. **Results:** A total of 1,538,864 patients from 773 hospitals were identified as undergoing resting TTE in the ICU with DEFINITY[®] in 51,141 (3.3%) patients and no contrast agent use in 1,487,723 (96.7%) patients. After adjusting for patient, clinical, and hospital characteristics, an adjusted analysis for subsequent TTE and TEE showed that during the index hospitalization, patients in the Definity[®] cohort were less likely to undergo a subsequent TTE or TEE as compared to those in the no contrast cohort (odds ratio=0.704 for TTE, odds ratio=0.841 for TEE; $p < 0.0001$ for both). Adjusted mean ICU LOS for the Definity[®] cohort was approximately 10% shorter than that of the no contrast cohort (4.15 vs. 4.59 days, $p < 0.0001$). Compared to the no contrast cohort, patients receiving DEFINITY[®] were more likely to start use of parenteral inotrope (3.8% vs. 2.4%), end use of parenteral inotrope (0.6% vs. 0.3%), start use of parenteral pressor (12.8% vs. 11.6%) and end use of parenteral pressor (4.3% vs. 3.2%) on the day of, or one day after the index TTE (all $p < 0.0001$). **Conclusions:** DEFINITY[®]-enhanced echocardiography in the ICU setting (in comparison with non-contrast TTE) was associated with lower rates of subsequent TTE and TEE during the index hospitalization and shorter ICU LOS.

P2-115

Correlation of Microvascular Perfusion Patterns Observed in the Acute Setting of Takotsubo Cardiomyopathy with Angiogram Findings, Electrocardiography, Biomarkers, and Recovery of Systolic Function

Chetaj Mahabir, Lalit Wadhvani, Sourabh Aggarwal, Gregory Pavlides, Feng Xie, Thomas R. Porter. University of Nebraska Medical Center, Omaha, NE

Background: Takotsubo cardiomyopathy (TC) is defined as transient systolic dysfunction associated with characteristic clinical and laboratory findings. Although the prognosis has been considered good, morbidity and mortality may be worse when microvascular perfusion is affected. Our objective was to determine how microvascular flow, measured with real time myocardial contrast echocardiography (RTMCE) correlates with angiographic and biomarkers obtained, and ultimately how this affects recovery of systolic function. **Methods:** 47 patients presenting acutely with TC from January 2012 - July 2017 that had RTMCE using intermittent high mechanical index (HMI) impulses and continuous infusions of ultrasound contrast were included. The presence of microvascular obstruction (MVO) was defined as either a persistent myocardial contrast defect during the plateau phase of the infusion or reduced microvascular blood flow (delay in replenishment > 4 seconds following HMI impulses). The segmental extent of the resting wall motion (WM) abnormality (17 segment model), TIMI flow at angiography, peak troponin levels, and presence of transient ST changes on EKG were correlated with the presence of MVO, as was subsequent recovery of systolic function (LVEF). **Results:** MVO was seen in 23 patients (49%). There was no difference in demographic variables, peak troponin levels, presence of ST segment abnormalities on EKG, or TIMI flow in the left anterior descending in the MVO versus no MVO groups. However, patients with MVO were more likely to have a larger extent of resting WM abnormality (7.7 ± 2.0 segments MVO group versus 5.4 ± 1.6 segments no MVO; $p < 0.001$), and had a lower rate of recovery of systolic function at follow up ($p = 0.02$ compared to no MVO group; Table). **Conclusion:** In the current era, the frequency of MVO in TC cardiomyopathy is over 48%. The presence of MVO is associated with larger functional abnormality in the acute setting, and less frequent recovery of systolic function.

Poster Session 2 (P2)

Monday, June 24, 2019

Table
Comparison between MVO and no MVO

	Group 1 (MVO)	Group 2 (no MVO)
Gender		
Male	5	5
Female	18	19
Diabetes	4/23 (17.4%)	7/24 (29.2%)
< TIMI 3 Flow	6/23 (26.1%)	2/24 (8.3%)
ST depression or elevation	2	6
Peak Troponin	1.2±1.3	3.8±8.0
Wall motion abnormality (number of segments involved)	7.7±2.0	5.4±1.6*
LVEF recovery on follow up within 1-6 months	11/19 (57.9%)	16/17 (94.1%)**

*p<0.001
**p=0.02

P2-116

Improving Visualization of Right Ventricular Size and Function in the ICU

Mohammed T. Essa, Jason Pereira, Michael Vaccarelli, Ian Crandall, Ifeoma Ugonabo, Lissa Sugeng. Yale School of Medicine, New Haven, CT

Background: Evaluation of the right ventricle (RV) is challenging especially in intensive care unit (ICU) patients. There is limited data on the use of contrast echo to better delineate the RV in this patient population. The purpose of this study is to determine the feasibility of using contrast echo (CE) to evaluate the right ventricular size, function and wall motion in ICU patients (pts). **Methods:** Thirty ICU pts who required CE for left ventricular opacification were included in this study. Patients with atrial or ventricular arrhythmias were excluded. Our transthoracic echocardiographic (TTE) protocol includes multiple two-dimensional echocardiographic imaging of the RV: parasternal long-axis, papillary level short-axis, an apical 4-chamber and apical RV focused view which were obtained with and without CE (unenhanced = UE). A dedicated RV view is acquired by maintaining a non-foreshortened left ventricular 4-chamber view, narrowing the sector size to focus on the RV. RV end-diastolic dimensions at the base (RVBASE), mid (RVMID), and longitudinal (RVLONG), RV end-diastolic area (RVEDA), RV end-systolic area (RVESA), and fractional area change (FAC) were measured with and without CE. In the RV focused view, RV contractility was assessed with a wall motion score index (WMSI), on CE and UE. Inter- and intra-observer variability was performed. **Results:** All 30 patients were analyzed by 2 independent observers. Patients had a mean age of 66 ± 15 years, 47% were female with a BMI of 32 ± 10 kg/m² and BSA 1.95 ± 0.3. RVBASE, RVMID, RVEDA, RVESA and SAX measurements were significantly larger on CE versus UE measurements. No significant difference was seen in PLAX RVOT and RV long diameters. There was a significant difference in WMSI (0.9 ± 0.08 vs 1.2 ± 0.08; UE vs CE images, P < 0.05). Inter and intra-observer variability were generally lower on CE vs UE (table2). From basal and mid RV diameter cutoffs for enlargement, 8 (27%) and 9 (30%) of cases respectively were reclassified to enlarged according to 2015 ASE recommendations for RV sizing, P < 0.05. **Conclusion:** Expanding the role of CE to include evaluation of RV size, function and wall motion is feasible in the ICU patients. CE in the assessment of the RV improves visualization and reduces variability in measurements.

Table 1. RV Parameters on Unenhanced (UE) & Contrast Enhanced (CE) Images.

RV Parameters	2D UE (n=30)		2D CE (n=30)		Difference	P Value
	Mean	SD	Mean	SD	CE-UE	
RV Base (cm)	3.74	0.60	4.04	0.51	0.31 ± 0.54	< 0.05
RV Mid (cm)	2.86	0.43	3.23	0.43	0.36 ± 0.48	< 0.05
RV Long (cm)	7.52	0.95	7.73	0.97	0.21 ± 0.72	NS
RV EDA (cm ²)	20.69	4.55	23.14	5.20	2.45 ± 4.64	< 0.05
RV ESA (cm ²)	13.85	4.48	15.85	4.49	1.99 ± 3.48	< 0.05
FAC (%)	33.66	12.33	31.53	11.44	-2.12 ± 9.6	NS
WMSI	0.88	0.43	1.20	0.45	0.31 ± 0.36	< 0.05
PLAX RVOT (cm)	3.0	0.55	3.13	0.59	0.13 ± 0.47	NS
SAX RV (cm)	2.24	0.63	2.63	0.72	0.39 ± 0.7	< 0.05

Table 2. Reproducibility of RV measurements on 2DE and CE

RV Parameters	Inter-observer variability %		Intra-observer variability %	
	2D UE Mean %	CE Mean %	2D UE Mean %	CE Mean %
RV BASE (cm)	13.7 ± 13.6	7.1 ± 5.4	7.9 ± 8.8	7.9 ± 9.6
RV MID (cm)	17.3 ± 10.3	6.4 ± 7.5	11.9 ± 5.7	4.8 ± 7.5
RV LONG (cm)	5.8 ± 5.1	5.9 ± 5.3	5.5 ± 3.1	4.5 ± 3.2
RV EDA (cm ²)	15.4 ± 12.2	14.9 ± 9.7	7.2 ± 5.3	8.1 ± 5.0
RV ESA (cm ²)	19.5 ± 17.2	16.8 ± 11.4	12.8 ± 10.3	8.1 ± 5.8
FAC %	37.2 ± 20.4	24.5 ± 24.8	29.1 ± 33.8	12.5 ± 6.6
PLAX RVOT (cm)	16.8 ± 6.5	17.3 ± 12.8	6.8 ± 5.6	5.7 ± 6.7
SAX RV (cm)	31.3 ± 21.3	13.7 ± 12.5	10.8 ± 9.8	5.7 ± 4.8

P2-117

Routine Use of Contrast Echocardiography in the Evaluation of Hypertrophic Cardiomyopathy

Srikanth Yandrapalli, Abdallah Sanaani, Mallory O'Shea, Srihari Naidu, Daniel Spevack, Tanya Dutta. Westchester Medical Center, Valhalla, NY

Background: The use of echocardiographic contrast enhancement (CE) is recommended to better visualize the left ventricle. CE may provide significant benefit in the setting of poor visualization and high index of suspicion for hypertrophic cardiomyopathy (HCM). Data are lacking regarding the implications of CE on various wall measurements in the evaluation of HCM. **Methods:** 100 consecutive pre-CE and post-CE transthoracic echocardiograms (TTE) of patients referred to our HCM clinic were evaluated by 2 blinded observers. The left ventricular basal septal, mid-septal, and basal inferolateral walls in the parasternal long axis view, and basal lateral and apical walls in the apical 4-chamber images were measured. Poorly visualized segments were recorded as uninterpretable. Categorical variables and continuous variables were compared using the Pearson chi-square and the t-test respectively. Inter-observer reliability between pre-CE and post-CE measurements were analyzed using the concordance correlation coefficient. Comparisons were done between interpretable measurements. **Results:** Of the 1000 segments measured by both observers, 35 (3.5%) were not seen pre-CE versus only 5 (0.5%) post-CE (P<0.001). Apical visualization improved with CE (31 poorly visualized apical segments pre-CE versus 0 segments post-CE, P<0.001). Of the 200 TTE interpretations by both observers combined, TTEs with at least 1 uninterpretable segment decreased from 32 (16%) without CE to 5 (2.5%) after CE (P<0.001). Use of CE resulted in significant reductions in reported measurements for basal septal, mid septal, and apical segments; **Figure 1.** While the inter-observer reliability was poor at baseline, use of CE modestly improved inter-observer agreement for all segments except the mid septum; **Figure 2.** **Conclusion:** CE in the routine evaluation of HCM improved readability, apex visualization, and modestly improved inter-observer agreement. CE use also resulted in mild but significant reductions in reported measurements.

Figure 1: Within-observer differences in measurements with contrast enhancement.

Wall segment	Observer 1				Observer 2			
	Pre-contrast measurement (mean±SD)	Post-contrast measurement (mean±SD)	Mean difference (±SD) (mm)	P value	Pre-contrast measurement (mean±SD)	Post-contrast measurement (mean±SD)	Mean difference (±SD) (mm)	P value
Basal septum	16.2±5.9	14.8±5.5	1.5±3.2	<0.001	15.7±5.4	14.2±5.2	1.4±3.6	<0.001
Mid septum	16.1±6.5	13.8±6.9	2.3±3.7	<0.001	15.6±5.9	12.9±6.3	2.7±4.3	<0.001
Basal inferolateral	9.3±3.0	9.1±3.0	0.1± 2.4	0.67	8.9±2.9	9.5±3.2	-0.6± 2.7	0.031
Basal lateral	9.0±3.3	9.1±3.5	-0.14±3.2	0.656	8.3±3.2	8.7±4.0	-0.5±3.1	0.102
Apex	8.3±3	6.9±2.6	1.3±3.5	0.001	7.5±3.3	6.5±2.2	1.1±2.7	<0.001

Figure 2: Inter-observer agreement between pre-contrast and post-contrast wall measurements.

Wall segment	Concordance correlation coefficient for pre-contrast inter-observer measurements	Concordance correlation coefficient for post-contrast inter-observer measurements
Basal septum	0.73	0.78
Mid septum	0.78	0.77
Basal inferolateral	0.48	0.55
Basal lateral	0.28	0.59
Apex	0.41	0.49

P2-118

Clinical Significance of Contrast-Enhanced Ultrasonography for Assessment of the Vasa Vasorum in Young Patients with Familial Hypercholesterolemia

Nobutaka Noto, Tomoo Okada, Masataka Kato, Akiko Komori, Yayoi Yoshino, Shino Jimbo, Mamoru Ayusawa, Ichiro Morioka. Nihon University, Tokyo, Japan

Background: Although proliferation of the adventitial vasa vasorum (VV) detected by contrast-enhanced ultrasound (CEUS) of the carotid arteries is considered to occur before the development of atherosclerotic plaque, its clinical significance in young patients with familial hypercholesterolemia (FH) remains unclear. **Methods:** To investigate the association between carotid VV by CEUS and the structural changes in the carotid wall, 26 FH patients without carotid plaque (median age: 28.3 years) and 8 age-matched healthy control subjects were enrolled to measure the mean carotid intima-media thickness (CIMT) and elastic property (Ep). CEUS was performed in contrast harmonic imaging mode after a bolus injection of Sonazoid (perflubutane, GE Healthcare, Norway). We set the region of interests (ROIs) in the lumen (L) and the near wall of the common carotid artery (W), and a time-intensity curve was generated for each area. The enhanced intensity (EI) [peak intensity - baseline intensity] and the ratio of EI (EIW/EIL) to quantify VV were calculated. The FH patients were divided into 3 groups according to the CIMT based on differences from the age-matched normal control values (n=35) or the use of HMG-CoA reductase inhibitors (statins) (G-1 (n=8): CIMT < 0.55 mm [SD < +2.0] without

Poster Session 2 (P2)

Monday, June 24, 2019

statins; G-2 (n=9): $0.55 \leq \text{CIMT} < 0.61 \text{ mm} [+2.0 \leq \text{SD} < +2.5]$ without statins; G-3 (n=9): $\text{CIMT} \geq 0.61 \text{ mm} [\text{SD} \geq +2.5]$ with statins), and these variables were compared among the groups. **Results:** There was no significant difference in age (p=0.07), sex (p=0.97), or EIL (p=0.52) among the 4 groups. Compared with controls, G-1, G-2, and G-3 had a significantly greater Ep (KPa) (p=0.003). In contrast, G-2 had a significantly greater EIW/EIL than the controls, G-1, and G-3 (0.56 ± 0.11 vs. 0.31 ± 0.05 vs. 0.36 ± 0.05 vs. 0.34 ± 0.07 , respectively p<0.001); however, there was no significant difference between the controls and G-3 (p=0.33). Excluding G-3, CIMT was correlated with EIW (r=0.81), EIW/EIL (r=0.75), and Ep (r=0.75) in the 3 groups. Multiple linear regression analysis demonstrated EIW/EIL to be a significant determinant of CIMT ($\beta=0.504$, p<0.001). When we defined a CIMT value of over +2.0 SD as a marker of atherosclerosis in patients without statins, patients with an EIW/EIL value over 0.49 were more likely to have (OR=36.0, AUC=0.92) atherosclerosis. **Conclusion:** Our study suggested that a greater EIW/EIL indicates proliferation of carotid VV and statins attenuate this proliferation in the absence of CIMT changes. Thus, carotid CEUS may provide a noninvasive method to monitor therapeutic interventions in young FH patients, independent of CIMT.

P2-119

Ultrasound Enhancing Agents Significantly Improve the Accuracy of Transthoracic Echocardiography for the Diagnosis of Hypertrophic Cardiomyopathy

Huazhen Chen, Edward Chu, Asaf Rabinovitz, Steve Liao, Lori Croft, Martin Goldman. Icahn School of Medicine at Mount Sinai, New York, NY

Background: Hypertrophic cardiomyopathy (HCM) is the most common inherited cardiomyopathy characterized by left ventricular (LV) hypertrophy without a secondary etiology. On transthoracic echocardiography (TTE), HCM is diagnosed when LV wall thickness exceeds 15mm and is most frequently seen in the LV basal septum and apex. Inability to visualize LV walls, the apex and possible aneurysm can lead to misdiagnosis of HCM, which can have serious implications for patients, their families, and the need for additional medical evaluation. Ultrasound enhancing agents (UEA) are used to enhance LV opacification and endocardial border definition thereby improving TTE diagnostic accuracy. We studied the use of UEA to improve the diagnostic accuracy of TTE for HCM. **Methods:** TTE images were reviewed for 78 patients who underwent evaluation for known or suspected HCM at Mount Sinai Hospital. Thickness of the LV basal septum was measured in the parasternal long axis view. Apical HCM was defined as LV apical hypertrophy in a "spade" like morphology at end-systole in the apical 4 chamber view. Presence of an apical aneurysm was assessed in the apical 2, 3 and 4 chamber views. Indication for implantable cardioverter-defibrillator (ICD) was defined as basal septal hypertrophy $\geq 30\text{mm}$. The primary endpoint was a change in diagnosis or severity of HCM based on the additional information provided by post-UEA TTE over pre-UEA TTE. These changes included the presence or absence of LV basal septal HCM, LV apical HCM, LV apical aneurysm, and indication for ICD. **Results:** Of the 78 patients (age 61.0 ± 4.0 years, male 64%), 61 patients (78%) had technically difficult, pre-UEA TTE studies. Use of UEA led to a change in HCM diagnosis from baseline pre-UEA study in 33 patients (42%, p=0.0002): 16 patients were found to have new HCM or aneurysm, 14 patients were found to not have HCM, and 3 patients had a change in location of HCM. There were a total of 39 anatomical changes resulting from the use of UEA: 18 changes related to LV basal septum HCM diagnosis (7 false negatives, 12 false positives, p<0.0001), 11 changes related to LV apical HCM diagnosis (6 false negatives, 5 false positives, p<0.0001), 7 changes related to LV apical aneurysm diagnosis (7 false negatives, p=0.012) and 2 changes related to need for ICD (2 false negatives, p=0.0385). **Conclusion:** UEA significantly improved TTE diagnosis of HCM by allowing better delineation of endocardial borders, quantification of LV wall thickness, and visualization of LV apical anatomy. Routine use of UEA should be considered in HCM patients referred for TTE.

P2-120

Detection of Acute Rejection in Heart Transplantation at the Early Stage Using Two-dimensional Speckle Tracking Imaging and Intercellular Cell Adhesion Molecule-1-targeted Myocardial Contrast Echocardiography

Chen Zhao¹, Chengcheng Hu², Jiawei Tian¹, Shouqiang Li¹, Dandan Yu¹, Xiaoping Leng¹. ¹The 2nd Affiliated Hospital of Harbin Medical University, Harbin, China; ²The Hospital of Longjiang Forest Industry, Harbin, China

Background: Heart transplantation is the only effective treatment for patients with end-stage heart failure. For whom postoperative rejection is one of the major risk factors which may affect the cardiac function and long-term survival, especially the acute rejection. Early detection of acute rejection is crucial to improve survival and guide clinical treatment. In this study, we sought to investigate whether two-dimensional speckle tracking imaging (2D-STI) and intercellular cell adhesion molecule (ICAM)-1-targeted myocardial contrast echocardiography could detect the acute cellular rejection of heart transplantation at the early stage. **Methods:** The abdominal heterotopic heart transplantation model was successfully established using Wistar and SD rats. Forty-eight rats were divided into allografts group (ALLO, n=24) and isografts group (ISO, n=24). Echocardiography, 2D-STI and ICAM-1-targeted myocardial contrast echocardiography were performed at 1,3,5 day after transplantation respectively. After ultrasound imaging, transplanted hearts were harvested for Hematoxylin-eosin staining and immunofluorescence histochemical to

evaluate acute cellular rejection and ICAM-1 expression. **Results:** No obvious differences between ALLO group and ISO group were observed at day 1. Echocardiographic parameters such as left ventricular wall thickness in end diastole, left ventricular end-diastolic diameter, left ventricular ejection fraction and fractional shortening showed significant statistical differences in ALLO group at 5 days after surgery compared with day 3 (all p<0.05). There were obvious difference between ALLO group and ISO group in left ventricular wall thickness in end diastole, left ventricular end-diastolic diameter, left ventricular ejection fraction and fractional shortening at 5 days after transplantation surgery (all p<0.05). Compared with that in ISO group, global circumferential strain and strain rate, circumferential strain of endo-myocardium decreased in ALLO group at day 3 post-transplantation (all p<0.05). Compared with ISO group, all strain parameters in ALLO decreased significantly at postoperative day 5 (all p<0.05). Myocardial contrast echocardiography using ICAM-1-targeted microbubbles showed that the video intensity in ALLO group was significantly higher than that in ISO group at the day 3 and day 5 postoperative (all p<0.05). **Conclusion:** 2D-STI and myocardial contrast echocardiography using ICAM-1-targeted microbubbles are sensitive and useful for detecting heart transplant acute rejection at the early stage.

P2-121

Role of Contrast-Enhanced Ultrasound Sonography in the Medical Diagnostics of the Disease Activity in Patients with Takayasu Arteritis

Xiaoping Leng¹, Chen Zhao¹, Dandan Yu¹, Yue Liu², Shouqiang Li¹, Jiawei Tian¹. ¹The 2nd Affiliated Hospital of Harbin Medical University, Harbin, China; ²The Affiliated Zhongshan Hospital of Dalian University, Dalian, China

Background: The accurate diagnosis of Takayasu arteritis and the evaluation of its activity can bring significant challenges. In this study, we sought to investigate a correlation between clinical activity and enhancement of vessel wall acquired by contrast-enhanced ultrasound sonography (CEUS) in patients with Takayasu arteritis, and to evaluate whether CEUS can be used to assess the disease activity of Takayasu arteritis. **Methods:** 20 patients diagnosed with Takayasu arteritis with their carotid arteries affected were enrolled and divided into the active group and the inactive group according to the National Institutes of Health scoring method. The white blood cell counts, C-reactive protein counts and erythrocyte sedimentation rate were obtained. Conventional ultrasound was performed to acquire the external diameter of the artery, intima-media thickness of the arterial wall, percent area stenosis, peak systolic velocity, end diastolic velocity, and resistance index. CEUS were performed to acquire the enhanced intensity, derived peak intensity, and time to peak. **Results:** The analysis showed that compared with the inactive group, the external diameter of the artery and intima-media thickness of the arterial wall were significantly higher in the active group (6.50 ± 1.80 vs. $9.20 \pm 4.00\text{mm}$, 1.80 ± 0.40 vs. $2.40 \pm 0.70\text{mm}$, p<0.05). The enhanced intensity and derived peak intensity were also significantly higher in the active group (38.20 ± 10.62 vs. $80.80 \pm 23.60\text{IU}$, 46.20 ± 10.20 vs. $90.30 \pm 24.60\text{IU}$, p<0.05). Meanwhile, the enhanced intensity and derived peak intensity showed good correlation with C-reactive protein counts and erythrocyte sedimentation rate. **Conclusion:** CEUS can increase the effectiveness of conventional ultrasound in differentiating active and inactive Takayasu arteritis.

P2-122

Bifurcating Left Ventricular Outflow Pattern in Hypertrophic Obstructive Cardiomyopathy: 3D Echocardiography-Based Fluid Dynamics Simulation

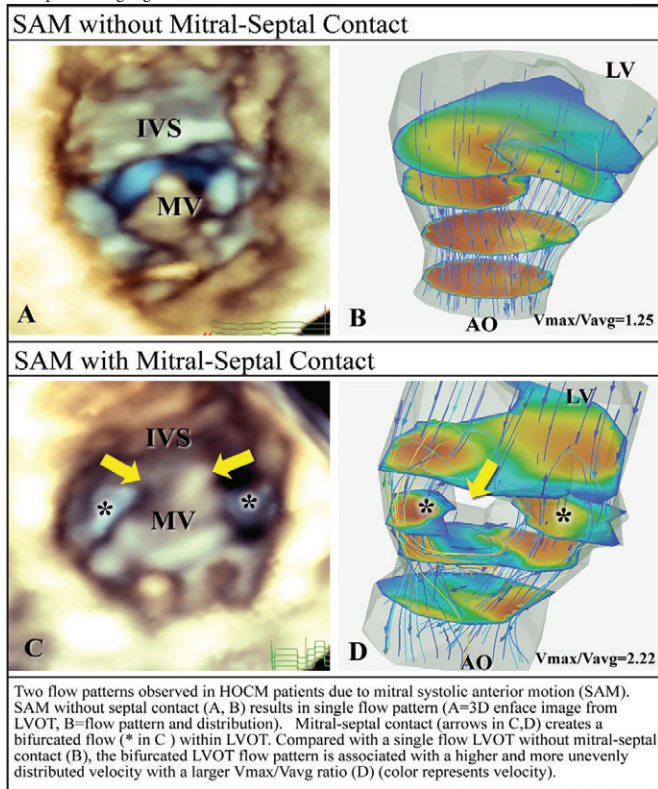
Hongning Song, Xin Zeng, Mayooraan Namasivayam, Danita Y. Sanborn, Mark D. Handschumacher, Robert A. Levine, Judy Hung. Massachusetts General Hospital, Boston, MA

Background: Obstruction in Hypertrophic Obstructive Cardiomyopathy (HOCM) results from dynamic left ventricular outflow tract (LVOT) narrowing. We used three-dimensional echocardiography (3DE) of LVOT geometry to simulate outflow fluid dynamics and better understand the mechanisms and hydrodynamics of LVOT obstruction. **Methods:** 20 HOCM patients with mitral leaflet systolic anterior motion (SAM) were retrospectively assessed by 3DE, with images post-processed using grey scale thresholding to separate blood pool from myocardium in late systole. Fluid simulation was performed to simulate LVOT flow dynamics using maximum velocity assessed by echo Doppler. The flow pattern, minimal LVOT area, maximal and average velocity within the obstructed plane and simulated LVOT gradient were measured using flow simulation software (Discovery AIM, ANSYS, USA). **Results:** Patients were divided based on two distinct LVOT flow patterns (Fig.1) resulting from mitral leaflet-septal contact: bifurcated flow (BF) group in patients with mitral-septal contact (N=14) and single flow (SF) group in patients without mitral-septal contact (N=6). Septal thickness was not different between the two groups (p=0.8); The minimal LVOT area showed highly negative correlation with the LVOT velocity by Doppler in all patients (R=-0.8). Minimal area of LVOT in the BF group was significantly smaller than in SF group ($1.75 \pm 0.79\text{cm}^2$ vs. $3.00 \pm 1.44\text{cm}^2$, p=0.02). Fluid simulation modeling showed that in order to maintain the same flow across the LVOT, the BF group required a higher increase in LV pressure than the SF group ($50.0 \pm 21.7\text{mmHg}$ vs. $17.5 \pm 11.3\text{mmHg}$ BF vs SF groups, p<0.01). The BF group also had higher nonuniformity of flow velocity distribution across the LVOT area, measured as ratio of maximum to

Poster Session 2 (P2)

Monday, June 24, 2019

average velocity (2.10 ± 0.70 vs. 1.45 ± 0.14 , $p < 0.01$). **Conclusion:** Mitral leaflet-septal contact in patients with HOCM creates a unique bifurcated LVOT orifice geometry and flow pattern. This bifurcating flow pattern and smaller LVOT area require a higher LV afterload to maintain stroke volume with a more nonuniform distribution [that may incur added pressure losses]. These results support the reduction of SAM-septal contact as a therapeutic target goal for HOCM.

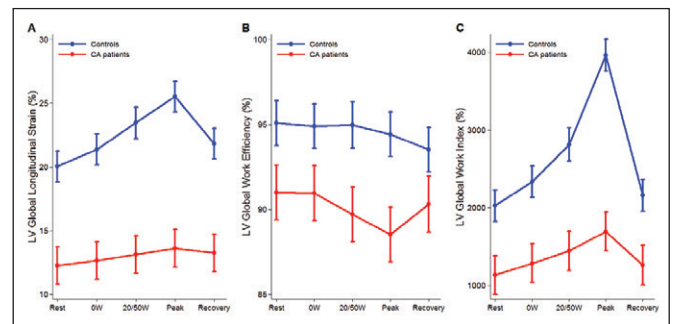


P2-123

Left Ventricular Pressure-Strain Derived Myocardial Work at Rest and During Exercise in Cardiac Amyloidosis Patients

Tor S. Clemmensen¹, Fabian Mikkelsen¹, Hans Eiskjær¹, Sven-Olof Granstam², Frank A. Flachkamp¹, Jens Sørensen^{1,2}, Steen H. Poulsen¹. ¹Aarhus University Hospital, Aarhus, Denmark; ²Uppsala University Hospital, Uppsala, Sweden

Background: Left ventricular pressure strain derived myocardial work index (LVMWI) is a novel non-invasive method for LV function evaluation in relation to LV pressure dynamics. LV global longitudinal strain (LVGLS) has proven benefit for diagnosis and risk stratification in patients suffering cardiac amyloidosis (CA), but LVGLS does not adjust for loading conditions. The present study aimed to characterize LVMWI at rest and during exercise in CA patients. **Methods:** A total of 145 subjects were included consisting of 91 CA patients and 54 healthy controls. All patients underwent comprehensive 2D echocardiographic evaluation at rest. Furthermore, a subgroup 27 CA patients and 41 controls underwent a semi-supine exercise stress echocardiography. **Results:** CA patients had significantly lower LVGLS, LVMWI and LV global work efficiency (LVGWE) than controls (all $p < 0.0001$). The reduction in LV myocardial performance was more pronounced in the basal segments, which led to significant alterations in the average apical-to-basal segmental ratios between CA patients and controls (LVGLS: 2.6 [1.8-3.8] versus 1.3 [1.2-1.5]; LVMWI: 2.5 [1.7-3.7] versus 1.2 [1.1-1.5]; LVGWE: 1.1 [1.0-1.3] versus 1.0 [1.0-1.1], all $p < 0.0001$). The average increase of LVMWI from rest to peak exercise was 1974 mmHg% (95% CI: 1699;2250, $p < 0.0001$) in controls and 496 mmHg% (95% CI: 156;835, $p < 0.01$) in CA patients. LVGLS increased 5.6% (95% CI: 3.9;7.3, $p < 0.0001$) in controls and only 1.2% (95% CI: -0.9;3.3, $p = 0.26$) in CA patients (between groups: $p < 0.0001$) from rest to peak exercise. The LVMWI increase in CA patients was mediated by the apical segments ($p < 0.0001$), whereas there was no significant increase in LVMWI in the mid-ventricular or basal segments. LVGWE remained stable during exercise in controls (Δ -0.6%, 95% CI -2.5;1.2, $p = 0.50$) but decreased significantly in CA patients (Δ -2.5%, 95% CI -4.8;-0.2, $p < 0.05$), Figure 1. **Conclusion:** CA patients have significantly reduced magnitude of LVMWI compared with healthy controls. With exercise, the differences are even more pronounced. Even though LVMWI increased in CA patients with exercise, LVGWE decreased suggesting inefficient myocardial energy exploitation. **Figure 1:** Margin plots showing A: LVGLS, B: LVGWE, C: LVMWI during exercise in CA patients (red) and controls (blue).



P2-124

Serial Echocardiography Defines Adaptive Cardiac Hypertrophy Following Creation of Arteriovenous Fistulae

Shin-rong Lee, Nicole Guerrero, Stephanie Thorn, Ricardo Avendano, Albert J. Sinusas, Alan Dardik. Yale University, New Haven, CT

Background: Arteriovenous fistulae (AVF) are surgically created shunts, connecting an artery to a vein, and are the preferred mode of vascular access for patients requiring hemodialysis. These shunts induce high flows and can have significant cardiovascular effects, which may be harmful or beneficial. To this point, while some advocate ligating AVF for patients with stable renal transplants, others recommend creating central AVF to treat refractory hypertension. Therefore, we performed serial echocardiography in a mouse model of AVF with modest shunt rates to examine the cardiac effects of AVF. We hypothesize that AVF would induce an adaptive hypertrophic response. **Methods:** 9-11wk old male C57Bl/6 mice were subjected to sham (n=5) or AVF (n=6) surgery, created by needle puncture (25G) of the infrarenal aorta into the vena cava. Fistula patency was confirmed post-operatively with abdominal pulse-wave doppler. Transthoracic echocardiography was performed before surgery, and on days 3, 10, and 21 after surgery using standardized cardiac views and imaging modes with a high-resolution ultrasound system. Images were analyzed offline for assessment of indices of systolic and diastolic function and changes in chamber size. 2-way ANOVA and t-test were used for statistical testing. **Results:** Mice with AVF had similar weight gain ($p = 0.98$) and wet lung mass (d35; $p = 0.7$), but increased cardiac mass (d35, AVF vs sham: 249 ± 7 vs 179 ± 6 mg, $p < 0.01$) compared to sham-operated mice. Cardiac output increased relative to baseline (19.5 ± 1.3 ml/min) at all subsequent timepoints after AVF (d3: 28.3 ± 1.5 ; d10: 32.2 ± 1.6 ; d21: 38.0 ± 3.4 , $p < 0.05$). At day 21, left atrial area (AVF vs sham: 8.9 ± 0.7 vs 6.6 ± 1.1 mm², $p = 0.02$) and LV end diastolic volume (LV_{EDV}; 108 ± 5.5 vs 64 ± 8.4 ul, $p < 0.01$) were enlarged. LV anterior wall (LV_{AW}; AVF vs sham: 0.97 ± 0.01 vs 0.8 ± 0.03 mm, $p < 0.01$) and LV posterior wall (LV_{PW}; 0.85 ± 0.03 vs 0.72 ± 0.02 mm, $p < 0.01$) significantly thickened at day 10, though LV_{AW}/LV_{EDV} and LV_{PW}/LV_{EDV} were decreased. Apart from a brief increase at day 3 (AVF vs sham: 70.7 ± 2.0 vs 59.7 ± 3.6 %, $p < 0.05$), LV ejection fraction remained unchanged after AVF. Diastolic function as estimated by mitral E/E', and right heart indices such as estimated mean pulmonary artery pressure and tricuspid annular plane systolic excursion were also unaltered by AVF at any time point. **Conclusion:** AVF with modest shunt rates are well-tolerated without development of heart failure or diastolic dysfunction, but generate an adaptive hypertrophic response. Further work to characterize their histopathologic correlates and molecular underpinnings are necessary.

P2-125

Validation of Echocardiographic Indices of Pulmonary Hemodynamics and Right Ventricular Performance in Neonatal Murine Hypoxia: Clinical Implications for Group 3 Pulmonary Hypertension

Kel Vin Woo¹, Philip T. Levy¹, Amanda Hauck², Aaron Hamvas², David Ornitz¹, Gautam K. Singh¹. ¹Washington University, Saint Louis, MO; ²Northwestern University, Chicago, IL

Background: Of half million premature born infants annually, up to 40% develop bronchopulmonary dysplasia and pulmonary hypertension (Group III PH) with high mortality from subsequent right ventricular (RV) failure. Reliable noninvasive tool for early detection of RV dysfunction and PH, validated against right heart catheterization (RHC) lacks in clinical care of premature infants. The aims of this study in mouse model of Group III PH were to determine which echocardiographic (echo) indices of RV mechanics and pulmonary hemodynamics reliably predict PH by RHC and validate them for diagnostic capability against histological phenotype of Group 3 PH in adult and neonatal mice. **Methods:** We assessed echo indices of RV morphometry and mechanics against invasive indices of RV hemodynamics from RHC in 6-week-old adult mice exposed to 2 weeks of hypoxia or normoxia. We applied echo measures that predicted PH confirmed by RHC and histology in 6-week-old mice to evaluate PH characteristics in neonatal mice exposed to 2 weeks of hypoxia. **Results:** Six-week-old hypoxia challenged mice developed PH with elevated RV systolic pressure (RVSP) by RHC, RV hypertrophy, and neomuscularization of pulmonary vessels. Echo derived RV free wall (RVFW) thickness correlated with RV:left

Poster Session 2 (P2)

Monday, June 24, 2019

ventricle + septum mass ratios. Tricuspid valve annulus tissue Doppler imaging (TV TDI), tricuspid annular plane systolic excursion (TAPSE), and pulmonary artery acceleration measures (PAAT), all correlated with RHC-derived RVSP in adult mice, indicating decreased RV function and elevated afterload (Figure 1A). TAPSExPAAT, a measure of RV work capacity, was decreased in mice with PH. In hypoxic neonatal mice, PAAT, TV TDI, TAPSE, and TAPSExPAAT were decreased and RVFW thickness increased, correlating robustly with histologic phenotype of PH (Figure 1B). **Conclusion:** Echocardiographic indices of RV hemodynamics, morphology, and function provide reliable estimates of invasive RVSP and RV phenotype in Group III PH in adult mice. When applied to Group III PH in neonatal mice, these measures robustly correlated with histological evidence of PH. These validated echocardiographic indices of RV mechanics and pulmonary hemodynamics can reliably be applied for early detection of PH and RV dysfunction in premature infants and adults with Group 3 PH.

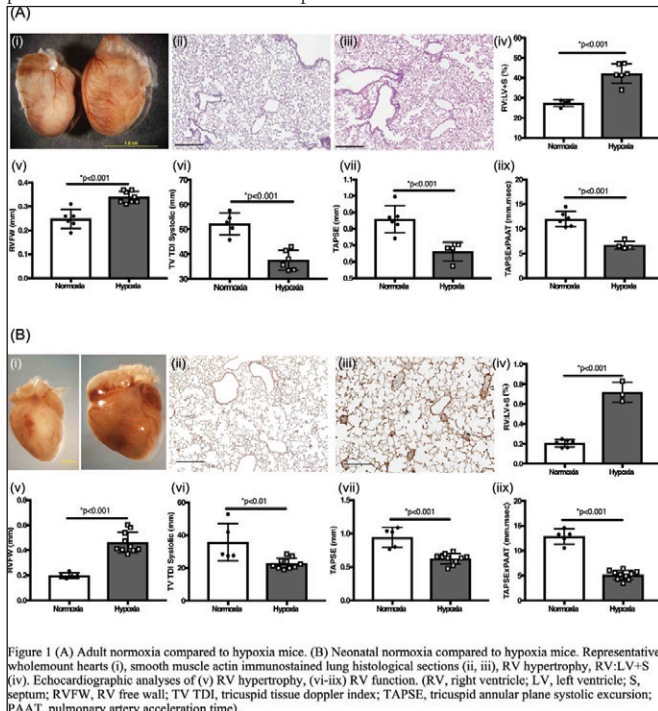


Figure 1 (A) Adult normoxia compared to hypoxia mice. (B) Neonatal normoxia compared to hypoxia mice. Representative wholemount hearts (i), smooth muscle actin immunostained lung histological sections (ii, iii), RV hypertrophy, RV:LV+S (iv). Echocardiographic analyses of (v) RV hypertrophy, (vi-ix) RV function. (RV, right ventricle; LV, left ventricle; S, septum; RVFW, RV free wall; TV TDI, tricuspid tissue doppler index; TAPSE, tricuspid annular plane systolic excursion; PAAT, pulmonary artery acceleration time).

P2-126

Surgical Pulmonary Embolectomy for Acute Pulmonary Embolism Improves Right Ventricular Function on Echocardiography

Yogita Rochlani, Tonusri Nag, Syed Ahsan, Monica Lopez-Islas, Ramin Malekan, Joshua B. Goldberg, Daniel Spevack, Tanya Dutta. Westchester Medical Center, White Plains, NY

Background: Acute pulmonary embolism (PE) remains a potentially lethal diagnosis largely due to right ventricular (RV) failure. Use of transthoracic echocardiography (TTE) for assessment of the RV is integral in the management of PE. Patients with hemodynamically significant acute PE can be treated with surgical embolectomy (SE). There is limited literature on TTE assessment of the RV in patients with acute PE treated with SE. In a large series of SE performed at our institution, we compared TTE parameters of RV structure and function in the pre- and post-operative period. **Methods:** All patients who underwent SE for acute massive or submassive PE between 2005 and 2018 at our institution with pre-and postoperative TTE data were included. TTE parameters of RV structure (RV/LV diameter ratio and RV end-diastolic area) and function [tricuspid regurgitation severity and fractional area change for RV (RVFAC)] were compared pre-and post-operatively. Logistic regression analysis was used to identify predictors of normal RV function postoperatively as indicated by RVFAC. **Results:** Among 120 SE performed for massive or submassive PE, 64 met inclusion criteria [mean age 58 (±13) years, 61% male, 20% massive PE, mean body mass index (BMI) 33 (±8) kg/m²]. TTE was performed a mean of 7.7 days post-operatively. As detailed in table 1, all TTE parameters of RV function showed significant improvement in the postoperative period prior to hospital discharge. On regression analysis, RV function preoperatively, as indicated by the RVFAC, was the best predictor for normal postoperative RV function after adjusting for age, sex, BMI, RV/LV ratio and RV end-diastolic area. 47 of the 64 patients (73%) had an RV FAC of <35% preoperatively. 45 of the 47 patients (96%) had improvement in their RVFAC post-operatively of which 25 (53%) normalized to >35%. 20 patients (43%) had improvement in RV function but the RVFAC did not return to normal. **Conclusions:** In one of the largest series of SE for acute massive or sub-massive PE, SE resulted in improvement in RV function based on TTE parameters in the post-operative period. Preoperative RV function

best predicted post-operative RV recovery. Structural parameters of RV size did not predict post-operative improvement in RV function.

Table 1: Comparison of pre and post-operative RV echocardiographic parameters

Echocardiographic Parameters	Pre-operative	Post-operative	P value
RV/LV ratio	1.15 (±0.34)	0.85 (±0.23)	<0.001
Moderate to severe tricuspid regurgitation	11 (17%)	4 (6%)	0.05
Right Ventricular End Diastolic Area (cm ²)	30 (±9)	24 (±8)	<0.001
Fractional Area Change for Right Ventricle (%)	28 (±12)	41 (±12)	<0.001

P2-127

Myocardial Deformation Abnormalities Prevalent Among Human Immunodeficiency Virus Infected Children on Long Term Antiretroviral Therapy

Benjamin Acheampong, David Parra, Jonathan Soslow. Vanderbilt University, Nashville, TN

Background: The improved availability of highly active antiretroviral therapy (HAART) for HIV infected children in sub-Saharan Africa has led to a decline in prevalence of overt clinical cardiovascular disease. However, the incidence of subclinical dysfunction, which could be a precursor to overt dysfunction later in life, is unclear. We hypothesized that Ghanaian HIV infected children on long term HAART may have abnormal myocardial strain and strain rate. **Methods:** HIV infected (HIV+) children aged 9 - 243 months (mo) from a tertiary teaching hospital, Cape Coast, Ghana were recruited. HIV exposed but uninfected (HIV-) children aged 1 - 221 mo were used as controls. Cardiac assessment included longitudinal strain, longitudinal strain rate, circumferential strain and circumferential strain rate from 2-dimensional images from apical 4-chamber and short axis images at the level of the papillary. Strain values below the 5th percentile were considered abnormal. Most recent CD4 count, viral load, duration of treatment and first line therapy available were obtained from the medical records. The two-sample t-test, Wilcoxon rank sum test and linear regression were used to assess differences among the groups and to compare means and test relationships between strain, CD4 count (n=36) and viral load. **Results:** Among 113 children, 77 were HIV+ and 36 were HIV-. The HIV+ group was slightly older (median age (IQR) 123 (65,159) mo vs 21(8,110) mo p<0.001). The median (IQR) duration of treatment among the HIV+ children were 30 (17,72) months. The median (IQR) CD4 count (n=36) was 731 (445,1173) cells/m³; median (IQR) viral load (n=26) was 2429 (279,176615) copies/ml. Circumferential strain rate was significantly impaired in the HIV+ compared with the control group (1.45 ± 0.03 vs 1.58 ± 0.04, p=0.02). There was no significant difference in the longitudinal strain (21.2 ± 0.4 vs 21.7, p=0.4); circumferential strain (26.6 ± 0.5 vs 27.8 ± 0.7, p=0.2) and longitudinal strain rate (1.1 ± 0.03 vs 1.2 ± 0.03, p=0.1) among the groups. Abnormal global longitudinal strain and strain rate was present in 22% (n=17) vs 11% (n=4) and 27% (n=21) vs 3% (n=1) between the HIV+ and HIV- children respectively. Circumferential strain and circumferential strain rate abnormalities were seen in 4% (n=3) vs 3% (n=1) and 27% (n=21) vs 0% between the HIV+ and HIV- groups. There was no association between CD4 count, viral load, duration of treatment and first line therapy and strain abnormalities. **Conclusion:** HIV infected children on long term HAART demonstrate cardiac strain abnormalities compared with HIV exposed but uninfected children in sub-Saharan Africa.

P2-128

ESC Sudden-death Risk Model in Hypertrophic Cardiomyopathy: Incremental Value of Left Ventricular Strain in Intermediate-risk Patients

Tomás F. Cianciulli, María C. Saccheri, Omar Prieto, Jorge A. Lax, Luciana J. Puente, María S. Bidonde, Luis A. Morita, Juan A. Gagliardi. Hospital Argerich, Capital Federal, Argentina

Background: Hypertrophic cardiomyopathy (HCM) is the most frequent cause of sudden death in young people, but not all patients who are candidates for the prevention of sudden death with an implantable cardioverter defibrillator (ICD) are adequately identified. No study has demonstrated an association of strain with the formula for calculating the risk of sudden death proposed by the European Society of Cardiology in 2014. The aim of our study was to determine the relationships of GLS and regional strain with the risk score of sudden cardiac death in patients with HCM according to the risk formula. **Methods:** A total of 74 patients with HCM between the ages of 16 and 80 years were included and divided into 3 groups: low risk (n=46), moderate risk (n=12), and high risk (n=16). GLS and regional strain were correlated in these 3 groups. Echocardiographic study was performed using a Vivid 7 device and EchoPAC software. **Results:** Analysis of the ROC curves showed that a strain > -15.7% indicated high risk with a specificity of 60.3% and sensitivity of 93.8%. The presence of ≤ 3 segments with strain > -10% indicated low risk with a specificity of 82.1% and sensitivity of 65.2%. These data could be useful in patients with intermediate risk of sudden death who are candidates for the implantation of an ICD.

Poster Session 2 (P2)

Monday, June 24, 2019

	LOW-RISK (4%)	INTERMEDIATE-RISK (4%-6%)	HIGH-RISK (>6%)	P
Patients (n, %)	46 (62.2%)	12 (16.2%)	16 (21.6%)	--
Age (years)	48.8 ± 16.5	36.5 ± 15.7	43.6 ± 17.8	0.05
Male (n, %)	28 (60.9%)	5 (41.7%)	8 (50%)	0.43
Ejection fraction (%)	70.4 ± 10.1	75.8 ± 14.4	68.5 ± 13.3	0.34
GLS (%)	-16.5 ± 3.6	-14.8 ± 5.1	-11.2 ± 3.5	<0.0001
Number of segments with strain > -10% (median and interquartile range)	2 (0-5)	4.5 (2-8.5)	7 (6-11)	<0.0001

Conclusions: A reduction in GLS consistent with the sudden death risk model was used to define low- and high-risk models. A GLS > -15.7% was highly correlated with high risk, whereas patients with ≤ 3 segments with strain > -10% are highly likely to be at low risk. In patients with intermediate risk of sudden death, GLS can provide additional information for deciding whether or not to implant an ICD. With the widespread observation of ventricular strain in daily practice, the reduction of strain is a promising tool for the stratification of patients with HCM according to the risk of sudden death.

P2-129

Chagas Cardiomyopathy in Patients of Mayan Origin in Yucatan: Experience from the ASEF/ANCAM Global Health Initiative

Federico M. Asch¹, Pedro Gutierrez-Fajardo², Hilda Peralta-Rosado³, Verónica Bravo-Rendón⁴, Martín Ibarrola⁵, Eric Kruse⁶, Tracy Lawrence⁷, Rachel Marcus¹, Carolina Melendez⁸, Adriana Ortega-Gutierrez⁹, Rhonda Price¹⁰, Emma Rosas-Munive¹¹, Madeline Schiminger¹², Allison Sterk¹³, Benigno Valderrábano-Salas¹⁴, Miguel A. Corona Franco¹⁵, Roberto M. Lang⁶. ¹MedStar Health Research Institute and MedStar Heart and Vascular Institute, Washington DC and Baltimore, MD; ²Hospitales Mac Bernardette, Guadalajara, Mexico; ³Hospital General Agustín O'Horan de Mérida, Mérida, Mexico; ⁴Instituto del Corazón de Querétaro, Santiago de Querétaro, Mexico; ⁵Centro Cardiovascular Bella Vista, Buenos Aires, Argentina; ⁶University of Chicago, Chicago, IL; ⁷Cigna, Glendale, CA; ⁸Baylor Scott & White The Heart Hospital, Plano, TX; ⁹Unidad Médica de Alta Atención de Yucatan, Mérida, Mexico; ¹⁰American Society of Echocardiography, Durham, NC; ¹¹Hospital General de México, Mexico City, Mexico; ¹²Johns Hopkins Hospital, Baltimore, MD; ¹³Great Ormond St Hospital, London, United Kingdom; ¹⁴Hospital Regional de Alta Especialidad Bicentenario de la Independencia, Mexico City, Mexico; ¹⁵Philips HealthCare Mexico, Naucalpan de Juárez, Mexico

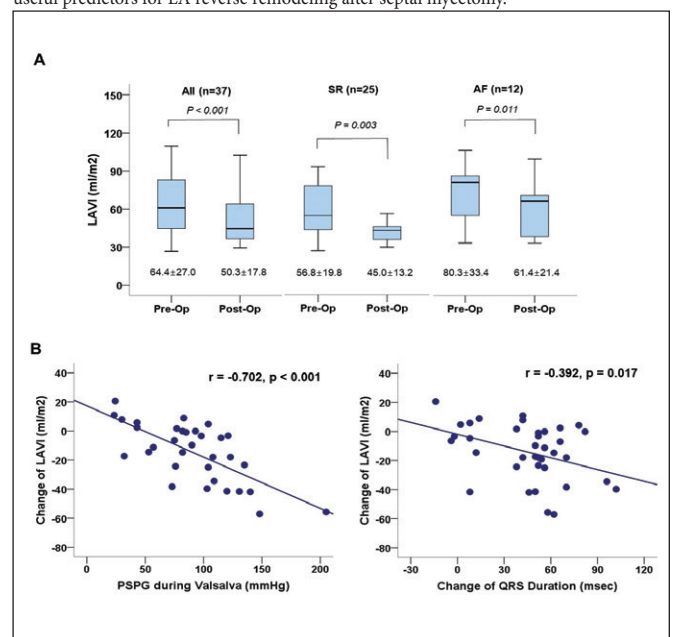
Background: Chagas disease (ChD) is a parasitic infection highly prevalent in Latin America that can induce cardiomyopathy in a minority of infected individuals. The American Society of Echocardiography Foundation and the National Association of Cardiologists of Mexico (ANCAM) organized a global health initiative in collaboration with the Mexican national and state Governments to investigate the prevalence and provide care for patients with Chagas cardiomyopathy (ChCM) in the state of Yucatan, Mexico. **Methods:** Patients of Mayan origin with a positive serology for ChD during blood bank screenings, underwent a comprehensive cardiac exam with comprehensive state-of-the-art echo and EKG. 2D and 3D echocardiographic datasets were used to measure left ventricular (LV) size and function global and regional wall motion abnormalities and for the presence of characteristic apical aneurysms (AN). LV ejection fraction (EF) was evaluated by 3D Heart Model (Philips) or 2D Simpsons rule when 3D was unavailable. ChCM was diagnosed on the basis of (+) serology and either characteristic abnormal EKG (right bundle or fascicular blocks, QRS>110 msec or abnormal ST/T) or echocardiograms (LV wall motion abnormalities -WMA- or AN). **Results:** A total of 156 consecutive patients with (+) serology were evaluated. Mean age was 43±12 years, 33% were female and mean body surface area was 1.71 m². Blood Pressure was 123±15 / 76±15 mmHg, LV EF was 59±7% and none had history of coronary or rheumatic disease. In these patients, 64 were diagnosed with ChCM (41%), 31% by echocardiography and 10% only by EKG. Of the 49 patients with abnormal echocardiograms, 16 had a normal EKG, 30 had LV AN, 1 RV AN, 7 had only WMA and 11 had AN and WMA. Location of the AN was apical in 39, septal in 2, and in the inferior wall and RV in 1. The AN were small and rarely coexisted with global LV dysfunction. Patients were asymptomatic and engaged for follow-up by cardiologists at the local hospital. **Conclusion:** In Mayan patients infected with Chagas in the state of Yucatan, the prevalence of cardiomyopathy was 41% and most cases had apical AN, while only 10% had abnormal EKG with normal echo. 33% of those with abnormal Echo had normal EKG, highlighting the value of imaging in addition to EKG. Diagnosis at early stages in this outreach activity will allow treatment and probably impact long term outcomes.

P2-130

Factors Associating Left Atrial Reverse Remodeling After Septal Myectomy in Patients with Obstructive Hypertrophic Cardiomyopathy

Kang-Un Choi, Chi Young Shim, Jah Yeon Choi, Purevjargal Lkhagvasuren, Geu-Ru Hong, Jong-Won Ha. Severance Cardiovascular Hospital, Seoul, Republic of Korea

Backgrounds: Surgical septal myectomy may induce left atrial (LA) reverse remodeling by relieving left ventricular (LV) outflow track dynamic obstruction in patients with hypertrophic obstructive cardiomyopathy (HOCM). We aimed to define clinical, echocardiographic, and electrocardiographic factors associated with LA reverse remodeling after septal myectomy in patients with HOCM. **Methods:** A total of 53 patients with symptomatic HOCM who underwent surgical septal myectomy from 2006 to 2018 were retrospectively analyzed. Patients were excluded if they did not perform a postoperative echocardiogram at 1 year or underwent a valve replacement at the same time. Finally, clinical, echocardiographic, and electrocardiographic variables before and 1 year after the surgery were comprehensively analyzed in 37 patients. **Results:** After septal myectomy, there were significant decreases in LA volume index (64±27 vs. 50±18 ml/m², p<0.001) and tricuspid regurgitation maximum velocity (2.8±0.7 vs. 2.5±0.4 m/s, p=0.001) through improvements of LV diastolic indices. LA volume reduction was significant after septal myectomy regardless of sinus rhythm or atrial fibrillation (Figure 1A). The change of LA volume index was strongly correlated with preoperative peak systolic pressure gradient (PSPG) during Valsalva maneuver (reflecting preoperative LV afterload) and significantly correlated with change of QRS duration (suggesting effective septal reduction) (Figure 1B). In multivariate analyses, a higher preoperative PSPG during Valsalva (β= -0.704, p<0.001) and a prolonged Δ QRS (β=-0.296, p=0.040) were independently associated with LA reverse remodeling after adjusting confounding factors. **Conclusion:** Septal myectomy shows LA reverse remodeling by improving LV diastolic function regardless of cardiac rhythm. Preoperative hemodynamic burden on LV and electrocardiographic changes are useful predictors for LA reverse remodeling after septal myectomy.



P2-131

Inferior Vena Cava Collapsibility Index Assessed by 3D Echocardiography: A Novel Tool for the Assessment of Right Atrial Pressure in Heart Failure Patients

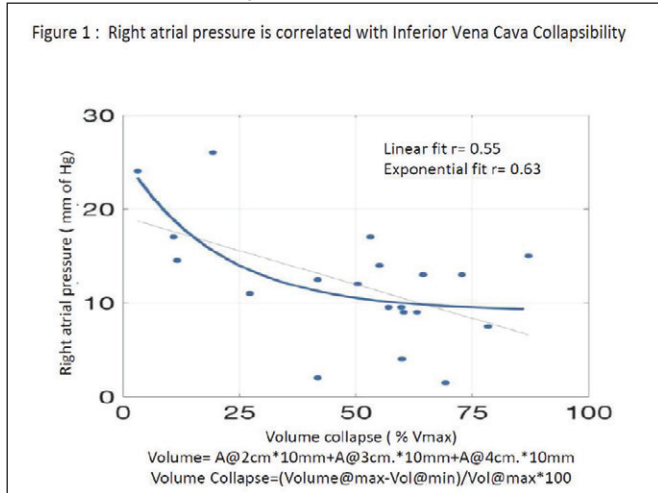
Jayant Raikhelkar¹, Kalie Kebed¹, Akhil Narang², Eric Kruse¹, Sarah Weatherford¹, Teruhiko Imamura¹, Friedrich Wetterling³, Ann Nguyen¹, Gabriel Sayer¹, Roberto Lang¹, Nir Uriel¹. ¹University of Chicago, Chicago, IL; ²Northwestern University, Chicago, IL; ³Fire 1 Ltd, Dublin, Ireland

Background: Inferior vena cava (IVC) size and respirophasic collapsibility by 2D transthoracic echocardiography (2DE) have previously been shown to correlate weakly with right atrial pressure (RAP) in patients with acute decompensated heart failure (ADHF). Accurate 2DE dimensions are reliant on obtaining the correct imaging plane and the assumption that the mostly elliptical IVC shape is circular, a limitation that 3D echocardiography (3DE) can overcome. The aim of study was to determine the relationship between invasively obtained RAP and IVC collapsibility as determined by 3DE in patients with ADHF. **Methods:** Simultaneous measurements of RAP and 3DE recordings of the IVC were performed in ADHF patients during clinically indicated right heart catheterizations. Cross-sectional area and major and minor axis dimensions (Tomtec) were obtained at rest

Poster Session 2 (P2)

Monday, June 24, 2019

and end inspiration. An IVC collapsibility index was calculated for cross-sectional area (3DE) using the following equation: ((Maximum area- Minimum area)/ Maximum area) * 100. **Results:** 20 patients were enrolled. Mean age was 59 ± 16 years, 52% were male, and 60% of the patients were African American. 80% of the patients were NYHA class III or IV, mean creatinine was 1.9 ± 1.4 mg/dl, mean NT-proBNP was 6729 ± 6142 pg/mL and mean left ventricular ejection fraction was 31 ± 17%. Mean RA pressure was 12.7 ± 6.5 mm of Hg. RAP and IVC volume did not correlate well (r=0.17), regardless of whether RAP was low or high. There was a strong correlation between RAP and IVC collapsibility index (r= 0.63) (Figure 1). **Conclusion:** 3DE derived IVC collapsibility index is a novel noninvasive tool to assess RAP. RAP does not appear to correlate to IVC size or volume as measured by 3DE in patients with ADHF. Further studies are needed to characterize this parameter's role in patient management.



P2-132

Diastolic Function and Left Atrial Strain Abnormalities in Obese, and Type II Diabetic Adolescents and Young Adults

Jeremy M. Steele, Elaine M. Urbina, Philip R. Khoury, Justin T. Tretter, Tarek Alsaied. Cincinnati Children's Hospital, Cincinnati, OH

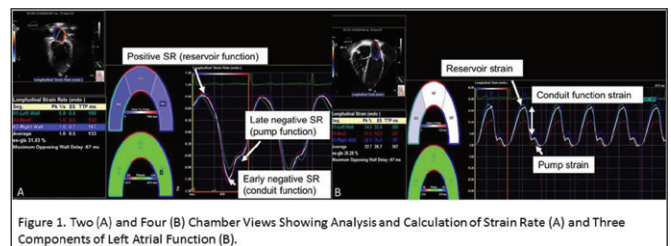
Background: Adults with obesity and type 2 diabetes related to obesity are at increased risk of left ventricular diastolic heart failure. Measurements of left atrial (LA) function has been shown to provide early detection and improved prognostic and diagnostic information in the assessment of diastolic function. Whether diastolic function abnormalities related to obesity and type 2 diabetes start in adolescence and early adulthood is not known. Our objective was to evaluate diastolic and LA function measures differences in adolescents and young adults with obesity and type 2 diabetes. **Methods:** We performed an analysis of echocardiographic measures of diastolic function, LA volumetric data, LA function, and LA strain analysis in patients without congenital heart disease. LA function measures were averaged over 3-5 cardiac cycles, using R-R interval. LA analysis was obtained in the 2 and 4 chamber views and averaged. Groups were compared by analysis of variance, Wilcoxon rank sums and Kruskal-Wallis test. **Results:** 113 patients were analyzed (43 normal weight, 30 obese, 40 type 2 diabetes). Obese and type 2 diabetes group had lower E/A, lower septal and lateral e' and higher septal and lateral E/e' as compared to controls. There was no difference between the groups with regards to LA volumetric assessment (Table 1). Obese and type 2 diabetic patients had significantly lower atrial reservoir strain compared to normal weight patients (p=0.01). In addition, obese and type 2 diabetic patients also had higher early global strain rates which is a measure of LA conduit function (p = 0.02). **Conclusions:** Abnormal diastolic function measures can be detected in adolescents and young adults with obesity and type 2 diabetes. LA function and strain analysis was able to detect evidence of decreased reservoir strain and conduit strain rate in these patients although LA volume was normal. The use of LA function strain may provide early detection of diastolic function abnormalities in this patient population.

Table 1. Demographics, Left Atrial Volumetric and Function Data

Variable	Normal weight (n = 43)	Obese (n=30)	Type 2 Diabetes (n=40)	p-value
Age (years)	21.7 (+/- 4.5)	21.4 (+/- 3.3)	25.7 (+/- 3.3)	
Male (n)	27	9	11	
BMI (Kg/m2)	23.7 (+/- 3.6)	35.7 (+/- 6.9)	34.9 (+/- 6.5)	0.001
LA EDV	17.9 (+/- 6.1)	20.1 (+/- 7.3)	17.4 (+/- 7.2)	0.3
LA ESV	49.4 (+/- 14)	55 (+/- 15.7)	48.4 (+/- 19.5)	0.2
LA EF	62.6 (+/- 8.6)	62.4 (+/- 10.6)	62.1 (+/- 11.9)	0.9
FAC	48.5 (+/- 6.6)	48.1 (+/- 8.4)	46.9 (+/- 9.7)	0.6
Booster Function	15.6 (+/- 6.2)	13.3 (+/- 5.3)	12.3 (+/- 7.1)	0.06
Reservoir Function	52.6 (+/- 10.4)	48.1 (+/- 10.2)	46.2 (+/- 9.9)	0.01
Conduit Function	38.1 (+/- 9.1)	35.2 (+/- 9.1)	36.6 (+/- 10.9)	0.6
Global Strain Rate	1.9 (+/- 0.5)	1.8 (+/- 0.4)	1.7 (+/- 0.4)	0.05
Early Strain Rate	-2.5 (+/- 1.0)	-2.2 (+/- 0.8)	-1.9 (+/- 0.7)	0.02
Late Strain Rate	-0.07 (+/- 0.4)	-0.01 (+/- 0.3)	-0.1 (+/- 0.4)	0.3
Septal e'	13.3 (+/- 2.2)	11.7 (+/- 1.7)	9.9 (+/- 2.2)	0.0001
Septal a'	7.1 (+/- 1.7)	6.6 (+/- 1.6)	7.9 (+/- 2.1)	0.02
Lateral e'	17.5 (+/- 3.1)	16.2 (+/- 2.5)	13.8 (+/- 3.8)	0.0001
Lateral a'	6.7 (+/- 1.7)	6.9 (+/- 2.1)	8.1 (+/- 2.1)	0.003
Septal e'/a'	8.7 (+/- 1.2)	7.8 (+/- 0.9)	7.8 (+/- 1.1)	0.001
Lateral e'/a'	11.3 (+/- 2.4)	9.8 (+/- 1.5)	9.8 (+/- 2.1)	0.002
Mitral Valve E' Wave	91.6 (+/- 17.7)	98 (+/- 13.7)	91.6 (+/- 17.4)	0.7
Mitral Valve A' Wave	42.1 (+/- 12.2)	48.4 (+/- 12.4)	62.5 (+/- 20.5)	0.001
E/A	15.3 (14.0, 16.9)	13.9 (12.8, 14.8)	11.8 (10.2, 14.1)	0.0001
Septal E'/e'	6.9 (5.9, 7.7)	7.8 (7.1, 9.0)	8.9 (8.0, 10.3)	0.0001
Lateral E'/e'	5.1 (4.3, 6.2)	5.6 (5.2, 6.5)	6.2 (5.0, 8.3)	0.009
Average E'/e'	6.1 (5.1, 6.7)	6.7 (6.1, 7.2)	7.3 (6.1, 8.8)	0.0001

Values are given as either means of the group ± standard deviation with p-values obtained using ANOVA or medians with interquartile range (25th-75th percentile) with p-values obtained using Kruskal-Wallis

LA (left atrium)-EDV (end diastolic volume)-ESV (end systolic volume)-EF (ejection fraction)-FAC (fractional area change).



P2-133

Differential Impact of Sleep Disorder Breathing Parameters on Cardiac Dysfunction

Osama Mukarram, Andre Gabriel, Min J. Kim, Kai Chen. University of Connecticut, Farmington, CT

Background: Cardiomyopathy, particularly heart failure with preserved ejection fraction has been linked to Sleep Disordered Breathing (SDB). Traditionally Apnea Hypopnea Index (AHI) is used to classify the severity of SDB. While this severity classification has guided clinical therapy of SDB, the impact of sleep parameters on cardiac pathophysiology and subsequent diastolic dysfunction remain to be evaluated. We hereby investigated the correlation of different sleep parameters with cardiac function. **Methods:** Data from 283 consecutive patients undergoing Polysomnography (PSG) and echocardiogram between January 2015 and December 2017 at University of Connecticut cardio-pulmonary laboratory was analyzed. Subjects with left ventricular ejection fraction < 50% or significant valvular heart disease were excluded. Four sleep study parameters including AHI, Respiratory Disturbance index (RDI), Lowest Nocturnal Desaturation (LND) and Sleep Efficiency (SE) were analyzed. We studied how each of these four parameters correlate with echocardiographic markers of diastolic function; the mitral annular relaxation velocity e' (medial and lateral), Tricuspid Regurgitation velocity (TR), and Pulmonic Valve Acceleration Time (PVAT), respectively. Spearman's rank correlation was used to analyze the correlation between PSG parameters and makers of diastolic dysfunction. According to AHI classification of SDB we had 25% patients with SDB, 35% with mild SDB and 40% with severe SDB. **Results:** Our patient population comprised of 60% females and 40% males. Mean age of our patients was 55.9 ± 8.0 years, mean BMI 35.7 ± 8.8. AHI failed to demonstrate statistically significant correlation with either e', TR, or PVAT. In contrast, LND showed strong correlation with e' (p<0.05) and PVAT (p<0.01), inverse correlation with TR (p<0.001), suggesting the lowest O2 saturation level is an important predictor of diastolic dysfunction. Similarly, both RDI and SE showed a significant correlation with e' (p<0.05) respectively, but not with TR or PVAT. There was a strong correlation between AHI and LND (p<0.001). **Conclusion:** Studies of SDB have focused on severe SDB population represented by highest AHI score. Our study shows the use of AHI may not be reliable when predicting the severity of cardiac dysfunction in patients with SDB. In fact LND seems to be the most significant determinant in cardiac remodeling from the perspective of diastolic function and pulmonary circulation. Our work highlights the importance of other parameters of SDB beyond the traditional AHI score when evaluating SDB patients for cardiac dysfunction.

Poster Session 2 (P2)

Monday, June 24, 2019

P2-134

The Evaluation of Right Heart Function with Exercise Stress Echocardiography in Patients with Connective Tissue Disease

Yi Wang, Lixue Yin. Sichuan Provincial People's Hospital, Chengdu, China

Background: Pulmonary hypertension is one of the most common complications in patients with Connective Tissue Disease (CTD). Patients are usually at the late stage and have irreversible right heart dysfunction when diagnosed as pulmonary hypertension with the rest echocardiography. Early detection of right heart dysfunction before pulmonary hypertension is essential to ensure that patients receive timely and appropriate treatment for this progressive disease. We aimed to use exercise stress echocardiography to detect early right heart dysfunction in patients with CTD and without pulmonary hypertension.

Methods: Treadmill exercise stress echocardiography was performed in 19 CTD patients without pulmonary hypertension at rest and 20 sex & age matched healthy volunteers. Parameters of RV systolic function (RV fractional area change, Doppler tissue s' velocity, and systolic strain and strain rate) and diastolic function (peak E and A velocity, Doppler tissue e' , a' and early and late diastolic strain rate) were evaluated at baseline and after exercise, with the difference (Δ) being systolic and diastolic reserve. **Results:** No significant difference in the body weight, height, age, sex, blood pressure, RV and LV function at rest between the two groups. The RV systolic reserve decreased significantly in CTD group ($\Delta s'$: 5.8 ± 2.1 vs $8.3 \pm 2.5 \text{ cm}^{-1}$, $p < 0.01$; ΔSr : 2.5 ± 0.8 vs $2.8 \pm 0.7 \text{ s}^{-1}$). Similar RV diastolic reserve was found in CTD group ($\Delta e'$: 2.8 ± 1.5 vs $3.9 \pm 2.3 \text{ cm}^{-1}$, $p < 0.05$; $\Delta a'$: 5.8 ± 2.5 vs $10.9 \pm 6.3 \text{ cm}^{-1}$, $p < 0.05$; $\Delta E-Sr$: 0.8 ± 0.2 vs $1.2 \pm 0.5 \text{ s}^{-1}$, $p < 0.05$; $\Delta A-Sr$: 0.9 ± 0.3 vs $1.3 \pm 0.6 \text{ s}^{-1}$, $p < 0.05$).

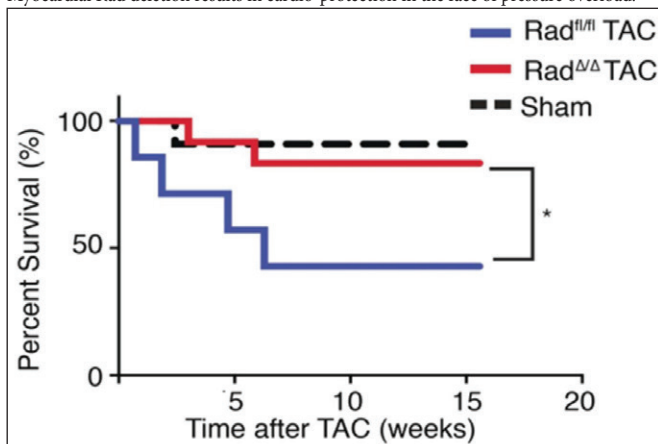
Conclusion: Treadmill exercise echocardiography could detect right heart dysfunction early before diagnosed as pulmonary hypertension with rest echocardiography in patients with CTD. RV reserve after exercise might be a promising parameter to detect pulmonary vascular disease early in CTD patients.

P2-135

Loss of Cardiomyocyte Rad Prevents Cardiac Dysfunction

Bryana M. Levitan, Brooke Ahern, Douglas A. Andres, Jonathan Satin. University of Kentucky, Lexington, KY

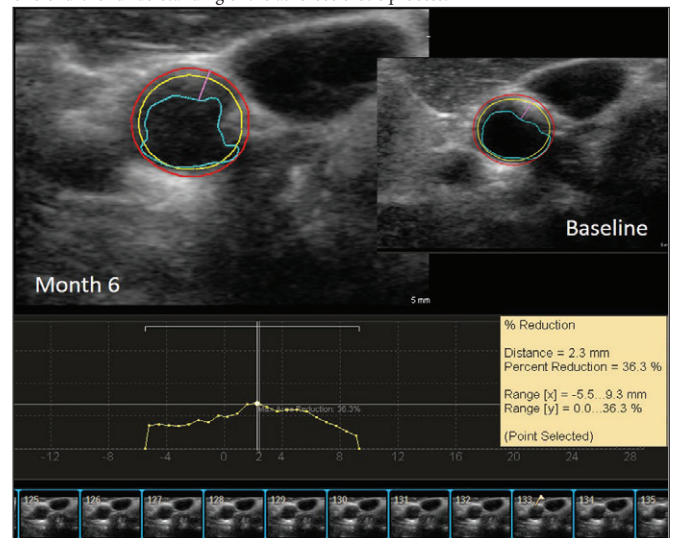
Background: Systemic hypertension causes pathologic cardiac remodeling that leads to left ventricular hypertrophy, arrhythmia and ultimately heart failure. Our lab utilized a mouse model with cardiac restricted Rad to evaluate to impact of Rad loss in the setting of pressure overload. **Methods:** Mice were genetically modified to allow myocardium-restricted, inducible Rad gene rearrangement leading to Rad protein loss. We induced Rad-loss before undergoing surgical transthoracic aorta constriction (TAC) to create pressure overload. Mice were followed by echocardiography (Visual Sonics 3100) at baseline, 2 weeks post Rad-loss induction, 1 week post TAC, 1 month post TAC and 3 months post TAC. Modified parasternal long axis, parasternal short axis and m-mode images were acquired and assessed at all time points. PicoSirus red staining was performed on short axis cross sections of all groups to assess for fibrosis. **Results:** All animals demonstrated normal cardiac systolic function and chamber dimensions at baseline. The Rad loss with TAC had no difference in survival than the control animals with Sham, while the control animals with TAC suffered significant death ($p = 0.002$). Control animals with TAC demonstrated increased left ventricular internal dimensions at 3 months ($p = 0.003$) with decreased ejection fraction at 3 months ($p = 0.0003$). Animals with Rad deletion were no different by echo parameters than Sham animals at 3 months. Animals with TAC demonstrated an increase in fractional fibrotic area over animals with sham ($p = 0.003$ for both control and Rad deletion groups). Heart weight to body weight ratio increased in the control animals with TAC ($p = 0.02$), but remained unchanged in the Rad deletion groups. **Conclusions:** Myocardial Rad deletion results in cardio-protection in the face of pressure overload.



P2-136

Three-Dimensional Plaque Quantification Reveals Progression of Atherosclerosis in Response to Carnitine Therapy in Patients with Metabolic SyndromeAmer M. Johri¹, Marie-France Héту¹, Daren K. Heyland¹, Julia E. Herr¹, Patrick Norman², Murray F. Matangi³, Stephen A. LaHaye¹, Fraser W. Saunders⁴, J. David Spence⁵. ¹Queen's University, Kingston, ON, Canada; ²Kingston General Health Research Institute, Kingston, ON, Canada; ³The Kingston Heart Clinic, Kingston, ON, Canada; ⁴Southeastern Ontario Vascular Laboratory, Kingston, ON, Canada; ⁵Stroke Prevention & Atherosclerosis Research Centre, London, ON, Canada

Background: L-carnitine (L-C) has been investigated as a potential therapy for cardiovascular (CV) disease, but its direct effects on human atherosclerosis are unknown. Epidemiological studies suggest a possible reduction of CV risk factors following treatment, whereas animal studies have shown that L-C may increase pro-atherogenic metabolites. The purpose of this study was to determine whether L-C therapy led to atherosclerosis progression or regression by direct quantification of carotid atherosclerotic lesions in patients with metabolic syndrome (MetS). **Methods:** This study was a Phase 2, prospective, parallel, double blinded, randomized, placebo-controlled, two-center trial. MetS was defined according to the International Diabetes Federation harmonized definition, for presence of 3 of 5 risk factors: elevated waist circumference; elevated triglycerides; reduced HDL; elevated blood pressure; elevated glucose or HbA1c; or treated. Participants were recruited from the Kingston and London Health Sciences Centres. Participants with a baseline carotid total plaque volume (TPV) $\geq 50 \text{ mm}^3$ were randomized to placebo or 2 g L-C daily for 6 months. Plaque progression was quantified by 3D ultrasound for change in TPV and reduction in vessel lumen area (% area stenosis; Fig. 1). Absolute differences were assessed on the raw scale, while percent change on the log scale. Analysis of covariance (ANCOVA) was used to assess within- and between-arm differences. **Results:** A total of 157 participants completed the study (L-C n=76, placebo n=81). No difference between arms was found in the TPV. However, there was progression of plaque stenosis in the treatment arm: the L-C group had an increase in stenosis of 9.8% ($p = 0.01$) higher than the placebo, and a 2.7% ($p = 0.03$) greater absolute change. Total cholesterol and LDL levels (0.10 mmol/L and 0.05 mmol/L, respectively) were higher in the intervention arm compared to the placebo arm (-0.06 mmol/L and -0.07 mmol/L). **Conclusion:** We observed progression of atherosclerosis with L-C therapy compared to placebo in patients with MetS. The clear lack of benefit of L-C therapy in this population raises serious concerns for its further use as a potential therapy. Given its association with pro-atherogenic metabolites our study offers further understanding of the atherosclerotic process.



P2-137

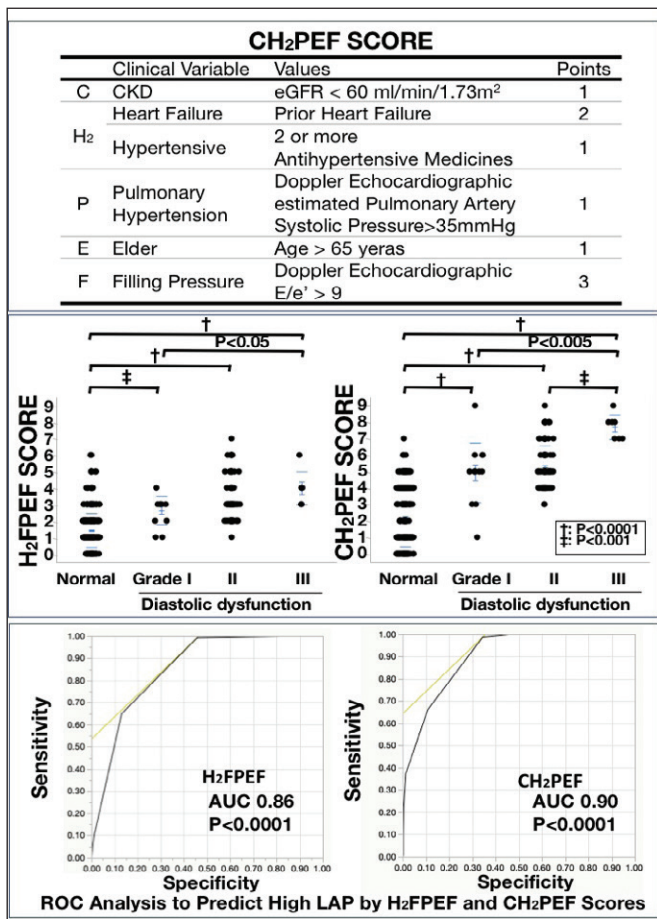
H₂FPEF Score as Modified H₁FPEF Score Discriminate High Left Atrial Pressure in Japanese Patients with HFpEF and Sinus RhythmTomoyuki Watanabe¹, Masumi Iwai-Takano². ¹Health Co-op. Watari Hospital, Fukushima, Japan; ²Fukushima Medical University, Fukushima, Japan

Background: H₁FPEF score, which relies on clinical characteristics and echocardiography, was developed for discrimination heart failure with preserved ejection fraction (HFpEF) from noncardiac dyspnea. However, it remains unclear the relationship between H₁FPEF score and the grade of diastolic dysfunction by echocardiography, and whether the usefulness of H₁FPEF score is ethnic dependence. Thus, we evaluated in Japanese population with preserved EF 1) whether it is possible to detect high left atrial pressure (LAP) (LV diastolic dysfunction with grade II or III) using H₂FPEF score, and 2) whether there is the ethnic dependence of selected variables for H₂FPEF score. **Methods:** We

Poster Session 2 (P2)

Monday, June 24, 2019

enrolled 858 patients (69.5±15.7 years, 441 female) with preserved EF (>50%) and sinus rhythm, who were assessed grade of diastolic dysfunction according to ASE guideline. Exclusion criteria were persistent atrial fibrillation, significant valvular heart disease, severe mitral annulus calcification, post-pacemaker implantation, pulmonary arterial hypertension, constrictive pericarditis, and cases with indeterminate of assessment for diastolic function. We evaluated the relationship between H₂FPEF score and the grade of diastolic function. Moreover, we assessed the utility of variables in H₂FPEF score in Japanese, and evaluated whether there is a necessity of modified H₂FPEF score depending on the race. **Results:** 181 of 858 patients had high LAP. H₂FPEF score significant correlated with the grade of diastolic function (P<0.001). However, the cut off value of H₂FPEF score for detection of high LAP was 2 (AUC 0.86, sensitivity 54.3% and specificity 99.4%). In multivariable analysis, the predictors of high LAP were filling pressure (β=0.31), prior heart failure (β=0.26), hypertension (β=0.15), elder (β=0.12), CKD (β=0.10) and pulmonary hypertension (β=0.09), but not AF and BMI. Thus, we modified H₂FPEF score to CH₂PEF score. In ROC analysis to detect high LAP using CH₂PEF score, the cut off value was 4 (AUC 0.90, sensitivity 98.9% and specificity 65.7%). **Conclusions:** H₂FPEF score is useful to discriminate high LAP, however, there is the ethnic dependence of selected variables in H₂FPEF score. Our data suggests that CH₂PEF score as modified H₂FPEF score is possible to discriminate high LAP in Japanese with sinus rhythm.



patients (24%) had no prior history of atrial arrhythmia compared to controls (5%), p=0.04. A significant proportion of patients (CA 39% vs controls 33%, p=0.78) were chronically anticoagulated for at least 4 weeks prior to index TEE. After a median follow up of 59 days (44-134), LAAT resolved in 9/21(43%) CA patients vs 35/42 (83%) controls (p=0.003) despite adequate anticoagulation in all patients except 2 (1 CA patient and 1 control). **Conclusion:** LAAT failed to resolve in the majority of patients with CA despite adequate anticoagulation. Further research is needed to determine reasons for persistence of LAAT in CA patients and to determine more effective anticoagulation strategies.

	Cardiac amyloidosis (n=21)	Controls (n=42)	P value
Age	61.7± 11.04	63.8± 11.33	0.49
Male	15/21 (71%)	27/42 (64%)	0.77
LVEF<50%	17/21 (81%)	19/42 (45%)	0.008
Sinus rhythm	5/21 (24%)	2/42 (5%)	0.04
Paroxysmal atrial fibrillation	4/21 (19%)	7/42 (16%)	1.0
Persistent atrial fibrillation	12/21 (43%)	33/42 (50%)	0.09
Duration of arrhythmia <48 hours	3/16 (19%)	5/40 (13%)	0.68
CHA2DS2-VASc ≥2	17/21 (81%)	34/42 (81%)	1.0
Anticoagulated prior to LAAT diagnosis	12/21 (57%)	20/42 (48%)	0.6
Treated with warfarin after LAAT diagnosis	17/21 (81%)	39/42 (93%)	0.21
Treated with direct oral anticoagulants after LAAT diagnosis	3/21 (14%)	1/42 (2%)	0.1
Treated with heparin after LAAT diagnosis	1/21 (5%)	2/42 (5%)	1.0

P2-139

Characteristics of Left Ventricular Apical Sparing Ratio and Pressure-strain Derived Global Work Index in Patients with Cardiac Amyloid and Hypertrophic Obstructive Cardiomyopathy

Anne Dybro, Anders H. Larsen, Tor S. Clemmensen, Henrik Vase, Steen H. Poulsen. Aarhus University Hospital, Aarhus N, Denmark

Background: The relative apical sparing (APS) pattern of longitudinal strain (LS) is characterized by decreased deformation from apex towards the basal left ventricular segments. APS has been reported in patients with cardiac amyloidosis (CA) and hypertrophic obstructive cardiomyopathy (HOCM). In both disease entities, severe myocardial thickness are present and other echocardiographic features are often comparable. We compared the APS ratios in HOCM, wild type transthyretin CA (wt-CA), and healthy controls. Furthermore, we assessed myocardial systolic function by global myocardial work index (GWI) to determine the diagnostic value of GWI in differentiating wt-CA patients from HOCM patients. **Method:** A total of 50 patients (HOCM: n=20; wt-CA: n = 30) and 30 controls underwent two-dimensional speckle-tracking echocardiography with LS analysis and assessment of non-invasive brachial artery cuff pressure. APS ratio was calculated as mean LS of the six apical segments divided by mean LS of the six mid and six basal segments. GWI, defined as the left ventricle pressure-strain loop area, was calculated as the product of LS and systolic blood pressure. In HOCM patients, the gradient of the left ventricular outflow tract was multiplied by 0.7 and added to the systolic blood pressure. **Results:** APS ratio was significantly higher in wt-CA and HOCM patients in comparison with controls. Furthermore, the APS ratio tended to be higher in wt-CA patients than HOCM patients (P<0.08). GWI was significantly higher in HOCM than wt-CA patients (P<0.001). GWI was able to discriminate wt-CA from HOCM at a cut-point of 1584 mmHg% (sensitivity: 87%; specificity: 85%; AUC 0.96). **Conclusion:** The APS ratio is significantly higher in HOCM and in particular in wt-CA. Analysis of the left ventricular pressure-strain loop demonstrated that GWI differed between the two diseases, being high in HOCM patients and low in CA. These findings may be useful in the diagnostic process and evaluation of myocardial function in these two diseases with myocardial thickness.

P2-138

Resolution of Left Atrial Appendage Thrombus in Patients with Cardiac Amyloidosis

Edward A. El-Am, Martha Grogan, Sri Harsha Patlolla, Kyle W. Klarich, Omar F. Abou-Ezzeddine, Naser M. Ammash, Rowlens M. Melduni, Angela Dispenzieri, Vuyisile T. Nkomo. Mayo Clinic, Rochester, MN

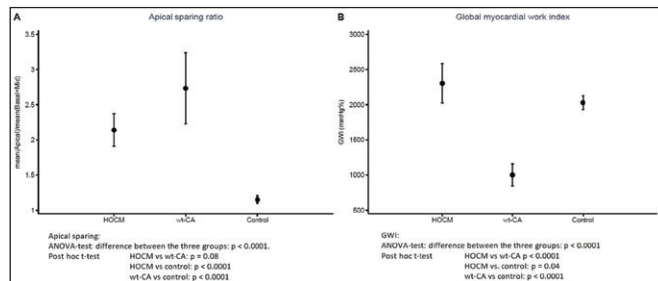
Background: Cardioversion cancellation rate is high in patients with cardiac amyloidosis (CA) because of left atrial appendage thrombus (LAAT) despite adequate anticoagulation. There are no previous studies examining LAAT resolution in CA. **Methods:** CA patients with LAAT diagnosed by transesophageal echocardiogram (TEE) were identified retrospectively and age- and sex-matched 2:1 with controls with LAAT. All patients had follow up TEE assessing thrombus resolution. **Results:** 21 CA patients with LAAT were matched to 42 controls. The mean age was 63±11 years and 67% were men. Patient characteristics are summarized in the Table. Amyloidosis was of the AL type in 12 (57%), ATTRwt type in 8 (38%) and ATTRmut type in 1 (5%). A significant proportion of CA

Poster Session 2 (P2)

Monday, June 24, 2019

Demographics and results				
	HOCM (N=20)	wt-CA (N=30)	Control (N=30)	p
Age	61 ± 12	76 ± 11	55 ± 11	<0.001
Blood pressure (mmHg)				
Systolic	125 ± 19	125 ± 21	124 ± 14	<0.97
Diastolic	77 ± 10	78 ± 11	74 ± 10	<0.74
IVS (cm)	1.85 ± 0.3	1.73 ± 0.4	0.8 ± 0.1	<0.001
PW (cm)	1.1 ± 0.2	1.4 ± 0.3	0.8 ± 0.1	<0.001
LVEF (%)	72 ± 8.2	48 ± 14.3	62 ± 4.5	<0.001
E/e'	16 (12-19)	21 (12-27)	8 (6-9)	<0.001
LS (%)				
Apical	25.4 ± 5.5	15.9 ± 4.7	21.8 ± 3.2	<0.001
Mid	14.6 ± 3.8	9.1 ± 3.6	19.8 ± 1.7	<0.001
Basal	9.8 ± 3.2	5.1 ± 4	17.9 ± 1.6	<0.001
MWI (mmHg%)				
Apical	3534 ± 1084	1517 ± 614	2234 ± 466	<0.001
Mid	1987 ± 692	912 ± 430	2004 ± 288	<0.001
Basal	1387 ± 436	556 ± 426	1844 ± 234	<0.001

Data are expressed as mean ± SD or median (interquartile range).
IVS, interventricular septum diameter; PW, posterior wall diameter; LVEF, left ventricular ejection fraction; E/e', ratio between early mitral inflow velocity and mitral annular early diastolic velocity; LS, longitudinal strain; MWI, myocardial work index.
Comparisons by one-way ANOVA and Kruskal Wallis test.



P2-140

Incidence and Variables Associated with Arrhythmias During Dobutamine Atropine Stress Echocardiography Among Patients with Chagas Disease

Daniela C. Rassi^{1,2,3}, Viviane Tiemi Hotta⁴, Rogerio Gomes Furtado², Marcelo Luiz Campos Vieira⁴, Fabio de Paula Turco², Luciano Henrique Melato², Colandy Nunes Dourado², Luiz Rassi, Jr.², Salvador Rassi¹. ¹Clinical Hospital of University Federal of Goiás, Goiânia, Brazil; ²CDI - Centro de Diagnóstico por Imagem, Goiânia, Brazil; ³Hospital São Francisco de Assis, Goiânia, Brazil; ⁴Heart Institute of University of São Paulo, São Paulo, Brazil

Background: Dobutamine stress echocardiography (DSE) is an important tool in the diagnosis of coronary artery disease. However, there is hesitation in clinical practice for using it in patients with Chagas disease (CD) due to the arrhythmogenic potential of this heart condition. This study aimed to evaluate the incidence and predictors of arrhythmias during DSE in a population of patients with CD. **Methods:** A population of 205 consecutive patients with CD and suspected coronary heart disease was assessed through a retrospective database analysis. CD was confirmed in all patients by serological testing. **Results:** The mean age of the patients selected was 64 years, the mean ejection fraction was 62.3% and 65.4% of the patients were female. Significant arrhythmias occurred as follows: nonsustained ventricular tachycardia in 7.3% of patients; supraventricular tachycardia and sustained ventricular tachycardia in 1%; and atrial fibrillation in 0.5%. Nonsignificant arrhythmias occurred as follows: premature ventricular contractions in 48% of patients and bigeminy in 4.4%. Values for the wall motion score index at rest greater than 1.12 and 1.18 were independently correlated with the occurrence of non-significant arrhythmias (odds ratio [OR] = 2.90, $p < 0.001$) and significant arrhythmias (OR = 4.23, $p = 0.044$), respectively. **Conclusion:** DSE should be considered a safe exam in patients with CD despite the known increased risk of arrhythmias in this group of patients. The occurrence of arrhythmias was low in this study. Abnormal wall motion score index values at rest was associated with the occurrence of significant and non-significant arrhythmias during the test.

P2-141

Relationship Between Systemic Lupus Erythematosus Disease Activity Index Scores and Right Ventricle Function

WenHui Deng^{1,2}, Jing Wang^{1,2}, MingXing Xie^{1,2}, Qing Lv^{1,2}. ¹Department of Ultrasound, Union Hospital, Tongji Medical College, HUST, Wuhan, China; ²Hubei Province Key Laboratory of Molecular Imaging, Wuhan, China

Background: Right ventricular (RV) performance has been demonstrated to be an important independent predictor of cardiovascular morbidity and mortality in patients with systemic lupus erythematosus (SLE). Some evidence has demonstrated that disease

activity could increase the risk of organ damage. **Objectives:** This study investigated the use of three-dimensional speckle tracking echocardiography (3DSTE) and tissue doppler imaging (TDI) to assess the systolic and diastolic RV function in patients with SLE, and the relationship of RV dysfunction and SLE Disease Activity Index (SLEDAI). **Methods:** Fifty SLE patients and fifty age and gender matched healthy (control group) were conducted on 3DSTE and TDI in 2018. Global longitudinal systolic strain of RV septal wall (GLS sep) and Global longitudinal systolic strain of RV free wall (GLS free), EF, EDV, ESV, FAC were obtained by 3DSTE. Pulmonary hypertension (PH) was defined as peak tricuspid regurgitation velocity (TRV) of ≥ 2.9 m/s based upon 2015 ESC guideline. SLE disease activity was assessed using the SLE Disease Activity Index (SLEDAI). Medical records, including patient characteristics, age at diagnosis, duration of disease, BSA, heart rate, diagnosis criteria, cumulative organ damage, laboratory data, were evaluated. **Results:** Compared with controls, the right ventricle's systolic function parameters, including GLS (sep), GLS (free), FAC, RVMPI, were significantly reduced in SLE patients. While assessing the right ventricle's diastolic function, there were no significantly difference between SLE patients and controls. A statistically was found that RVMPI, GLS as an index of right ventricle systolic function parameters impairment had closely relation in the SLEDAI scores. The multivariable regression analysis showed that patients with higher SLEDAI scores had higher rates of PH. **Conclusions:** Echocardiography is a useful noninvasive technique for detecting subclinical RV systolic dysfunction in SLE patients. Disease activity may contribute to RV myocardial impairment and PH.

P2-142

Correlates and Clinical Significance of Right Ventricular Dysfunction in Patients with Preserved Left Ventricular Systolic Function Undergoing Transcatheter Aortic Valve Replacement

Andreas Kyvernitakis, Garima Dahiya, Aditya Joshi, Orestis Pappas, Rahul Sinha, David M. Lasorda, Georgios Lygouris, Robert WW Biederman, Manreet Kanwar, Amresh Raina. Allegheny General Hospital, Pittsburgh, PA

Background: Right ventricular dysfunction (RVD) and pulmonary hypertension are frequent comorbidities in patients with severe aortic stenosis (AS). Little is known about the correlates of RVD in AS patients with preserved left ventricular ejection fraction (LVEF), the change in RVD post transcatheter aortic valve replacement (TAVR) and the impact of RVD on prosthetic aortic valve assessment post TAVR. **Methods:** We reviewed records of patients with severe AS and LVEF $\geq 55\%$ who underwent TAVR at our institution. We analyzed pre-, 1 and 12 month post-procedural transthoracic echocardiograms. The presence of RVD was defined as TAPSE < 16 mm and/or Tissue Doppler S' velocity < 10 cm/s. Variables were compared using paired t-tests and repeated-measures ANOVA. **Results:** 148 patients (median age 83, 61% women) were included. Of these, 33 (22%) had RVD prior to TAVR while 115 (78%) did not. LVEF was similar between groups with and without RVD (65 vs. 66%; $P=0.52$) as was mean grade of LV diastolic dysfunction (1.45 vs 1.56; $P=0.46$). TAPSE (14.4 vs 22.6 mm; $P < 0.001$) and TDS' (9 vs 13 cm/s; $P < 0.001$) were as expected lower in patients with RVD, but estimated PASP (35 vs 35 mm Hg; $P=0.97$), as well as E/e' ratio (19.7 vs 17.6; $P=0.13$) were similar. LV mass index was higher in RVD patients (116 vs. 106 g/m²; $P=0.05$), as was LV posterior wall (12.2 vs 11.2 mm; $P=0.02$) and interventricular septum thickness (13.7 vs. 12.7 mm; $P=0.05$). At 1 month post TAVR, there was a non-significant increase in TAPSE in the RVD group (14.4 vs 15.4mm; $P=0.29$) which did not increase further at 12 months (15.5 mm), whereas TAPSE decreased at 1 month in the cohort without RVD (22.7 vs 21.1 mm, $P=0.004$) before stabilizing at 12 months (21.1 mm). In patients without RVD, LVEF remained stable post TAVR ($P=0.99$), however, in the RVD cohort, LVEF decreased progressively post TAVR, albeit still within normal range (66.4% pre vs 63.6% at 1 month and 61.5% at 12 months; $P=0.02$). Finally, prosthetic aortic valve gradients post TAVR were lower at 1 month in RVD patients (mean gradient 12.8 vs 10.9 mm Hg; $P=0.01$) and remained lower at 12 month follow up (13.7 vs 10.6 mm Hg; $P=0.001$). **Conclusion:** RVD is common in patients with severe AS and preserved LVEF undergoing TAVR. RVD was not associated with grade of LV diastolic dysfunction, PASP or E/e' ratio but was associated with worse LV mass index and LV thickness. Our data suggest that in patients with normal LVEF, RVD may not improve post TAVR and paradoxically LVEF may decrease in those with RVD, while prosthetic aortic valve gradients may be lower on routine assessment.

Poster Session 2 (P2)

Monday, June 24, 2019

P2-143

Feasibility of Transthoracic Doppler Echocardiography-Based Measurement of Coronary Flow Reserve in Heart Failure with Preserved Ejection Fraction

Juliet Ryan¹, Sara Svedlund², Antti Saraste³, Camilla Hage⁴, Ru-San Tan⁵, Lauren Beussink-Nelson¹, Maria Lagerstrom Fermer⁶, Malin A. Broberg⁶, Carolyn S.P. Lam⁵, Lars H. Lund⁴, Li-Ming Gan⁶, Sanjiv J. Shah¹.
¹Northwestern University, Chicago, IL; ²Institute of Medicine, Sahlgrenska University Hospital, University of Gothenburg, Gothenburg, Sweden; ³Heart Center, Turku University Hospital, University of Turku, Turku, Finland; ⁴Department of Medicine, Cardiology Unit and Heart and Vascular Theme, Karolinska Institutet, Stockholm, Sweden, Stockholm, Sweden; ⁵National Heart Centre Singapore, Duke-National University of Singapore, Singapore, Singapore; ⁶Early Clinical Development, IMED Biotech Unit, AstraZeneca, Gothenburg, Sweden

Background: Transthoracic Doppler echo (TDE)-based coronary flow reserve (CFR) has been extensively validated but is not widely used in clinical or research settings. CFR, used for the diagnosis of coronary microvascular dysfunction (CMD; defined as CFR<2.5), is increasingly recognized as a potential pathophysiological factor in heart failure with preserved ejection fraction (HFpEF). We sought to demonstrate the feasibility of TDE-CFR in HFpEF in the setting of a multi-center study (PREvalance Of Microvascular dysfunction in HFpEF [PROMIS-HFpEF]). **Methods:** PROMIS was an observational study conducted at 5 centers. Experienced cardiac sonographers with no prior TDE-CFR experience attended a 1-week intensive training on the TDE-CFR technique. After completion of training, all sites began enrollment. TDE-CFR was attempted in all enrolled patients who did not have contraindications to adenosine. Doppler images of the distal LAD coronary artery were captured at rest/baseline and during a 5-10 min adenosine infusion. CFR was calculated as the ratio of mean diastolic coronary flow velocity mean velocity during adenosine hyperemia / rest. All CFR measurements and quality assessments were made by a core lab blinded to all other echo and clinical information. **Results:** A total of 234 patients with HFpEF (none of whom had unrevascularized epicardial CAD) were enrolled and underwent adenosine TDE of the LAD. CFR was successfully obtained and measured in 203/234 (87%) of the study patients. The overall prevalence of CMD was 75% (95% CI 69-81%). In approximately half (n=15/31) of the patients with unmeasurable CFR, Doppler acquisition of the LAD was attempted but coronary flow could not be visualized. In the rest of these patients (n=16/31), Doppler recordings were made but were deemed not of sufficient quality by the CFR core lab. The only differences between groups were 6-minute walk distance, which was longer in those with successful CFR (329±118 vs. 278±130 meters, p=0.026), and history of revascularized epicardial CAD, which was lower in those with successful CFR (20% vs. 39%, p=0.018). There were no differences between groups in terms of obesity (36% vs. 48%, p=0.20), BMI (30±9 vs. 31±7 kg/m², p=0.32), atrial fibrillation, or lung disease. **Conclusions:** TDE-CFR is feasible in the majority of patients with HFpEF and provides important information on the presence of CMD, which is common and pathophysiologically important in this patient population. With appropriate training, experienced cardiac sonographers can learn and successfully perform the TDE-CFR acquisition technique, even in obese patients.

P2-144

Utility of Echocardiography for Cardiac Amyloidosis in Patients with Suspected Cardiomyopathy

Ian C. Chang, Christopher G. Scott, Alexander T. Lee, Kyle W. Klarich, Angela Dispenzieri, Martha Grogan. Mayo Clinic, Rochester, MN

Background: Cardiac amyloidosis commonly leads to increased myocardial thickness and may mimic other forms of cardiomyopathies. At Mayo Clinic, patients with suspected primary or hypertrophic cardiomyopathy (HCM) are evaluated at the Cardiomyopathy Clinic and echocardiography is routinely acquired to rule out HCM-mimickers, such as cardiac amyloidosis. A relative apical sparing strain pattern has been suggested to be a specific marker for amyloidosis. We sought to determine the utility of echocardiography for the diagnosis of amyloidosis in this outpatient population. **Methods:** We studied consecutive, newly referred patients to the Cardiomyopathy Clinic at Mayo Clinic from January 2011 to December 2017. Patients referred to the Amyloidosis Clinic or with prior diagnosis of amyloidosis were excluded. The diagnosis of amyloidosis was determined using clinical designation in the Mayo Clinic dysproteinemia database. Using classification trees, echocardiographic variables with the ability to discriminate between amyloid and non-amyloid patients were identified to determine the diagnostic utility. **Results:** Of the 3134 patients, 3016 (96%) had an echocardiogram and 42 (1.3%) were diagnosed with amyloidosis. Compared to non-amyloid patients, those with amyloidosis were older, more likely to be male, have lower ejection fraction, cardiac index, average global longitudinal strain (LS), relative apical sparing with a higher apical to basal LS ratio (ABSR), higher estimated RV systolic pressure, LV mass index, and thicker LV walls (Table). When available, of all the echocardiographic markers, ABSR best discriminated between patients with and without amyloidosis; all patients with amyloidosis had ABSR > 1.4, and 4.4% (37/849) of patients with ABSR > 1.4 had amyloidosis. When used in patients with posterior wall thickness (PWT) ≥ 12 mm, the diagnostic yield of ABSR > 1.4 increased to 6.4% (34/524). No patient with ABSR ≤ 1.4 was diagnosed with amyloidosis. **Conclusions:**

Among new patients with suspected cardiomyopathy, use of ABSR in patients with PWT ≥ 12 mm could increase the diagnostic yield for amyloidosis to 6.4% and potentially rule out amyloidosis when ABSR ≤ 1.4. Additional research is needed to determine the subset of patients who might benefit most from screening echocardiography for amyloidosis.

Table. Characteristics of study patients with suspected cardiomyopathy, N = 3134			
	Non-amyloid (N=3092)	Amyloidosis (N=42)	p-value
Age (years)	56.5 (15.7)	68.2 (9.9)	<0.001
Male gender	1760 (57%)	34 (81%)	0.002
Creatinine (mg/dL)	1.0 (0.9, 1.2)	1.2 (1.0, 1.4)	<0.001
NTproBNP (pg/mL)	506.5 (175.0, 1250.0)	1764.5 (945.0, 4827.0)	<0.001
Echocardiogram available	2976 (96%)	40 (95%)	0.73
LVEF (%)	67.0 (62.0, 71.0)	55.0 (43.0, 64.0)	<0.001
LV septal wall thickness (mm)	14.0 (11.0, 18.0)	17.0 (15.5, 19.0)	<0.001
LV posterior wall thickness (mm)	11.0 (10.0, 13.0)	15.5 (13.0, 18.0)	<0.001
LV cardiac index (ml/m ² /min)	3.0 (2.6, 3.6)	2.4 (2.1, 3.2)	<0.001
LV mass index (g/m ²)	122.0 (98.0, 156.5)	168.5 (147.0, 195.0)	<0.001
Left atrial volume index (mL/m ²)	41.0 (33.0, 53.0)	42.0 (37.0, 53.0)	0.5
Estimated RV systolic pressure (mmHg)	32.0 (26.0, 39.0)	41.5 (32.0, 46.0)	<0.001
Average global LV longitudinal strain (%)	-16.0 (-18.0, -12.0)	-10.0 (-12.0, -8.0)	<0.001
Average apical LV longitudinal strain (%)	-18.0 (-22.0, -13.0)	-16.0 (-19.0, -13.0)	0.2
Average mid-ventricular LV longitudinal strain (%)	-16.0 (-19.0, -12.0)	-10.0 (-12.0, -8.0)	<0.001
Average basal LV longitudinal strain (%)	-14.0 (-17.0, -11.0)	-5.0 (-8.0, -4.0)	<0.001
Average apical to basal LV longitudinal strain ratio	1.3 (0.9, 1.7)	2.5 (2.1, 4.0)	<0.001

Data are presented as number (percentage), mean (standard deviation) or median (interquartile range). EF = ejection fraction, LV = Left ventricular, RV = right ventricular

P2-145

Associations Between Cardiac Biomarkers and Echocardiographic Measures in Chronic Kidney Disease

Nathan R. Stein¹, Leila R. Zelnick², Amanda H. Anderson³, Robert H. Christenson⁴, Christopher R. deFilippi⁵, Rajat Deo⁶, Alan S. Go⁷, Jiang He³, Bonnie Ky⁸, James P. Lash⁹, Stephen L. Seliger⁴, Elsayed Z. Soliman⁹, Michael G. Shlipak¹, Nisha Bansal². ¹University of California, San Francisco, San Francisco, CA; ²University of Washington School of Medicine, Seattle, WA; ³Tulane University School of Public Health and Tropical Medicine, New Orleans, LA; ⁴University of Maryland School of Medicine, Baltimore, MD; ⁵Inova Heart and Vascular Institute, Falls Church, VA; ⁶Perelman School of Medicine at the University of Pennsylvania, Philadelphia, PA; ⁷Kaiser Permanente, Oakland, CA; ⁸University of Illinois College of Medicine, Chicago, IL; ⁹Wake Forest School of Medicine, Winston-Salem, NC

Background: Subclinical changes to cardiac structure and function detected with echocardiography precede the development of clinical heart failure in persons with chronic kidney disease (CKD). Circulating cardiac biomarkers may reflect these pathophysiological changes. This study investigated associations between established biomarkers (N-terminal pro-B-type natriuretic peptide [NT-proBNP] and high sensitivity troponin T [hsTnT]) and novel biomarkers (growth differentiation factor 15 [GDF-15], Galectin-3 [Gal-3], and soluble ST-2 [sST-2]) with echocardiographic measurements in persons with CKD. **Methods:** Among 2,101 participants with mild to moderate CKD in the Chronic Renal Insufficiency Cohort, biomarker levels measured at baseline were evaluated with echocardiographic measurements from year 1. These included measures of left ventricular mass index (LVMI), end-systolic volume (LVESV), end-diastolic volume (LVEDV), ejection fraction (LVEF), and left atrial diameter (LAD). Multivariable linear regression analyses tested associations of each biomarker with each echocardiographic measurement, adjusting for age, sex, race/ethnicity, prior cardiovascular disease, diabetes, smoking, kidney function, uric acid, blood pressure, BMI, and medication use. **Results:** GDF-15, modeled as a continuous predictor (per standard deviation higher), was significantly associated with higher LVMI (1.0 g/m^{2.7}, CI 0.4 - 1.7), LVESV (0.4 mL/m^{2.7}, CI 0.0 - 0.7), and LVEDV (0.6 mL/m^{2.7}, CI 0.1 - 1.1), but not with LVEF (-0.2%, CI -0.7 - 0.3) or LAD (0.0 cm, CI -0.03 - 0.04), after adjusting for covariates. Gal-3 and sST-2 were not significantly associated with any echocardiographic measurements. Higher levels of NT-proBNP were associated with a higher LVMI (2.2 g/m^{2.7}, CI 1.6 - 2.8), higher LVESV (1.2 mL/m^{2.7}, CI 0.8 - 1.5), higher LVEDV (1.4 mL/m^{2.7}, CI 1.0 - 1.8), lower LVEF (-1.1%, CI -1.6 - -0.7), and higher LAD (0.13 cm, CI 0.10 - 0.16). Higher levels of hsTnT were associated with a higher LVMI (2.2 g/m^{2.7}, CI 1.6 - 2.8), higher LVESV (0.8 mL/m^{2.7}, CI 0.5 - 1.1), higher LVEDV (1.0 mL/m^{2.7}, CI 0.7 - 1.4), lower LVEF (-0.7%, CI -1.1 - -0.3), and higher LAD (0.06 cm, CI 0.02 - 0.09). **Conclusion:** In patients with CKD, the novel biomarker GDF-15, a marker of inflammation and tissue injury in cardiovascular and non-cardiovascular cell types, was associated with echocardiographic measurements of subclinical cardiovascular disease. GDF-15 may highlight biological pathways that contribute to development of cardiovascular disease, in addition to those reflected by NT-proBNP and hsTnT.

Poster Session 2 (P2)

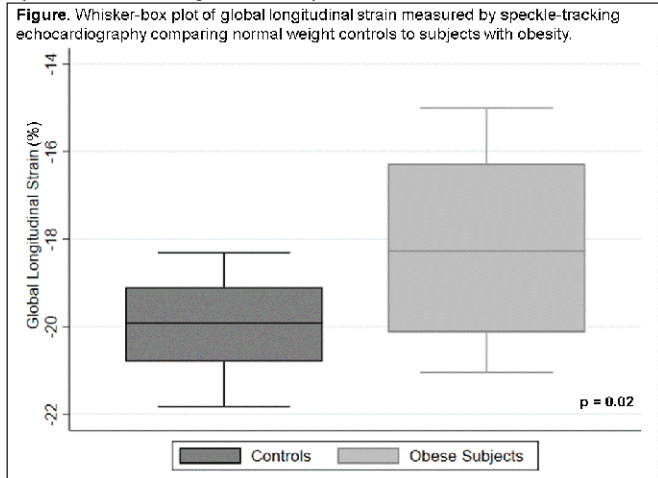
Monday, June 24, 2019

P2-146

Global Longitudinal Strain is Diminished in Young Children with Obesity

Erin A. Paul¹, Nikhil Pasumarti², Thomas J. Starc², Vidhu V. Thaker², Aviva B. Sopher², Jennifer A. Woo Baidal², Michael Rosenbaum², Ameer M. Shah².
¹Children's Hospital at Montefiore, Albert Einstein College of Medicine, Bronx, NY; ²New York-Presbyterian Morgan Stanley Children's Hospital, Columbia University Medical Center, New York, NY

Background: Subclinical cardiac dysfunction defined as diminished global longitudinal strain (GLS) with normal ejection fraction (EF) has been identified in adolescents with obesity using speckle-tracking echocardiography. Studies in early childhood are lacking, and the age of onset of dysfunction is unknown. We hypothesized that GLS is diminished in young children with obesity compared to counterparts with healthy body mass index (BMI). **Methods:** Normotensive children with obesity, ages 2 to 9 years, were prospectively recruited between July 2017 and June 2018 from the Families Improving Health Together Clinic, a multidisciplinary obesity program, and compared to retrospectively-identified sex- and age-matched normal weight controls. We excluded children with hypertension, cardiac disease, and obstructive sleep apnea. GLS was performed using TomTec software. Left ventricular (LV) volumes, EF, and mass were measured by the 5/6 area length method. Wilcoxon matched-pairs signed-ranks test was used to compare groups. **Results:** The median [IQR] age in both groups was 8 [6, 9] years and 50% were male. BMI differed significantly between groups with a median of 25 [25, 29] kg/m² (n=12) in the obese children versus 16 [15, 17] kg/m² (n=12) in controls (p<0.001). Similarly, the median BMI percentile was uniformly ≥95th percentile in the obese group and 54 [34, 70] in controls; 7 subjects had class 2 obesity, and 4 subjects had class 3 obesity. GLS was significantly decreased in subjects with obesity (-18.3 [-20, -16] % vs. -19.9 [-21, -19] %, p = 0.02, Figure). While none of the controls had a GLS below -18, half of the obese cohort did. The systolic blood pressures, LV EF, end-diastolic and end-systolic volumes were not significantly different between groups. Although LV mass was increased in the obese children compared to controls (57 [48, 70] g vs. 44 [35, 50] g, p = 0.04), LV mass indexed to height^{2.7} was not different between groups. **Conclusion:** GLS is diminished in this group of young children with obesity. This suggests that preventive measures and treatment for obesity must be enacted early in life. These results encourage a larger, prospective study to further characterize the timing of onset and risk factors for development of abnormal myocardial mechanics in pediatric obesity.



P2-147

Short-Term Impacts of Transjugular Intrahepatic Portosystemic Stent Shunt on Right Ventricular Function Assessed by Three-Dimensional Echocardiography

Y.J. Zhao, H.Y. Chen, J.F. Wang, J.J. Luo, Y.G. Su, Xianhong Shu. Zhongshan Hospital, Fudan University, Shanghai, China

Background: We aimed to evaluate the short-term impacts of transjugular intrahepatic portosystemic stent shunt (TIPS) on right ventricular function in patients with liver cirrhosis. **Methods:** Two-dimensional (2D) and three-dimensional (3D) echocardiography were performed in twenty patients with intractable esophageal varices or refractory ascites before and 3 months after TIPS. Right ventricular end-diastolic area (RVEDA), right ventricular end-systolic area (RVESA), right atrial area (RAA), right ventricular end-diastolic diameter (RVEDD), pulmonary arterial systolic pressure (PASP), tricuspid annulus plane systolic excursion (TAPSE), the maximum diameter of inferior vena cava (IVCmax) and the minimum diameter of inferior vena cava (IVCmin) were measured by conventional echocardiography. RV fractional area change (FAC) was calculated according to RVEDA and RVESA, and inferior vena cava collapse index (IVC-CI) was calculated according to IVCmax and IVCmin. End diastolic volume (EDV), end systolic volume (ESV) and ejection fraction (EF) of right ventricular body (RVB), right ventricular

outflow tract (RVOT), right ventricular inflow tract (RVIT) and global right ventricle (RV) were measured by TOMTEC software using 3D full-volume pyramid datasets. **Results:** 1. After TIPS, 3D echocardiography detected a significant increase in right ventricular volume and contraction. (Before vs After TIPS: RVOT-EDV : 17.42±7.70 vs. 21.46±8.28 ; RVIT-EDV , 0.89±24.11 vs. 59.72±19.50; RVB-EF, 0.30±0.13 vs. 0.41±0.13; RVIT-EF, 0.57±0.09 vs. 0.65±0.08; global RVEF, 0.51±0.08 vs. 0.59±0.08; all p<0.01). 2. Although 2D echocardiography failed to detect the difference in right ventricular volume and contraction before and after tips, PASP worsened obviously and IVC-CI decreased significantly, indicating a rise in right atrium pressure and a decline in right ventricular diastolic function. (Before vs aAfter TIPS: PASP, 32.5±4.77 vs. 37.05±8.14, p<0.01; IVC-CI, 0.27±0.11 vs. 0.21±0.07, p<0.05). **Conclusion:** TIPS can cause right ventricular overload, and diastolic dysfunction. 3D echocardiography can detect changes of right ventricular volume and ejection fraction in a more sensitive way than 2D echocardiography.

P2-148

Echocardiographic Findings of Trypanosoma Cruzi Seropositive Blood Donors

Vera M. C. Salemi¹, Antonio Ribeiro², Claudia Oliveira³, Marcia Menezes⁴, Andre Antunes⁴, Julio Ferreira-Filho¹, Fabio Fernandes¹, Barbara Ianni¹, Charles Mady¹, Anna Carneiro-Proietti¹, Ester Sabino¹, Vandana Sachdev⁵.
¹Heart Institute (InCor), University of São Paulo Medical School, São Paulo, Brazil; ²Hospital das Clínicas e Faculdade de Medicina da Universidade Federal de Minas Gerais, Belo Horizonte, Brazil; ³Campos Dona Lindu da Universidade Federal de São João Del Rei, Divinópolis, Brazil; ⁴Centro de Ciências Biológicas e da Saúde- Prontosocor, Montes Claros, Brazil; ⁵National Heart, Lung and Blood Institute, Bethesda, MD

Introduction: Chagas' disease is caused by the protozoan Trypanosoma cruzi and is endemic in South and Central Americas. Due to immigration of infected individuals, it is becoming an increasing problem in non-endemic developed countries. Echocardiography is a noninvasive tool that allow the evaluation of cardiac morphology and function in different stages of Trypanosoma cruzi-infected patients. The objective of this study is to detect early echocardiographic findings in T. cruzi seropositive compared to patients with advanced Chagas' cardiomyopathy and seronegative blood donors (controls). **Methods:** This study population was derived from a retrospective cohort, in which 499 T. cruzi seropositive blood donors [(no Chagas' cardiomyopathy (CC-) and with CC (CC+)] identified by blood bank screening and 488 seronegative blood donors (controls) matched, and 101 previously diagnosed cases of severe Chagas' disease cardiomyopathy (CCC) followed at tertiary university hospital, were enrolled to perform complete echocardiographic study (NHLBI Retrovirus Epidemiology Donor Study-II). Distributions of data were examined for normality by using Kolmogorov-Smirnov tests. Bivariate analyses were developed for the groups and covariables were analyzed. Then, logistic regression model was developed with the use of a forward elimination approach. **Results:** Left ventricular systolic dimension, relaxation variable and wall motion score (WMS) were found in the early phase of the disease. Whereas, WMS, relaxation variable and particularly, left ventricular systolic dimension allowed the detection of the advanced stage of Chagas' disease. The multivariate analysis results are shown at the Table.

Variables	Controls vs CC -adjusted OR (CI95%)	Controls vs CC+adjusted OR (CI95%)	Controls vs CCCadjusted OR (CI95%)
LVEDD/BSA (mm/m ²)	1.44 (1.08-1.94)	3.29(2.05-5.26)	
LVESD/BSA (mm/m ²)			68.3 (10.5-444.41)
Ejection Fraction (%)		0.45 (0.26-.077)	
E' septum (cm/s)			3.17 (1.12-8.9)
E' average (cm/s)		0.72(0.52-0.99)	
IVRT (ms)	1.67 (1.38-2.02)	1.58 (1.19-2.11)	
Wall Motion Score	0.10(0.02-0.46)		9.26(3.27-26.2)

CC, Chagas cardiomyopathy; E' average, E' septum + lateral/2; IVRT, isovolumic relaxation time; LVEDD/BSA, left ventricular end-diastolic dimension corrected by body surface area; LVESD/BSA, left ventricular end-systolic dimension corrected by body surface area
Conclusions: In this largest echocardiographic evaluation of cardiac function, echocardiographic alterations were detected in the different stages of Chagas' disease. Future studies using new echocardiographic modality such as myocardial deformation imaging would improve the diagnosis of early cardiac involvement in this disease.

Poster Session 2 (P2)

Monday, June 24, 2019

P2-149

Relationship of Left Ventricular Mechanics and Mechanical Dispersion to Exercise Capacity in Patients with Hypertrophic Cardiomyopathy

Xiu-Zhang Lu, Xiao-Peng Wu, Yi-Dan Li, Yi-Dan Wang, Qi-Zhe Cai, Lan-Lan Sun, Wei-Wei Zhu, Wei Jiang, Xiao-Guang Ye. Beijing Chao Yang Hospital, Beijing, China

Background: Impaired exercise capacity is associated with adverse cardiovascular events in patients with hypertrophic cardiomyopathy (HCM). We aimed to investigate the association between left ventricular mechanics and mechanical dispersion (MD) and exercise capacity in HCM patients by exercise speckle-tracking echocardiography. **Methods:** Sixty-five HCM patients (40 with obstructive, 25 with non-obstructive) and 25 control subjects were recruited in this study. Left ventricular mechanics, MD and exercise capacity were evaluated by two-dimensional speckle-tracking imaging and exercise echocardiography, and the following parameters of left ventricular mechanics were recorded at rest and during exercise: left ventricular global longitudinal strain (LVGLS), the ratio of peak early diastolic mitral inflow to annulus velocity (E/e'); MD was evaluated by the standard deviation of time to maximal myocardial shortening of left ventricular longitudinal strain; Left ventricular mechanical reserve was defined as the difference of LVGLS (Δ LVGLS) between peak exercise and rest; Exercise capacity was evaluated by metabolic equivalents (METs). The association between left ventricular mechanics and MD and exercise capacity was explored. **Results:** Compared with the controls, non-obstructive patients had higher E/e' and MD and lower absolute value of LVGLS, Δ LVGLS, and METs at rest and during exercise. Moreover, E/e' and MD were further increased, while LVGLS and METs were further decreased in obstructive patients. LVGLS, E/e' and MD measured at peak exercise were associated with METs ($r = -0.68, -0.54$ and -0.43 , all $P < 0.001$, respectively). The multiple linear regression analysis revealed that the parameters of LVGLS and E/e' during exercise are independently correlated with exercise capacity. Receiver operating characteristic curve analysis showed LVGLS during exercise had better predictive value of exercise intolerance (METs < 7) in HCM patients with an area under the curve of 0.793, a sensitivity of 86.5%, and a specificity of 64.3%. **Conclusion:** HCM patients have lower left ventricular mechanics and mechanic reserve and higher MD. Moreover, obstructive patients have more severe impairment of left ventricular mechanics and exercise capacity. Exercise intolerance is associated with impaired left ventricular mechanics and higher MD, which can predict the reduced exercise capacity and may be helpful for risk stratification in HCM patients.

P2-150

Right and Left Ventricular Dysfunction Relates with Clinical Severity in Patients with Parkinson Disease

Risako Fujiwara¹, Masumi Iwai-Takano², Nobuyuki Ohte³. ¹Research Institute for Brain and Blood Vessels-Akita, Akita, Japan; ²Fukushima Medical University, Fukushima, Japan; ³Nagoya City University Graduate School of Medical Sciences, Nagoya, Japan

Backgrounds: Several investigators have reported that cardiac sympathetic nerve dysfunction is appeared in patients with Parkinson's disease (PD). However, it remains unclear whether PD has left ventricular (LV) and right ventricular (RV) dysfunction. In this study, we assessed whether 1) LV and RV dysfunction occurs in PD, 2) the cardiac dysfunction relates with clinical severity in patients with PD. **Methods:** We examined LV and RV function in 38 patients with PD (PD group) and age-matched 17 control subjects (C group) using conventional, tissue Doppler (tissue velocity of the mitral (septal and lateral LV-s', e', a') and tricuspid (RV-s') valve annuli), and strain echocardiography (LV global longitudinal strain (GLS)) in the three-apical views by 2D speckle tracking method (EchoPac™). Patients with previous cardiac disease and atrial fibrillation were excluded. In addition, PD patients were divided into two groups according to the Hoehn and Yahr scale (clinical severity of PD), i.e., HY mild group (n=25): HY I to III, and HY severe group (n=13): HY scale IV and V. We compared indices of echocardiography between the HY mild group and the HY severe group. **Results:** There was no significant difference in the age (74.2±8.1 vs 71.4±7.0 years), the LV ejection fraction (65.9±4.5 vs 68.5±6.2%), or the LV E/A (0.76±0.27 vs 0.82±0.13) between the PD and the C groups. In the PD group compared to the C group, LV end diastolic volume index (48.5±11.8 vs 41.3±11.6 ml/m², P<0.05), LV mass index (93.0±37.7 vs 79.3±14.3 mm/m², P<0.05) and LV-E/e' (12.6±6.2 vs 10.2±1.9, P<0.05) were significantly increased, in contrast LV-e' (4.9±1.4 vs 5.7±1.0 cm/s, P<0.01), LV-s' (5.2±1.2 vs 5.8±0.9 cm/s, P<0.05), RV-s' (9.8±1.9 vs 10.9±1.8, P<0.05) and GLS (-20.7±2.7 vs -22.4±2.5%, P<0.05) were significantly decreased. In PD patients, significant differences in the age, LV-s', LV-e', LV-E/e', and RV-s' between the HY mild group and the HY severe group were also observed. In multivariable analysis, independent predictors of the HY scale were the age (P<0.01) and the RV-s' (P<0.05). **Conclusions:** Cardiac dysfunction, which is not acknowledged as a decrease in LV ejection fraction, is clarified by using GLS and LV-s', LV-e' and RV-s' in patients with PD. Especially, RV systolic dysfunction may be related to the clinical severity of PD.

P2-151

Size and Function Evaluation of Left and Right Ventricles in Chagas Patients without Known Cardiomyopathy

Diego Medvedofsky¹, Pedro Gutierrez-Fajardo², Hilda Peralta-Rosado³, Verónica Bravo-Rendón⁴, Martín Ibarrola⁵, Eric Kruse⁶, Tracy Lawrence⁷, Rachel Marcus¹, Carolina Melendez⁸, Adriana Ortega-Gutierrez⁹, Rhonda Price¹⁰, Emma Rosas-Munive¹¹, Madeline Schiminger¹², Allison Sterk¹³, Benigno Valderrábano-Salas¹⁴, Miguel A. Corona Franco¹⁵, Roberto M. Lang⁶, Federico M. Asch¹. ¹MedStar Health Research Institute and MedStar Heart and Vascular Institute, Washington, DC; ²Hospitales Mac Bernardette, Guadalajara, Mexico; ³Hospital General Agustín O'Horan, Mérida, Mexico; ⁴Instituto del Corazón, Querétaro, Mexico; ⁵Centro Cardiovascular, Bella Vista, Argentina; ⁶University of Chicago, Chicago, IL; ⁷Cigna, Glendale, CA; ⁸Baylor Scott & White The Heart Hospital, Plano, TX; ⁹Unidad Médica de Alta Atención, Yucatán, Mexico; ¹⁰American Society of Echocardiography, Durham, NC; ¹¹Hospital General de México, Mexico City, Mexico; ¹²Johns Hopkins Hospital, Baltimore, MD; ¹³Great Ormond St Hospital, London, United Kingdom; ¹⁴Hospital Regional de Alta Especialidad Bicentenario de la Independencia, Mexico, Mexico; ¹⁵Philips Healthcare, Mexico, Mexico

Background: Chagas disease (ChD) is a parasitic infection diagnosed by serology. It is highly prevalent in Latin America and can induce cardiomyopathy in a minority of infected individuals. The American Society of Echocardiography Foundation and ANCAM organized a global health initiative in collaboration with the Mexican national and state Governments to investigate the prevalence of ChD cardiomyopathy (Yucatán, Mexico) in patients known to be carriers of the infection but without a previous cardiac examination. ChD cardiomyopathy is usually diagnosed by conventional echocardiography and EKG. We aim to describe myocardial deformation findings by speckle tracking echocardiography (STE) in patients with Chagas infection and investigate its potential role in diagnosis of cardiomyopathy. **Methods:** Patients with a positive serology for ChD during blood bank screenings, underwent a comprehensive cardiac exam with echo and EKG. Offline strain STE analysis of both left and right ventricles (LV, RV) was performed (TOMTEC) from which size and function parameters were derived. Indices included LV end-diastolic and end-systolic (ED, ES) volumes, ejection fraction (EF) and global/regional longitudinal strain (LS) and RV ED and ES areas, fractional area change (FAC) and free-wall (FW) LS. Normal cutoff values recommended by guidelines were used: 52/54% for LVEF (male/female), 35% for RV FAC and -20% for both LV global LS and RV FW LS. Bull's Eye with 18 segments was created for LV LS. **Results:** From a total of 156 consecutive patients (43±12 years, 33% females), some were lost due to technical problems or poor image quality: 138 and 96 patients were analyzed for the LV and RV respectively. LV ED and ES volumes were 104±29 and 43±19 ml, EF 59±7% and global LS -22±3%. RV ED and ES areas were 20±5 and 11±3 cm², FAC 45±6% and free wall LS -26±4%. Patients with abnormal LV EF were 12 (9%), LV global LS 17 (12%), RV FAC 6 (6%) and RV free wall LS were 4 (4%). Bull's Eye of the LV showed that inferior and infero-septal segments had lower LS in basal than in apical segments, opposite to the pattern in all other walls (Figure) **Conclusion:** Our STE findings in patients with ChD suggest LV GLS is more sensitive than LV EF to identify patients with abnormal LV function and that patients have an atypical regional function pattern affecting the inferior and inferolateral walls

